1-1-2014

Development of Spinal Neuronal Hyperexcitability and Structural Plasticity after Cervical Facet Injury: Implications for Modulating Persistent Pain

Nathan Crosby
University of Pennsylvania, nated.crosby@gmail.com

Development of Spinal Neuronal Hyperexcitability and Structural Plasticity after Cervical Facet Injury: Implications for Modulating Persistent Pain

Abstract
Chronic neck pain is a prevalent and costly condition that commonly develops after whiplash injuries. The cervical facet joint and its capsular ligament are frequently identified as a source of pain in patients, particularly those with whiplash-associated disorders. Spinal neuronal hyperexcitability is a common feature of persistent pain that can be induced by enhanced excitatory signaling in the dorsal horn. Spinal dorsal horn neurons develop hyperexcitability after painful facet joint injury, but the neurophysiological mechanisms that lead to spinal hyperexcitability and persistent pain after facet joint loading remain unclear. This thesis uses a rat model of painful facet joint injury to define the peripheral and spinal signals that promote dorsal horn neuronal hyperexcitability. In particular, the development of spinal hyperexcitability is evaluated by characterizing neuronal activity at multiple times within the first day after painful facet joint injury. To evaluate the role of injury-induced joint afferent activity in the potentiation of excitatory signaling and spinal neuronal excitability, afferent activity is blocked at various times after painful facet joint injury. Excitatory synaptogenesis and the mechanisms inducing synaptogenesis are evaluated to determine whether structural plasticity in the spinal cord contributes to facet-mediated pain. Spinal cord stimulation (SCS) is an effective clinical therapy that attenuates chronic pain by modulating spinal hyperexcitability, but the mechanisms and effectiveness of SCS for persistent neuropathic or joint-mediated pain remain unclear. This thesis evaluates the use of a novel mode of SCS, burst SCS, in rat models of cervical radiculopathy and painful facet joint injury. The role of GABA signaling in the inhibitory effects of burst SCS on dorsal horn neurons is assessed by applying GABA receptor antagonists to the spinal cord during the application of burst SCS. Studies in this thesis demonstrate that afferent discharge induced by injurious loading of the facet joint initiates excitatory synaptic and structural changes in the spinal cord that promote neuronal hyperexcitability, but SCS can attenuate persistent pain by reducing spinal hyperexcitability. This thesis provides a foundation for future investigations into the mechanisms underlying the transduction of mechanical joint injury to centrally-mediated pain and the development of effective therapies for chronic pain.

Degree Type
Dissertation

Degree Name
Doctor of Philosophy (PhD)

Graduate Group
Bioengineering

First Advisor
Beth A. Winkelstein

DEVELOPMENT OF SPINAL NEURONAL HYPEREXCITABILITY AND STRUCTURAL PLASTICITY AFTER CERVICAL FACET INJURY: IMPLICATIONS FOR MODULATING PERSISTENT PAIN

Nathan D. Crosby

A DISSERTATION

in

Bioengineering

Presented to the Faculties of the University of Pennsylvania in

Partial Fulfillment of the Requirements for the

Degree of Doctor of Philosophy

2014

Supervisor of Dissertation

_____

Beth A. Winkelstein, Professor of Bioengineering

Graduate Group Chairperson

_____

Jason A. Burdick, Professor of Bioengineering

Dissertation Committee
David F. Meaney, Professor and Chair of Bioengineering
Gordon Barr, Associate Professor of Psychology in Anesthesiology and Critical Care
Wenqin Luo, Assistant Professor of Neuroscience
Iyad Obeid, Associate Professor of Electrical and Computer Engineering, Temple Univ.

ACKNOWLEDGMENTS

I am immensely grateful to my advisor, Dr. Beth Winkelstein, for her support throughout my training. Her mentorship and guidance will benefit me throughout the rest of my professional career, and I hope to continue to gain from her insight and experience in the years to come. I would also like to thank the members of my committee, Dr. David Meaney, Dr. Gordon Barr, Dr. Wenqin Luo, and Dr. Iyad Obeid, for their commitment to my success and their insight during the development and completion of this work.

I would like to thank Dr. Melanie Goodman-Keiser for the training and assistance she provided during our collaboration. Her experience and advice were instrumental for designing the experiments, analyzing the data, and interpreting the findings in the studies in this thesis using spinal cord stimulation.

I am very grateful to the past and present members of the Spine Pain Research Lab for their support and constant friendship over the years. I would especially like to thank those lab members that contributed directly to my research, including Kyle Quinn, Ling Dong, Christine Weisshaar, Martha Zeeman, Jenell Smith, Jeff Kras, Ben Bulka, and Taylor Gilliland.

I would like to thank my family for their unending encouragement and their commitment to seeing me achieve my goals. Finally, I would like to thank my wife, Erika. We leaned on each other frequently as we both navigated graduate school over the last several years, and I am eternally grateful for her love, patience, perseverance, and unwavering dedication.

ABSTRACT

DEVELOPMENT OF SPINAL NEURONAL HYPEREXCITABILITY AND STRUCTURAL PLASTICITY AFTER CERVICAL FACET INJURY: IMPLICATIONS FOR MODULATING PERSISTENT PAIN

Nathan D. Crosby

Beth A. Winkelstein

Chronic neck pain is a prevalent and costly condition that commonly develops after whiplash injuries. The cervical facet joint and its capsular ligament are frequently identified as a source of pain in patients, particularly those with whiplash-associated disorders. Spinal neuronal hyperexcitability is a common feature of persistent pain that can be induced by enhanced excitatory signaling in the dorsal horn. Spinal dorsal horn neurons develop hyperexcitability after painful facet joint injury, but the neurophysiological mechanisms that lead to spinal hyperexcitability and persistent pain after facet joint loading remain unclear. This thesis uses a rat model of painful facet joint injury to define the peripheral and spinal signals that promote dorsal horn neuronal hyperexcitability. In particular, the development of spinal hyperexcitability is evaluated by characterizing neuronal activity at multiple times within the first day after painful facet joint injury. To evaluate the role of injury-induced joint afferent activity in the potentiation of excitatory signaling and spinal neuronal excitability, afferent activity is blocked at various times after painful facet joint injury. Excitatory synaptogenesis and the mechanisms inducing synaptogenesis are evaluated to determine whether structural plasticity in the spinal cord contributes to facet-mediated pain. Spinal cord stimulation

(SCS) is an effective clinical therapy that attenuates chronic pain by modulating spinal hyperexcitability, but the mechanisms and effectiveness of SCS for persistent neuropathic or joint-mediated pain remain unclear. This thesis evaluates the use of a novel mode of SCS, burst SCS, in rat models of cervical radiculopathy and painful facet joint injury. The role of GABA signaling in the inhibitory effects of burst SCS on dorsal horn neurons is assessed by applying GABA receptor antagonists to the spinal cord during the application of burst SCS. Studies in this thesis demonstrate that afferent discharge induced by injurious loading of the facet joint initiates excitatory synaptic and structural changes in the spinal cord that promote neuronal hyperexcitability, but SCS can attenuate persistent pain by reducing spinal hyperexcitability. This thesis provides a foundation for future investigations into the mechanisms underlying the transduction of mechanical joint injury to centrally-mediated pain and the development of effective therapies for chronic pain.

TABLE OF CONTENTS

Page

LIST OF TABLES

Page

LIST OF FIGURES

Page

CHAPTER 1

Introduction and Background

1.1. Introduction

Chronic pain affects at least one in three adults in the United States, and has an estimated annual cost of over $635 billion (Roehr, 2011). Costs associated with painful spine conditions alone increased by 65% to $85.9 billion between 1997 and 2005, reaching expenditures similar to the costs associated with diabetes and cancer (Martin et al., 2008). The prevalence of spine pain has been reported at 26-66% in the general population, with a 30-50% annual incidence of neck or cervical spine pain (Hogg-Johnson et al., 2008; Linton et al., 1998; Martin et al., 2008). Whiplash injuries are a primary cause of cervical spine pain, and account for up to 53% of the injuries from motor vehicle accidents (Freeman et al., 1999). The annual incidence of whiplash-associated pain has been reported to be at least 300 per 100,000 people in the United States (Holm et al., 2008). Furthermore, up to 50% of the patients with whiplash injuries develop chronic pain that is resistant to conservative interventions, like exercise and physical therapy (Sterling et al., 2012). Recent increases in clinical interventions for chronic neck pain (Manchikanti et al., 2013), and the fact that motor vehicle collisions continue to be a leading cause of emergency room visits (Quinlan et al., 2004), suggest a continued growth in the prevalence of whiplash injuries.

Many different tissues in the cervical spine have the capacity to generate pain from injurious mechanical loading owing to their innervation by nerve fibers that detect and transmit painful signals (Antonacci et al., 1998; Inami et al., 2001; McLain, 1994; Rhalmi et al., 1993). Among those tissues with the potential to generate pain, the cervical facet joints are most commonly implicated as the source of chronic pain after whiplash (Barnsley et al., 1995; Lord et al., 1996; Manchikanti et al., 2004). The facet joints are bilateral articulations between each pair of vertebrae that guide the motions of the vertebrae. Each joint is enclosed by a facet capsular ligament, or facet capsule, that is highly innervated with primary afferent nerve fibers that detect both low-threshold mechanical stimulation and noxious, painful stimulation (Cavanaugh et al., 1989; McLain, 1994; Yamashita et al., 1990). Those primary afferent fibers converge in the dorsal horn of the spinal cord, where they transmit sensory information to second-order neurons that integrate and project signals supraspinally (Steeds, 2009).

The cervical facet joints are at risk for excessive loading during abnormal motions of the cervical spine. Biomechanical studies of human volunteers and cadaveric subjects have determined that the facet joint can undergo injurious motions during simulated low-velocity rear-impact collisions (Bogduk and Yoganandan, 2001; Deng et al., 2000; Kaneoka et al., 1999; Panjabi et al., 1998c; Winkelstein et al., 2000). These abnormal motions of the facet joint can cause tensile and shear loading of the facet capsular ligament, resulting in strains exceeding the physiologic limit of the capsule (Panjabi et al., 1998b; Pearson et al., 2004; Siegmund et al., 2001). In a goat model of tensile loading of the facet joint, facet capsule stretch has also been shown to activate the nerve fibers that innervate the joint (Chen et al., 2006; Lu et al., 2005a), suggesting that joint loading

has the potential to induce painful signals that are transmitted from the joint to the spinal cord. Despite evidence of the transduction of mechanical loading to potentially painful neural signals, the relationship between facet joint loading and the development of persistent joint-mediated pain is still unclear.

Nociceptive pain is the normal sensory response to stimulation that exceeds the activation threshold of nociceptors, which are the nerve fibers that specifically respond to noxious stimuli (Loeser and Treede, 2008). Nociception typically persists only in the presence of continued suprathreshold stimulation, but pathological pain can develop after tissue damage and persist even in the absence of noxious stimulation (Coderre et al., 1993; Steeds, 2009). Chronic pain can be maintained by *central sensitization*, a state in which the second-order neurons that integrate sensory information in the spinal dorsal horn become hyperexcitable (Latremoliere and Woolf, 2009; Loeser and Treede, 2008). Both nociceptive and nonpainful signals that converge in the spinal cord can be amplified by increased excitability and decreased activation thresholds of the dorsal horn neurons. Central sensitization is initiated by a period of sustained afferent discharge (Seltzer et al., 1991a; Wall et al., 1974), which can occur after excessive loading of the joint that leads to increased firing of the primary afferents that innervate the facet capsule (Lu et al., 2005a); despite this notion, no study has defined the role of afferent firing from the facet joint in the onset of central sensitization.

Central sensitization is associated with widespread changes in the spinal cord that enhance neuronal excitability and promote persistent pain after tissue injury. For example, potentiation of excitatory glutamatergic signaling can amplify nociception by increasing the firing of neurons in the spinal regions that integrate and transmit painful

signals (Basbaum et al., 2009; Latremoliere and Woolf, 2009). Structural plasticity, like the growth of new excitatory synapses, can also promote aberrant nociception in the spinal cord by increasing the number of excitatory inputs to the dorsal horn neurons (Jaken et al., 2010; Peng et al., 2010). Noxious loading of the rat facet joint has been shown to induce dorsal horn neuronal hyperexcitability and spinal modifications that contribute to the potentiation of glutamatergic signaling (Dong and Winkelstein, 2010; Lee et al., 2004a; Lee et al., 2008; Quinn et al., 2010b). However, the neurophysiological mechanisms that underlie the development and maintenance of spinal hyperexcitability after excessive loading of the facet joint are unknown.

Central sensitization leads to the development of *hyperalgesia*, defined as a general increase in pain sensitivity, and *allodynia*, defined as a painful response to a typically non-noxious stimulus (Loeser and Treede, 2008). Hyperalgesia can develop both at the site of injury (*primary hyperalgesia*) or at remote locations in which there is no tissue injury (*secondary hyperalgesia*) because of the amplification of nociceptive signals as they converge in the spinal cord from widespread anatomical regions (Coderre et al., 1993). Many of the symptoms exhibited by patients with whiplash-associated pain are indicative of central sensitization, including decreased pain thresholds in the neck and back, and at distant sites with no tissue damage, like the head, arms, and legs (Banic et al., 2004; Curatolo et al., 2001; Curatolo et al., 2004; Herren-Gerber et al., 2004; Jansen et al., 2008; Lord et al., 1996). In order to prevent the development of persistent pain or treat the symptoms of pain after facet joint injury, the timeline and factors affecting the onset of facet joint pain must be elucidated. However, despite the development of

primary and secondary hyperalgesia after whiplash, the relationship between facet joint injury and the development of centrally-mediated pain has not been defined.

Current treatment strategies for facet joint-mediated pain focus on reducing pain by eliminating nociceptive input from symptomatic facet joints using peripheral nerve blocks or neurotomy; however, the effects of those treatments invariably are only temporary and patients require periodic re-intervention (Barnsley et al., 1995; Lord et al., 1996; Manchikanti et al., 2008). The inability of peripheral interventions to permanently reverse central sensitization after its onset is common across many different models of neuropathic and inflammatory pain (Araujo et al., 2003; Shankarrapa et al., 2012; Xie et al., 2005). For patients with facet joint-mediated pain after whiplash, conventional treatment strategies, including physical therapy, pharmacological interventions, or blocking nerve conduction from the facet joint, fail to target the hyperexcitability of the neurons in the spinal dorsal horn that contribute to persistent pain (Lord et al., 1996; Manchikanti et al., 2008; Peeters et al., 2001). Direct modulation of spinal hyperexcitability, as occurs with spinal cord stimulation, may be more effective for treating persistent pain after the development of central sensitization (Cameron, 2004; Compton et al., 2012; Simpson, 1997). Yet, the effectiveness and mechanisms of spinal cord stimulation for the reduction of spinal hyperexcitability require further investigation.

The next sections of this chapter provide relevant background information about the cervical spine and facet joint anatomy, neuroanatomy, facet joint injury and whiplash kinematics, central sensitization, in vivo animal models for the study of facet joint pain, and spinal cord stimulation. Additional background information related to the specific studies is also provided at the beginning of each chapter as relevant.

1.2. Background

1.2.1. Cervical Spine and Facet Joint Anatomy

The cervical spine is comprised of seven articulating vertebrae that are supported by soft tissues, including ligaments, musculature, and cartilage. Each pair of bony vertebrae is connected by the collagenous intervertebral discs ventrally, and by the bilateral articulating facet (or zygapophyseal) joints posterolaterally (Fig. 1.1a). The facet joints are formed by contact of the superior and inferior articular facets of two adjacent vertebrae (Fig. 1.1a). The articulating surfaces of the facet joints are covered by articular cartilage and lubricated by synovial fluid to allow the vertebral bodies to rotate with respect to each other during normal head and neck motion (Fig. 1.1b). The joints guide and limit motions of the head and neck, while protecting the spinal cord from mechanical loading (Lang, 1993; Watson et al., 2009). The joint space and synovial fluid are

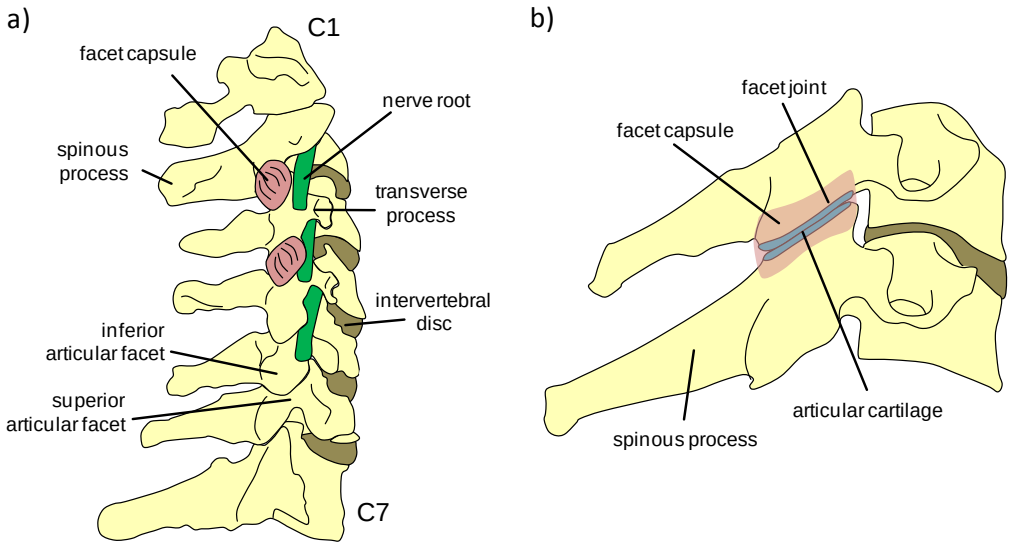

Fig. 1.1. Lateral view of the human cervical spinal column. **(a)** The facet joints are formed by the superior and inferior articulating processes of each pair of vertebrae (adapted from Benzel, 2012). **(b)** The articulating surfaces of the facet joints are covered with cartilage (blue), and the facet capsule (red) encloses the joint space.

enclosed by the facet capsular ligament, or facet capsule (Fig. 1.1b) (Jaumard et al., 2014), which is a heterogeneous, fibrous structure composed of dense bundles of collagen and elastic fibers (Yamashita et al., 1996).

The cervical facet joints are innervated by the medial branches of the dorsal primary rami immediately superior and inferior to the joint, although the joint can be innervated to a lesser degree by the dorsal rami of more distant spinal levels (Bogduk and Marsland, 1988; Kras et al., 2013a; Ohtori et al., 2001). The facet capsule, in particular, is innervated by mechanosensitive nerve fibers that are activated by capsule stretch (Cavanaugh et al., 1989; McLain, 1994; Yamashita et al., 1990). Many mechanosensitive fibers in the capsule exhibit proprioceptive properties, suggesting that the capsule communicates information about head and neck position and movement (McLain and Pickar, 1998). The capsule also contains free nerve endings that are typically associated with nociceptors, the nerve fibers that specifically respond to painful stimuli (Cavanaugh et al., 1989; McLain, 1994). A subset of the nerve fibers in the capsule express substance P (SP) and calcitonin gene-related peptide (CGRP), two neuropeptides with demonstrated roles in nociception, further suggesting that the facet joint is likely capable of signaling pain under excessive mechanical loading conditions (Beaman et al., 1993; Inami et al., 2001; Kallakuri et al., 2004; Ohtori et al., 2000; Yamashita et al., 1993).

1.2.2. Neuroanatomy and Neurophysiology of Nociception

Sensory signals are transmitted from the periphery to the spinal cord through primary afferent nerve fibers. Primary afferents project axons distally from the dorsal root ganglia (DRG) to innervate peripheral targets and centrally to the spinal cord (Grant

and Robertson, 2004). Primary afferents are classified into several groups (Aα/β, Aδ, C) based on their structure and function. Aα and Aβ fibers (also called group I and II fibers) have large, myelinated axons and rapid conduction velocities (Guyton and Hall, 1996). They generally respond to innocuous mechanical stimuli or movement, and are classified as low-threshold mechanoreceptors or proprioceptors. The other two types of fibers, Aδ (group III) and C fibers (group IV), are classified as nociceptors and contribute to the sensation of pain (Steeds, 2009). Aδ fibers are thinly myelinated, with smaller diameters and slower conduction velocities than Aβ fibers, and are thought to evoke sharp, pricking pain and "fast" pain (Basbaum et al., 2009; Guyton and Hall, 1996; Meyer et al., 2006). C fibers have small-diameter, unmyelinated axons with relatively slow conduction velocities, and transmit "slow" pain and diffuse pain from heat and pressure (Basbaum et al., 2009; Meyer et al., 2006). C fibers are further classified as peptidergic fibers, if they express SP and CGRP, or non-peptidergic fibers, based on the expression of the purinergic ATP receptor, P2X3, or binding of isolectin B4 (Braz et al., 2005; Snider and McMahon, 1998).

Nociceptive pain is established in response to stimuli (mechanical, chemical, thermal, etc.) that exceed the activation thresholds of nociceptive afferent fibers. Nociception is a protective response designed to warn of impending tissue damage, so it typically continues only in the presence of noxious stimuli (Costigan et al., 2009). However, repetitive stimulation of afferent fibers can temporarily sensitize them by inducing wind-up, which is a progressive increase in dorsal horn neuronal firing in response to repetitive stimulation of nociceptive afferents (Woolf and Salter, 2000), or

afterdischarge, which is a continuation of afferent firing after the termination of the initiating stimulus (Li et al., 1999).

Afferents synapse in the spinal cord with three main classes of second-order neurons (Fig. 1.2). Nociceptive-specific neurons (NS), or high-threshold (HT) neurons, receive input only from nociceptive afferents, therefore they are only activated by noxious stimuli (Dostrovsky and Craig, 2006; Steeds, 2009). Wide dynamic range (WDR) neurons receive input from non-nociceptive *and* nociceptive afferents, and exhibit a graded response to innocuous and noxious stimuli (Baron, 2006; Basbaum et al., 2009; Dostrovsky and Craig, 2006; Steeds, 2009). Low-threshold mechanoreceptors (LTM) only process light touch sensation from innocuous stimuli.

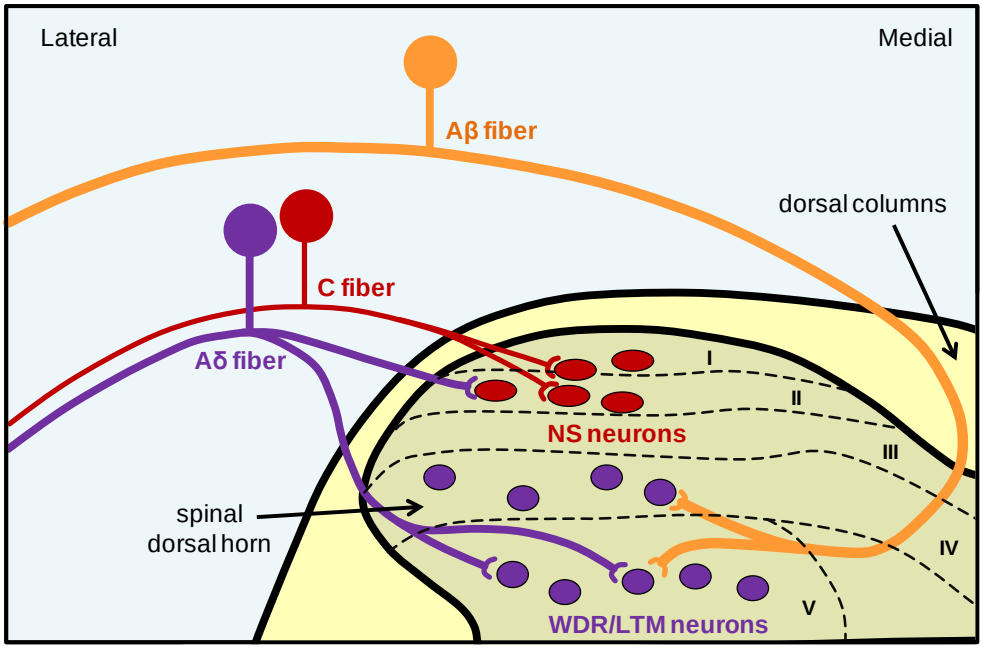

Fig. 1.2. Primary afferent connections in the spinal dorsal horn. The superficial laminae (I-II) contain nociceptive-specific (NS) neurons that receive input from C and Aδ fibers. The deep laminae (III-VI) contain wide dynamic range (WDR) and low-threshold mechanoreceptive (LTM) neurons that receive input from Aδ and Aβ fibers (adapted from Basbaum et al., 2009). Also shown are the dorsal columns, where some Aβ fibers collateralize without first synapsing in the dorsal horn.

Primary afferents synapse with second-order neurons in the dorsal horn region of the spinal cord. The dorsal horn is organized into laminae, or layers, that contain specialized populations of second-order neurons, and receive input from specific groups of afferent fibers (Fig. 1.2) (Grant and Koerber, 2004; Molander et al., 1989; Rexed, 1952; Todd and Koerber, 2006; Watson et al., 2009). For example, the most dorsal, superficial laminae (laminae I and II) almost exclusively contain NS neurons and the central terminals of nociceptive Aδ and C fibers (Fig. 1.2) (Basbaum et al., 2009; Todd and Koerber, 2006). In contrast, Aβ mechanoreceptors and some additional Aδ fibers terminate largely at WDR and LTM neurons in the deeper laminae (laminae III-VI) (Fig. 1.2) (Basbaum et al., 2009; Grant and Robertson, 2004; Todd and Koerber, 2006).

Secondary neurons project supraspinally from the dorsal horn, carrying sensory information to the brain. Most nociceptive signals are conveyed to the brainstem and thalamus through the spinothalamic and spinoreticular tracts (Fig. 1.3) (Basbaum et al., 2009; Watson et al., 2009). For projection of low-threshold mechanical signals, some Aβ fibers collateralize into the dorsal horn and send mechanosensory information through the spinothalamic and spinoreticular pathways (Fig. 1.3) (Yaksh and Luo, 2001; Steeds, 2009). However, a large number of Aβ fibers also project directly through the dorsal columns, carrying proprioceptive and light touch signals to the brainstem without first synapsing in the dorsal horn (Figs. 1.2 and 1.3) (Steeds, 2009; Watson et al., 2009).

1.2.3. Whiplash Kinematics and Facet Joint Injury

The facet joint and its capsular ligament are among the cervical spinal tissues with the potential to generate pain during its excessive mechanical loading. Distension of

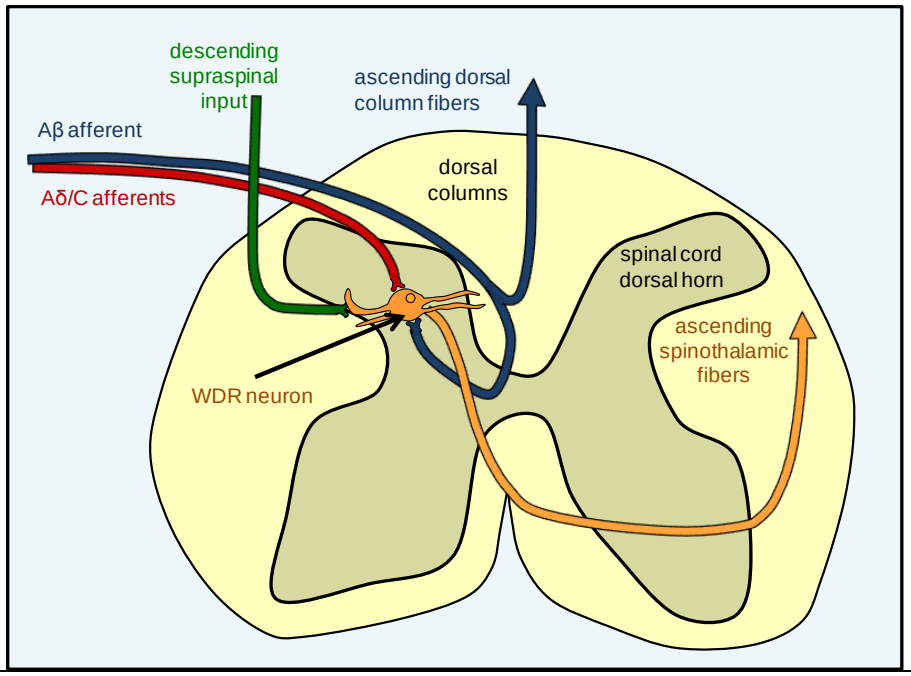

Fig. 1.3. Ascending pathways from the spinal dorsal horn. Input from primary afferent fibers converges in the spinal dorsal horn, and then continues through spinothalamic tract projections that convey sensory information to the brain. Aβ fibers can also project supraspinally through the dorsal columns (adapted from Baron, 2006).

the cervical facet joints in normal subjects by intra-articular injection of fluoroscopic contrast medium produces neck pain in distributions similar to those observed after whiplash (Dwyer et al., 1990). Additionally, the cervical facet joints have been implicated as the source of pain in 54-60% of whiplash patients using diagnostic blocks of symptomatic joints with intra-articular injection of local anesthetics (Barnsley et al., 1995; Lord et al., 1996; Manchikanti et al., 2004). The lower cervical levels (C5-C7) are the most common source of neck and shoulder pain (Barnsley et al., 1995; Bogduk and Marsland, 1988). Local anesthetic block or radiofrequency ablation of the medial branches of the dorsal rami that innervate the symptomatic facet joints attenuates pain (Aprill, 1990; Lord et al., 1996; Manchikanti et al., 2004), further supporting the role of the facet joints as a primary source of pain following whiplash.

Facet joint injury has been hypothesized to result from excessive loading of the facet capsular ligament beyond its physiologic limit. Biomechanical studies using human volunteers and post-mortem human subjects have defined the kinematics of the head and cervical spine during simulated low-velocity rear-impact collisions (Deng et al., 2000; Ono et al., 1997; Panjabi et al., 1998a; Pearson et al., 2004; Sundararajan et al., 2004; Winkelstein et al., 2000; Yoganandan et al., 2001). Based on high-speed X-ray imaging of the cervical spine during rear impact, the spine forms an S-shaped curvature within the first 100-120ms after impact, with the upper cervical spine undergoing flexion and the lower cervical spine being extended (Fig. 1.4) (Bogduk and Yoganandan, 2001; Kaneoka et al., 1999; Panjabi et al., 1998c). Extension and vertebral retraction at the lower cervical spinal levels produces tensile and shear loading across the facet joints and capsular ligaments (Fig. 1.4) (Luan et al., 2000; Panjabi et al., 1998b; Panjabi et al., 1998c; Siegmund et al., 2001; Winkelstein et al., 2000).

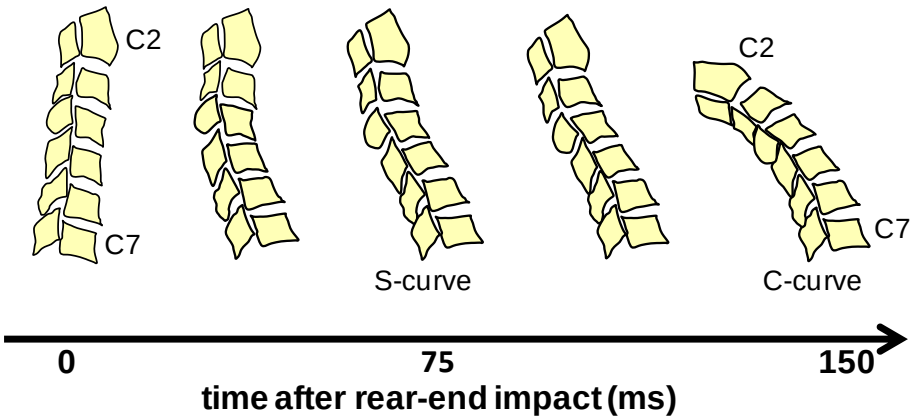

Fig. 1.4. Deformation of the cervical spine during rear-impact. Abnormal motions of the cervical spine, including excessive extension in the lower cervical levels, can induce excessive strains in the facet capsule that exceed the physiologic levels (adapted from Croft, 2000).

Facet capsule strains from joint loading during low-speed rear impacts can be as high as five times the peak strains that are observed for the same cervical levels during normal neck bending (Panjabi et al., 1998b; Pearson et al., 2004). Capsule strains during simulated rear-impact collisions are the greatest at the lower cervical facet joints, peaking at 38.5±24.6% strain at the C5/C6 joint and 39.9±26.3% strain at the C6/C7 joint during 8g accelerations (Pearson et al., 2004), potentially explaining the prevalence of symptomatic C5-C7 facet joints reported after whiplash (Barnsley et al., 1995; Bogduk and Marsland, 1988). Capsular strains can be further increased by more complicated out-of-plane head postures, such as a turned head (Sundararajan et al., 2004; Winkelstein et al., 2000).

Up to 77% of the nerve fibers that innervate the cervical facet capsule are activated by physiologic or noxious stretching of the capsule in a goat model of tensile facet joint loading, and the discharge of nerve fibers is directly related to the magnitude of facet capsule stretch (Chen et al., 2006; Lu et al., 2005a; Lu et al., 2005b). Although mechanosensitive fibers are activated by strains as low as 10%, a subpopulation of high-threshold nociceptors are only activated by noxious strains of 47.2±9.6% (Lu et al., 2005a). Many activated fibers also exhibit afterdischarge, which is a continuation of afferent firing after the termination of the initiating stimulus, for up to 30 minutes after the facet joint is returned to the unloaded configuration (Cavanaugh et al., 1989; Lu et al., 2005a). Those studies collectively establish the role of nerve fibers in transducing the magnitude of facet joint loading into proprioceptive and nociceptive signals. However, no study has investigated the role of discharge and afterdischarge of capsule-innervating fibers in the development of persistent facet-mediated pain.

1.2.4. Central Sensitization

Sensory signals are processed in the spinal dorsal horn by the convergence of excitatory input from afferent fibers, local excitation and inhibition from interneurons, and descending supraspinal inhibition (Fig. 1.3). Nociception can, therefore, be augmented or suppressed by changes in those convergent inputs that alter dorsal horn neuronal excitability. Central sensitization is a state in which nociceptive signaling is amplified by spinal neuronal hyperexcitability, resulting in persistent pain that outlasts the inciting injury or tissue damage (Latremoliere and Woolf, 2009). Central sensitization is characterized by altered neuronal function in the spinal cord that includes increased spontaneous activity, reduced thresholds for activation, heightened responses to both non-noxious and noxious stimuli, and expansion of receptive fields (Coderre et al., 1993; Latremoliere and Woolf, 2009; Woolf, 1983; Woolf and Salter, 2000). Those functional changes in the central nervous system (CNS) result in spontaneous pain, painful responses to typically non-noxious stimuli like light touch (allodynia), and hypersensitivity to noxious stimuli at the site of injury (primary hyperalgesia) and at regions distant from the site of injury (secondary hyperalgesia) (Coderre et al., 1993; Lamotte et al., 1991).

Central sensitization is initiated by sustained afferent firing that occurs during noxious stimulation or tissue injury (Seltzer et al., 1991a; Wall et al., 1974). Blocking the increased afferent discharge that accompanies nerve injury effectively reduces the subsequent development of central sensitization in models of neuropathic pain (Dougherty et al., 1992; Gonzales-Darder et al., 1986; Seltzer et al., 1991a). Blocking injury-induced afferent discharge is also a foundational concept for the use of preemptive

analgesia in order to reduce postoperative pain (Coderre et al., 1993; Woolf and Chong, 1983; Woolf and Wall, 1986). Once spinal neuronal hyperexcitability develops, neurons can return to a baseline state in the absence of continuing afferent discharge, but hyperexcitability can be maintained by low levels of firing, such as the ectopic discharge that develops in damaged neural tissue (Devor, 2009; Devor et al., 1992; Djouhri et al., 2006; Koltzenburg et al., 1992; Xie et al., 2005). Although excessive stretch of the facet capsule has been shown to induce increased firing of the afferents that innervate the joint (Chen et al., 2006; Lu et al., 2005a), no study has evaluated the role of injury-induced afferent discharge from the joint in the development and maintenance of persistent facet-mediated pain.

Many of the changes in the spinal dorsal horn that are associated with central sensitization involve altered glutamatergic signaling. Glutamate is the primary excitatory neurotransmitter in the CNS (Sheng and Lin, 2001; Yaksh, 2006). Glutamate activates several different ionotropic and metabotropic receptors on the post-synaptic membrane (Fig. 1.5a). Ionotropic α-amino-3-hydroxy-5-methyl-4-isoxazolepropionic acid receptors (AMPAR) are permeable to Na^+ and K^+ currents and mediate rapid excitatory neurotransmission (Yaksh, 2006). N-methyl-D-aspartate receptors (NMDARs) are a second class of ionotropic receptor that are activated by glutamate in a voltage-dependent manner and, once activated, allow calcium influx into the postsynaptic terminal (Fig. 1.5b) (Petrenko et al., 2003; Sheng and Lin, 2002; Yaksh 2006). Metabotropic glutamate receptors (mGluRs) are a family of G protein-coupled receptors that mediate slower synaptic responses. Glutamate binding to group 1 metabotropic receptors, namely

mGluR1 and mGluR5, can also contribute to calcium influx by releasing calcium from intracellular stores (Fig. 1.5b) (Sheng and Lin, 2002; Yaksh, 2006).

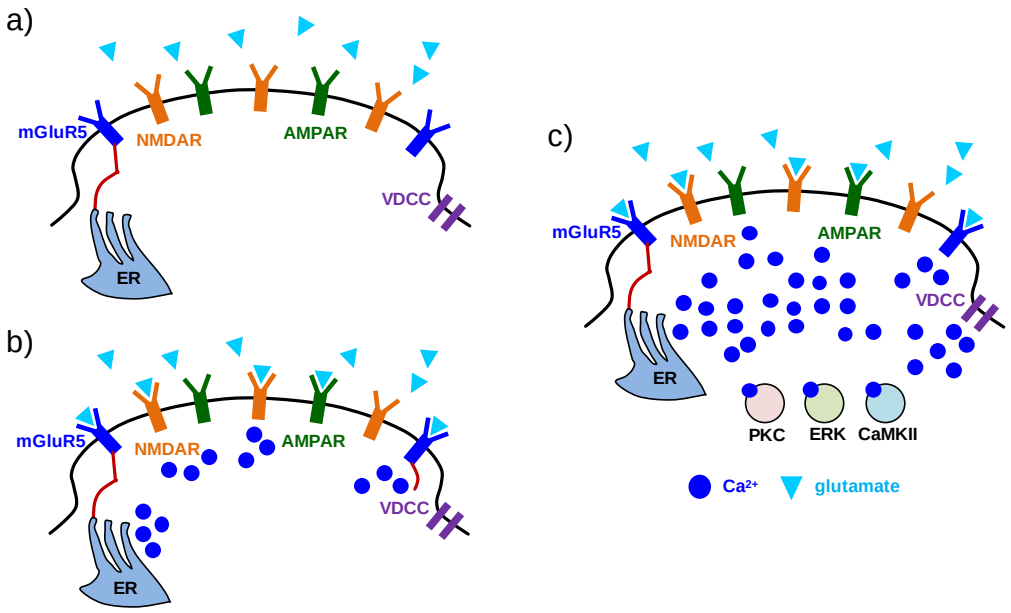

Fig. 1.5. The initiation of central sensitization in the dorsal horn. **(a)** Glutamatergic signaling activates ionotropic (AMPAR, NMDAR) and metabotropic (mGluR5) receptors. **(b)** NMDAR and mGluR5 activation cause calcium influx from external and intracellular sources like the endoplasmic reticulum (ER). **(c)** Calcium influx activates kinases (PKC, ERK, and CamKII) and voltage-dependent calcium channels (VDCC) to increase membrane excitability and the strength of excitatory synapses, leading to neuronal hyperexcitability (adapted from Latremoliere and Woolf, 2009).

Central sensitization is induced by increases in intracellular calcium from NMDAR and group 1 mGluR activation during sustained afferent discharge in the dorsal horn (Fig. 1.5) (Petrenko et al., 2003; Soliman et al., 2002; Woolf and Thompson, 1991; Young et al., 1997). Calcium influx activates calcium-dependent kinases, including PKC, PKA, CamKII, and ERK, that act on numerous targets to directly influence excitatory signaling (Fig. 1.5c) (Kawasaki et al., 2004; Latremoliere and Woolf, 2009). For example, phosphorylation of AMPARs and NMDARs at multiple sites increases their activation kinetics and trafficking to the membrane, enhancing membrane excitability

(Daulhac et al., 2011; Liu and Salter, 2010; Petrenko et al., 2003; Ultenius et al., 2006). Activation of calcium-dependent kinases also leads to transcriptional changes that alter expression of proteins in primary afferent and dorsal horn neurons to further enhance spinal excitability (Kawasaki et al., 2004; Latremoliere and Woolf, 2009).

Temporal and spatial management of glutamate concentrations in synapses is important for preventing aberrant signaling and excitotoxicity. Glutamate signaling is, therefore, regulated by astrocytic and neuronal transporters that remove glutamate from the synapse (Danbolt, 2001; Liaw et al., 2005). The excitatory amino acid transporters (EAAT1-5) are one family of glutamate transporters that are crucial for the regulation of extracellular glutamate concentrations in the spinal dorsal horn (Queen et al., 2007). EAAT1 and EAAT2 are homologous to two glutamate transporters in the rat, glutamate aspartate transporter (GLAST) and glial glutamate transporter 1 (GLT1), and are expressed primarily on astrocytes. A third member of the transporter family, EAAT3, is neuronally expressed and is homologous to the rat glutamate transporter EAAC1 (Queen et al., 2007). In rodent models of neuropathic pain, downregulation of GLAST and GLT1 contributes to persistent behavioral sensitivity (Hu et al., 2009; Sung et al., 2003; Xin et al., 2009), but dorsal horn expression of those astrocytic transporters has not been evaluated in the context of facet joint-mediated pain.

Astrocytes can also contribute to central sensitization and pathological pain after tissue injury. Astrocytes can be activated by excitatory signaling molecules, including substance P, glutamate, and ATP, that are released by primary afferent nociceptors in response to tissue damage or noxious stimulation (Milligan and Watkins, 2009). Once activated, astrocytes increase their expression of glial fibrillary acidic protein (GFAP),

vimentin, and nestin, which are intermediate filament proteins that form part of the intracellular cytoskeletal network, resulting in hypertrophy of cellular processes (Benveniste, 1992; Pekny and Nilsson, 2005). Activated astrocytes in the dorsal horn also release substances that can both enhance neuronal excitability (i.e., excitatory neurotransmitters, growth factors, and prostaglandins) and promote spinal inflammation (i.e., pro-inflammatory cytokines) (Benveniste, 1992; Watkins et al., 2001). Astrocytes may play a particularly important role in facet joint-mediated pain, because spinal GFAP is upregulated in conjunction with the development of persistent behavioral sensitivity after injurious facet joint loading (Lee et al., 2004a; Lee et al., 2008). Separately, anti-inflammatory treatments and spinal treatments that attenuate neuronal excitability reduce GFAP expression in parallel with attenuation of behavioral sensitivity, further supporting the contribution of astrocyte activation to facet-mediated pain (Dong et al., 2013a; Dong et al., 2013b).

1.2.5. Spinal Structural Plasticity

Spinal structural plasticity, which is broadly defined as changes in the number, distribution, and connectivity of neurons in the spinal cord, has the potential to modify CNS processing of sensory signals by introducing aberrant synaptic connections between neurons that do not normally synapse. For example, after peripheral nerve injury, low-threshold Aβ afferents may sprout from the deep laminae of the dorsal horn into the superficial laminae and synapse with nociceptive dorsal horn neurons, producing painful sensation from normally innocuous stimuli (Woolf et al., 1992). Electron microscopy and immunolabeling show increases in synapses and synaptic proteins in the superficial

dorsal horn in conjunction with the onset of behavioral sensitivity after nerve injury, supporting the potential role of dorsal horn synaptogenesis in neuropathic pain (Chou et al., 2002; Chung et al., 1989; Jaken et al., 2010; Lin et al., 2011; Peng et al., 2010). Although synaptogenesis may contribute to spinal hyperexcitability by altering the connectivity of nociceptive and non-nociceptive afferents and second-order neurons, the mechanisms promoting synaptogenesis after injury are unknown.

Astrocytes are important regulators of synapse assembly in the CNS. In the absence of astrocytes, neurons develop only small numbers of immature synapses in vitro (Ullian et al., 2001; Christopherson et al., 2005); astrocytes or astrocyte-conditioned cell culture media significantly increase the number of functional, mature synapses on cultured CNS neurons (Christopherson et al., 2005). Blocking astrocyte activation after peripheral nerve injury in the neonatal CNS prevents injury-induced synaptogenesis (Lo et al., 2011), suggesting that astrocytes mediate synaptogenesis in pathological settings as well. Studies have identified several astrocyte-derived extracellular matrix proteins with synaptogenic properties, including hevin, secreted protein acidic and rich in cysteine (SPARC), and the thrombospondins (TSP1-5) (Christopherson et al., 2005; Kucukdereli et al., 2011). The thrombospondins in particular have been characterized as astrocyte-secreted factors necessary for CNS synaptogenesis during development (Christopherson et al., 2005; Ehlers, 2005; Eroglu et al., 2009; Risher and Eroglu, 2012). One member of the thrombospondin family, TSP4, is localized to synapses in the CNS and neuromuscular junctions (Arber and Caroni, 1995). Gene array analysis and subsequent studies of TSP4 protein expression found upregulation of spinal TSP4 in multiple models of neuropathic pain, implicating TSP4 in the development of behavioral sensitivity and

dorsal horn neuronal hyperexcitability (Kim et al., 2009; Kim et al., 2012; Li et al., 2014a; Zeng et al., 2013). However, despite the synaptogenic properties of TSPs, the mechanisms by which TSP4 contributes to behavioral sensitivity and neuronal hyperexcitability remain unclear.

1.2.6. In Vivo Animal Models of Facet-Mediated Pain from Joint Trauma

Whiplash injuries can produce a variety of symptoms that are collectively termed "whiplash-associated disorders" (Jansen et al., 2008; Spitzer et al., 1995). The symptoms of whiplash-associated disorders may include neck and back pain, dizziness, tinnitus, headache, paresthesias, temporomandibular joint pain, and disturbances in concentration, vision, or memory (Barnsley et al., 1995; Jansen et al., 2008; Lord et al., 1996). Patients with whiplash-associated disorders demonstrate painful responses to stimuli that are normally non-noxious (allodynia), increased sensitivity to noxious stimuli (hyperalgesia), and local and widespread decreases in the activation thresholds of spinal reflexes (Banic et al., 2004; Curatolo et al., 2001; Moog et al., 2002; Sheather-Reid and Cohen, 1998; Van Oosterwijck et al., 2013). The body is divided into *dermatomes* that correspond to the regions that are innervated by each spinal level (Fig. 1.6). Whiplash-associated pain symptoms often develop in a dermatome-specific fashion, depending on the spinal level of the symptomatic facet joints (Dwyer et al., 1990). For example, the C6 and C7 levels of the spinal cord receive primary afferent innervation from the arms, shoulders, and back, including the C6/C7 facet joints (Fig. 1.6). Those anatomical regions, collectively called the C6 and C7 dermatomes, commonly develop decreased pain thresholds after noxious stimulation of C6/C7 facet joint (Aprill, 1990; Dwyer et al., 1990).

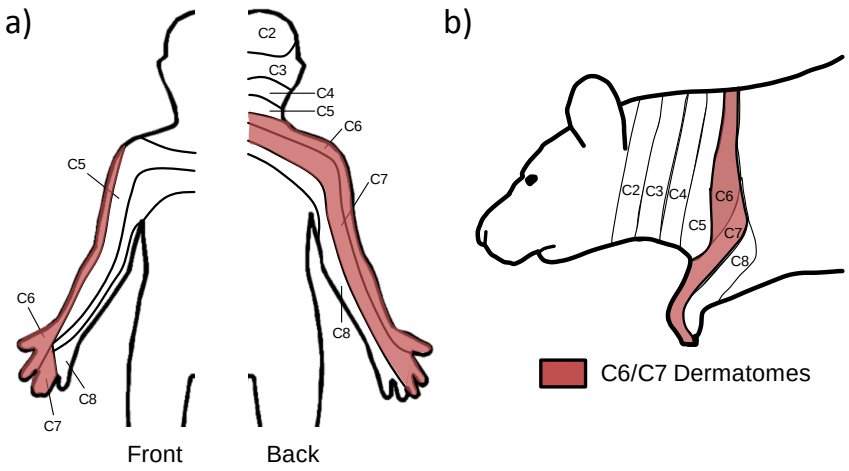

Fig. 1.6. Patterns of sensory innervation in the cervical region of the human and rat. Pain commonly develops in the C6 and C7 dermatomes after noxious stimulation or loading of the C6/C7 facet joints. **(a)** The C6/C7 dermatomes are highlighted on a human dermatomal map. **(b)** Corresponding innervation patterns and locations of behavioral hypersensitivity after painful C6/C7 facet joint injury are shown for the rat (adapted from Takahashi and Nakajima, 1996).

The cervical spine anatomy, neurophysiology, and dermatomal distribution of the rat are similar to those of the human (Fig. 1.6), enabling the use of rat models to investigate the biomechanical and neurophysiological mechanisms underlying persistent pain. A rat model of facet joint loading has been developed to evaluate the development of persistent facet-mediated pain. Facet joint loading is induced in rats by distracting the facet joint to induce capsule stretch and simulate the injurious tensile strains that occur in the capsule during whiplash (Dong et al., 2012; Lee et al., 2004a; Lee et al., 2008; Pearson et al., 2004; Siegmund et al., 2001). Behavioral sensitivity develops one day after injurious C6/C7 facet joint loading and persists for up to six weeks (Rothman et al., 2008). Pain develops in the shoulders, neck, and forepaws in a dermatome-specific pattern similar to the symptoms that develop following noxious stimulation of the human cervical facet capsule (Fig. 1.6) (Crosby et al., 2014a; Curatolo et al., 2001; Dong et al.,

2012; Dwyer et al., 1990; Lee et al., 2008; Van Oosterwijck et al., 2013). However, physiologic strains in the facet capsule do not induce behavioral sensitivity in the rat, and capsule transection that alleviates mechanical loading of the capsule prevents the development sensitivity (Dong et al., 2012; Lee and Winkelstein, 2009; Winkelstein and Santos, 2008). Together, these findings suggest that capsule strain magnitude plays a key role in the initiation of persistent facet joint pain.

Injurious C6/C7 facet joint loading that produces pain in rats induces spinal modifications that are associated with central sensitization. Neurons in the dorsal horn of the spinal cord develop hyperexcitability by day 7 after painful facet joint injury (Dong et al., 2013a; Quinn et al., 2010b), including increased responses of WDR neurons to both non-noxious and noxious mechanical stimulation of the forepaw (Quinn et al., 2010b). Intrathecal treatment with gabapentin, a neuropathic pain drug that reduces neuronal excitability, attenuates spinal hyperexcitability and behavioral sensitivity (Dong et al., 2013a), further supporting that neuronal sensitization contributes to persistent facet-mediated pain.

Spinal hyperexcitability may be facilitated by increases in excitatory glutamatergic signaling in the dorsal horn after painful facet joint injury. Metabotropic glutamate receptor mGluR5 is upregulated in the dorsal horn seven days after painful facet injury, while neuronal glutamate transporter EAAC1 expression is decreased at that time point (Dong and Winkelstein, 2010). Increases in mGluR5 and decreases in EAAC1 correlate to the magnitude of capsule strain, suggesting that mechanotransduction of facet capsule loading alters spinal glutamatergic signaling (Dong and Winkelstein, 2010). Painful facet joint injury also increases spinal expression of PKCε (Dong et al., 2012), a

member of one kinase family that contributes to neuronal hyperexcitability in central sensitization (Chen and Huang, 1992; Kawasaki et al., 2004). Although some components of glutamate signaling have been characterized after painful facet joint injury, many glutamate signaling proteins that play important roles in central sensitization have not been studied after facet joint injury, including the activation of NMDA receptors and the expression of astrocytic glutamate transporters GLAST and GLT1.

Spinal glial activation also develops after painful facet joint injury in the rat, as measured by an increase in GFAP expression in spinal astrocytes at day 7 after injury (Lee et al., 2004a; Weisshaar et al., 2010). Astrocyte activation has been reported to be modulated by the magnitude of facet capsule stretch, because GFAP expression exhibits a graded response to sham procedures, physiologic or injurious levels of facet capsule stretch, and joint distraction that causes rupture of the capsule (Lee et al., 2004a; Lee et al., 2008). Intrathecal gabapentin treatment that reduces spinal hyperexcitability also attenuates the injury-induced increase in GFAP in the dorsal horn (Dong et al., 2013a), suggesting that GFAP expression is modulated by spinal neuronal activity. However, the relationship between mechanical facet joint injury and the spinal neuronal and glial activation that may contribute to persistent pain has not been fully defined.

1.2.7. Spinal Cord Stimulation

Spinal cord stimulation (SCS) is used to treat a wide range of chronic neuropathic pain conditions by directly modulating neuronal activity in the spinal dorsal horn (Cameron, 2004; Compton et al., 2012; Simpson, 1997). Common clinical indications include failed back surgery syndrome, complex regional pain syndrome, ischemic pain,

peripheral neuropathy, and cervical and lumbar radiculopathy (Alo et al., 2002; Cameron, 2004; Compton et al., 2012; Stojanovic and Abdi, 2002). SCS has also been used to treat whiplash-associated pain in a small number of patients (Kirvela and Kotilainen, 1999; Van Buyten et al., 2001). Conventional tonic SCS administers continuous electrical pulses to the dorsal columns of the spinal cord using various pulse frequencies (40-60Hz) and pulse widths (0.2-0.5ms) (De Ridder et al., 2010; Guan, 2012; Tang et al., 2014). Activation of Aβ fibers is believed to induce orthodromic (forward-propagating) signals from Aβ fibers to the brain are believed to be the cause of the tingling paresthesias in the stimulated dermatome(s) that frequently accompany tonic SCS (De Ridder et al., 2010; Tang et al., 2014). Aβ fibers can collateralize in the dorsal horn and synapse with inhibitory interneurons (Yaksh and Luo, 2001), so Aβ activation in the dorsal columns can also cause antidromic (backward-propagating) signals that activate those inhibitory interneurons to attenuate nociception (Melzack and Wall, 1965; Mendell, 2014). Many studies report decreased dorsal horn neuronal excitability during and after SCS, supporting the assertion that activation of Aβ afferents in the dorsal columns suppresses persistent painful signals at the dorsal horn level (Guan, 2012; Guan et al., 2010; Yakhnitsa et al., 1999).

Based on studies in animal models, the attenuation of neuronal firing by γ-aminobutyric acid (GABA) has been proposed as a key mechanism of action for tonic SCS. GABA is the primary inhibitory neurotransmitter in the spinal cord, and acts through $GABA_A$ (ligand-gated) and $GABA_B$ (G-protein-coupled) receptors that are localized to inhibitory synapses (Malcangio and Bowery, 1996; Yaksh, 2006). After peripheral nerve injury, rats with behavioral sensitivity have less extracellular GABA in

the dorsal horn compared to uninjured rats, suggesting that a disinhibition of dorsal horn neuronal activity leads to persistent pain (Drew et al., 2004; Stiller et al., 1996). However, dorsal horn GABA levels are increased during tonic SCS (Linderoth et al., 1994; Stiller et al., 1996), suggesting that SCS acts by enhancing spinal inhibitory GABA signaling. The GABA receptor agonist, baclofen, enhances pain-suppression during SCS (Cui et al., 1997), but GABA receptor antagonists abolish the analgesic effects of dorsal column stimulation (Cui et al., 1996), further supporting the role of inhibitory GABA signaling in the effects of tonic SCS.

Despite extensive reports that SCS is effective for treating chronic pain, the mean success rate of SCS in clinical studies is only 58%, and that rate has improved little in the last several decades (Cameron, 2004; Zhang et al., 2014). Recently, new modes of SCS have been developed with the aim of improving pain relief. Burst stimulation is one novel mode of SCS that delivers short bursts of pulses rather than continuous pulses of stimulation (De Ridder et al., 2010). Burst SCS reduces pain in patients with chronic neuropathic pain better than tonic stimulation without inducing the paresthesia that is typically associated with tonic SCS (De Ridder et al., 2013; De Vos et al., 2014). However, the mechanisms underlying the analgesic effects of burst SCS are unknown, and a better understanding of the neurophysiology and mechanisms of burst SCS may be required to more effectively design and administer novel SCS therapies.

1.3. Overview

The overall aim of this thesis is to define the development of spinal neuronal hyperexcitability and structural plasticity after painful facet joint injury, and to evaluate

the modulation of spinal hyperexcitability for the treatment of persistent pain. Using a rat model of painful cervical facet joint injury, the temporal development of spinal neuronal hyperexcitability is evaluated by quantifying spontaneous and evoked neuronal activity at times between facet joint injury and the onset of behavioral sensitivity. To establish the role of facet joint injury-induced afferent firing in the induction of neuronal hyperexcitability, afferent activity is transiently blocked at times during the development of spinal hyperexcitability. Structural plasticity is assessed by quantifying excitatory synapse density in the spinal dorsal horn and characterizing the role of thrombospondin-4 in persistent facet-mediated pain. Lastly, the effectiveness and mechanisms of burst SCS are evaluated for the attenuation of spinal neuronal hyperexcitability in models of painful facet joint injury and cervical radiculopathy.

The studies in this thesis are organized into chapters that summarize the relevant experiments. Chapter 2 details the hypotheses and specific aims of this thesis. Chapter 3 presents the studies that establish the temporal development of spinal neuronal hyperexcitability after painful facet joint injury (Aim 1a). Chapter 4 presents the studies related to Aims 1b-1d that evaluate the role of injury-induced afferent discharge in spinal neuronal hyperexcitability and the potentiation of glutamatergic signaling. Chapter 5 presents studies defining the role of dorsal horn excitatory synaptogenesis in promoting persistent pain (Aim 2). In Chapter 6, the studies related to Aim 3a are presented, including the optimization of burst spinal cord stimulation for the attenuation of spinal hyperexcitability. Chapter 7 extends the findings from Chapter 6, comparing burst SCS to conventional tonic SCS for the treatment of neuropathic pain and persistent joint-mediated pain (Aims 3b and 3c). Additional studies in Chapter 7 also evaluate

GABAergic signaling as a potential mechanism for the action of burst SCS (Aim 3b). Finally, in Chapter 8 all of the studies are synthesized in the broader context of facet-mediated pain, along with limitations and implications of this work for future research.

CHAPTER 2

Rationale, Context and Hypotheses

2.1. Rationale and Context

Chronic neck pain affects a substantial portion of the general population annually (Hogg-Johnson et al., 2008; Martin et al., 2008). Cervical facet joint-mediated pain is prevalent after neck trauma, during which the cervical facet joints are susceptible to injurious loading (Bogduk and Yoganandan, 2001; Pearson et al., 2004; Winkelstein et al., 2000). The cervical facet joint is implicated as a source of pain in 54-60% of whiplash pain cases (Barnsley et al., 1995; Freeman et al., 1999; Lord et al., 1995; Manchikanti et al., 2004). Patients with facet joint-mediated pain experience decreased pain thresholds both in the neck and at distant sites in which there is no tissue damage, like the upper and lower limbs (Banic et al., 2004; Curatolo et al., 2001; Curatolo et al., 2004; Koelbaek et al., 1999). Those widespread symptoms are characteristic of central sensitization, a state in which hyperexcitability of spinal neurons amplifies the nociceptive signals that converge in the dorsal horn from diverse anatomical regions, leading to extensive pain hypersensitivity (Curatolo et al., 2004; Moog et al., 2002).

Studies of cervical spine kinematics during simulated low-velocity rear impacts suggest that excessive loading of the facet capsular ligament is a primary injury mechanism for persistent pain (Panjabi et al., 1998b; Pearson et al., 2004; Winkelstein et

al., 2000). Strains in the facet capsule can exceed physiologic levels by nearly five-fold during low-speed rear impacts (Pearson et al., 2004), and approach the strain thresholds for activation of nociceptive fibers in the facet joint (Lu et al., 2005a). In animal models of painful facet joint injury, excessive facet capsule stretch induces behavioral hypersensitivity to mechanical stimuli and spinal neuronal hyperexcitability (Dong et al., 2013a; Lee et al., 2004b; Lee and Winkelstein, 2009; Quinn et al., 2010b). However, despite evidence implicating facet capsule stretch in the initiation of persistent facet joint-mediated pain, the temporal relationship between mechanical loading of the facet joint sufficient to induce pain and the development of spinal hyperexcitability is still unclear.

Spinal neuronal hyperexcitability after painful facet joint injury may be maintained by excitatory synaptic plasticity, which includes changes in synapse strength or structure that enhance neurotransmission. Plasticity in the dorsal horn can promote aberrant firing in nociceptive neurons by potentiating excitatory signaling at glutamatergic synapses and/or inducing excitatory synaptogenesis (Dong and Winkelstein et al., 2010; Kawasaki et al., 2004; Latremoliere and Woolf, 2009; Peng et al., 2010; Ultenius et al., 2006; Woolf et al., 2000). However, it remains unknown if plasticity in the spinal cord that promotes neuronal hyperexcitability is induced by painful facet joint injury. Therefore, the **central aim** of this thesis is to define the development, maintenance, and modulation of spinal hyperexcitability after painful facet joint injury using an established rat model of painful C6/C7 facet joint distraction. The **overall hypothesis** is that injury-induced afferent activity from the facet joint initiates the development of spinal neuronal hyperexcitability by potentiating excitatory signaling and inducing excitatory synaptogenesis in the spinal dorsal horn.

The first aim of this thesis determines the time after painful facet joint injury at which behavioral sensitivity and dorsal horn neuronal hyperexcitability develop by measuring mechanical hyperalgesia and neuronal excitability in the spinal dorsal horn within the first day following painful injury (Aim 1a). In order to evaluate the role of afferent discharge following joint injury in the initiation of spinal modifications that promote neuronal hyperexcitability, intra-articular bupivacaine injections were used to block afferent activity at a range of times from immediately after injury (within minutes) to day 4 after injury, and behavioral sensitivity and spinal neuronal excitability were measured at day 7 (Aims 1b-1d). Collectively, those studies define the temporal development of spinal hyperexcitability after painful facet joint injury and evaluate the relevance of the timing of joint interventions for the attenuation of persistent pain.

Persistent facet-mediated pain may be maintained by structural modifications in the spinal cord, like the development of new excitatory synapses that enhance dorsal horn neuronal excitability (Jaken et al., 2010; Peng et al., 2010; Woolf et al., 1995). The synaptogenic protein thrombospondin-4 (TSP4) has recently been implicated in the development of neuropathic pain after peripheral nerve injury (Kim et al., 2012; Risher and Eroglu, 2012). Injury-induced TSP4 is largely expressed by activated astrocytes in the spinal dorsal horn (Kim et al., 2012). Although astrocytic TSP4 can induce synaptogenesis (Christopherson et al., 2005; Eroglu et al., 2009), it is unclear whether TSP4 contributes to persistent pain by inducing *excitatory* synaptogenesis in the spinal cord. Spinal astrocytic activation is evident after painful facet joint injury (Lee et al., 2004a; Weisshaar et al., 2010), so astrocyte-derived thrombospondin proteins may play a key role in mediating persistent pain after facet joint injury. Studies in Aim 2 quantify

changes in the number of excitatory synapses in the dorsal horn (Aim 2a) and define the temporal expression of TSP4 in the dorsal root ganglia (DRG) and spinal cord after painful facet joint injury (Aim 2b). Lastly, the role of spinal TSP4 in persistent facet-mediated pain is evaluated by blocking TSP4 expression (Aim 2c) and augmenting levels of spinal TSP4 prior to facet joint loading (Aim 2d-e), in separate studies.

Analgesics often fail to provide sustained treatment of persistent pain after the development of spinal hyperexcitability has already occurred (Lin et al., 2011; Lord et al., 1996; Xie et al., 2005). However, spinal cord stimulation (SCS) offers effective analgesia for otherwise intractable chronic pain by directly modulating neuronal activity in the spinal dorsal horn (Cameron, 2004; Guan, 2012; Simpson, 1997). Conventional tonic SCS inhibits nociceptive signals in the dorsal horn by applying *continuous* electrical stimulation to the dorsal columns of the spinal cord. However, novel modes of stimulation have been developed recently to improve the effectiveness of SCS for reducing pain. Burst SCS is one such mode of SCS that delivers *periodic* bursts of electrical stimulation rather than continuous tonic pulses (De Ridder et al., 2010). Despite studies showing the clinical effectiveness of burst SCS for treating chronic pain, the mechanisms underlying its attenuation of pain remain only speculative (De Ridder et al., 2013; De Vos et al., 2013). Studies in the first two aims of this thesis focus on the development of spinal hyperexcitability as a key feature of central sensitization, so studies in Aim 3 evaluate the effectiveness of spinal cord stimulation for modulating spinal hyperexcitability and attenuating persistent pain, after painful facet joint injury and in a more traditional model of neuropathic pain.

In Aims 3a and 3b, studies evaluate burst SCS for the treatment of neuropathic pain using an established model of painful cervical nerve root compression (Hubbard and Winkelstein, 2005; Hubbard et al., 2008; Zhang et al., 2013). The burst stimulation parameters are optimized for neuropathic pain in Aim 3a. Burst SCS is then compared directly to conventional tonic SCS for the attenuation of dorsal horn neuronal activity (Aim 3b). Inhibitory γ-aminobutyric acid (GABA) signaling has been shown to play a key role in the decrease of dorsal horn activity during tonic SCS (Cui et al., 1996; Stiller et al., 1996), but the potential role of GABA signaling in burst SCS is not known. Therefore, Aim 3b also evaluates the role of GABA signaling in burst SCS to determine if that mechanism contributes to its attenuation of dorsal horn neuronal activity. Lastly, SCS has not been tested for reduction of the spinal hyperexcitability that is associated with persistent pain from other etiologies. As such, in Aim 3c, both burst and tonic SCS are evaluated for the attenuation of dorsal horn neuronal activity after painful facet joint injury.

2.2. Overall Hypothesis and Specific Aims

The overall goal of this dissertation is to elucidate when and how facet capsule stretch leads to spinal hyperexcitability that promotes persistent pain, and to define the role of synaptic plasticity and synaptogenesis in that process. The **overall hypothesis** of this thesis is that the increased primary afferent activity from the facet joint that is initiated by painful facet joint injury potentiates excitatory neuronal signaling and induces excitatory synaptogenesis in the spinal dorsal horn. These changes lead to hyperexcitability of dorsal horn neurons that amplifies nociceptive signals as they are

transmitted to the spinal cord. Blocking the injury-induced signals that initiate excitatory changes in the spinal cord can prevent the development of persistent neuronal hyperexcitability and behavioral sensitivity. In addition, it is hypothesized that hyperexcitability of dorsal horn neurons after a painful injury may be attenuated by direct stimulation of the spinal dorsal columns using both tonic and burst modes of SCS. These overarching hypotheses have three sub-hypotheses that are tested in the following associated aims and sub-aims.

Hypothesis 1. Painful facet joint injury induces an increase in neuronal excitability in the dorsal horn of the spinal cord that parallels the temporal development of sustained mechanical hyperalgesia. Neuronal hyperexcitability is initiated by increased discharge of afferents from the facet joint that is induced during painful capsule stretch. Attenuation of afferent activity from the facet joint immediately following stretch of its capsule prevents the subsequent development of spinal neuronal hyperexcitability. However, blocking afferent activity *after* hyperalgesia has already developed does not reduce behavioral sensitivity or dorsal horn neuronal hyperexcitability at later time points.

Aim 1. Define the relationship of a painful mechanical facet joint capsule injury to the development of spinal neuronal hyperexcitability, using an in vivo rat model of painful facet joint injury. Evaluate the role of afferent activity from the injured joint in the induction and maintenance of dorsal horn neuronal hyperexcitability by blocking joint afferent activity with intra-articular injections of bupivacaine, a fast-acting local anesthetic that transiently blocks axonal conduction. After bupivacaine injection, measure

the subsequent behavioral sensitivity, dorsal horn neuronal excitability, and potentiation of glutamatergic signaling in the spinal cord.

1a. Determine the time after painful facet joint injury at which dorsal horn neurons develop hyperexcitability by quantifying the evoked firing response of spinal neurons to non-noxious and noxious mechanical stimuli at 6 hours or day 1 after painful facet injury.

1b. Determine if the initial painful facet capsule stretch or ongoing joint afferent firing is responsible for hyperalgesia and spinal hyperexcitability by eliminating primary afferent activity from the joint using intra-articular injections of bupivacaine, either immediately or at day 4 after the capsule stretch, in separate studies.

1c. Define the spinal expression of a panel of excitatory neuronal and glial signaling proteins (mGluR5, NR1/pNR1, ERK/pERK, GLAST, GLT1, GFAP) by Western blot at day 7 after injury, following bupivacaine treatment at the times specified in Aim 1b.

1d. Identify the time period after painful facet joint injury during which afferent input from the facet joint induces sustained spinal neuronal hyperexcitability. Administer single intra-articular doses of bupivacaine to the bilateral facet joints at different times throughout the period when hyperexcitability develops (immediately, 4 hours, 8 hours, day 1, or day 4), and measure behavioral sensitivity and spinal neuronal excitability at day 7 after injury.

Hypothesis 2. Excitatory synaptogenesis in the dorsal horn contributes to facet joint-mediated pain and spinal hyperexcitability following capsule stretch. The release of the

synaptogenic protein thrombospondin-4 (TSP4) from activated astrocytes induces excitatory synaptogenesis that contributes to behavioral sensitivity and hyperexcitability of dorsal horn neurons after painful facet joint injury.

Aim 2. Determine if painful facet joint injury induces excitatory synaptogenesis in the spinal dorsal horn. Define the temporal expression of TSP4 in the DRG and spinal cord after painful facet joint injury. Evaluate the role of TSP4 in dorsal horn synaptogenesis and the development of behavioral sensitivity by blocking spinal TSP4 expression or augmenting spinal TSP4 levels prior to physiologic or painful levels of joint loading.

2a. Quantify excitatory synapse density in the superficial and deep laminae of the spinal dorsal horn at day 7 after painful facet joint injury by counting synapsin-labeled puncta (pre-synaptic marker) colocalized with homer (post-synaptic marker). In order to evaluate the effects of analgesic gabapentin treatment on excitatory synaptogenesis, quantify excitatory synapse density in the dorsal horn at day 7 in rats receiving intrathecal gabapentin treatments that have been previously shown to reduce spinal hyperexcitability after painful facet joint injury.

2b. Evaluate TSP4 expression in the DRG and spinal cord at days 1 and 7 after a painful facet joint injury to determine if upregulation of TSP4 is induced and over what time course.

2c. Administer intrathecal antisense oligonucleotides designed against a segment of TSP4 mRNA to block TSP4 protein expression before, and continuously following, painful facet joint injury. Measure behavioral sensitivity and quantify TSP4 expression and synapse densities at day 7 after painful injury to determine whether

increased spinal TSP4 is necessary for the development of hyperalgesia and excitatory synaptogenesis in the dorsal horn.

2d. Administer TSP4 intrathecally in naïve rats to evaluate the role of spinal TSP4 in the development of behavioral sensitivity. Define the threshold dose of TSP4 for inducing behavioral sensitivity, and identify separate TSP4 doses that: (1) induce behavioral sensitivity and (2) do not induce behavioral sensitivity.

2e. Administer TSP4 prior to facet joint loading to determine whether pre-injury levels of TSP4 mediate behavioral sensitivity and/or dorsal horn neuronal excitability. Apply sham surgical procedures, nonpainful but physiologic joint loading, or painful facet joint loading after TSP4 treatments defined in Aim 2d to determine if spinal TSP4 levels modulate the hyperalgesia and/or spinal hyperexcitability that develop after painful facet loading.

Hypothesis 3. Dorsal horn neuronal hyperexcitability can be reduced by spinal cord stimulation of the dorsal columns. Burst SCS is more effective than conventional tonic SCS for attenuating spinal hyperexcitability. Since tonic SCS utilizes GABAergic signaling to inhibit aberrant dorsal horn neuronal activity, and because burst and tonic SCS both reduce pain symptoms, burst SCS also reduces neuronal firing through a GABAergic mechanism.

Aim 3. Separately evaluate the effectiveness of burst SCS to attenuate symptoms of persistent pain following painful nerve root compression and painful facet joint injury. Optimize the stimulation conditions and parameters needed to maximize the effectiveness

of burst SCS for the reduction of dorsal horn neuronal firing during noxious mechanical stimulation of the forepaw. Evaluate the role of GABA signaling as a potential mechanism of action for burst SCS.

3a. Optimize the burst stimulation parameters for attenuating dorsal horn neuronal hyperexcitability after painful nerve root compression. Determine how the parameters of the burst waveform (pulse number, pulse frequency, pulse width, burst frequency, and amplitude) alter the effectiveness of burst SCS by measuring dorsal horn neuronal firing in response to noxious mechanical stimulation, and the percentage of dorsal horn neurons responding to stimulation. Identify the set of burst parameters that is most effective in reducing dorsal horn neuronal firing following burst SCS.

3b. Assess the effectiveness of burst SCS compared to tonic SCS for attenuating neuronal firing in the spinal dorsal horn after painful nerve root compression. In separate groups, apply the $GABA_A$ antagonist, bicuculline, or the $GABA_B$ antagonist, CGP35348 to the dorsal spinal cord continuously on day 7 after painful nerve root compression to determine whether burst SCS reduces firing in dorsal horn neurons through modulation of GABA signaling.

3c. Evaluate the effectiveness of burst SCS compared to tonic SCS for attenuating spinal neuronal hyperexcitability on day 7 after painful facet joint injury by quantifying dorsal horn neuronal firing after burst and tonic SCS.

The aims in this thesis are organized into chapters summarizing the relevant experimental studies. Aim 1a is presented in Chapter 3 to establish a timeline for the

development of spinal neuronal hyperexcitability after painful facet joint injury. Studies investigating Aims 1b-1d are presented in Chapter 4 evaluating the role of afferent discharge from the facet joint in the development of persistent pain. Chapter 5 reports studies addressing Aim 2 to evaluate the role of excitatory synaptogenesis in behavioral and neuronal hypersensitivity. Aim 3a is presented in Chapter 6 to optimize the parameters of burst spinal cord stimulation for the attenuation of spinal hyperexcitability, and Chapter 7 compares burst to conventional tonic SCS for treatment of neuropathic pain and persistent joint-mediated pain, and evaluates GABAergic signaling as a potential mechanism for the effects of burst SCS (Aims 3b and 3c). Lastly, Chapter 8 summarizes the main findings of this thesis in the broader context of cervical spine injury and persistent pain, including limitations and implications of this work for future research.

CHAPTER 3

Spinal Neuronal Plasticity is Evident within One Day after a Painful Cervical Facet Joint Injury

This chapter was adapted from:

Crosby ND, Weisshaar CL, Winkelstein BA. Spinal neuronal plasticity is evident within 1 day after a painful cervical facet joint injury. *Neuroscience Letters* 2013; 542:102-106.

3.1. Overview

Chronic facet joint-mediated pain is prevalent in the both the lumbar and cervical regions of the spine (Manchikanti et al., 2004; Schwarzer et al., 1995). Spinal syndromes are responsible for an estimated annual cost of over $85 billion in the United States (Martin et al., 2008). The facet joints in the cervical spine have been reported as the source of pain in 54-60% of individuals who experience chronic pain from whiplash (Barnsley et al., 1995; Lord et al., 1996, Manchikanti et al., 2004). Many cadaveric studies report abnormal motions of the cervical facet joints and excessive facet capsular ligament stretch during neck injury that may lead to chronic neck pain (Bogduk and Yoganandan, 2001; Panjabi et al., 1998b; Pearson et al., 2004; Winkelstein et al., 2000). Clinically, chronic cervical spine pain symptoms include decreased pain thresholds, secondary hyperalgesia that extends into the extremities, enlarged receptive fields, and insensitivity of pain to peripheral administration of local anesthetics (Banic et al., 2004;

Curatolo et al., 2001; Curatolo et al., 2004; Herren-Gerber et al., 2004; Munglani, 2000). Those symptoms are characteristic of central sensitization, a state in which spinal neuronal hyperexcitability potentiates nociceptive responses to the non-noxious and noxious stimuli that converge in the spinal dorsal horn from widespread anatomical regions (Latremoliere and Woolf, 2009). However, despite the development of persistent pain after mechanical injury to the cervical facet joint, it is not known how early the spinal changes occur after injurious loading of the joint, and the physiologic sequelae leading to chronic pain from that injury remain unclear.

In a rat model of painful facet joint injury, hyperalgesia develops as early as day 1 and persists through day 7 after injury (Dong et al., 2012; Lee et al., 2008; Lee and Winkelstein, 2009). Spinal neuronal hyperexcitability is also evident at day 7 after painful facet injury (Quinn et al., 2010b), but dorsal horn neuronal activity has not been measured at earlier time points. This chapter addresses the objectives outlined in Aim 1a in order to characterize the temporal development of spinal hyperexcitability after painful facet joint injury. Behavioral sensitivity was measured at 6 hours or 1 day after sham or painful facet joint injury, in separate groups. Spontaneous activity and neuronal firing evoked by non-noxious and noxious mechanical stimuli applied at the forepaw were also quantified at 6 hours or 1 day after sham or painful facet joint injury. The work in this chapter defines the onset of behavioral sensitivity and spinal hyperexcitability to provide context for the studies in Aims 1b-1d, which evaluate the role of afferent activity from the injured facet joint in inducing spinal neuronal hyperexcitability.

3.2. Background

The facet capsular ligament is innervated by both proprioceptive and nociceptive mechanoreceptors that project to the spinal cord at largely the same spinal level as the facet joint from which they originate (Chen et al., 2006; McLain, 1993; Ohtori et al., 2001; Yamashita et al., 1990). During facet capsule stretch, afferents that innervate the capsule have been shown to increase their firing rates with increases in applied capsular strain (Lu et al., 2005a). Increased peripheral neuronal input to the spinal cord can be sufficient to produce long-lasting central sensitization via increased excitability of dorsal horn neurons, leading to hyperalgesia and allodynia as early as minutes or hours after the initial discharge of afferent firing (Cook et al., 1987; Koltzenburg et al., 1992; Ren and Dubner, 1998; Wall and Woolf, 1986; Woolf, 1983). Central sensitization has been studied in several models of chronic joint-mediated pain, including knee inflammation and temporomandibular joint disorders (Hathaway et al., 1995; Lam et al., 2008; Martindale et al., 2007), but such models do not investigate mechanical injury to the joint. Transient mechanical facet joint trauma induces sustained behavioral sensitivity and neuronal hyperexcitability by day 7 after injury (Lee and Winkelstein, 2009; Quinn et al., 2010b). Yet, it is not known how early such putative spinal changes develop after painful facet injury and how the timing of the onset of spinal involvement relates to pain.

Central sensitization often involves plasticity among wide dynamic range (WDR) neurons in the spinal cord, a subpopulation of second-order cells found largely in the deep laminae (III-VI) of the dorsal horn (Christensen and Hulsebosch, 1997; Hains et al., 2003c; Hao et al., 1992; Zhang et al., 2005). WDR neurons receive input from both non-nociceptive and nociceptive neurons, so they are involved in the integration and

supraspinal projection of both innocuous and painful sensation (Baron, 2006; D'Mello and Dickenson, 2008). WDR neurons develop hyperexcitability to both mechanical and thermal stimuli in a variety of pain models in addition to expansion of their receptive fields, and are believed to mediate the hyperalgesia and allodynia that manifest during central sensitization (Cata et al., 2006; Coghill et al., 1993; Hains et al., 2003c; Hao et al., 1991; Martindale et al., 2007; Zhang et al., 2005). Painful facet joint injury induces WDR neuronal hyperexcitability at day 7 after injury, along with a shift among second-order dorsal horn neurons to the multi-receptive WDR phenotype (Quinn et al., 2010b). However, plasticity in dorsal horn neurons remains undefined at earlier time points after painful facet joint injury.

This study investigates the development of hyperalgesia and dorsal horn neuronal hyperexcitability in the spinal cord during the first day after painful facet joint injury, and tests the hypothesis that spinal neuronal hyperexcitability develops concurrently with hyperalgesia within one day after injury. Painful cervical facet joint injury was imposed and behavioral sensitivity measured in the forepaw at either 6 hours or 1 day. Extracellular potentials were recorded from neurons in the deep laminae of the dorsal horn at those times in order to assess spontaneous firing and evoked responses to peripheral non-noxious and noxious mechanical stimuli.

3.3. Methods

3.3.1. Study Design and Facet Joint Injury

All experimental procedures were approved by the University of Pennsylvania Institutional Animal Care and Use Committee and carried out under the guidelines of the

Committee for Research and Ethical Issues of the International Association for the Study of Pain (Zimmerman, 1983). Male Holtzman rats (350-464g) were divided into two groups designated to undergo behavioral and electrophysiological testing at either 6 hours (n=4 injury, n=4 sham) or 1 day (n=6 injury, n=6 sham). Normal rats (n=6) were also included for both assays as an additional control group. All statistical analyses were performed using JMP9 (SAS; Cary, NC) with α=0.05.

Rats were anesthetized with isoflurane (4% for induction, 2-3% for maintenance). Injurious distraction of the C6/C7 facet joints was administered using a custom loading device as previously described (Lee and Winkelstein, 2009). Rats were placed in a prone position and the paraspinal musculature was separated to bilaterally expose the laminae and facet capsules of the cervical vertebrae from C5-T1. The C6 and C7 vertebrae were attached to a custom loading device using microforceps. The C6 vertebra was then distracted 0.7mm rostrally to stretch the facet capsule across the joint. Polystyrene beads were placed on the C6 and C7 vertebrae and a grid of beads was placed on the right C6/C7 facet capsule to track motions during the imposed capsule stretch (Fig. 3.1). A Phantom v4.3 CCD camera (Vision Research; Wayne, IN) recorded the bead marker positions at a rate of 500fps. The bead marker positions before joint distraction and also at the peak of imposed capsule stretch were used to calculate the vertebral and capsular distraction magnitudes and the maximum principal strains on the facet capsule during each joint distraction (Fig. 3.1). Although there is a negative slope of the facet capsule running from the rostral insertion to the caudal insertion site, that angle of incline is small enough that the strains can be calculated using a single camera (Lee et al., 2004a). A sham group was included in which the facet capsule was kept intact without any joint

distraction imposed in order to control for the effects of surgical procedures. Following surgery, incisions were closed using 3-0 polyester suture and surgical staples, and rats were monitored during recovery in room air. Vertebral and capsule distractions and capsule strains were compared between the 6 hour and 1 day injury groups using Student's t-tests.

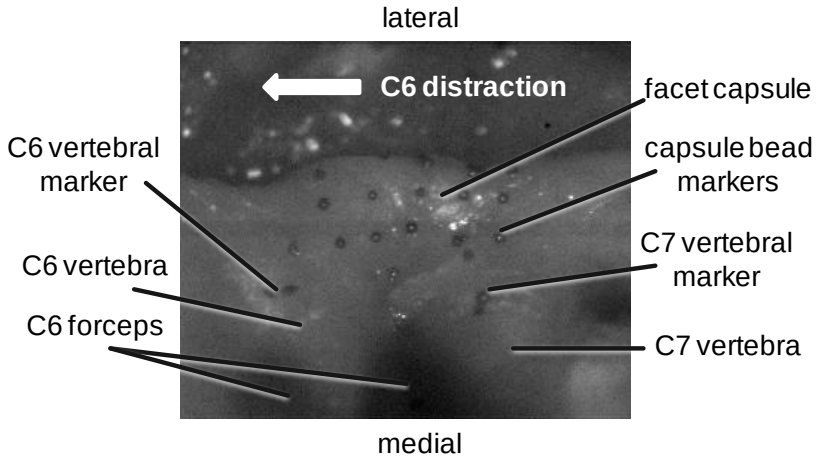

Fig. 3.1. The right facet joint of the rat with vertebral and capsule bead markers. Vertebral markers were placed on the laminae of the C6 and C7 vertebrae to measure joint distraction magnitudes. A grid of bead markers on the facet capsule was used to quantify capsule distraction and capsule strain.

3.3.2. Assessment of Mechanical Hyperalgesia

Mechanical hyperalgesia in the left and right forepaws was assessed preoperatively and at either 6 hours or 1 day after injury to evaluate behavioral hypersensitivity. Hyperalgesia was measured by quantifying the paw withdrawal threshold in response to application of a series of von Frey filaments (1.4, 2, 4, 6, 8, 10, 15, and 26g) to the plantar surface of the forepaws (Chaplan et al., 1994; Hubbard and Winkelstein, 2005; Lee et al., 2008). Beginning with the 1.4g filament, each filament was applied to the forepaw five times, in order of increasing buckling weight. A response was considered as positive if the rat reacted to the filament by withdrawing, licking, or

shaking the stimulated forepaw. The first filament magnitude to elicit a positive response was recorded as the paw withdrawal threshold if the next larger filament strength also evoked a positive response. If the next filament failed to elicit a positive response, testing was continued until two consecutive filaments both elicited a positive response (Lee and Winkelstein, 2009). A rat failing to respond to any of the filaments was assigned the maximum threshold, 26g, for that round. The paw withdrawal threshold for each rat was averaged from three rounds of repeated testing separated by at least ten minutes to provide an adequate rest period (Dong et al., 2012; Kras et al., 2013b). A repeated-measures ANOVA compared paw withdrawal thresholds between the sham and injury groups at each time point.

3.3.3. Spinal Cord Electrophysiological Recordings

Immediately after testing for hyperalgesia at the designated time point (6 hours or 1 day) following surgery, extracellular electrophysiological recordings were acquired in order to assess neuronal excitability in the dorsal horn of the spinal cord. Rats were anesthetized with sodium pentobarbital (45mg/kg, i.p.) and given supplementary doses (5-10mg/kg, i.p.) as needed based on toe pinch, corneal, and palpebral reflexes (Field et al., 1993). The C6 and C7 vertebrae were exposed by separating the paraspinal musculature that was dissected during the original facet joint distraction surgery. A bilateral laminectomy and dural resection at C6 and C7 exposed the spinal cord. A tracheotomy was performed and rats were connected to a ventilator and CO_2 monitor to control respiration during the recording session (CWE; Ardmore, PA). A lateral thoracotomy was also performed to alleviate intrathoracic pressure and to isolate the

spinal cord from any movement of the thoracic wall that is induced by respiration. Rats were then immobilized on a stereotaxic frame (David Kopf Instruments; Tujunga, CA) using ear bars and a vertebral clamp at T2 to stabilize the cervical spine (Fig. 3.2). The forepaws were inverted and secured to the stereotaxic frame, exposing the plantar surface of the paw for mechanical stimulation. Core temperature was maintained at 35-37ºC using a temperature controller with a rectal probe (Physitemp; Clifton, NJ). The spinal cord was bathed in 37ºC mineral oil for the duration of recording to prevent drying.

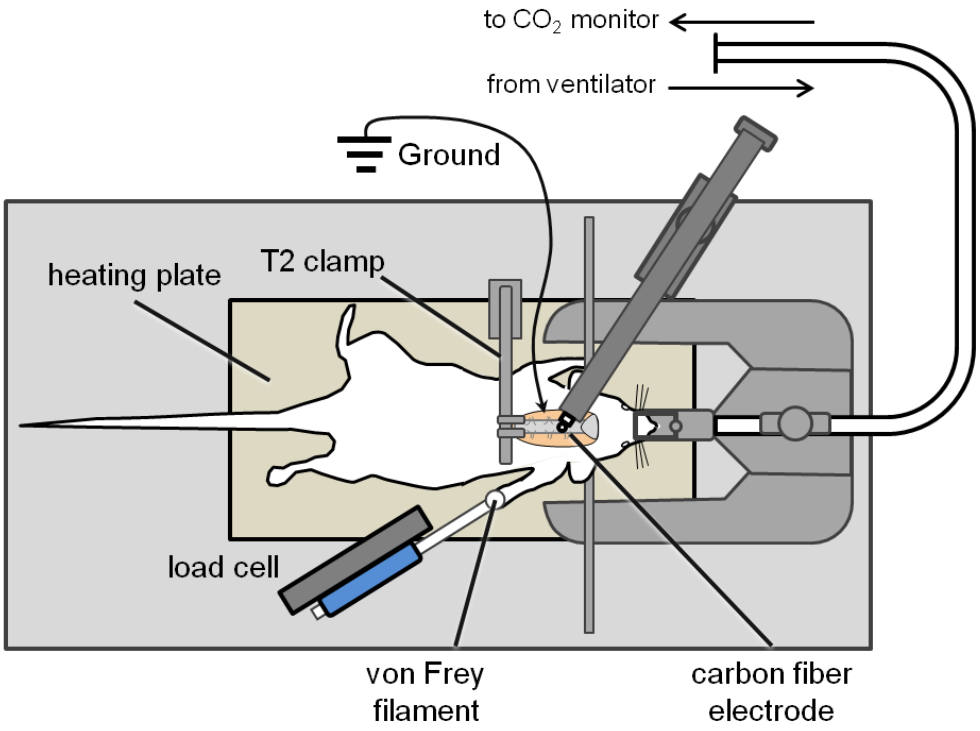

Fig. 3.2. Schematic of the instrumentation for extracellular electrophysiological recordings. Rats were mounted on a stereotaxic frame with ear bars and a clamp at T2. Body temperature and respiration were monitored and controlled for the duration of recording. A carbon fiber electrode was lowered into the dorsal horn of the spinal cord to record neuronal firing during mechanical stimulation of the forepaw. Mechanical stimuli were coupled to a load cell to synchronize the application of stimuli with electrophysiological recordings.

Extracellular potentials were recorded continuously using a carbon fiber electrode (Carbostar-1; Kation; Minneapolis, MN). Signals were amplified with a gain of 10^3 and conditioned using a bandpass filter between 0.3kHz and 3kHz (World Precision Instruments; Sarasota, FL). The signal was processed with a 60Hz HumBug adaptive filter (Quest Scientific; North Vancouver, BC), digitally sampled at 25kHz (Micro1401, CED; Cambridge, UK), and monitored with a speaker for audio feedback (A-M Systems; Carlsborg, WA) (Fig. 3.3). Mechanical stimuli were attached to a load cell whose signal was also sampled and recorded at 25kHz in order to synchronize stimulus application with the electrophysiological data (Fig. 3.3).

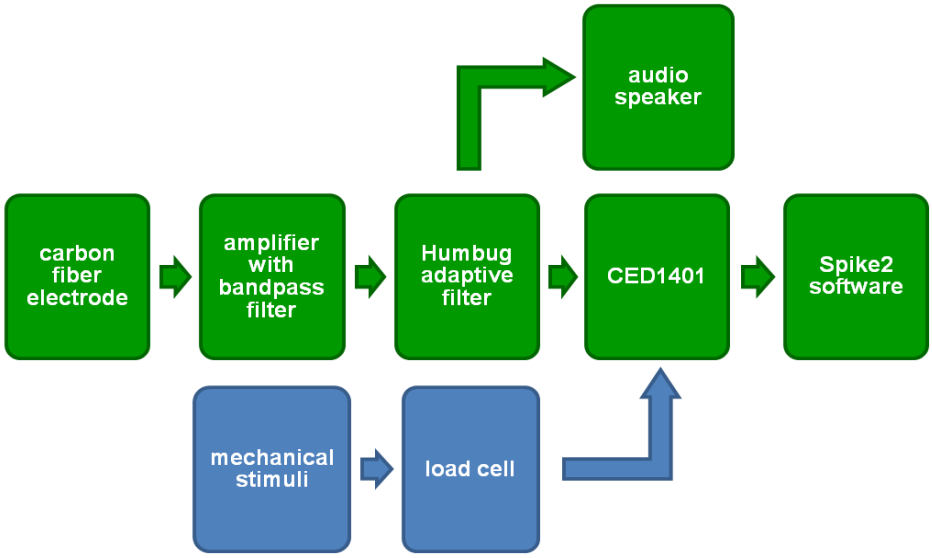

Fig. 3.3. General scheme for data collection and processing of electrophysiological recordings. Extracellular potentials and stimulus loads were conditioned and recorded using Spike2. Voltage potentials were also used for audio feedback during recording.

Neuronal activity within the dorsal horn was recorded by lowering the electrode through the pial surface of the C6 or C7 spinal cord with a micropositioner (Narishige; Tokyo, Japan). Mechanically-sensitive neurons were identified by brushing of the plantar surface of the forepaw on the side ipsilateral to the electrode. A neuron was selected for

recording if the brushing evoked activity with an estimated signal-to-noise ratio of at least two, and if the evoked activity did not increase in amplitude when the electrode was lowered further into the dorsal horn. Once selected, the neuron was mechanically stimulated at the forepaw with a series of non-noxious and noxious stimuli (Fig. 3.4), including a two-second baseline period before each stimulus, ten seconds of light brushing, five consecutive one-second stimulations at one-second intervals with a series of von Frey filaments (1.4g, 4g, 10g, 26g), followed by ten seconds of noxious pinch with a 60g vascular clip (Hains et al., 2003a; Quinn et al., 2010b). At least 30 seconds were allowed between stimuli in order to prevent wind-up of mechanically-sensitive neurons (Fig. 3.4). The von Frey filaments were chosen to be logarithmically spaced and span the range of filaments used for measuring hyperalgesia. The specifics of the spike recording protocol are described in detail in Appendix A.

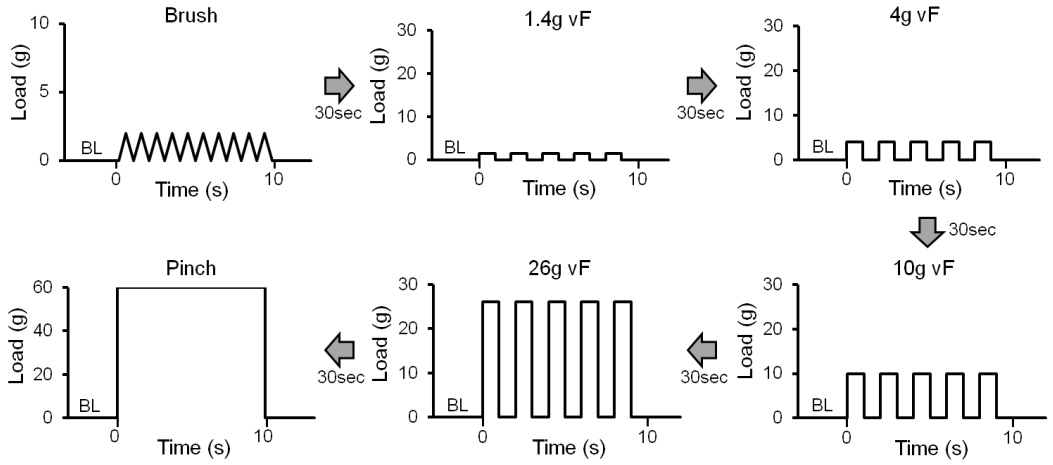

Fig. 3.4. Protocol for mechanical stimulation of the forepaw during recording of dorsal horn neuronal firing. Baseline firing (BL) was recorded for two seconds before each stimulus. Light brush was applied for ten seconds, followed by five applications of 1.4g, 4g, 10g, and 26g von Frey (vF) filaments each over a ten-second period. Noxious pinch was applied for ten seconds with a 60g vascular clip.

3.3.4. Electrophysiological Data Analysis

Voltage recordings from each neuron were spike-sorted using Spike2 software (CED; Cambridge, UK) to ensure that spikes from only one neuron were considered at a time. Baseline firing was established before each stimulus by totaling the number of spikes in the two-second baseline period prior to stimulation (Fig. 3.4). To evaluate spontaneously active neurons, the number of neurons with no spikes and the number of neurons with more than one spike in the baseline period before application of the brush stimulus was counted for each time point in each of the injury and sham groups. Evoked responses were quantified for the brush and pinch stimuli by summing the spikes over the ten seconds that each stimulus was administered. For the von Frey filament stimuli, spikes were considered to be evoked by a single von Frey stimulus if they occurred during the one-second application or the one-second rest period immediately following stimulus application; each filament had a total of five spike counts since each filament was applied to the forepaw five times (Fig. 3.4). Baseline firing was subtracted from the spike counts for each stimulus to quantify the evoked response. Spike counts for each stimulus were log-transformed due to a positive skew in the distributions of the spike totals. Residuals were plotted after transformation to confirm a normal distribution. The spike sorting protocol is described in detail in Appendix A.

Pearson's Chi-square test was used to evaluate differences in the number of spontaneously firing cells in each group. Evoked responses to the brush and pinch stimuli were tested between groups using a mixed-effect ANOVA with neurons nested within rats and rats nested within groups; post-hoc Tukey's HSD tested for differences between the individual groups. For the von Frey stimuli, a mixed-effect ANOVA with the same

nesting structure and post-hoc analysis was used to test the differences between groups, von Frey stimulus magnitudes, stimulus order, and their interactions. Neurons having evoked responses with Studentized residuals greater than two were excluded from statistical analysis as outliers.

3.4. Results

The vertebral distractions for the injury groups tested at 6 hours (0.53±0.31mm) and 1 day (0.63±0.16mm) are not significantly different from each other. The capsule distractions (0.31±12mm for the 6 hour injury group; 0.29±0.12mm for the 1 day injury group) and the maximum principal strains in the capsule (28±14% for 6 hour group; 21±14% for 1 day group) also are not significantly different between the 6 hour and 1 day injury groups. The detailed mechanical data for each facet joint distraction are summarized in Appendix B. Paw withdrawal threshold (PWT) at 6 hours is not changed from baseline (BL) for the injury group (9.0±4.3g BL; 10.2±3.4g at 6 hours) or the sham group (11.7±3.2g BL; 12.9±6.2g at 6 hours) (Fig. 3.5). At 1 day, the PWT of the sham group (13.4±7.9g) also is not changed from BL responses (12.8±10.4g); however, the PWT is significantly reduced ($p=0.012$) at 1 day after painful facet joint injury (12.0±6.6g BL; 6.5±3.3g at day 1) (Fig. 3.5). The baseline PWT for each group is not different from the PWT (10.2±4.4g) measured in normal rats (Fig. 3.5). Paw withdrawal thresholds for each rat on each day can be found in Appendix C.

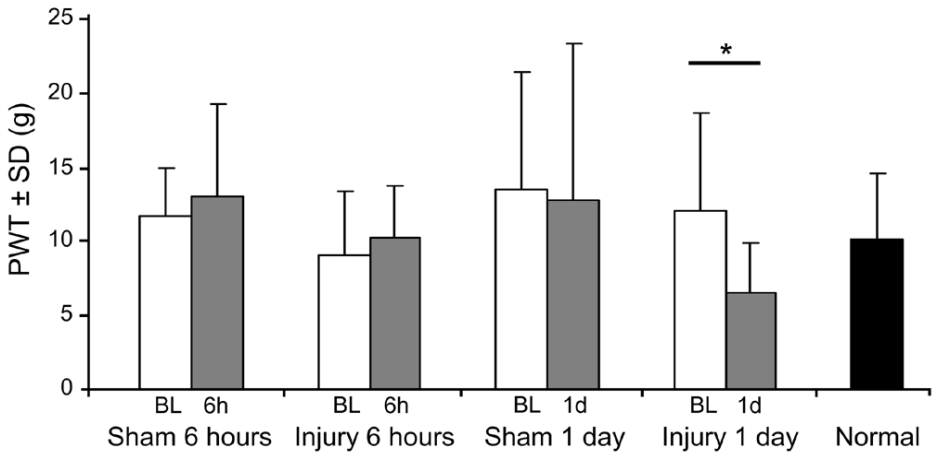

Fig. 3.5. Mechanical hyperalgesia at 6 hours or 1 day after painful facet joint injury. Paw withdrawal threshold (PWT) at baseline (BL) for the 6 hour and 1 day groups is not different from normal. At 6 hours (6h), PWT is not different from baseline in the sham or injury groups. PWT is significantly reduced (*p=0.012) from baseline at 1 day (1d) after injury but is unchanged at that time point in the sham group.

A total of 229 neurons (46±13 neurons/group) was recorded at an average depth of 636±170μm in the dorsal horn (Table 3.1), which is a depth included in laminae III-VI in the rat spinal cord (Watson et al., 2009). Of the 229 neurons, 31 neurons were removed from analysis as outliers because their evoked responses had Studentized residuals greater than two (6±4 neurons/group). Appendix D lists the spike counts for each individual neuron from each rat.

Table 3.1. Total number of neurons recorded for each spinal cord level.

	C6	C7	C6/C7 Total	Avg. Depth ± SD
Injury, 6h	22	19	41	633±167μm
Sham, 6h	25	11	36	656±175μm
Injury, 1d	29	12	41	652±152μm
Sham, 1d	27	15	42	607±170μm
Normal	33	36	69	646±174μm
Totals	136	93	229	636±170μm

6h = 6 hours; 1d = 1 day; Avg. = average; SD = standard deviation

Spontaneous firing is increased at both 6 hours and 1 day after injury, although firing at 1 day after sham procedures is not different from normal (Fig. 3.6). Two groups of neurons were classified based on spontaneous activity during the baseline period prior to stimulation: neurons with no baseline firing (Fig. 3.6a) and those with baseline firing rates greater than one spike/sec (Fig. 3.6b). Eighty percent of neurons in the normal group have no spontaneous firing and 5% have firing greater than one spike/sec. At 6 hours after injury or sham procedures, the percentages of neurons with no spontaneous firing (68% after injury, 64% after sham) and spontaneous firing greater than one

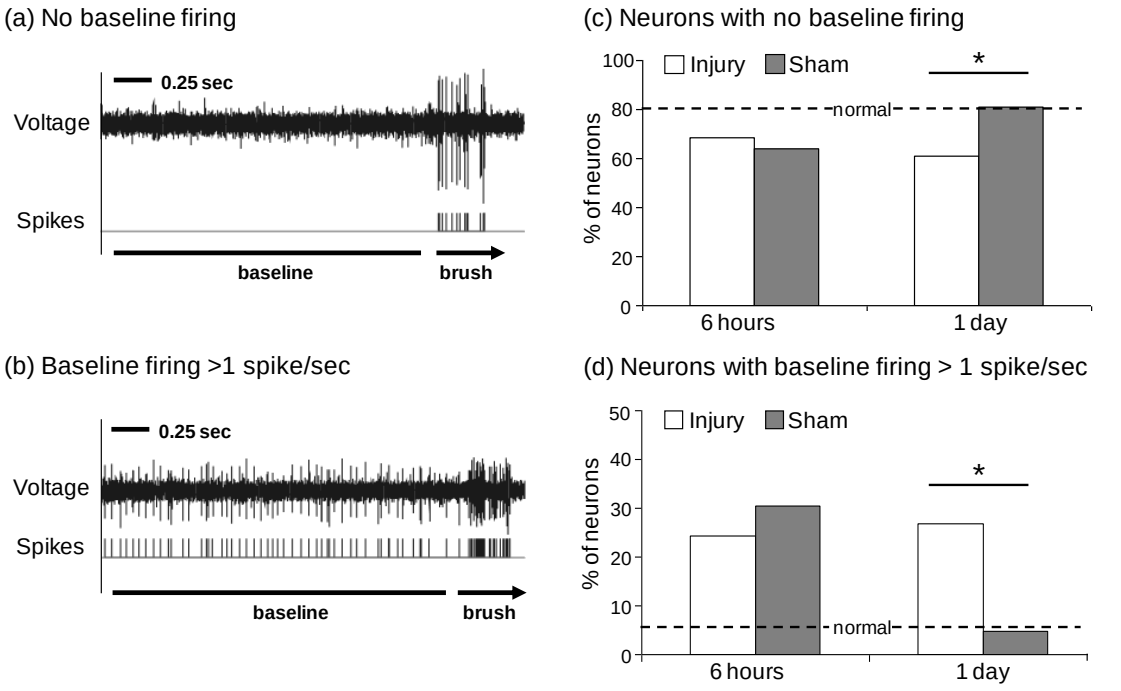

Fig. 3.6. Spontaneous firing in the spinal dorsal horn. Example recorded voltage potentials from neurons with **(a)** no baseline firing and **(b)** baseline firing greater than one spike/sec. **(c)** The number of quiescent neurons (presented as the percentage of total recorded neurons in each group) is unchanged at 6 hours relative to sham at that time point, but at 1 day is significantly lower after injury compared to sham (*p=0.038). **(d)** The number of active neurons exhibits a similar trend with a significantly greater number of neurons (*p=0.006) at 1 day after injury. Percentages of cells in the normal group are shown (dotted line) for **(c)** and **(d)**.

spike/sec (24% after injury, 31% after sham) are not different (Fig. 3.6). However, 1 day after injury the percentages of neurons with no spontaneous firing (61% after injury, 81% after sham, $p=0.038$) and spontaneous firing greater than one spike/sec (27% after injury, 5% after sham, $p=0.006$) are significantly different (Fig. 3.6).

Overall, evoked firing is elevated at 6 hours and 1 day after injury, but firing returns to normal levels in the sham group at 1 day (Figs. 3.7 and 3.8). The evoked responses for light brushing and noxious pinch are not different between the 6 hour sham (107±15 spikes for brush, 78±15 spikes for pinch), 6 hour injury (91±12 spikes for brush, 79±11 spikes for pinch), or 1 day injury groups (89±8 spikes for brush, 77±15 spikes for pinch) (Fig. 3.8a); each is also elevated over normal (48±4 spikes for brush, 29±5 spikes for pinch) for both brush ($p<0.004$) and pinch ($p<0.0001$). The evoked responses for the injury group at 1 day also are significantly higher than the sham responses at that time point (59±7 spikes for brush, 32±5 spikes for pinch) for light brush ($p=0.003$) and noxious pinch ($p=0.014$) (Fig. 3.8a). Likewise, evoked responses for the 4g, 10g, and 26g von Frey filaments are not different between any of the groups at 6 hours or the injury group at day 1. However, for the 4g, 10g, and 26g filaments, each of the 6 hour sham, 6 hour injury, and 1 day injury groups exhibit significantly elevated firing over both sham at day 1 ($p<0.004$) and normal ($p<0.017$) (Fig. 3.8b). For the 1.4g filament, only the 6 hour sham and 1 day injury groups demonstrate evoked firing that is significantly greater than at 1 day after sham ($p<0.03$) and normal responses ($p<0.007$) (Fig. 3.8b). There is no difference from normal evoked responses for any stimulus applied at 1 day after a sham procedure.

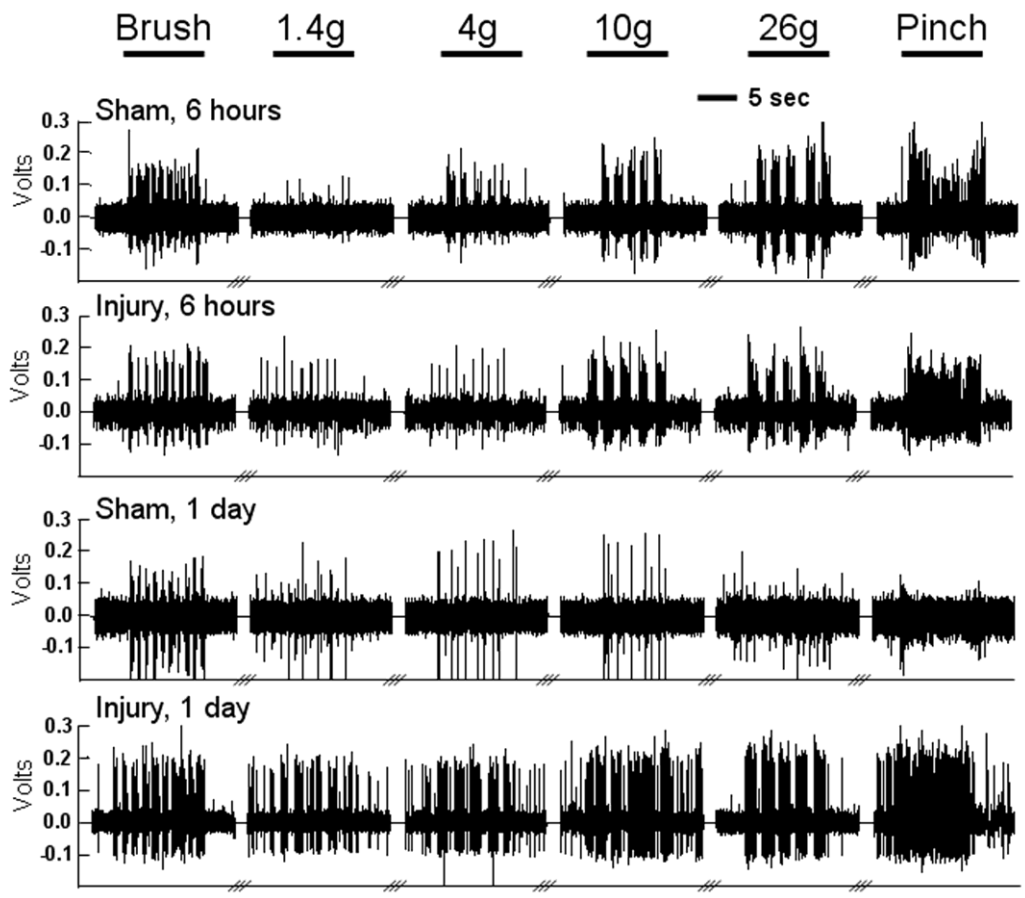

Fig. 3.7. Representative firing for sham and injured rats at 6 hours or 1 day. Voltage recordings are presented prior to spike sorting to demonstrate the relative differences in neuronal activity in response to light brush, von Frey filament (1.4-26g) and noxious pinch stimuli. Sham and injured rats have similar firing at 6 hours, but at 1 day after the injury there is demonstrably more neuronal firing relative to sham.

3.5. Discussion

This study demonstrates that neuronal hyperexcitability in the dorsal horn develops within the first day after transient mechanical facet joint injury, corresponding to the development of hyperalgesia (Figs. 3.5-3.8). Although neuronal hyperexcitability is evident at 1 day after painful facet joint injury, neither behavioral nor neuronal responses are different from sham at 6 hours after the injury (Figs. 3.5-3.8). The hyperexcitability in dorsal horn neurons at day 1 is measured as an increase over sham in both spontaneous

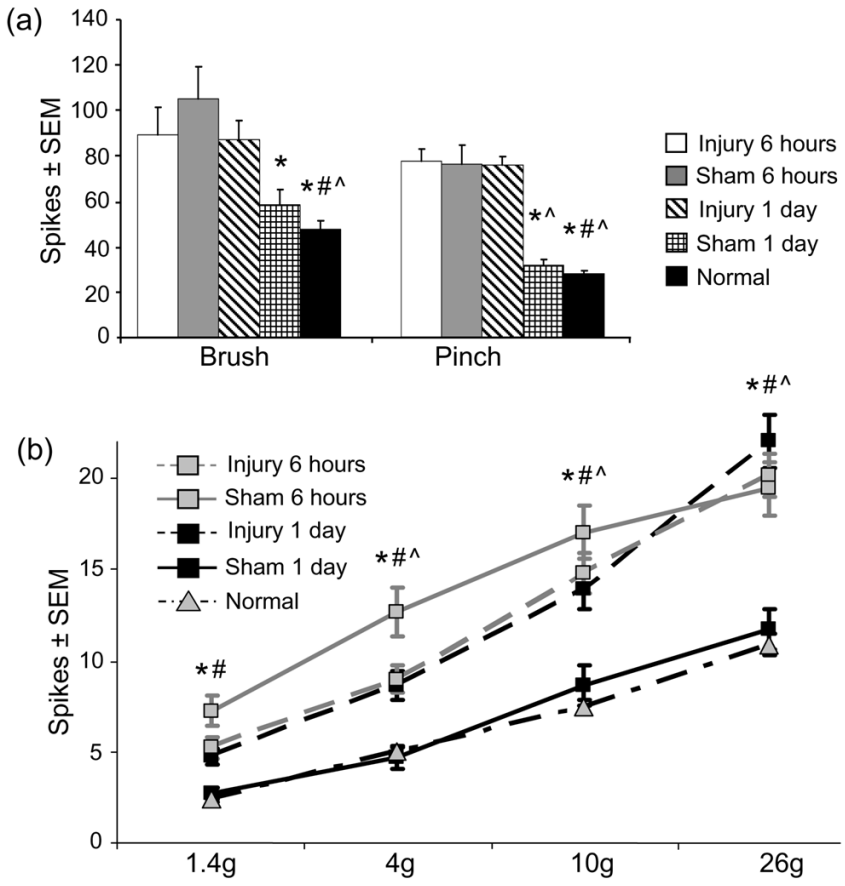

Fig. 3.8. Evoked firing in the spinal dorsal horn. **(a)** Normal rats and those at 1 day after sham exhibit significantly lower evoked responses to light brush and noxious pinch than those at 1 day after painful injury (*p≤0.014). Only normal rats are significantly lower than those at 6 hours after sham (#p<0.0008) and 6 hours after injury (^p<0.004). **(b)** In response to von Frey filament stimuli, normal rats and those at 1 day after sham exhibit significantly less evoked firing than those at 1 day after injury (*p<0.03), 6 hours after sham (#p<0.0006), and 6 hours after injury (^p<0.017).

firing and responses evoked by non-noxious and noxious mechanical stimuli (Figs. 3.6-3.8). These results suggest that spinal neuronal hyperexcitability indicative of central sensitization develops early after facet joint injury and plays a role in the development of the behavioral sensitivity that is known to persist at later time points in this model (Lee and Winkelstein, 2009; Quinn et al., 2010b).

The mechanical parameters defining the extent of facet joint injury, including vertebral distractions, capsule distractions, and maximum principal capsule strains, are not different between the two groups studied at 6 hours and 1 day after injury, indicating that those two groups received the same injury. The vertebral distractions for both painful injury groups (0.53±0.31mm for 6 hour; 0.63±0.16mm for 1 day) are not different from those previously reported to induce microstructural damage in the capsular ligament (Quinn et al., 2010a), and to produce persistent pain (Lee et al., 2004a; Lee and Winkelstein, 2009). Furthermore, the capsular strains measured in this study (28±14% and 21±14% for the 6 hour and 1 day groups, respectively) are similar to those strains induced in the C5-C7 facet capsules during whiplash injury (Pearson et al., 2004). Strains greater than 10% have been shown to be sufficient to activate the nociceptive fibers that innervate the facet joint in a caprine model (Lu et al., 2005b). Increases in afferent discharge after nerve injury have been shown to induce neuropathic pain, and blocking afferent activity after injury can suppress the development of behavioral sensitivity (Seltzer et al., 1991a). Therefore, the levels of facet joint distraction in this study that produce persistent pain may induce neuronal hyperexcitability by increasing afferent discharge from the injured joint. Studies in Chapter 4 further evaluate the role of primary afferent discharge from the cervical facet joint in the initiation of spinal hyperexcitability.

There are no behavioral or electrophysiological differences between the injury and sham groups at 6 hours, and behavioral sensitivity at 6 hours after injury is not different from baseline, indicating that the potentiation of nociception in the dorsal horn has not yet occurred at that time. However, at 6 hours, 31% of neurons in sham rats and 24% in injured rats exhibit spontaneous firing greater than one spike/sec, similar to those

percentages found at day 1 after injury (27%) (Fig. 3.6). Both spontaneous and evoked firing are elevated over normal for injury *and* sham at 6 hours, suggesting that afferent activity may be acutely potentiated by the initial surgical procedure itself without causing secondary behavioral sensitivity. However, the neuronal activity largely returns to that of normal levels over the following hours in sham controls, while aberrant spontaneous activity and spinal hyperexcitability persist after injury (Figs. 3.6-3.8). It is possible that the increased firing that is observed at 6 hours after the sham and injury procedures relative to normal responses (Fig. 3.8) may be due, in part, to interactions between the isoflurane used for the initial surgery and the pentobarbital used for the electrophysiology procedures. However, the sham group received the same anesthesia as the painful injury group, so the direct comparison of behavioral sensitivity and neuronal activity between those two groups at 6 hours is not affected by any potential anesthesia interactions.

Mechanical hyperalgesia in this study is measured in the forepaw, a site remote from the injury, which is consistent with clinical reports of secondary hyperalgesia and centrally-mediated pain following whiplash (Curatolo et al., 2004; Herren-Gerber et al., 2004). The development of mechanical hyperalgesia parallels the onset of persistent spinal neuronal hyperexcitability within the first day after facet joint injury (Figs. 3.5 and 3.8). The significant decrease in PWT at that same time point (Fig. 3.5) is consistent with other studies of behavioral sensitivity after painful facet joint injury, in which sensitivity was induced at day 1 after injury (Lee et al., 2008; Weisshaar et al., 2010). In fact, in the current study, facet capsule stretch reduces PWTs to below the baseline 10-15g threshold in normal rats, suggesting the recruitment of typically non-nociceptive Aβ afferents for nociception. Aβ afferents may acquire nociceptive functionality through de novo

expression of neuromodulators, like substance P, that are typically associated with nociceptive fibers (Latremoliere and Woolf, 2009). Low-threshold afferents may also sprout processes into the superficial dorsal horn and structurally integrate into nociceptive pathways by synapsing with nociceptive-specific dorsal horn neurons (Woolf et al., 1992). Regardless of the mechanism, the activation of nociceptive neurons in the dorsal horn by typically non-nociceptive low-threshold mechanosensitive fibers can directly cause aberrant pain in response to innocuous stimuli, and supports the assertion that facet joint loading that produces pain also initiates modifications in the spinal processing of sensory information that leads to behavioral hypersensitivity.

Spontaneous activity in primary afferents is a potential mechanism for the initiation and long-term maintenance of central sensitization (Devor, 2009; Latremoliere and Woolf, 2009). In this study, a greater percentage of dorsal horn neurons (27%) exhibit spontaneous firing at day 1 after painful injury compared to each of sham exposed (5%) and normal rats (5%) (Fig. 3.6). This finding is supported by reports that up to one-third of primary sensory neurons develop spontaneous activity after peripheral nerve axotomy (Devor, 2005; Devor, 2009). The development of spontaneous activity also corresponds to the onset of tactile allodynia after peripheral nerve injury (Devor, 2009; Sun et al., 2005). Indeed, ectopic activity in nociceptive Aδ and C fibers may contribute to central sensitization and neuropathic pain after injury (Cook et al., 1987; Djouhri et al., 2006; Wall and Woolf, 1986). However, other work examining the role of afferent firing in the development of neuropathic pain has shown that allodynia can be induced by Aβ fibers in the absence of C fiber activation (Devor, 2009; Liu et al., 2000). Although spontaneous Aδ and C fiber activity and low-threshold Aβ fibers each have been

proposed as contributors to central sensitization after injury (Devor, 2009; Djouhri et al., 2006; Liu et al., 2000), WDR neurons receive input from both non-nociceptive and nociceptive afferents (Baron, 2006). As such, the presence of WDR spontaneous activity alone in this study does not determine whether low-threshold afferents or nociceptors mediate the development of central sensitization after painful facet joint injury. However, ectopic firing in C fibers develops weeks after injury while the majority of spontaneous firing in the immediate hours or days after injury occurs in the low-threshold touch-sensitive Aβ fibers (Devor, 2009). Based on Devor's study (2009), the development of aberrant spontaneous activity between 6 hours and 1 day after painful facet joint injury (Fig. 3.6) suggests that Aβ fibers are likely to be the source of that ectopic activity. Ultimately, better classification of the primary afferents is necessary during spinal electrophysiological recordings to determine which afferent populations are involved in the ectopic firing that is observed here.

The temporal responses after this painful joint injury mimic the timing of changes after peripheral nerve injury, in which up to 27% of A fibers, but not C fibers, begin spontaneously firing between 6 and 30 hours after the injury (Michaelis et al., 1995). Given the similarity to neuropathic pain models in both the timing and scope of ectopic firing observed in this study, it should be noted that this painful facet joint model is a ligamentous injury and not an explicit nerve injury. However, axonal swelling indicative of secondary axotomy has been reported in a similar caprine model of facet capsule stretch (Kallakuri et al., 2008). Nonetheless, taken together with the literature, the increased spontaneous activity in the spinal cord evident at day 1 after painful facet joint injury suggests that the etiology of pain and central sensitization following mechanical

joint injury may be similar to peripheral neuropathic injuries. As such, studies of the initiation and development of neuropathic pain in nerve injury models may provide valuable insight for continued elucidation of the biomechanical and neurophysiological mechanisms underlying persistent facet joint-mediated pain.

Evoked activity is elevated over sham in neurons recorded at day 1 after painful facet joint injury (Fig. 3.7 and 3.8). There is a significantly greater evoked response to light brush and the 4g von Frey filament at day 1 after injury (Fig. 3.8), both of which are non-noxious stimuli that do not elicit a behavioral response in uninjured rats and do not typically activate high-threshold nociceptors (Kitagawa et al., 2005). These results suggest that the Aβ fibers that transduce non-noxious mechanosensation may have a role in the early development of spinal hyperexcitability following painful facet joint injury. The evoked responses to noxious stimuli, including the 10g and 26g von Frey filaments and 60g pinch, are also significantly greater at day 1 after injury (Fig. 3.8). WDR neurons receive input from non-nociceptive and nociceptive afferent populations (Baron et al., 2006), so the consistent increase in excitability across both non-noxious and noxious stimuli supports the involvement of WDR neurons in the development of central sensitization after painful facet joint injury.

The increases in evoked activity following both non-noxious and noxious stimuli are consistent with the hyperexcitability that has been reported at day 7 after this facet joint injury (Quinn et al., 2010b). These similarities in spinal hyperexcitability at two different time points suggest that the mechanisms of neuronal plasticity associated with the development of sustained spinal hyperexcitability begin between 6 hours and 1 day after a facet capsule stretch. One potential mechanism may involve protein kinase C

epsilon (PKCε), an important downstream regulator of excitatory glutamate signaling and N-methyl-D-aspartate (NMDA) glutamate receptor activation (Xu et al., 2007). NMDA receptor activation is a key step in the induction and maintenance of sensitization since it is an important glutamatergic receptor in the dorsal horn (Latremoliere and Woolf, 2009). PKCε is upregulated in the DRG at day 7 and in the spinal dorsal horn at day 1 after painful facet joint injury (Dong et al., 2012; Weisshaar et al., 2010). The increased PKCε in the DRG and spinal cord may potentiate the excitability of primary afferents and dorsal horn neurons, respectively, by increasing the depolarizing inward currents through activated NMDA receptors and voltage-dependent ion channels (Deriemer et al., 1985; Weisshaar et al., 2010). Potentiation of the glutamatergic system is believed to play a key role in the amplification of nociception that causes pain hypersensitivity after nerve injury; consequently, many pharmacological interventions for neuropathic pain are designed to modulate glutamatergic signaling (Kawasaki et al., 2004; Ultenius et al., 2006; Yaksh, 1999). Expression of some glutamatergic signaling proteins has been characterized after painful facet joint injury (Dong et al., 2012; Dong and Winkelstein, 2010; Weisshaar et al., 2010). However, future studies should more fully evaluate the potentiation of spinal glutamatergic signaling after facet joint injury, including the activation of NMDA glutamate receptors and the secondary signaling molecule, ERK. Activation of each of those glutamatergic signaling proteins has been reported to promote central sensitization by increasing spinal neuronal excitability (Kawasaki et al., 2004; Ultenius et al., 2006). Understanding their role in the overall potentiation of glutamatergic signaling and the onset of persistent joint-mediated pain may provide a foundation for the development of effective analgesic treatments after joint injury.

3.6. Conclusions and Integration

Dorsal horn neuronal hyperexcitability develops between 6 hours and 1 day after painful facet joint injury, and parallels the onset of behavioral hypersensitivity (Crosby et al., 2013). Those results support the hypothesis that electrophysiological and behavioral hypersensitivity develop concurrently early after painful facet joint injury. The findings from this study suggest that spinal modifications play a key role in promoting mechanical hyperalgesia by potentiating firing in the WDR neurons that integrate and transmit non-nociceptive and nociceptive mechanosensation (Baron, 2006; Christensen and Hulsebosch, 1997; Hains et al., 2003a; Zhang et al., 2005). Additionally, the increase in aberrant spontaneous activity at day 1 suggests that ectopic firing develops in parallel with spinal neuronal hyperexcitability and mechanical hyperalgesia. Ectopic activity in afferent fibers may directly contribute to the increase in spinal neuronal excitability by maintaining low levels of excitatory input to the dorsal horn.

Overall, data in this chapter provide evidence that spinal neuronal hyperexcitability contributes to the development of persistent facet-mediated pain within the first day after painful facet joint injury. However, spinal hyperexcitability and behavioral sensitivity do not develop until at least 6 hours after painful joint injury (Crosby et al., 2013), so there is a critical, and likely short, time between injury and the development of persistent elevated spinal responses. That potential temporal window before the onset of spinal hyperexcitability may provide an opportunity to attenuate the subsequent development of persistent pain, and could have importance in the design of more effective acute treatments for traumatic joint injuries. However, the role of afferent

activity in the initiation of persistent pain and the importance of the timing of that afferent activity from the injured joint has not been established.

Studies in Chapter 4 evaluate the role of afferent firing from the facet joint in the induction of spinal hyperexcitability by blocking afferent activity at different times in the hours following painful joint injury. Furthermore, the neuronal hyperexcitability that develops after painful facet joint injury likely directly contributes to persistent pain, but the spinal modifications that result in hyperexcitability have not been fully elucidated. Subsequent chapters of this thesis evaluate if spinal plasticity is induced by painful facet joint injury and the mechanisms that may contribute to neuronal hyperexcitability, including potentiation of excitatory glutamate signaling (Chapter 4) and excitatory synaptogenesis (Chapter 5).

CHAPTER 4

Early Afferent Activity from the Injured Facet Joint Potentiates Spinal Sensitization

This chapter was adapted from:

Crosby ND, Gilliland TM, Winkelstein BA. Early afferent activity from the facet joint after painful trauma to its capsule potentiates neuronal excitability and glutamate signaling in the spinal cord. *Pain* 2014; 155(9):1878-1887.

4.1. Overview

Painful facet joint injury induces dorsal horn neuronal hyperexcitability and spinal modulation of excitatory glutamatergic signaling, both of which are indicative of central sensitization, as early as one day after injury (Crosby et al., 2013; Dong et al., 2010; Dong et al., 2012; Quinn et al., 2010b; Weisshaar et al., 2010; Winkelstein, 2004). Direct injury to peripheral nerve fibers can induce significant discharge from the damaged afferents that is believed to be a primary contributor to central sensitization (Blenk et al., 1996; Chi et al., 1993; Seltzer et al., 1991a; Seltzer et al., 1991b; Wall et al., 1974). Painful facet joint injury may lead to central sensitization in a similar fashion via an increase in firing of the afferents that innervate the joint, during and after noxious facet capsule stretch (Chen et al., 2006; Lu et al., 2005a). Treatments that block the initial afferent discharge after nerve injury are more effective for attenuating neuropathic pain than treatments that are given after pain has already developed (Araujo et al., 2003; Lin et

al., 2011; Seltzer et al., 1991a). Those studies indicate that effective intervention for chronic pain relies, in part, on understanding the timing of the afferent firing that initiates sensitization. Despite this, the temporal relationship between afferent discharge and the development of persistent facet joint pain after mechanical joint injury is not defined.

The studies of the temporal development of spinal hyperexcitability after painful facet joint injury in Chapter 3 suggest that the onset of hyperalgesia and aberrant spinal neuronal hyperexcitability does not occur for at least 6 hours after facet joint injury (Crosby et al., 2013). During that time before the onset of hyperalgesia, noxious stretch of the cervical facet capsule increases discharge and afterdischarge from the afferent fibers that innervate the capsule. However, the role of that increased afferent firing in the induction and maintenance of spinal hyperexcitability is unknown. This chapter summarizes the experiments under Aims 1b-1d, which determine the role of facet injury-induced afferent discharge in the initiation of behavioral sensitivity, spinal hyperexcitability, and the potentiation of glutamatergic signaling in the spinal cord.

Intra-articular bupivacaine was administered immediately, or at day 4, after painful injury to the bilateral C6/C7 facet joints to block the afferent firing from the joint. Mechanical hyperalgesia was assessed through day 7 to measure behavioral sensitivity. Dorsal horn neuronal activity, and the spinal expression of glial fibrillary acidic protein (GFAP) and glutamate signaling proteins, including the secondary signaling molecule, ERK1/2, the NR1 subunit of NMDA glutamate receptors, the metabotropic glutamate receptor mGluR5, and astrocytic glutamate transporters GLAST and GLT-1, were each quantified at day 7 to evaluate the development of, and mechanisms that may promote, spinal hyperexcitability. Studies also evaluated the importance of the timing of peripheral

intervention after painful facet joint injury by transiently blocking joint afferent firing at times throughout the development of spinal hyperexcitability, and subsequently measuring behavioral sensitivity and spinal hyperexcitability at day 7.

4.2. Background

The cervical facet joints are at risk for injury during abnormal neck motions and have been implicated as a source of pain in up to 60% of chronic neck pain cases (Barnsley et al., 1995; Lord et al., 1996; Manchikanti et al., 2004). Current treatments for facet joint-mediated pain include intra-articular injection of analgesics or corticosteroids, and nerve block or radiofrequency neurotomy of the medial branches of the dorsal ramus that innervates the joint (Barnsley and Bogduk, 1993; Lander, 2007; Lord et al., 1996b; Manchikanti et al., 2008). Although these treatments can provide relief in some patients, that relief is often only temporary. It is unclear whether the effectiveness of local interventions for spinal joint pain depends on the timing of the treatment relative to the traumatic event and/or the onset of pain, or the development of spinal modifications that enhance neuronal excitability and amplify nociception.

Interrupting the neuronal signals that initiate central sensitization has been a focus of therapeutic approaches to preemptively reduce postoperative pain (Chen et al., 2014; Wei et al., 2013; Woolf and Chong, 1993), and to alleviate neuropathic pain following nerve injury (Seltzer et al., 1991a; Xie et al., 2005). For nerve injury, early intervention blocking discharge from the injured fibers is more effective for reducing or preventing neuropathic pain than treatments initiated after central sensitization has already

developed (Araujo et al., 2003; Gonzales-Darder et al., 1986; Seltzer et al., 1991a; Seltzer et al., 1991b; Shankarrapa et al., 2012; Xie et al., 2005). Although injury to the cervical facet joint and its capsule is primarily a ligamentous injury, the facet capsule *is* innervated with primary afferent fibers that exhibit signs of secondary damage after excessive loading of the facet joint (Chen et al., 2006; Kallakuri et al., 2008; Kras et al., 2013a; McLain, 1994; Yamashita et al., 1990). Evidence of axonal damage in the facet capsule suggests that the pain after facet joint injury is due, at least in part, to neuropathic mechanisms. In fact, capsule stretch in a caprine model of facet joint distraction induces transient increases in the firing of afferents that innervate the facet capsule, similar to the increases in afferent firing that accompany nerve injury (Chen et al., 2006; Kallakuri et al., 2008; Lu et al., 2005a). Painful facet joint injury also leads to the development of ectopic firing and hyperexcitability in dorsal horn neurons (Crosby et al., 2013; Quinn et al., 2010b). Despite evidence of enhanced facet capsule afferent activity and spinal neuronal hyperexcitability after joint injury, the temporal relationship between capsule afferent activity, spinal hyperexcitability, and pain after mechanical facet joint injury has not been defined and could help to inform timing of effective treatments.

Potentiation of excitatory glutamatergic signaling in the dorsal horn can contribute to the spinal hyperexcitability that is associated with central sensitization (Latremoliere and Woolf, 2009). Glutamate signaling from primary afferents activates both ionotropic (i.e., AMPA, NMDA) and metabotropic (i.e., mGluR1-5) receptors at excitatory synapses in the dorsal horn (Yaksh, 2006). Increases in afferent input to the dorsal horn can overstimulate glutamate receptors, especially NMDA receptors and mGluR5, whose activation causes increases in intracellular calcium concentrations

(Latremoliere and Woolf, 2009; Petrenko et al., 2003). Activation of calcium-dependent secondary signaling molecules like PKC and ERK1/2 can then lead to further potentiation of NMDA receptor activity, including phosphorylation of the NR1 subunit (pNR1), and changes in the expression of proteins like mGluR5 that can enhance dorsal horn neuronal excitability (Kawasaki et al., 2004; Ultenius et al., 2006). Glutamatergic signaling is normally regulated by astrocytic and neuronal transporters that remove glutamate from the synapse and prevent overstimulation of glutamate receptors (Danbolt, 2001; Liaw et al., 2005). However, downregulation of the astrocytic glutamate transporters, GLAST and GLT1, in the dorsal horn can prevent clearance of synaptic glutamate, and contributes to the persistent behavioral sensitivity that is evident after nerve injury (Sung et al., 2003; Xin et al., 2009). Some modifications in glutamatergic signaling have been measured in the dorsal horn after painful facet joint injury, including upregulation of mGluR5 and PKC (Dong et al., 2012; Dong and Winkelstein, 2010; Weisshaar et al., 2010). However, the roles of many glutamatergic signaling proteins that play important roles in central sensitization have not been studied in the context of facet joint injury, including activation of the secondary signaling molecule ERK1/2, phosphorylation of NMDA-NR1, and the expression of the astrocytic glutamate transporters GLAST and GLT1. Furthermore, the role of afferent discharge from the facet joint in the potentiation of spinal glutamatergic signaling after painful joint injury has not been evaluated.

These studies investigate the role of afferent activity from the facet joint in inducing behavioral sensitivity and spinal modifications indicative of central sensitization in a rat model of facet capsule trauma. It was hypothesized that the afferent activity from the facet joint capsule that occurs early after joint injury is critical for initiating spinal

hyperexcitability, and that quieting peripheral inputs from the joints *after* hyperexcitability is established is ineffective at attenuating central sensitization. To test these hypotheses, painful facet capsule stretch was imposed followed by intra-articular injection of bupivacaine at two times after injury, in separate groups – immediately after capsule stretch and at day 4, after spinal hyperexcitability is established (see Chapter 3) (Crosby et al., 2013). Behavioral sensitivity was measured through day 7 and then evoked activity was recorded from dorsal horn neurons to assess neuronal excitability. Spinal expression of ERK, pERK1/2, NR1, pNR1, mGluR5, GLAST, and GLT1 were quantified to determine the role of afferent activity in potentiating glutamatergic signaling and in enhancing neuronal excitability in the dorsal horn. Glial activation can also contribute to spinal hyperexcitability, so spinal GFAP expression was quantified as an indicator of astrocytic activation (Watkins et al., 2001). Expanding that work in a second study, bupivacaine was administered to quiet joint afferent activity at 4 hours, 8 hours, or 1 day after injury, times throughout the period when spinal hyperexcitability develops (Crosby et al., 2013). Mechanical hyperalgesia was measured through day 7, and dorsal horn neuronal excitability was assessed at day 7 in order to determine the extent to which the timing of afferent inputs modulates the transition to sustained pain.

4.3. Methods

All experimental procedures were approved by the University of Pennsylvania Institutional Animal Care and Use Committee and carried out under the guidelines of the Committee for Research and Ethical Issues of the International Association for the Study

of Pain (Zimmerman, 1983). Male Holtzman rats (395±30g) were housed under USDA- and AAALAC-compliant conditions with free access to food and water.

4.3.1. Facet Joint Injury with Immediate or Delayed Intra-articular Bupivacaine

Separate groups of rats received a bilateral intra-articular injection of bupivacaine either immediately after injury (*inj-BP0h*, n=12) or delayed until day 4 after injury (*inj-BPd4*, n=12). Similarly, separate groups of rats received control injections of the saline vehicle immediately following either the injury (*inj-VEH0h*, n=13) or a sham surgery (*sham-VEH0h*, n=12); as with the delayed bupivacaine treatment, groups also received saline vehicle at day 4 after injury (*inj-VEHd4*, n=11) or sham surgery (*sham-VEHd4*, n=12). Mechanical hyperalgesia was assessed prior to and at days 1, 3, 5, and 7 after surgery, and compared to baseline and between groups using repeated-measures ANOVA with post-hoc Tukey's HSD tests. On day 7, extracellular electrophysiological recordings were acquired from a subset of rats that received intra-articular injections of bupivacaine (*inj-BP0h, inj-BPd4*, n=6 per group) or saline (*inj-VEH0h*, n=7; *sham-VEH0h, inj-VEHd4, sham-VEHd4*, n=6 per group). Spinal cord tissue was collected after electrophysiology for Western blot analysis of ERK, pERK1/2, NR1, pNR1, mGluR5, GLAST, GLT1, and GFAP expression. Spinal cord samples were also collected from the remaining rats (n=5-6 per group) to assess region-specific expression of mGluR5, pNR1, and GFAP by immunohistochemical analysis. Evoked neuronal firing and protein expression were compared between groups for each injection time by ANOVA with a post-hoc Tukey's HSD test.

4.3.2. Painful Facet Joint Capsule Injury

The surgical methods used to impose painful facet joint injury are detailed in Section 3.3.1 of Chapter 3, and have been previously described (Dong and Winkelstein, 2010; Lee et al., 2004a). Rats were anesthetized with isoflurane (4% induction, 2-3% maintenance) and placed in a prone position. An incision was made along the midline of the back of the neck to expose and separate the paraspinal musculature. The bilateral vertebral laminae and facet joints from C5 to T1 were exposed, the soft tissue was resected, and the interspinous ligaments cut to enable attachment of the C6 and C7 vertebrae to a custom loading device (Dong and Winkelstein, 2010; Lee et al., 2004a). The C6 vertebra was distracted 0.7mm rostrally while the C7 vertebra was held fixed to stretch the facet capsules across the bilateral C6/C7 joints (Dong and Winkelstein, 2010). Beads were placed on the C6 and C7 vertebrae and in a grid on the right C6/C7 facet capsule to track motions during the imposed capsule stretch. A Phantom v4.3 CCD camera (Vision Research; Wayne, IN) monitored the bead marker positions, which were used to calculate vertebral and facet capsule displacements, and maximum principal strains on the facet capsule surface during each joint distraction. Separate rats underwent surgical procedures for a sham injury with attachment to the loading device but with no joint distraction applied. Following surgery, incisions were closed using 3-0 polyester suture and surgical staples, and rats were monitored during recovery in room air.

4.3.3. Intra-articular Bupivacaine Injections

Intra-articular injections of 0.5% bupivacaine or 0.9% saline solution were given in a volume of 10μL injected into the left and right facet joints using a 10μL

microsyringe with a 33G beveled needle (Hamilton; Reno, NV). The microsyringe was held in the joint for at least 30 seconds after injection before it was slowly removed in order to prevent fluid leakage from the joint space. For those treatments given immediately after injury, intra-articular injections were administered following the injury or sham facet joint loading, prior to closing the surgical incisions. For the intra-articular injections made on day 4, rats were anesthetized with isoflurane (4% induction, 2-3% maintenance), the paraspinal musculature was separated to re-expose the C6/C7 facet joints and injections were performed as described above. All incisions were closed using 3-0 polyester suture and surgical staples, and rats were monitored during recovery in room air.

4.3.4. Assessment of Mechanical Hyperalgesia

Mechanical hyperalgesia was evaluated in all rats prior to and after injury and/or treatment, using methods described in Section 3.3.2 of Chapter 3 and detailed previously (Dong et al., 2012; Kras et al., 2013b). A series of weighted von Frey filaments was applied to the left and right forepaws in increasing weight (1.4, 2, 4, 6, 8, 10, 15, and 26g). Each filament was applied five times. If a rat responded to two consecutive filament weights by withdrawing, licking, or shaking the forepaw, the lower of those filament weights was recorded as the paw withdrawal threshold, with a maximum threshold of 26g. Testing was repeated in three rounds and the average of all rounds was calculated for each rat, by averaging the left and right paw withdrawal thresholds (mean±SD) (Dong et al., 2012; Kras et al., 2013b).

4.3.5. Spinal Cord Electrophysiology and Analysis of Neuronal Excitability

Electrophysiological recordings were acquired on day 7 after painful facet joint injury, using methods described in Section 3.3.3 of Chapter 3. Briefly, rats were anesthetized with sodium pentobarbital (45mg/kg, i.p.) and given supplementary doses (5-10mg/kg, i.p.) as needed based on toe pinch reflexes. The C6/C7 spinal cord was exposed by performing a bilateral laminectomy and dural resection, and the rat was immobilized on a stereotaxic frame (David Kopf Instruments; Tujunga, CA). Extracellular potentials were recorded using carbon fiber electrodes (Carbostar-1; Kation Scientific; Minneapolis, MN). Potentials were amplified with a gain of 10^3 and conditioned using a bandpass filter between 0.3kHz and 3kHz (World Precision Instruments; Sarasota, FL) and a 60Hz HumBug adaptive filter (Quest Scientific; North Vancouver, BC). Signals were then digitally sampled at 25kHz (Micro1401, CED; Cambridge, UK), and monitored with a speaker for audio feedback (A-M Systems; Carlsborg, WA).

The electrode was lowered by a micropositioner (Narishige; Tokyo, Japan) into the spinal dorsal horn by entering the pial surface of the C6 or C7 spinal cord. Neurons were selected for recording if they were responsive to mechanical stimulation of the forepaw by brushing with a cotton swab (Christensen and Hulsebosch, 1997; Crosby et al., 2013; Quinn et al., 2010b). Once selected, a neuron was mechanically stimulated at the forepaw with a series of non-noxious and noxious stimuli, including a two-second baseline period before each stimulus, ten seconds of light brushing, five consecutive one-second stimulations at one-second intervals with a series of von Frey filaments (1.4, 4, 10, and 26g), and concluding with ten seconds of noxious pinch with a 60g vascular clip

(Crosby et al., 2013; Hains et al., 2003a; Quinn et al., 2010b). Each stimulus was separated by at least 30 seconds to prevent wind-up of mechanically sensitive neurons, which is a progressive increase in dorsal horn neuronal firing in response to repetitive stimulation of nociceptive afferents (Woolf and Salter, 2000). The von Frey filaments were chosen to represent the range of stimuli used to evaluate mechanical hyperalgesia and their application was synchronized with the electrophysiological recordings. The spike recording protocol is presented in detail in Appendix A.

Voltage potentials were sorted with Spike2 (CED; Cambridge, UK) to ensure that spikes from only one neuron were considered for each recording site. Evoked firing was counted for a given stimulus (light brush, each von Frey filament, or pinch) by totaling the number of spikes during mechanical stimulation and subtracting spontaneous firing as determined by the firing counted during the preceding two-second baseline period (Hains et al., 2003b). The spike sorting and counting protocol is detailed in Appendix A. The distribution of evoked spike counts was positively skewed, so spike counts for each stimulus were transformed by calculating the $\log_{10}$ of each spike count. Residuals were plotted after transformation to confirm a normal distribution, and subsequent statistical analyses were performed on the log-transformed spike counts. Evoked neuronal firing was compared between the *inj-BP*, *inj-VEH*, and *sham-VEH* groups at each treatment time (immediately or at day 4) by ANOVA with a post-hoc Tukey's HSD test.

4.3.6. Western Blot Analysis of Spinal Cord Tissue

Rats were transcardially perfused with 300mL of chilled phosphate-buffered saline (PBS). The C6/C7 spinal cord tissue was collected and homogenized in lysis buffer

(50mM Tris-HCl, 1% Triton X-100, 150mM NaCl, 1mM EDTA, pH 8.0) with protease and phosphatase inhibitors (Sigma-Aldrich Corp; St. Louis, MO). SDS-PAGE was performed by loading spinal cord protein (50μg per well) onto a polyacrylamide gel (Invitrogen; Carlsbad, CA) and running for 75 minutes at 150V. Protein was transferred to a polyvinylidene difluoride (PVDF) membrane using an iBlot (Invitrogen). Gels were cut into strips for high molecular weight (75-250kDa) or low molecular weight proteins (25-75kDa). Multiple high molecular weight or low molecular weight strips were transferred onto single PVDF membranes to allow synchronous detection of numerous proteins from the same protein samples and comparative analysis across multiple gels that were run simultaneously (Kiyatkin and Aksamitiene, 2009). Membranes were blocked for one hour in 5% dry-milk blocking reagent in Tris-buffered saline (TBS).

The membranes incubated overnight at 4ºC with primary antibodies for the secondary signaling molecule, ERK1/2, as an indicator of neuronal activation (mouse, 1:2000; Cell Signaling; Boston, MA), phosphorylated ERK1/2 (pERK1/2; rabbit, 1:1000; Cell Signaling; Boston, MA), the ionotropic glutamate receptor NMDA subunit, NR1 (rabbit, 1:1000; Millipore; Billerica, MA) and its phosphorylated form (pNR1; rabbit, 1:667; Millipore; Billerica, MA), the metabotropic glutamate receptor mGluR5 (rabbit, 1:1250; Millipore; Billerica, MA), the astrocytic glutamate transporters GLAST (rabbit, 1:2000; Abcam; Cambridge, MA) and GLT1 (rabbit, 1:500, Abcam; Cambridge, MA), glial fibrillary acidic protein for activated astrocytes (GFAP; rabbit, 1:1000; Dako; Carpinteria, CA), or β-tubulin as a protein loading control (mouse, 1:2000; Covance; Princeton, NJ). The PVDF membrane was washed in TBS with 0.1% Tween, followed by two hour incubation at room temperature with IRDye goat anti-mouse 680 and goat anti-

rabbit 800 secondary antibodies (1:10,000; Li-Cor Biosciences; Lincoln, NE). Each membrane was imaged using an Odyssey Imaging System (Li-Cor Biosciences; Lincoln, NE). The fluorescence intensity of each target protein band was analyzed using the Odyssey 2.1 software and normalized to the corresponding β-tubulin fluorescence to control for the amount of protein loaded.

4.3.7. Fluorescent Immunohistochemistry of Spinal Cord Tissue

Rats were transcardially perfused first with 250mL of chilled PBS, then 300mL of 4% paraformaldehyde (PFA). The C6/C7 spinal cord was dissected and removed, post-fixed overnight in 4% PFA, and then submerged in 30% sucrose solution for 5-7 days for cryoprotection. Spinal cords were embedded in OCT medium and frozen, and then 14μm cryosections were mounted on Fisher Superfrost slides. Sections were blocked for two hours at room temperature with 10% normal goat serum with 0.3% Triton-X, and then labeled overnight at 4ºC with primary antibodies for pNR1 (rabbit, 1:500; Abcam; Cambridge, MA), mGluR5 (rabbit, 1:1000; Millipore; Billerica, MA), or GFAP (mouse, 1:500; Millipore; Billerica, MA). Slides were rinsed with PBS and labeled with goat anti-mouse Alexa 488 and goat anti-rabbit Alexa 568 secondary antibodies, then coverslips were mounted with Fluorogel medium (Electron Microscopy Sciences; Hatfield, PA). The spinal dorsal horns were imaged at 200x using an Olympus BX51 microscope, and analyzed using densitometry techniques in a customized MATLAB code (see Appendix E) to quantify the percentage of pNR1-, mGluR5-, or GFAP-positive pixels in each image (Dong et al., 2012; Kras et al., 2014a). The percentage of positive pixels in the

injury groups with vehicle or bupivacaine treatment were normalized to sham values and compared by one-way ANOVA with post-hoc Tukey's HSD test.

4.3.8. Painful Facet Joint Injury with Intra-articular Bupivacaine during the Development of Spinal Hyperexcitability

A separate study was performed to determine if blocking afferent activity at times during the development of spinal sensitization affects the onset of hyperalgesia and spinal neuronal hyperexcitability. Intra-articular bupivacaine injections were used to temporarily quiet facet joint afferent firing in separate groups with injections at additional times early after the injury (4 hours, 8 hours, or day 1). Hyperalgesia and spinal hyperexcitability are first observed 6-24 hours after painful facet joint injury (Crosby et al., 2013), so those bupivacaine treatment times are during the development of sensitivity. Rats underwent painful facet joint capsule injury as described in Section 4.3.3 and received bilateral intra-articular injections of bupivacaine at 4 hours (*inj-BP4h*, n=5), 8 hours (*inj-BP8h*, n=6), or day 1 (*inj-BPd1*, n=6) after injury. Mechanical hyperalgesia was assessed prior to injury and at days 1 and 7 after injury; behavioral responses were compared to pre-injury baseline responses by repeated-measures ANOVA with a post-hoc Tukey's HSD test. On day 7, electrophysiological recordings were made to quantify dorsal horn neuronal activity as described in Section 4.3.6. Evoked neuronal firing was compared between bupivacaine-treated groups by ANOVA with a post-hoc Tukey's HSD test. Behavioral and electrophysiological data from the groups that received intra-articular bupivacaine immediately or at day 4 after injury (see Section 4.3.2) were included in these statistical comparisons to compare the effects of immediate or delayed

bupivacaine to those treatments that occurred at different times throughout the development of spinal hyperexcitability.

4.4. Results

4.4.1. Immediate, but not Delayed, Intra-articular Bupivacaine Attenuates Mechanical Hyperalgesia after Painful Facet Joint Injury

The vertebral distraction, the average distraction across the facet capsule, and the average maximum principal strain in the capsule are not different for any group that received painful facet joint injury (Table 4.1). A detailed report of the mechanical data from the painful joint distraction for each rat can be found in Appendix B. Facet capsule stretch with immediate saline vehicle treatment (*inj-VEH0h*) induces a significant decrease from the baseline paw withdrawal threshold (PWT) ($p<0.027$) on all testing days after injury (Fig. 4.1a). The PWT is not different from baseline on any day after the sham injury with vehicle treatment (*sham-VEH0h)* (Fig. 4.1a). Rats receiving intra-articular bupivacaine immediately after injury (*inj-BP0h*) do not develop sensitivity, with a PWT not different from baseline on any day (Fig. 4.1a). The overall effect of treatment

Table 4.1. Facet joint distraction and capsule mechanical measurements.

	Vertebral Distraction ± SD (mm)	Avg. Capsule Distraction ± SD (mm)	Avg. MPS ± SD (%)
inj-VEH0h	0.75±0.19	0.35±0.08	23.88±9.58
inj-VEHd4	0.70±0.07	0.36±0.07	31.16±8.79
inj-BP0h	0.79±0.19	0.30±0.06	27.50±8.00
inj-BP4h	0.71±0.17	0.35±0.23	31.47±20.10
inj-BP8h	0.70±0.17	0.38±0.12	25.88±6.81
inj-BPd1	0.64±0.17	0.29±0.14	25.72±14.31
inj-BPd4	0.63±0.16	0.31±0.12	24.41±15.14

Avg. = average; MPS = maximum principal strain; SD = standard deviation

is also significant, with PWTs for the *inj-VEH0h* group being lower than those for the *sham-VEH0h* ($p<0.0001$) and *inj-BP0h* groups ($p<0.0001$) (Fig. 4.1a). The behavioral response after either injury or sham with vehicle injection at day 4 is the same as when a vehicle injection is given immediately after injury or sham, respectively. Specifically, the *inj-VEHd4* group exhibits significant decreases in PWT from baseline ($p<0.003$) on all days after injury and PWT remains at baseline levels in the *sham-VEHd4* group (Fig. 4.1b). Unlike the bupivacaine treatment given immediately (Fig. 4.1a), bupivacaine given

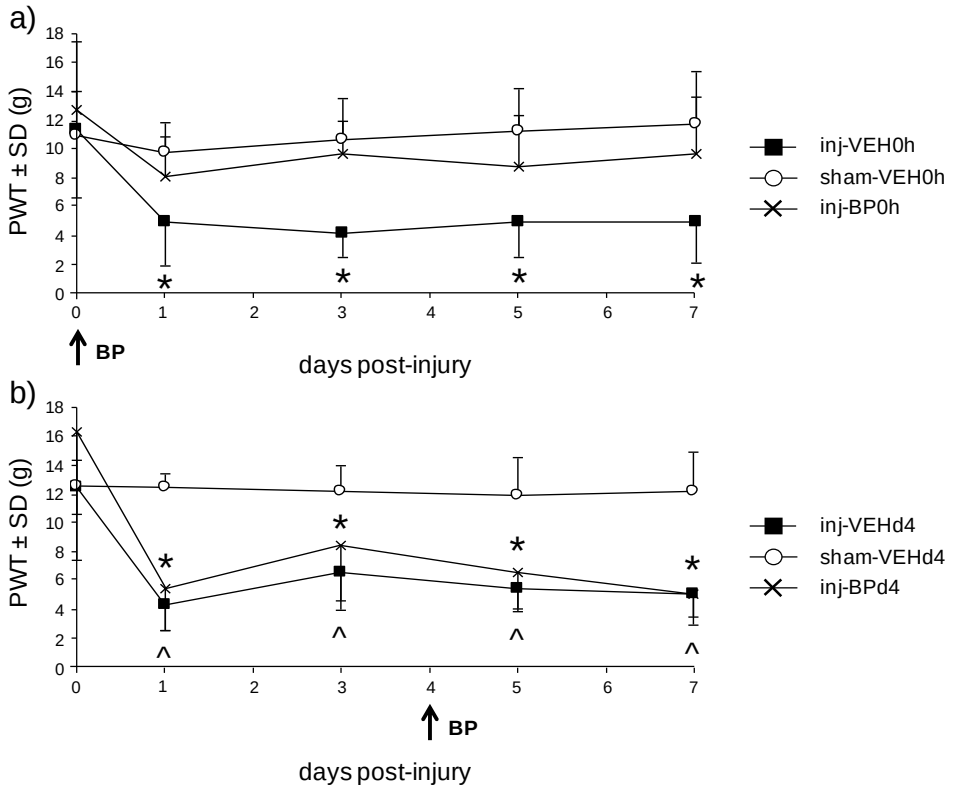

Fig. 4.1. Behavioral sensitivity after intra-articular bupivacaine (BP) given either at injury or 4 days later. **(a)** Paw withdrawal threshold (PWT) decreases from baseline on all days (*$p<0.027$) after injury with immediate intra-articular saline (*inj-VEH0h*), but PWT after bupivacaine treatment at the time of injury (*inj-BP0h*) is not different from baseline on all days, as is observed with sham (*sham-VEH0h*). **(b)** In contrast, intra-articular bupivacaine given at 4 days after injury (*inj-BPd4*) has no effect on PWT, with decreased PWT compared to baseline on all days (*$p<0.003$), similar to the injury with a saline vehicle injection (*inj-VEHd4*) (^$p<0.0001$).

at day 4 after injury (*inj-BPd4*) does not attenuate sensitivity, exhibiting decreases from the baseline PWT on all testing days ($p<0.0001$) (Fig. 4.1b). Furthermore, the PWTs are significantly lower overall for both of the groups receiving treatment on day 4 (*inj-VEHd4*, *inj-BPd4*) relative to *sham-VEHd4* ($p<0.0001$). A summary of the individual paw withdrawal thresholds for each rat on each day is provided in Appendix C.

4.4.2. Dorsal Horn Neuronal Hyperexcitability is Prevented by Immediate Bupivacaine Injection

Neuronal activity in the dorsal horn was recorded from a total of 370 neurons (62±4 neurons per group) at an average depth of 638±177μm below the pial surface. Rats receiving saline vehicle immediately after injury (*inj-VEH0h*) exhibit increases in evoked firing of dorsal horn neurons during light brushing and 4g, 10g, and 26g von Frey filament stimulation, relative to sham ($p<0.026$) (Fig. 4.2). However, immediate bupivacaine treatment (*inj-BP0h*) significantly reduces the number of spikes evoked by light brushing ($p<0.0001$), noxious pinch ($p=0.004$), and all of the different strength von Frey filaments ($p<0.0001$), compared to the *inj-VEH0h* group (Fig. 4.2). Immediate bupivacaine reduces neuronal firing levels below those of the sham group during brush, pinch, and 1.4g von Frey filament stimulation ($p<0.0007$) (Fig. 4.2). Firing is also increased after injury with a day 4 vehicle treatment (*inj-VEHd4*) during all stimuli ($p<0.045$). In contrast to immediate bupivacaine treatment, bupivacaine given 4 days after injury (*inj-BPd4*) does not alter neuronal firing on day 7 from those responses of the matched vehicle group (*inj-VEHd4*) (Fig. 4.2). In fact, evoked firing is increased in the *inj-BPd4* group over sham for all mechanical stimuli ($p<0.035$) (Fig. 4.2). Raw spike

counts for baseline firing, light brush, von Frey filament stimulation, and noxious pinch are detailed in Appendix D for each neuron from each rat.

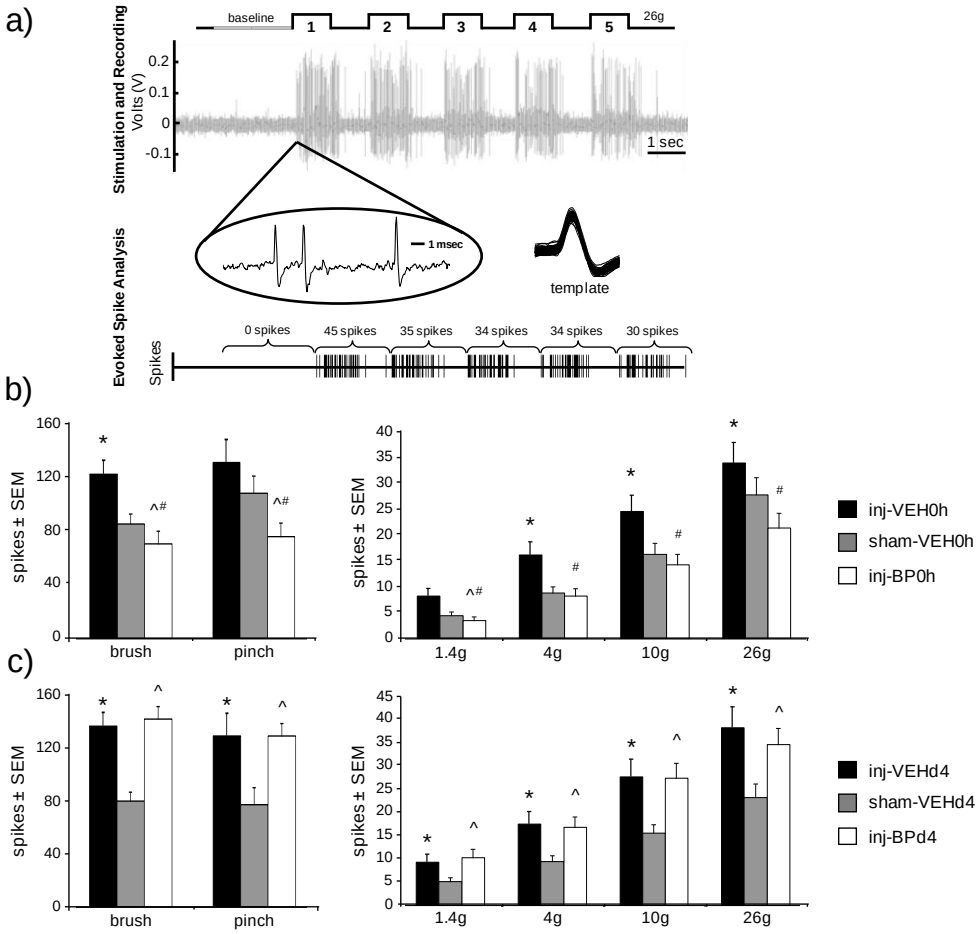

Fig. 4.2. Extracellular spike activity in the spinal dorsal horn 7 days after facet joint injury. **(a)** Traces indicate the filament application, raw extracellular voltage recording, and neuron identification and spike counts. Neuronal firing was sorted and spikes were counted during a baseline period and mechanical stimulation of the forepaw; a representative response to five applications of a 26g von Frey filament 7 days after facet joint injury is shown. **(b)** Firing increases after injury (*inj-VEH0h*) over sham (*sham-VEH0h*) during light brush, 4g, 10g, and 26g von Frey filament stimulation (*$p<0.026$). Immediate bupivacaine attenuates firing in response to all stimuli after injury (#$p\leq0.004$). Bupivacaine treatment (*inj-BP0h*) also reduces activity below that of sham for brush, pinch, and the 1.4g von Frey filament (^$p<0.0007$). **(c)** During all stimuli, for injections at day 4, neuronal firing is increased over sham (*sham-VEHd4*) after injury with either vehicle injection (*inj-VEHd4*) (*$p<0.045$) and after bupivacaine injection (*inj-BPd4*) (^$p<0.035$).

4.4.3. Excitatory Signaling is Modified by Immediate Bupivacaine Injection

Several glutamatergic signaling proteins are increased in the spinal cord at day 7 after painful facet joint injury and are attenuated with immediate bupivacaine administration in the joint (Fig. 4.3). Phosphorylated ERK1/2 ($p<0.012$), pNR1 ($p<0.029$), mGluR5 ($p<0.026$), and GLAST expression ($p<0.023$) all increase after injury, regardless of whether vehicle treatment is given at the time of injury or at day 4 (Fig. 4.3). However, immediate bupivacaine treatment prevents those increases in the expression of pERK1/2, pNR1, mGluR5, and GLAST (Figs. 4.3a and 4.3b), with expression in the *inj-BP0h* group being significantly different for each protein compared to that of the *inj-VEH0h* group ($p<0.029$), and not different from sham levels (Figs. 4.3a and 4.3b). GLT1 expression significantly decreases after injury with vehicle injection either immediately ($p=0.032$) or at day 4 ($p=0.0001$). Immediate bupivacaine treatment also prevents the decrease in GLT1, with expression significantly higher than the *inj-VEH0h* group ($p=0.049$) and not different from sham. Bupivacaine administered at day 4 after injury does not prevent the increases in pERK1/2 ($p=0.048$), pNR1 ($p=0.034$), mGluR5 ($p=0.0003$), and GLAST ($p=0.0006$), or the decrease in GLT1 ($p=0.0001$), that are typically evident over sham (Figs. 4.3c and 4.3d). Total ERK1/2 and NR1 protein levels are not different from sham in any injury or treatment group. Spinal cord protein levels quantified by Western blot are detailed for each rat in Appendix F.

GFAP expression, unlike the other proteins quantified in this study that are involved in excitatory signaling, is not attenuated by immediate bupivacaine treatment (Fig. 4.3). In fact, GFAP significantly increases over sham after injury with immediate vehicle injection ($p=0.002$), and is similarly increased even after immediate bupivacaine

treatment (p=0.006) (Fig. 4.3a). For vehicle treatment given at day 4, GFAP expression is increased over sham (p=0.046), but is not different from sham levels with bupivacaine treatment given at day 4 (Fig. 4.3c).

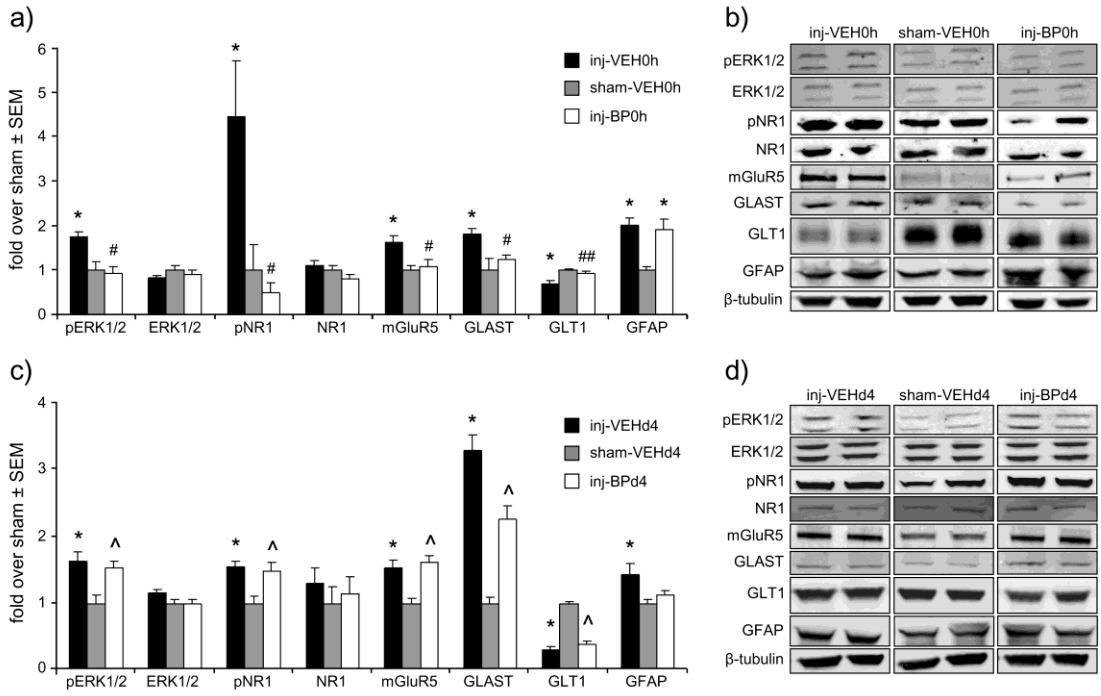

Fig. 4.3. Western blot of spinal cord at day 7. **(a,b)** Facet joint injury (*inj-VEH0h*) increases pERK1/2, pNR1, mGluR5, GLAST and GFAP, and decreases expression of GLT1 (*p≤0.032). Immediate bupivacaine treatment (*inj-BP0h*) prevents such increases, with significantly lower expression (#p<0.029) of pERK1/2, pNR1, mGluR5, and GLAST than *inj-VEH0h* and no differences from sham (*sham-VEH0h*). Immediate bupivacaine also prevents the decrease in GLT1 expression that is evident after injury (##p=0.049). However, GFAP expression remains significantly elevated over sham (*) and is not different from the *inj-VEH0h* group. **(c,d)** Injury with vehicle treatment at day 4 (*inj-VEHd4*) induces the same changes relative to sham as does injury with vehicle treatment at the time of injury (*inj-VEH0h*) (*p≤0.046). However, pERK1/2, pNR1, mGluR5, GLT1, and GLAST remain at injury levels with bupivacaine treatment at day 4 (*inj-BPd4*), and are significantly elevated over sham (^p≤0.048). Total ERK1/2 and NR1 expression is unchanged in all groups.

Increases in pNR1 and mGluR5 occur in the superficial dorsal horn after painful facet joint injury with vehicle treatment immediately after injury (p≤0.046) (Fig. 4.4).

Likewise, increases in pNR1, mGluR5, and GFAP are localized to the superficial dorsal horn after painful injury with vehicle treatment at day 4 ($p \leq 0.003$) (Fig. 4.4). Immediate bupivacaine treatment decreases dorsal horn expression of pNR1 and mGluR5 to sham levels ($p < 0.0001$), but treatment at day 4 does not alter the injury-induced increases in pNR1 and mGluR5 ($p \leq 0.0009$) (Fig. 4.4). GFAP labeling remains elevated over sham when injury is followed by immediate ($p < 0.0001$) or day 4 ($p = 0.024$) bupivacaine treatment (Fig. 4.4). Densitometry quantifications of immunolabeling in the spinal cord for each rat are detailed in Appendix G.

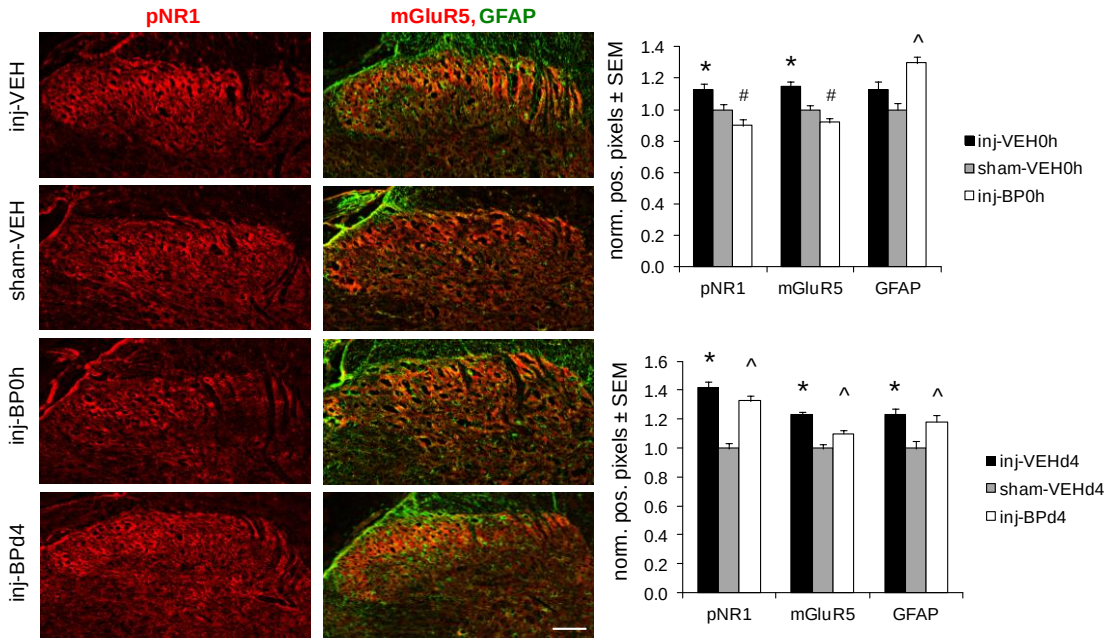

Fig. 4.4. Immunolabeling of phosphorylated NR1 (pNR1), mGluR5, and GFAP in the spinal dorsal horn. Representative images of **(a-d)** pNR1 (red) and **(e-h)** mGluR5 (red) and GFAP (green) after injury, sham, and injury with immediate or day 4 bupivacaine treatment. **(i)** The percentage of pNR1- and mGluR5-positive pixels increases in the dorsal horn after injury with immediate vehicle treatment (*inj-VEH0h*) (*$p \leq 0.046$). Immediate bupivacaine treatment (*inj-BP0h*) prevents increases in pNR1 and mGluR5 (#$p < 0.0001$), but GFAP remains increased (^$p < 0.0001$). **(j)** The percentages of pNR1-, mGluR5-, and GFAP-positive pixels increase after injury with day 4 vehicle treatment, relative to sham levels (*$p \leq 0.003$). However, delayed bupivacaine (*inj-BPd4*) does not prevent the increases in pNR1, mGluR5, and GFAP (^$p \leq 0.024$). Scale bar=100µm.

4.4.4. Intra-articular Bupivacaine within 8 Hours after Injury Attenuates Hyperalgesia and Spinal Hyperexcitability

Bupivacaine treatment administered 4 hours after painful facet joint injury prevents the development of mechanical hyperalgesia. Paw withdrawal thresholds at day 1 and day 7 are not different from baseline when rats receive intra-articular bupivacaine up to 4 hours after injury (Fig. 4.5); this is consistent with the PWT responses of the group receiving bupivacaine treatment immediately after injury in the first study (Figs. 4.1a and 4.5). However, paw withdrawal thresholds decrease from baseline values on both day 1 ($p<0.006$) and day 7 ($p<0.0002$) if intra-articular bupivacaine is given at either 8 hours or 1 day after painful facet joint injury (Fig. 4.5). That finding is similar to the PWT pattern for the group with bupivacaine treatment at day 4 after injury (*inj-BPd4*) (Figs. 4.1b and 4.5).

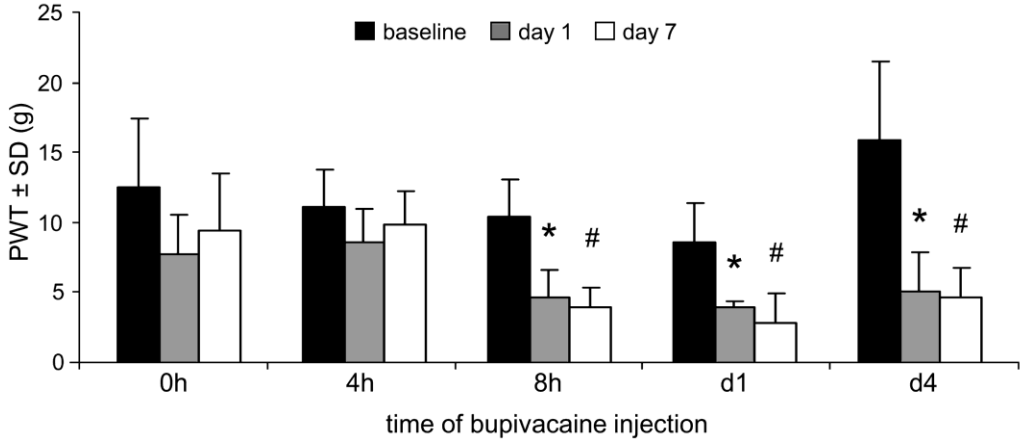

Fig. 4.5. Hyperalgesia after bupivacaine administered during spinal sensitization onset. Bupivacaine administered immediately (0h) or 4 hours (4h) after facet joint injury prevents any change from baseline paw withdrawal threshold (PWT) at day 1 and day 7 after injury. However, when bupivacaine treatment is given at 8 hours (8h), day 1 (d1), or day 4 (d4) after the injury, PWTs are significantly decreased from baseline levels on day 1 (*$p<0.006$) and day 7 (#$p<0.0002$).

Evoked firing in dorsal horn neurons on day 7 exhibits the same general pattern as the behavioral responses (Figs. 4.5 and 4.6), with attenuation of firing by intra-articular bupivacaine injections that are given before 8 hours. Firing evoked by light brushing is significantly lower in the *inj-BP0h* ($p<0.0001$) and *inj-BP4h* ($p<0.0001$) groups than in the groups receiving bupivacaine at later time points (*inj-BP8h*, *inj-BPd1*, *inj-BPd4*) (Fig. 4.6). The evoked neuronal response to noxious pinch is lower in the groups receiving bupivacaine immediately ($p<0.0001$), 4 hours ($p<0.002$), or 4 days after injury ($p<0.018$) than in either of the groups receiving intra-articular injections at either 8 hours or 1 day. Neuronal firing evoked by any of the von Frey filaments is also significantly lower after bupivacaine treatments given immediately after injury ($p<0.0001$) or 4 hours later ($p<0.045$) compared to the firing evoked in the groups receiving bupivacaine injection at later times: 8 hours, day 1, or day 4 post-injury (Fig. 4.6). Immediate bupivacaine administration does attenuate firing significantly more than the 4 hour treatment at each von Frey filament strength ($p<0.0001$). In addition, firing is significantly greater in the group receiving bupivacaine at 8 hours after injury compared to those groups with treatment at day 1 and day 4 after injury, for stimulation with isolated filament strengths (Fig. 4.6b).

4.5. Discussion

Behavioral sensitivity and dorsal horn neuronal excitability are induced within hours after painful facet joint injury by afferent activity from the injured joint (Figs. 4.1 and 4.2) (Crosby et al., 2013). The fast-acting anesthetic, bupivacaine, given in the facet

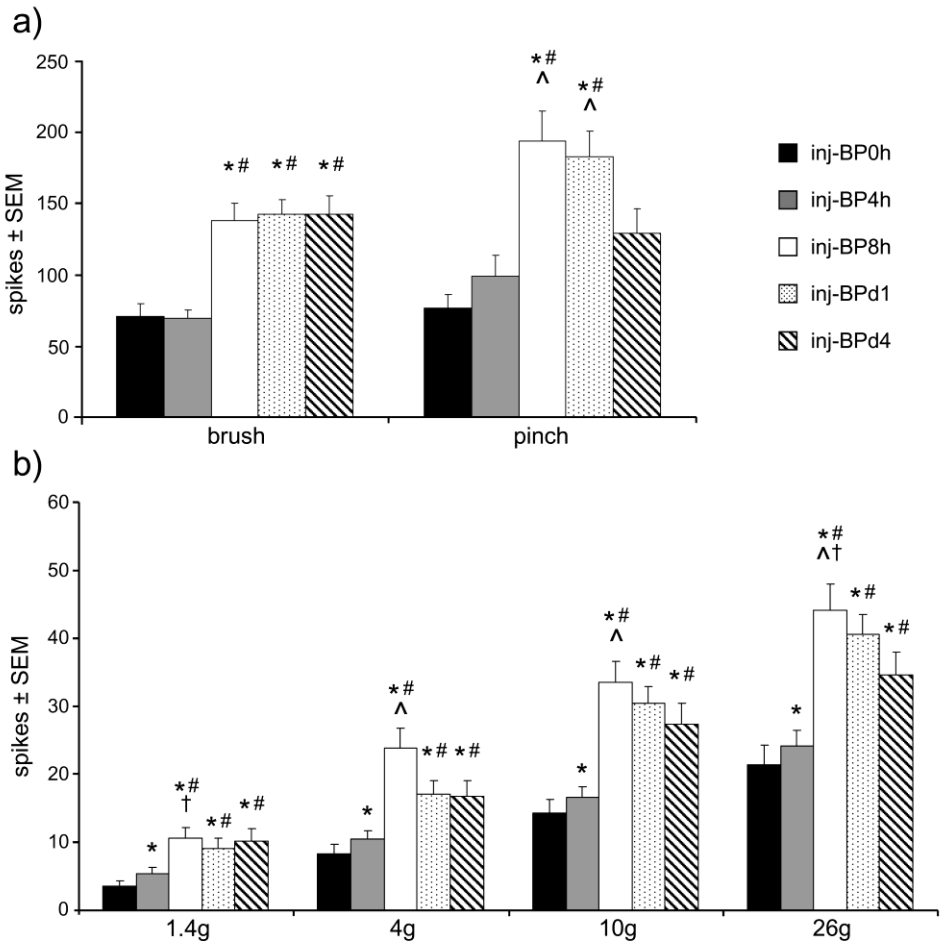

Fig. 4.6. Evoked spike activity in the dorsal horn after painful facet joint injury varies with timing of intra-articular bupivacaine. **(a)** Neuronal firing evoked by light brush is significantly higher when bupivacaine is administered at times later than 4 hours after injury than when it is given immediately (*inj-BP0h*) (*p<0.0001) or at 4 hours (*inj-BP4h*) (#p<0.0001). Firing during a noxious pinch is increased in the *inj-BP8h* and *inj-BPd1* groups compared to the *inj-BP0h* (*p<0.0001), *inj-BP4h* (#p<0.002), and *inj-BPd4* (^p<0.018) groups. **(b)** Similarly, firing evoked by stimulation by all of the magnitudes of von Frey filaments is significantly greater when bupivacaine is administered 8 hours (*inj-BP8h*), 1 day (*inj-BPd1*), or 4 days after injury (*inj-BPd4*) than when it is given immediately (*inj-BP0h*) (*p<0.0001) or at 4 hours (*inj-BP4h*) (#p<0.045). Firing is also greater after treatment given at 4 hours (*inj-BP4h*) than it is when given at the time of injury (*inj-BP0h*) for all von Frey filament stimuli (*p<0.0001). There is also significantly more evoked firing in the *inj-BP8h* group than the *inj-BPd1* group for stimulation by the 1.4g and 26g filaments (†p<0.0003) and the *inj-BPd4* group for the 4g, 10g, and 26 filaments (^p<0.0001).

joint immediately after painful facet joint injury prevents the development of behavioral sensitivity (Fig. 4.1). Immediate bupivacaine treatment also reduces neuronal hyperexcitability and potentiation of excitatory glutamate signaling in the dorsal horn at day 7 (Figs. 4.2-4.4). The same attenuation of behavioral sensitivity and evoked dorsal horn neuronal firing is measured after intra-articular bupivacaine given at 4 hours after injury, but is not observed with later treatment times (Figs. 4.5 and 4.6). Systemic infusion of corticosteroids given at up to 8 hours after a motor vehicle collision reduces patient disability and chronic pain from whiplash-associated disorders (Pettersson et al., 1998), but this report is the first to our knowledge that utilizes peripheral joint injections in a controlled study in which the time after injury is known. Understanding the timing of the sequelae leading from facet joint injury to spinal hyperexcitability is important for the development of more effective treatments for facet joint pain. Indeed, the findings in this study support the notion that joint afferent fiber blocks must be given within a tightly regulated temporal window with respect to the development of spinal hyperexcitability in order to prevent the transition to persistent pain.

Intra-articular bupivacaine given at the time of facet joint injury that is known to cause pain prevents both the onset of mechanical hyperalgesia and dorsal horn neuronal hyperexcitability on day 7 (Figs. 4.1 and 4.2), suggesting that afferent inputs from the injured joint immediately after capsule loading are *critical* to induce sustained central sensitization. The painful joint injury used in this model induces joint capsular strains with the same magnitude as those strains that increase firing and afterdischarge for up to 30 minutes in unmyelinated C fibers that innervate the capsule (Chen et al., 2006; Lee et al., 2004a; Lu et al., 2005a). Stimulation of primary afferent C fibers is sufficient to

induce hyperexcitability of second-order dorsal horn neurons that long-outlasts their initial stimulation (Cook et al., 1987; Wall and Woolf, 1986). Furthermore, both capsule transection before injury that removes any local loading in the capsule (Winkelstein and Santos, 2008), and selective chemical ablation of spinal C fiber populations prior to painful facet joint injury (Weisshaar and Winkelstein, 2014), each prevent the development of behavioral sensitivity. So, C fiber afferents in the facet joint and its capsule likely play an important role in transducing mechanical loading of that joint's capsule into nociceptive signals that regulate spinal sensitization. However, in addition to C fibers, Aβ and Aδ fibers have also been shown to innervate the facet joint (Kallakuri et al., 2004; Kras et al., 2013a; McLain, 1994; Yamashita et al., 1990). Bupivacaine does not selectively act on C fibers (Gissen et al., 1982; Tabatabai and Booth, 1990), so the effects of intra-articular bupivacaine on the development of spinal hyperexcitability in this study cannot be attributed solely to the block of firing in any specific subpopulation of primary afferents. A fibers and C fibers are believed to have distinct contributions to the temporal development of central sensitization after nerve injury (Devor, 2009), so understanding the specific roles of Aβ, Aδ, and C fibers in the mechanotransduction of noxious facet joint loading and the induction of persistent facet-mediated pain will be critical for effective timing and targeting of analgesic treatments.

Early afferent activity from an injured facet joint potentiates excitatory signaling that contributes to dorsal horn neuronal hyperexcitability (Figs. 4.2-4.4). Although this study did not classify the phenotypes of the neurons from which recordings were made, the increased responses to both innocuous and noxious mechanical stimuli (Figs. 4.2 and 4.6) suggests that there is enhanced excitatory signaling at the synapses between the

primary afferents and the wide dynamic range (WDR) neurons that integrate both non-nociceptive and nociceptive signals (Christensen and Hulsebosch, 1997). Peripheral afferent firing due to facet capsule loading may depolarize WDR neurons sufficiently to remove the heavily voltage-dependent magnesium block on ionotropic NMDA glutamate receptors (Dingledine et al., 1999; Mayer et al., 1984). Once NMDA receptors are activated, they allow rapid calcium influx that induces numerous downstream effects leading to neuronal hyperexcitability (Kawasaki et al., 2004; Latremoliere and Woolf, 2009). For example, calcium-dependent activation of the secondary signaling molecule, PKC, can increase NR1 phosphorylation in the dorsal horn after facet injury (Dong et al., 2012; Kawasaki et al., 2004). Activation of NR1, together with the increases in pERK1/2 and mGluR5 that are evident after injury (Figs. 4.3 and 4.4), can further enhance glutamate signaling and neuronal excitability (Brenner et al., 2004; Chen and Huang, 1992; Kawasaki et al., 2004; Latremoliere and Woolf, 2009). Additionally, decreases in spinal GLT1 (Fig. 4.3), the primary transporter responsible for synaptic glutamate uptake, may impair the clearance of glutamate from synapses in the dorsal horn, increasing aberrant excitatory neurotransmission (Danbolt, 2001; Ramos et al., 2010).

Since bupivacaine was used at a 0.5% concentration in the current study, it is expected to have a duration of action lasting for several hours (Dyhre et al., 1997; Klein et al., 1998). Unfortunately, the specific time between 4 hours and 8 hours after injury when joint intervention becomes ineffective is not determined explicitly here since each bupivacaine administration likely blocks afferent activity for several hours. Nonetheless, silencing afferent firing for a period of several hours before the development of spinal plasticity likely returns dorsal horn neurons to their resting membrane potential and

allows NMDA receptors to recover their magnesium block, slowing the influx of calcium and the resulting potentiation of excitatory signaling (Dingledine et al., 1999). In the absence of enhanced glutamatergic signaling, behavioral sensitivity and dorsal horn neuronal hyperexcitability are not evident after facet joint loading that typically induces persistent pain (Figs. 4.1 and 4.2). Therefore, the results in this study support that the potentiation of glutamatergic signaling that is induced by afferent firing after painful facet joint injury plays a key role in the development and maintenance of spinal hyperexcitability.

In contrast to the robust effects of immediate bupivacaine injection, blocking afferent firing with intra-articular bupivacaine at 8 hours or later after painful facet joint loading does not prevent mechanical hyperalgesia or spinal hyperexcitability (Figs. 4.1-4.6). This suggests that once spinal hyperexcitability has developed after facet joint loading, that hyperexcitability remains even without continued peripheral input from the joint. After central sensitization is induced, lower levels of activity, like ectopic firing in injured nerve fibers, are sufficient to maintain sensitization (Devor, 2009; Koltzenburg et al., 1992). In the absence of continuing input to the spinal cord, allodynia and spontaneous pain can diminish, but those behavioral hallmarks of central sensitization return with the re-establishment of ectopic activity (Gracely et al., 1992; Xie et al., 2005). Despite being ineffective for reducing behavioral sensitivity (Fig. 4.1), bupivacaine given at day 4 does reduce spinal neuronal firing compared to both the 8 hour and/or 1 day treatment times, especially in response to noxious mechanical stimuli (Fig. 4.6). It is possible that the partial attenuation of spinal hyperexcitability after bupivacaine treatment at day 4 is due to the effect of transiently eliminating ectopic activity from injured

primary afferents just three days before the electrophysiological recordings were made. Groups receiving bupivacaine treatment at 8 hours or 1 day may experience the same transient reduction of spinal hyperexcitability, but hyperexcitability likely redevelops fully in the 6-7 days prior to electrophysiological recordings. Studies measuring hyperalgesia and dorsal horn neuronal activity for extended post-treatment periods would better assess the persistence of hyperexcitability after delayed bupivacaine treatment.

Mechanical hyperalgesia (Fig. 4.1b), dorsal horn neuronal firing (Fig. 4.2c), and spinal expression of excitatory signaling proteins (Fig. 4.3b) after bupivacaine treatment at day 4 all remain elevated over sham responses at day 7. Those increases over sham suggest that, despite lower neuronal firing after bupivacaine treatment at day 4 relative to bupivacaine treatment at 8 hours or day 1 (Fig. 4.6), none of those delayed treatments fully attenuate central sensitization. The timing of peripheral intervention is an important consideration for the treatment of neuropathic pain and the preemptive treatment of postoperative pain (Seltzer et al., 1991a; Shankarappa et al., 2012; Woolf and Chong, 1993). This study shows that, as with neuropathic injury, early intervention is also critical for preventing the transition to persistent centrally-mediated pain for other types of traumatic injury, including mechanical joint loading, for which the timing of treatment after injury has rarely been considered.

The differential effects of early (immediate or 4 hour) and delayed (8 hour, 1 day, or 4 days) silencing of afferent activity after facet injury (Figs. 4.5 and 4.6) suggest that there is a critical period lasting several hours after injury during which inputs from the joint are necessary to initiate central sensitization. That timing identified in the rodent should not necessarily be taken as directly translating to that in the human due to lifespan

differences between species. In adulthood, each day for a rat corresponds to roughly 30 days for a human, leading to difficulties in defining conditions in the rat as being "chronic" and in translating rodent models of persistent pain to analogous chronic human conditions (Sengupta, 2013). Nevertheless, studies in humans have reported that systemic infusion of corticosteroids up to 8 hours after neck trauma significantly reduces chronic pain and the incidence of disability 6 months after injury (Pettersson et al., 1998). The reduction of pain by early intervention in humans supports the relevance of the current findings in a rat model showing that that analgesic joint intervention occurring up to 8 hours after painful facet joint injury prevents the development of persistent pain.

Central hypersensitivity is maintained, in part, by nociceptive input to the spinal cord (Herren-Gerber et al., 2004), but many studies also suggest that aberrant spontaneous activity from injured afferent fibers is important for the maintenance of central sensitization (Crosby et al., 2013; Devor, 2009; Djouhri et al., 2006). Pharmacological treatments to suppress aberrant spontaneous activity can transiently reduce behavioral sensitivity, but ectopic discharge from injured afferents resumes and restores sensitivity as the effects of the treatment diminish (Liu et al., 2000; Xie et al., 2005). The critical period for facet joint intervention in this study corresponds to the time before ectopic afferent activity develops, which occurs between 6 and 24 hours after painful facet injury in the rat (Crosby et al., 2013). As such, the onset of spontaneous firing from injured primary afferent fibers likely represents a temporal threshold after which sensitization persists despite blockade of joint afferent activity with nerve blocks or neurotomy (Lord et al., 1996; Manchikanti et al., 2008).

The results of this study are consistent with previous reports of pain attenuation by anesthetic treatment administered early after nerve injury, before the onset of ectopic activity (Araujo et al., 2003; Lin et al., 2011; Shankarappa et al., 2012; Xie et al., 2005; Zhang et al., 2005). Xie et al. (2005) found that a local nerve block reduces mechanical hypersensitivity in rats when applied immediately after nerve injury and continued for 3-5 days, but not when administered ten days after injury. Although the current findings (Figs. 4.5 and 4.6) support a transition to centrally-mediated responses, after which peripheral nerve block is ineffective, this study used a local, short-duration anesthetic block. It remains unclear whether other clinically-relevant joint interventions or nerve blocks with longer durations of action could be effective at permanently reversing pain hypersensitivity and spinal hyperexcitability after they have already developed. However, clinical studies and data from other models of persistent pain do suggest that delayed treatment is not likely to permanently reverse pain regardless of the treatment mode or its duration of action (Araujo et al., 2003; Manchikanti et al., 2008; Roy et al., 1988; Shankarappa et al., 2012; Xie et al., 2005).

Despite early intra-articular bupivacaine reducing behavioral and spinal neuronal hypersensitivity, spinal GFAP expression at day 7 after painful facet joint injury and immediate bupivacaine treatment remains increased at levels comparable to those after injury and vehicle treatment (Figs. 4.3 and 4.4). Further, the increase in GFAP after painful facet joint injury with immediate bupivacaine treatment is similar to previously reported increases in GFAP in dorsal horn astrocytes after painful facet joint injury alone (Lee et al., 2004a; Weisshaar et al., 2010). These results suggest that spinal glial activation may not be sufficient to induce pain after mechanical joint injury, despite

previous reports that activated astrocytes are a substantial contributor to pathological pain (Watkins et al., 2001). It is possible that the quantification of GFAP in this study is not sufficient to characterize the effects of intra-articular bupivacaine treatment on the *activation* of astrocytes after painful facet injury. For example, astrocyte activation often involves upregulation of a collection of intermediate filaments (IF), including GFAP, vimentin, and nestin, that form an intracellular cytoskeletal network (Pekny and Nilsson, 2005). Early bupivacaine treatment may attenuate the upregulation of vimentin and/or nestin, preventing the expansion of the IF network that is critical for astrocytic activation even without reducing GFAP expression. Future studies could evaluate different hallmarks of astrocyte activation, like vimentin or nestin expression, or the hypertrophy of cellular processes that results from IF upregulation (Pekny and Nilsson, 2005; Watkins et al., 2001), to better characterize the role of astrocytic activation in persistent pain after facet joint injury.

Facet joint loading induces spinal inflammation as early as day 1 after injury (Kras et al., 2014a; Lee et al., 2008), so it is also possible that the astrocytic activation observed even after attenuation of spinal hyperexcitability by early bupivacaine treatment may result from inflammatory signals that are independent of spinal sensitization (Benveniste, 1992). Pro-inflammatory cytokines IL-1 and TNFα promote astrocyte activation (Milligan and Watkins, 2001). Blocking IL-1 or TNFα receptors after painful facet joint injury prevents the upregulation of GFAP, but does not attenuate hyperalgesia (Dong, 2013), further supporting the existence of distinct inflammatory and neuropathic mechanisms after painful facet joint injury. This has significant implications for the

effective treatment of facet joint-mediated pain, since multi-faceted therapies may be necessary to simultaneously address both spinal inflammation and neuropathic pain.

4.6. Conclusions and Integration

The studies in this chapter suggest that silencing afferent activity from the facet joint early after its injury is critical to block the development of spinal sensitization. Local intervention at the facet joint to block afferent activity can prevent spinal hyperexcitability, but only when initiated before the development of spontaneous firing in injured capsule-innervating afferent fibers. Conventional treatments for chronic facet joint pain, including intra-articular anesthetic injections and medial branch nerve ablation, often fail to offer lasting relief from pain symptoms (Lord et al., 1996b; Manchikanti et al., 2008). The findings of the current study suggest reasoning for why it is that such joint interventions have limited success clinically, and indicate that early joint interventions are most effective for the long-term prevention of persistent pain. One clinical study evaluating treatment protocols for whiplash-associated disorders found no difference between treatment at 96 hours (considered to be "early intervention") and treatment at 2 weeks post-injury (Rosenfeld et al., 2000). In another study, despite the onset of symptoms within 24 hours after a motor vehicle accident, patients were considered to be in the acute phase of whiplash-associated pain for up to one month post-injury (Chien et al., 2010). Rather than treating whiplash-associated disorders in a reactionary manner, clinical treatment paradigms may need to evolve as the mechanisms of facet joint injury and joint-mediated pain are better understood. Based on the studies in

this thesis, early intervention should be considered in the first hours following traumatic joint injury in order to more effectively manage, or prevent, chronic joint-mediated pain.

Together, the studies in Chapter 3 and Chapter 4 support the hypothesis in Aim 1 that discharge from afferents innervating the facet joint plays a key role in the development of persistent pain after joint loading. Dorsal horn neuronal hyperexcitability is sustained by dysregulation of excitatory glutamate signaling that potentiates neuronal firing. In addition to the enhancement of excitatory signaling at existing synapses, the development of new synapses in the dorsal horn may further contribute to aberrant nociception by increasing the frequency and/or intensity of excitatory input to nociceptive dorsal horn neurons. It is also possible that increases in synaptic proteins like mGluR5 may be due to an overall increase in synapse number instead of, or in addition to, upregulation at existing synapses. Studies in Chapter 5 evaluate excitatory synaptogenesis as an additional potential mechanism of plasticity in the spinal cord that could promote the hyperexcitability that is observed in this model (Crosby et al., 2013; Crosby et al., 2014a; Quinn et al., 2010b). Given the development of dorsal horn neuronal hyperexcitability after painful facet joint injury, treatments that directly attenuate spinal neuronal activity or modulate the mechanisms that promote dorsal horn neuronal hyperexcitability may attenuate joint pain.

CHAPTER 5

Thrombospondin-4 Induces Excitatory Synaptogenesis and Primes the Spinal Cord for the Development of Sensitization Leading to Pain after Facet Joint Loading

Parts of this chapter were adapted from:

Crosby ND, Zaucke F, Kras JV, Dong L, Luo ZD, Winkelstein BA. Thrombospondin-4 and excitatory synaptogenesis promote spinal sensitization after painful mechanical joint injury. Submitted.

5.1. Overview

Painful facet joint injury induces spinal hyperexcitability that develops within the first day after injury and persists at least through day 7 (Crosby et al., 2013; Quinn et al., 2010b). The changes in dorsal horn neuronal activity that are observed after painful facet joint injury are characteristic of central sensitization, including the development of ectopic activity and increases in evoked firing in response to both non-noxious and noxious mechanical stimuli (Chapters 3 and 4) (Crosby et al., 2013; Crosby et al., 2014a). Spinal hyperexcitability can be maintained by synaptic changes that increase the activity of dorsal horn neurons, including the potentiation of excitatory glutamatergic signaling (Crosby et al., 2014a; Dong and Winkelstein, 2010; Weisshaar et al., 2010). As

demonstrated in Chapter 4, those changes can include increases in the expression and activation of glutamate receptors and decreases in glial glutamate transporter 1 (GLT), the primary transporter responsible for clearing glutamate from synapses to prevent aberrant neurotransmission (Crosby et al., 2014a).

Once spinal hyperexcitability develops, it can be maintained by low levels of afferent activity, causing decreased pain thresholds (i.e., increased sensitivity) that outlast the initial injury (Koltzenburg et al., 1992). The persistence of spinal hyperexcitability may be due, in part, to long-term structural modifications in the spinal cord, including excitatory synaptogenesis, which alter the dorsal horn processing of sensory signals (Jaken et al., 2010; Woolf et al., 1992; Woolf et al., 1995). Synapse densities increase in the dorsal horn after nerve injury in conjunction with the development of allodynia, suggesting that synaptogenesis contributes to neuropathic pain (Chung et al., 1989; Jaken et al., 2010; Peng et al., 2010). However, the spinal signals initiating synaptogenesis remain unclear. Thrombospondin-4 (TSP4) is one member of a family of extracellular matrix proteins that induces synaptogenesis (Christopherson et al., 2005). TSP4 expressed by activated astrocytes has been implicated in the development of neuropathic pain after peripheral nerve injury (Christopherson et al., 2005; Kim et al., 2012; Risher and Eroglu, 2012). Since spinal astrocytic activation has been reported after painful facet joint injury in our model (Lee et al., 2004a; Weisshaar et al., 2010), astrocyte-derived TSP4 may contribute to persistent pain after facet joint injury. However, the roles of TSP4 in synaptogenesis and the development of facet-mediated pain remain unknown.

Blocking facet joint afferent firing immediately after joint distraction reduces the potentiation of glutamatergic signaling, spinal hyperexcitability, and behavioral

sensitivity (Chapter 4) (Crosby et al., 2014a), indicating that many of the spinal modifications that contribute to hyperexcitability are induced by the discharge of nerve fibers that innervate the facet joint. Astrocytic release of TSP-family proteins can be stimulated by ATP (Tran and Neary, 2006), a molecule that acts as a neurotransmitter and contributes to nociception (Burnstock, 2000). It is possible that primary afferent discharge after painful facet joint injury induces TSP4 expression in spinal astrocytes, but the potential role of joint afferent activity in the induction of spinal TSP4 release and TSP4-mediated excitatory synaptogenesis is unknown. In addition to inducing synaptogenesis, TSP4 has also been shown to enhance excitatory neurotransmitter release from presynaptic terminals (Kim et al., 2012). Increased levels of TSP4 in the spinal cord may potentiate the activation of dorsal horn neurons by primary afferent firing, augmenting the effects of noxious peripheral stimuli, like excessive stretch of the facet capsule. However, the effects of increasing the *pre-injury* levels of a spinal molecule like TSP4 that enhances neuronal excitability have not been investigated for facet joint loading. Together, the studies in this chapter address the objectives outlined in Aim 2 to determine whether painful loading of the facet joint induces excitatory synaptogenesis in the spinal dorsal horn, and to evaluate the role of TSP4 in synaptogenesis and the development of persistent pain.

5.2. Background

The cervical facet joints are a common source of chronic pain, and are susceptible to injury during neck trauma and degeneration (Hogg-Johnson et al., 2008). Abnormal motions of the cervical facets can load the joint tissues that are innervated by

mechanoreceptive and nociceptive fibers, including the facet capsular ligament (Pearson et al., 2004; Siegmund et al., 2009). Facet joint loading that produces pain initiates a host of changes in the spinal cord that are characteristic of central sensitization, including hyperexcitability and increased spontaneous activity in dorsal horn neurons (Crosby et al., 2013; Quinn et al., 2010b). Even with this evidence of centrally-mediated pain, local joint injections and radiofrequency neurotomy are used clinically to manage chronic facet joint pain, despite the effectiveness of such local therapies being limited (Boswell et al., 2005). Effective clinical treatment requires a better understanding of the spinal mechanisms contributing to central sensitization from joint pain.

Structural plasticity, including neurite outgrowth and synaptogenesis, is one mechanism by which pain can be maintained through the potentiation of both nociceptive and non-nociceptive pathways (Jaken et al., 2010; Latremoliere and Woolf, 2009; Woolf et al., 1992). Although overall increases in synapse number are observed in the dorsal horn in neuropathic pain states (Jaken et al., 2010; Lin et al., 2011; Peng et al., 2010), the spinal signals initiating synaptogenesis remain unclear. The TSP family of extracellular matrix proteins promotes synaptogenesis (Christopherson et al., 2005; Eroglu et al., 2009; Lo et al., 2011). The thrombospondins are glycoproteins that are produced by numerous cell types and have widely varying roles in cell signaling (Adams, 2001; Adams and Lawler, 2004). For example, platelets, fibroblasts, skeletal muscle, endothelial cells, and astrocytes and neurons in the CNS each express one or more TSP isoform (Adams, 2001; Arber and Caroni, 2004; Christopherson et al., 2005; Stenina et al., 2003). Astrocytic expression of each of the five TSP isoforms has been shown to promote synaptogenesis; retinal ganglion cells treated with TSP1-5 or with astrocyte-conditioned media containing

TSPs develop more synapses than controls using matching isolated cell cultures (Christopherson et al., 2005). Expression of TSPs can be radically altered in pathophysiological conditions (Adams and Lawler, 2004; Chen et al., 2000). In particular, thrombospondin-4 (TSP4) is upregulated in spinal astrocytes following peripheral nerve ligation and enhances excitatory synaptic transmission in the dorsal horn, although TSP1 and TSP2 are unchanged after that injury (Kim et al., 2012). Despite its potential involvement in spinal hyperexcitability that develops with pain from neural trauma, the role of TSP4 in joint-mediated pain and synaptogenesis is unknown.

Given the involvement of TSP4 in neuropathic pain and its potential to induce structural modifications in neurons (Christopherson et al., 2005; Kim et al., 2012), it is hypothesized that TSP4 plays a role in joint-mediated pain by promoting dorsal horn excitatory synaptogenesis following painful facet joint loading. As such, studies in this chapter investigate the role of TSP4 in synaptogenesis and the development and maintenance of persistent pain. Synapses can be quantified in the spinal cord by immunolabeling pre- and post-synaptic markers and identifying their colocalized puncta (Ippolito and Eroglu, 2010). Synapsin is a pre-synaptic protein that regulates neurotransmitter release in synapses throughout the peripheral and central nervous systems (De Camilli et al., 1983), and homer is a structural protein that binds metabotropic glutamate receptors in excitatory post-synaptic terminals (Brakeman et al., 1997); so, the colocalization of synapsin and homer was used to quantify excitatory synapses in the spinal cord at day 7 after painful facet joint loading. To determine whether TSP4 dysregulation may contribute to facet joint-mediated pain, TSP4 protein

levels were quantified by Western blot and immunolabeling in the DRG and spinal cord on day 7 after painful facet joint loading.

In a separate study, antisense oligonucleotides designed against the TSP4 mRNA were delivered intrathecally prior to, and for seven days, after painful facet joint loading in order to block the spinal expression of TSP4 (Fig. 5.1). Behavioral sensitivity was assessed through day 7 and excitatory synapses were quantified in the dorsal horn at day 7 after painful facet joint loading in order to determine whether TSP4 expression is required to induce synaptogenesis and persistent pain. Although TSP4 can induce synaptogenesis, gabapentin blocks the synaptogenic activity of TSP4 by preventing it from binding to its neuronal receptor (Eroglu et al., 2009). As such, in separate rats, intrathecal gabapentin was administered immediately after painful facet joint loading in order to antagonize the synaptogenic activity of TSP4 (Fig. 5.1). Hyperalgesia and excitatory synapses in the dorsal horn were quantified at day 7 in those studies to further evaluate the role of TSP4 in synaptogenesis and persistent pain. Because primary afferent activity after painful facet joint loading has been shown to contribute to spinal hyperexcitability by initiating the potentiation of excitatory signaling in the dorsal horn (Crosby et al., 2014a), a study was performed to determine whether afferent firing from the facet joint also induces TSP4 expression and excitatory synaptogenesis. Joint afferent firing was blocked either immediately, or four days, after painful joint loading using intra-articular injections of bupivacaine (Fig. 5.1), and TSP4 expression and excitatory synapses were quantified in the dorsal spinal cord at day 7. Lastly, to determine whether spinal TSP4 levels facilitate the development of joint-mediated pain, intrathecal TSP4

was administered prior to different severities of facet joint distraction that separately simulate either physiologic or injurious loading of tissues in the joint (Fig. 5.1).

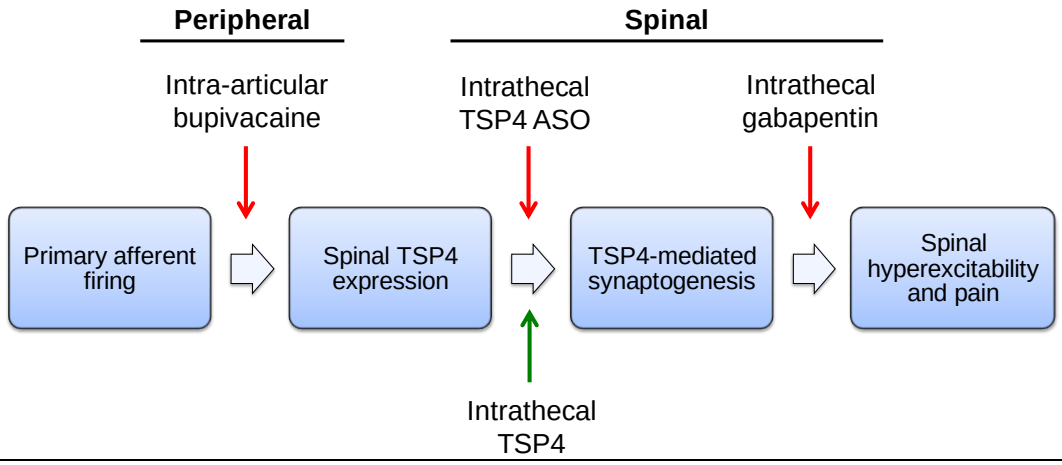

Fig. 5.1. Schematic showing the peripheral and spinal treatments used to evaluate the potential relationships between facet joint loading, spinal TSP4 expression, spinal neuronal sensitization and pain. Studies used treatments to block (red) or augment (green) TSP4 protein levels and activity in the spinal cord. Bupivacaine was administered in the facet joints to block joint afferent firing after facet joint loading. Intrathecal TSP4 antisense oligonucleotides (ASO) and intrathecal TSP4 protein were used to decrease or increase spinal TSP4 levels, respectively. Gabapentin was used intrathecally to block the synaptogenic activity of TSP4.

5.3. Methods

5.3.1. Facet Joint Distraction

All surgical procedures were performed using adult male Holtzman rats (362-464g) under inhalation isoflurane anesthesia (4% induction, 2-3% maintenance). Facet joint loading was performed by distracting the bilateral C6/C7 facet joints, which has been described previously to produce physiologic or injurious tissue loading under different magnitudes of distraction (Dong and Winkelstein, 2010; Lee et al., 2004a; Lee and Winkelstein, 2009). Facet joint distraction was applied using the methods described in detail in Section 3.3.1 of Chapter 3 (Crosby et al., 2013; Crosby et al., 2014a). Briefly,

the C6 and C7 vertebrae were attached to a custom loading device using microforceps and the C6 vertebra was distracted rostrally to stretch the bilateral facet capsules across the C6/C7 joints. In separate rats, distraction of 0.2mm was applied for physiologic loading and 0.7mm distraction was imposed for injurious loading (Dong et al., 2012; Lee and Winkelstein, 2009). Bead markers were placed on the C6 and C7 vertebrae and the right C6/C7 facet capsule to quantify the vertebral and capsule displacements, and the maximum principal strain (MPS) on the facet capsule surface during each applied distraction. Vertebral and capsule distractions and capsule MPS during physiologic and injurious loading were compared using Student's t-tests. Sham surgeries included all of the same procedures with no joint distraction applied in order to control for the effect of the surgical procedures.

5.3.2. Assessment of Mechanical Hyperalgesia

Mechanical hyperalgesia was assessed pre-operatively and on days 1, 3, 5, and 7 after facet joint distraction. Hyperalgesia was measured by quantifying the paw withdrawal threshold (PWT) in the forepaws of each rat during application of a series of von Frey filaments (1.4, 2, 4, 6, 8, 10, 15, and 26g) to the plantar surface of the forepaws (Hubbard and Winkelstein, 2005; Lee and Winkelstein, 2009). Detailed methods for behavioral assessment of mechanical hyperalgesia are presented earlier in Section 3.3.2 of Chapter 3. PWT was compared over time and between groups by repeated-measures ANOVA with a post-hoc Tukey's HSD test.

5.3.3. Western Blot Analysis of DRG and Spinal Cord Tissue

To measure the temporal expression of TSP4 in the DRG and spinal cord, TSP4 was quantified by Western blot on day 1 after sham (n=6) or painful facet joint loading (n=8), or on day 7 after sham (n=8) or painful loading (n=8). Rats were anesthetized with sodium pentobarbital (65mg/kg, i.p.) and transcardially perfused with 300mL of PBS. The C6 DRG and C6/C7 spinal cord were removed and homogenized in lysis buffer containing 50mM Tris HCl (pH 8.0), 1% Triton X-100, 150mM NaCl, 1mM EDTA, and protease and phosphatase inhibitors (Sigma-Aldrich Corp; St. Louis, MO). Protein samples (25μg for DRG, 50μg for spinal cord) were loaded on a polyacrylamide gel for SDS-PAGE (Invitrogen; Carlsbad, CA) and run for 75 minutes at 150V. Protein was transferred to a polyvinylidene difluoride (PVDF) membrane using an iBlot gel transfer device (Invitrogen; Carlsbad, CA). Membranes were blocked for one hour with 5% dry milk blocking reagent in 0.1% Tween-20 Tris-buffered saline (TBS-T) and incubated overnight at 4ºC with rabbit anti-TSP4 (1:1000; Santa Cruz; Dallas, TX) and mouse anti-β-tubulin (1:2000; Covance; Princeton, NJ). The PVDF membranes were washed in TBS-T three times for ten minutes each time, followed by a two-hour incubation at room temperature with goat anti-rabbit 800 and goat anti-mouse 680 IRDye fluorescent secondary antibodies (1:10,000; Li-Cor Biosciences; Lincoln, NE). Membranes were imaged using an Odyssey Imaging System (Li-Cor Biosciences; Lincoln, NE). The fluorescence of each TSP4 band was analyzed using the Odyssey 2.1 software to quantify the intensity of the pixels within the bands and normalized to the corresponding β-tubulin fluorescence as a protein loading control for each sample. TSP4 levels were compared between groups and over time by two-way ANOVA with post-hoc Tukey's HSD test.

5.3.4. Immunolabeling of Spinal Cord Tissue

To quantify the region-specific expression of TSP4, spinal cord sections were immunolabeled for TSP4 on day 7 after sham (n=4) or painful facet joint loading (n=6). Sections were colabeled for GFAP in order to specifically quantify astrocytic TSP4 expression, because spinal TSP4 expression after nerve injury has been shown to be mainly in astrocytes (Kim et al., 2012). Rats were anesthetized with sodium pentobarbital (65mg/kg, i.p.) and transcardially perfused with 250mL of PBS followed by 250mL of 4% paraformaldehyde (PFA). The C6 and C7 spinal cord segments were removed and post-fixed in 4% PFA overnight, then cryopreserved in 30% sucrose in PBS for seven days at 4ºC. Samples were freeze-mounted in OCT medium (Fisher Scientific; Waltham, MA) and axial cryosections (14μm each, 5-6 sections per rat) were mounted on Superfrost Plus slides (Fisher Scientific; Waltham, MA).

Sections were blocked in 10% goat serum in PBS for one hour at room temperature. Sections were then incubated overnight at 4°C with chicken anti-TSP4 (1:1000; from F. Zaucke; Cologne, Germany) and rabbit anti-GFAP (1:500; Dako, Denmark) in 10% goat serum with 0.3% Triton-X PBS. The specificity of the chicken anti-TSP4 antibody was characterized for immunolabeling of rat TSP4 (Fig. 5.2) (Dunkle et al., 2007). Sections were incubated for two hours at room temperature with goat anti-chicken Alexa 488 and goat anti-rabbit Alexa 568 fluorescent secondary antibodies (1:1000, Invitrogen; Carlsbad, CA), and then incubated with DAPI (1:10,000, Invitrogen; Carlsbad, CA) for ten minutes. After rinsing in PBS and deionized water, slides were air-dried and cover slips were applied with Fluorogel mounting medium (EMS; Hatfield, PA). Each tissue section was imaged with using a Zeiss LSM510 confocal microscope.

Separate images of subregions of the spinal cord (superficial dorsal horn, deep dorsal horn, and dorsal columns) were analyzed by densitometry using a MATLAB code (see Appendix E) to quantify the percent of TSP4- or GFAP-positive or colocalized pixels in each dorsal horn region (Dong et al., 2013b; Hubbard et al., 2008).

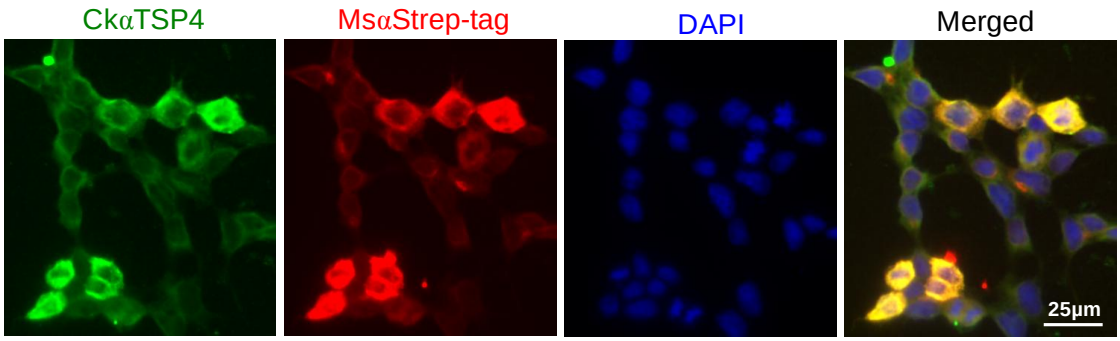

Fig. 5.2. TSP4 antibody specificity. A mouse anti-StrepII antibody (red) was used to label transfected 293/EBNA cells in which all TSP4 protein is tagged with a StrepII peptide. The StrepII antibody detected the StrepII tag on all recombinant TSP4 protein. The cells were colabeled with a chicken anti-rat TSP4 antibody (green) and DAPI. The TSP4 labeling was highly colocalized with the StrepII labeling, indicating that the TSP4 antibody specifically detected recombinant TSP4 in the 293/EBNA cells.

5.3.5. Synapse Quantification in the Dorsal Horn

Spinal cord sections were immunolabeled as described in Section 5.3.4 with mouse anti-synapsin (1:100; Synaptic Systems; Goettingen, Germany) and rabbit anti-homer (1:200; Synaptic Systems; Goettingen, Germany) to quantify synapse densities in the dorsal horn at day 7 after sham (n=4) or painful (n=6) facet joint loading. Because synapsin is a general synaptic marker and homer is a glutamatergic synaptic marker (Brakeman et al., 1997; De Camilli et al., 1983), excitatory synapses were quantified by counting the colocalization of synapsin- and homer-positive puncta. Synapses were quantified using previously published methods (Ippolito and Eroglu, 2010). The detailed protocol for identifying and quantifying synapses is presented in Appendix H. Image

stacks were acquired from the superficial or deep dorsal horn at 0.33μm increments up to 3μm of depth using a Zeiss LSM510 confocal microscope. The maximum intensity projection of each set of three sequential images was used to generate a single image ($0.02mm^2$ tissue area) corresponding to 1μm of tissue depth. The custom MATLAB code used to generate maximum intensity projections is included in Appendix E. Because irregular surface topology of the spinal cord sections and lack of antibody penetration led to large variations in labeling efficiency in the outermost and innermost maximum intensity projections, only the middle projection from each spinal cord section was analyzed, corresponding to tissue at 1-2μm from the surface of each section.

The Puncta Analyzer plugin for ImageJ (National Institutes of Health; Bethesda, MD) was used to identify puncta exhibiting colocalization of synapsin and homer in each maximum intensity projection. The area of the tissue parenchyma, excluding any holes and/or gaps in the tissue sections, was quantified using a custom MATLAB code, which can be found in Appendix E. The number of colocalized puncta in the superficial or deep dorsal horn was normalized to the corresponding tissue area for the image of that dorsal horn region. The synapse number per area was then averaged across all rats in each group and compared between groups using Student's t-test.

5.3.6. Intrathecal Injections

Rats were anesthetized with isoflurane (4% for induction, 2-3% for maintenance) and placed in a prone position. The skin over the dorsal aspect of the lumbar spine was shaved and cleaned with Betadyne solution. A 30-gauge needle attached to a microinjector (Hamilton; Reno, NV) was inserted perpendicular to the spine in the

dorsal-ventral direction, along the midline between the L5 and L6 spinous processes. The needle was angled approximately 30° to the right or left and lowered into the spinal canal between the laminae of the L5 and L6 vertebrae, with placement in the cauda equina confirmed by the presence of a reflexive tail flick or hindpaw flinch. Antisense or mismatch oligonucleotides, gabapentin, saline, recombinant TSP4, or StrepII-tag peptide were administered in single bolus injections (Fig. 5.1). The needle was held in place for 30-60 seconds before removing it in order to prevent leakage of the injected solutions from the lumbar spine. Rats were then monitored during recovery in room air.

5.3.7. Intrathecal Oligonucleotide Treatment

Antisense oligonucleotides were used to block spinal TSP4 expression, as reported previously (Kim et al., 2012). Antisense oligonucleotides were designed against a segment of the TSP4 mRNA using the sequence, CCATCATTGTTGCTATCTTCC, with stabilizing modifications as described previously (Kim et al., 2012). An equal length random sequence of nucleotides, ACCATCGTTGTTACTTTCTCC, was used as a mismatch control for the oligonucleotide treatment. Antisense (75µg/rat/day, n=11) and mismatch (75µg/rat/day, n=12) oligonucleotides were delivered by bolus 25µL intrathecal injections. Injections were administered daily beginning three days before injurious facet joint distraction and continuing for seven days after joint distraction because the effectiveness of previous TSP4 antisense treatments peaked on the third day of repeated injections (Kim et al., 2012). TSP4 expression was quantified by Western blot as described in Section 5.3.3 using fresh spinal cord tissue collected on day 7 after painful facet joint loading (n=5 antisense, n=6 mismatch). Excitatory synapses were

quantified in the dorsal horn as described in Section 5.3.5 using separate spinal cord tissue samples that were also collected as described above on day 7 after joint loading (n=6 antisense, n=6 mismatch).

5.3.8. Intrathecal Gabapentin Treatment

Gabapentin was administered to block TSP4 binding to its neuronal receptor, the α2δ-1 subunit of voltage-gated calcium channels (Eroglu et al., 2009; Luo et al., 2002; Rose and Kam, 2002) to determine if TSP4 induces synaptogenesis after painful facet joint loading by interacting with α2δ-1. Rats received intrathecal injections of gabapentin (*Inj-GBP*, n=6) or a saline vehicle treatment (*Inj-VEH*, n=6) after painful facet joint loading. Gabapentin (4.2μg in 30μL saline) was administered 90 minutes prior to injurious facet joint distraction. A second dose was administered one day after injurious joint distraction, immediately following behavioral assessment on that day. Saline vehicle injections (30μL) were administered under the same paradigm to control for the effects of the intrathecal injections. The gabapentin concentration and treatment times were optimized previously for the attenuation of behavioral sensitivity in dose-response studies (Dong et al., 2013a). Excitatory synapses were quantified as described in Section 5.3.5 using spinal cord tissue samples that were collected on day 7 after painful joint loading.

5.3.9. Intra-articular Bupivacaine Treatment

To evaluate the role of injury-induced joint afferent activity in the induction of spinal TSP4 expression and synaptogenesis, rats received bilateral intra-articular injections of bupivacaine immediately after painful facet joint loading (*Inj-BP0h*, n=6) or

delayed until day 4 after painful joint loading (*Inj-BPd4*, n=6) (Crosby et al., 2014a). Separate groups of rats received control injections of the saline vehicle immediately following a sham surgery (*Sham-VEH0h*, n=6) or a painful joint loading (*Inj-VEH0h*, n=6). As with the delayed bupivacaine treatment, rats also received saline vehicle at day 4 after sham surgery (*Sham-VEHd4*, n=6) or painful joint loading (*Inj-VEHd4*, n=5). Intra-articular injections of 0.5% bupivacaine or 0.9% saline solution were injected into the left and right facet joints in a volume of 10µL using a microsyringe with a 33-gauge beveled needle (Hamilton; Reno, NV). Detailed methods for the immediate or delayed intra-articular injections of bupivacaine or saline are presented in Section 4.3.3 of Chapter 4 (Crosby et al., 2014a). On day 7 after sham or painful joint loading, spinal cord samples were collected to quantify immunolabeling of spinal astrocytic TSP4 and dorsal horn excitatory synapses as described in Sections 5.3.4 and 5.3.5.

5.3.10. Recombinant TSP4 Purification and Intrathecal TSP4 Injections

Full length TSP4 protein was recombinantly expressed in 293/Ebstein-Barr nuclear antigen (EBNA) cells using methods described previously by Hansen et al. (2011) for COMP, another TSP family member. Briefly, 293/EBNA cells were stably transfected with cDNA for rat TSP4 (GenBank accession no. X89963) with a StrepII tag. Cell culture media were collected every other day and stored at -20°C with 1.2mM N-ethylmaleimide (NEM) and 1.2mM phenylmethylsulfonyl fluoride (PMSF) to inhibit protease activity. Secreted TSP4-StrepII protein in the cell media was purified with a Streptactin affinity chromatography column (1.5mL; IBA; Goettingen, Germany), then

concentrated from the elution fractions using Amicon Ultra centrifugal filters with a 50kDa threshold (Millipore; Billerica, MA) and stored at -80°C.

To assess the dose-response of spinal TSP4 and behavioral sensitivity, purified recombinant TSP4 (20, 30, 45, or 60µg/rat) was administered intrathecally in 25µL bolus injections. Based on a previous study showing that hindpaw sensitivity returns to baseline levels by ten days after intrathecal TSP4 treatment (Kim et al., 2012), hyperalgesia in the forepaw was assessed for ten days after TSP4 injection (n=6 rats per group). Intrathecal injection of 60µg StrepII peptide was used to control for the presence of the StrepII tag on recombinant TSP4 protein (n=6). Paw withdrawal thresholds for each group were compared to baseline on each day after TSP4 injection using a repeated-measures ANOVA with a post-hoc Tukey's HSD test.

In separate rats, the effect of increased spinal TSP4 on the development of hyperalgesia after joint loading was tested by intrathecally injecting 20µg or 60µg TSP4 three days before sham, physiologic (Phys), or injurious (Inj) facet joint loading (*20µg TSP4+Sham*, *20µg TSP4+Phys*, *60µg TSP4+Sham*, *60µg TSP4+Phys*, *60µg TSP4+Inj*, n=6-7 per group). Separate rats received 60µg intrathecal injections of StrepII peptide prior to sham or physiologic loading of the facet joint (*60µg StrepII+Sham*, *60µg StrepII+Phys*, n=6 per group) to control for the presence of the StrepII tag on the TSP4 protein. Hyperalgesia was assessed in all rats through day 7 after joint loading, and paw withdrawal thresholds for each group were compared to baseline on each day using a repeated-measures ANOVA with a post-hoc Tukey's HSD test.

5.3.11. Electrophysiological Recording of Spinal Dorsal Horn Neurons

To evaluate the effect of increased spinal TSP4 on the development of neuronal hyperexcitability after facet joint loading, dorsal horn neuronal activity was recorded on day 7 from a subset of rats that received intrathecal TSP4 or StrepII injections prior to joint loading (*60µg StrepII+Sham*, *20µg TSP4+Phys*, *60µg TSP4+Phys*, *60µg TSP4+Inj*, n=6 rats per group). Briefly, using methods detailed in Section 3.3.3 of Chapter 3 (Crosby et al., 2013; Crosby et al., 2014a), rats were anesthetized with sodium pentobarbital (45mg/kg, i.p.) and given supplemental doses (5-10mg/kg, i.p.) as needed based on toe pinch reflexes. A bilateral laminectomy and dural resection were performed to expose the C6/C7 spinal cord. Rats were then immobilized on a stereotaxic frame to stabilize the cervical spine (David Kopf Instruments; Tujunga, CA). Core temperature was maintained at 35-37ºC using a temperature controller with a rectal probe (Physitemp; Clifton, NJ). The exposed spinal cord was bathed in 37ºC mineral oil to prevent drying of the spinal cord.

A carbon fiber electrode (Kation; Minneapolis, MN) was used to record neuronal activity in the C6/C7 spinal dorsal horn. Neurons were mechanically stimulated at the forepaw with ten seconds of light brushing, five consecutive one-second stimulations at one-second intervals with a series of von Frey filaments (1.4g, 4g, 10g, 26g), and ten seconds of noxious pinch applied by a 60g vascular clip (Crosby et al., 2013; Crosby et al., 2014a; Hains et al., 2003a; Quinn et al., 2010b). Voltage recordings from each neuron were sorted using Spike2 (CED; Cambridge, UK). For the brush and pinch stimuli, spikes were summed over the ten seconds that the stimulus was administered. For the von Frey filament stimuli, spikes were summed for each separate application of the filament

(Quinn et al., 2010b). Therefore, each filament strength had a total of five spike counts since each filament was applied to the forepaw five times. Baseline spike counts recorded prior to mechanical stimulation were subtracted from the spike counts for each stimulus to isolate the evoked response, and spike counts for each stimulus were log-transformed due to a positive skew in the distributions of the spike totals. Detailed protocols for recording and counting evoked firing are provided in Appendix A.

5.4. Results

5.4.1. Facet Joint Distraction Inducing Mechanical Hyperalgesia Also Increases Excitatory Synapses in the Spinal Dorsal Horn

Rats develop mechanical hyperalgesia at day 1 that persists through day 7 after injurious loading of the bilateral C6/C7 facet joints. Paw withdrawal threshold decreases significantly on all days after painful joint loading relative to baseline ($p<0.0001$) (Fig. 5.3). PWT is significantly lower than the sham group after painful joint loading overall

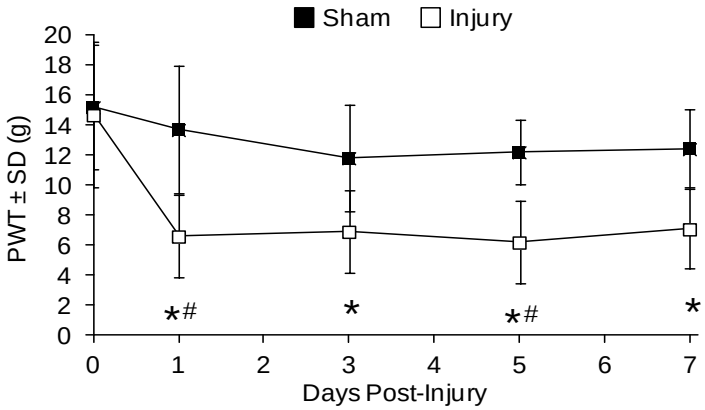

Fig. 5.3. Mechanical hyperalgesia after painful facet joint loading. Paw withdrawal threshold (PWT) decreases on all testing days after painful facet joint loading, relative to baseline (*$p<0.0001$). PWT also decreases compared to the sham group on days 1 and 5 after painful joint loading (#$p\leq0.024$).

($p<0.0001$), as well as on days 1 and 5 ($p\leq0.024$) (Fig. 5.3). A summary of the individual paw withdrawal thresholds for each rat on each day for this study is provided in Appendix C.

To determine whether the number of dorsal horn synapses is altered in rats with sustained hyperalgesia, synapses were quantified in the C6/C7 dorsal horn at day 7 after painful joint distraction (Fig. 5.4) (Ippolito and Eroglu, 2010; Ullian et al., 2001). The

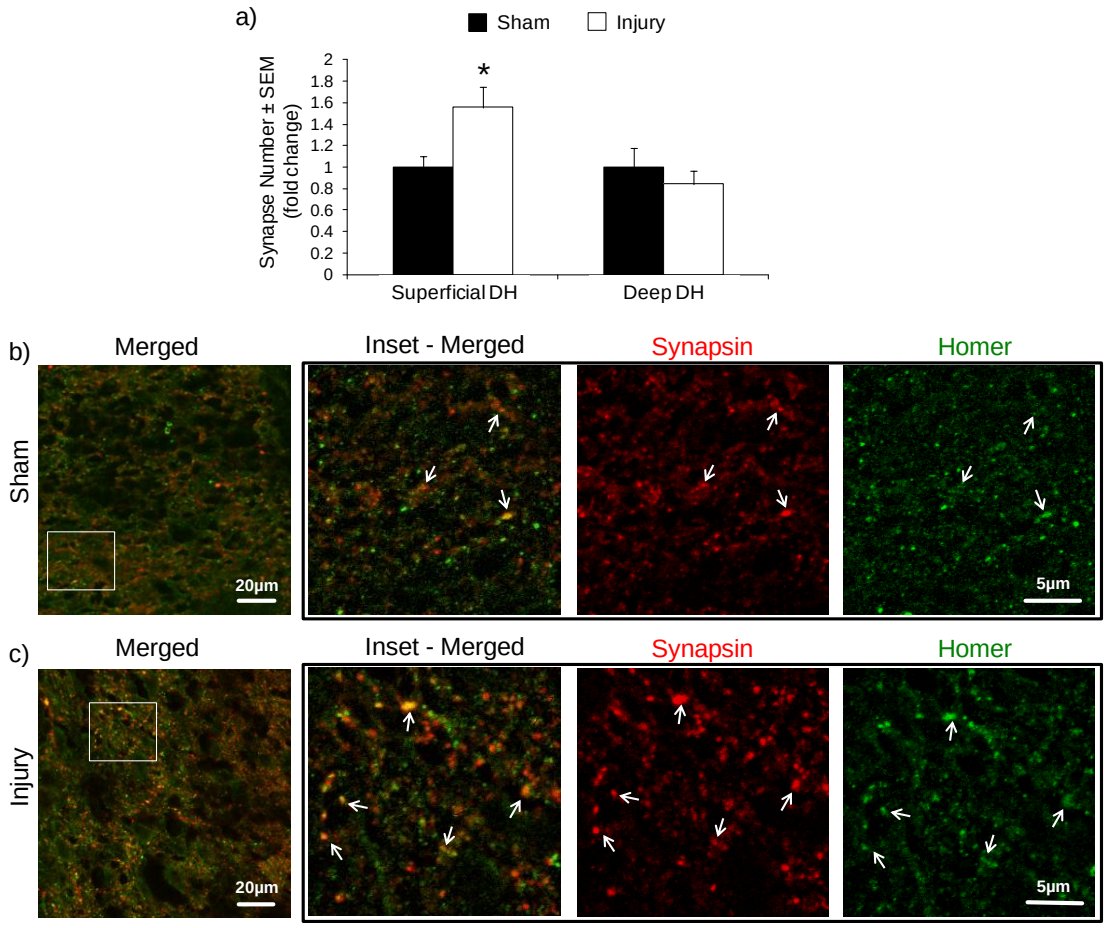

Fig. 5.4. Quantification of excitatory synapses in the superficial and deep laminae of the dorsal horn. **(a)** The number of excitatory synapses increases in the superficial dorsal horn (DH) after painful facet joint injury (*p=0.032), but synapse number does not change in the deep DH. **(b,c)** Representative immunolabeling of synapsin (red) and homer (green) in the superficial dorsal horn after sham **(b)** or painful facet joint injury **(c)**. Colocalization (merged, yellow) represents synaptic puncta (arrows).

number of excitatory synapses increases in the superficial dorsal horn after painful facet joint loading (p=0.032) (Fig. 5.4), suggesting that injury-induced synaptogenesis in the dorsal horn is evident with the presence of sustained hyperalgesia after facet joint distraction. Synapse number is not altered in the deep laminae of the dorsal horn (Fig. 5.4). Synapse counts in the dorsal horn for each rat are presented in Appendix I.

5.4.2. Altered Expression of TSP4 Parallels the Development of Sustained Mechanical Hyperalgesia

TSP4 decreases in the DRG (p=0.012) and increases in the spinal cord (p=0.002) at day 7 after painful joint loading (Fig. 5.5). TSP4 expression also increases in the C6 DRG and decreases in the C6/C7 spinal cord at day 1, but not significantly. The quantification of DRG and spinal TSP4 by Western blot is presented in Appendix F.

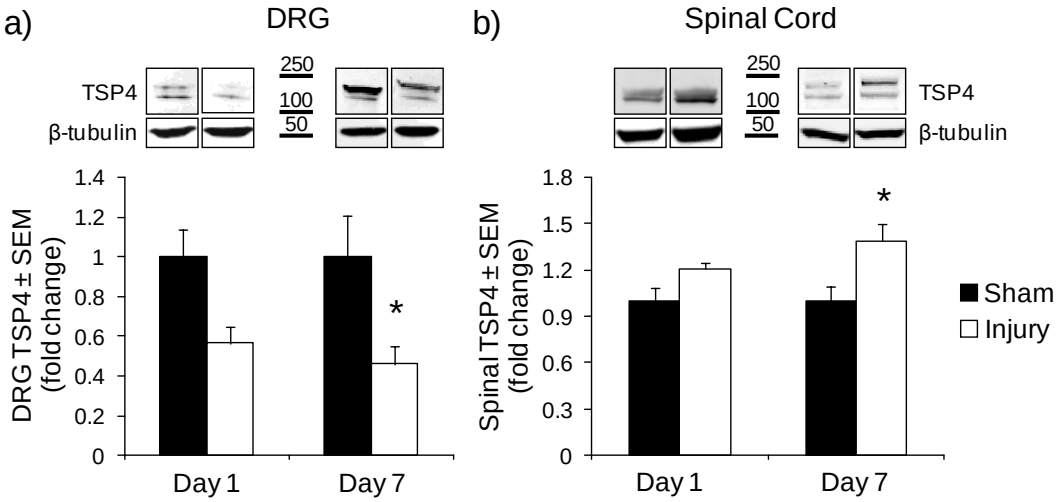

Fig. 5.5. Western blot quantification of DRG and spinal TSP4. **(a)** Expression of TSP4 decreases in the C6 dorsal root ganglion (DRG) at day 7 after painful facet joint injury, relative to sham (*p=0.012). **(b)** Spinal TSP4 expression increases relative to sham at day 7 after painful joint injury (*p=0.002). TSP4 bands are normalized to β-tubulin as a loading control.

Because significant changes in TSP4 expression are evident at day 7, a time when hyperalgesia is also sustained (Fig. 5.3), TSP4 expression and synapse density in the spinal cord are evaluated at day 7 in the remaining studies in this chapter.

Immunolabeling was used to quantify region-specific expression of TSP4 at day 7 after painful facet joint loading in the superficial dorsal horn, deep dorsal horn, and dorsal columns of the C6/C7 spinal cord (Fig. 5.6). Total TSP4 labeling significantly increases after painful joint loading only in the dorsal columns (p=0.0082) (Fig. 5.6). The amount of colocalized GFAP and TSP4, indicating astrocytic TSP4, increases in both the superficial dorsal horn (p=0.036) and the dorsal columns (p=0.024) (Fig. 5.6).

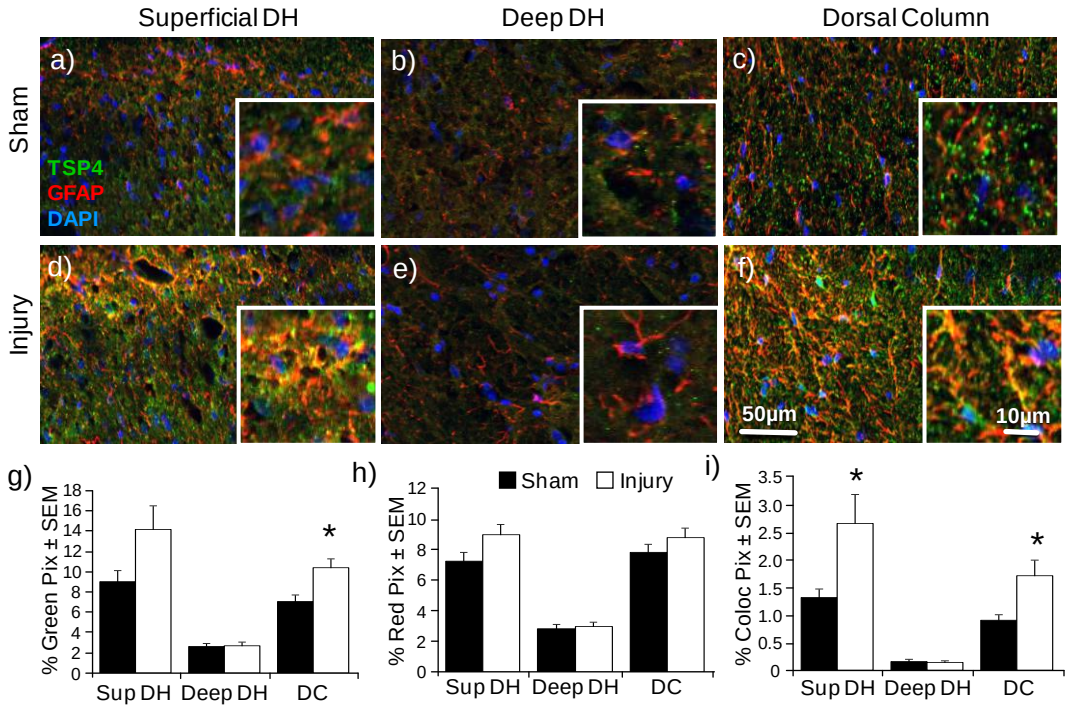

Fig. 5.6. Immunolabeling of TSP4 and GFAP in the spinal cord. TSP4 (green), GFAP (red) and DAPI (blue) are labeled in the superficial dorsal horn (Sup DH) **(a,d)**, deep dorsal horn (Deep DH) **(b,e)**, and dorsal columns (DC) **(c,f)**, after sham or painful facet joint injury. **(g)** TSP4 increases in the dorsal columns (p=0.0082), but **(j)** GFAP is unchanged in any dorsal horn region. **(k)** The colocalization of TSP4 and GFAP (yellow) increases in the superficial DH and dorsal columns (*p≤0.036).

Densitometric quantifications of TSP4 and GFAP for each rat are included in Appendix G. These results support that spinal TSP4 expression is altered following injurious facet joint distraction; in particular, astrocytic expression of TSP4 increases in the dorsal regions of the spinal cord where it may potentiate signaling of the nociceptive primary afferent fibers terminating in the superficial dorsal horn.

5.4.3. Blocking Spinal TSP4 Expression Prevents Behavioral Sensitivity and Synaptogenesis after Painful Facet Joint Loading

To determine whether the increase in spinal TSP4 at day 7 contributes to hyperalgesia, TSP4 expression was blocked prior to painful facet joint loading using intrathecal antisense oligonucleotides. Rats receiving daily intrathecal injection of mismatch oligonucleotides display decreases in PWT on all days following painful facet joint loading ($p<0.0001$), similar to rats receiving painful joint distraction with no treatment (Fig. 5.7a). However, TSP4 antisense oligonucleotides block the development of hyperalgesia after painful facet joint loading ($p<0.0001$) (Fig. 5.7a). Western blot analysis of TSP4 on day 7 confirms that antisense oligonucleotide treatment reduces TSP4 in the C6/C7 spinal cord relative to TSP4 levels after mismatch oligonucleotide treatment ($p=0.049$) (Fig. 5.7b). Paw withdrawal thresholds for rats receiving antisense or mismatch oligonucleotide treatment are detailed in Appendix C, and the quantification of spinal TSP4 by Western blot for each rat is presented in Appendix F.

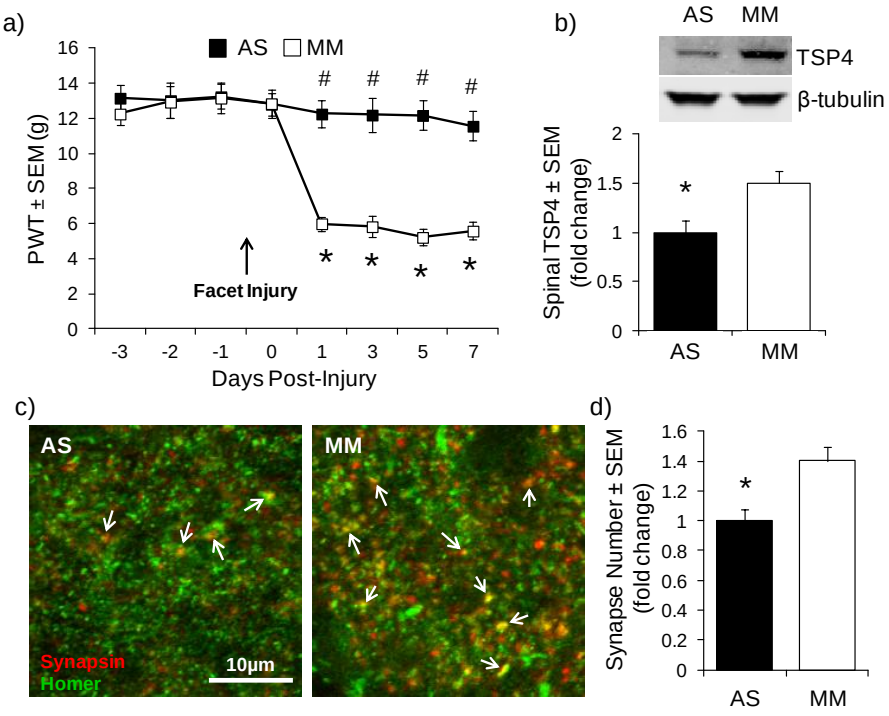

Fig. 5.7. TSP4 antisense oligonucleotides prevent hyperalgesia and spinal excitatory synaptogenesis. **(a)** Paw withdrawal threshold (PWT) decreases relative to baseline after painful facet joint loading in rats receiving mismatch oligonucleotides (MM) (*p<0.0001). Antisense oligonucleotides (AS) prevent hyperalgesia (#p<0.0001 vs. MM) **(b)** AS treatment reduces spinal TSP4 expression on day 7 compared to MM-treated rats (*p=0.049) **(c)** Representative labeling of synapsin (red) and homer (green); colocalization (yellow) represents synaptic puncta (arrows). **(d)** AS treatment reduces the number of excitatory synapses relative to MM treatment (*p=0.001).

Given the synaptogenic properties of TSP4 and its upregulation in the same dorsal horn regions where excitatory synapses also increase in this model (Figs. 5.4 and 5.6), TSP4 may contribute to persistent hyperalgesia by inducing excitatory synaptogenesis. To test this hypothesis, synapses were quantified in the superficial dorsal horn after injurious joint distraction in rats that received antisense or mismatch oligonucleotide treatment. Fewer excitatory synaptic puncta are observed in the superficial dorsal horn at day 7 after painful facet joint loading in rats undergoing daily antisense oligonucleotide treatment, relative to rats that receive mismatch oligonucleotides (p=0.001) (Fig. 5.7).

These data suggest that spinal TSP4 plays a role in the development of hyperalgesia after injurious joint loading, likely through the initiation of excitatory dorsal horn synaptogenesis. Synapse counts in the dorsal horn for each rat after antisense or mismatch oligonucleotides are included in Appendix I.

5.4.4. Intrathecal Gabapentin Reduces Injury-Induced Hyperalgesia and Dorsal Horn Excitatory Synaptogenesis

PWT is unchanged from baseline at day 7 after painful facet joint loading in rats that receive gabapentin treatment (Fig. 5.8a). However, PWT decreases in vehicle-treated rats on day 7 after injurious joint distraction, relative to baseline (p=0.0001) and to the gabapentin-treated group (p=0.01). Gabapentin also prevents the injury-induced increase in excitatory synapses that is typically observed in the superficial dorsal horn (p=0.0002)

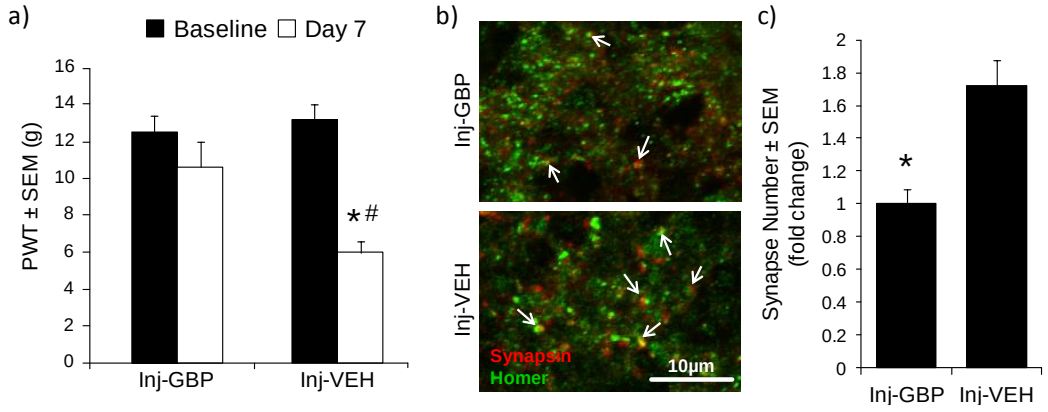

Fig. 5.8. Gabapentin attenuates mechanical hyperalgesia and excitatory synaptogenesis after painful facet joint loading. **(a)** Paw withdrawal threshold (PWT) decreases on day 7 after painful joint loading in rats receiving saline vehicle (*Inj-VEH*) (*p=0.0001 vs. baseline, #p=0.01 vs. gabapentin (*Inj-GBP*)). **(b)** Representative immunofluorescent labeling of synapsin (red) and homer (green) in the superficial dorsal horn. Colocalization (yellow) indicates synaptic puncta (arrows). **(c)** Gabapentin prevents the injury-induced increase in excitatory synapses. (*p=0.0002).

(Fig. 5.8). These results further support the role of TSP4-mediated synaptogenesis in persistent pain after facet joint loading. Paw withdrawal thresholds for each rat after intrathecal gabapentin or vehicle treatment are presented in Appendix C, and the corresponding synapse counts in the dorsal horn are detailed in Appendix I.

5.4.5. Immediate Intra-articular Bupivacaine Prevents Hyperalgesia and Excitatory Synaptogenesis

Blocking injury-induced afferent firing early after painful facet injury prevents the development of hyperalgesia and spinal hyperexcitability (Crosby et al., 2014a). As such, afferent activity from the joint was blocked to determine if that activity after painful joint loading *also* induces the dysregulation of TSP4 and excitatory synaptogenesis. Astrocytic TSP4 increases in the superficial dorsal horn and dorsal columns at day 7 after painful joint loading with immediate saline vehicle treatment (*Inj-VEH0h*) over the corresponding sham levels (*Sham-VEH0h*) ($p<0.0001$) (Fig. 5.9). However, immediate bupivacaine treatment (*Inj-BP0h*) attenuates those increases in astrocytic TSP4 in the superficial dorsal horn and dorsal columns ($p<0.0001$) (Fig. 5.9). In contrast, although astrocytic TSP4 increases in the dorsal horn and the dorsal columns after painful joint loading with vehicle treatment given at day 4 (*Inj-VEHd4*) ($p\leq0.0061$), bupivacaine administered at day 4 (*Inj-BPd4*) does *not* attenuate spinal TSP4 expression ($p\leq0.048$) (Fig. 5.9). Immediate bupivacaine treatment also prevents the injury-induced increase in excitatory synapses in the superficial dorsal horn at day 7 after painful joint loading ($p<0.0001$), but synapse numbers increase despite the administration of bupivacaine at

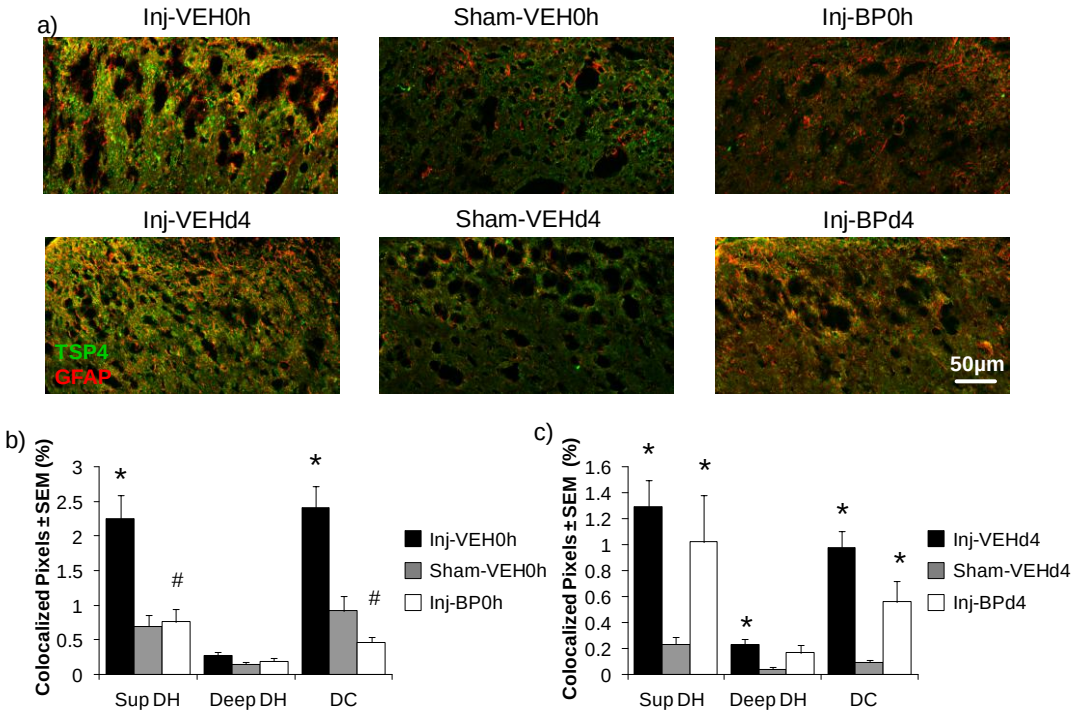

Fig. 5.9. Immediate intra-articular bupivacaine prevents TSP4 upregulation after painful facet joint loading. **(a)** TSP4 (green) and GFAP (red) in the superficial dorsal horn of rats receiving sham or painful facet joint injury followed by immediate (*Inj-VEH0h*, *Sham-VEH0h*) or day 4 intra-articular vehicle injections (*Inj-VEHd4*, *Sham-VEHd4*) or bupivacaine injections (*Inj-BP0h*, *Inj-BPd4*). **(b,c)** Densitometric quantification of colocalized TSP4 and GFAP (yellow) in the superficial dorsal horn (Sup DH), deep dorsal horn (Deep DH), and dorsal columns (DC). **(b)** Increases in astrocytic TSP4 after painful joint loading (*$p<0.0001$ vs. *Sham-VEH0h*) are prevented by immediate bupivacaine (#$p<0.0001$ vs. *Inj-VEH0h*). **(c)** However, increases in astrocytic TSP4 after painful joint loading (*$p\leq0.048$ vs. *Sham-VEHd4*) are not blocked by bupivacaine at day 4.

day 4 ($p\leq0.043$) (Fig. 5.10). Appendix G summarizes the quantification of astrocytic TSP4 for each rat in this study, and the dorsal horn synapse counts for each rat are itemized in Appendix I. These results support that afferent activity initiated early after painful facet joint loading induces the upregulation of spinal TSP4 and excitatory synaptogenesis.

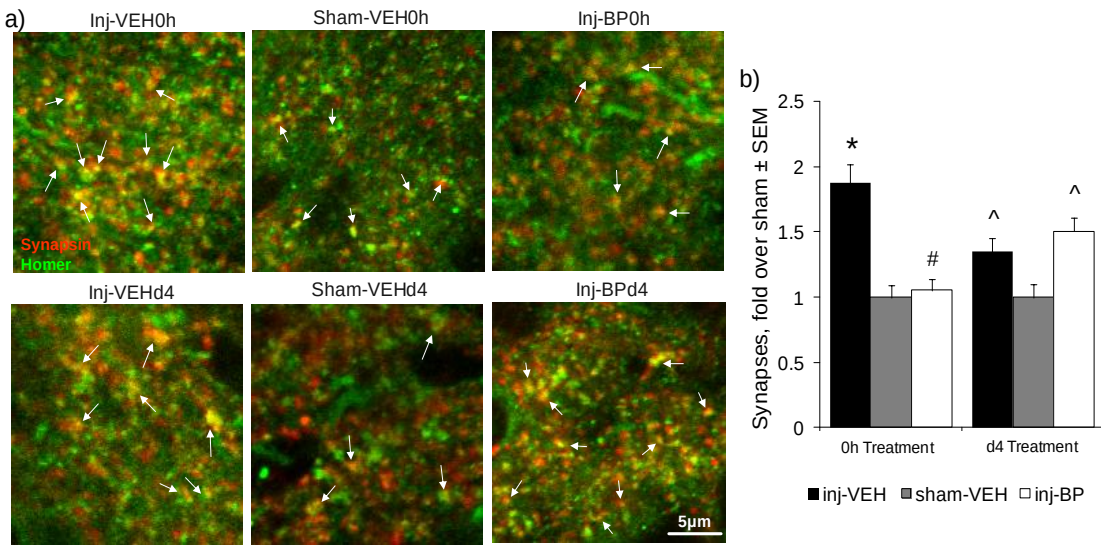

Fig. 5.10. Immediate intra-articular bupivacaine prevents excitatory synaptogenesis. **(a)** Representative immunolabeling of synapsin (red) and homer (green) to identify synaptic puncta (yellow, arrows). Synapses were counted in the superficial dorsal horn of rats receiving sham or painful facet joint injury followed by immediate (*Inj-VEH0h*, *Sham-VEH0h*) or day 4 vehicle injections (*Inj-VEHd4*, *Sham-VEHd4*), or bupivacaine injections (*Inj-BP0h*, *Inj-BPd4*). **(b)** Increases in excitatory synapses after painful joint loading (*$p<0.0001$ vs. *Sham-VEH0h*) are prevented by immediate bupivacaine (#$p<0.0001$ vs. *Inj-VEH0h*), but not by bupivacaine at day 4 (*$p\leq0.043$ vs. *Sham-VEHd4*).

5.4.6. Spinal TSP4 Potentiates Hyperalgesia and Neuronal Hyperexcitability Induced by Facet Joint Loading

In addition to synaptogenesis, TSP4 may contribute to spinal hyperexcitability by enhancing excitatory input from primary afferent fibers to the dorsal horn (Kim et al., 2012). Since facet joint loading increases firing of the afferents that innervate the facet capsule (Lu et al., 2005a), increased spinal TSP4 levels may potentiate hyperalgesia and neuronal excitability after nonpainful or painful loading of the facet joint. To identify the dose-response of spinal TSP4 and behavioral sensitivity, mechanical hyperalgesia was assessed in the forepaw after intrathecal administration of full-length recombinant TSP4 protein with a StrepII tag for affinity purification (Fig. 5.11).

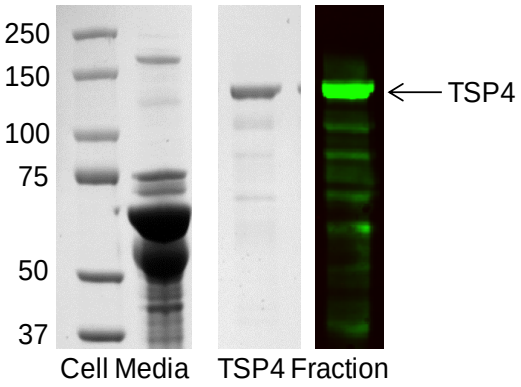

Fig. 5.11. Purification of recombinant TSP4. The Coomassie-stained SDS-PAGE gel (Cell Media) shows the protein bands in cell culture media collected from transfected 293/EBNA cells. The Coomassie-stained gel and immunolabeled membrane (TSP4 Fraction) show the elution fraction containing TSP4 after Streptactin affinity purification.

Mechanical hyperalgesia develops after an intrathecal bolus injection of 30µg ($p \leq 0.043$), 45µg ($p \leq 0.014$), or 60µg ($p \leq 0.011$) of TSP4 (see Appendix B for paw withdrawal thresholds for each rat) (Fig. 5.12). Hyperalgesia peaks 3-4 days after injection and behavioral sensitivity is most prolonged, lasting for 2-6 days, following the 60µg dose (Fig. 5.12). Injection of either 20µg TSP4 or of 60µg StrepII peptide, as a control, does not induce any sensitivity (Fig. 5.12). These results suggest that intrathecal TSP4 is sufficient to induce mechanical hyperalgesia in the forepaw, but that

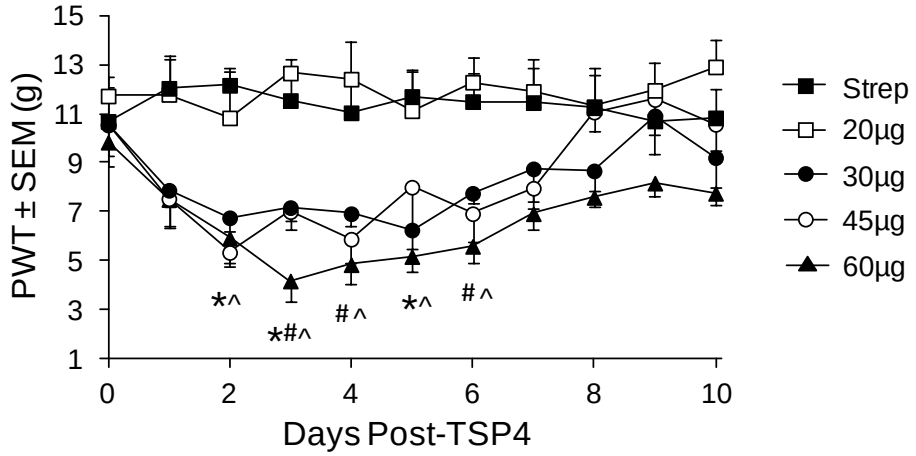

Fig. 5.12. Dose-response of intrathecal TSP4 and mechanical hyperalgesia in the forepaw. Injections of 30µg (*$p \leq 0.043$), 45µg (#$p \leq 0.014$), or 60µg (^$p \leq 0.011$) of TSP4 induce decreases in paw withdrawal threshold (PWT) in the forepaw that peak 3-4 days after injection. Injection of either the 60µg StrepII peptide (Strep), to control for the StrepII tag on the TSP4 protein, or the 20µg TSP4 do not induce sensitivity.

subthreshold doses can be administered that do not independently produce sensitivity. As such, two doses of TSP4 were used for further studies: a non-sensitizing dose (20µg) and a sensitizing dose (60µg).

To determine whether spinal TSP4 potentiates the development of hyperalgesia and spinal hyperexcitability after facet joint loading, non-sensitizing or sensitizing doses of recombinant TSP4 were administered three days before sham, physiologic, or injurious loading the facet joint. Physiologic loading of the C6/C7 facet joint induces lower vertebral and capsule distraction, joint loading and facet capsule strain than injurious distraction ($p<0.0001$) (Fig. 5.13); a detailed summary of the mechanical data from the

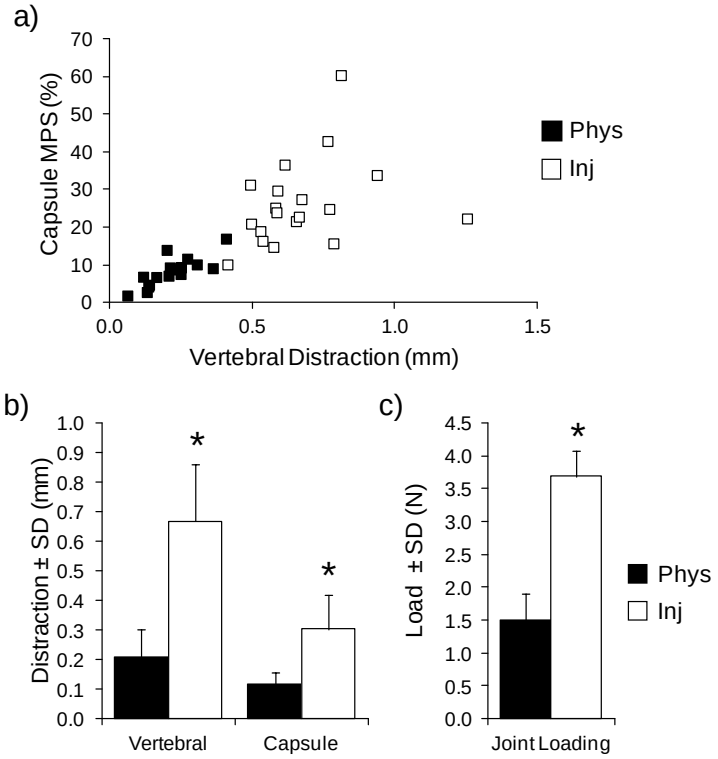

Fig. 5.13. Mechanical characterization of facet joint loading. **(a)** Injurious (Inj) loading imposes greater C6/C7 vertebral distraction and generates higher maximum principal strains (MPS) in the facet capsule than physiologic (Phys) loading. **(b)** Vertebral and capsule distraction, and **(c)** load across the facet joint are significantly higher during injurious loading than physiologic loading (*$p<0.0001$).

joint distraction for each rat is included in Appendix B. Neither injection of StrepII peptide with either sham or physiologic loading, nor injection of the non-sensitizing 20µg dose of TSP4 with sham loading, induce sensitivity (Fig. 5.14a). Those data confirm that non-sensitizing TSP4 and physiologic loading alone are insufficient to induce behavioral sensitivity. The combination of either 20µg or 60µg TSP4 with physiologic facet joint loading produces sustained hyperalgesia that persists through day 7 ($p \leq 0.01$) (Fig. 5.14a). However, the effects of TSP4 and facet joint loading on behavioral sensitivity are not

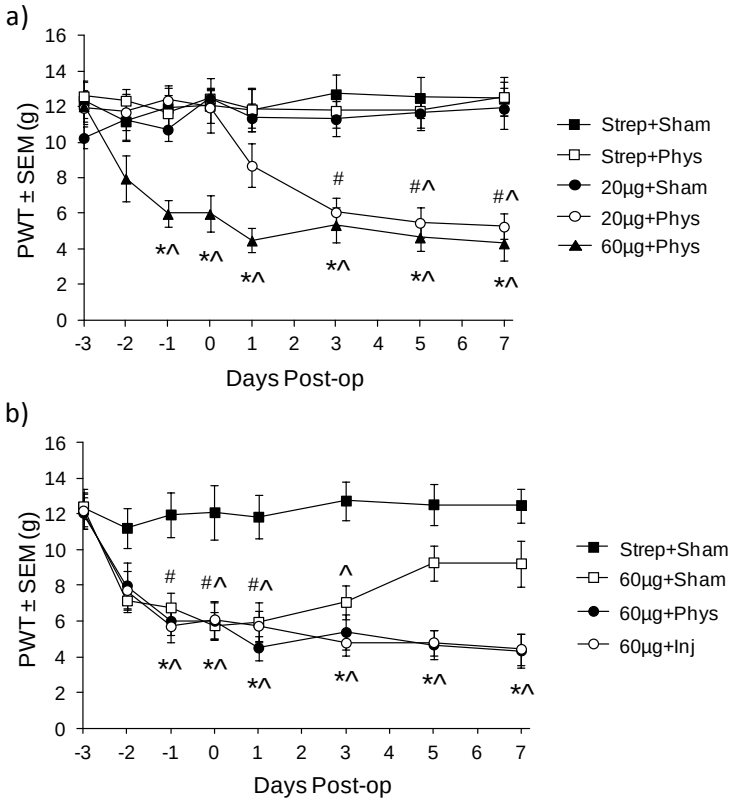

Fig. 5.14. Spinal TSP4 facilitates hyperalgesia after facet joint loading. Rats received non-sensitizing (20µg) or sensitizing (60µg) intrathecal TSP4, or a StrepII peptide control (Strep) three days before sham, physiologic (Phys), or injurious (Inj) facet joint distraction. **(a)** TSP4 potentiates the development of hyperalgesia after joint loading (*$p \leq 0.01$ *60µg+Phys* vs. baseline, #$p \leq 0.0002$ *20µg+Phys* vs. baseline, ^$p \leq 0.013$ vs. *Strep+Sham*). **(b)** Sensitivity induced by TSP4 is not increased further by any magnitude of facet joint loading (*$p \leq 0.01$ *60µg+Phys* and *60µg+Inj* vs. baseline, #$p \leq 0.028$ *60µg+Sham* vs. baseline, ^$p \leq 0.028$ vs. *Strep+Sham*).

cumulative – sensitivity develops after injection of 60µg TSP4 ($p \leq 0.028$), but is not increased further by physiologic or injurious joint loading (Fig. 5.14b). Appendix B presents the paw withdrawal thresholds for each rat on each day.

Increased spinal TSP4 also potentiates the development of dorsal horn neuronal hyperexcitability at day 7 after facet joint loading. Neuronal firing evoked by light brush or noxious pinch increases over firing levels in the sham group when 20µg or 60µg TSP4 is followed by physiologic loading ($p \leq 0.0057$) (Fig. 5.15). Likewise, von Frey filament stimulation (1.4, 4, 10, and 26g) also evokes greater firing when 20µg or 60µg TSP4 is followed by physiologic loading, compared to neuronal firing in the sham group ($p \leq 0.013$) (Fig. 5.15). Neuronal activity after either 20µg or 60µg TSP4 with physiologic joint loading is increased to the same level as when 60µg TSP4 is followed by injurious joint loading (Fig. 5.15). These results indicate that the facet joint loading that occurs during normal physiologic events can induce the same sustained neuronal hyperexcitability as a painful facet joint injury, when superimposed on preexisting increased spinal TSP4 levels. The effects of increased spinal TSP4 and facet loading on neuronal firing are not additive, because evoked firing after 60µg TSP4 with physiologic loading is not different from neuronal firing after 60µg TSP4 with injurious loading (Fig. 5.15). Evoked spike counts for each neuron from each rat are itemized in Appendix E.

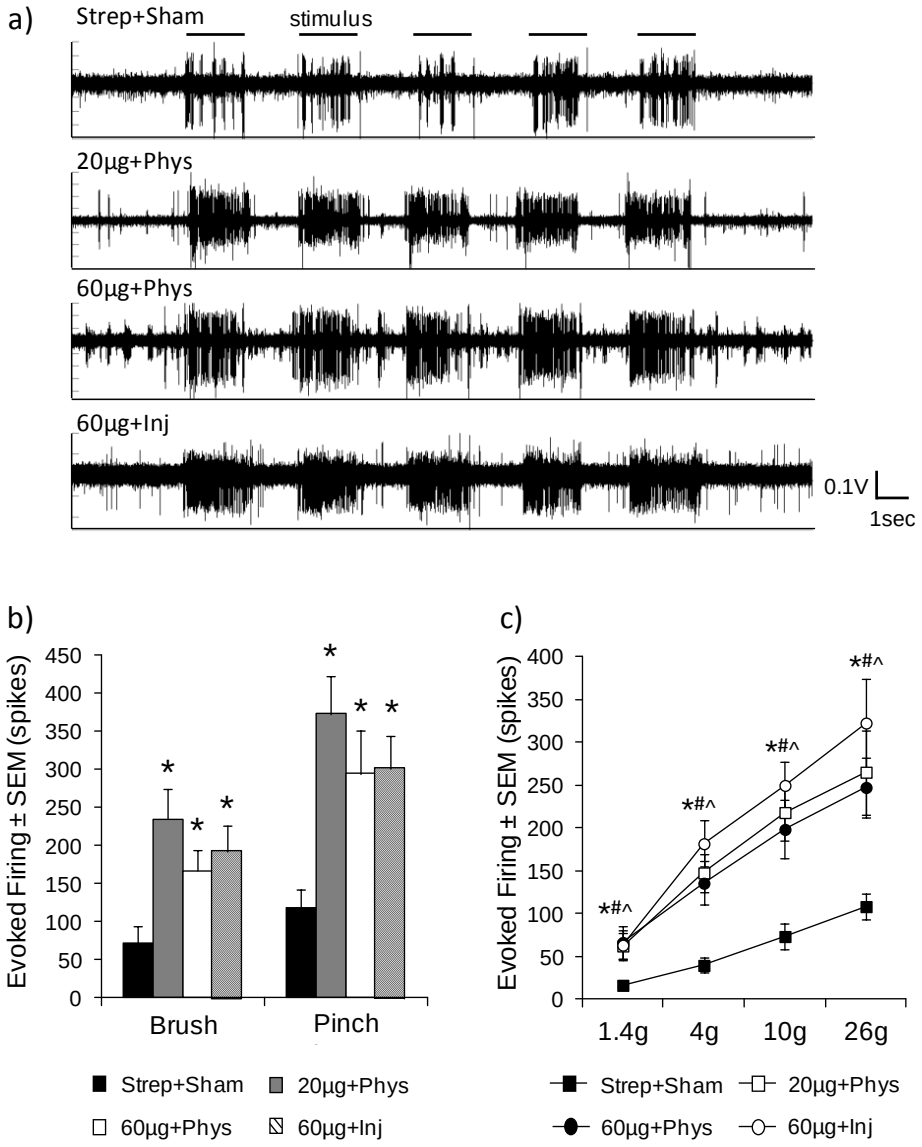

Fig. 5.15. Spinal TSP4 potentiates dorsal horn neuronal hyperexcitability after facet joint loading. **(a)** Representative neuronal firing in response to five stimulations with a noxious 26g von Frey filament for a subset of groups (*Strep+Sham*, *20µg+Phys*, *60µg+Phys*, *60µg+Inj*). **(b)** Neuronal firing in response to light brush and pinch is elevated when facet loading is preceded by non-sensitizing or sensitizing TSP4 treatment (*p≤0.0057 vs. *Strep+Sham*). **(c)** Neuronal firing is also elevated over sham levels in response to 1.4, 4, 10, and 26g von Frey filaments when facet loading is preceded by non-sensitizing or sensitizing TSP4 treatment (*p≤0.008 for *20µg+Phys*, #p≤0.013 for *60µg+Phys*, ^p≤0.024 for *60µg+Inj*).

5.5. Discussion

Painful facet joint loading induces excitatory dorsal horn synaptogenesis along with dysregulation of thrombospondin-4 (TSP4) in both the DRG and spinal cord paralleling the time course of sustained mechanical hyperalgesia (Figs. 5.3-5.6). Of note, although this study only evaluates hyperalgesia through day 7, behavioral sensitivity persists for up to six weeks after the same injurious facet joint loading (Rothman et al., 2008). Additional studies characterizing the long-term effects of painful facet joint loading on spinal TSP4 expression and dorsal horn hyperexcitability would provide insight into the chronic mechanisms that maintain persistent facet joint pain. Nonetheless, the peripheral and spinal treatments used in this collection of studies suggest a mechanism for the induction of structural plasticity in the spinal cord at day 7 after painful facet joint injury. Blocking afferent activity immediately after painful joint loading prevents injury-induced increases in spinal TSP4 and excitatory synapses (Figs. 5.9 and 5.10). Blocking injury-induced TSP4 expression or antagonizing the synaptogenic activity of TSP4 attenuates dorsal horn synaptogenesis (Figs. 5.7 and 5.8). Together, these results suggest that astrocytic TSP4 expression is stimulated by afferent discharge from the facet joint early after painful joint loading, resulting in TSP4-mediated excitatory synaptogenesis. That increase in excitatory synapses could contribute to the spinal neuronal hyperexcitability that is observed after painful facet joint injury (Crosby et al., 2013; Crosby et al., 2014a; Quinn et al., 2010b) by increasing the number of excitatory inputs on neurons in the dorsal horn and lowering the intensity of primary afferent stimulation required to activate those dorsal horn neurons.

The peripheral and central neurochemical changes associated with inflammatory and neuropathic pain can differ substantially (Honore et al., 2000), emphasizing the need to define those mechanisms for each pain state, especially for joint-mediated pain which often includes both inflammatory and neuropathic characteristics (Bove et al., 2006; Dong and Winkelstein, 2010; Kras et al., 2013b; Kras et al., 2014a; Lee and Winkelstein, 2009; Quinn et al., 2010b). Although not a direct neural tissue insult, injurious facet joint distraction can produce pain through the induction of secondary axonal damage and increased discharge and afterdischarge of fibers innervating the facet joint (Crosby et al., 2014a; Lu et al., 2005a; Kallakuri et al., 2008). In this study, the downregulation of TSP4 in the DRG and upregulation of spinal astrocytic TSP4 after painful facet loading (Fig. 5.5) are consistent with reports of TSP4 dysregulation in neuropathic pain after lumbar spinal nerve ligation, spinal cord contusion, and trigeminal nerve injury (Kim et al., 2012; Li et al., 2013; Zeng et al., 2013). TSP4 can also be expressed in neurons (Arber and Caroni, 1995); but although neuronal TSP4 could contribute to the increase in spinal TSP4 in this study, this is not likely since TSP4 expression occurs mostly in astrocytes and not neurons after painful nerve injury (Kim et al., 2012). The similarities in the spatiotemporal regulation of TSP4 in the DRG and spinal cord after painful joint loading and neural trauma strongly suggest that there are common mechanism(s) by which TSP4 contributes to spinal sensitization and chronic pain, regardless of the inciting event. Therefore, blocking the upregulation or activity of TSP4 may serve as an effective therapeutic approach for a wide range of chronic pain conditions.

Given the synaptogenic properties of thrombospondins (Christopherson et al., 2005), upregulation of TSP4 in the superficial dorsal horn could lead to the increase in

the number of excitatory synapses that is observed in that region (Figs. 5.4-5.6). However, given that hyperalgesia is observed at day 1, the temporal mechanism by which this synaptogenesis develops is not known. Preventing TSP4 expression or blocking TSP4 activity with gabapentin abolishes injury-induced hyperalgesia and those increased synapses (Figs. 5.7 and 5.8), suggesting that increased spinal TSP4 is requisite for synaptogenesis through interaction with its neuronal receptor, α2δ-1. Gabapentin has also been shown to reduce spinal astrocytic activation and dorsal horn neuronal hyperexcitability in this same painful joint distraction model (Dong et al., 2013a), suggesting that gabapentin may prevent TSP4 activity that is critical for the development of facet-mediated pain. Gabapentin likely does not remain active until day 7 when synapse numbers were evaluated (Field et al., 1997). So, it is also possible that gabapentin given at the time of injury prevents the initial increase in spinal TSP4, similar to the administration of intra-articular bupivacaine early after injury (Fig. 5.9), rather than blocking TSP4 activity after its upregulation.

The relative increase in excitatory synapses (1.56-fold) in the superficial dorsal horn after painful facet joint loading (Fig. 5.4) is similar to the range of increases in synapses reported in that spinal region after peripheral nerve injury (Jaken et al., 2010; Li et al., 2014b; Lin et al., 2011; Peng et al., 2010). Retinal ganglion cell cultures treated with TSP1 develop synapses that are post-synaptically silent due to a lack of functional AMPA glutamate receptors, despite normal structural appearance (Christopherson et al., 2005). The synaptogenic domains of the TSP1 protein are conserved across all members of the TSP family (Eroglu et al., 2009), so it is possible that newly developed synapses in the dorsal horn induced by TSP4 after painful facet joint loading are similarly not

functional. In the current study, synaptic puncta are identified based only on labeling of pre- and post-synaptic structural components; future studies should electrophysiologically evaluate the functionality of synapses that are induced by TSP4 after joint loading (Christopherson et al., 2005; Ullian et al., 2001).

An increase in functional excitatory synapses after painful facet joint loading could amplify nociceptive signals via increasing activation of second-order nociceptive neurons by the Aδ and C fibers that terminate in the superficial laminae of the dorsal horn (Basbaum et al., 2009). Alternately, nerve injury may induce sprouting of Aβ fibers from the deep dorsal horn into the superficial laminae (Woolf et al., 1992). Although the evidence supporting sprouting of Aβ fibers in the dorsal horn after nerve injury is disputed (Hughes et al., 2003), the increase in excitatory synapses could indicate new connections of low-threshold afferents into nociceptive pathways in the superficial dorsal horn, resulting in the hypersensitivity to innocuous mechanical stimuli that is observed after painful joint loading (Fig. 5.3). Additional studies of spinal structural plasticity are needed to determine which pre- and post-synaptic dorsal horn neuronal populations, if any, form aberrant connections during excitatory synaptogenesis.

Bupivacaine treatment immediately after painful facet joint loading attenuates spinal TSP4 upregulation and excitatory synaptogenesis (Figs. 5.9 and 5.10). However, bupivacaine administered at day 4 after joint loading does not reduce spinal TSP4 or synaptogenesis (Figs. 5.9 and 5.10), indicating that joint afferent input is not required to maintain the increase in excitatory synapses after spinal hyperexcitability has already developed. Early afferent activity after painful facet joint loading induces other synaptic changes that promote neuronal excitability, including the upregulation of glutamate

receptors and downregulation of astrocytic glutamate transporters (Crosby et al., 2014a). Injury-induced afferent discharge may directly induce TSP-mediated synaptogenesis by increasing spinal astrocytic TSP4 expression, since excitatory signaling molecules like ATP have been shown to stimulate astrocyte release of other members of the thrombospondin family (Tran and Neary, 2006). The subsequent increase in excitatory synapses could contribute to increases in neuronal glutamate signaling proteins like mGluR5 and phosphorylated NR1 at day 7 after painful facet joint loading (Crosby et al., 2014a). Together, the results of this study suggest that afferent discharge from the facet joint initiates TSP4-mediated synaptogenesis in the spinal cord, and the subsequent increase in excitatory synapses may underlie the potentiation of glutamatergic signaling and the spinal neuronal hyperexcitability that are observed after painful joint loading.

Increased spinal TSP4 is sufficient to induce mechanical hyperalgesia, but it also potentiates the development of dorsal horn neuronal hyperexcitability after mechanical loading of the facet joint (Figs. 5.12-5.15). Low-threshold mechanosensitive and nociceptive afferents in the facet capsule are differentially activated by capsule strains produced during physiologic and injurious joint loading, respectively (Dong et al., 2012; Lu et al., 2005a). However, in the presence of increased spinal TSP4, even physiologic joint loading is sufficient to induce hyperalgesia and dorsal horn neuronal hyperexcitability (Fig. 5.14). These findings suggest that TSP4 sensitizes the non-nociceptive spinal pathways that are activated by physiologic joint loading, possibly by facilitating presynaptic excitatory neurotransmitter release from Aβ afferents terminating in the dorsal horn (Kim et al., 2012). The specific mechanisms by which TSP4 facilitates excitatory neurotransmission remain unclear (Kim et al., 2012), but TSP-family proteins

have been shown to regulate calcium signaling at the plasma and endoplasmic reticular membranes (Duquette et al., 2014), and altering presynaptic calcium levels could enhance excitatory neurotransmitter release (Neher and Sakaba, 2008). Collectively, these results implicate increased spinal TSP4 in priming the spinal cord for the development of dorsal horn neuronal hyperexcitability in response to afferent activity induced by joint loading, and decreasing the mechanical threshold for pain from joint loading. Repeated exposure to joint loading that upregulates TSP4, or higher endogenous levels of spinal TSP4, may therefore present a higher risk for the development of persistent joint-mediated pain.

5.6. Conclusions and Integration

In summary, the studies in this chapter demonstrate that TSP4 plays an important role in the development and maintenance of persistent pain after facet joint loading. The dysregulation of TSP4 after painful joint loading, in conjunction with behavioral sensitivity and increased excitatory synapse density, indicates a relationship between TSP4 expression, spinal structural plasticity, and persistent joint-mediated pain. Evidence of excitatory synaptogenesis in the spinal dorsal horn in association with joint pain, and the absence of synaptogenesis with decreased TSP4 expression or analgesic gabapentin treatment, support a TSP4-mediated mechanism as driving the hyperalgesia and neuronal hyperexcitability that develop after painful facet joint loading. TSP4 also facilitates the mechanotransduction of joint loading to initiate hyperalgesia and spinal hyperexcitability. By lowering the threshold of mechanical loading to the joint that induces persistent pain, increased spinal TSP4 could increase risk for the development of facet joint-mediated pain in individuals undergoing any magnitude of facet loading. These findings suggest

that the spinal cord is sensitive to "priming" by pro-excitatory or pro-nociceptive molecules, like TSP4, that may lower the threshold for afferent firing-induced sensitization of dorsal horn neurons from any type of noxious stimulation, not just mechanical loading of the cervical facet joints. Identifying the molecules and the spinal concentrations of those molecules that may cause spinal cord priming is important to understand the relationships between noxious stimulation, including mechanical joint loading, and the development of persistent pain.

This study also emphasizes the finding from Chapter 4 that peripheral intervention after painful facet joint injury is only effective for blocking hyperalgesia and spinal hyperexcitability when administered early after joint loading. In addition to synaptic changes that potentiate excitatory glutamatergic signaling (Chapter 4), the studies in this chapter indicate that structural changes develop in the spinal cord within the first seven days after painful joint loading that could permanently alter the spinal processing of non-nociceptive and nociceptive signals. Collectively, the studies in this thesis suggest that extensive spinal modifications underlie the onset of spinal neuronal hyperexcitability after painful joint injury, and spinal hyperexcitability can be difficult to effectively treat after it has developed. Spinal cord stimulation (SCS) is an effective therapy for chronic pain that directly modulates dorsal horn neuronal activity rather than pharmacologically targeting one or more of the spinal mechanisms that contribute to neuronal hyperexcitability (Compton et al., 2012; Guan, 2012). As such, Chapters 6 and 7 evaluate the effectiveness and mechanisms of SCS for the attenuation of spinal neuronal hyperexcitability in models of cervical radiculopathy and painful facet joint injury.

CHAPTER 6

Optimization of Burst Spinal Cord Stimulation Parameters in a Rat Model of Neuropathic Pain

Parts of this chapter were adapted from:

Crosby ND, Goodman-Keiser MD, Smith JR, Zeeman ME, Winkelstein BA. Stimulation parameters define the effectiveness of burst spinal cord stimulation in a rat model of neuropathic pain. *Neuromodulation* 2014; doi:10.1111/ner.12221.

6.1. Overview

Spinal neuronal hyperexcitability is a key feature of central sensitization that develops after many different types of neural or soft tissue injuries, including painful facet joint injury and compression of the dorsal nerve root that leads to cervical radiculopathy (Crosby et al., 2013; Hanai et al., 1996; Nicholson et al., 2014a; Quinn et al., 2010b; Smith et al., 2013; Zhang et al., 2013). Injury-induced spinal modifications, including potentiation of glutamatergic signaling and synaptogenesis detailed in Chapters 4 and 5, can contribute to neuronal hyperexcitability by altering nociceptive signaling and excitatory neurotransmission (Crosby et al., 2014a; Dong et al., 2012; Kim et al., 2012). As a result, spinally-mediated pain that becomes chronic is often refractory to conventional treatments, such as physical therapy, neck immobilization, or pharmacological interventions, that fail to target the amplification of nociception at the spinal level (Peeters et al., 2001). Spinal cord stimulation (SCS) attenuates chronic pain

by directly modulating neuronal hyperexcitability in the spinal dorsal horn (Cameron, 2004; Compton et al., 2012; Simpson, 1997). Despite the use of SCS to treat chronic pain, the mechanisms underlying its analgesic effects remain unknown. Because cervical radiculopathy is a common indication for SCS (Alo et al., 2002; De Ridder et al., 2013; Rizvi and Kumar, 2013), that injury is ideal for studying the potential mechanism(s) of action, and effectiveness, of SCS for treating chronic neuropathic pain.

Traditional SCS stimulates the dorsal columns of the spinal cord with continuous, tonic pulses of current to inhibit nociception in the dorsal horn (Guan et al., 2010; Qin et al., 2012; Tang et al., 2014). The reported success rate of SCS for pain relief in clinical studies varies widely and, overall, has improved little in the last several decades (Cameron, 2004; Zhang et al., 2014). Recently, novel modes of stimulation have been developed to improve the effectiveness of SCS by modifying the delivery of stimulation in order to increase the inhibition of nociception in the spinal cord. Burst SCS is one mode of stimulation that shows greater clinical effectiveness than conventional tonic stimulation while also reducing paresthesia, a major side-effect of tonic SCS (De Ridder et al., 2010; De Vos et al., 2013). However, the optimization, effectiveness, and mechanisms of burst SCS are unclear, especially for cervical radiculopathy.

Studies in this chapter and Chapter 7 evaluate burst SCS for modulating spinal neuronal firing after the development of persistent radicular pain. In particular, the studies in this chapter are outlined in Aim 3a, with the goal of optimizing the parameters and conditions of burst SCS for attenuating spinal hyperexcitability. Using an established rat model of C7 dorsal nerve root compression that induces radicular pain (Hubbard and Winkelstein, 2005; Zhang et al., 2013), burst SCS was applied to the C4 dorsal columns

to determine its effect on spinal neuronal firing. The effectiveness of SCS was measured by the reduction of dorsal horn neuronal activity during noxious mechanical stimulation of the forepaw. The optimization of the stimulation parameters in this study identifies the most effective settings for burst SCS for use in the studies presented in Chapter 7, in which the efficacy of burst and tonic SCS are compared for attenuating spinal neuronal hyperexcitability after painful nerve root compression or facet joint injury.

6.2. Background

Spinal cord stimulation (SCS) is used to treat a wide range of chronic pain conditions by administering electrical stimulation to the dorsal columns of the spinal cord. Traditional SCS uses a tonic paradigm to deliver continuous pulses of various frequencies, pulse widths, and intensities to the spinal cord and is commonly used to manage cervical and lumbar axial and radicular pain (Alo et al., 2002; Compton et al., 2002; Stojanovic and Abdi, 2002). Those parameters can be modulated, along with electrode configuration and placement on the spinal cord, to maximize pain relief for individual patients (De Vos et al., 2013; Rizvi and Kumar, 2013). However, tonic stimulation induces paresthesia in the stimulated dermatomes. Although paresthesia can be used to guide electrode placement and SCS programming, many patients prefer paresthesia-free stimulation (De Vos et al., 2013).

Burst SCS is an alternative mode of stimulation that uses small bursts of pulses of stimulation rather than continuous pulses. Burst SCS has been recently reported to reduce neuropathic pain better than tonic SCS without generating paresthesia in the majority of

patients (De Ridder et al., 2010; De Ridder et al., 2013; De Vos et al., 2013). De Ridder et al. (2013) found that burst SCS decreased visual analog scale (VAS) pain scores more than tonic SCS for back pain and general pain perception in patients undergoing brief trials with each stimulation modality, including those with cervical radicular pain. Patients report greater pain relief from burst SCS than from tonic SCS in a placebo-controlled trial (De Ridder et al., 2013), as well as when burst SCS is introduced after at least six months of tonic stimulation (De Vos et al., 2013). Furthermore, burst SCS has been shown to be more effective than tonic SCS for attenuating visceral nociception in a rat model of colorectal distension (Tang et al., 2014). Although burst SCS has been postulated to provide improved pain relief over tonic SCS via delivering more charge per second to the spinal dorsal columns (De Ridder et al., 2010), the role of charge delivery in burst SCS has not been investigated.

The burst SCS waveform is highly adaptable by modifying any of the parameters that control the shape of the waveform – the number of pulses per burst, the frequency of pulses within each burst, the pulse width, the frequency of bursting, or the amplitude (Fig. 6.1). To date, the clinical and preclinical studies using burst SCS have used the same stimulation parameters: 5 pulses per burst, 500Hz pulse frequency, 1ms pulse width, and 40Hz burst frequency (De Ridder et al., 2010; De Ridder et al., 2013; De Vos et al., 2013; Tang et al., 2014). Even though tonic SCS is frequently optimized for pain management on a patient-by-patient basis by adjusting pulse width, frequency, and amplitude (Alo et al., 1999; Smits et al., 2013), there have been no studies, clinical or preclinical, investigating the optimization of burst SCS for neuropathic pain with respect to any of the parameters defining the stimulation waveform or the charge delivery.

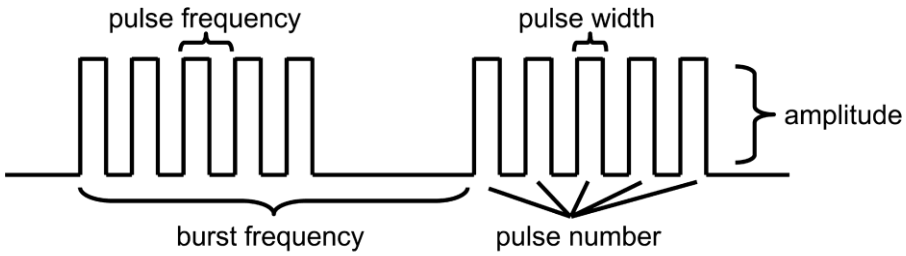

Fig. 6.1. Schematic of a burst SCS waveform. Five parameters define the shape of the stimulation: pulse number, pulse frequency, pulse width, burst frequency, and amplitude.

Cervical radiculopathy and cervical brachialgia are neuropathic pain conditions that cause neck, shoulder, and arm pain from compression of the cervical spinal nerves and/or nerve roots, and are common indications for SCS (Alo et al., 2002; De Ridder et al., 2013; Rizvi and Kumar, 2013). However, the stimulation parameters associated with effective burst SCS have not been systematically evaluated for these indications. This study tests the hypotheses that burst SCS is effective in reducing dorsal horn neuronal firing associated with cervical radicular pain, and that altering burst SCS parameters modulates the effects of stimulation on neurons in the spinal dorsal horn. A model of nerve root compression that induces behavioral sensitivity and spinal neuronal hyperexcitability in the rat is used to evaluate neuronal activity immediately before and after application of burst SCS (Nicholson et al., 2014a; Smith et al., 2013; Zhang et al., 2013). The effects of burst SCS are measured specifically in wide dynamic range (WDR) and high-threshold (HT) dorsal horn neurons, because those two dorsal horn neuronal populations are responsible for processing nociceptive signals (Steeds, 2009). In order to evaluate the sensitivity of burst SCS effectiveness to each burst parameter (Fig. 6.1), each parameter is varied across a range of several values that could be used for clinical

application of burst SCS. This study also investigates the modulation of charge per burst as a potential mechanism for the sensitivity of burst SCS to changes in the stimulation parameters.

6.3. Methods

6.3.1. Nerve Root Compression Surgery

Male Holtzman rats (386-466g) were housed under USDA- and AAALAC-compliant conditions with free access to food and water. All experimental procedures were approved by the University of Pennsylvania Institutional Animal Care and Use Committee and carried out under the guidelines of the Committee for Research and Ethical Issues of the International Association for the Study of Pain (Zimmerman, 1983).

Compression of the right C7 dorsal nerve root was performed with rats (n=8) under isofluorane inhalation anesthesia (4% for induction, 2-3% for maintenance) using procedures previously described (Hubbard and Winkelstein, 2005; Rothman and Winkelstein, 2007; Rothman and Winkelstein, 2010). With the rat in a prone position, the C6 and C7 vertebrae were exposed by making a midline incision from the base of the skull to the T2 vertebra and separating the overlying muscular tissue. A C6/C7 hemilaminectomy and partial facetectomy on the right side exposed the C7 dorsal nerve root between the dorsal root ganglion and the spinal cord. A 10gf microvascular clip (World Precision Instruments; Sarasota, FL) was inserted through a small incision in the dura to compress the nerve root for 15 minutes. After the surgical procedure, incisions were closed using 3-0 polyester sutures and surgical staples. Rats were monitored during recovery in room air, and then returned to normal housing conditions.

6.3.2. Assessment of Mechanical Hyperalgesia

Behavioral sensitivity was assessed by measuring mechanical hyperalgesia in both forepaws of each rat prior to surgery (baseline) and on days 1, 3, 5, and 7 after nerve root compression. Hyperalgesia was assessed separately in the ipsilateral and contralateral forepaws by quantifying the paw withdrawal threshold (PWT) during application of a series of weighted von Frey filaments (1.4, 2, 4, 6, 8, 10, 15, and 26g) to the plantar surface of the paw (Chang and Winkelstein, 2011; Hubbard and Winkelstein, 2005; Zhang et al., 2013). Each filament was applied five times to determine if the rat displayed a positive response to that filament weight; a positive response was taken as withdrawing, licking, or shaking of the paw. If the rat displayed a positive response to two consecutive filaments, the lower of the two filament weights was recorded as the PWT. Rats not responding to any of the filaments were assigned the maximum PWT of 26g. On each designated day, testing was repeated in three rounds separated by at least ten minutes, and the average threshold from the three rounds was calculated for each paw and each rat. A repeated-measures ANOVA compared the PWTs between the ipsilateral and contralateral forepaws at each time point.

6.3.3. Electrophysiological Recordings and Burst Spinal Cord Stimulation

After hyperalgesia testing on day 7, extracellular electrophysiological recordings were acquired in the spinal dorsal horn to measure neuronal firing before and after burst SCS. Rats were anesthetized with sodium pentobarbital (50mg/kg, i.p.) and given supplemental doses (5-10mg/kg, i.p.) as needed based on toe pinch, corneal, and palpebral reflexes (Field et al., 1993). A bilateral laminectomy and dural resection from

C3 to C7 were performed to expose the spinal cord. Rats were then immobilized on a stereotaxic frame (David Kopf Instruments; Tujunga, CA) using ear bars and a vertebral clamp at T2 to stabilize the cervical spine. Core temperature was maintained at 35-37ºC using a temperature controller with a rectal probe (Physitemp; Clifton, NJ), and the exposed spinal cord was bathed in 37ºC mineral oil for the duration of recording to prevent drying.

A monopolar platinum ball electrode was placed on the surface of the dorsal columns at the C4 level (Fig. 6.2), and a grounding electrode was attached to the incised skin on the neck. Constant-current burst spinal cord stimulation was applied using an S48 Grass stimulator with a photoelectric stimulus isolation unit (Grass Technologies; Warwick, RI). The motor threshold (MT) for each rat was identified as the stimulation

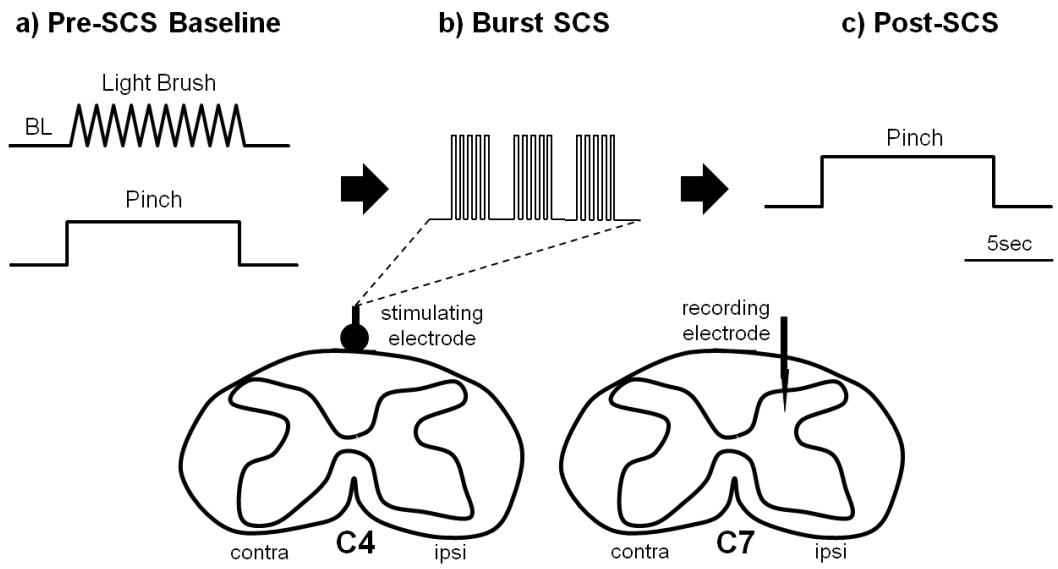

Fig. 6.2. Stimulation protocol for burst SCS optimization. Burst SCS was applied to the dorsal columns at the C4, and neuronal firing was recorded in the C7 dorsal horn ipsilateral to the site of nerve root compression. **(a)** Spontaneous firing was recorded in a 10sec baseline (BL) period, followed 10sec of light brush and 10sec of noxious pinch at the forepaw. **(b)** Burst SCS was applied for 10sec. **(c)** A 10sec pinch was applied to the forepaw to record evoked firing immediately after SCS.

intensity at which small contractions were first observed in the paraspinal musculature or forelimbs. Extracellular potentials were recorded by lowering a carbon fiber electrode (Kation Scientific; Minneapolis, MN) into the C7 spinal dorsal horn on the side ipsilateral to the compressed nerve root. Signals were amplified with a gain of 10^3 and conditioned using a bandpass filter between 0.3 and 3kHz (World Precision Instruments; Sarasota, FL). The signal was processed with a 60Hz HumBug adaptive filter (Quest Scientific; North Vancouver, BC), digitally sampled at 25kHz (Micro1401, CED; Cambridge, UK), monitored with a speaker for audio feedback (A-M Systems; Carlsborg, WA) and recorded using Spike2 software (CED; Cambridge, UK).

The carbon fiber electrode was lowered into the spinal cord until a recording site in the dorsal horn was identified where evoked firing from mechanically-sensitive neurons was detected during light brushing and noxious pinch of the ipsilateral forepaw. To evaluate changes in neuronal activity due to burst SCS, the neuron (or neurons, if multiple waveforms could be differentiated at a single recording site) underwent multiple spinal cord stimulation trials (Fig. 6.2). Each stimulation trial consisted of: (1) at least ten seconds of recording to establish baseline spontaneous firing; (2) ten seconds of light brushing and ten seconds of noxious pinch of the forepaw by forceps in order to classify the neuron as WDR or HT, and to establish pre-SCS evoked firing; (3) ten seconds of burst spinal cord stimulation (Fig. 6.1); (4) ten seconds of noxious forepaw pinch to record post-SCS evoked firing; and, (5) at least 20 minutes of rest in order to allow the neuron to recover from the effects of burst SCS.

For each recording site, the first stimulation trial applied burst SCS consisting of 7 pulses per burst at 500Hz with a 1000μs pulse width, a burst frequency of 40Hz, and

amplitude of 90% MT. From that reference parameter set, each of the five parameters was varied individually in subsequent stimulation trials with the remaining four parameters held constant (Table 6.1). At least three separate values were tested for each parameter (Table 6.1), in consecutive stimulation trials at the same recording site. The different values for each parameter were tested in a random order to avoid any effect of the order of application. At the lowest pulse frequency (250Hz), the inter-burst interval was not long enough for each burst to contain 7 pulses with 1000μs width, so bursts of 5 pulses were applied when testing different pulse frequencies.

Table 6.1. Burst SCS conditions and parameter values.

Pulse Number	Pulse Frequency	Pulse Width	Burst Frequency	Amplitude
3 pulses	250Hz	250μs	20Hz	30% MT
5 pulses	333Hz	500μs	40Hz*	60% MT
7 pulses*	500Hz*	750μs	60Hz	90% MT*
		1000μs*		

*reference parameter set; MT = motor threshold

6.3.4. Electrophysiological Data Analysis

Voltage potentials from each recording site were spike-sorted using Spike2 (CED; Cambridge, UK) to differentiate waveforms from individual neurons. A detailed protocol for spike sorting is included in Appendix A. Each neuron was classified as either WDR, if firing was evoked by both light brush and noxious pinch, or HT, if firing was only evoked by a noxious pinch. Low threshold (LT) neurons responding only to light mechanical stimuli were not included in this study since LT neurons do not respond to noxious pinch, which was used as the test stimulus. Pre- and post-SCS firing were determined by counting the number of spikes evoked by noxious pinch in the ten seconds

before, and the ten seconds immediately following, the application of burst SCS. Voltage potentials during SCS were not visible due to the large artifacts from stimulation that masked neuronal activity; therefore, measurements of neuronal responses were only performed before and after SCS. Baseline spontaneous activity was subtracted from the spike counts for each pinch in order to isolate the neuronal response evoked by the noxious pinch itself.

Two metrics of neuronal activity were used to evaluate the effects of burst SCS on dorsal horn neuronal firing. First, the percent change in evoked neuronal firing after burst SCS was calculated relative to the firing evoked before SCS. Neurons having a negative percent change in firing after burst SCS (i.e., a reduction in spikes) were considered to be responsive to burst SCS. The percentage of responsive neurons for each set of stimulation parameters was used as a second measure of SCS efficacy. A bivariate linear regression tested for correlation between each parameter and changes in neuronal firing among responsive neurons only. The effect of each parameter on the percentage of neurons responding to burst SCS was tested using Fisher's exact test.

The charge per burst delivered to the spinal cord was calculated for each parameter by integrating the waveform of the constant-current stimulation over time during a single burst. Changes in WDR and HT neuronal firing were averaged at each charge value across all stimulation trials. The correlations between charge per burst and percent changes in neuronal firing were then tested separately for WDR and HT neurons using bivariate linear regression. Percentages of responsive WDR and HT neurons in each stimulation trial were binned by charge per burst; bins were chosen to span the full

range of charge values, in ten equal increments of 0.1μC. All statistical analyses were performed with α=0.05 using JMP9 (SAS; Cary, NC).

6.4. Results

The paw withdrawal threshold (PWT) of the ipsilateral forepaw is significantly reduced from baseline on each of days 1, 3, 5, and 7 after injury ($p<0.017$) (Fig. 6.3). The contralateral PWT is not significantly different from baseline throughout the seven day period after injury (Fig. 6.3). In addition, the PWT of the ipsilateral forepaw is significantly lower than the PWT of the contralateral forepaw on all days following nerve root compression ($p<0.019$), despite the ipsilateral and contralateral PWTs not being different at baseline (Fig. 6.3). Appendix J includes the paw withdrawal thresholds for each rat on each day after nerve root compression.

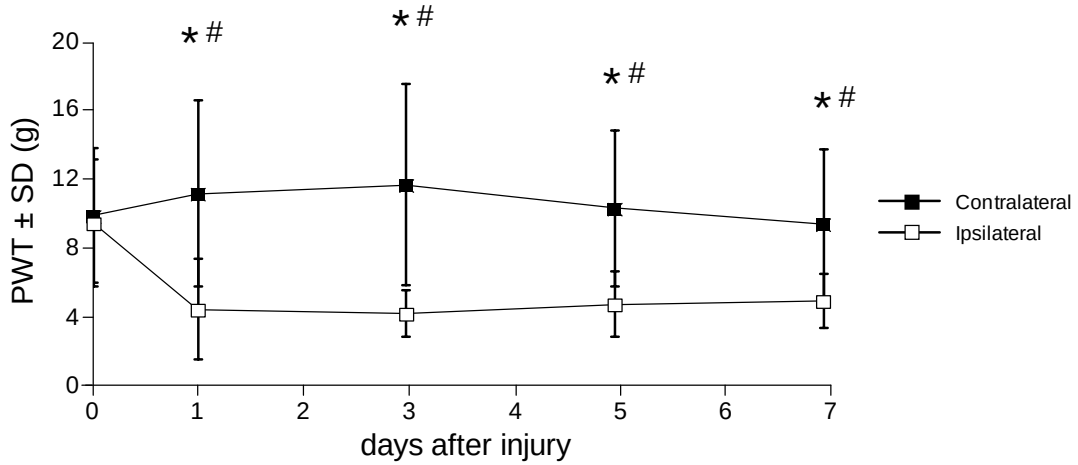

Fig. 6.3. Mechanical hyperalgesia after painful cervical nerve root compression. Nerve root compression induces a significant decrease in paw withdrawal threshold (PWT) for the ipsilateral forepaw compared to both baseline (*$p<0.017$) and the contralateral forepaw (#$p<0.019$) on each day after injury.

Neuronal firing was recorded at 25 different sites in the spinal cord (3.0±1.1 recording sites per rat). At each recording site, 4.1±1.4 stimulation trials were performed. Each of the five burst parameters was tested at 6.8±1.8 separate recording sites. Of the 25 recording sites, nine sites with stable signals were used to test multiple parameters consecutively. Neuronal firing evoked by noxious pinch is reduced to varying degrees based on the burst parameters (Fig. 6.4). Among the neurons that are responsive to burst SCS (n=191 neurons from all recording sites and stimulation trials), pulse number (p=0.0018), pulse width (p=0.0001), and amplitude (p=0.0086) are each significantly correlated to reductions in evoked neuronal firing after burst SCS (Fig. 6.5). Neuronal firing is reduced more with each increase in those parameters. Pulse frequency and burst frequency are not correlated to changes in neuronal firing after burst SCS (Fig. 6.5). Evoked spike counts for each neuron from each rat are included in Appendix D.

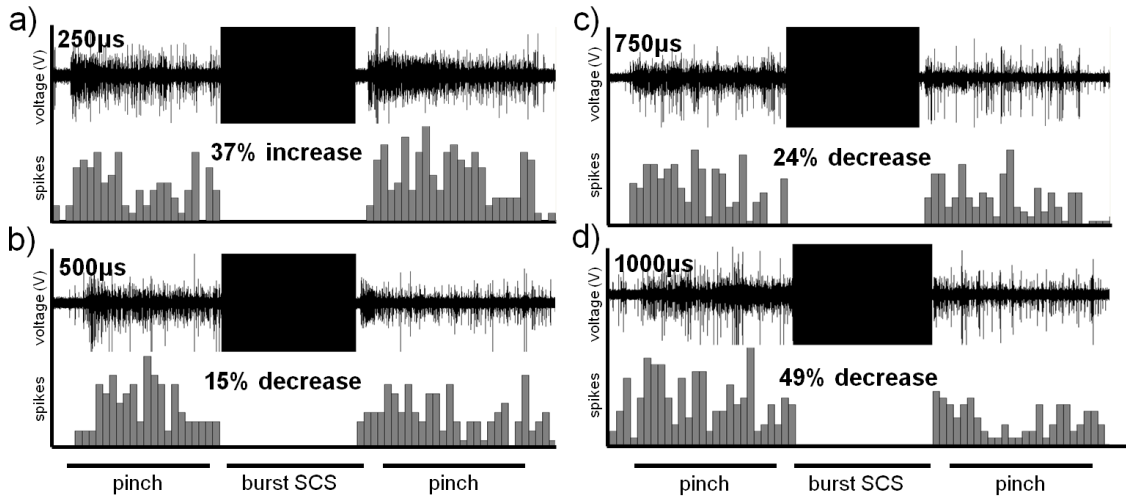

Fig. 6.4. Attenuation of neuronal firing by burst SCS. Neuronal firing evoked by noxious pinch of the ipsilateral forepaw is attenuated by burst SCS to varying degrees depending on the burst parameters. In this representative neuron, activity is suppressed more as pulse width increases from **(a)** 250µs to **(b)** 500µs, **(c)** 750µs, and **(d)** 1000µs. In this case, the other parameters are fixed: pulse number=7; pulse frequency=500Hz; burst frequency=40Hz; amplitude=90% MT.

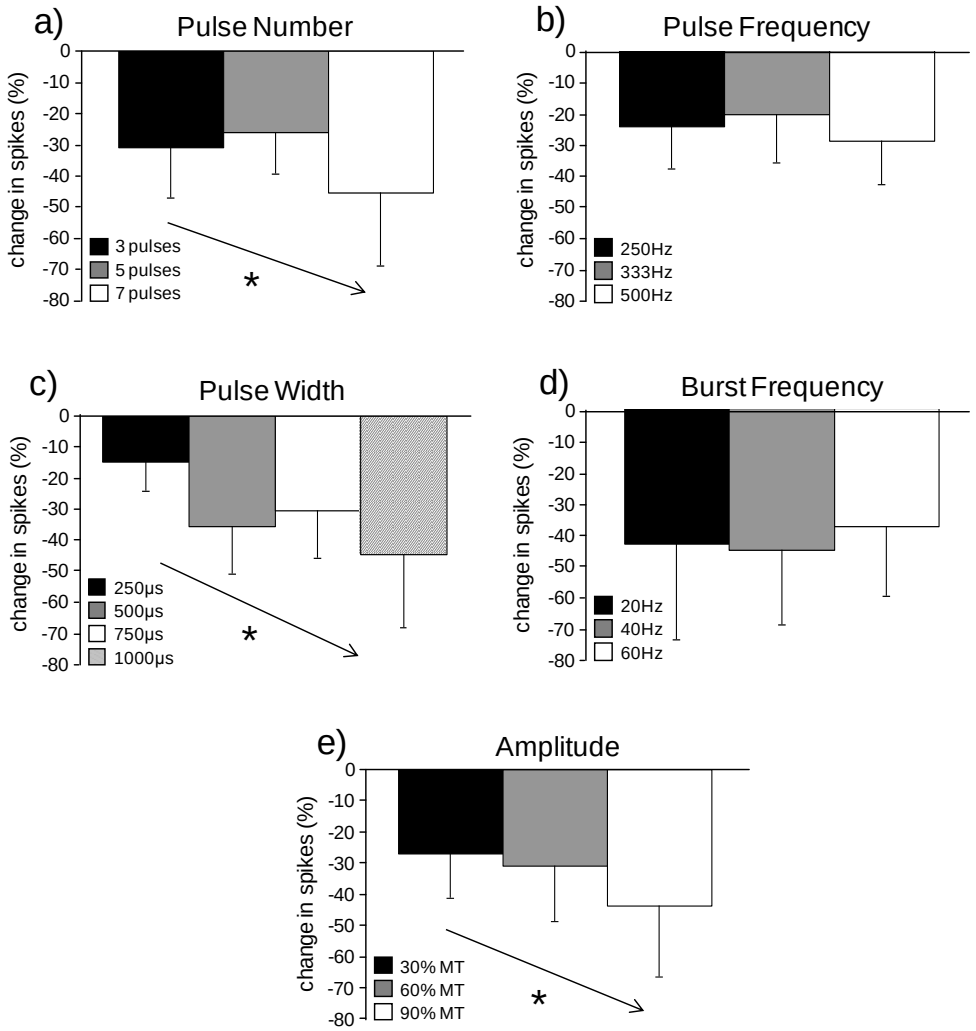

Fig. 6.5. Effect of burst parameters on the attenuation of neuronal firing. The change in neuronal firing for each set of parameters after burst SCS is shown as the percent change in spikes relative to pre-SCS baseline firing: **(a)** pulse number, **(b)** pulse frequency, **(c)** pulse width, **(d)** burst frequency, and **(e)** amplitude. Asterisks and arrows indicate significant negative correlations between each of pulse number ($p=0.0018$), pulse width ($p=0.0001$), and amplitude ($p=0.0086$), and the reduction in neuronal activity after burst SCS.

The percentage of responsive neurons exhibiting a reduction in firing after burst SCS is significantly related to the pulse frequency ($p=0.05$) and the amplitude of stimulation ($p=0.023$) (Fig. 6.6). As the pulse frequency and amplitude increase, the

percentage of responsive neurons also increases. Although the percentage of responsive neurons also increases with higher pulse numbers (p=0.13) and pulse widths (p=0.078), those relationships are not significant (Fig. 6.6). Altering burst frequency has no effect on the percentage of responsive neurons (Fig. 6.6).

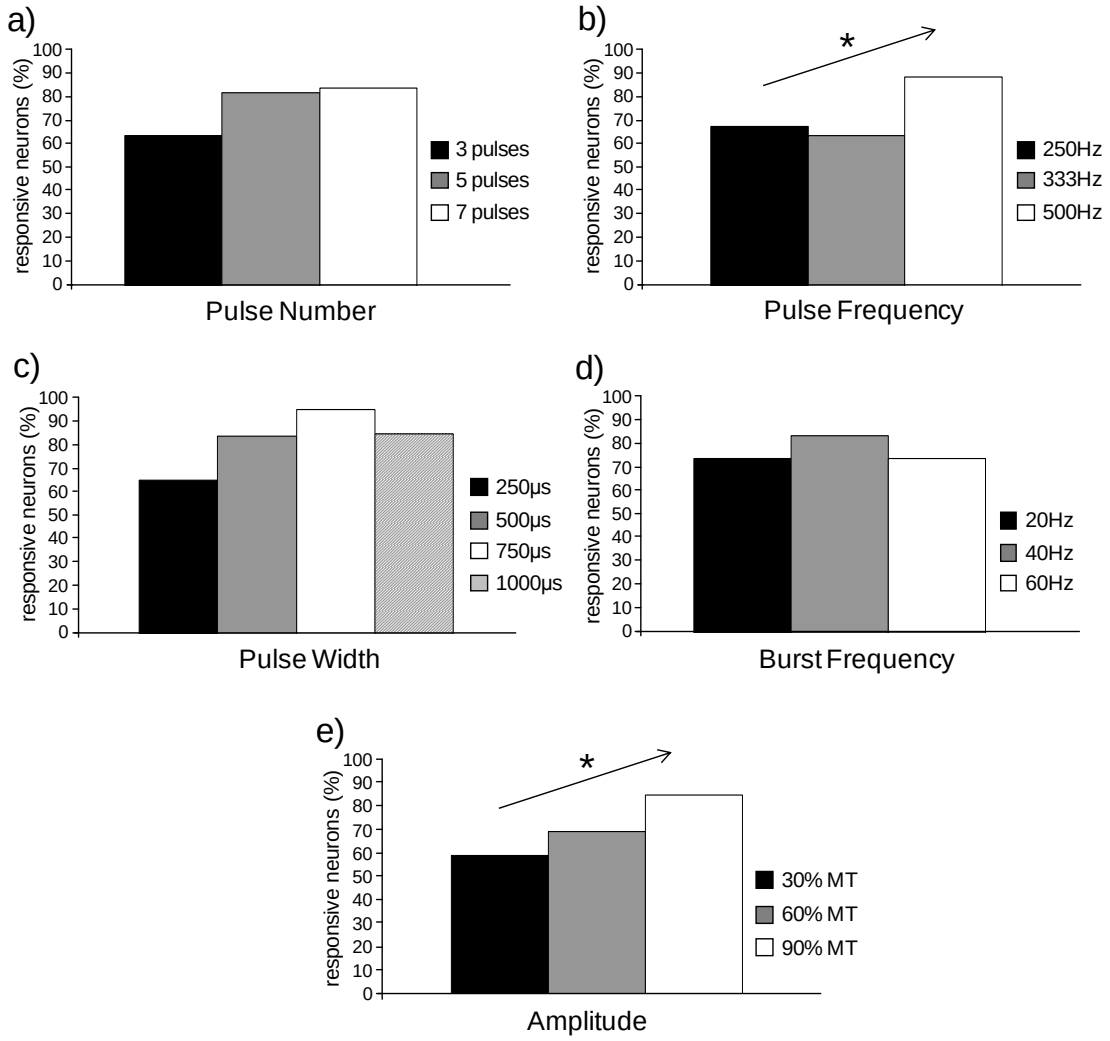

Fig. 6.6. Effect of burst parameters on the percentage of responsive neurons. The percentage of neurons responding to burst SCS with a decrease in evoked firing is shown for each level of the burst parameters: **(a)** pulse number, **(b)** pulse frequency, **(c)** pulse width, **(d)** burst frequency, and **(e)** amplitude. Asterisks and arrows indicate significant positive correlations between each of pulse frequency (p=0.05) and amplitude (p=0.023), and the percentage of responsive neurons.

Charge per burst delivered to the spinal cord is highest for the reference parameter set (7 pulses, 500Hz pulse frequency, 1000μs pulse width, 40Hz burst frequency, 90% MT amplitude), ranging from 0.76-1.07μC, with some variation due to the differences in motor threshold between rats (Fig. 6.7a). Pulse number, pulse width, and amplitude are each directly proportional to the charge per burst, so changes in each of those parameters results in a wide range of charges per burst during stimulation trials (Fig. 6.7a). Pulse frequency and burst frequency do not affect charge per burst (Fig. 6.7a), aside from the variation due to motor threshold differences between rats.

Charge per burst is negatively correlated with changes in neuronal firing among responsive WDR neurons (n=141) after burst SCS (R^2=0.30, p=0.0017) (Fig. 6.7b). Among responsive HT neurons (n=50), neuronal firing also decreases as charge per burst increases, although that correlation is not significant (R^2=0.14, p=0.13). The total percentage of neurons responding to SCS increases nonlinearly with charge per burst, exhibiting a step transition from 65% responding (35% not responding) at charges below 0.5μC, to 80-85% of neurons responding (15-20% not responding) at charges above 0.5μC (Fig. 6.7c). The percentage of WDR neurons responding to burst SCS remains high, averaging 83±6% across all charge values (Fig. 6.7c). But, the responsiveness of HT neurons exhibits a large increase from 45±4% at charges below 0.5μC to 78±7% at charges above 0.6μC; no HT neurons were recorded after stimulation having a charge per burst between 0.5μC and 0.6μC (Fig. 6.7c).

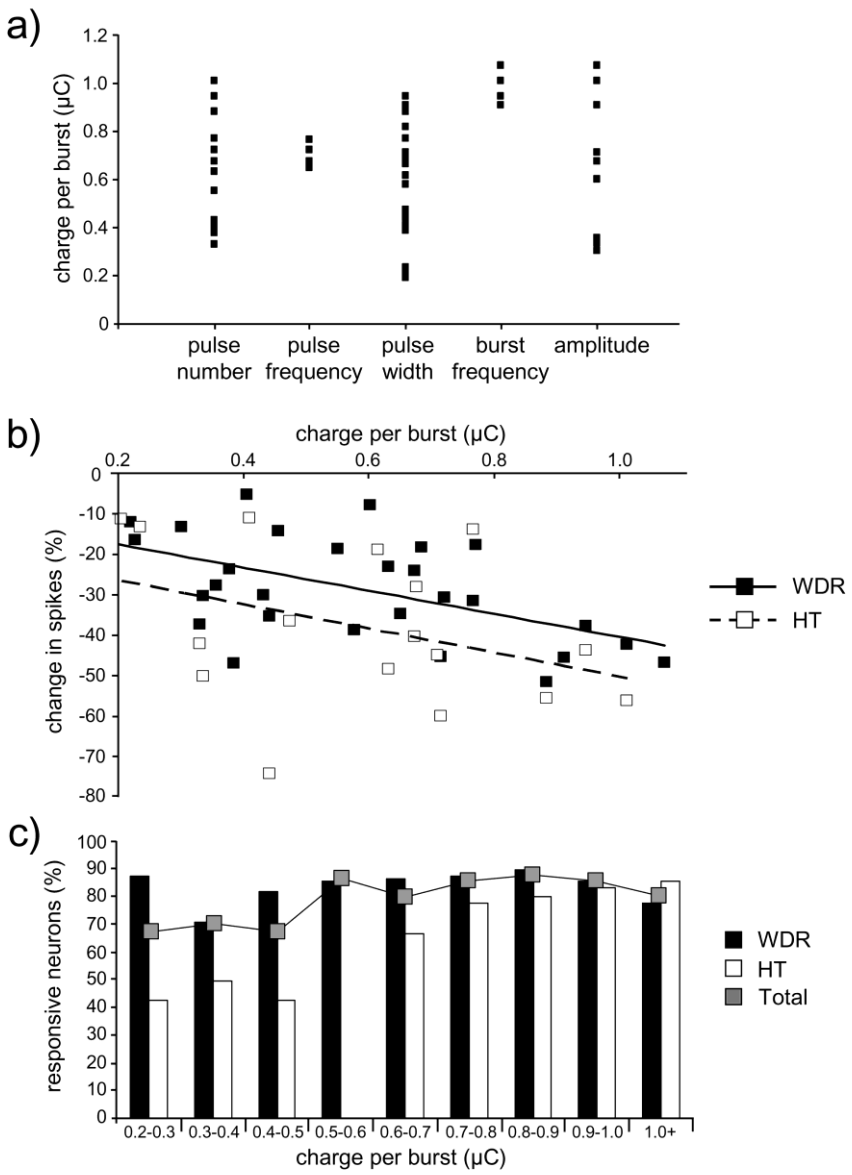

Fig. 6.7. Charge per burst determines the effectiveness of burst SCS. **(a)** Pulse number, pulse width, and amplitude have the greatest range of charges tested across the stimulation trials associated with each parameter. Charge is constant across all pulse frequencies and across all burst frequencies, aside from small variations due to motor threshold differences between rats. **(b)** Percent change in firing of wide dynamic range (WDR) and high threshold (HT) neurons is negatively correlated to charge per burst, but the correlation is significant only for WDR neurons ($p=0.0017$). **(c)** The percentage of WDR neurons responding to SCS is unchanged by charge per burst. The percentage of HT neurons and total percentage of all neurons responding to burst SCS exhibit a step response, increasing when charge per burst exceeds 0.5μC. No HT neurons were collected in the 0.5 to 0.6μC per burst range.

6.5. Discussion

This study demonstrates that burst SCS reduces dorsal horn neuronal responses to noxious stimulation of the forepaw after painful compression of the cervical nerve root in rats (Figs. 6.3-6.5). Changes in neuronal activity following burst SCS are mediated by the stimulation parameters that define the burst waveform. Three parameters in particular – number of pulses per burst, pulse width, and amplitude – are each significantly correlated to the changes in evoked neuronal firing after burst SCS (Fig. 6.5). Pulse frequency has a significant effect on the percentage of recorded neurons responding to burst SCS (Fig. 6.6). Furthermore, the charge per burst delivered to the spinal cord is correlated to the decrease in responses of both WDR and HT neurons after burst SCS (Fig. 6.7). Together, these findings show that the effects of burst SCS are highly dependent on the burst stimulation parameters, suggesting that the reduction of pain symptoms by burst SCS could be maximized by optimizing the burst parameters on a patient-by-patient basis.

The effectiveness of burst SCS, as measured by changes in dorsal horn neuronal firing after stimulation, varies with the parameters and conditions of the burst stimulation. For example, the most effective burst SCS paradigm is found when using the reference parameter settings (7 pulses at 500Hz and 1000μs width, 40Hz bursts, and 90% MT amplitude), after which neuronal firing is reduced by 44.8±23.3% across the 84.7% of neurons that respond to SCS (Figs. 6.5 and 6.6). When the pulse width is adjusted from 1000μs to 250μs, neuronal firing is reduced only 15.1±9.4%, with 65.4% of neurons responding to stimulation (Figs. 6.5 and 6.6). At its maximum effectiveness, burst SCS suppresses up to 44.8% of neuronal activity, which is comparable to the only other study that has applied burst SCS in an animal model of pain (Tang et al., 2014). That study

demonstrates that burst SCS reduces firing in lumbar dorsal horn neurons by up to 41.5% during noxious pinch and up to 22.6% during colorectal distension (Tang et al., 2014), suggesting that burst SCS may similarly suppress both nociceptive and chronic neuropathic pain.

The attenuation of spinal neuronal firing in this study of neuropathic pain suggests that burst SCS reduces signaling in pain pathways in the dorsal horn that include WDR and HT secondary neurons. Inhibiting firing of WDR and HT neurons likely reduces aberrant nociception after neural tissue injury, because those are the two second-order neuronal populations in the dorsal horn that process painful signals (Steeds, 2009). Those findings are consistent with reductions in the visual analog scale (VAS) pain scores reported after burst SCS in a clinical study (De Ridder et al., 2013). Although burst SCS decreases neuronal activity by attenuating firing in dorsal horn neurons that exhibit hyperexcitability after nerve root compression (Nicholson et al., 2014a; Smith et al., 2013; Zhang et al., 2013), studies measuring behavioral sensitivity after SCS are needed in order to draw more direct conclusions about the modulation of pain by burst SCS.

The reduction in neuronal response to noxious pinch following burst SCS is significantly correlated to charge per burst delivered during stimulation (Fig. 6.7b). SCS causes antidromic signaling, in which stimulated axons in the dorsal columns conduct action potentials from the site of stimulation back into the dorsal horn (Oakley and Prager, 2002). Antidromic activation of spinal inhibitory interneurons by large-diameter Aβ fibers suppresses firing in dorsal horn neurons to block nociceptive signaling, as proposed by the gate theory of pain and supported by reports of attenuation of dorsal horn excitability by dorsal column stimulation (Daniele and MacDermott, 2009; Dubuisson,

1989; Guan, 2012; Guan et al., 2010; Linderoth and Foreman, 1999; Melzack and Wall, 1965; Yakhnitsa et al., 1999). The current required to activate a stimulated axon increases with the distance of the axon from the point of stimulation (Brocker and Grill, 2013). Therefore, increased charge delivery may enhance current penetration and subsequent antidromic activation of large-diameter Aβ fibers in the dorsal columns (Compton et al., 2012; Holsheimer, 2002), resulting in the increased attenuation of WDR and HT neuronal activity that is observed at higher charges (Figs. 6.5 and 6.7b). The charge per burst is also nonlinearly related to the percentage of neurons responding to burst SCS, most notably an increase in responsive HT neurons at higher charges (Fig. 6.7c). As charge delivery increases, stimulation may activate fibers of decreasing diameter that have higher activation thresholds (Holsheimer, 2002; Kreis and Fishman, 2009), increasing the number of active dorsal column fibers and overall inhibitory tone in the dorsal horn. The percentage of responsive WDR neurons remains constant and is higher than HT neurons at low charge values (Fig. 6.7c), suggesting that WDR neurons are more susceptible than HT neurons at low charges to the stimulation-induced attenuation of dorsal horn neuronal firing (Guan et al., 2010; Yakhnitsa et al., 1999).

Despite the increase in responsive HT neurons observed at higher charges, a subset of neurons (15-40% of both WDR and HT neurons) never respond to burst SCS regardless of increasing burst parameters (Figs. 6.5 and 6.7c). Computational models of fiber recruitment during dorsal column stimulation suggest that SCS activates fibers that are located only near the surface of the dorsal columns (Holsheimer et al., 2002). It is possible that the unresponsive dorsal horn neurons may be those that are inhibited only by activity in deeper dorsal column fibers that are not recruited by burst SCS in this

study. However, additional computational models of dorsal column fiber activation during SCS suggest that multi-contact arrays can offer greater control of stimulation field breadth and depth and may activate deeper dorsal column fibers more efficiently to reduce firing in non-responsive dorsal horn neuronal populations (Manola et al., 2007; Sankarasubramanian et al., 2011).

Among the individual parameters investigated here, pulse number, pulse width, and amplitude each have substantial influence on the effectiveness of burst SCS, correlating to reductions in neuronal firing and/or increases in the percentage of responsive neurons (Figs. 6.5 and 6.6). Pulse number, pulse width, and amplitude are also the only parameters that are directly proportional to charge per burst and have the greatest range of charges tested across stimulation trials (Fig. 6.7a). These results further support that modulation of charge per burst is the underlying factor that regulates the effectiveness of burst SCS. Increases in pulse frequency result in a greater percentage of neurons responding to burst SCS, especially at the highest pulse frequency (500Hz) (Fig. 6.6b). Afferent fibers are activated in a frequency-specific fashion by sine-wave stimulation, with the large diameter Aβ fibers found in the dorsal columns progressively activated as stimulation frequencies increase from 5 to 250 to 2000Hz (De Ridder et al., 2013; Koga et al., 2005; Tang et al., 2014). Studies of frequency-dependent neuronal activation have not been performed with the square-wave stimulation used in SCS. Nonetheless, increases in burst SCS pulse frequency may selectively activate more Aβ fibers in the dorsal columns and inhibit greater numbers of WDR and HT neurons in the dorsal horn without changing charge per burst. Yet, higher pulse frequencies do not directly result in a corresponding decrease in neuronal firing. Therefore, increased

stimulation frequency may also require accompanying changes in other parameters that *do* increase charge per burst in order to enhance suppression of neuronal firing.

This study investigates the parameters that collectively define the shape and intensity of burst stimulation, but other elements of SCS can be modified to adjust charge delivery. For example, monopolar electrodes deliver higher charge densities than bipolar and tripolar stimulation, suggesting that electrode configuration plays an important role in determining charge densities at the surface of the spinal cord (Wesselink and Boom, 1998). Electrodes with small surface areas also yield higher charge densities by concentrating current delivery on a smaller contact area (Wesselink and Boom, 1998). It is also important to note that, as with any animal model, additional studies are needed to fully evaluate the optimization and relative effectiveness of burst SCS in the human. Although animal models enable focused evaluation of specific mechanisms, the findings do not always translate to the human, owing in part to the differences in the delivery of SCS in preclinical and clinical studies. This study used a monopolar ball-shaped electrode, which despite common use in preclinical studies (Tang et al., 2014; Yakhnitsa et al., 1999), may deliver current differently from the directed stimulation applied by insulated bipolar electrode arrays that are used clinically. Therefore, further studies are needed to characterize burst SCS using more clinically relevant stimulation, including larger multi-electrode arrangements with cathode and anode configurations that can steer current to optimize therapeutic outcomes in patients (Manola et al., 2007).

6.6. Conclusions and Integration

The high variability in published outcomes after SCS treatment suggests that understanding of SCS parameters and optimization of stimulation are needed to effectively manage pain (Cameron, 2004; De Vos et al., 2013; Tang et al., 2014; Zhang et al., 2014). The studies in this chapter show that burst SCS is effective for reducing neuronal responses to noxious stimulation in the dorsal horn after painful nerve root compression (Figs. 6.4-6.6) (Crosby et al., 2014b). However, the attenuation of neuronal firing is highly dependent on the parameters of the burst stimulation. Charge per burst is significantly correlated to the effectiveness of burst SCS (Fig. 6.7), indicating that changing the parameters to increase the amount of charge delivered to the spinal cord may, in turn, increase pain relief in patients. This study indicates that patient-specific optimization of burst SCS by modulating its stimulation parameters may provide a greater range of therapeutic approaches for spinal cord stimulation. In studies evaluating the administration of tonic SCS for chronic pain, subjects unanimously preferred patient-controlled stimulation in which amplitude, frequency, and electrode programming could be modified to individually maximize pain relief (Alo et al., 1998; Alo et al., 1999). The results of the current study suggest that, as burst SCS becomes more widely used, similar efforts should be made to maximize analgesia by optimizing, or giving patients more control over, the burst parameters that directly modulate the effectiveness of stimulation.

This work characterizes the sensitivity of burst SCS to changes in the stimulation parameters (Crosby et al., 2014b), providing context for further studies of burst SCS for the treatment of persistent pain. Studies presented in Chapter 7 directly compare burst and tonic stimulation for the attenuation of dorsal horn hyperexcitability; those studies

also evaluate the role of GABAergic signaling in the mechanism of burst SCS. Previous preclinical and clinical studies of burst SCS efficacy used stimulation with bursts of 5 pulses at 500Hz with a 1000μs pulse width, a burst frequency of 40Hz, and amplitude of 90% MT (De Ridder et al., 2010; De Ridder et al., 2013; Tang et al., 2014). Although this work demonstrates that increasing the pulse number to 7 pulses per burst could further attenuate dorsal horn firing and reduce pain symptoms (Crosby et al., 2014b), additional studies of burst SCS in Chapter 7 use this parameter set with 5 pulses per burst to better compare findings in that study with previously published findings.

CHAPTER 7

Evaluating Burst and Tonic Spinal Cord Stimulation for Attenuating Spinal Hyperexcitability

Parts of this chapter were adapted from:

Crosby ND, Weisshaar CL, Goodman-Keiser MD, Smith JR, Zeeman ME, Winkelstein BA. Burst & tonic spinal cord stimulation differentially activate GABAergic mechanisms to attenuate pain in a rat model of cervical radiculopathy. Submitted.

7.1. Overview

Spinal cord stimulation (SCS) is a neurostimulation therapy for chronic pain conditions that are refractory to conventional pharmacological therapies (Guan, 2012). Traditional tonic SCS directly modulates spinal neuronal activity by applying continuous pulses of electrical stimulation to the spinal dorsal columns (Compton et al., 2012). Animal models of persistent pain have offered significant insight into the mechanisms underlying tonic SCS (Linderoth and Foreman, 2006). For example, in a rat model of peripheral nerve injury, tonic SCS has been shown to attenuate the excitability of dorsal horn neurons by stimulating spinal release of the inhibitory neurotransmitter, γ-aminobutyric acid (GABA) (Linderoth et al., 1994; Stiller et al., 1996). Those findings led to the use of GABA agonists to enhance SCS-induced analgesia in human patients (Lind et al., 2004). However, the success rate of tonic SCS varies widely in clinical

studies (Alo et al., 2002; Buyten et al., 2001; Cameron, 2004; Ohnmeiss et al., 1996), so novel modes of SCS have been developed to improve pain relief. Burst SCS, a novel mode of stimulation that applies periodic *bursts* of pulses rather than continuous pulses, has been shown to offer greater reduction of pain than tonic SCS (De Ridder et al., 2010; De Ridder et al., 2013; De Vos et al., 2014). However, the mechanisms underlying the analgesic effects of burst SCS and its reported increase in effectiveness over tonic SCS are poorly understood.

The studies in this chapter address the objectives outlined in Aims 3b and 3c to evaluate the effectiveness of burst SCS and tonic SCS for attenuating spinal hyperexcitability in two established rat models of persistent pain from cervical spine trauma – nerve root compression and facet joint distraction. Because burst SCS reduces pain in patients more effectively than tonic SCS (De Ridder et al., 2010), it was hypothesized that burst SCS would be more effective than tonic SCS for attenuating spinal hyperexcitability. Since tonic SCS acts via GABAergic mechanisms in the dorsal horn to inhibit nociception (Cui et al., 1996; Linderoth et al., 1994), studies here evaluate the role of GABA signaling in the effects of burst SCS after nerve root compression to test the hypothesis that burst SCS also inhibits dorsal horn activity through GABA signaling. In Chapter 6, the effectiveness of burst SCS was found to depend on the parameters of the burst stimulation program. Studies in this chapter use the burst parameters from Chapter 6 that were determined to optimally attenuate dorsal horn neuronal firing, and that also match the parameters used in previous clinical and preclinical studies of burst SCS (De Ridder et al., 2010; Tang et al., 2014). Burst and tonic SCS were applied separately to the dorsal columns on day 7 after painful nerve root

compression to compare the effects of each mode of SCS on dorsal horn neuronal excitability. To determine whether GABA signaling is a necessary component of burst SCS-induced dorsal horn inhibition, $GABA_A$ or $GABA_B$ receptor antagonists were applied to the spinal cord during the administration of burst and tonic SCS on day 7 after painful nerve root compression. In separate rats, burst and tonic SCS were applied on day 7 after painful facet joint injury to compare burst and tonic SCS for the modulation of the spinal hyperexcitability that develops after mechanical joint injury.

7.2. Background

Spinal cord stimulation has been in use for decades to manage chronic, intractable pain from a wide range of indications (Cameron, 2004), including neuropathic pain from injury of neural tissues. In particular, SCS is commonly used to manage chronic pain in the cervical and lumbar spines by delivering pulses of varying frequencies and intensities to the dorsal columns of the spinal cord (Alo et al., 2002; Compton et al., 2012; Stojanovic and Abdi, 2002). Despite many positive reports of SCS being effective for treating chronic pain, the reported success rate of SCS in clinical studies has improved little (Cameron, 2004; Zhang et al., 2014). Better understanding the neurophysiology of chronic pain and defining the mechanisms that underlie SCS-induced analgesia may help to more effectively design and administer SCS therapies.

Conventional tonic SCS administers continuous pulses of stimulation to the dorsal columns from electrodes implanted on the dorsal surface of the spinal cord (Cameron, 2004). Tonic SCS often induces paresthesias, which are aberrant cutaneous tingling or prickling sensations that develop in the anatomical regions where the stimulation is

applied (De Ridder et al., 2010; De Vos et al., 2014). In an effort to improve pain relief and to reduce such side-effects as paresthesia, novel modes of stimulation have been developed. Burst SCS is one such mode of SCS that uses periodic bursts of stimulation for pain management rather than the continuous pulses that are used in tonic SCS (De Ridder et al., 2010). Burst SCS reduces back pain and general pain more effectively and induces less paresthesia than tonic SCS (De Ridder et al., 2013). Furthermore, up to 60% of patients with diabetic neuropathy or failed back surgery syndrome experience greater pain reduction after switching from tonic SCS to burst SCS (De Vos et al., 2014). However, the mechanisms underlying the analgesic effects of burst SCS and its potential increase in effectiveness relative to tonic SCS are still unidentified.

Many neurophysiological and neurochemical mechanisms have been proposed as responsible for the analgesic effects of SCS, including modulation of GABA signaling in the dorsal horn. GABA is the primary inhibitory neurotransmitter in the spinal cord, and acts through $GABA_A$ (ligand-gated) and $GABA_B$ (G-protein-coupled) receptors to inhibit neuronal activity (Malcangio and Bowery, 1996; Yaksh, 2006). Allodynia after nerve injury is often accompanied by decreased GABA levels in the dorsal horn (Drew et al., 2004; Stiller et al., 1996), suggesting a disinhibition of neuronal firing. Tonic SCS has been shown to stimulate GABA release in the dorsal horn that inhibits neuronal firing and attenuates the release of excitatory neurotransmitters like glutamate (Cui et al., 1997; Linderoth et al., 1994).

$GABA_A$ or $GABA_B$ receptor antagonists are commonly used to determine the separate roles of GABA signaling through each receptor subtype. Bicuculline is a competitive antagonist of $GABA_A$ receptors that prevents receptor activation by GABA

or a GABA agonist (Curtis et al., 1970). Bicuculline blocks the rapid synaptic inhibition that is typically mediated by $GABA_A$ receptors, resulting in the disinhibition of spinal motor reflexes (Sivilotti and Woolf, 1994). Similarly, CGP35348 has been used to selectively block $GABA_B$ receptor activation (Olpe et al., 1990). Although CGP35348 does not induce rapid spinal disinhibition like bicuculline (Sivilotti and Woolf, 1994), blocking $GABA_B$ receptors can modulate the analgesic effects of tonic SCS (Cui et al., 1997). Based on those findings, $GABA_B$ agonists like baclofen have been used clinically to enhance the effects of SCS, especially in patients that do not experience sufficient pain relief from SCS alone (Lind et al., 2004; Lind et al., 2008). Despite GABA signaling being implicated in the inhibition of nociception by SCS, studies have been performed only with tonic SCS, and the role of GABA signaling in the analgesic effects of burst SCS is unknown.

Cervical radiculopathy and cervical brachialgia are neuropathic pain conditions that cause neck, shoulder, and arm pain from spinal nerve and/or nerve root compression, and are commonly treated with tonic SCS (Alo et al., 2002; De Ridder et al., 2010; Rizvi and Kumar, 2013). However, no study has directly investigated the relative effectiveness of burst and tonic SCS in modulating spinal neuronal hyperexcitability and dorsal horn inhibition in the context of radicular pain. Furthermore, despite the prevalence of persistent facet-mediated pain, few patients with that indication receive spinal cord stimulation therapies (Kirvela and Kotilainen, 1999; Van Buyten et al., 2001), and no study has evaluated burst SCS for the treatment of persistent facet joint-mediated pain. As such, the studies in this chapter directly compare burst and tonic SCS for the attenuation of dorsal horn neuronal activity in rat models of painful nerve root

compression and painful facet joint injury, both of which induce sustained hyperalgesia and spinal neuronal hyperexcitability (Lee and Winkelstein, 2009; Nicholson et al., 2014a; Quinn et al., 2010b; Smith et al., 2013).

In the first study (detailed in Section 7.3), rats underwent a painful nerve root compression and hyperalgesia was assessed through day 7. To evaluate the effects of burst and tonic SCS on spinal hyperexcitability on day 7, dorsal horn neuronal firing was evaluated before and at several times up to 15 minutes after administering each mode of SCS. Since SCS has been shown to attenuate hyperexcitability in wide dynamic range (WDR) neurons in the dorsal horn (Crosby et al., 2014b; Yakhnitsa et al., 1999), the effects of burst and tonic SCS were specifically evaluated in WDR neurons. In separate groups of rats, the role of GABA signaling in burst and tonic SCS was compared administering bicuculline or CGP35348 to the spinal cord prior to the application of SCS and recording of spinal neuronal activity. In a second study (detailed in Section 7.4), rats underwent painful facet joint injury and hyperalgesia was assessed through day 7. Both burst and tonic SCS were applied at day 7 after painful facet joint injury, as in the first study that evaluated both modes after painful nerve root compression. Dorsal horn neuronal firing was quantified before and at times up to 15 minutes after administering each mode of SCS to compare the effects of each on dorsal horn activity after a painful joint injury.

7.3. Burst and Tonic SCS after Painful Nerve Root Compression: The Role of GABA Signaling

7.3.1. Methods

Male Holzman rats (368-470g) were housed under USDA- and AAALAC-compliant conditions with free access to food and water. All experimental procedures were approved by the University of Pennsylvania Institutional Animal Care and Use Committee and carried out under the guidelines of the Committee for Research and Ethical Issues of the International Association for the Study of Pain (Zimmerman, 1983).

Painful Cervical Nerve Root Compression

Compression of the right C7 dorsal nerve root was performed using procedures described in detail in Section 6.3.1 of Chapter 6, and have been previously reported (Hubbard et al., 2005; Rothman et al., 2007; Rothman et al., 2010). Briefly, rats (n=17) were anesthetized with inhaled isoflurane (4% for induction, 2-3% for maintenance). With the rat in a prone position, a midline incision was made along the back of the neck from the base of the skull to the T2 vertebra. After exposing the C6 and C7 vertebrae, a C6/C7 hemilaminectomy and partial facetectomy on the right side exposed the C7 dorsal nerve root between the dorsal root ganglion and the spinal cord. The nerve root was compressed for 15 minutes with a 10gf microvascular clip (World Precision Instruments; Sarasota, FL) inserted through a small incision in the dura (Fig. 7.1). Incisions were closed using 3-0 polyester suture and surgical staples, and rats were monitored during recovery.

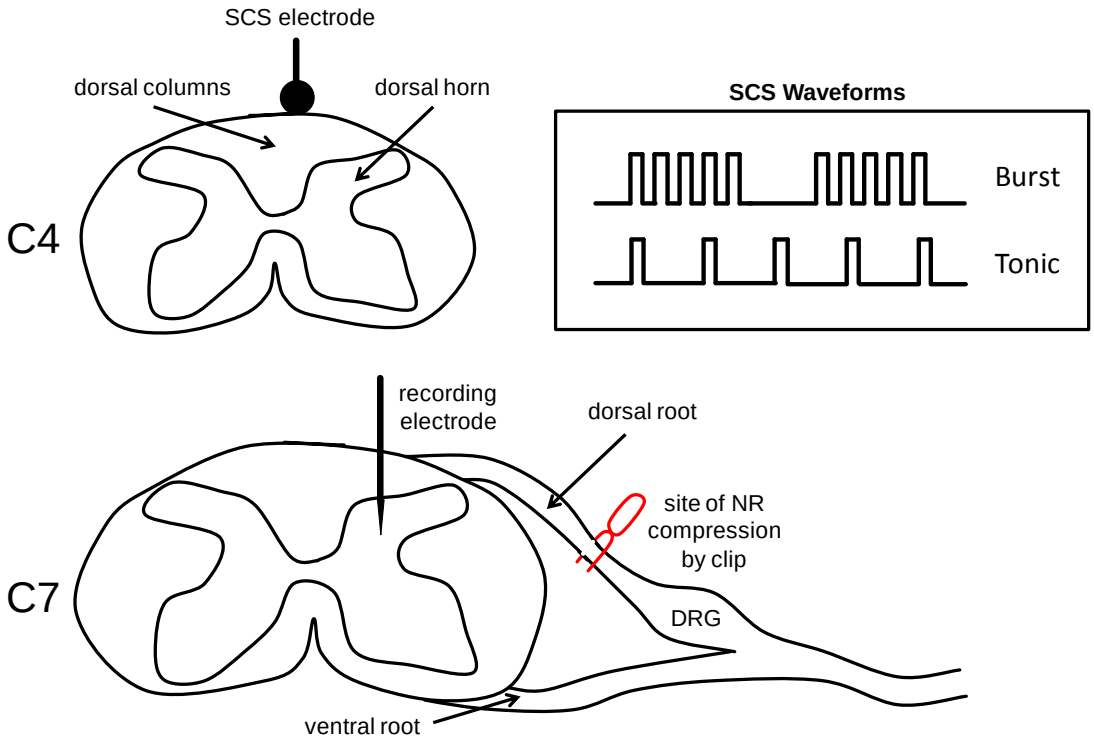

Fig. 7.1. Schematic of a C7 nerve root compression and application of SCS. Painful nerve root (NR) compression was applied to the right C7 dorsal nerve root proximal to the dorsal root ganglion (DRG) with a microvascular clip. On day 7 after NR compression, monopolar burst and tonic SCS waveforms (inset) were applied to the dorsal columns of the C4 spinal cord using a monopolar ball electrode. Evoked neuronal firing was recorded in the C7 dorsal horn ipsilateral to the site of NR compression during mechanical stimulation of the forepaw.

Assessment of Mechanical Hyperalgesia

Mechanical hyperalgesia was evaluated in the ipsilateral and contralateral forepaws of each rat prior to surgery (baseline) and at days 1, 3, 5, and 7 after nerve root compression. Detailed methods for behavioral testing after nerve root compression can be found in Section 6.3.2 of Chapter 6. Hyperalgesia was measured by applying a series of weighted von Frey filaments (1.4, 2, 4, 6, 8, 10, 15, and 26g) to the plantar surface of each forepaw to identify the paw withdrawal threshold (PWT) (Chang and Winkelstein, 2011; Hubbard and Winkelstein, 2005). The average threshold from three rounds of

testing was calculated separately for the ipsilateral and contralateral forepaws of each rat. A repeated-measures ANOVA compared PWTs to baseline and between the ipsilateral and contralateral forepaws at each time point.

Electrophysiological Recordings and Spinal Cord Stimulation

Extracellular electrophysiological recordings were acquired in the dorsal horn on day 7 after painful nerve root compression (n=8 rats) to assess neuronal firing before and after burst and tonic SCS. Rats were anesthetized with sodium pentobarbital (50mg/kg, i.p.) and given supplemental doses (5-10mg/kg, i.p.) as needed based on toe pinch reflexes. With the rat in a prone position, an incision was made along the back of the neck from the base of the skull to the T2 vertebra. A bilateral laminectomy and dural resection were performed to expose the spinal cord from C3 to C7. A tracheotomy was performed and rats were connected to a ventilator and CO_2 monitor to control respiration throughout the recording session (CWE; Ardmore, PA). A lateral thoracotomy was also performed to alleviate intrathoracic pressure and to isolate the spinal cord from any movement of the rat during ventilation. Rats were immobilized on a stereotaxic frame (David Kopf Instruments; Tujunga, CA) using ear bars and a vertebral clamp at T2 to stabilize the cervical spine. The spinal cord was bathed in 37°C mineral oil for the duration of recording, and core temperature was maintained at 35-37°C using a temperature controller with a rectal probe (Physitemp; Clifton, NJ).

A monopolar platinum ball electrode was placed over the C4 dorsal columns (Fig. 7.1), and a grounding electrode was attached to the incised skin on the neck. Constant current stimulation was applied using a Grass stimulator with a photoelectric stimulus

isolation unit (S48 Stimulator; Grass Technologies; Warwick, RI). The motor thresholds for burst and tonic SCS were separately identified in each rat to be the stimulation intensities at which small contractions were first observed in the paraspinal musculature or forelimbs. Burst SCS was applied using parameters that were determined in Chapter 6 to optimally attenuate spinal hyperexcitability: 40Hz burst frequency, 90% of the motor threshold (MT), and each burst contained 5 pulses per burst, 500Hz pulse frequency, 1ms pulse width, and 90% MT amplitude (Crosby et al., 2014b). Tonic SCS delivered pulses at 40Hz with a pulse width of 0.3ms and amplitude of 90% MT (Tang et al., 2014).

A carbon fiber electrode (Carbostar-1, Kation Scientific; Minneapolis, MN) was lowered into the C7 spinal dorsal horn ipsilateral to the compressed nerve root using a micropositioner (Fig. 7.1) (Narishige; Tokyo, Japan). Extracellular potentials were amplified with a gain of 10^3 and conditioned using a bandpass filter between 0.3kHz and 3kHz (World Precision Instruments; Sarasota, FL). The signal was processed with a 60Hz HumBug adaptive filter (Quest Scientific; North Vancouver, BC), digitally sampled at 25kHz (Micro1401, CED; Cambridge, UK). Voltage potentials were monitored with a speaker for audio feedback (A-M Systems; Carlsborg, WA) and recorded using Spike2 software (CED; Cambridge, UK).

As the electrode was lowered into the spinal cord, light brushing and noxious pinch of the ipsilateral forepaw were used to identify mechanically-sensitive wide dynamic range (WDR) neurons and their receptive fields on the paw. Once a neuron was identified, baseline evoked neuronal firing was recorded during mechanical stimulation of the forepaw consisting of five consecutive one-second applications of the non-noxious 1.4g and noxious 26g von Frey filaments, and ten seconds of noxious pinch with forceps

(Fig. 7.2) (Hains et al., 2003a; Quinn et al., 2010b). A baseline period of two seconds was recorded before each stimulus to quantify spontaneous firing (Fig. 7.2). Burst SCS was then applied for five minutes, during which period the evoked firing could not be recorded because artifacts from the stimulation masked neuronal activity. After SCS, evoked activity was recorded during 1.4g von Frey, 26g von Frey, and pinch stimulation immediately (0 minutes) and recording was repeated again at 2, 5, 10, and 15 minutes post-SCS (Fig. 7.2). The stimulation protocol was then repeated in the same neuron using tonic SCS. The protocol was reversed to apply tonic SCS before burst SCS in alternating neurons in order to avoid any effects of the order of burst and tonic SCS application.

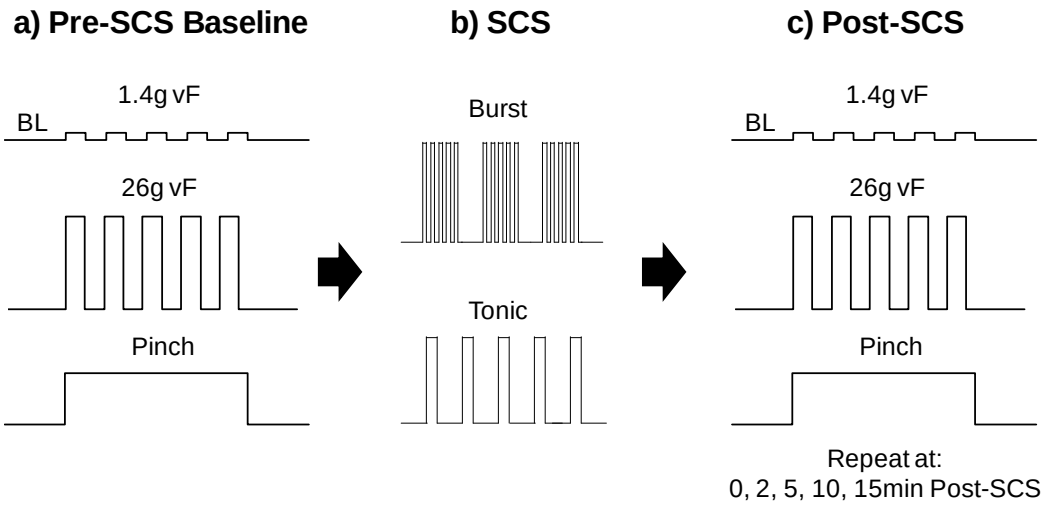

Fig. 7.2. Stimulation protocol for recording evoked neuronal activity after burst or tonic SCS. **(a)** Evoked activity is recorded before SCS during (Pre-SCS Baseline) 1.4g von Frey (vF) filament, 26g vF, and noxious pinch stimulation. Baseline (BL) spontaneous firing is subtracted to isolate the evoked response. **(b)** Burst or tonic SCS is applied for 5 minutes. **(c)** Evoked firing is then recorded during 1.4g vF, 26g vF, and noxious pinch stimulation at 0, 2, 5, 10, and 15 minutes after the SCS application (Post-SCS).

Spinal Superfusion of GABA Receptor Antagonists

Separate groups of rats received spinal application of either the $GABA_A$ receptor antagonist, bicuculline (n=2), or the $GABA_B$ receptor antagonist, CGP35348 (n=7), for the duration of the SCS and dorsal horn electrophysiological recordings on day 7 after a painful nerve root compression. Rats were mounted on the stereotaxic frame and the burst and tonic motor thresholds were determined. The exposed spinal cord from C3 to C7 was then covered with agar (1g agar/40mL 0.9% saline), but agar was cleared from the C7 spinal cord to form a well for superfusion of the drug solutions. Agar was also cleared from the C4 spinal cord to allow contact of the stimulating electrode with the spinal cord. Bicuculline and CGP35348 (Abcam; Cambridge, MA) were solubilized in artificial cerebrospinal fluid (Harvard Apparatus; Holliston, MA). The concentrations of bicuculline (1mM) and CGP35348 (10mM) were chosen based on previous studies applying them to the dorsal spinal cord with effective modulation of spinal GABA signaling (Brumley et al., 2007; Buesa et al., 2006; Buesa et al., 2008; Wang et al., 2013). Peak dorsal horn drug concentrations have been shown to occur after 15-30 minutes of drug superfusion (Beck et al., 1995), so bicuculline or CGP35348 was applied to the C7 spinal cord for 20 minutes before the stimulation and recording protocols were initiated; drug solutions were refreshed every 20-30 minutes throughout the recording session.

Electrophysiology Analysis and Statistics

Voltage potentials from each recorded neuron were sorted and counted using Spike2 software (CED; Cambridge, UK). Pre- and post-SCS firing were determined by counting the spikes evoked separately by the 1.4g filament, 26g filament, and noxious

pinch in the baseline period prior to SCS, and at each time point after SCS. Spontaneous firing was subtracted from the spike counts for each mechanical stimulus in order to isolate firing evoked by the forepaw stimulus. For each of the 1.4g filament, 26g filament, and pinch stimuli, a repeated-measures ANOVA was used to compare the number of evoked spikes between the pre-SCS baseline and evoked firing at each post-SCS time point. Changes in neuronal firing immediately (0 minutes) after SCS were calculated as the percent change in spikes relative to the pre-SCS baseline (Crosby et al., 2014b). For neurons in which both burst and tonic stimulation protocols were completed without losing the signal from the recorded neuron, paired Student's t-tests compared the percent changes in evoked firing immediately after burst SCS to the changes in firing after tonic SCS.

7.3.2. Results

The PWT in the ipsilateral forepaw is significantly reduced from baseline at days 1, 3, 5, and 7 after painful nerve root compression ($p<0.0001$) (Fig. 7.3). PWTs in the ipsilateral and contralateral forepaws are not different from each other at baseline, but the PWT decreases in the ipsilateral forepaw relative to the contralateral side on all days after painful nerve root compression ($p<0.0001$) (Fig. 7.3). The PWT in the contralateral forepaw is unchanged from baseline (Fig. 7.3). Individual PWTs for each rat on each day after painful nerve root compression are summarized in Appendix J.

The average motor threshold is significantly lower for burst SCS relative to tonic SCS ($p\leq0.0002$) (Table 7.1). A total of 49 neurons was recorded following burst SCS and 51 neurons were recorded after tonic SCS (Table 7.1). In 39 of those neurons, paired

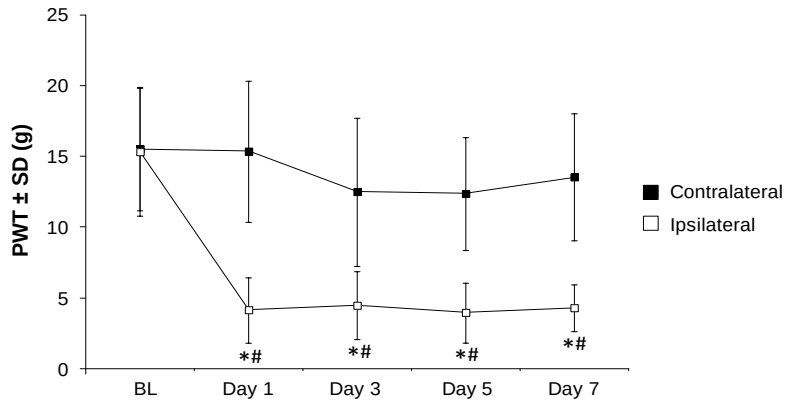

Fig. 7.3. Mechanical hyperalgesia after painful nerve root compression. Paw withdrawal threshold **(**PWT) decreases in the ipsilateral forepaw compared to baseline (*p<0.0001) and compared to the contralateral forepaw (#p<0.0001) after C7 nerve root compression.

Table 7.1. Summary of rat and SCS data for groups receiving painful nerve root compression or NR compression with GABA receptor antagonists.

			Paw Withdrawal Threshold at Day 7 (% of BL)		Motor Threshold (µA)		Total # of Neurons Recorded (# per Rat±SD)	
Group	**Rats**	**Weight (g)**	**Ipsilateral**	**Contralateral**	**Burst**	**Tonic**	**Burst**	**Tonic**
NRC	n=8	412±36	33±11%*	76±26%	182±60	324±68#	49 (6.1±1.5)	51 (6.4±2.3)
NR + Bic	n=2	433±52	20±8%	77±24%	160±0	270±14	10 (5.0±0.0)	10 (5.0±1.4)
NRC + CGP	n=7	396±18	25±10%*	105±34%	183±23	319±58#	29 (4.1±1.3)	30 (4.3±1.7)

NRC = nerve root compression; Bic = bicuculline; CGP = CGP35348
BL = baseline; SD = standard deviation
*p<0.0001, Day 7 vs. BL; #p<0.0002, Tonic vs. Burst

firing data were collected after both burst and tonic SCS. Firing evoked by the 26g filament is significantly reduced by 32±5% from baseline immediately after burst SCS (p<0.0001), and significantly reduced by 26±7% from baseline after tonic SCS (p=0.0014) (Fig. 7.4). Likewise, firing during noxious pinch decreases by 43±4% immediately after burst SCS (p<0.0001), and by 37±4% after tonic SCS (p<0.0001) (Fig. 7.4). The percent reductions in firing after burst and tonic SCS are not different from

each other during either the 26g filament or noxious pinch stimulation (Fig. 7.4). Neuronal firing evoked by 1.4g filament stimulation of the ipsilateral forepaw is not changed from baseline after either mode of stimulation (Fig. 7.4).

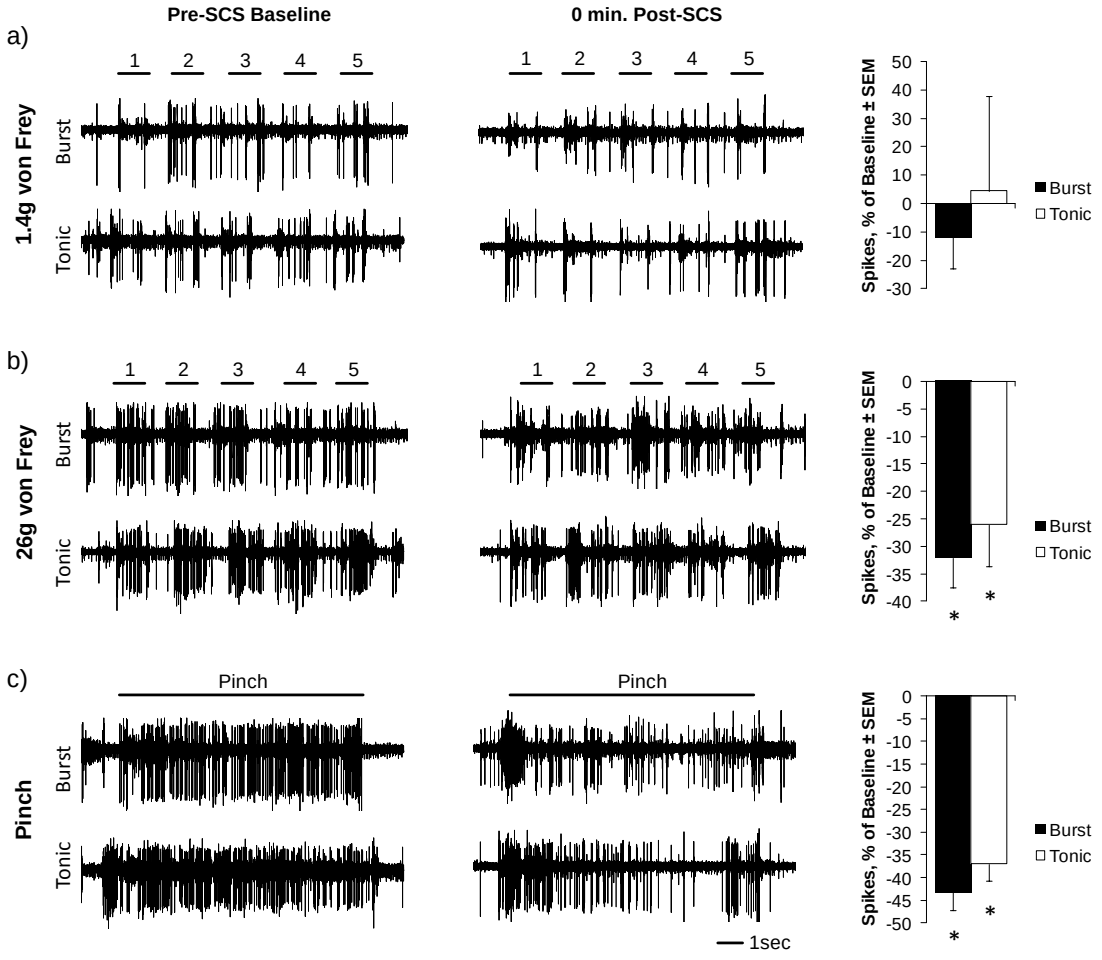

Fig. 7.4. Evoked dorsal horn neuronal activity after burst and tonic SCS application. Neuronal firing was quantified in the C7 spinal cord before (Pre-SCS Baseline) and immediately after (0 min. Post-SCS) burst and tonic SCS at day 7 following painful nerve root compression in response to forepaw stimulation. **(a)** No change in neuronal firing is observed during stimulation of the ipsilateral forepaw by a 1.4g von Frey filament after burst or tonic SCS. Firing is significantly reduced after burst or tonic SCS during **(b)** 26g von Frey filament (*$p \leq 0.0014$) and **(c)** noxious pinch stimulation (*$p < 0.0001$).

The suppressive effects of both burst and tonic SCS on dorsal horn neuronal firing evoked by noxious stimulation are sustained for up to ten minutes after the cessation of SCS (Fig. 7.5). The number of spikes evoked by a 26g von Frey filament stimulation of the ipsilateral forepaw decreases from baseline levels immediately (at 0 minutes) and at 2 minutes after burst SCS ($p \leq 0.0004$). However, after tonic SCS the evoked firing remains decreased during 26g filament stimulation at those times and also at 5 minutes and 10 minutes ($p \leq 0.035$) (Fig. 7.5). The number of spikes evoked during noxious pinch

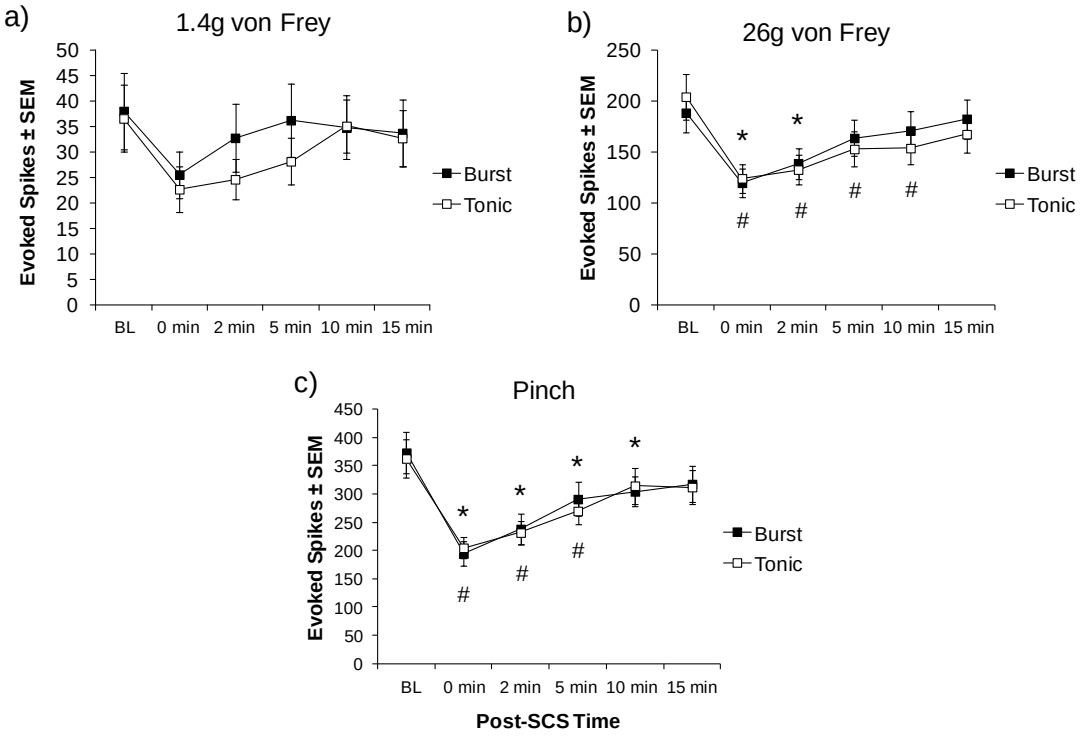

Fig. 7.5. Evoked spike counts for up to 15 minutes after the cessation of burst and tonic SCS application following painful nerve root compression. **(a)** Burst and tonic SCS do not change firing evoked by 1.4g von Frey filament stimulation of the ipsilateral forepaw, relative to the pre-SCS baseline (BL) firing. **(b)** The 26g von Frey filament evokes fewer spikes than at baseline for up to two minutes following the application of burst SCS (*$p \leq 0.0004$), and up to ten minutes after tonic SCS (#$p \leq 0.035$). **(c)** Noxious pinch evokes fewer spikes than at baseline for up to ten minutes after burst SCS (*$p \leq 0.034$), and up to five minutes after tonic SCS (#$p \leq 0.0016$).

stimulation decreases from baseline at all of the time points measured up to 10 minutes after burst SCS ($p \leq 0.034$), although pinch-evoked firing decreases from baseline only at 0 minutes, 2 minutes, and 5 minutes after tonic SCS ($p \leq 0.0016$) (Fig. 7.5). The number of spikes evoked by forepaw stimulation with the non-noxious 1.4g filament is not different from baseline at any recorded time point after burst or tonic stimulation (Fig. 7.5). Of note, despite differences in the duration of the effects of burst and tonic SCS on evoked neuronal activity, evoked firing is not different after burst SCS compared to tonic SCS for any mechanical stimulus at any pre- or post-SCS time point.

The $GABA_A$ receptor antagonist, bicuculline, does not affect the attenuation of neuronal firing by burst or tonic SCS (Fig. 7.6). Ten neurons were recorded from rats that received spinal superfusion of bicuculline; all ten neurons had paired data after burst and tonic SCS (Table 7.1). After superfusion of the spinal cord with bicuculline, burst SCS significantly reduces neuronal firing by 27±11% during application of the 26g von Frey filament to the ipsilateral forepaw ($p=0.012$) and by 25±14% during noxious pinch ($p=0.008$) (Fig. 7.6a). Likewise, in the presence of bicuculline, tonic SCS significantly attenuates neuronal firing by 31±14% during 26g filament stimulation ($p=0.028$) and by 31±18% during noxious pinch ($p=0.021$) (Fig. 7.6b). The attenuation of firing by burst or tonic SCS with bicuculline treatment is not different from the changes in firing following burst or tonic SCS without that $GABA_A$ receptor antagonist present (Fig. 7.6).

The $GABA_B$ receptor antagonist, CGP35348, differentially modulates the effects of burst and tonic SCS in the dorsal horn. A total of 30 neurons were recorded from rats that received spinal superfusion of CGP35348, and 27 of those neurons had paired data for both burst and tonic SCS (Table 7.1). In the presence of CGP35348, burst SCS

significantly attenuates dorsal horn neuronal firing by 36±4% ($p<0.0001$) and by 44±4% ($p<0.0001$) during 26g filament and noxious pinch stimulation of the ipsilateral forepaw, respectively (Fig. 7.6a). That suppression of evoked firing is not different from the attenuation of neuronal activity after burst SCS with no GABA receptor antagonist (Fig. 7.6a). However, CGP35348 abolishes the effects of tonic SCS, with no change from baseline firing during the 26g filament stimulation (4±8% change from baseline) or the

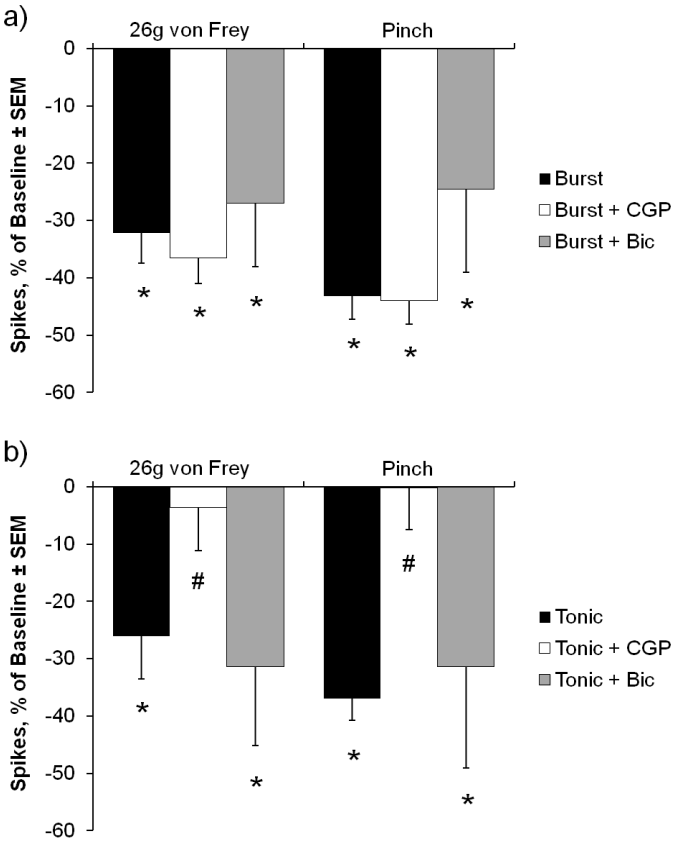

Fig. 7.6. Effects of GABA receptor antagonists on the attenuation of dorsal horn neuronal firing by burst or tonic SCS. **(a)** Burst SCS alone, burst SCS with CGP35348 (Burst+CGP), and burst SCS with bicuculline (Burst+Bic) treatment attenuate neuronal firing in response to noxious ipsilateral forepaw stimulation by both the 26g von Frey filament and pinch (*$p\leq0.017$). **(b)** Tonic SCS alone and tonic SCS with bicuculline (Tonic+Bic) attenuate neuronal firing evoked by both 26g and pinch stimulation (*$p\leq0.028$). However, tonic SCS with CGP35348 (Tonic+CGP) does not induce any change in neuronal firing from baseline, and that percent change from baseline is significantly less than the percent change after tonic SCS alone (#$p\leq0.049$).

noxious pinch (0.2±7.3%) (Fig. 7.6b). The reduction in firing after tonic SCS with CGP35348 is significantly less than the attenuation of firing after tonic SCS with no $GABA_B$ receptor antagonist for all mechanical stimuli ($p \leq 0.049$) (Fig. 7.6b). Raw spike counts for each dorsal horn neuron from each rat are included in Appendix E.

7.4. Burst and Tonic SCS after Painful Facet Joint Injury

7.4.1. Methods

Painful Facet Joint Injury and Assessment of Mechanical Hyperalgesia

Male Holtzman rats (338-450g) underwent injurious distraction of the C6/C7 facet joints (n=8) as previously described (Crosby et al., 2013; Crosby et al., 2014a; Lee and Winkelstein, 2009). Detailed methods for the bilateral facet joint distraction can be found in Section 3.3.1 of Chapter 3. Briefly, under isoflurane anesthesia (4% for induction, 2-3% for maintenance), the C6 and C7 vertebrae were exposed and attached to a custom loading device using microforceps. The C6 vertebra was then distracted 0.7mm rostrally to stretch the bilateral facet capsules across the facet joints. Incisions were closed using 3-0 polyester suture and surgical staples, and rats were monitored during their recovery in room air. Hyperalgesia was assessed bilaterally in the forepaws before (baseline) and at days 1, 3, 5, and 7 after joint injury using methods described in detail in Section 7.3.1, in order to confirm the development of hyperalgesia after joint distraction.

Electrophysiological Recordings and Spinal Cord Stimulation

On day 7 after painful facet joint injury, extracellular electrophysiological recordings were acquired using the methods described in Section 7.3.1. Briefly, rats were anesthetized with sodium pentobarbital (50mg/kg, i.p.) and given supplementary doses (5-10mg/kg, i.p.) as needed. The spinal cord was exposed from C3 to C7 and a monopolar platinum ball electrode was placed over the C4 dorsal columns. The motor thresholds were identified during the application of burst SCS and tonic SCS using a Grass stimulator with a photoelectric stimulus isolation unit (S48 Stimulator, Grass Technologies; Warwick, RI). Burst SCS parameters (5 pulses per burst, 500Hz pulse frequency, 1ms pulse width, 40Hz burst frequency, 90% MT amplitude) were chosen based on the optimization of burst stimulation for attenuating dorsal horn neuronal firing in Chapter 6 (Crosby et al., 2014b). Tonic SCS parameters (40Hz pulse frequency, 0.3ms pulse width, 90% MT amplitude) were based on previous studies evaluating tonic SCS in animal models of neuropathic pain (Qin et al., 2012; Tang et al., 2014).

A carbon fiber electrode (Carbostar-1; Kation Scientific; Minneapolis, MN) was lowered into the C6/C7 spinal dorsal horn to record neuronal activity. Baseline evoked firing of dorsal horn neurons was recorded during mechanical stimulation of the forepaw consisting of five consecutive one-second applications of 1.4g and 26g vF filaments, and ten seconds of noxious pinch with forceps (Fig. 7.2). Spontaneous firing was recorded for two seconds before each new mechanical stimulus. Burst SCS was then applied for five minutes, and evoked activity was recorded during 1.4g, 26g, and pinch stimulation immediately (0 minutes) and again at 2, 5, 10, and 15 minutes post-SCS (Fig. 7.2). The stimulation protocol was repeated in the same neuron using tonic SCS. The order of

application of burst SCS and tonic SCS was reversed in alternating neurons to avoid any effects of the order of application on neuronal firing. Spontaneous firing was subtracted from the spike counts for each mechanical stimulus to isolate evoked firing. Changes in neuronal firing were calculated as the percent change in spikes immediately after SCS relative to the pre-SCS baseline. Paired Student's t-tests compared the percent changes in neuronal firing immediately after burst SCS to the changes after tonic SCS. A repeated-measures ANOVA was used to compare the number of evoked spikes between the pre-SCS baseline and evoked firing at 0, 2, 5, 10, and 15 minutes after SCS.

7.4.2. Results

The paw withdrawal threshold is significantly reduced from baseline on days 1, 3, 5, and 7 after painful facet joint injury ($p<0.0001$) (Fig. 7.7). PWTs for each rat on each day after painful facet joint injury are summarized in Appendix B. The average motor threshold is significantly lower for burst SCS than for tonic SCS in rats undergoing electrophysiological recordings on day 7 after painful facet joint injury ($p<0.0001$) (Table

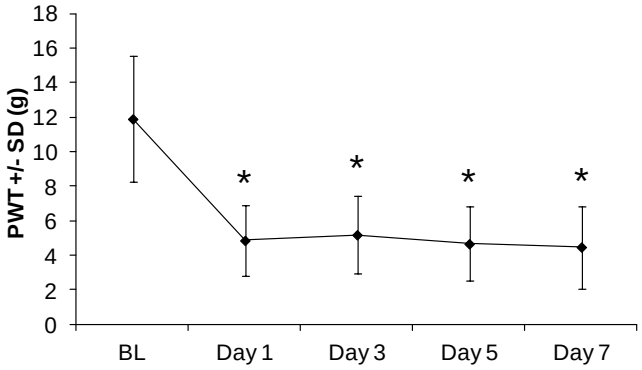

Fig. 7.7. Mechanical hyperalgesia after painful facet joint injury. Paw withdrawal threshold (PWT) significantly decreases relative to baseline (BL) after painful facet joint injury (*$p<0.0001$).

7.2). A total of 35 neurons was recorded after burst SCS and 38 neurons were recorded after tonic SCS (Table 7.2). In 31 of those neurons, paired firing data were collected after both burst and tonic SCS. Immediately after burst SCS, neuronal firing evoked by the 26g filament decreases by 24±5% ($p<0.0001$), and firing evoked by the noxious pinch decreases by 42±4% ($p<0.0001$) (Fig. 7.8). Tonic SCS reduces neuronal firing by 31±4% ($p<0.0001$) and 42±4% ($p<0.0001$) during 26g filament and pinch stimulation, respectively (Fig. 7.8). The reductions in firing after burst and tonic SCS are not different from each other during either the 26g filament stimulation or the noxious pinch (Fig. 7.8). Firing evoked by 1.4g stimulation is unchanged after burst and tonic SCS.

Table 7.2. Summary of rat and SCS data after a painful facet joint injury.

		Motor Threshold (μA)		**# of Neurons Recorded**	
Rat #	**Weight (g)**	**Burst**	**Tonic**	**Burst**	**Tonic**
213	438	145	290	3	3
214	422	170	280	4	5
217	338	150	270	5	5
218	378	120	200	8	8
219	370	165	290	6	7
220	376	150	250	4	4
221	360	145	255	3	4
222	450	150	260	2	2
Avg ± SD	392±40	149±15	262±29*	4.4±1.9 (35 total)	4.8±2.0 (38 total)

SD = standard deviation; *$p<0.0001$ vs. Burst

Neuronal firing evoked by noxious stimulation is reduced for a longer time after tonic SCS than after burst SCS, but only burst SCS reduces firing evoked by non-noxious stimulation. The number of spikes evoked by the 26g filament ($p\leq0.037$) and the noxious pinch ($p<0.0001$) decreases significantly from baseline at 0, 2, and 5 minutes after burst

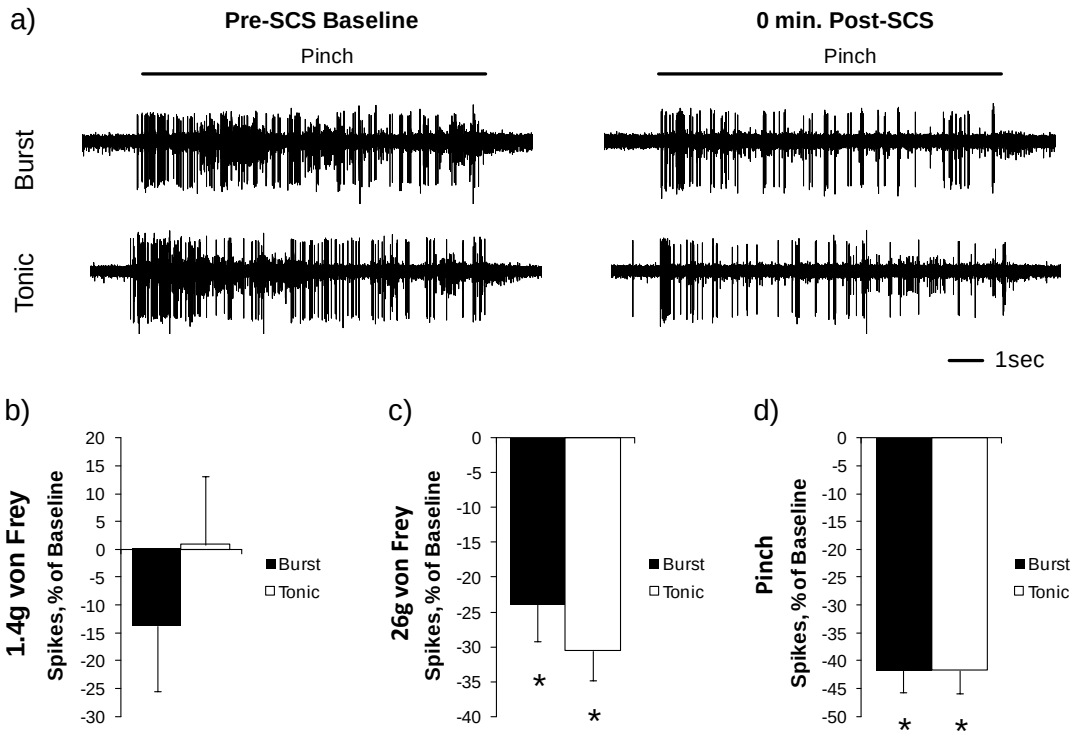

Fig. 7.8. Representative firing and quantification of neuronal activity after burst and tonic SCS on day 7 following painful facet joint injury. **(a)** Representative firing evoked by noxious pinch before (Pre-SCS Baseline) and immediately after (0 min. Post-SCS) burst and tonic SCS. **(b)** No change in neuronal firing is observed during stimulation with the 1.4g von Frey filament after burst or tonic SCS. Firing is significantly reduced after burst and tonic SCS during **(c)** 26g von Frey filament (*$p<0.0001$) and **(d)** noxious pinch stimulation (*$p<0.0001$).

SCS (Fig. 7.9). Tonic SCS reduces firing evoked by the 26g filament ($p\leq0.0011$) and noxious pinch ($p\leq0.042$) for at least 10 minutes after stimulation, a longer period of time than after burst SCS (Fig. 7.9). The total number of spikes evoked by the 1.4g filament stimulation decreases from baseline values at all times after burst SCS ($p\leq0.041$) (Fig. 7.9a). Tonic SCS does not induce any change in firing evoked by the 1.4g filament. However, the number of spikes recorded at each time after burst SCS is not different from the firing recorded after tonic SCS for any mechanical stimulus. Raw spike counts for each dorsal horn neuron from each rat are listed in Appendix E.

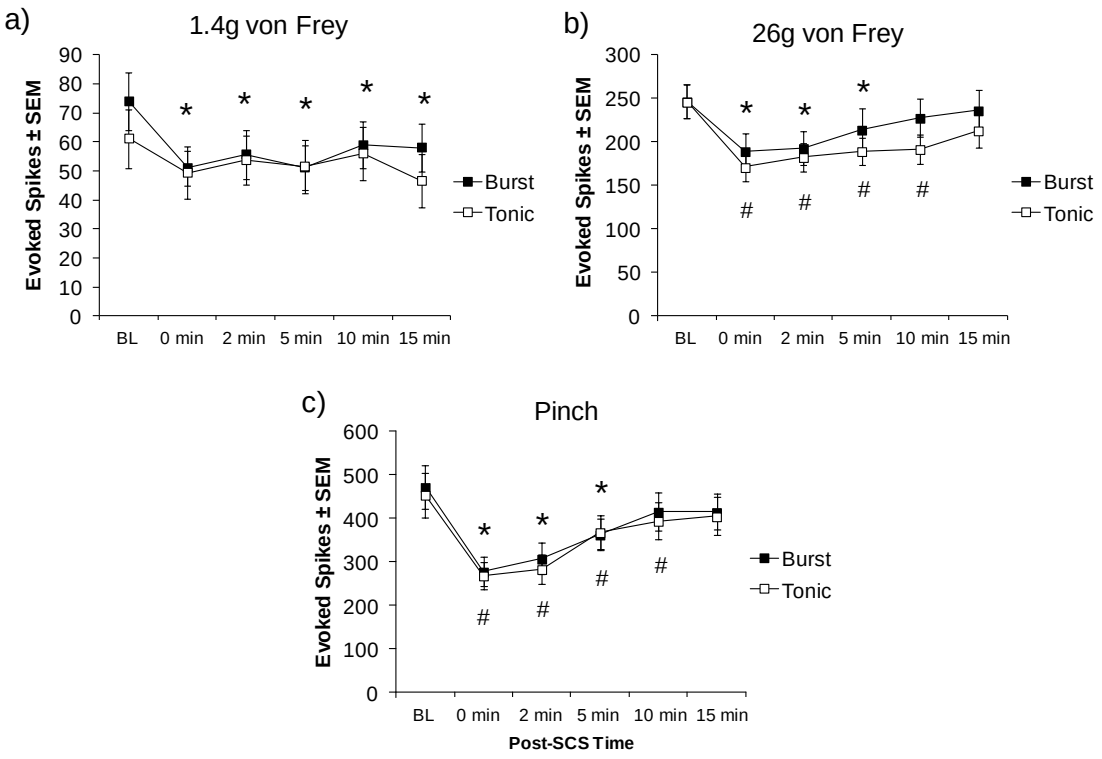

Fig. 7.9. Evoked spike counts for up to 15 minutes after the cessation of burst and tonic SCS application following painful facet joint injury. **(a)** Burst SCS reduces the number of spikes evoked by 1.4g stimulation (*p≤0.041). **(b)** Stimulation with the 26g von Frey filament evokes fewer spikes after application of burst SCS (*p≤0.037) or tonic SCS (#p≤0.0011). **(c)** Pinch stimulation evokes fewer spikes after application of burst SCS (*p<0.0001) or tonic SCS (#p≤0.042).

7.5. Discussion

Burst SCS reduces neuronal firing during noxious mechanical stimulation of the forepaw seven days after painful compression of the C7 dorsal nerve root (Figs. 7.3-7.6) and seven days after painful C6/C7 facet joint injury (Figs. 7.7-7.9). However, the attenuation of neuronal firing in the dorsal horn after burst SCS is not different from the decreases in firing that occur after tonic SCS for either injury model (Figs. 7.4 and 7.8). Tonic SCS is believed to activate GABA signaling in the dorsal horn as a primary mechanism of action (Linderoth et al., 1994; Cui et al., 1996), which is supported by the

ineffectiveness of tonic SCS in the presence of the $GABA_B$ receptor antagonist (Fig. 7.6b). However, the effects of burst SCS are not abolished by either of the $GABA_A$ or $GABA_B$ receptor antagonists (Fig. 7.6a). Collectively these results suggest that, despite similar attenuation of spinal hyperexcitability by burst and tonic SCS, GABA signaling does not contribute to burst SCS-induced analgesia after painful nerve root compression.

Burst SCS reduces neuronal hyperexcitability seven days after painful cervical nerve root compression or painful facet joint injury. Each of those injuries in the cervical spine induces increased evoked dorsal horn neuronal firing during noxious stimulation of the forepaw by between two and three times the neuronal activity normally observed in controls (Crosby et al., 2014a; Dong et al., 2013a; Nicholson et al., 2014a; Quinn et al., 2010b). But, each of burst and tonic SCS significantly reduces that hyperexcitability in dorsal horn WDR neurons (Figs. 7.4 and 7.8). This attenuation of neuronal hyperexcitability has also been reported for pharmacological interventions that attenuate behavioral hypersensitivity after nerve root compression and joint injury in the rat (Crosby et al., 2014a; Dong et al., 2013a; Nicholson et al., 2014a; Nicholson et al., 2014b; Smith et al., 2013). Tonic SCS has been reported to reduce allodynia after peripheral nerve injury by normalizing the responses of hyperexcitable WDR neurons to mechanical stimulation (Yakhnitsa et al., 1999). The relationship between dorsal horn neuronal activity and behavioral hypersensitivity during tonic SCS suggests that the attenuation of WDR neuronal activity in the dorsal horn likely contributes to the analgesic effects of burst SCS as well (Figs. 7.4-7.5 and 7.8-7.9). However, dorsal horn neuronal firing was quantified in this study immediately *after* the cessation of SCS because artifacts from the electrical stimulation prevented the recording of voltage

potentials during SCS. Pairing electrophysiological recordings of dorsal horn neuronal activity with studies that actively assess pain-related behaviors *during* stimulation would more directly relate changes in spinal neuronal activity to burst SCS-induced analgesia.

After painful facet joint injury, dorsal horn neuronal firing evoked by 1.4g filament stimulation decreases from baseline levels at all times through 15 minutes after burst SCS, but firing is unchanged from baseline levels after tonic SCS (Fig. 7.9). The attenuation of firing in response to innocuous stimulation may reflect the inhibition of WDR neuronal activity, because WDR neurons receive low-threshold input in addition to their role in nociceptive processing (Steeds, 2009). However, when considered as a percent change from baseline, no differences in 1.4g filament-evoked firing are observed after either burst or tonic SCS (Fig. 7.8). Furthermore, firing in response to 1.4g filament stimulation is not consistently elevated over control firing levels after painful facet joint injury (Crosby et al., 2014a; Nicholson et al., 2014b; Quinn et al., 2010b), so any decrease in 1.4g filament-evoked spikes after burst SCS likely does not contribute to SCS-induced analgesia.

The burst SCS-induced reduction of evoked neuronal activity by up to 43% after painful nerve root compression and up to 42% after painful facet joint injury is similar to the only other study that has applied burst SCS in an animal model of pain, in which burst SCS reduced lumbar dorsal horn neuronal firing by 41.5% in response to noxious cutaneous pinch (Tang et al., 2014). SCS has been proposed to inhibit activity in the spinal cord by activating Aβ fibers in the dorsal columns that synapse with inhibitory interneurons in the dorsal horn (Dubuisson, 1989; Guan, 2012). Aβ fiber stimulation can directly activate inhibitory interneurons in the superficial laminae of the dorsal horn and

reduce activity in the nociceptive neurons in that dorsal horn region (Daniele and MacDermott, 2009). These findings support that SCS may act, at least in part, by the gate theory of pain, which proposes that low-threshold stimulation induces dorsal horn inhibition to attenuate nociception (Melzack and Wall, 1965; Mendell, 2014). Persistent pain states can differ greatly in their pathophysiology and peripheral and spinal mechanisms, potentially altering the spinal mechanisms that induce dorsal horn inhibition. For example, nerve root compression causes axonal degeneration and neuroinflammation in the injured nerve root itself (Chang and Winkelstein, 2011; Hubbard and Winkelstein, 2008), whereas mechanical facet joint injury induces extensive synaptic and structural changes in the dorsal horn that enhance spinal neuronal excitability (Chapters 3-5) (Crosby et al., 2014a; Crosby et al., 2014c; Dong et al., 2012; Weisshaar et al., 2010). However, regardless of the etiology of pain, nociceptive signals from the periphery are transmitted by Aδ and C fiber nociceptors that synapse with second-order WDR and nociceptive-specific (NS) neurons in the dorsal horn (Basbaum et al., 2009). The comparable reduction of spinal neuronal activity by burst SCS in animal models of nociceptive pain (Tang et al., 2014), neuropathic pain (Fig. 7.4), and joint pain (Fig. 7.8) suggests that, at the cellular level, burst stimulation attenuates nociception in the dorsal horn to a similar extent regardless of the inciting event and the specific altered peripheral or central nervous system functions that may contribute to pain.

Burst SCS may therefore provide an effective therapy for patients with chronic pain conditions that are currently infrequently treated with SCS, including persistent facet joint-mediated pain. However, studies are needed to assess the cost-effectiveness of SCS for the treatment of less commonly indicated pain conditions that may benefit from

increased use of SCS. For example, evaluations of the cost-effectiveness of SCS for the treatment of failed back surgery syndrome, the most common indication for SCS, show that SCS becomes more cost-effective than conventional pain therapies within 2-3 years after implantation of a stimulator (Bell et al., 1997; Kumar et al., 2002). Similar cost-benefit analyses for other chronic pain conditions would ultimately determine whether burst SCS offers utility for their treatment, relative to conventional therapeutic approaches.

Burst and tonic SCS differ in the relative duration of their effects on the neuronal firing evoked by noxious stimulation after painful nerve root compression. For example, burst SCS reduces pinch-evoked spikes compared to baseline levels for up to ten minutes after the cessation of SCS, but tonic SCS reduces firing for only up to five minutes (Fig. 7.5). During 26g filament stimulation, the opposite is observed, with burst SCS reducing the number of evoked spikes for up to two minutes and tonic SCS reducing the number of evoked spikes for a longer period, up to ten minutes after the SCS ends (Fig. 7.5). Similar differences between burst and tonic SCS are observed after painful facet joint injury (Fig. 7.9). However, despite these apparent differences in the duration of the effects of each mode of SCS after nerve root compression or facet joint injury, the evoked spike counts are not different between burst and tonic SCS for any noxious or non-noxious stimulus at any of the post-SCS times (Figs. 7.5 and 7.9). Neuronal activity was only quantified for up to 15 minutes after the end of SCS; but, since firing returned to baseline levels by 15 minutes (Figs. 7.5 and 7.9) no differences between burst and tonic SCS would be expected at any later time point. These results suggest that, overall, neither mode of SCS is more or less effective at attenuating spinal neuronal hyperexcitability.

Burst SCS was hypothesized to reduce neuronal firing more effectively than tonic SCS, because burst SCS reduces VAS pain scores significantly more than does tonic SCS in patients with chronic neuropathic pain (De Ridder et al., 2010; De Ridder et al., 2013; De Vos et al., 2014). However, no differences were observed between burst and tonic SCS for attenuating spinal neuronal excitability after nerve root or facet joint injury (Figs. 7.4-7.5 and 7.8-7.9). This study used a single electrode for monopolar stimulation, whereas patients often receive bipolar stimulation from large arrays of implanted electrodes (Alo et al., 1998; Manola et al., 2007). Monopolar and multipolar stimulation can differ significantly in their delivery of electrical current; for example, monopolar electrodes deliver higher charge densities than bipolar and tripolar stimulation (Wesselink and Boom, 1998). The unexpected similarity between the two modes of SCS in this study may, therefore, be due to the use of monopolar stimulation instead of more clinically relevant electrode configurations. Furthermore, using the same monopolar stimulation as this study, Tang et al. (2014) reported no significant differences in the effects of burst and tonic SCS on lumbar dorsal horn neuronal firing in response to noxious pinch. However, that study found visceromotor reflexes to be more attenuated after burst SCS than after tonic SCS (Tang et al., 2014). That finding suggests that additional metrics other than evoked dorsal horn neuronal firing may be more sensitive to differences in burst and tonic stimulation, as was detected by their dissimilar activation of GABA signaling in the dorsal horn (Fig. 7.6) and reduction of chronic neuropathic pain in patients (De Ridder et al., 2010; De Ridder et al., 2013).

The electrophysiological metrics used in the current study describe the neuronal effects of burst and tonic SCS in hyperalgesic rats; however, patient-reported pain scores

incorporate additional factors that were not explicitly studied here, including spontaneous pain, emotional perceptions of pain, and the presence or absence of paresthesia during SCS (De Vos et al., 2014; Fernandez and Turk, 1992; Price, 2000). Paresthesia may play a particularly important role in determining pain outcomes during SCS because of the widely varying positive and negative experiences patients associate with paresthetic sensation (De Vos et al., 2014). For example, many patients favor paresthesia-free modes of stimulation, but some patients that switch from tonic to burst SCS report a preference for paresthesia as desirable feedback for adjusting stimulation parameters or as a distraction from underlying pain (De Vos et al., 2014). In studies of SCS using animal models of pain, additional behavioral assessments that incorporate measures of paresthesia, spontaneous pain, and the affective dimensions of pain may better evaluate those effects of burst SCS that are more clinically relevant and capture all aspects of pain.

Tonic SCS has been reported to attenuate nociception in the dorsal horn by stimulating the release of GABA (Cui et al., 1996). Aβ fiber stimulation can activate GABAergic interneurons in the superficial dorsal horn (Daniele and MacDermott, 2009), producing GABA release and facilitating the spinal inhibition of nociceptive signals (Dubuisson, 1989; Stiller et al., 1996). However, the attenuation of dorsal horn neuronal firing after tonic SCS with spinal superfusion of the $GABA_A$ antagonist, bicuculline, is not different from the effects of SCS alone on day 7 after painful nerve root compression (Fig. 7.6). These findings are consistent with a previous study that found the effects of SCS to be independent of signaling through $GABA_A$ receptors after nerve injury (Cui et al., 1996). Although some $GABA_A$ receptors can be found in the dorsal horn, they are more abundant in the ventral horn in association with motoneurons, and the analgesic

effects of $GABA_A$ receptor agonists like muscimol are attributed to supraspinal mechanisms, not inhibition of firing in the dorsal horn (Malcangio and Bowery, 1996). As such, bicuculline was administered during SCS in only two rats, but blocking $GABA_A$ receptors did not modulate the effectiveness of either burst *or* tonic SCS (Fig. 7.6), so further experiments with superfusion of bicuculline were not pursued.

In contrast to the role of $GABA_A$ receptors, tonic SCS activates $GABA_B$ receptors to inhibit nociception in the dorsal horn (Cui et al., 1996; Cui et al., 1997). The $GABA_B$ receptor antagonist, CGP35348, abolishes the effects of tonic SCS (Fig. 7.6b), further supporting the role of $GABA_B$ receptor activation in tonic SCS-induced spinal inhibition. However, neuronal firing is significantly reduced from baseline after burst SCS despite the spinal superfusion of CGP35348 (Fig. 7.6a), indicating that $GABA_B$ receptor activation is not required for burst SCS-induced inhibition in the dorsal horn. Burst SCS has a significantly lower motor threshold than tonic SCS (Tang et al., 2014) which was also determined in our study (Tables 7.1 and 7.2), and burst SCS requires a lower amplitude than tonic SCS to relieve pain in patients (De Ridder et al., 2010). It is possible that the burst SCS amplitudes that attenuate dorsal horn neuronal firing are too low to activate the release of GABA in the spinal dorsal horn, and instead activate other non-GABAergic mechanisms to inhibit nociception in the spinal cord.

Spinal superfusion of drug solutions can lead to steep drug concentration gradients in the dorsal horn, which can be greatly affected by metabolism or uptake of the drug (Beck et al., 1995). Because CGP35348 reduces the effectiveness of tonic SCS on dorsal horn WDR neuronal firing (Fig. 7.6b) the effective concentration in the deep dorsal horn was taken as sufficient to inhibit GABA signaling. However, other drug

delivery methods, like intrathecal injection or dorsal horn microdialysis (Cui et al., 1996; Cui et al., 1997), may produce more uniform drug concentrations and inhibition of GABA signaling. Nonetheless, based on studies with a radiolabeled neuropeptide showing that peak dorsal horn concentrations occur after 15-30 minutes of superfusion (Beck et al., 1995), GABA receptor antagonist solutions were refreshed every 20-30 minutes in order to maintain drug concentrations in the dorsal horn. Furthermore, burst and tonic SCS were applied sequentially during recording of the same dorsal horn neurons, so any differential effects of the two modes of SCS are not due to differences in drug penetration or efficacy between rats.

In addition to inducing GABA release, tonic SCS also stimulates release of serotonin, acetylcholine, and noradrenaline, each of which contribute to the inhibitory effects of SCS on dorsal horn neurons (Levin and Hubschmann, 1980; Linderoth et al., 1992; Schechtmann et al., 2008). Many of the inhibitory effects of those additional neurotransmitters are attributed to secondary activation of GABAergic interneurons in the dorsal horn (Chen and Pan, 2004; Song et al., 2011; Zhang et al., 2009), and those effects would also be blocked by the GABA receptor antagonists administered in this study. However, serotonin and noradrenaline can exhibit direct inhibitory effects on dorsal horn projection neurons (Grudt et al., 1995; North and Yoshimura, 1984; Sonohata et al., 2004), so it is possible that burst SCS attenuates nociception by activating inhibitory neurotransmitter systems that partially act independently of GABA signaling. Dorsal column stimulation can also directly inhibit dorsal horn neuronal firing, either by presynaptically depolarizing primary afferents to block excitatory neurotransmission, or producing hyperpolarizing inhibitory potentials in dorsal horn neurons (Narikawa et al.,

2000; Shimoji et al., 1982). Further studies are required to determine what non-GABAergic neurotransmitter systems or neurophysiological mechanisms may be activated during burst SCS to inhibit nociception in the dorsal horn.

7.6. Conclusions and Integration

Overall, studies in this chapter demonstrate that burst SCS attenuates dorsal horn neuronal firing after both painful nerve root compression and painful facet joint injury, supporting burst SCS as an effective therapy for persistent pain from cervical neural tissue and mechanical joint injuries. However, burst and tonic SCS reduce neuronal firing to the same degree in both models of persistent pain. Those findings do not support the hypothesis that burst SCS attenuates spinal hyperexcitability more effectively than tonic SCS. That hypothesis was based on clinical data showing increased effectiveness of burst SCS over tonic SCS for reducing chronic pain (De Ridder et al., 2013; De Vos et al., 2014), but patient-reported pain scores in clinical studies incorporate many additional dimensions of pain that are not directly quantified here. The behavioral and dorsal horn neuronal responses to mechanical stimulation that were used in this study measure spinal-level reflexes and electrophysiology, but do not account for any potential cognitive, affective, or other supraspinal contributions to pain perception (Fernandez and Turk, 1992; Price, 2000). It is possible that behavioral testing that more comprehensively assesses spontaneous pain and/or the psychosocial aspects of chronic pain may show burst SCS to be more effective than tonic SCS in animal models of persistent cervical spine pain.

The similarities between SCS modes in their suppression of dorsal horn neuronal activity suggest that their neurophysiological mechanisms of action in the spinal cord may be similar. However, GABA receptor antagonists do not alter the effects of burst SCS, so that mode likely does not rely on GABA release and activation of GABA receptors to inhibit spinal neuronal firing. Therefore, these results do not support the hypothesis that burst SCS activates GABAergic mechanisms to reduce nociception in the spinal dorsal horn. Other neurochemical and neurophysiological mechanisms may reduce spinal neuronal firing during burst SCS, either by stimulating non-GABAergic inhibitory neurotransmitter release or directly blocking firing in dorsal horn projection neurons. Although continued studies are needed to elucidate the specific mechanisms underlying the effects of burst stimulation, the work in this chapter demonstrates that burst SCS is an effect modulator of dorsal horn neuronal activity and, by attenuating spinal hyperexcitability, can inhibit the aberrant nociception that develops in multiple different models of chronic pain.

CHAPTER 8

Synthesis and Future Work

8.1. Introduction

Excessive loading of the facet joint has been implicated as a likely mechanism to produce pain during abnormal motions of the cervical spine, based on biomechanical studies that demonstrate excessive loading of the cervical facet joints during neck trauma (Deng et al., 2000; Kaneoka et al., 1999; Ono et al., 1997; Siegmund et al., 2001; Yoganandan et al., 2001). Clinical studies have identified the facet joint as a primary source of whiplash-associated pain, further supporting that mechanical facet joint loading can lead to chronic pain (Barnsley et al., 1995; Lord et al., 1996). Many patients with whiplash-associated disorders exhibit symptoms that are characteristic of central sensitization, including decreased pain thresholds both at the back of the neck and shoulders and at the upper and lower limbs (Banic et al., 2004; Curatolo et al., 2004; Herren-Gerber et al., 2004).

Facet joint loading in the rat that induces pain also induces spinal neuronal hyperexcitability, possibly through the potentiation of glutamatergic signaling (Dong et al., 2012; Quinn et al., 2010; Rothman et al., 2008; Weisshaar et al., 2010). Because structural modifications in the spinal cord can contribute to central sensitization, painful facet joint loading could also initiate excitatory synaptogenesis in the dorsal horn, as

occurs after peripheral nerve injury (Jaken et al., 2010; Kim et al., 2012). Elucidating the mechanisms in the spinal cord that promote neuronal hyperexcitability can lead to more effective treatments for persistent pain after joint injuries, like those that result from excessive facet joint loading. Therefore, the purpose of this thesis was to define the temporal establishment and maintenance of spinal neuronal hyperexcitability after painful facet joint injury, and to evaluate the use of spinal cord stimulation to modulate neuronal activity in the dorsal horn for the attenuation of cervical spine pain.

8.2. Summary and Synthesis of Major Findings

Painful facet joint injury induces both mechanical hyperalgesia and dorsal horn neuronal hyperexcitability within the first day after injury, despite evidence that neither is evident six hours after joint injury (Chapter 3) (Crosby et al., 2013). The timing of the development of spinal hyperexcitability in the rat is consistent with the clinical experience of many patients that do not exhibit pain symptoms until hours or days after neck trauma (Chien et al., 2010). However, intra-articular injection of the fast-acting anesthetic, bupivacaine, in the bilateral facet joints is only effective for preventing the development of pain when that treatment is administered before 8 hours after injurious facet joint loading in the rat (Chapter 4) (Crosby et al., 2014a). These results suggest that the *timing* of any localized joint intervention is a crucial consideration for the effective treatment of sustained joint-mediated pain. This temporal importance of interventional therapy after facet joint injury is supported by the finding that early systemic treatment with corticosteroids (up to 8 hours after injury) is effective for reducing long-term disability in patients with whiplash-associated pain (Pettersson et al., 1998). Although the

studies in this thesis only evaluated behavioral sensitivity through day 7, a preliminary study showed that paw withdrawal threshold decreases significantly through day 14 after painful facet joint injury (Fig. 8.1). Furthermore, although the temporal development and maintenance of sensitivity in the rat may not directly translate to chronic pain in humans due to lifespan differences between the two species (Sengupta, 2013), the hyperalgesia that is evident at day 7 after facet joint injury in the rat continues, and does not diminish, for at least six weeks (Rothman et al., 2008), so the behavioral sensitivity at day 7 that is observed in the studies in this thesis can be considered as "persistent" pain.

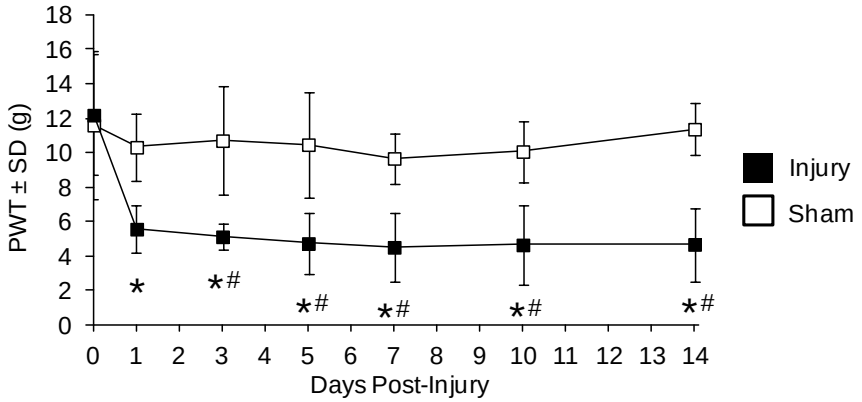

Fig. 8.1. Quantification of hyperalgesia through day 14 after painful facet joint injury. Rats underwent painful facet joint injury (n=6) or sham procedures (n=5). Paw withdrawal threshold (PWT) decreases significantly through day 14 after painful facet joint injury relative to baseline (*$p<0.0001$). PWT also decreases relative to sham on days 3, 5, 7, 10, and 14 (#$p\leq0.037$).

The primary afferent fibers that innervate the joint are activated by strain in the facet capsule in a goat model of tensile facet joint loading (Chen et al., 2006; Lu et al., 2005a). Low-threshold fibers are activated at strains as low as 10%, and nociceptor firing is maximally activated at 44% strain (Lu et al., 2005a). In the studies in this thesis that evaluate the role of primary afferent firing in the induction of facet joint-mediated pain,

injurious joint distraction of 0.7mm generates average maximum principal strains of 27±12% and peak maximum principal strains of 45±25% on the surface of the facet capsule (Chapter 4) (Crosby et al., 2014a). Those strains in the capsule, which are similar to the strains measured in other studies of painful facet joint loading in the rat (Dong et al., 2012; Lee et al., 2004a), are of sufficient magnitude to activate and saturate firing in both the low-threshold and nociceptive afferents that innervate the joint (Lu et al., 2005a). Because of the demonstrated role of afferent discharge in the initiation of neuropathic pain after peripheral nerve injury, this firing in facet joint afferents presents a likely mechanism for the induction of facet-mediated pain.

Excessive primary afferent activation induced by painful facet joint injury is associated with neuronal and astrocytic modifications, including the potentiation of glutamatergic signaling and the upregulation of astrocytic TSP4, that promote spinal neuronal hyperexcitability (Fig. 8.2) (Chapters 4 and 5) (Crosby et al., 2014a; Crosby et al., 2014c). Overstimulation of dorsal horn neurons increases intracellular calcium concentrations that can trigger secondary signaling pathways to alter the expression of glutamatergic signaling proteins (Kawasaki et al., 2004; Latremoliere and Woolf, 2009). That mechanism may contribute to the increases in mGluR5, pNR1, and pERK, and the decreases in GLT1 that are observed after painful joint loading (Fig. 8.2) (Chapter 4) (Crosby et al., 2014a; Dong et al., 2012; Weisshaar et al., 2010). Astrocytes also express receptors for excitatory neurotransmitters like glutamate and ATP (Milligan and Watkins, 2009), so in addition to neuronal excitation, injury-induced afferent discharge may directly stimulate astrocytes in the dorsal horn.

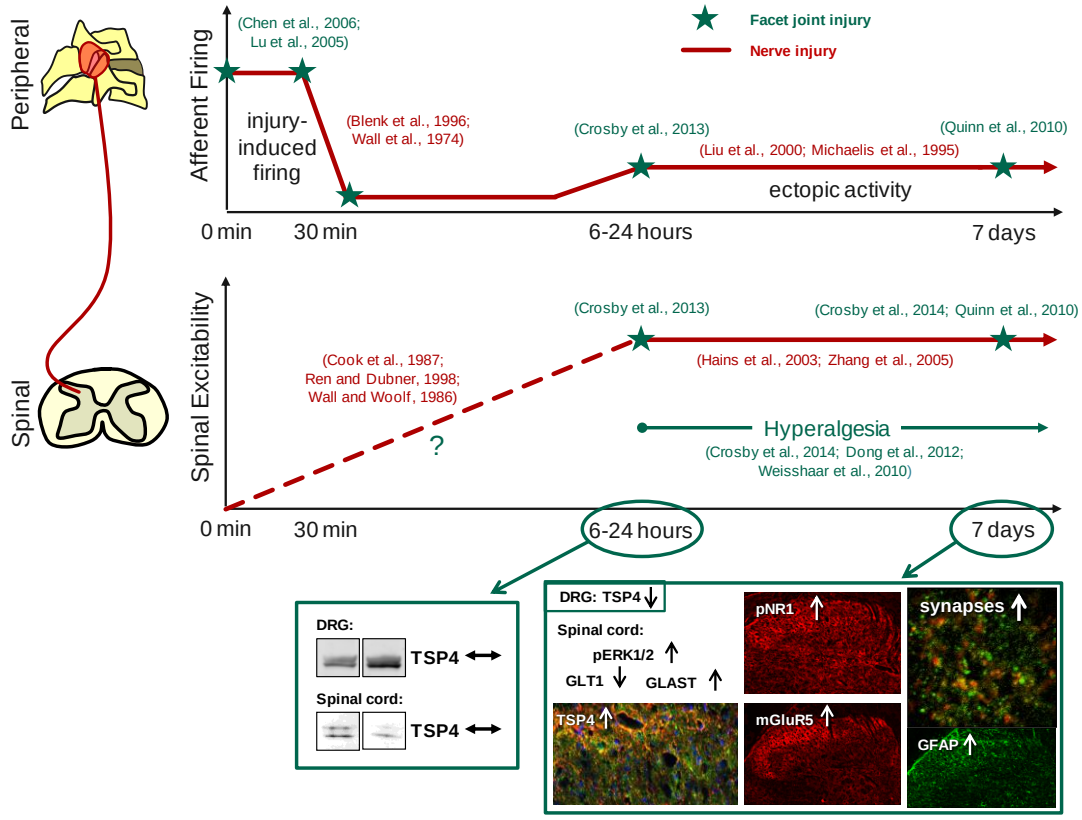

Fig. 8.2. Temporal development of synaptic and structural modifications in the spinal cord that promote spinal hyperexcitability and behavioral sensitivity after facet joint injury. The time course of peripheral and spinal mechanisms contributing to persistent pain after facet joint injury (green) are compared with the mechanisms of neuropathic pain after nerve injury (red). Injurious facet capsule stretch induces primary afferent activity, followed by the onset of spontaneous activity in the first 24 hours that persists at least through day 7 after injury. Ectopic firing was measured by proxy using the spontaneous activation of neurons in the dorsal horn. These peripheral mechanisms are similar to the injury-induced afferent discharge and ectopic activity that are believed to promote neuropathic pain after a peripheral nerve injury. In the spinal cord, hyperexcitability develops within 24 hours after facet joint injury and also persists through at least day 7. The onset of spinal hyperexcitability after nociceptor activation can be rapid, but the exact timeline of the development of sensitization in the first 24 hours after facet joint injury remains unclear. Behavioral sensitivity develops concurrently with spinal hyperexcitability at day 1, and persists. Spinal hyperexcitability is promoted by neuronal and astrocytic modifications that were measured at day 7 after injury, including the potentiation of glutamatergic signaling, spinal TSP4 upregulation, and TSP4-mediated synaptogenesis.

Once activated, astrocytes can contribute directly to neuronal hyperexcitability by increasing spinal levels of excitatory neurotransmitters, neuropeptides (i.e., substance P), growth factors, and prostaglandins, each of which has sensitizing effects on dorsal horn neurons (Watkins et al., 2001). In particular, excitatory neurotransmitter release by astrocytes activates AMPA receptors on neurons that contribute to neuronal firing in the spinal dorsal horn (Watkins et al., 2001). Similarly, astrocyte activation by excitatory neurotransmission can lead to the increase in astrocytic TSP4 that is observed after painful facet joint injury (Fig. 8.2) (Chapter 5) because expression of TSP1, a thrombospondin-family protein that is closely related to TSP4, has been shown to be induced by the excitatory neurotransmitter, ATP (Tran and Neary, 2006). Astrocytic TSP4 can enhance the neuronal release of excitatory neurotransmitters, like glutamate (Kim et al., 2012). Increased glutamate release in the dorsal horn may overactivate second-order dorsal horn neurons, especially after the downregulation of GLT1 (Chapter 4), which is the primary glutamate transporter responsible for clearing excess synaptic glutamate (Danbolt, 2001). By facilitating the activation of dorsal horn neurons through excitatory neurotransmitter and TSP4 release, astrocyte activation may substantially contribute to the increases in neuronal excitability that occur after painful joint injury.

TSP4 plays a particularly important role in the development of behavioral sensitivity and spinal hyperexcitability after painful facet joint injury. TSP4 has synaptogenic properties (Eroglu et al., 2009), and blocking injury-induced spinal TSP4 expression prevents excitatory synaptogenesis (Chapter 5) (Crosby et al., 2014c). As such, elevated spinal TSP4 likely causes the increase in excitatory synapses that is observed in the dorsal horn at day 7 after painful facet joint injury (Fig. 8.2) (Chapter 5)

(Crosby et al., 2014c). TSP4 is upregulated in the spinal cord at day 7 after painful facet joint loading, but nerve injury-induced synapse development has been reported to occur over the course of at least 3-5 days (Lo et al., 2011). Spinal TSP4 levels exhibit similar trends at day 1 as at day 7, so the observed increase in synapses at day 7 may be induced by increases in TSP4 that are observed beginning at day 1 (Chapter 5). Although new excitatory synapses may require several days to develop after painful facet joint injury, spinal hyperexcitability and behavioral sensitivity develop within the first day after injury. Together, these results indicate that TSP4-mediated synaptogenesis contributes to behavioral sensitivity and spinal hyperexcitability by day 7 after painful facet joint injury. But, the temporal development of hyperexcitability in the first day after injury precludes the involvement of synaptogenesis in the initial induction of facet joint-mediated pain.

The studies in this thesis demonstrate that the potentiation of glutamate signaling and the excitatory synaptogenesis that are both induced by primary afferent discharge contribute to persistent facet joint-mediated pain. But, multiple different signaling pathways can lead to the development of spinal hyperexcitability (Latremoliere and Woolf, 2009). For example, painful facet joint injury leads to an increase in expression of nerve growth factor (NGF) in the facet capsule and the DRG, which can initiate the later development of prostaglandin-mediated inflammatory pain (Kras et al., 2014a; Kras et al., 2014b). NGF is an inflammatory mediator that can also directly sensitize primary afferent nociceptors (McMahon, 1996), potentially increasing afferent input to the dorsal horn and contributing to the development of spinal hyperexcitability (Kras et al., 2014b). Spinal inflammation can also contribute to astrocyte activation by stimulating astrocytic receptors for pro-inflammatory cytokines like IL-1 and TNFα (Benveniste, 1992;

Milligan and Watkins, 2001). Indeed, blocking IL-1 and TNFα receptors prevents the spinal upregulation of GFAP after painful facet joint injury (Dong, 2013); however, blocking IL-1 and TNFα does not attenuate hyperalgesia after facet injury (Dong, 2013). Furthermore, spinal GFAP expression remains increased despite the attenuation of hyperalgesia and spinal hyperexcitability by intra-articular injection of bupivacaine immediately after injury (Chapter 4) (Crosby et al., 2014a). Therefore, astrocyte activation after painful facet joint injury is likely due, at least in part, to inflammatory mechanisms that are independent of injury-induced afferent discharge.

Both peripheral and spinal interventions can prevent or reduce persistent pain after facet joint injury by modulating joint afferent firing and/or the sensitization of spinal neurons (Fig. 8.3). However, those treatments are most effective when administered immediately or early after facet joint injury. Intra-articular bupivacaine administered up to 4 hours after joint injury prevents the development of hyperalgesia and spinal hyperexcitability by blocking the potentiation of glutamatergic signaling, TSP4 upregulation, and excitatory synaptogenesis. But, if bupivacaine treatment is not administered until after spinal hyperexcitability develops, it is ineffective at attenuating joint-mediated pain (Fig. 8.3) (Chapters 4 and 5) (Crosby et al., 2014a; Crosby et al., 2014c). Similarly, spinal administration of gabapentin at the time of injury prevents the development of hyperalgesia, spinal hyperexcitability, astrocyte activation, and the increase in excitatory synapses that are all observed after painful facet injury (Fig. 8.3) (Chapter 5) (Crosby et al., 2014c; Dong et al., 2013a). Since gabapentin binds to the α2δ-1 subunit of voltage-dependent calcium channels and has been reported to inhibit calcium influx (Dooley et al., 2002; Stefani et al., 1998), it may attenuate spinal hyperexcitability

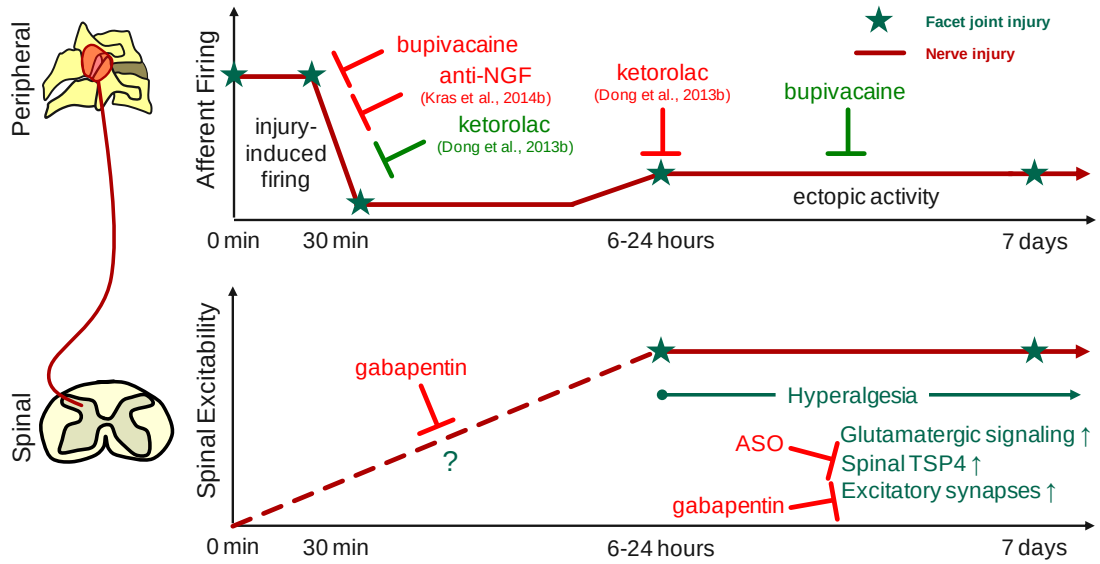

Fig. 8.3. Timing of peripheral and spinal interventions and effects on hyperalgesia and spinal neuronal hyperexcitability. The timing of peripheral and spinal interventions is a significant factor in determining whether they are effective (red) or ineffective (green) in attenuating hyperalgesia and/or spinal neuronal hyperexcitability. Immediate, but not delayed, intra-articular bupivacaine blocks injury-induced afferent discharge, preventing the subsequent development of hyperalgesia and spinal hyperexcitability. Anti-NGF antibodies are also effective when given immediately after injury, indicating that inflammatory mechanisms also contribute to the development of facet joint pain. In contrast, anti-inflammatory treatments like ketorolac are effective at day 1, but not when given immediately after injury. In the spinal cord, daily intrathecal antisense oligonucleotides (ASO) prevent TSP4 expression, and reduce subsequent excitatory synaptogenesis. Intrathecal gabapentin given at the time of injury and again at day 1 blocks the synaptogenic activity of TSP4 to prevent synaptogenesis, and may also reduce calcium influx in dorsal horn neurons to attenuate the potentiation of glutamatergic signaling.

by reducing calcium currents in dorsal horn neurons and preventing the calcium-mediated changes in excitatory glutamatergic signaling that would be induced by afferent discharge. Gabapentin also blocks the synaptogenic activity of TSP4 through that α2δ-1 subunit (Eroglu et al., 2009; Luo et al., 2002), so it may also reduce persistent pain by antagonizing the activity of TSP4 (Fig. 8.3). However, that mechanism is less probable

because TSP4 is not significantly upregulated at day 1 when the gabapentin treatment likely ceases to be effective (Fig. 8.2) (Chapter 5) (Crosby et al., 2014c).

Localized joint interventions that target NGF-mediated inflammatory pain can also reduce behavioral sensitivity and spinal hyperexcitability. Intra-articular injection of an anti-NGF antibody at the time of facet joint injury effectively prevents the development of behavioral sensitivity and spinal hyperexcitability (Kras et al., 2014b). However, intra-articular injection of the nonsteroidal anti-inflammatory drug ketorolac, is not effective when administered at the time of injury, while it does reduce sensitivity when administered at day 1 (Fig. 8.3) (Dong et al., 2013b). Ketorolac disrupts the synthesis of prostaglandins (Dong et al., 2013b). As such, these results indicate that NGF is likely an early mediator of facet joint pain, but additional mechanisms, like prostaglandin synthesis, may contribute to the maintenance of inflammatory pain at later times. Both spinal and local joint interventions can reduce facet joint-mediated pain by targeting one of several neuropathic and inflammatory mechanisms that converge to promote central sensitization. However, blocking joint afferent activity *after* afferent discharge has already induced spinal plasticity is ineffective (Chapter 4) (Crosby et al., 2014a), just as blocking prostaglandin synthesis *before* prostaglandins contribute to pain does not reduce sensitivity (Fig. 8.3) (Dong et al., 2013b). Therefore, the timing of each intervention relative to the temporal development of the targeted mechanism is a crucial consideration for effective treatment of facet joint pain.

The magnitudes of facet joint distraction and the resulting local strain in the facet capsule play a key role in the induction of facet joint-mediated pain, because the afferent fibers that innervate the joint are activated in a strain-dependent manner (Chen et al.,

2006; Lu et al., 2005a). Low-threshold mechanosensitive and nociceptive afferents in the facet capsule are differentially activated by the capsule strains that are produced during physiologic and injurious joint loading, respectively (Dong et al., 2012; Lu et al., 2005a). Physiologic joint loading alone does not initiate behavioral sensitivity, or the dorsal horn neuronal hyperexcitability or inflammatory cascades that promote pain (Dong et al., 2011; Lee and Winkelstein, 2009; Quinn et al., 2010). However, when spinal TSP4 levels are increased, physiologic loading of the facet joint *does* induce sustained behavioral sensitivity and spinal hyperexcitability (Chapter 5) (Crosby et al., 2014c). In addition to its synaptogenic properties, TSP4 can potentiate the pre-synaptic release of excitatory neurotransmitters (Kim et al., 2012), possibly by strengthening the pre-synaptic calcium currents that stimulate neurotransmitter release (Neher and Sakaba, 2008). Increased spinal TSP4 may enhance excitatory neurotransmitter release at the synapses between primary afferents and dorsal horn neurons, increasing the temporal and spatial summation of excitatory post-synaptic potentials and the likelihood of dorsal horn neuronal activation. This priming of dorsal horn neuronal firing may facilitate the initiation of spinal hyperexcitability in response to the non-noxious primary afferent signals that are typically induced by physiologic joint loading. Spinal TSP4 can be upregulated by painful facet joint loading (Crosby et al., 2014c) or peripheral nerve injury (Kim et al., 2012; Li et al., 2014a), but it remains unclear whether nonpainful mechanical loading of joint or neural tissue is sufficient to increase spinal TSP4 levels. Nonetheless, higher spinal TSP4 levels prime the development of neuronal hyperexcitability in response to cervical spine motions and/or facet capsule strains that are within the normal, physiologic range. Therefore, higher endogenous levels of spinal TSP4, or increased spinal TSP4

from either previous nerve injury or injurious joint loading, may present a higher risk for the development of joint-mediated pain.

Central sensitization often involves hyperexcitability of the wide dynamic range (WDR) neurons in the spinal dorsal horn that integrate non-nociceptive and nociceptive signals from primary afferents (Basbaum et al., 2009; Christensen and Hulsebosch, 1997; Hains et al., 2003c; Hao et al., 1992; Zhang et al., 2005). Dorsal horn WDR neurons are sensitized within one day after painful facet joint injury (Chapter 3) (Crosby et al., 2013), and WDR hyperexcitability persists for at least seven days (Quinn et al., 2010b). Since neuronal hyperexcitability can amplify nociceptive signals in the dorsal horn, direct modulation of the excitability of dorsal horn neurons can effectively reduce aberrant nociception. That strategy is exemplified by the use of spinal cord stimulation (SCS) to modulate spinal neuronal activity for attenuating pain symptoms (Guan et al., 2010; Yakhnitsa et al., 1999). Conventional tonic SCS reduces behavioral sensitivity after peripheral nerve injury by attenuating WDR neuronal hyperexcitability (Yakhnitsa et al., 1999). Studies in this thesis evaluated burst SCS, a novel mode of stimulation, to determine potential mechanisms that may underlie its analgesic effects. Similar to tonic SCS, the anti-nociceptive effects of burst SCS are likely related to its attenuation of WDR hyperexcitability, because burst SCS inhibits neuronal activity most effectively in WDR neurons (Chapter 6) (Crosby et al., 2014b).

Burst SCS reduces neuronal hyperexcitability in the spinal dorsal horn after a painful nerve root compression. However, the burst stimulation waveform is defined by five parameters (pulse number, pulse frequency, pulse width, burst frequency, and amplitude), and the reduction in neuronal activity is highly dependent on the values of

those parameters (Chapter 6) (Crosby et al., 2014b). Although individual parameters can alter the effectiveness of burst SCS, modulating the charge delivery to the spinal cord is the underlying factor that determines the effectiveness of burst SCS (Chapter 6) (Crosby et al., 2014b). Burst SCS was originally hypothesized to reduce pain more than tonic SCS because burst stimulation delivers significantly more charge over time than traditional tonic SCS (De Ridder et al., 2010). The amount of charge delivered *per burst* is correlated to the attenuation of neuronal activity, but a 50% increase or decrease in burst frequency, and therefore in the amount of charge *per second*, does not alter the effectiveness of burst SCS (Chapter 6) (Crosby et al., 2014b). The insensitivity of spinal neuronal activity to changes in burst frequency suggests that charge delivery over time is less important for burst-SCS induced analgesia than charge delivery during each individual burst. These results showing the sensitivity of burst SCS to charge delivery provide a framework for the optimization of burst SCS on a patient-by-patient basis by indicating those parameters that have the greatest effect on SCS efficacy, but further comparisons between burst and tonic SCS are needed to evaluate the role of charge delivery in the differential effects of the two SCS modes for reducing chronic pain.

Burst SCS reduces spinal neuronal hyperexcitability to the same extent in rat models of painful cervical nerve root compression and mechanical facet joint injury (Chapter 7). Dorsal column stimulation has been proposed to inhibit neuronal activity in the dorsal horn by activating Aβ fibers that collateralize into the dorsal horn and synapse with inhibitory interneurons (Guan et al., 2010; Yaksh and Luo, 2006). Inhibitory interneurons that are activated by Aβ fiber stimulation can directly influence the activity of dorsal horn projection neurons, especially the nociceptive-specific neurons in the

superficial laminae and the WDR neurons in the deeper laminae that contribute to pain signaling (Daniele and MacDermott, 2009; Dubuisson, 1989; Yakhnitsa et al., 1999). Burst SCS has been evaluated in a limited number of clinical studies, most commonly in patients with back pain from failed back surgery syndrome (FBSS) (De Ridder et al., 2010; De Ridder et al., 2013; De Vos et al., 2014), and studies are needed to test the effectiveness of burst SCS in patients with indications other than FBSS. However, dorsal horn neuronal firing is attenuated by burst SCS to the same extent in rat models of neuropathic pain and joint pain (Chapter 7), and in a model of acute nociceptive pain (Tang et al., 2014). Therefore, the mechanisms of SCS-induced dorsal horn inhibition are likely conserved regardless of the pathophysiological basis of the pain, and burst stimulation may be effective for analgesia in patients with a wide range of chronic pain conditions.

Studies in this thesis indicate that burst SCS does not reduce dorsal horn neuronal hyperexcitability more than tonic SCS after painful cervical nerve root compression or painful cervical facet joint injury (Chapter 7). Therefore, it was hypothesized that burst and tonic stimulation act through a similar mechanism, namely the activation of inhibitory GABA signaling in the dorsal horn. $GABA_B$ receptor antagonists abolish the effects of tonic SCS but not burst SCS (Chapter 7), indicating that, unlike with tonic SCS (Cui et al., 1996), burst stimulation-induced analgesia is not mediated by GABA signaling. Burst SCS requires a significantly lower amplitude than tonic SCS for effective analgesia (Chapter 7) (De Ridder et al., 2010), so it has been proposed that burst SCS inhibits dorsal horn firing via subthreshold stimulation of Aβ fibers (i.e., without inducing firing of the Aβ fibers) (De Ridder et al., 2010). Therefore, it is possible that

burst SCS inhibits neuronal activity in the dorsal horn with subthreshold stimulation that does not activate the inhibitory interneurons that release GABA. Instead, burst SCS may increase the dorsal horn levels of other neurotransmitters that potentially have lower thresholds for release during stimulation. Serotonin, for example, is increased in the dorsal horn during tonic SCS (Linderoth et al., 1992) and can have inhibitory effects on nociceptive dorsal horn neurons (Grudt et al., 1995). Selective antagonism of serotonin receptors in the dorsal horn during the application of SCS in rats with neuropathic pain indicates that a subset of receptors are activated and contribute to dorsal horn inhibition during tonic SCS, independent of GABA signaling (Song et al., 2011); however, the role of serotonin signaling in the effects of burst SCS are unknown. Future studies should continue to evaluate these potential inhibitory mechanisms of burst SCS, because understanding the mechanisms underlying the effects of that mode of stimulation is necessary to improve its effectiveness as a treatment for chronic pain.

8.3. Limitations and Future Work

The studies presented in this thesis demonstrate that afferent firing from the facet joint early after joint loading induces potentiation of glutamatergic signaling and excitatory synaptogenesis in the dorsal horn that collectively promote spinal neuronal hyperexcitability. However, neuronal hyperexcitability can be directly modulated by spinal cord stimulation to inhibit aberrant nociception in the dorsal horn. This work contributes to a better understanding of the mechanisms underlying the development and treatment of persistent pain from mechanical loading of tissues in the cervical spine, but there are several assumptions and limitations that require consideration. As such, this

section addresses important limitations and also outlines additional studies that could be performed to build upon the findings in this thesis.

The ectopic activity that develops within one day after painful facet joint injury (Chapter 3) (Crosby et al., 2013) may promote spontaneous pain by activating nociceptive neurons in the dorsal horn in the absence of peripheral afferent stimulation (Devor, 2009; Djouhri et al., 2000). Indeed, spontaneous pain, or ongoing pain, is observed in a majority of patients with whiplash-associated disorders (Kosek and Januszewska, 2008). However, the presence or severity of spontaneous pain was not measured in the studies in this thesis. Ongoing pain has been evaluated in rat models of neuropathic pain and formalin-induced pain by quantifying abnormal spontaneous behaviors like lifting or licking of the affected forepaw (Djouhri et al., 2006; Kawasaki-Yatsugi et al., 2012; Shi et al., 2010). Operant behavioral assessments may also reveal the presence of ongoing pain, including conditioned place preference (CPP) testing, in which rats are conditioned to environments that are linked to positive (i.e., analgesic) or negative (i.e., aversive) stimuli (Sufka, 1994). In that testing paradigm, rats with spontaneous pain show an increased preference for an environment that has previously been associated with an analgesic treatment (Davoody et al., 2011; King et al., 2009). However, difficulties in reliably, sensitively, and quantitatively measuring spontaneous pain in rats have prevented the acceptance of a consensus methodology for acquiring such data (Mogil and Crager, 2004). As better measures are developed to objectively measure spontaneous pain in animal models, future studies should evaluate spontaneous pain as a potentially important component of joint-mediated pain after facet injury.

A large majority of animal studies of pain and analgesia have historically included only male subjects, despite the fact that the prevalence of clinical pain conditions is higher in women (Greenspan et al., 2006; Mogil and Chanda, 2005). This effect is observed for whiplash-associated pain as well, since pressure pain thresholds are lower for women than for men both at the site of injury in the neck and at distant sites in the upper limbs (Sterling et al., 2003). The sex-dependent differences in pain thresholds after rear impacts may be due in part to different cervical spine kinematics; women experience greater facet joint shear loading and joint distraction than men, especially at the lower cervical levels (Stemper et al., 2004). The studies in this thesis used only male rats, and the findings may, therefore, be limited by their exclusion of female animals. Future studies including both female and male subjects are needed in order to evaluate if there are any potential sex differences in the mechanisms that promote facet-mediated pain.

Although injury-induced afferent activity from the facet joint has been shown to initiate spinal hyperexcitability and sustained behavioral sensitivity (Chapter 4) (Crosby et al., 2014a), the specific roles of subpopulations of primary afferent fibers in the induction of spinal hyperexcitability were not evaluated in this thesis. A fibers and C fibers are believed to have distinct contributions to the temporal development of central sensitization after nerve injury (Devor, 2009), so understanding the temporal contributions of primary afferent fiber subpopulations to the induction and maintenance of persistent facet-mediated pain may be critical for effective timing and targeting of analgesic treatments. C fiber nociceptors in the facet joint may play a particularly important role in the development of central sensitization, because selective chemical ablation of spinal peptidergic C fibers prior to painful facet joint injury prevents the

development of behavioral sensitivity (Weisshaar et al., 2014). Peptidergic C fibers also mediate the sensitivity that is induced by intra-articular NGF (Kras et al., 2014b). However, degeneration of C fibers can trigger secondary structural changes in the spinal dorsal horn (Bailey and Ribeiro-Da-Silva, 2006), so ablating C fibers at their central terminals may cause unanticipated modifications in the spinal processing of pain signals that confound any determination of the contributions of the ablated afferent population to persistent pain. Instead, future studies could use pharmacological compounds that selectively and transiently block subpopulations of afferent fibers, like substance P antagonists that inhibit peptidergic C fiber activity (Xu et al., 1992), to determine the individual roles of fiber types in the development and maintenance of pain after injurious facet joint loading.

Excitatory synaptogenesis contributes to persistent facet joint-mediated pain, but the studies in this thesis only evaluated synapses at day 7. The temporal development of excitatory synaptogenesis and the potential contributions of other synapse populations (i.e., inhibitory synapses) to spinal hyperexcitability are unknown. Synapses in hippocampal neuron cultures begin to develop by day 4 after plating the neurons, but do not reach maturity for 10-12 days (Basarsky et al., 1994), and synaptogenesis occurs over the course of several weeks after CNS injury (Wells and Tripp, 1987). Based on those timelines for the development of synapses in the CNS, a preliminary study evaluated excitatory and inhibitory synapses at day 14 after painful facet joint injury to determine whether structural modifications continue to develop after day 7. Excitatory synapses were identified by immunolabeling bassoon, a pre-synaptic structural protein, and homer, as described in Section 5.3.5 of Chapter 5. Inhibitory synapses were quantified by

immunolabeling bassoon and the inhibitory post-synaptic marker, gephyrin, which is a structural protein that organizes GABA and glycine receptors at inhibitory synapses (Tretter et al., 2012; Zeilhofer, 2005). Excitatory synapse density significantly increases in the superficial dorsal horn by 1.40-fold over sham levels at day 14 after painful facet joint injury (p=0.019) (Fig. 8.4a). The increase in excitatory synapses at day 14 is similar to the 1.56-fold increase at day 7 (Chapter 5), showing that the structural changes in the spinal cord that promote spinal hyperexcitability are sustained and likely contribute to the persistence of behavioral sensitivity at day 14 (Fig. 8.1).

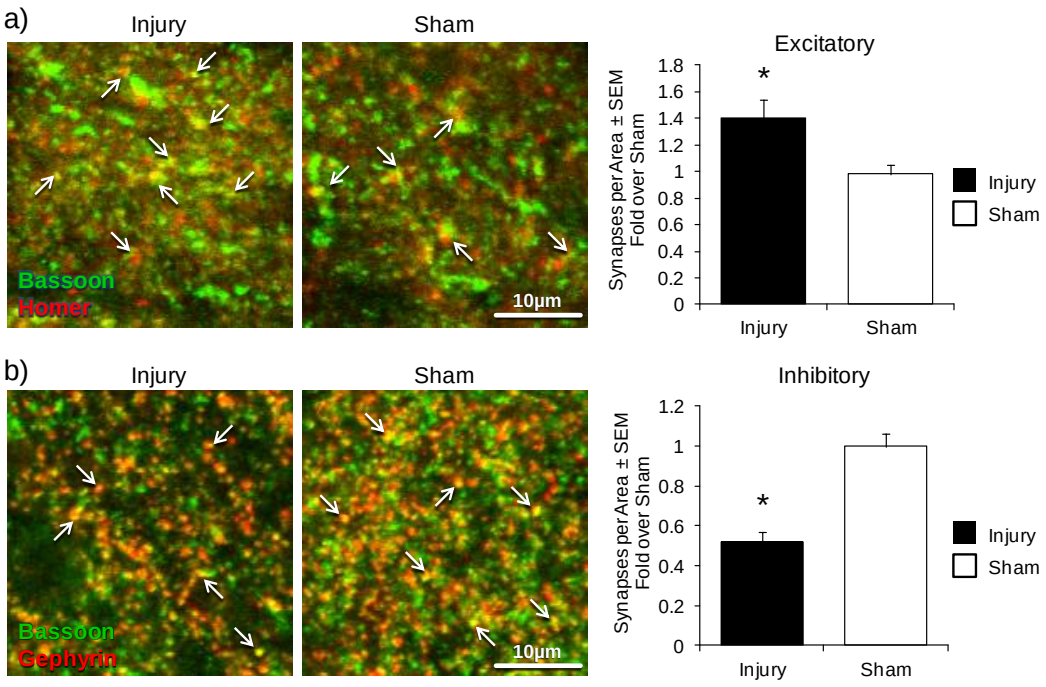

Fig. 8.4. Quantification of excitatory and inhibitory synapses at day 14 after painful facet joint injury. **(a)** Representative images showing the immunolabeling of bassoon (green) and homer (red) in the superficial dorsal horn at day 14 after painful facet joint injury (n=6) or sham surgery (n=5); excitatory synaptic puncta (yellow, arrows) are increased over sham levels (*p=0.019). **(b)** The number of inhibitory synapses, identified by colocalization (yellow, arrows) of bassoon (green) and gephyrin (red) decreases at day 14 (*p<0.0001).

Inhibitory synapse density decreases to 51% of sham levels in the superficial dorsal horn at day 14 after painful facet joint injury ($p<0.0001$) (Fig. 8.4b), suggesting a decrease in spinal inhibition that could amplify nociceptive signals by potentiating neuronal firing in response to excitatory afferent input (Zeilhofer, 2005). Decreases in gephyrin-labeled synaptic puncta in the dorsal horn could indicate fewer functional GABA and/or glycine receptors at inhibitory synapses, or complete degeneration of those inhibitory synapses (Todd, 2010). However, peripheral nerve injury induces spinal disinhibition without any change in immunolabeling of GABA or $GABA_A$ receptors (Moore et al., 2002; Polgar and Todd, 2008), so the loss of gephyrin-positive puncta in this preliminary study may instead correspond to a decrease in glycinergic synapses. The decrease in inhibitory synapses at day 14 shows that structural changes in the spinal cord persist for at least two weeks after facet joint injury, and likely contribute to the hyperalgesia that is sustained at that time point (Fig. 8.1). If the numbers of excitatory and inhibitory synapses change concurrently, it could indicate a shift of inhibitory synapses to an excitatory phenotype rather than degeneration of inhibitory synapses and development of new excitatory terminals. Alternately, it is possible that excitatory synaptogenesis precipitates the loss of inhibitory synapses, and spinal disinhibition develops in response to the hyperexcitability of dorsal horn neurons. Ultimately, further studies are needed to define the temporal development of both excitatory and inhibitory structural modifications in the spinal cord after painful facet joint injury.

One of the greatest impediments to characterizing injury-induced synapse growth or loss in vivo is differentiating preexisting synapses from those that develop after injury. Mouse models have been increasingly used for the study of pain (Mogil, 2009), though

recapitulating a model of painful facet joint injury in the mouse would be complicated by physiological and behavioral differences between species. For example, some considerations that are intended to reduce stress-related changes in nociception in the rat, like handling the rats to habituate them for behavioral testing, may actually increase stress in mice and confound the use of behavioral assays to measure nociception (Wilson and Mogil, 2001). Nonetheless, the powerful genetic technologies available in mice may overcome some of the obstacles to the in vivo study of synaptogenesis (Holtmaat et al., 2013). The use of fluorescent reporter genes like GFP or tdTomato with cell-type-specific expression patterns may allow the determination of which primary afferent and/or dorsal horn neuronal populations are involved in the gain or loss of synapses after injury (Cavanaugh et al., 2009; Holtmaat et al., 2013; Kain et al., 1995). Alternately, synaptic proteins can be identified in a cell-type-specific fashion using Synaptic Tagging with Recombination (STaR), a transgenic approach that alters selected synaptic proteins to include a GFP reporter or a small peptide tag that can be detected by immunolabeling (Chen et al., 2014). Increases in synaptic proteins within one neuronal subpopulation after injury may indicate the development of new synapses associated with those neurons.

The studies in this thesis did not consider supraspinal changes that could contribute to spinal hyperexcitability and/or persistent pain. Descending pathways from the brain have dual inhibitory and facilitatory roles in spinal dorsal horn processing of nociceptive signals (Millan, 2002; Vanegas and Schaible, 2004). Chronic pain is often associated with concurrent disinhibition and increased facilitation from descending pathways that collectively promote spinal neuronal hyperexcitability (Blom et al., 2014; Porreca et al., 2002; Vanegas and Schaible, 2004). The brain can also contribute to

persistent pain by amplifying *ascending* nociceptive signals from the spinal dorsal horn. Nociceptive neurons project from the spinal dorsal horn to the thalamus (Basbaum et al., 2009), and thalamic neurons can become hyperexcitable after peripheral nerve injury in rats, promoting behavioral sensitivity (Fischer et al., 2009; Miki et al., 2000). As such, future studies of facet joint injury should consider these potentially multifaceted supraspinal contributions to persistent pain by electrophysiologically assessing neuronal activity in the thalamus and the brain regions that modulate descending facilitation and inhibition, like the rostroventral medulla and the periaqueductal gray (Porreca et al., 2002; Vanegas and Schaible, 2004).

Another recently developed technology, Time-Specific Tagging for the Age Measurement of Proteins (TimeSTAMP), uses protease degradation of an engineered epitope tag to allow detection of only recently translated proteins (Lin et al., 2008). TimeSTAMP has been employed to identify newly developing synapses in vitro, and may provide the ability to characterize injury-induced synaptogenesis in vivo (Lin et al., 2008). To date, STaR and TimeSTAMP have been developed for use in vitro or in vivo in Drosophila, so significant work would be required to adapt these technologies to investigate synaptogenesis in rodent models of persistent pain. Nonetheless, these technologies could provide insight about the time course of injury-induced synaptogenesis and the neuronal populations that develop new excitatory synapses or lose inhibitory input.

The application of spinal cord stimulation in the different pain models used in this thesis contrasts substantially with the delivery of stimulation that is used clinically. A single, monopolar, ball-shaped electrode was used to administer electrical pulses to the

dorsal columns in the studies in this thesis (Chapters 6 and 7) (Crosby et al., 2014b), based on previous techniques for the administration of SCS in animal models of acute nociceptive pain (Qin et al., 2012; Tang et al., 2014). However, humans often receive implantation of arrays of up to 16 electrodes that can be programmed in different patterns as cathodes, anodes, or inactive terminals. Electrode arrangement and programming is known to be a significant variable in the effectiveness of stimulation by altering the charge density and steering the depth and location of current delivery (Alo et al., 1998; Alo et al., 1999; Manola et al., 2007; Shankarasubramanian et al., 2011; Wesselink and Boom, 1998). As such, the attenuation of dorsal horn neuronal firing by monopolar burst SCS in rats may not directly correspond to the effects of burst SCS in humans that receive multielectrode stimulation. Furthermore, dorsal horn neuronal firing was quantified immediately *after* the cessation of SCS because artifacts from the electrical stimulation prevented the recording of voltage potentials *during* SCS. In clinical studies, pain scores are reported *during* stimulation (De Ridder et al., 2010; De Vos et al., 2013). Although SCS is a clinically-approved therapy for many chronic pain conditions, studies in rodent models of pain form the foundation of understanding the mechanisms that underlie SCS-induced analgesia and provide potential insight for improved effectiveness of SCS. As such, due to those limitations listed above, the electrophysiological recordings of dorsal horn neuronal activity in these rat studies should be considered together with studies that employ more clinically-relevant stimulation, like bipolar stimulation from an implanted electrode array, and actively assess pain-related behaviors during stimulation.

Clinical studies of the effectiveness of SCS often rely on patient-reported pain scores to determine whether stimulation attenuates pain symptoms (De Ridder et al., 2010; De Vos et al., 2013; Van Buyten et al., 2001). Some measures, like the visual-analog scale (VAS), require patients to rate their pain on a linear scale (Downie et al., 1978), whereas other methods, like the McGill Short Form, seek to differentiate the sensory and affective components of pain (Melzack, 1987). The affective dimension of pain includes the unpleasant emotional associations with pain that lead to aversive behavior (Price, 2000). Psychosocial and affective dimensions are important contributors to chronic pain in both humans and rats (Johansen et al., 2001; LaBuda and Fuchs, 2000; Price, 2000), including those with whiplash-associated disorders (Drottning et al., 1995). The measurements of mechanically-evoked hyperalgesia and dorsal horn neuronal activity used in this thesis assess the spinal integration of sensory signals, but those outcomes likely do not fully characterize the effects of SCS on pain. More comprehensive behavioral assays may better evaluate SCS-induced analgesia by incorporating the psychosocial and affective components of pain (Vierck et al., 2008). CPP testing offers one potential behavioral assay to evaluate the effects of an analgesic treatment like SCS without relying on reflexive nociceptive behaviors to indicate the severity or presence of pain (Sufka, 1994). CPP has not been employed in a rodent model of pain to study the effectiveness of spinal cord stimulation, but its use could significantly increase the clinical relevance of studies using SCS in animal models of pain.

In summary, the studies presented in this thesis define the mechanisms that contribute to spinal hyperexcitability after mechanical facet joint injury. Painful facet joint injury produces afferent discharge from the facet joint that initiates spinal neuronal

hyperexcitability. The initiation of spinal hyperexcitability by facet joint afferent activity is similar to the mechanisms that induce central sensitization after a peripheral nerve injury. In one respect, the studies in this thesis are important *because* of the demonstrated similarities between the development of spinal neuronal hyperexcitability after facet joint injury and peripheral nerve injury. Those similarities support the potential application of therapies, like gabapentin administration, that have been used previously to successfully treat neuropathic pain in order to treat patients with facet joint-mediated pain. However, it is also important to continue to separately evaluate mechanisms of injury, nociception, and central sensitization after mechanical facet joint loading because injurious facet joint distraction induces soft tissue damage and inflammation that may lead to differences from neuropathic pain that are not defined in this thesis.

Joint afferent discharge induces synaptic plasticity in the dorsal horn by day 7 that potentiates excitatory glutamatergic signaling and amplifies pain sensation. Injury-induced afferent activity also leads to the dysregulation of TSP4 expression in the DRG and spinal cord, possibly as early as day 1, which can stimulate TSP4-mediated excitatory synaptogenesis. Synaptogenesis likely develops over the course of several weeks, and coincides with a loss of inhibitory synapses in the dorsal horn; together these spinal structural modifications contribute to the maintenance, but not the initial development, of spinal hyperexcitability. Additional work is needed to further evaluate the development of spinal hyperexcitability and its contribution to the initiation and maintenance of pain. In particular, more comprehensive behavioral assays are needed to characterize the spontaneous, evoked, and affective components of persistent pain after facet joint injury.

The studies in this thesis also show that burst spinal cord stimulation is an effective treatment to modulate spinal hyperexcitability. Despite its apparent clinical effectiveness (De Ridder et al., 2013; De Vos et al., 2014), additional studies are still needed to elucidate the mechanisms underlying the analgesic effects of burst SCS, because defining those mechanisms can lead to novel uses of the stimulation to improve analgesia. For example, the role of GABA signaling in the analgesic effects of tonic SCS was not reported until nearly 40 years after the first implanted electrodes were used to deliver tonic SCS (Cameron, 2004; Cui et al., 1996; Linderoth et al., 1994). After the importance of GABA signaling was discovered, intrathecal delivery of the GABA agonist, baclofen, was used to enhance the effects of tonic SCS, especially in patients that were previously non-responsive to SCS alone (Lind et al., 2004; Lind et al., 2008). Overall, this work provides a foundation for future investigations into the synaptic and structural mechanisms that promote hyperexcitability of dorsal horn neurons after painful facet joint injury. With a more comprehensive understanding of the peripheral and spinal sequelae that cause persistent pain from excessive facet joint loading, better pharmacological or electrical stimulation therapies can be developed to modulate spinal hyperexcitability and effectively treat chronic pain.

APPENDIX A

Protocols for Electrophysiological Recordings and Analysis

This appendix details the protocols for identifying and recording evoked potentials from dorsal horn neurons (Section A.1), and sorting spikes to quantify spontaneous and evoked neuronal firing (Section A.2). These protocols were used for the studies of dorsal horn neuronal excitability in Chapters 3-5. These protocols were also modified for use in studies of the effects of spinal cord stimulation on spinal neuronal excitability Chapters 6 and 7; detailed methods for those studies can be found in Section 6.3 of Chapter 6 and Section 7.3 of Chapter 7. In addition, the electrophysiological data from the studies in Chapters 3-7 are summarized in Appendix D.

A.1. Protocol for Identification and Recording of Dorsal Horn Neurons

1. In preparation for making spinal dorsal horn recordings, surgically expose the spinal cord, mount the rat on a stereotaxic frame, and instrument the rat for monitoring and control of body temperature and respiration (see Section 3.3.3 of Chapter 3 for detailed surgical methods) (Crosby et al., 2013; Crosby et al., 2014a).
2. Initialize the Spike2 program (CED; Cambridge, UK) for data acquisition and record continuously for the duration of the recording session. The recording file should include one channel for input from the recording electrode in the spinal cord, one

channel for input from the load cell, and one channel to record keystrokes for internal notation. The Spike2 Training Course Manual includes detailed information for customization of data acquisition.

3. Beginning at the C6 spinal cord, create a small hole in the pia mater using a sharp Dumont forceps, approximately midway in the mediolateral direction between the midline and the dorsal rootlets. Lower a carbon fiber electrode (Carbostar-1, Kation; Minneapolis, MN) using a micropositioner until the tip of the electrode reaches the surface of the spinal cord just above the hole in the pia mater.
4. Brush the forepaw continuously with a cotton swab while slowly lowering the electrode into the spinal cord in increments of 25-50µm. Once a mechanically-evoked response is identified in the audio feedback from the electrode, optimize the position of the electrode to maximize the signal-to-noise ratio of the evoked response in the voltage channel of Spike2.
5. Identify the location of the receptive field on the forepaw that evokes the maximal neuronal response and mark that location with a felt-tip pen to ensure that mechanical stimuli are applied consistently in that same location.
6. Record the identification number of the neuron in the keystroke channel to denote the beginning of the stimulation protocol. Acquire 30 seconds of baseline spontaneous firing data by passively recording neuronal activity without mechanically stimulating the forepaw or moving the rat.
7. Apply ten brush strokes to the plantar surface of the forepaw at the previously marked location in the receptive field of the neuron at a rate of approximately one stroke per second. Synchronize each brush stroke with a tap on the load cell to denote the time

of each brush stroke in the load cell channel. Wait 30 seconds before applying the next stimulus.

8. Apply a series of von Frey filaments to the forepaw that span the range of the filaments used for behavioral testing (1.4, 4, 10, and 26g). Apply each filament five times for one second, with a one-second rest in between each application. Tap the load cell during each application to denote the time of the stimulation in the load cell channel. Wait 30 seconds between the applications of different filament strengths.
9. Apply noxious pinch to the forepaw for ten seconds using a 60g vascular clip. Press the load cell during noxious pinch to denote the time of the stimulation in the load cell channel.
10. Once pinch stimulation ends and the stimulation protocol is complete, continue lowering the electrode to search for another neuron. To avoid recording from the same neuron, a second evoked response in the same spinal cord location must be separated from the first recorded neuron by at least 100μm of depth, and/or have a different receptive field on the forepaw. If the electrode reaches the boundary of the dorsal horn approximately 1000μm below the pial surface, return to Step 3 and begin the search and recording protocol at a new location caudal to the previous hole in the pia mater.
11. After recording 10-15 neurons from the C6/C7 spinal cord in each rat, terminate the surgery and collect the cervical spinal cord if tissue analysis will be performed.

A.2. Protocol for Sorting and Counting Spikes

Once data collection is complete, spike sorting can be performed offline to identify and quantify firing from individual neurons. The Spike2 Training Course Manual provides a detailed tutorial for spike sorting, but a brief protocol is outlined here.

1. The Spike2 file for each rat includes all neurons from a recording session. Export the voltage potential, load cell, and keyboard channels into a separate file for each individual neuron.
2. Apply a digital bandpass filter to the voltage potential channel with a passband of 0.3-3kHz. Create a new channel that contains the filtered voltage data. Perform all subsequent spike sorting steps on the filtered data.
3. Identify a detection threshold in the voltage channel for identifying spikes. The threshold should be above the noise in the system, but low enough such that evoked spikes surpass the threshold. A detection threshold can also be set to detect the downward deflection of voltage potentials, below the noise level of the voltage recording. The threshold should be separately adjusted to an appropriate level for each individual neuron.
4. Voltage potentials are sorted as individual spikes called WaveMarks, which can be counted to quantify neuronal firing. Create a new WaveMark channel to generate spike templates and sort the voltage potentials according to those templates. In the WaveMark dialogue box, set the detection threshold to the level identified in Step 3, and set the template width from -0.3ms to +0.4ms (Fig. A.1). Set the sensitivity of spike template generation and matching of evoked potentials to those templates using the settings in Fig. A.2.

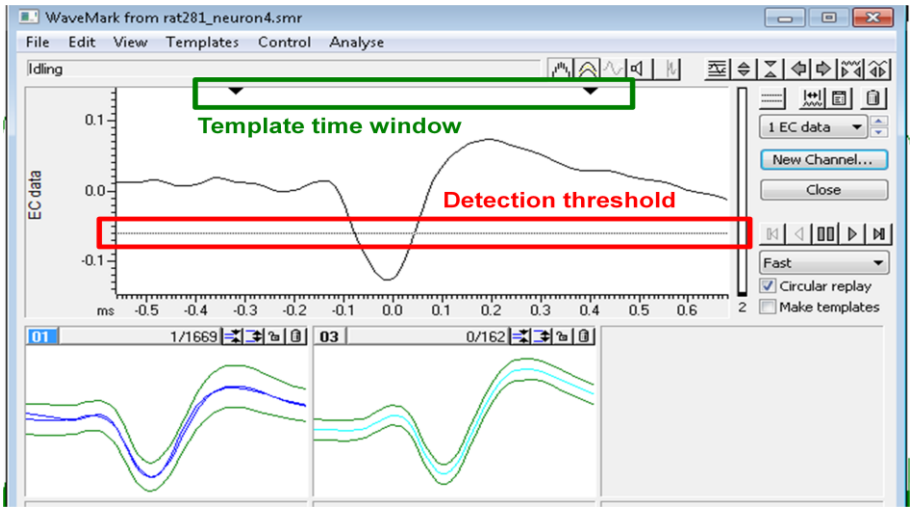

Fig. A.1. Spike template detection. This dialogue box controls the detection of spikes and the creation of a new WaveMark channel. Set a detection threshold in the voltage channel to discriminate spikes from noise in the system. The detection threshold (red) should be adjusted for each individual neuron. Set the time range (green) to adjust the width of spike templates to -0.3ms to +0.4ms.

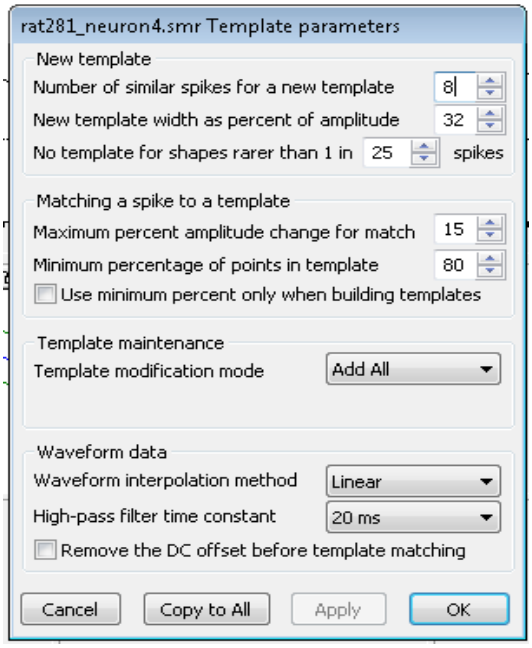

Fig. A.2. Spike template parameter dialogue box. The parameters in the "New template" section of this dialogue box control the generation of spike templates based on the spike shapes detected in the voltage recording. Parameters in the section labeled "Matching a spike to a template" control the sensitivity of the matching of voltage potentials to spike templates. The parameter values displayed here were used for spike sorting in all of the studies in this thesis.

5. If Spike2 generates multiple similar templates, they can be combined by clicking and dragging one template and releasing it on top of the similar template in the WaveMark dialogue box.
6. Choose the spike template that represents the neuronal firing evoked by mechanical stimulation of the forepaw. For quantification of the spikes, create a new channel that contains only the spikes assigned to that template.
7. Quantify the number of spikes evoked by ten seconds of light brushing. Record the number of spikes in the two seconds immediately before brushing as the baseline spontaneous firing.
    a. Use the load cell channel to identify the beginning and end of each stimulus (Fig. A.3). Slide two vertical cursors to the beginning and end of the stimulation period to quantify the number of spikes in between the two cursors (Fig. A.3).
8. Quantify the number of spikes evoked during the application of the von Frey filaments. Each evoked response includes the spikes during the one-second filament application plus the subsequent one-second rest period (Fig. A.3). Each filament weight, therefore, includes five separate evoked spike counts, one for each application of the filament (Fig. A.3). Record the number of spikes in the two seconds immediately before each filament weight as baseline spontaneous firing.
9. Quantify the number of spikes evoked during ten seconds of noxious pinch. Record the number of spikes in the two seconds immediately before noxious pinch as the baseline spontaneous firing.
10. Repeat Steps 2-9 for each individual neuron.

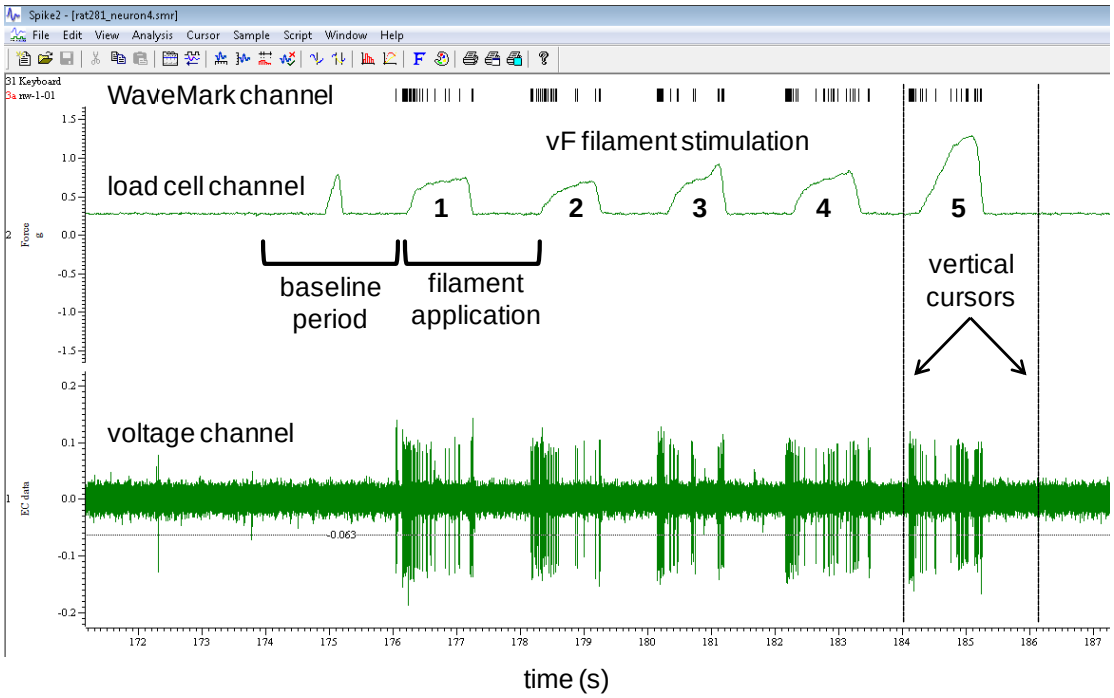

Fig. A.3. Quantification of evoked firing during von Frey filament stimulation. Shown is the Spike2 interface that is displayed after creation of a new WaveMark channel. Neuronal firing is shown for five applications of a von Frey filament, denoted by each displacement in the load cell channel (#1-5). Spontaneous firing is quantified in the two-second baseline period. Evoked firing is counted for each filament application, including the one-second stimulus plus the subsequent one-second rest period. Vertical cursors are used to mark the beginning and end of each filament application (shown here for filament application #5), and evoked spikes are counted for the time enclosed by the vertical cursors.

APPENDIX B

Facet Joint Distraction Mechanics and Facet Capsule Strains

This appendix includes the force, displacement, and strain data measured across the C6/C7 facet joint for each rat that underwent mechanical joint distraction. The load was measured by a load cell attached to the C7 forceps on the facet joint distraction device. Vertebral and capsule distraction magnitudes were determined during joint displacement based on the relative changes in the position of bead markers that were placed on the laminae of the C6 and C7 vertebrae and the C6/C7 facet capsule. Maximum and average maximum principal strains (MPS), strains in the rostral-caudal direction (x-strain), and strains in the medial-lateral direction (y-strain) were also calculated on the surface of the facet capsule. Strains were calculated using LS-DYNA (LSTC; Livermore, CA) based on the relative positions of the bead markers on the facet capsule before joint displacement and at the time of maximum vertebral distraction, as described previously (Dong and Winkelstein, 2010; Lee et al., 2004b).

In Table B.1, the mechanical data are presented for rats that were tested for hyperalgesia and neuronal hyperexcitability at 6 hours (*Injury-6h*) or 1 day (*Injury-d1*) after painful facet joint injury in the studies presented in Chapter 3. Table B.2 lists the mechanical data for all rats that underwent sham or painful facet joint injury followed by intra-articular injection of bupivacaine (BP) or saline vehicle (VEH) immediately (*inj-*

BP0h, *inj-VEH0h*), 4 hours (*inj-BP4h*), 8 hours (*inj-BP8h*), 1 day (*inj-BPd1*) or 4 days (*inj-BPd4*, *inj-VEHd4*) after injury, in the studies presented in Chapter 4. Lastly, Table B.3 summarizes the mechanical data for the rats that underwent either physiologic or injurious facet joint loading with intrathecal TSP4 treatment three days prior to joint distraction in the studies presented in Chapter 5.

Table B.1. Facet joint distraction mechanics for rats that were tested for hyperalgesia at 6 hours or 1 day after painful facet joint injury (Chapter 3).

Group	Rat #	Load (N)	Vertebral Distraction (mm)	Average Capsule Distraction (mm)	Maximum MPS (%)	Average MPS (%)	Maximum x-strain (%)	Average x-strain (%)	Maximum y-strain (%)	Average y-strain (%)
Injury-6h	30	3.94	0.86	0.43	84.28	40.79	32.40	6.39	31.42	4.98
	31	4.37	0.25	0.20	21.19	11.89	16.52	6.72	16.90	1.83
	32	2.72	0.73	0.35	38.08	20.40	32.44	13.15	12.54	5.07
	33	2.14	0.28	0.17	32.11	11.74	16.36	6.39	5.55	2.21
Injury-d1	13	3.37	0.87	0.49	119.68	52.99	96.57	26.67	27.25	7.22
	18	4.59	0.56	0.16	64.71	30.59	32.10	14.21	27.60	5.54
	20	4.47	0.54	0.28	37.50	24.40	27.00	16.50	21.30	3.81
	21	4.84	0.47	0.29	26.50	20.40	21.90	14.80	5.50	2.64
	27	3.82	0.69	0.33	31.62	15.53	15.81	10.11	18.33	6.82

Table B.2. Facet joint distraction mechanics for bupivacaine treatment study (Chapter 4).

Group	Rat #	Load (N)	Vertebral Distraction (mm)	Average Capsule Distraction (mm)	Maximum MPS (%)	Average MPS (%)	Maximum x-strain (%)	Average x-strain (%)	Maximum y-strain (%)	Average y-strain (%)
inj-VEH0h	45	4.58	0.70	0.28	22.0	17.4	21.1	15.5	8.8	1.2
	48	4.45	0.77	0.28	18.7	13.7	11.5	5.8	10.4	5.2
	50	5.51	0.46	0.38	36.1	25.3	33.0	16.8	17.4	2.6
	52	5.10	0.66	0.24	36.2	25.8	18.7	14.5	15.9	8.1
	53	3.76	1.07	0.48	62.4	33.2	44.4	26.5	12.1	3.8
	54	4.21	0.83	0.41	44.7	38.1	32.2	22.3	5.7	-2.7
	72	3.33	0.76	0.35	15.8	13.5	14.1	11.2	4.3	-1.0
inj-VEHd4	52a	3.50	0.65	0.35	40.0	30.8	30.8	18.9	7.4	0.5
	54a	3.36	0.80	0.44	63.3	43.1	41.5	29.5	7.2	-0.9
	66	3.04	0.65	0.37	22.7	19.2	19.4	13.6	-1.1	-2.8
	69	2.38	0.73	0.40	38.3	34.8	22.6	18.5	5.3	1.1
	71	3.05	0.65	0.24	29.6	27.8	9.6	7.9	16.7	13.0
inj-BP0h	41	4.89	0.66	0.29	53.4	26.1	23.0	9.9	10.5	3.8
	42	4.03	0.63	0.23	93.8	33.6	49.0	18.3	48.0	6.7
	43	4.47	0.89	0.38	85.9	28.7	70.4	18.1	25.8	4.6
	46	5.09	0.60	0.31	27.9	18.3	24.4	13.6	13.0	6.0
	49	4.59	0.86	0.31	28.9	19.4	24.0	12.7	12.7	3.7
	51	2.95	1.09	0.24	54.8	38.9	29.4	17.3	33.0	5.3
inj-BP4h	88	2.73	1.11	0.89	123.7	76.4	89.4	52.4	29.6	10.1
	89	3.50	0.64	0.30	27.2	22.2	19.2	12.0	16.8	8.6
	90	3.84	0.62	0.25	29.9	19.6	15.9	13.6	22.6	7.5
	91	3.18	0.73	0.15	46.8	30.4	34.1	10.5	33.2	12.1
	92	3.39	0.74	0.28	23.1	17.9	18.7	11.7	16.8	10.6
	93	3.60	0.58	0.27	55.3	27.8	29.0	11.2	44.5	14.3
	117	3.30	0.66	0.23	23.5	15.1	18.1	10.2	3.3	-1.7
	118	3.16	0.57	0.43	106.5	42.3	106.2	40.7	6.9	-4.1
inj-BP8h	111	3.31	0.70	0.37	59.6	36.7	55.3	22.4	18.9	10.1
	112	3.05	0.73	0.45	18.8	16.8	35.9	15.1	6.0	-7.8
	113	3.77	0.45	0.19	55.0	23.4	12.6	5.3	37.0	10.1
	114	3.16	0.90	0.44	52.9	34.3	31.7	23.2	25.5	4.6
	124	3.28	0.54	0.37	34.4	17.8	31.4	14.9	2.7	-0.4
	125	2.62	0.99	0.60	54.4	30.5	51.1	27.6	6.8	-7.0
	126	3.06	0.71	0.27	39.3	24.9	25.5	13.0	32.3	3.5
	127	2.89	0.71	0.32	61.2	23.9	57.8	16.6	7.5	2.1
	128	3.63	0.57	0.40	78.3	24.6	78.0	20.7	2.0	-4.7
inj-BPd1	82	4.14	0.58	0.26	35.2	21.3	17.6	11.3	27.6	10.3
	83	3.68	0.66	0.20	81.0	42.0	33.8	18.9	33.0	8.2
	84	4.08	0.53	0.15	43.6	22.4	9.3	4.2	35.7	15.3
	85	3.33	0.60	0.21	35.3	21.4	21.4	12.0	9.8	5.8
	86	3.76	0.45	0.21	37.4	18.7	29.3	9.2	35.3	9.5
	87	3.19	0.76	0.37	25.1	17.0	25.0	14.0	8.4	0.8
	119	2.94	1.01	0.61	73.8	57.2	69.8	51.0	7.3	-3.1
	120	2.94	0.70	0.37	22.7	18.2	20.9	13.9	8.9	1.8
	122	3.68	0.49	0.23	19.2	13.3	17.6	10.1	6.6	-0.5
inj-BPd4	53a	3.83	0.53	0.29	43.2	22.3	42.9	14.9	17.5	4.0
	56	3.20	0.78	0.35	30.4	25.9	17.5	15.2	3.3	1.4
	63	3.87	0.55	0.17	21.2	15.9	15.1	8.8	11.1	5.2
	64	2.93	0.89	0.52	70.1	53.7	30.0	18.1	15.8	1.7
	67	3.03	0.54	0.24	15.2	12.8	10.1	8.6	8.3	4.4
	70	4.11	0.51	0.28	21.3	15.9	8.7	6.4	12.6	5.9

Table B.3. Facet joint distraction mechanics for TSP4 treatment study (Chapter 5).

Group	Rat #	Load (N)	Vertebral Distraction (mm)	Average Capsule Distraction (mm)	Maximum MPS (%)	Average MPS (%)	Maximum x-strain (%)	Average x-strain (%)	Maximum y-strain (%)	Average y-strain (%)
Physiologic Joint Loading	245	1.35	0.14	0.12	6.9	4.7	2.5	0.9	6.4	2.0
	246	0.72	0.21	0.10	11.4	7.1	0.8	-1.2	11.2	5.2
	247	0.71	0.41	0.11	31.8	17.0	24.0	2.2	2.8	-14.0
	248	1.12	0.07	0.13	0.0	-2.5	24.6	4.3	19.8	10.1
	271	1.68	0.20	0.18	25.8	14.0	18.4	9.3	2.0	-1.1
	274	1.39	0.25	0.12	10.2	9.2	6.5	4.7	4.6	1.8
	275	1.46	0.22	0.12	9.9	8.8	7.6	6.6	2.5	2.2
	280	1.53	0.12	0.05	8.8	6.8	2.5	-1.2	2.3	-0.3
	282	1.76	0.21	0.13	12.8	9.3	10.0	6.1	4.7	3.3
	283	1.93	0.16	0.09	8.5	6.8	5.4	3.7	6.0	-0.2
	284	2.08	0.13	0.09	6.5	4.2	2.5	2.2	0.4	-3.0
	288	1.70	0.25	0.12	12.6	9.4	6.9	5.3	4.7	-0.4
	289	1.39	0.27	0.12	15.0	11.6	7.7	5.6	8.1	3.7
	290	1.55	0.30	0.14	13.8	10.1	9.5	6.1	1.6	0.5
	296	1.35	0.36	0.21	10.2	9.1	9.6	7.1	0.4	-2.3
	297	2.26	0.06	0.05	3.1	1.9	1.5	0.6	1.4	1.1
	298	1.33	0.25	0.14	8.3	7.6	6.4	2.7	4.2	2.4
	299	1.61	0.13	0.09	3.8	2.8	3.1	1.9	0.6	-1.2
Injurious Joint Loading	226	3.18	0.57	0.27	24.6	14.8	38.2	16.8	7.0	1.9
	227	3.63	1.25	0.34	34.2	22.3	30.5	14.8	7.0	1.9
	228	3.54	0.94	0.42	60.4	33.9	36.9	25.7	20.5	0.2
	253	3.17	0.67	0.38	36.3	27.5	14.6	8.3	17.6	10.6
	254	3.81	0.65	0.31	26.7	21.6	19.9	16.2	-2.1	-7.8
	255	3.65	0.58	0.41	33.9	25.2	31.3	22.8	-0.6	-4.4
	256	4.48	0.78	0.17	18.1	15.7	12.6	1.9	10.3	5.8
	257	4.13	0.49	0.13	40.5	31.3	12.3	3.1	19.5	11.2
	258	3.77	0.50	0.23	25.0	21.0	11.6	8.3	10.7	6.6
	259	4.05	0.59	0.28	35.8	29.7	24.5	18.1	8.6	4.3
	260	3.35	0.77	0.38	29.6	24.9	21.6	19.4	16.7	6.1
	261	4.08	0.61	0.47	64.6	36.6	32.1	20.6	8.3	-12.8
	262	4.04	0.41	0.18	12.0	10.1	8.6	7.3	0.4	-2.6
	263	3.04	0.81	0.47	98.9	60.4	67.7	35.6	9.9	6.5
	264	4.02	0.53	0.13	27.7	19.0	10.2	7.1	17.9	10.9
	281	3.55	0.58	0.29	26.6	24.0	20.3	15.7	7.1	6.1
	291	3.27	0.66	0.29	26.6	22.8	14.0	11.4	6.8	4.8
	292	3.44	0.76	0.45	93.4	42.9	49.7	30.6	6.7	-2.4
	293	3.84	0.54	0.18	27.3	16.4	9.7	7.9	11.3	1.8

APPENDIX C

Mechanical Hyperalgesia after Facet Joint Injury

This appendix summarizes the results for the assessment of mechanical hyperalgesia for each rat included in the studies in Chapters 3-7. Mechanical hyperalgesia is reported as the average of the left and right paw withdrawal thresholds (PWT) for each rat over three rounds of testing on each day. Table C.1 details the PWTs at baseline and at 6 hours or day 1 after a sham or painful facet joint injury (Chapter 3). Table C.2 includes PWTs for the rats that underwent sham or painful facet joint injury followed by intra-articular bupivacaine (BP) or vehicle (VEH) injections immediately (*inj-BP0h*, *inj-VEH0h*, *sham-VEH0h*), or at 4 hours (*inj-BP4h*), 8 hours (*inj-BP8h*), day 1 (*inj-BPd1*), or day 4 (*inj-BPd4*, *inj-VEHd4*, *sham-VEHd4*) after injury, for the studies presented in Chapter 4. For those studies, hyperalgesia was assessed prior to injury (BL) and on days 1, 3, 5, and 7 after injury.

The PWTs for the rats that underwent sham or painful facet joint injury for the characterization of DRG and spinal TSP4 expression at day 1 or day 7 after injury in Chapter 5 are summarized in Table C.3. Those rats were originally tested by Ling Dong and the behavioral responses have been previously published (Dong et al., 2011; Dong et al., 2012; Dong and Winkelstein, 2010). The PWTs for the rats that received daily intrathecal TSP4 antisense or mismatch oligonucleotides beginning three days before painful facet joint injury (Chapter 5) are presented in Table C.4. For those studies,

hyperalgesia was assessed through day 7 after the injury. Table C.5 details the PWTs at baseline, day 1, and day 7 after painful facet joint injury for the rats that received gabapentin (*Inj-GBP*) or vehicle treatment (*Inj-VEH*) in the studies presented in Chapter 5 that evaluate the effect of gabapentin on TSP4-induced synaptogenesis. Those rats were originally tested by Ling Dong and the behavioral responses were previously published (Dong et al., 2013a). The PWTs for the rats that received intrathecal injection of 20µg, 30µg, 45µg, or 60µg TSP4 or 60µg StrepII peptide to characterize the dose-response of TSP4 and mechanical hyperalgesia (Chapter 5) are listed in Table C.6. Hyperalgesia was assessed daily for ten days following injections.

Based on the PWTs in Table C.6, two doses were identified for use in the TSP4 treatment studies reported in Chapter 5 to evaluate the role of increased spinal TSP4 in facilitating spinal hyperexcitability after facet joint loading – a non-sensitizing dose (20µg) and a sensitizing dose (60µg). Table C.7 presents the PWTs for the rats in those studies that received a single intrathecal injection of 20µg or 60µg TSP4 after baseline testing, three days before either a sham, physiologic (Phys), or injurious (Inj) loading of the facet joint (*20µg TSP4+Sham*, *20µg TSP4+Phys*, *60µg TSP4+Sham*, *60µg TSP4+Phys*, *60µg TSP4+Inj*). Hyperalgesia was then assessed on days 1, 3, 5, and 7 after joint loading. Separate rats received 60µg intrathecal injections of StrepII peptide prior to sham or physiologic loading of the facet joint (*60µg StrepII+Sham*, *60µg StrepII+Phys*), to control for the presence of the StrepII tag on the recombinant TSP4 protein. Lastly, Table C.8 details the PWTs for the rats included in the studies in Chapter 7 using burst or tonic spinal cord stimulation; painful facet joint injury was applied seven days before

spinal cord stimulation, and hyperalgesia was assessed at baseline (BL) and on days 1, 3, 5, and 7 after injury.

Table C.1. Paw withdrawal thresholds at 6 hours or day 1 after sham or painful facet joint injury (Chapter 3).

Group		Rat #	BL	6h
6 hours	Sham	34	12.50	18.83
		37	15.17	10.67
		38	9.17	17.00
		39	7.67	5.33
	Injury	30	8.33	9.33
		31	4.67	6.00
		32	14.33	14.00
		33	7.00	11.67
Group		**Rat #**	**BL**	**D1**
Day 1	Sham	6	26.00	26.00
		17	24.78	26.00
		24	6.33	3.33
		26	4.50	5.67
		28	8.00	6.00
		29	18.67	9.67
	Injury	13	8.78	3.67
		18	22.33	11.17
		20	4.00	2.33
		21	7.67	8.83
		27	19.67	7.67

Table C.2. Paw withdrawal thresholds for bupivacaine treatment study (Chapter 4).

Group	Rat #	BL	D1	D3	D5	D7
inj-VEH0h	45	18.40	5.33	5.00	5.00	9.33
	48	12.50	10.67	6.50	6.33	5.00
	50	10.00	5.00	4.33	8.00	6.00
	52	7.83	1.60	2.47	1.80	1.70
	53	8.25	4.00	3.43	4.00	3.33
	54	6.25	2.13	2.23	2.23	2.13
	72	17.33	6.67	6.00	7.67	7.67
sham-VEH0h	78	14.75	11.83	11.00	11.83	16.83
	79	7.83	6.00	8.67	8.33	8.33
	80	14.25	9.50	11.50	16.83	8.83
	81	8.50	10.67	10.33	10.67	10.33
	133	8.92	11.00	10.50	11.33	16.00
	134	12.33	10.50	12.67	9.33	11.00
inj-BP0h	41	16.75	10.17	14.33	13.33	16.83
	42	11.20	7.67	7.67	5.33	10.33
	43	12.30	12.50	7.00	7.67	5.67
	46	7.17	8.00	8.33	7.00	9.17
	49	9.86	4.67	6.50	7.00	6.67
	51	20.08	6.50	15.17	13.33	10.17
inj-VEHd4	52	13.42	7.00	6.33	7.00	6.67
	54a	7.58	3.33	9.17	3.67	5.00
	65	7.83	2.90	4.67	4.67	3.67
	66	10.50	3.33	4.67	5.33	5.33
	69	20.50	6.33	8.00	5.67	4.00
	71	14.75	5.00	8.00	7.67	7.67
sham-VEHd4	135	12.42	12.50	12.67	13.00	11.33
	136	10.00	11.50	9.00	9.00	10.17
	137	14.75	13.00	12.17	10.67	9.33
	138	12.00	12.17	14.17	10.67	13.00
	139	12.08	11.33	12.17	11.83	11.83
	140	13.83	13.67	12.50	16.17	16.83
inj-BPd4	53	18.33	5.00	8.83	10.17	7.00
	56	11.94	7.33	8.00	6.00	6.67
	63	23.25	5.67	15.83	7.00	6.00
	64	17.00	9.83	9.33	8.00	6.50
	67	17.92	4.67	6.33	7.00	3.67
	70	7.67	1.70	3.00	2.67	2.03
inj-BP4h	91	8.42	7.67	8.67	9.00	7.00
	92	9.92	7.67	8.67	9.00	8.33
	93	16.50	14.17	14.17	16.00	11.33
	117	8.00	7.83	8.33	9.75	8.83
	118	17.00	19.67	16.00	13.75	17.83
inj-BP8h	124	10.17	3.33	2.50	4.00	4.00
	125	16.92	9.75	7.33	4.67	5.67
	126	16.83	8.50	7.00	8.00	7.00
	127	13.83	8.50	7.00	7.00	7.00
	128	11.67	7.50	12.50	7.00	7.00
inj-BPd1	83	7.50	4.00	1.50	1.50	1.50
	86	13.33	5.00	2.67	4.33	3.00
	87	18.75	11.83	19.00	14.33	14.50
	119	10.08	5.67	6.33	5.50	5.00
	120	22.42	7.67	6.67	8.00	6.00
	122	9.92	6.00	3.00	4.00	5.00

Table C.3. Paw withdrawal thresholds after sham or painful facet joint injury for characterization of TSP4 expression (Chapter 5).

Group	Rat #	BL	D1	D3	D5	D7
Sham	LD50	25.39	24.17	22.33	26.00	23.33
	LD55	17.25	18.83	17.00	15.17	15.17
	LD56	25.08	26.00	24.17	24.17	26.00
	LD60	16.92	18.67	15.17	19.67	18.67
	LD252	14.17	8.33	12.50	11.00	10.17
	LD253	13.00	12.50	14.17	14.17	14.17
	LD256	16.83	11.33	9.83	14.00	14.17
	LD257	7.83	6.33	8.83	8.83	7.33
	LD262	16.83	14.17	8.67	10.17	13.83
	LD263	13.33	14.17	8.67	12.50	12.17
	LD267	14.17	19.67	18.67	12.17	12.50
	LD270	24.17	20.50	13.33	15.00	15.17
	LD272	18.67	16.00	---	---	---
	LD274	8.33	8.50	---	---	---
	LD275	14.33	16.00	---	---	---
	LD281	16.83	16.00	---	---	---
	LD293	18.67	17.00	---	---	---
	LD300	16.00	11.50	---	---	---
Injury	LD47	15.17	7.00	4.00	5.00	3.67
	LD48	17.33	5.67	7.67	8.33	8.00
	LD49	18.25	8.00	8.33	7.00	7.67
	LD52	21.72	6.33	8.33	8.67	7.00
	LD53	18.58	12.50	9.50	7.00	8.67
	LD54	9.75	4.57	3.57	4.33	5.67
	LD254	13.33	6.33	7.33	9.83	10.17
	LD255	15.17	13.00	11.83	8.00	7.00
	LD248	15.00	5.33	6.33	4.67	6.67
	LD249	9.33	3.67	5.00	2.67	2.67
	LD264	16.83	4.67	3.33	2.90	3.67
	LD265	17.83	9.67	7.00	6.00	8.33
	LD266	20.50	9.00	10.83	10.50	10.67
	LD268	26.00	6.33	5.33	5.33	8.00
	LD271	16.83	5.67	5.33	6.00	6.67
	LD273	8.67	4.67	---	---	---
	LD278	15.17	5.33	---	---	---
	LD279	6.67	2.57	---	---	---
	LD280	11.00	3.67	---	---	---
	LD287	20.50	10.33	---	---	---
	LD292	12.50	6.67	---	---	---
	LD296	12.50	9.50	---	---	---
	LD299	12.17	6.00	---	---	---

Note – Spinal cord and DRGs were harvested on day 1 from rats #272-300 in the Sham group and rats #273-299 in the Injury group, so those rats only underwent behavioral testing at baseline (BL) and post-operative day 1 (D1). Rat numbers in this table refer to animals originally tested and presented by Ling Dong (LD) (Dong et al., 2011; Dong et al., 2012; Dong and Winkelstein, 2010).

Table C.4. Paw withdrawal thresholds after painful facet joint injury with administration of TSP4 antisense or mismatch oligonucleotides (Chapter 5).

Group	Rat #	BL	D-2	D-1	D0	D1	D3	D5	D7
Injury + TSP4 Antisense Oligonucleotides	229	14.67	14.83	14.17	13.33	13.33	14.17	10.17	9.17
	236	10.75	8.33	8.67	8.33	7.00	8.00	8.00	8.00
	231	10.33	12.17	13.33	13.00	11.00	10.17	10.17	9.83
	237	15.08	13.75	16.00	13.75	12.50	12.00	12.00	12.50
	241	14.67	12.50	12.50	13.75	13.33	10.50	11.25	10.17
	253	17.75	20.50	15.25	12.50	17.50	15.00	14.17	14.17
	254	12.50	10.00	9.50	10.00	9.67	9.33	10.83	9.00
	255	13.42	15.00	15.00	15.00	12.17	18.67	18.67	17.83
	256	12.00	13.00	13.75	15.00	14.17	12.17	12.67	12.67
	259	14.25	13.33	12.50	15.00	11.67	9.00	11.67	12.50
	260	9.33	9.83	15.00	11.25	12.50	15.17	14.33	11.33
Injury + TSP4 Mismatch Oligonucleotides	232	13.58	15.00	16.83	13.33	7.33	7.33	4.00	3.67
	233	15.08	16.00	13.33	16.83	6.33	7.00	7.33	7.33
	234	8.17	8.67	9.00	9.50	4.33	3.00	4.00	3.33
	238	9.83	9.50	11.25	10.75	6.67	4.33	4.00	6.33
	239	12.92	15.00	13.75	13.75	8.00	7.50	5.00	8.33
	240	12.83	12.00	12.50	12.00	5.33	6.33	7.00	4.67
	257	12.33	12.50	13.75	12.50	5.33	6.00	6.00	6.33
	258	13.17	19.25	16.50	16.50	7.33	9.83	8.00	6.00
	261	11.75	9.00	7.00	15.25	3.00	3.33	3.00	3.00
	262	9.42	10.75	13.75	8.00	5.33	4.33	3.00	5.00
	263	14.67	13.75	17.75	15.00	6.67	7.00	6.33	7.67
	264	13.33	13.75	12.50	10.75	6.33	4.00	5.00	5.33

Table C.5. Paw withdrawal thresholds for gabapentin treatment study (Chapter 5).

Group	Rat #	BL	D1	D3	D5	D7
Inj-GBP	LD301	14.83	10.50	14.17	17.83	14.17
	LD303	11.67	9.67	10.00	9.67	10.50
	LD305	16.83	9.00	11.67	16.00	12.50
	LD306	14.17	11.67	13.00	12.17	9.67
	LD307	12.17	7.33	9.83	13.33	8.67
	LD308	12.17	7.00	11.67	16.00	13.33
	LD355	9.33	7.33	8.67	8.67	7.00
	LD356	8.00	8.00	14.17	12.50	16.83
Inj-VEH	LD302	15.17	7.00	7.33	6.00	7.00
	LD304	13.00	6.00	6.33	3.67	3.67
	LD337	17.83	4.67	5.33	6.33	5.00
	LD338	15.17	7.00	9.33	9.67	8.00
	LD339	10.83	3.67	5.00	4.67	5.33
	LD341	10.17	4.67	4.33	5.67	5.67
	LD357	13.33	7.67	7.00	7.00	8.83
	LD358	11.67	4.33	5.67	5.33	6.33
	LD359	11.67	8.00	6.33	5.67	4.00

Note – Rat numbers in this table refer to animals originally tested and presented by Ling Dong (LD) (Dong et al., 2013).

Table C.6. Paw withdrawal thresholds for TSP4 dose-response study (Chapter 5).

	Rat #	BL	D1	D2	D3	D4	D5	D6	D7	D8	D9	D10
20µg TSP4	141	9.33	14.17	9.75	12.00	15.00	9.50	13.75	15.00	14.17	13.75	13.33
	142	11.33	14.33	5.00	12.00	12.50	15.00	13.75	13.75	10.00	13.25	13.33
	143	11.33	11.00	3.50	13.75	15.00	13.75	12.00	9.50	11.83	10.75	13.33
	202	11.88	10.75	7.50	11.25	11.50	7.00	10.75	10.75	10.75	12.00	15.00
	204	11.50	5.50	10.00	12.00	5.50	6.50	8.50	7.50	6.00	7.00	7.50
	206	15.00	15.00	15.00	15.00	15.00	15.00	15.00	15.00	15.00	15.00	15.00
30µg TSP4	186	8.83	7.50	4.50	9.00	8.00	8.00	6.50	6.50	6.00	---	7.50
	187	10.17	7.50	6.50	5.50	7.00	3.50	7.00	7.00	9.00	---	8.00
	188	10.17	7.00	7.00	7.50	6.00	7.00	9.50	7.00	12.00	---	9.75
	190	12.63	8.50	7.50	7.50	7.00	4.50	7.50	9.00	8.00	10.25	8.00
	192	13.75	10.75	8.50	8.00	8.50	8.50	8.50	15.00	9.00	15.00	15.00
	194	7.75	6.00	6.50	5.50	5.00	6.00	7.50	8.00	8.00	7.50	7.00
45µg TSP4	144	13.33	8.67	10.25	9.50	6.00	10.25	4.50	7.50	11.00	10.75	10.17
	145	15.00	12.17	10.75	7.50	9.75	13.25	10.25	9.75	12.50	13.75	14.17
	146	8.33	6.33	11.25	8.00	6.50	12.00	9.75	10.00	12.67	12.50	9.83
	201	11.38	8.50	7.00	7.00	6.00	6.00	7.00	7.50	12.50	12.50	12.50
	203	7.75	6.00	4.50	4.00	4.00	2.00	3.00	4.50	10.25	5.00	6.50
	205	7.50	3.50	4.50	6.00	3.00	4.50	7.00	8.50	7.50	15.00	10.25
60µg TSP4	183	8.67	6.00	6.50	2.50	5.00	4.00	4.50	7.00	7.00	---	6.50
	184	10.67	7.50	4.00	3.50	7.00	6.00	8.00	9.00	8.50	---	8.50
	185	13.33	12.50	8.50	4.50	5.00	6.00	5.50	6.00	8.00	---	8.50
	189	11.63	7.50	9.00	8.00	7.00	6.50	7.00	8.00	8.00	9.50	9.00
	191	7.75	7.00	5.00	3.00	2.50	6.00	4.00	7.00	8.00	8.00	8.00
	193	7.00	4.50	2.50	3.50	2.50	2.50	4.50	4.50	6.00	7.00	6.00
60µg StrepII	195	15.00	13.75	12.50	13.75	12.50	12.00	12.50	12.50	13.75	15.00	12.50
	196	8.75	7.50	9.00	7.50	8.00	8.50	8.50	9.00	8.00	9.00	9.00
	197	8.50	8.50	13.25	9.75	7.00	8.50	8.00	6.00	5.50	5.50	6.50
	198	15.00	15.00	12.50	12.50	12.50	12.50	13.75	11.25	10.25	8.50	11.25
	199	9.38	13.75	13.75	13.75	13.75	15.00	15.00	15.00	15.00	15.00	15.00
	200	7.50	13.75	12.00	12.00	12.50	13.75	11.25	15.00	15.00	11.25	10.75

Note – Hyperalgesia responses on day 9 for rats #183-188 are not available due to the confounding effects of excessive noise in the behavior testing environment.

Table C.7. Paw withdrawal thresholds for TSP4 treatment study (Chapter 5).

	Rat #	BL	D-2	D-1	D0	D1	D3	D5	D7
20µg TSP4 + Sham	272	9.00	9.50	11.25	13.75	12.50	15.00	10.50	12.00
	273	11.83	12.50	12.00	12.50	12.50	10.50	13.33	13.75
	302	8.33	8.00	8.00	10.00	8.67	10.00	7.33	8.00
	303	9.75	9.00	9.50	12.50	9.17	8.00	12.17	9.00
	304	10.58	13.75	12.50	12.50	13.33	12.50	12.50	13.75
	305	12.17	15.00	11.25	13.75	12.17	12.00	14.17	15.00
20µg TSP4 + Phys	243	9.92	9.33	11.50	9.17	5.00	4.33	4.00	3.67
	246	9.50	8.67	11.25	10.83	7.00	5.33	4.67	5.67
	248	14.17	14.17	13.75	14.17	7.00	8.67	10.17	8.33
	274	14.17	13.75	13.75	13.75	7.33	5.00	5.33	6.33
	282	12.42	12.17	12.00	13.75	11.83	6.33	5.33	6.00
	283	14.58	15.00	15.00	13.75	14.17	9.00	5.67	4.33
	284	9.00	.9.00	9.50	8.50	8.67	4.00	3.33	2.67
60µg TSP4 + Sham	277	12.33	6.00	9.00	7.50	9.33	8.67	11.33	11.83
	278	9.50	6.00	3.50	3.00	2.67	4.67	6.67	6.67
	279	13.33	9.00	7.00	5.50	6.33	8.67	9.50	9.83
	285	13.33	8.83	6.50	6.00	5.67	7.67	10.50	10.50
	286	11.42	5.33	5.50	4.50	3.33	3.67	6.00	4.33
	287	14.58	7.67	9.00	8.00	8.33	9.00	11.67	12.17
60µg TSP4 + Phys	244	13.75	7.00	7.00	4.67	5.00	7.00	6.00	4.00
	245	14.58	10.17	8.50	9.83	7.00	7.33	6.67	8.00
	280	11.83	7.00	3.50	4.50	2.33	1.90	2.03	1.70
	288	8.50	5.00	4.50	3.50	3.33	3.67	2.67	3.33
	289	12.75	13.25	7.00	8.50	5.33	8.00	6.33	6.33
	290	10.92	5.50	5.50	5.00	4.00	4.33	4.33	2.67
60µg TSP4 + Inj	223	14.17	8.00	7.83	6.67	7.67	4.33	6.33	4.33
	227	11.33	11.83	5.33	9.83	4.33	4.00	3.33	2.67
	281	8.50	5.50	4.00	3.50	3.67	4.00	2.80	3.23
	291	14.58	7.50	7.00	6.00	7.33	5.67	7.00	5.33
	292	10.33	4.50	2.50	3.00	3.33	3.00	3.67	2.67
	293	14.17	9.00	7.50	7.50	8.00	7.67	5.67	8.33
60µg StrepII + Sham	270	8.33	7.50	6.50	6.50	7.00	7.67	7.67	8.00
	276	15.00	15.00	15.00	15.00	14.17	15.00	15.00	14.17
	294	10.67	11.25	13.75	12.50	12.50	14.17	13.33	13.75
	295	14.58	12.50	10.75	15.00	15.00	13.33	14.17	13.75
	300	13.33	12.50	13.75	15.00	12.67	13.75	14.17	13.25
	301	12.33	8.50	12.00	8.50	9.67	12.50	10.83	12.00
60µg StrepII + Phys	271	11.33	12.50	13.75	12.00	12.50	12.17	12.50	13.75
	275	13.33	12.00	9.00	10.25	9.83	7.67	8.67	9.50
	296	14.17	13.75	13.75	13.75	15.00	14.17	15.00	15.00
	297	9.17	9.75	11.25	13.25	9.67	10.17	9.67	9.00
	298	14.58	12.50	8.50	12.50	9.33	13.33	11.67	13.25
	299	13.17	13.75	13.75	13.25	15.00	13.33	13.33	15.00

Table C.8. Paw withdrawal thresholds after painful facet joint injury for spinal cord stimulation at day 7 (Chapter 7).

	Rat #	BL	D1	D3	D5	D7
Injury	213	12.42	5.67	5.67	4.00	3.33
	214	14.50	6.33	7.33	8.00	9.17
	217	8.00	2.33	3.33	3.00	2.67
	218	13.75	7.33	6.33	4.00	2.67
	219	7.17	2.00	2.33	2.67	3.00
	220	17.00	6.33	8.17	7.67	7.00
	221	14.17	5.67	6.00	5.33	4.67
	222	8.17	3.23	2.33	2.67	3.33

APPENDIX D

Quantification of Dorsal Horn Neuronal Firing

This appendix lists the dorsal horn neuronal firing data for all of the rats in the studies presented in Chapters 3-7. A detailed protocol for the recording and analysis of these electrophysiological data is included in Appendix A. In the following tables, neurons are listed by the group and rat from which they were recorded. The depth column indicates the location depth in the dorsal horn where the electrode was placed for recording each neuron (μm below the pial surface of the spinal cord). The evoked spike counts are listed for each mechanical stimulus applied to the forepaw of each rat, including ten seconds of light brushing (Brush), five applications of each of four different von Frey (vF) filaments (1.4g, 4g, 10g, and 26g), and ten seconds of noxious pinch (Pinch). Baseline firing counts (BL) are presented for each mechanical stimulus as well. Missing cells in each table reflect that, for those neurons, the signal was lost during recording before completing the stimulation protocol.

Table D.1 lists the spike counts for the neurons recorded at 6 hours or day 1 after sham (*Sham 6h*, *Sham D1*) or painful facet joint injury (*Injury 6h*, *Injury D1*), in the studies presented in Chapter 3. Table D.2 presents the neuronal firing data on day 7 for the rats that underwent sham or painful facet joint injury followed by intra-articular bupivacaine (BP) or vehicle (VEH) injections immediately (*inj-BP0h*, *inj-VEH0h*, *sham-VEH0h*), or at 4 hours (*inj-BP4h*), 8 hours (*inj-BP8h*), day 1 (*inj-BPd1*), or day 4 (*inj-*

BPd4, *inj-VEHd4*, *sham-VEHd4*) after injury (from Chapter 4). Table D.3 details the neuronal firing data on day 7 for the rats that received intrathecal TSP4 treatments (20µg or 60µg) followed by sham, physiologic (Phys), or injurious (Inj) loading of the facet joint (*20µg+Phys*; *60µg+Phys*; *60µg+Inj*), for the studies presented in Chapter 5. That table also includes neuronal firing data on day 7 for the rats that received intrathecal injections of 60µg StrepII peptide before sham surgery (*Strep+Sham*).

Table D.4 lists the neuronal firing data for the optimization of the burst spinal cord stimulation (SCS) parameters on day 7 after painful nerve root compression in the studies presented in Chapter 6. The Stim Number column refers to the order in which each set of SCS parameters was applied to the neuron. The SCS parameters included pulse number (Pulse #), pulse frequency (Pulse Hz), pulse width (Pulse Width), burst frequency (Burst Hz), and amplitude (Amplitude). The charge per burst is also listed for each of the SCS parameter sets. In addition, the waveform identification codes from Spike2 (Spike2 Waveform ID) are presented for each neuron. The spikes associated with multiple waveforms were counted together if they corresponded to the same recorded neuron, and the waveform codes are indicated together (i.e., 01+02). Detailed methods for sorting spikes and combining waveforms are summarized in Appendix A.

Neurons were classified as wide dynamic range (WDR), if they fired in response to non-noxious and noxious stimuli, or high threshold (HT), if they fired only in response to noxious stimuli. Neurons that did not exhibit characteristic WDR or HT firing patterns were not classified (NC). Finally, baseline spontaneous firing (BL) and pre-SCS and post-SCS spike counts are listed based on the neuronal firing recorded in response to ten seconds of noxious pinch before and immediately following burst SCS.

Tables D.5-D.8 list the spike counts for all of the neurons recorded in the studies of burst and tonic SCS presented in Chapter 7. In each table, the spike counts are listed for each neuron during pre-SCS stimulation consisting of ten seconds of light brushing (Br), five applications of the 1.4g von Frey filament (1.4g vF) and the 26g von Frey filament (26g vF), and ten seconds of noxious pinch (Pinch). Baseline spontaneous firing counts are included for each mechanical stimulus (BL). Spike counts are also listed for 1.4g, 26g, and pinch stimuli applied at 0, 2, 5, 10, and 15 minutes post-SCS. Table D.5 lists the neuronal firing data after burst or tonic SCS on day 7 following painful nerve root compression. Table D.6 presents the spike counts after burst or tonic SCS on day 7 following painful nerve root compression with spinal superfusion of the $GABA_A$ receptor antagonist, bicuculline. Table D.7 presents the spike counts after burst or tonic SCS on day 7 following painful nerve root compression with spinal superfusion of the $GABA_B$ receptor antagonist, CGP35348. Lastly, Table D.8 details the spike counts after burst or tonic SCS on day 7 following painful facet joint injury, for studies presented in in Chapter 7.

Table D.1. Spike counts at 6 hours or 1 day after sham or painful facet injury (Chapter 3).

	Rat #	Neuron	Depth	Brush		1.4g vF						4g vF						10g vF						26g vF						Pinch	
				BL		BL	1	2	3	4	5	BL	1	2	3	4	5	BL	1	2	3	4	5	BL	1	2	3	4	5	BL	
Sham 6h	34	2	630	2	68	5	4	9	5	4	8	6	14	8	6	6	8	6	8	9	9	16	6	3	21	24	25	27	20	3	110
	34	3	470	0	48	0	2	2	2	0	2	0	5	2	5	6	4	0	5	7	3	4	8	0	4	8	4	2	8	0	73
	34	4	600	3	163	9	23	12	23	6	17	8	40	37	44	24	23	9	53	23	31	18	10	9	36	13	10	2	6	0	5
	34	6	530	3	103	2	26	19	9	22	15	0	13	10	12	5	0	0	18	14	13	21	12	2	11	17	18	10	3	0	29
	34	7	610	0	205	10	25	21	15	20	18	10	49	24	27	26	26	5	62	51	40	31	35	7	64	45	74	52	39	0	263
	34	8	480	0	140	0	11	3	6	6	5	0	14	10	9	16	18	0	23	14	19	11	7	0	4	20	35	15	23	0	13
	37	1	800	13	117	9	12	13	17	13	8	12	18	15	17	14	11	16	23	15	10	18	13	10	19	14	14	8	12		
	37	2	550	0	52	0	2	6	1	0	10	0	10	6	4	8	7	0	6	6	6	7	3	0	12	3	8	10	6	0	26
	37	3	780	4	222	14	31	31	25	20	26	2	42	25	26	26	25	10	53	52	29	36	24	12	37	33	44	34	22	5	207
	37	4	400	0	83	0	4	0	8	3	5	1	15	8	7	9	4	0	15	17	9	19	13	1	18	10	8	16	9	0	14
	37	5	770	21	135	15	18	14	20	18	16	18	29	23	18	19	23	20	34	23	19	24	21	5	44	32	26	25	29	8	106
	37	6	470	0	57	0	0	0	0	0	0	0	0	0	0	1	0	0	1	0	0	2	1	0	0	0	1	2	2	0	1
	37	7	600	0	264	0	7	4	2	3	8	1	40	40	25	30	26	0	50	35	29	24	20	1	76	47	40	33	37	0	288
	37	8	575	0	52	0	0	0	0	0	0	0	0	0	0	0	0	0	5	3	0	3	1	0	4	5	2	6	10	0	10
	37	9	750	13	166	5	23	21	21	21	20	9	21	24	21	9	21	13	40	38	30	28	38	8	23	30	26	35	21	11	191
	37	10	825	6	101	12	26	11	14	14	12	6	23	9	7	14	13	9	20	27	17	19	28	9	25	24	35	34	26	6	64
	37	11	510	0	357	0	1	6	1	6	3	0	38	45	31	35	16	0	63	44	91	97	78	0	94	84	54	43	48	0	187
	38	1	650	0	78	0	0	0	0	0	0	0	3	0	0	1	0	0	33	15	7	7	7	1	26	22	42	22	9	1	52
	38	2	600	1	69	3	6	3	6	3	8	6	6	5	5	6	6	4	9	11	12	9	10	6	15	14	9	8	16	4	71
	38	3	1120	8	123	4	18	17	21	19	32	24	32	20	22	21	21	6	80	18	17	32	10	6	38	26	22	60	39	0	212
	38	4	600	0	51	1	2	4	5	0	2	0	6	4	1	6	1	0	9	3	3	8	4	0	3	1	6	1	2	0	26
	38	5	300	0	38	2	3	11	8	3	6	0	8	3	29	3	7	0	17	19	11	13	7	0	28	20	12	11	11	0	121
	38	6	600	0	61	2	3	1	8	7	6	1	2	5	6	5	4	4	8	7	5	4	5	3	6	5	8	7	16	8	41
	38	7	640	23	184	0	6	2	2	3	2	0	0	3	2	9	0	0	8	3	2	1	7	0	3	7	5	5	8	0	129
	39	1	450	3	139	8	9	12	16	10	10	7	58	37	43	28	36	0	88	51	31	36	28	3	28	44	38	34	35	2	110
	39	2	595	0	202	0	2	2	1	1	5	0	16	10	7	5	8	0	19	24	19	18	18	0	31	27	24	30	29	0	130
	39	3	760	0	41	0	0	0	0	0	0	0	0	0	0	1	0	0	1	0	1	1	4	0	4	2	4	0	1	0	6
	39	4	590	0	193	1	29	3	7	61	18	0	25	28	16	19	22	1	26	51	42	17	19	1	39	34	32	38	24	0	10
	39	5	800	0	70	0	2	4	3	5	3	0	7	1	4	3	3	0	12	8	6	9	7	0	11	13	9	7	6	0	18
	39	6	610	1	74	2	10	9	4	6	4	2	15	15	9	11	13	4	22	14	12	17	12	6	24	24	25	14	11	4	84
	39	7	830	0	88	0	1	2	3	1	4	0	7	14	8	9	6	0	12	9	10	7	1	0	12	11	14	11	10	0	24
	39	8	1010	0	394	0	31	70	61	43	64	0	74	120	102	99	47	0	86	52	35	44	68	0	89	104	64	77	37	0	339
	39	10	690	0	30	0	14	8	7	7	4	2	10	14	5	5	19	0	12	11	7	5	8	0	6	14	11	10	7	0	67
	39	11	710	0	41	0	0	2	0	0	1	0	0	2	1	1	2	0	2	1	0	0	0	0	4	1	2	1	1	0	1
	39	12	650	0	119	0	6	1	4	3	4	0	14	5	7	8	7	2	9	9	11	8	18	0	15	14	10	15	4	0	36
	39	13	1050	0	34	0	0	0	0	0	1	0	0	2	0	3	2	0	11	11	8	5	4	0	7	4	4	7	4	0	5

Note – Table is continued on the next page.

	Rat #	Neuron	Depth	Brush		1.4g vF						4g vF						10g vF						26g vF						Pinch	
				BL		BL	1	2	3	4	5	BL	1	2	3	4	5	BL	1	2	3	4	5	BL	1	2	3	4	5	BL	
Injury 6h	30	1	250	0	49	0	0	1	0	0	1	0	22	12	14	9	12	0	31	35	24	32	32	0	33	33	27	32	11	0	83
	30	2	560	5	60	4	13	7	14	3	2	3	19	10	10	9	7	3	8	6	15	19	40	3	25	29	33	45	28	2	86
	30	3	300	0	111	0	0	0	1	0	0	0	0	0	0	0	1	0	1	1	1	0	2	0	10	29	23	23	18	0	126
	31	1	300	0	22	0	1	1	0	1	0	0	0	0	2	2	3	1	1	1	0	1	1	0	1	0	0	4	0	0	1
	31	2	400	0	32	0	0	0	1	0	1	0	3	3	2	1	0	0	2	4	3	4	2	0	6	6	5	5	2	0	7
	31	3	400	0	3	0	0	0	0	0	0	0	2	3	0	0	2	0	7	1	3	3	3	0	11	26	12	7	15	0	48
	31	4	650	4	60	3	7	2	4	1	0	0	1	0	0	3	0	2	8	6	3	5	4	0	9	11	12	15	4	0	
	31	5	600	0	242	0	5	2	4	2	4	0	13	11	8	5	8	1	19	3	10	9	7	1	38	33	43	33	20	1	37
	31	6	370	0	210	0	25	9	20	8	15	0	20	4	14	17	11	0	24	22	16	20	16	0	28	16	17	18	12	0	27
	31	7	560	0	14	0	0	0	0	0	0	0	0	0	0	0	0	0	2	1	0	1	1	0	8	5	8	11	4	0	10
	31	8	770	0	49	0	0	0	0	0	0	0	0	0	0	0	0	0	7	9	5	6	5	0	8	7	5	6	3	0	4
	31	9	550	0	169	0	10	11	17	13	13	0	33	6	26	26	22	0	20	17	19	40	41	0	32	35	52	28	29	0	57
	31	10	640	1	33	1	5	4	8	4	2	0	23	3	8	8	5	0	27	26	13	17	28	1	58	24	29	35	41	0	273
	32	1	580	1	39	2	3	2	2	3	3	1	2	5	9	2	6	0	6	4	4	4	4	3	18	4	6	6	7	5	95
	32	3	830	15	281	19	26	30	21	18	33	9	44	31	45	29	34	6	74	65	48	56	49	6	53	55	53	36	39	10	298
	32	4	970	0	80	1	2	1	1	3	3	0	2	4	2	1	3	0	1	5	4	3	4	0	12	10	6	9	8	0	56
	32	5	360	3	106	7	22	20	18	16	17	4	15	13	34	21	25	20	52	52	42	42	32	2	66	59	33	50	42	2	257
	32	6	710	23	219	34	37	43	49	39	36	40	36	34	27	35	28	40	40	27	51	33	41	56	64	59	63	56	56	31	283
	32	7	850	0	34	0	0	0	0	0	0	0	1	0	0	1	0	0	5	5	4	3	1	0	5	6	5	5	6	0	38
	32	8	400	0	62	9	19	31	25	20	26	12	18	12	14	15	16	14	8	19	21	21	16	8	13	10	12	14	28	0	110
	32	9	550	2	345	5	11	6	6	7	6	0	7	1	20	7	7	0	24	13	12	9	8	0	20	14	32	15	15	0	142
	32	10	500	0	157	1	1	3	2	4	2	0	15	12	8	4	9	0	7	4	11	10	10	1	16	22	15	10	14	0	57
	32	11	720	0	195	4	10	19	8	12	9	7	50	31	53	35	42	3	57	48	38	15	45	4	22	33	33	24	33	10	143
	32	12	670	2	43	1	4	3	4	3	4	0	9	10	3	4	5	0	7	5	14	5	9	0	10	15	9	10	5	0	60
	32	13	950	0	131	0	0	0	0	0	0	0	0	1	1	1	0	0	30	35	24	15	16	0	28	29	14	18	18	0	
	32	14	650	0	161	0	10	4	3	2	22	0	24	33	13	12	17	0	30	21	11	14	15	0	16	15	16	5	14	0	49
	32	15	700	6	63	7	7	11	14	7	10	5	9	13	14	6	7	0	15	6	3	8	7	0	9	2	8	6	10	0	33
	33	1	450	5	184	3	9	6	7	8	12	7	24	25	22	13	16	6	73	51	29	36	27	3	61	47	46	51	68	4	149
	33	2	590	27	178	23	54	42	64	35	70	20	52	40	33	39	42	22	56	56	31	24	29	17	55	32	14	11	14	12	136
	33	3	775	0	59	0	1	0	2	2	0	0	4	1	5	1	1	0	10	2	5	6	5	0	12	12	13	7	12	0	74
	33	4	530	0	98	0	2	2	0	3	6	0	10	14	4	6	7	0	6	5	8	2	11	0	10	11	8	14	21	0	134
	33	5	720	0	63	0	0	0	1	0	1	0	11	4	4	5	8	0	9	10	10	5	14	0	14	6	11	7	21	0	93
	33	6	830	0	217	0	42	18	37	23	30	0	46	32	38	49	34	0	69	72	42	51	55	14	69	54	85	76	114	54	350
	33	8	500	0	52	3	1	3	8	3	3	0	7	5	8	8	2	3	22	28	28	29	17	9	16	22	17	13	14	5	68
	33	9	680	0	156	0	3	2	3	1	6	0	2	3	2	1	1	0	35	27	31	27	24	0	27	34	40	29	50	0	233
	33	10	625	0	4	0	0	0	0	0	1	0	1	1	1	0	0	0	3	3	3	4	5	0	3	4	14	14	18	0	13
	33	11	710	0	24	1	2	0	0	1	7	0	3	8	5	4	8	0	11	8	9	14	7	0	36	29	28	32	33	1	142
	33	12	570	1	48	0	0	0	1	0	1	1	2	4	3	4	2	0	2	1	1	2	5	0	8	11	11	5	2	0	20
	33	13	810	0	114	0	0	2	3	0	0	2	4	3	5	7	2	0	15	6	6	4	6	0	51	41	62	18	25	0	105
	33	14	830	0	20	0	0	1	0	1	0	0	6	6	4	4	3	0	3	2	2	6	5	1	6	5	3	18	8	1	25
	33	15	770	0	21	0	0	0	0	0	1	0	0	1	1	0	3	0	4	4	1	5	2	0	4	5	2	4	1	0	7

Note – Table is continued on the next page.

	Rat #	Neuron	Depth	Brush		1.4g vF						4g vF						10g vF						26g vF						Pinch	
				BL		BL	1	2	3	4	5	BL	1	2	3	4	5	BL	1	2	3	4	5	BL	1	2	3	4	5	BL	
Sham D1	6	3	370	1	14	0	1	2	2	3	0	2	7	7	8	9	6	1	18	20	13	13	10	0	25	11	10	12	9	1	0
	6	4	450	0	6	0	0	0	0	0	0	0	0	0	1	1	0	0	3	3	2	1	3	0	4	3	3	1	5	0	0
	6	5	600	0	61	1	0	0	0	1	0	1	2	2	0	2	1	0	12	8	5	5	5	2	23	12	9	15	15	0	0
	6	6	770	0	39	0	1	2	2	0	1	0	1	2	1	1	0	0	7	2	3	4	4	1	10	5	7	4	2	0	0
	6	7	550	0	30	0	0	0	0	0	0	0	0	0	0	0	0	0	3	4	3	4	0	0	10	7	1	2	7	0	0
	6	10	450	0	29	0	0	0	0	0	0	0	1	0	0	2	0	1	4	1	1	1	2	0	7	7	5	2	4	0	1
	6	11	700	0	12	0	0	0	0	0	1	0	0	1	1	1	0	0	2	8	1	6	4	2	5	5	9	13	23	1	1
	17	1	780	2	22	1	1	0	2	1	2	1	1	1	1	2	2	1	2	1	4	6	4	0	8	4	2	2	5	0	10
	17	2	850	4	13	2	1	2	0	0	1	1	3	5	4	3	8	3	5	4	2	4	5	2	6	3	6	3	4	5	18
	17	3	600	0	71	4	5	3	4	6	4	2	4	5	1	2	2	8	13	9	3	2	6	2	2	5	1	2	3	0	23
	17	4	430	0	26	0	1	2	1	1	0	0	4	1	0	0	1	0	3	3	2	2	3	0	7	0	5	2	1	0	8
	17	5	550	0	44	0	0	0	1	0	2	0	3	0	4	1	0	0	6	5	4	3	5	0	5	6	1	7	7	0	23
	17	6	500	0	61	0	7	4	2	7	4	0	3	0	3	1	3	0	12	15	5	8	7	2	6	11	15	12	12	5	50
	17	7	650	0	40	0	5	3	3	1	2	0	10	8	3	5	3	1	7	4	6	5	6	1	7	15	8	6	1	0	20
	17	8	750	0	78	0	19	28	15	10	7	2	9	6	10	16	14	0	16	19	10	8	11	0	25	4	14	10	6	5	20
	17	9	450	0	121	2	2	2	1	1	2	1	4	2	4	4	3	0	8	3	7	6	3	2	15	6	14	16	8	1	16
	17	10	580	1	51	0	1	1	1	0	0	0	2	4	2	2	2	0	5	9	8	1	5	1	18	19	26	16	24	1	81
	17	11	700	0	101	0	4	3	2	0	1	1	5	7	5	5	3	0	5	5	8	6	9	0	19	20	49	23	25	1	113
	17	12	450	0	39	0	0	0	1	0	0	0	1	1	0	1	0	0	2	0	0	3	2	0	6	2	5	4	6	0	7
	24	1	530	0	169	0	2	3	5	1	0	0	2	1	3	2	2	0	3	1	6	5	3	0	7	5	9	2	5	3	48
	24	3	280	0	43	0	0	0	0	0	1	0	0	10	3	6	4	0	11	1	2	1	2	0	7	5	4	2	9	0	17
	24	5	1000	0	16	0	0	1	0	2	0	0	0	1	1	0	4	0	0	1	1	2	5	0	8	3	12	4	3	1	3
	24	6	380	0	25	0	0	0	0	1	0	0	0	0	0	0	0	0	0	1	2	0	2	0	2	2	1	0	1	0	13
	26	1	470	1	82	0	4	3	1	0	1	1	7	2	4	8	3	0	6	5	5	3	2	1	15	8	4	11	12	2	79
	26	2	625	0	130	0	7	5	6	5	5	0	11	13	9	11	6	0	18	12	16	14	11	1	20	16	15	14	17	0	74
	26	3	700	0	66	0	0	0	2	2	1	1	3	5	1	6	3	0	7	7	6	3	0	0	9	6	7	11	6	0	21
	26	4	310	1	82	2	5	6	3	5	1	4	4	5	9	6	6	1	4	2	2	5	5	3	9	9	14	12	10	0	34
	26	5	970	0	31	0	2	1	3	2	2	2	3	5	4	3	6	0	1	5	6	2	3	2	8	16	15	21	15	8	60
	26	6	510	0	81	0	0	0	0	0	0	0	1	1	2	1	2	0	6	4	0	1	0	0	0	6	2	4	4	0	11
	26	7	700	0	66	0	1	1	0	1	0	0	2	0	1	2	0	0	4	2	3	1	4	0	9	4	4	4	0	0	5
	26	8	460	0	184	0	10	5	17	13	5	0	8	4	9	9	10	0	10	12	13	14	17	0	13	9	15	21	20	2	31
	26	9	570	0	75	0	2	8	9	6	3	1	8	9	12	8	3	2	19	17	20	16	16	2	29	19	30	32	24	3	128
	26	10	700	1	99	0	4	4	2	2	8	0	11	8	14	14	5	0	13	27	27	12	11	0	34	39	46	36	29	0	60
	26	11	450	0	129	0	2	12	0	0	1	0	60	64	67	11	60	0	112	92	101	115	82	0	75	101	95	85	88	0	109
	28	1	550	0	37	0	0	0	0	0	1	0	1	0	1	2	3	0	3	2	4	3	7	0	40	9	8	18	16	0	50
	28	2	700	0	88	0	0	0	2	3	2	0	1	4	0	1	1	1	2	8	5	11	8	0	5	0	11	3	2	0	11
	28	3	670	0	29	0	0	0	0	0	0	0	4	5	3	0	0	0	3	1	8	6	5	0	2	3	0	0	1	0	8
	28	4	540	1	11	0	1	1	0	0	0	0	2	0	0	2	1	0	1	4	1	1	3	1	2	2	1	1	3	1	20
	28	5	750	0	31	0	2	0	2	2	4	0	2	3	2	0	1	1	1	2	3	1	4	0	4	1	3	1	0	0	3
	28	6	800	0	64	0	0	2	2	2	6	0	6	4	0	4	2	0	6	10	3	3	7	1	5	10	3	1	7	0	33
	28	7	910	0	138	0	32	0	0	0	19	0	13	6	4	0	15	0	30	17	39	9	10	0	23	19	16	10	25	0	86
	29	1	720	0	17	0	2	0	3	1	2	0	0	0	0	1	1	0	2	0	3	3	2	3	5	2	4	10	8	1	21

Note – Table is continued on the next page.

	Rat #	Neuron	Depth	Brush		1.4g vF						4g vF						10g vF						26g vF						Pinch	
				BL		BL	1	2	3	4	5	BL	1	2	3	4	5	BL	1	2	3	4	5	BL	1	2	3	4	5	BL	
Injury D1	13	1	650	0	147	0	2	3	0	2	2	2	12	6	6	13	7	0	12	8	8	8	10	1	49	8	13	26	40	3	137
	13	2	900	2	32	2	1	2	2	1	1	2	7	2	4	3	2	3	10	7	5	2	2	0	8	8	7	16	14	0	55
	13	3	750	0	49	2	1	3	2	2	3	3	5	2	4	1	5	2	7	6	3	4	2	2	10	8	3	5	5	3	27
	13	4	800	3	100	0	11	6	9	12	3	0	11	4	6	2	4	0	6	17	6	2	7	4	9	18	11	7	9	2	15
	13	5	650	1	101	1	4	1	4	2	1	3	14	6	11	5	10	2	20	11	10	8	3	2	38	23	16	31	17	2	15
	13	6	910	1	55	0	1	5	3	1	0	2	3	1	2	4	0	1	22	21	22	13	11	1	28	13	9	12	6	1	58
	13	8	850	1	32	2	6	0	2	1	3	1	6	6	3	5	7	2	8	9	8	8		2	25	24	15	11		0	32
	13	9	450	2	62	1	13	16	14	13	8	2	7	3	9	7	8	1	15	10	6	9	9	1	8	12	10	10	21	2	36
	13	9	450	2	33	0	6	3	2	2	4	2	9	5	9	7	3	0	10	9	18	2	4	2	14	20	20	18	9	2	73
	18	1	630	0	57	0	4	1	2	1	1	0	12	3	5	6	8	0	6	7	5	5	5	2	10	5	4	8	13	0	73
	18	2	470	0	92	0	2	1	0	1	1	0	2	4	4	3	3	0	8	5	7	5	8	0	22	13	17	14	12	0	29
	18	3	650	2	78	1	4	4	4	2	2	1	3	0	3	1	2	2	17	2	7	3	8	2	10	14	23	14	10	2	70
	18	5	630	0	39	0	1	0	0	2	2	0	2	0	6	3	0	0	3	1	2	2	2	0	5	6	3	3	1	0	28
	18	8	585	0	50	0	4	1	0	8	5	0	5	5	3	10	9	0	9	7	7	6	9	0	10	10	6	12	5	0	28
	20	1	530	0	57	1	0	2	0	2	1	1	3	4	8	10	8	1	6	8	6	7	11	1	17	14	11	13	18	3	79
	20	2	700	0	55	0	1	0	0	0	1	0	1	1	2	1	1	0	4	1	4	4	12	0	26	20	66	59	62	1	151
	20	3	760	1	86	0	1	0	0	0	0	0	1	8	2	0	1	0	6	10	2	5	15	1	79	85	76	55	39	0	126
	20	4	570	0	151	0	0	0	0	0	0	0	0	0	0	0	0	0	11	7	10	8	7	0	6	4	4	8	5	0	26
	20	5	650	0	80	0	4	5	6	3	4	0	4	5	3	3	0	0	7	4	5	3	7	0	14	6	4	2	3	0	48
	20	6	820	0	88	0	0	1	1	1	1	0	6	7	10	3	14	0	6	4	4	2	9	0	14	20	18	18	15	0	111
	20	8	550	28	357	13	17	16	15	20	14	9	34	35	42	34	26	16	48	40	38	34	31	11	102	84	76	46	56	17	527
	20	9	670	0	62	1	5	4	14	5	4	0	9	2	3	10	6	0	15	11	6	5	5	0	9	8	4	7	7	0	23
	20	11	650	2	110	1	0	4	5	12	11	0	9	1	6	3	4	0	15	20	27	11	9	1	34	29	61	7	11	3	429
	21	1	870	2	75	2	2	4	4	17	5	2	12	13	10	5	15	0	23	12	7	13	5	1	35	35	28	22	26	16	139
	21	2	810	0	161	3	8	19	19	17	20	3	30	23	21	15	13	2	23	19	13	27	20	0	28	14	20	21	19	1	51
	21	3	370	0	57	0	0	8	3	1	1	0	6	10	4	4	8	1	10	14	10	14	7	0	18	19	7	13	9	1	58
	21	4	450	0	107	1	13	5	14	5	8	1	16	13	13	22	26	1	29	39	30	25	38	1	45	42	41	27	25	5	85
	21	5	550	0	99	0	2	1	6	4	3	1	9	4	3	7	8	0	11	18	21	8	13	1	23	12	22	18	21	1	51
	21	6	700	0	57	0	4	11	10	7	9	0	22	22	11	16	14	0	23	32	27	23	16	0	27	28	22	29	19	12	90
	21	8	550	0	96	1	4	6	13	3	4	0	18	12	6	6	8	2	10	7	12	12	7	2	34	24	20	8	15	4	91
	21	9	570	0	66	0	0	0	1	0	0	0	1	0	0	0	0	0	3	0	1	4	1	0	11	10	9	11	6	0	5
	25	1	730	0	46	2	3	2	7	2	9	2	7	9	0	4	4	0	3	5	9	8	7	1	17	15	5	9	11	1	42
	25	2	500	2	155	0	1	0	1	0	2	0	1	1	1	2	2	0	53	40	36	60	55	1	59	57	48	42	46	1	20
	25	3	650	0	118	1	26	12	16	3	17	0	59	70	54	65	57	0	104	99	85	41	84	0	130	62	72	17	18	3	91
	25	4	750	1	154	3	13	13	14	14	13	4	28	24	20	18	13	14	27	28	37	32	37	0	47	37	36	36	32	2	174
	25	5	330	0	99	0	4	4	2	5	6	0	6	1	2	1	7	0	13	3	7	4	4	0	7	9	6	10	5	1	11
	25	6	1020	65	606	26	35	38	47	71	73	36	54	52	54	45	31	30	69	64	57	50	50	35	111	93	76	60	75	16	353
	25	7	630	0	124	0	0	0	0	5	0	0	33	24	0	30	1	0	53	3	16	69	20	0	46	24	43	27	26	0	181
	27	1	540	0	144	0	1	3	3	2	3	0	4	7	5	2	3	0	9	7	5	1	7	0	5	13	4	6	8	0	22
	27	2	630	0	87	0	1	1	0	0	0	0	3	1	2	1	2	0	10	0	2	0	1	0	15	6	1	1	4	0	18
	27	3	800	18	74	16	10	9	15	11	14	11	16	22	21	18	16	19	13	23	8	19	13	9	16	21	14	21	11	6	46

Note – Missing data points are from neurons that were lost during recording before completing the stimulation protocol.

Table D.2. Spike counts on day 7 for bupivacaine treatment study (Chapter 4).

	Rat #	Neuron	Depth	Brush		1.4g vF						4g vF						10g vF						26g vF						Pinch	
				BL		BL	1	2	3	4	5	BL	1	2	3	4	5	BL	1	2	3	4	5	BL	1	2	3	4	5	BL	
inj-VEH0h	45	1	590	3	97	5	10	8	2	2	2	2	7	5	7	14	9	4	10	5	11	10	8	9	34	19	18	25	19	8	65
	45	2	300	0	81	0	1	5	6	1	2	0	2	5	4	4	8	0	10	8	5	6	4	0	8	9	7	14	16	0	15
	45	3	670	1	116	3	16	3	7	7	8	1	13	7	5	10	8	0	31	31	45	26	18	2	43	36	43	13	20	5	57
	45	4	630	0	384	0	6	9	5	3	5	4	21	11	1	21	16	0	5	23	74	88	84	0	41	45	31	41	69	0	179
	45	5	820	0	61	0	0	1	0	0	0	0	18	8	0	6	13	0	38	28	17	26	20	0	18	24	19	14	18	0	47
	45	6	550	2	118	5	5	2	8	4	5	6	8	4	10	6	10	1	11	6	10	8	5	1	31	33	27	34	26	2	116
	45	7	650	3	64	0	1	4	2	3	0	2	8	9	5	3	6	0	12	0	3	3	0	4	10	12	9	11	7	1	66
	45	8	770	2	146	1	3	2	2	0	4	1	8	0	2	2	2	0	10	8	10	13	3	2	20	17	26	20	24	1	92
	45	9	830	0	82	0	0	0	1	3	1	1	13	10	13	8	4	3	42	33	37	32	17	1	52	44	25	51	45	0	69
	45	10	680	0	107	4	3	3	5	4	4	0	7	4	6	0	5	1	31	11	11	12	11	0	40	38	24	25	19	1	102
	45	11	680	0	90	0	9	3	1	3	3	1	4	8	7	3	3	0	6	4	8	5	5	0	8	8	9	8	14	0	21
	48	1	900	8	151	11	11	13	13	11	11	11	14	13	11	8	9	12	9	16	11	10	8	10	12	17	9	8	7	6	44
	48	2	500	5	141	0	9	15	14	10	19	0	16	20	22	18	10	0	31	34	25	28	26	0	40	16	33	26	19	0	40
	48	3	480	0	198	2	0	3	1	0	3	0	3	7	9	7	4	0	6	2	7	2	1	0	10	4	2	1	2	0	44
	48	4	640	0	24	0	2	0	1	1	0	5	3	6	8	11	4	4	9	6	11	9	6	2	11	6	11	5	11	0	48
	48	5	320	0	134	1	5	8	1	4	3	0	15	13	21	18	16	1	7	8	3	5	6	0	10	10	7	6	17	1	53
	48	6	610	0	136	0	17	16	16	15	11	0	26	17	31	21	24	0	17	20	16	20	14	1	13	5	9	8	9	0	15
	48	7	800	0	73	0	1	6	6	9	4	0	5	2	3	4	6	0	9	12	0	3	6	0	11	15	17	15	13	3	42
	48	8	950	2	264	7	11	7	10	9	12	8	12	15	11	13	18	2	20	16	26	17	27	2	31	13	32	16	24	1	51
	48	9	940	0	171	1	1	2	2	1	1	0	13	6	11	11	12	3	29	35	23	18	17	1	46	35	51	33	26	2	136
	50	1	650	4	115	2	4	6	7	8	6	4	11	10	10	11	10	12	32	25	15	25	19	6	24	51	28	29	34	2	148
	50	2	710	4	227	5	5	7	4	2	0	5	16	13	8	10	11	10	91	32	49	76	73	6	129	72	109	73	78	1	183
	50	3	770	8	113	3	4	8	4	8	7	1	13	12	12	12	5	3	17	12	4	4	10	13	32	37	39	22	21	0	118
	50	4	730	3	75	4	9	9	7	10	14	1	21	21	11	16	12	2	20	26	18	33	30	2	31	42	51	37	31	3	171
	50	5	810	17	208	8	18	11	17	18	14	11	29	30	24	17	19	6	55	44	31	54	36	10	109	73	69	48	53	7	149
	50	6	650	0	75	0	38	28	26	31	21	0	44	35	33	36	29	0	44	51	40	31	40	0	50	51	70	44	21	1	278
	50	7	840	0	144	0	4	4	16	22	9	1	12	14	27	20	5	1	37	8	24	22	14	0	29	27	19	24	28	3	185
	50	8	900	3	48	1	6	2	5	5	3	0	4	4	5	3	2	4	31	19	13	6	19	1	32	23	30	20	47	1	155
	50	9	360	0	153	0	16	5	7	14	12	0	20	24	21	22	27	0	30	25	19	20	23	1	26	19	18	20	9	0	25
	50	11	510	0	122	1	0	2	2	2	0	0	10	6	10	6	2	0	82	83	49	79	66	0	101	138	98	104	110	0	117
	50	12	770	3	114	1	13	10	6	3	4	3	5	13	7	6	8	0	21	13	15	6	17	1	38	39	24	17	31	3	115
	50	13	560	5	135	6	7	5	12	7	12	7	13	12	12	14	15	10	30	21	21	24	14	18	36	32	27	25	25	14	138
	52	1	620	4	44	3	13	11	6	8	4	3	18	17	14	14	20	6	18	31	30	64	45	4	48	65	78	78	71	4	472
	52	2	790	10	153	8	28	26	28	17	13	8	49	45	50	42	44	9	81	55	52	50	47	6	65	69	74	61	74	5	369
	52	3	690	3	314	4	59	61	45	43	48	6	91	73	68	57	58	10	77	59	30	30	45							4	405
	52	4	900	0	34	0	2	3	2	1	1	0	3	5	4	6	4	0	7	6	7	3	7	0	29	37	41	31	35	0	209
	52	5	710	3	77	6	24	11	10	5	2	9	24	21	11	13	32	0	54	48	51	40	41	0	74	56	55	49	62	0	270
	52	6	690	0	62	0	13	7	6	4	7	0	8	9	20	7	15	0	30	12	15	27	18	0	40	30	39	34	28	1	117
	52	7	750	2	122	6	14	20	10	14	17	3	20	17	25	19	15	0	30	36	32	31	22	0	40	31	26	26	21	1	71
	52	8	850	0	144	0	0	0	3	4	0	2	16	5	4	2	19	0	28	21	12	15	15	0	46	43	56	51	43	2	289
	52	9	770	0	74	0	4	2	1	2	4	0	1	2	2	6	4	0	7	6	6	5	9	0	13	10	12	15	16	0	36
	52	10	880	0	334	0	65	60	44	37	34	0	57	69	49	59	42	0	12	60	55	53	59	1	79	76	60	55	51	0	96
	52	11	600	0	245	0	11	4	7	2	6	0	84	91	77	84	82	10	145	83	154	143	163	106	262	217	189	191	#	18	459
	53	1	600	10	81	6	11	15	15	20	13	6	3	5	16	17	8	2	10	10	6	3	3	2	9	11	15	8	15		
	53	2	850	0	95	0	0	0	0	36	0	0	111	43	58	43	42	0	47	30	31	16	24	0	32	25	11	9	3	0	54
	53	3	680	0	160	5	38	42	34	30	34	2	31	47	64	84	62	1	55	69	61	86	135	0	196	210	65	25	5	11	313
	53	4	660	0	31	0	0	0	3	5	3	0	9	2	1	2	5	0	5	12	6	14	15	0	18	25	23	238	29		
	53	5	370	15	99	0	3	3	4	7	4	0	1	2	5	6	3	12	22	11	14	4	11	1	11	13	9	7	8	0	50
	53	6	380	2	49	0	68	36	35	34	38	1	102	45	88	2	87	0	68	6	93	74	59	0	103	78	70	96	2	0	188
	54	1	470	0	105	0	2	9	4	6	9	1	13	10	9	16	8	0	8	9	7	7	4	0	8	10	9	4	8	0	22
	54	2	750	12	417	1	19	7	9	11	12	0	19	18	26	24	20	0	9	30	24	22	25	1	53	40	34	19	36	0	67
	54	3	470	0	37	2	2	3	0	1	1	0	5	4	1	4	5	1	7	8	11	4	5	0	9	1	12	3	5	0	14
	54	4	580	0	82	0	5	3	0	8	4	0	5	10	5	3	2	0	24	26	17	11	8	0	25	8	15	20	12	0	21
	54	5	550	0	22	0	1	0	1	1	0	0	1	2	1	1	2	0	7	9	7	4	7	0	19	14	32	24	44	0	15
	54	6	710	0	111	0	8	1	5	2	3	0	10	8	7	5	6	0	33	20	17	4	22	0	26	29	10	22	14	0	116

Note – Table is continued on the next page.

	Rat #	Neuron	Depth	Brush		1.4g vF						4g vF						10g vF						26g vF						Pinch	
				BL		BL	1	2	3	4	5	BL	1	2	3	4	5	BL	1	2	3	4	5	BL	1	2	3	4	5	BL	
inj-VEH0h	54	7	410	0	31	0	0	0	2	0	0	0	0	0	0	0	3	0	1	1	5	1	2	0	0	3	1	3	4	0	9
	54	8	870	0	58	0	2	3	2	4	1	0	2	3	6	3	9	0	4	3	6	6	6	0	16	9	16	21	25	0	47
	72	2	720	10	284	16	42	32	27	53	46	19	80	74	62	63	56	20	76	67	60	68	59	13	74	65	63	50	45	19	400
	72	3	570	3	234	3	27	23	30	28	29	4	21	35	28	26	26	3	57	35	46	47	39	0	54	60	72	58	52	1	393
	72	4	490	0	143	0	3	1	0	9	0	0	5	9	7	8	6	1	46	27	44	47	31	0	75	73	67	70	56	2	221
	72	5	620	18	297	17	26	23	18	26	26	17	45	50	41	33	38	10	47	46	44	41	37	9	75	59	93	69	65	24	913
	72	6	500	8	213	15	20	24	32	31	31	10	43	35	32	14	24	18	52	31	30	28	25	15	66	54	30	42	18	7	127
	72	7	680	0	46	0	0	0	0	0	0	0	9	1	5	5	6	0	17	16	14	7	3	0	7	10	10	8	3	0	2
	72	9	680	0	127	0	3	7	2	6	3	0	11	8	5	7	9	0	18	12	13	7	16	0	33	31	25	29	15	0	103
	72	10	830	2	246	3	33	29	21	33	33	5	66	35	97	91	40	3	65	54	51	52	61	8	76	47	46	67	58	0	253
	72	11	910	7	264	3	47	30	20	16	9	9	37	52	36	30	15	6	89	53	46	48	50	3	85	65	62	72	80	3	309
sham-VEH0h	79	1	600	10	62	17	21	22	17	16	18	16	31	22	25	24	12	22	26	35	18	10	16	8	31	35	16	17	14	10	175
	79	2	710	3	35	1	8	4	8	6	8	5	4	18	7	9	7	1	8	12	6	3	5	2	14	18	19	13	11	0	101
	79	3	750	1	89	3	5	3	0	4	2	0	5	2	1	1	4	3	5	11	9	8	2	1	10	10	11	4	3	4	84
	79	4	550	0	110	0	1	7	5	3	2	0	9	6	6	2	1	3	23	17	18	18	12	6	55	50	55	36	42	0	221
	79	5	710	32	367	29	38	26	26	8	32	38	41	64	61	55	55	19	94	79	79	61	164	36	152	128	114	79	80	24	1280
	79	6	870	9	143	6	2	11	4	5	6	4	11	10	13	9	11	8	20	16	16	19	13	6	57	49	36	43	37	5	252
	79	8	760	3	60	2	16	7	5	12	11	4	7	15	10	2	4	4	5	6	4	8	5	2	14	8	17	25	21	2	52
	79	9	880	2	117	4	4	10	9	8	16	5	51	24	31	42	37	2	63	61	35	38	34	0	37	56	47	44	54	7	138
	79	11	665	4	125	10	28	16	17	18	19	13	52	30	21	35	7	6	36	43	32	31	24	16	52	33	26	21	20	25	241
	79	12	460	0	95	0	2	2	0	1	1	0	3	2	1	3	5	0	2	8	5	1	0	0	9	8	4	3	4	0	9
	79	13	580	3	108	3	7	10	0	5	5	0	8	4	17	5	8	0	12	15	18	10	16	0	18	15	15	23	13	6	110
	79	14	600	0	156	2	18	12	10	14	13	2	9	14	16	11	13	8	26	21	18	25	22	5	25	17	22	30	23	10	88
	79	16	830	0	142	2	21	11	3	1	4	1	19	9	12	10	12	5	36	10	22	18	12	0	28	48	43	25	14	4	163
	80	1	790	5	136	9	38	19	23	13	17	13	25	32	32	26	42	10	57	57	32	38	26	6	54	29	17	13	20	15	182
	80	2	900	0	78	0	0	0	1	1	0	0	1	1	0	0	0	0	1	1	2	0	3	0	15	11	6	19	20	0	58
	80	3	600	0	31	2	4	9	17	6	4	1	8	8	17	13	13	1	18	10	10	9	9	3	28	30	20	16	23	2	120
	80	4	710	0	32	0	0	0	0	0	1	0	3	1	0	1	0	0	4	3	6	5	2	0	9	21	26	10	22	0	134
	80	5	830	0	63	0	3	4	2	5	3	2	31	12	24	13	7	1	58	41	43	39	37	0	77	83	56	75	55	0	286
	80	6	730	0	64	1	5	9	4	7	1	1	16	13	11	11	4	0	29	21	16	31	26	1	34	36	29	32	32	0	139
	80	8	520	1	139	4	8	8	9	10	4	5	16	10	19	9	12	1	22	19	18	17	17	1	19	31	24	19	23	1	90
	80	9	380	0	65	0	0	1	2	1	0	0	6	5	5	6	3	0	25	21	22	13	16	0	33	35	30	35	27	0	48
	80	11	850	0	20	1	1	3	3	3	4	3	6	5	7	7	1	4	3	13	12	13	11	6	12	20	22	16	9	3	105
	80	12	350	2	62	1	2	0	0	0	2	0	4	7	6	7	4	0	11	8	8	7	3	0	24	31	17	19	17	0	108
	80	13	950	7	114	5	27	25	30	23	18	7	26	20	22	30	21	9	40	26	31	34	32	17	83	85	93	92	66	2	835
	81	1	270	0	78	0	1	1	1	0	1	0	5	1	4	2	4	0	16	15	5	14	17	0	17	17	12	7	7	0	48
	81	2	400	8	90	6	8	8	11	5	5	3	19	9	19	5	13	4	22	24	16	24	11	4	43	29	30	21	12	5	77
	81	3	610	5	183	11	17	27	26	16	31	14	41	32	17	25	33	22	32	29	30	34	18	10	43	41	50	37	45	7	184
	81	4	750	0	70	1	4	1	5	2	2	3	3	4	3	3	2	3	6	9	9	13	7	3	3	12	11	16	17	0	79
	81	5	870	17	129	18	22	16	14	18	11	12	29	17	13	23	22	9	28	34	18	24	31	7	30	35	32	39	38	4	213
	81	7	820	0	185	1	3	2	10	4	4	0	21	10	13	18	7	1	65	39	39	40	51	0	96	43	47	23	30	2	305
	81	8	430	0	44	0	6	3	3	1	3	0	14	8	12	8	13	0	21	11	17	16	20	1	23	17	26	25	14	3	142
	81	9	610	0	61	0	0	0	1	0	0	0	1	5	0	0	0	0	15	9	5	3	2	0	34	31	21	11	16	0	160
	81	10	630	0	84	0	0	2	1	1	3	0	3	4	3	5	1	0	9	5	4	3	6	0	9	6	5	5	9	0	9
	81	11	780	0	66	0	2	1	2	0	1	0	3	2	5	5	1	0	9	8	11	6	4	0	14	11	21	14	14	0	46
	81	12	890	5	283	8	8	13	10	5	10	6	21	17	16	16	18	4	46	71	35	70	50	6	134	145	142	106	#	7	176
	81	13	840	3	128	8	8	23	15	11	7	2	15	39	15	32	32	4	25	27	19	12	26	7	33	28	21	17	28	1	50
	133	1	700	7	248	4	16	8	21	10	8	3	14	20	17	10	15	5	30	23	22	32	32	6	21	4	13	13	6	4	32
	133	2	870	0	62	0	9	19	9	3	1	0	5	2	0	2	0	0	20	13	15	10	9	0	51	54	70	48	57	0	87
	133	3	640	12	99	24	17	27	32	29	27	24	37	22	30	18	27	37	37	37	41	37	32	20	37	46	34	53	49	28	501
	133	5	690	2	106	3	10	16	13	12	16	2	19	20	16	24	22	1	24	24	29	17	21	2	11	16	16	3	8	2	94
	133	6	330	0	32	0	0	2	0	0	0	0	5	4	4	2	3	1	18	3	8	2	4	1	11	5	8	9	12	0	60
	133	7	440	6	126	0	8	2	11	6	10	1	22	18	16	15	16	4	28	27	39	24	46	1	53	44	40	41	44	1	102
	133	8	570	0	52	0	3	5	4	0	4	1	6	5	9	0	1	0	17	19	12	23	10	0	11	10	12	7	10	1	56
	133	9	620	0	81	0	5	9	5	2	13	0	8	12	5	15	6	0	18	11	15	12	5	0	10	13	23	19	17	0	111

Note – Table is continued on the next page.

	Rat #	Neuron	Depth	Brush		1.4g vF						4g vF						10g vF						26g vF						Pinch	
				BL		BL	1	2	3	4	5	BL	1	2	3	4	5	BL	1	2	3	4	5	BL	1	2	3	4	5	BL	
sham-VEH0h	133	10	720	0	47	0	0	0	0	0	0	0	0	0	1	1	1	0	7	2	8	3	8	0	18	9	12	9	18	0	34
	133	12	790	8	205	22	37	32	29	30	20	11	44	40	29	25	27	11	50	43	27	33	25	14	74	62	39	62	49		
	133	13	830	1	61	3	6	9	7	7	6	0	6	14	6	8	3	1	17	4	12	5	10	2	8	13	5	9	5	3	55
	134	1	170	0	68	0	1	1	0	1	0	0	2	0	9	3	2	0	1	2	0	1	4	0	5	4	5	16	8	0	45
	134	2	580	10	270	11	34	35	20	24	21	17	47	39	32	28	32	18	57	49	42	31	36	11	62	63	69	52	88	14	479
	134	3	780	0	54	0	0	0	0	0	0	0	0	0	0	0	0	0	2	3	1	3	3	0	5	1	5	3	3	0	4
	134	4	460	1	54	1	9	8	7	7	10	0	2	3	1	2	3	0	9	2	5	6	2	1	15	19	8	5	8	0	69
	134	5	595	0	141	0	12	9	6	13	8	0	14	15	14	16	8	0	13	9	13	13	13	0	14	9	17	16	18	0	30
	134	8	640	2	42	3	5	5	1	6	6	7	14	8	5	6	6	1	13	11	14	14	6	0	18	22	31	31	39	0	62
	134	9	780	26	143	16	19	16	18	17	12	9	25	19	12	13	14	6	24	39	24	23	18	3	78	74	84	97	98	2	224
	134	10	770	8	78	0	2	0	6	4	8	4	17	20	12	9	13	0	43	33	27	25	28	0	62	67	51	61	65	0	65
	134	11	520	0	33	0	1	1	1	2	2	0	4	3	5	0	1	0	13	4	2	2	4	0	13	15	14	12	9	0	21
	134	12	560	0	90	0	0	0	0	0	0	0	4	6	8	2	1	0	5	5	4	5	6	0	9	6	7	5	5	0	22
	134	13	590	5	121	4	10	22	7	17	8	3	25	33	34	26	22	9	43	65	42	32	46	6	70	50	77	85	47	2	447
inj-BP0h	41	1	370	3	44	2	2	3	4	3	2	3	2	2	2	1	6	2	2	9	1	2	1	4	8	3	4	11	5	2	23
	41	2	820	0	27	0	0	0	0	0	0	0	1	1	0	0	0	0	19	11	10	9	9	0	32	22	21	17	18	0	77
	41	4	320	0	11	1	6	5	2	0	2	0	9	3	3	9	2	0	3	3	2	3	4	1	6	3	4	1	2		
	41	5	450	21	128	45	41	32	35	22	21	16	18	20	25	23	20	23	26	20	30	32	22	20	23	34	33	35	45	17	144
	41	6	400	0	67	0	2	3	8	5	5	0	3	2	0	0	0	0	7	8	6	15	9	0	43	18	24	25	46	1	204
	41	7	580	0	45	0	2	1	1	1	2	1	1	0	4	1	14	1	2	3	3	2	3	0	6	3	8	5	6	0	152
	41	8	700	2	66	0	4	9	2	7	9	1	15	26	6	0	3	0	31	30	48	39	32	0	32	40	40	37	41	1	225
	41	9	500	0	31	0	1	2	4	0	1	0	3	4	2	3	0	0	3	12	1	3	4	2	17	5	7	10	7	0	31
	41	10	520	0	53	1	1	3	2	0	1	2	3	4	5	5	3	2	6	8	10	7	8	0	19	6	6	8	7	0	9
	42	1	410	7	100	6	5	3	5	11	10	4	23	17	8	6	11	4	33	30	35	27	22	6	26	29	34	31	20	4	274
	42	2	500	4	60	3	4	9	8	4	8	1	21	17	10	19	18	2	24	17	8	19	19	5	19	24	21	21	18	5	111
	42	3	620	2	203	4	8	7	3	8	12	3	21	18	27	13	4	9	27	20	10	19	18	3	30	23	17	23	12	6	119
	42	4	570	0	223	0	0	0	0	0	0	0	8	8	9	4	3	0	15	16	10	6	1	0	50	46	47	47	28	0	186
	42	5	890	0	12	0	1	0	0	0	0	0	0	2	0	0	1	0	2	2	2	3	1	0	0	3	0	1	4	0	4
	42	6	340	0	118	0	3	5	2	2	3	0	15	8	9	3	4	0	10	15	9	11	10	0	14	16	13	14	18	0	41
	42	7	720	15	524	12	47	33	24	27	24	18	114	67	72	74	56	4	121	87	60	59	79	18	107	77	47	62	69	22	129
	42	8	720	0	21	3	5	1	1	1	2	0	0	3	3	18	1	4	10	7	1	1	7	3	10	17	5	6	5	11	117
	42	9	520	0	35	0	1	0	0	0	0	0	2	1	1	1	5	0	1	0	1	1	1	0	3	2	1	0	2	0	7
	42	10	600	0	29	0	0	2	0	0	0	0	3	4	3	1	6	0	8	10	10	8	11	2	16	15	11	16	10	0	60
	42	11	810	2	41	0	3	1	1	1	0	0	1	1	0	1	0	0	5	6	5	6	3	0	13	21	9	8	6	0	25
	43	1	510	0	12	0	2	1	0	1	2	0	2	3	1	5	2	0	1	2	4	3	1	0	5	5	5	3	4	0	26
	43	2	810	0	53	1	4	2	1	3	1	0	1	2	4	4	4	0	14	7	9	10	10	0	18	11	12	10	11	0	25
	43	3	950	3	33	3	1	2	1	2	3	3	5	1	5	2	4	4	6	7	8	4	8	0	3	2	1	3	2	1	10
	43	4	720	1	50	0	4	2	1	2	1	2	6	5	3	3	0	3	9	3	12	3	8	0	31	16	9	11	21	0	42
	43	5	720	2	69	5	10	8	6	9	10	10	18	13	16	12	17	4	29	24	26	24	37	0	30	21	21	24	19	7	202
	43	6	480	0	112	0	7	1	6	3	3	0	1	3	5	5	20	0	29	21	23	14	17	0	19	10	7	0	11	0	0
	43	7	730	3	95	4	18	23	22	17	13	3	8	13	12	11	14	1	11	9	12	17	16	5	17	18	10	11	16	3	81
	43	8	720	0	55	0	3	2	1	5	2	0	3	1	2	2	2	1	10	6	6	6	3	0	9	8	6	11	3	0	5
	43	8	720	14	151	5	2	20	20	22	10	3	0	23	38	28	21	4	55	66	44	36	28	14	70	61	59	40	57	1	130
	43	9	350	0	63	0	1	9	12	5	6	0	2	29	28	31	6	0	39	39	21	17	7	0	40	37	65	25	66	0	27
	43	10	690	0	91	0	9	17	20	10	10	3	35	34	22	18	12	0	43	45	47	38	28	5	42	48	45	48	32	2	178
	43	11	480	0	113	0	2	1	1	2	3	0	2	0	2	2	1	0	0	0	0	1	2	0	0	2	3	2	2	0	9
	46	1	520	1	22	5	3	3	6	6	7	2	4	1	5	7	20	2	12	5	7	12	3	2	19	15	12	12	12	7	56
	46	2	610	2	146	0	4	4	4	3	1	0	7	6	3	3	8	2	6	6	6	7	10	1	9	9	16	7	12	1	78
	46	3	810	0	55	0	0	0	0	1	0	0	9	9	8	3	3	0	26	20	26	17	13	0	36	25	29	24	16	0	81
	46	4	440	3	107	1	1	0	4	6	6	0	10	9	37	10	11	0	27	41	10	48	43	0	41	29	44	44	44	1	95
	46	5	670	0	35	0	0	0	0	0	0	0	0	0	0	0	0	0	0	0	0	0	0	0	4	1	0	1	2	0	15
	46	6	590	7	169	3	9	8	10	12	3	2	11	9	9	7	5	1	42	68	39	67	27	2	106	107	97	83	70	0	170
	46	7	530	0	85	0	0	2	4	1	9	0	19	17	20	26	8	0	22	9	12	8	20	2	16	18	23	35	42	7	101
	46	8	710	0	63	0	3	4	6	4	6	0	10	7	2	4	8	0	24	29	21	16	21	0	43	32	35	35	35	0	164
	46	9	620	0	69	0	2	4	1	0	2	0	2	0	1	1	3	0	6	3	2	2	4	0	8	5	5	10	9	0	42

Note – Table is continued on the next page.

	Rat #	Neuron	Depth	Brush		1.4g vF						4g vF						10g vF						26g vF						Pinch	
				BL		BL	1	2	3	4	5	BL	1	2	3	4	5	BL	1	2	3	4	5	BL	1	2	3	4	5	BL	
inj-BP0h	46	10	750	0	74	0	0	1	0	1	0	0	0	0	0	0	0	0	1	1	3	3	1	0	9	6	12	8	6	0	29
	46	11	500	0	68	0	10	7	8	5	10	0	18	17	28	14	7	0	31	34	64	52	44	0	39	31	31	43	28	0	283
	46	12	650	0	97	0	1	2	0	0	2	0	3	1	1	0	2	0	0	1	5	2	0	1	18	26	11	8	31	0	25
	49	1	800	0	150	0	2	1	0	0	0	0	2	1	0	0	0	0	1	0	0	2	1	0	0	0	4	2	0	0	3
	49	2	550	0	29	0	0	0	0	0	0	0	3	1	4	4	2	0	1	1	1	1	2	0	9	12	11	23	2	0	91
	49	3	580	0	65	0	17	4	4	1	2	0	14	4	15	22	11	0	32	22	38	33	27	0	35	52	57	32	33	0	49
	49	4	410	10	173	23	41	38	34	33	38	3	41	21	41	45	42	11	49	40	25	67	57	5	85	85	91	85	118	3	116
	49	5	300	1	35	0	1	0	1	0	1	1	1	1	1	0	0	0	9	4	2	1	3	0	5	13	9	17	12	0	18
	49	6	320	0	32	0	0	0	0	0	0	0	9	1	12	5	9	6	11	8	7	9	12	0	17	20	20	14	15	0	18
	49	7	870	0	21	0	0	1	0	0	5	0	23	3	9	12	7	0	20	19	20	26	16	0	24	33	32	30	19	0	88
	49	8	650	0	53	0	0	2	0	4	1	0	4	1	2	5	0	0	3	3	2	1	3	0	4	3	5	6	6	0	5
	49	9	460	0	51	0	0	0	0	0	3	0	2	1	2	2	1	0	12	4	2	6	4	0	9	7	5	11	10	1	69
	51	1	320	0	31	5	3	1	4	4	5	8	5	6	8	9	6	5	5	9	11	7	6	3	10	7	2	4	14	6	67
	51	2	1020	3	65	2	6	5	6	8	6	4	29	27	11	21	15	4	40	20	31	29	19	1	43	39	27	24	18	7	167
	51	3	260	0	130	0	33	26	24	24	30	0	38	33	27	25	31	0	25	18	22	22	25	0	34	39	27	28	35	0	58
	51	4	620	32	254	16	42	38	32	28	23	27	71	71	72	51	51	24	64	74	64	69	58	17	83	91	69	72	63	21	454
	51	5	830	0	15	0	2	2	3	3	4	1	14	8	8	9	7	2	22	31	27	11	11	3	24	37	17	29	18	7	280
	51	6	950	1	39	5	3	0	0	3	3	2	7	8	9	3	6	5	33	18	10	13	16	6	49	27	55	12	30	4	72
	51	7	480	3	123	4	11	12	15	2	20	3	16	12	11	6	10	1	19	19	13	22	12	6	48	32	27	45	32	3	156
	51	8	650	0	3	0	2	0	1	0	1	0	4	3	9	7	4	1	12	22	43	8	34	0	42	18	27	21	32	3	142
	51	9	520	0	62	0	1	2	5	3	7	0	2	2	3	6	5	1	11	7	8	8	12	0	20	14	11	9	12	1	32
	51	10	670	0	140	0	0	0	0	0	0	0	39	6	2	35	11	0	6	1	7	8	4	1	13	15	8	6	8	0	33
	51	11	410	0	36	0	0	0	0	0	0	1	10	8	2	4	0	1	24	17	16	8	18	0	31	28	27	20	23	0	10
	51	12	720	0	19	2	1	2	2	1	2	0	2	2	1	3	2	0	2	3	2	0	1	0	4	2	2	3	4	0	8
inj-VEHd4	52b	1	490	1	85	1	2	5	3	3	7	1	2	9	5	5	4	0	5	8	2	3	3	0	6	4	3	4	4	0	4
	52b	2	650	0	35	0	0	0	0	0	0	0	1	1	2	2	0	0	3	1	5	6	0	0	5	10	1	6	5	0	6
	52b	4	670	1	47	1	11	8	8	4	6	0	18	8	13	7	17	0	8	13	14	19	22	0	23	19	14	13	17	1	111
	52b	5	855	0	45	0	1	8	8	16	13	1	10	5	16	11	14	0	7	6	13	8	9	0	12	2	5	4	11	0	6
	52b	6	425	0	107	0	3	3	5	1	2	1	7	4	7	5	8	0	17	14	9	26	21	1	33	38	25	16	22	1	98
	52b	7	580	0	117	4	13	3	5	6	9	0	23	11	9	14	8	0	18	20	20	13	8	0	21	32	18	11	24	1	60
	52b	8	590	0	139	0	19	14	15	8	20	3	40	32	22	23	12	0	28	19	38	51	51	2	47	48	39	24	26	0	87
	52b	9	410	30	439	9	42	38	20	28	25	2	56	47	29	34	40	0	34	44	48	36	33	1	37	42	46	42	28	0	91
	52b	10	630	0	71	4	25	24	20	11	19	4	10	13	20	17	11	2	8	10	19	10	19	0	20	11	8	15	12	3	141
	52b	11	710	0	140	0	8	12	4	10	8	2	14	10	15	24	4	0	24	6	14	5	8	0	14	27	7	39	8	0	123
	52b	12	740	0	59	3	15	27	15	16	21	0	21	15	14	16	23	4	13	11	17	10	5	1	17	17	17	14	5	0	46
	52b	13	800	6	70	11	6	6	6	8	13	6	6	1	14	14	11	5	12	17	9	7	11	6	18	18	15	19	15	1	91
	54b	1	930	0	30	0	0	0	0	0	0	0	6	0	3	3	4	0	9	9	14	10	8	0	9	8	10	10	11	0	1
	54b	2	610	3	113	4	13	21	15	15	20	11	26	17	25	31	30	8	33	87	114	88	112	14	137	126	163	150	92	10	688
	54b	4	270	0	153	4	25	25	22	14	18	0	34	30	41	27	23	0	21	23	27	27	17	2	40	43	47	26	15	0	65
	54b	5	470	0	55	1	11	7	13	13	6	3	14	15	16	13	10	0	14	14	10	10	12	0	8	14	7	12	11	3	39
	54b	6	285	0	29	0	26	28	23	20	15	0	37	17	39	29	41	0	49	44	35	37	28	0	58	42	36	39	46	0	37
	54b	7	640	1	79	3	6	21	8	15	7	1	31	33	23	18	19	3	41	21	34	76	43	2	50	50	93	77	71	1	498
	54b	8	715	0	423	0	21	33	44	26	17	0	19	13	31	31	23	1	33	26	20	24	25	1	55	47	53	55	40	1	114
	54b	9	625	0	196	0	12	19	8	9	21	3	33	5	25	21	29	0	57	61	45	53	49	0	80	67	67	77	71	2	277
	54b	11	920	0	291	0	1	10	0	0	1	0	33	11	15	18	19	1	95	70	48	64	36	1	57	55	56	34	43	0	150
	54b	12	620	0	87	0	0	0	0	0	0	0	1	4	0	2	7	0	4	8	10	7	15	0	19	14	19	21	11	0	28
	54b	13	950	2	80	6	11	4	11	9	7	1	25	9	11	12	9	3	39	50	49	39	38	6	45	41	42	44	38	9	268
	66	1	600	5	177	5	13	4	6	14	6	8	14	15	9	11	22	6	36	32	40	42	32	2	42	55	35	32	32	4	224
	66	2	750	4	53	0	8	8	5	3	8	0	16	14	8	8	5	0	27	22	13	10	7	2	47	35	26	27	33	0	117
	66	3	820	2	145	0	2	13	10	4	12	2	4	10	1	7	9	0	17	23	24	24	17	1	30	25	24	28	27	3	49
	66	4	450	1	187	0	2	4	3	1	2	0	14	20	0	17	17	7	21	21	14	22	5	3	63	45	41	51	51	2	65
	66	5	370	0	108	0	2	2	3	3	1	0	2	2	5	2	3	0	2	4	2	3	3	0	1	1	2	1	2	0	7
	66	6	690	0	62	0	1	1	3	2	1	0	4	2	1	1	2	0	4	1	1	1	1	0	3	1	3	3	5	0	13
	66	7	790	0	120	0	51	33	41	35	40	0	56	80	85	46	77	0	79	56	85	69	53	0	52	46	62	47	77	0	62
	66	8	555	0	112	0	6	4	3	4	4	0	36	27	32	24	29	1	23	44	57	15	9	0	53	60	37	56	63	5	86

Note – Table is continued on the next page.

	Rat #	Neuron	Depth	Brush		1.4g vF						4g vF						10g vF						26g vF						Pinch	
				BL		BL	1	2	3	4	5	BL	1	2	3	4	5	BL	1	2	3	4	5	BL	1	2	3	4	5	BL	
inj-VEHd4	66	10	450	2	130	4	32	17	15	17	9	0	29	19	26	18	14	0	48	37	26	26	28	0	58	45	52	55	61	0	154
	66	12	440	0	456	0	12	8	13	10	14	0	14	14	9	23	16	0	21	16	16	30	15	0	52	49	39	42	30	0	54
	66	13	500	0	114	4	12	10	12	10	5	0	12	6	18	10	11	0	16	17	8	14	10	0	12	14	31	21	24	0	71
	66	14	640	0	185	0	6	4	10	8	5	0	15	16	9	14	11	0	60	62	70	75	63	0	134	114	121	102	110	0	119
	66	15	850	4	133	7	13	14	7	15	8	17	14	22	25	14	19	9	23	23	21	36	32	19	51	38	34	38	54	12	180
	66	16	280	0	66	0	44	33	76	32	47	0	54	#	82	89	76	0	89	107	100	146	12	0	48	87	74	71	64	0	80
	66	18	670	0	157	0	3	2	1	2	5	0	11	4	5	2	6	0	25	11	14	9	6	0	35	33	30	24	22	0	95
	66	19	450	0	65	0	2	0	3	4	2	0	4	1	3	7	1	0	8	18	13	10	14	0	18	20	8	10	14	0	31
	66	21	570	4	151	1	2	1	3	3	1	0	11	15	4	9	11	5	14	13	22	15	13	0	44	30	33	20	19	0	42
	69	1	570	8	85	11	11	0	2	7	11	5	10	2	14	7	2	0	3	9	5	9	2	9	24	14	16	12	17	4	42
	69	2	570	5	358	4	11	10	7	5	10	1	36	27	21	27	16	4	48	55	64	60	55	3	91	124	112	111	101	18	934
	69	4	400	0	157	1	4	6	12	13	1	0	28	28	24	36	36	0	29	20	44	25	39	0	47	36	30	22	24	0	151
	69	5	490	0	188	0	0	0	0	1	0	0	7	9	7	7	12	0	28	25	21	15	16	0	30	17	25	15	23	0	20
	69	6	650	0	209	2	14	12	10	4	5	0	14	21	21	19	9	0	21	10	15	10	8	0	41	33	29	21	32	0	124
	69	7	760	0	448	0	29	12	17	3	8	0	40	26	21	8	9	0	49	27	17	11	16	0	98	109	83	71	70	0	221
	69	8	500	19	240	15	26	18	20	21	17	23	33	33	19	27	25	13	32	23	33	39	41	20	56	54	67	52	53	13	170
	69	10	900	0	130	1	1	1	0	1	1	0	5	5	7	5	2	1	12	18	15	14	13	0	26	24	31	16	17	0	83
	71	1	535	21	151	14	23	28	20	21	18	16	41	27	32	29	28	16	91	71	72	67	50	24	107	102	78	84	79	14	163
	71	2	450	1	157	2	7	11	12	12	8	2	38	14	46	46	54	4	50	56	39	62	38	0	42	53	32	32	56	1	103
	71	3	600	11	132	10	31	41	17	21	16	10	43	27	25	32	14	21	61	36	34	30	34	11	41	53	25	31	37	13	471
	71	4	770	0	52	1	0	1	3	2	6	3	21	26	19	26	23	0	24	24	28	22	21	5	41	28	37	42	26	2	126
	71	6	690	6	112	3	17	22	13	12	6	1	32	27	22	19	15	1	54	29	38	29	19	2	56	37	43	40	37	1	94
	71	7	760	3	416	1	56	53	63	68	66	6	132	110	98	117	94	1	166	162	143	187	116	1	219	197	175	147	#	3	493
	71	8	480	1	172	0	11	3	5	10	17	0	24	9	19	27	18	0	35	35	32	16	24	0	36	40	45	52	42	1	84
	71	9	650	9	192	9	11	11	9	9	6	5	2	16	25	19	15	8	41	41	28	12	16	5	41	23	20	13	17	12	206
	71	10	530	2	70	0	6	6	9	3	6	0	7	7	9	5	6	0	15	19	12	23	21	1	30	30	23	33	23	0	145
	71	11	700	0	112	0	2	0	2	2	1	0	1	3	3	1	3	0	14	11	6	6	11	0	38	29	18	26	27	0	97
sham-VEHd4	135	1	620	0	63	0	3	5	6	5	8	0	17	10	10	15	11	0	37	27	26	24	24	0	53	47	48	38	39	0	56
	135	2	880	0	93	0	3	1	0	1	3	0	21	18	16	11	19	0	14	25	29	22	39	0	37	41	40	38	29	0	25
	135	3	660	0	19	0	1	2	2	2	1	1	5	2	2	2	1	0	5	7	1	1	4	0	5	2	3	3	8	0	14
	135	4	50	0	42	0	2	5	2	3	1	0	7	4	5	4	5	0	4	16	9	4	7	0	14	11	11	12	4	0	12
	135	5	750	0	82	0	1	0	0	0	1	0	11	3	6	4	6	0	26	34	17	30	19	0	24	27	30	11	25	0	13
	135	6	525	1	21	2	7	3	4	5	7	2	11	4	9	7	3	4	10	7	21	11	15	1	11	22	17	26	21	0	134
	135	7	700	0	86	0	3	5	3	4	5	1	32	8	15	10	12	0	19	22	17	23	31	0	39	27	16	23	13	2	51
	135	8	320	0	119	0	12	13	12	9	9	0	5	2	6	8	6	0	19	17	17	13	24	0	25	44	39	42	18	0	30
	135	9	90	0	76	0	0	0	0	0	0	0	1	1	1	0	1	0	10	10	3	7	27	0	7	17	3	3	33	0	79
	135	10	250	3	175	6	18	5	16	10	14	9	23	32	26	29	24	1	57	69	66	77	70	4	57	66	97	57	38		
	136	1	720	5	81	20	31	23	26	8	28	19	36	17	19	18	29	7	28	32	28	21	13	7	29	38	20	24	35	8	157
	136	2	480	0	45	0	3	3	0	3	3	0	3	2	2	6	1	0	7	3	0	5	5	0	7	8	9	7	3	0	11
	136	3	550	4	119	3	21	15	12	11	14	5	16	19	19	16	11	5	16	8	10	13	9	6	16	25	29	27	11	7	169
	136	4	650	0	149	0	10	4	1	0	1	0	4	3	2	8	6	0	2	2	0	1	5	0	3	9	10	7	9	0	33
	136	5	620	0	61	3	2	7	3	7	2	4	11	7	4	4	5	1	14	16	11	16	18	7	32	34	20	47	22	0	116
	136	6	710	0	115	1	7	9	6	5	6	0	8	5	7	6	7	0	11	13	11	11	9	0	25	19	18	10	17	0	91
	136	7	630	3	43	9	12	10	10	7	5	2	5	10	6	8	10	6	20	17	16	8	15	2	20	7	18	3	15	5	72
	136	9	210	0	68	0	3	1	1	0	0	0	5	6	3	2	7	0	10	4	3	13	15	0	11	8	6	3	13	0	16
	136	10	410	0	76	0	0	0	1	0	0	0	2	3	0	1	2	0	2	4	3	1	2	0	27	10	22	18	5	0	9
	136	11	590	1	39	0	12	6	7	10	16	1	9	9	14	17	18	1	13	2	17	9	7	1	19	10	5	9	12	2	96
	136	12	650	8	154	6	5	1	0	3	2	7	40	7	15	14	10	6	31	30	33	31	37	9	49	42	19	28	56	5	183
	137	1	500	0	29	1	5	5	6	4	4	0	8	3	4	6	5	0	8	4	3	6	1	0	9	9	9	8	8	0	24
	137	2	800	25	150	12	26	36	22	17	39	13	47	10	32	40	30	33	65	33	35	31	34	21	65	54	32	64	47	19	432
	137	4	600	0	90	0	5	6	3	9	9	0	20	14	7	13	23	0	33	18	15	21	21	1	17	27	18	19	23	0	19
	137	5	750	4	81	9	15	20	13	6	11	11	21	17	19	26	20	5	30	18	19	30	26	11	25	38	28	32	31	3	109
	137	7	450	0	139	0	10	6	6	6	3	0	5	7	7	8	11	0	10	5	8	9	3	0	6	11	11	9	9	0	0
	137	8	740	0	66	0	5	3	3	4	2	0	6	1	0	5	1	0	21	7	11	8	12	0	12	12	25	8	11	0	50
	137	9	770	0	141	0	7	1	5	4	6	0	9	6	5	12	8	0	20	16	14	9	10	0	31	20	27	22	11	0	30

Note – Table is continued on the next page.

	Rat #	Neuron	Depth	Brush		1.4g vF						4g vF						10g vF						26g vF						Pinch	
				BL		BL	1	2	3	4	5	BL	1	2	3	4	5	BL	1	2	3	4	5	BL	1	2	3	4	5	BL	
sham-VEHd4	137	10	650	4	96	3	29	23	19	9	8	6	17	22	17	18	11	4	28	42	38	15	20	1	45	38	36	37	35	2	137
	137	11	525	1	47	3	15	6	16	3	17	2	14	28	15	21	19	11	34	27	19	38	7	7	28	27	34	48	32	0	114
	137	12	540	0	180	10	41	11	15	20	11	7	18	33	20	19	26	9	29	36	18	9	23	2	40	28	30	47	32	14	137
	138	1	720	1	58	3	1	5	6	13	4	4	5	9	7	8	5	4	17	15	9	7	8	3	7	4	8	7	14	4	47
	138	2	520	0	14	0	1	1	0	1	2	1	10	5	3	7	6	1	12	10	7	8	8	0	10	7	11	12	13	0	42
	138	3	620	0	203	0	24	15	6	4	9	0	39	19	14	30	21	0	35	46	54	20	29	0	43	40	23	26	37	0	81
	138	4	740	0	22	0	0	0	0	0	0	0	0	1	1	3	0	0	4	7	2	4	2	0	10	9	6	8	2	0	11
	138	5	350	2	60	1	3	2	3	3	9	3	6	6	7	9	7	1	15	21	22	24	22	0	14	9	2	0	0		
	138	6	500	0	61	0	4	4	1	0	4	0	5	3	3	3	10	0	14	17	6	4	12	0	13	17	22	21	12	0	37
	138	7	450	1	92	1	0	1	1	4	2	0	23	9	9	5	11	0	33	39	26	31	21	0	89	88	82	77	65	0	115
	138	8	750	0	90	0	3	0	4	0	0	0	6	2	2	1	4	0	1	1	8	3	1	0	11	11	8	10	8	0	2
	138	9	650	0	66	0	25	23	21	17	15	1	19	24	26	16	22	0	20	11	17	13	16	0	20	9	9	23	23	0	25
	139	1	700	3	66	0	5	4	8	5	6	0	14	6	12	7	8	1	23	12	12	16	23	3	33	31	19	34	28	1	97
	139	2	850	0	27	0	0	0	1	0	0	0	1	1	2	1	1	0	6	2	1	6	3	0	3	3	5	2	1	0	5
	139	3	510	0	93	0	14	5	7	7	8	0	27	25	20	27	29	0	33	28	36	26	32	0	37	33	23	26	24	0	102
	139	4	620	0	52	0	4	6	3	3	2	0	16	5	7	6	5	0	20	13	17	8	11	0	28	31	27	17	15	0	39
	139	5	750	0	96	0	1	1	0	0	0	0	12	6	11	4	1	0	11	12	10	18	13	0	15	22	13	11	10	0	10
	139	6	280	0	59	0	5	0	3	5	2	0	19	5	8	5	1	0	19	39	10	15	13	2	41	22	20	58	58	6	81
	139	7	320	0	73	0	0	3	0	1	1	0	9	4	4	3	9	0	12	4	11	9	6	0	12	8	3	6	6	0	227
	139	8	710	1	70	4	15	11	10	11	8	4	23	21	21	17	11	4	14	11	9	9	7	6	7	7	11	17	8	2	155
	139	9	820	3	101	1	13	20	9	10	8	2	7	14	15	2	8	0	15	13	4	9	9	0	44	41	45	43	31	0	203
	139	10	720	0	53	0	9	2	2	8	5	0	12	6	6	1	14	0	22	19	11	15	17	0	30	27	45	27	33	0	72
	139	11	810	0	92	0	7	5	11	4	4	0	11	8	6	16	6	0	21	23	27	20	32	0	26	28	39	27	28	0	21
	140	1	700	0	42	0	1	0	2	2	0	0	1	2	5	0	2	0	2	14	6	1	3	0	25	24	17	13	11	0	16
	140	2	600	3	156	6	9	7	10	17	9	7	33	29	25	15	17	12	15	32	25	16	29	13	15	14	28	19	28	9	142
	140	3	650	9	204	21	19	20	17	11	18	10	66	45	36	52	64	26	62	59	89	70	90	20	118	115	104	112	#	9	564
	140	4	425	0	96	0	10	7	2	3	10	0	16	16	11	13	7	0	7	18	8	11	10	0	9	10	14	8	6	0	30
	140	6	600	8	319	0	5	12	27	10	7	0	34	34	37	8	37	0	86	61	57	33	42	0	144	115	121	106	#	0	361
	140	9	610	2	72	19	39	50	54	37	31	30	34	43	33	27	22	14	33	24	17	12	13	10	23	27	23	22	18	3	109
	140	10	720	0	61	0	7	9	6	7	13	0	4	3	5	9	2	0	6	14	10	10	8	0	12	4	13	12	9	0	57
	140	11	680	2	91	10	16	13	11	9	9	5	13	12	14	16	13	8	12	17	16	15	25	3	15	12	12	12	16	5	52
	140	12	760	0	43	0	0	0	0	0	0	0	5	6	4	2	3	0	27	6	9	5	5	0	45	27	30	21	15	0	80
inj-BPd4	53b	1	890	0	124	0	15	37	23	21	9	0	16	15	3	14	17	0	3	4	14	14	17	0	7	3	10	6	15	0	25
	53b	2	890	0	160	0	27	27	18	12	13	0	36	22	35	41	25	0	35	27	36	42	23	0	39	44	39	44	12	4	120
	53b	4	880	0	10	0	1	0	1	0	1	0	2	1	0	0	1	0	1	0	2	1	2	0	3	0	2	3	5	0	5
	53b	5	660	1	48	2	5	4	9	5	6	0	15	16	7	7	6	0	5	4	10	9	6	2	10	7	9	11	11	0	21
	53b	6	760	2	134	1	12	12	23	17	4	4	22	16	26	19	9	3	31	30	22	16	17	3	32	36	35	32	20	2	160
	53b	7	830	0	110	2	8	9	6	7	4	0	10	7	11	8	9	2	16	15	27	16	15	0	44	32	26	30	28	1	110
	53b	8	610	0	93	0	3	3	2	3	1	0	4	0	4	2	1	0	4	4	2	2	1	0	14	4	2	3	3	0	3
	53b	9	1000	0	119	0	1	3	0	2	1	0	0	4	0	1	2	2	18	12	7	17	11	0	19	11	11	12	13	0	28
	53b	10	790	3	133	1	7	5	10	7	2	0	10	7	10	7	1	0	9	11	12	10	7	1	18	13	18	8	13	0	38
	53b	11	890	0	191	1	5	3	3	1	6	0	8	6	6	4	12	1	11	10	11	15	11	0	8	13	14	12	8	0	35
	53b	12	800	2	102	10	12	15	18	18	20	11	19	17	16	13	16	10	49	50	46	32	41	10	64	80	89	82	72	7	558
	56	1	780	9	169	14	9	12	11	4	14	8	19	19	13	18	25	10	25	35	41	32	33	7	33	42	25	32	25	8	118
	56	2	870	13	117	14	22	30	25	23	28	12	21	18	19	19	19	17	36	25	17	24	20	6	44	46	47	32	36	10	200
	56	3	830	21	324	21	48	34	33	36	24	17	33	42	43	37	34	24	79	70	105	93	113	22	148	137	126	116	78	20	634
	56	4	1040	0	135	0	1	9	3	7	5	0	10	4	4	2	5	0	10	18	20	13	4	0	30	17	14	36	45	0	34
	56	5	430	0	43	1	0	0	1	1	3	0	6	2	7	7	2	0	6	5	5	16	9	1	25	23	56	20	23	2	53
	56	6	720	0	42	0	10	13	8	8	6	0	8	5	9	10	11	2	19	7	12	9	5	0	8	8	10	18	15	0	41
	56	7	840	11	177	11	27	34	18	26	14	5	28	36	31	31	18	9	60	43	32	26	20	6	75	49	57	51	44	15	167
	56	8	650	1	35	2	3	2	3	1	4	0	4	2	6	2	2	0	17	19	6	6	11	1	20	18	15	10	16	1	72
	56	9	460	2	74	0	0	0	0	0	0	0	2	2	3	3	2	0	3	3	4	4	5	1	11	15	18	25	19	2	33
	56	10	600	0	68	2	9	2	15	12	3	0	18	17	10	18	13	0	10	11	16	11	10	0	15	18	22	7	13	0	92
	56	11	740	2	121	0	2	3	2	2	1	0	4	3	0	3	4	0	15	6	4	6	2	0	12	19	11	10	9	0	12
	56	12	745	2	61	1	1	2	2	3	2	0	1	1	2	1	2	4	3	9	2	4	3	0	19	15	11	27	30	1	15

Note – Table is continued on the next page.

	Rat #	Neuron	Depth	Brush		1.4g vF						4g vF						10g vF						26g vF						Pinch	
				BL		BL	1	2	3	4	5	BL	1	2	3	4	5	BL	1	2	3	4	5	BL	1	2	3	4	5	BL	
inj-BPd4	63	1	600	0	51	1	7	8	5	4	3	3	14	8	5	8	4	2	17	6	6	5	6	1	7	8	4	8	12	3	26
	63	2	760	3	112	6	18	16	7	7	14	9	19	21	15	18	6	14	21	18	14	19	24	13	36	33	35	21	25	8	111
	63	3	870	1	288	0	42	30	31	24	37	1	58	42	46	30	31	0	54	42	36	31	21	0	54	43	30	32	27	3	139
	63	4	875	41	607	37	78	65	#	47	60	19	82	78	68	52	65	35	115	98	90	90	78	22	101	101	105	101	#	13	360
	63	5	950	25	130	0	7	0	7	6	2	7	29	24	11	14	21	1	34	38	34	48	37	2	56	56	57	52	55	4	155
	63	6	310	0	96	0	0	0	0	0	0	0	28	18	16	17	10	0	50	53	48	48	40	0	57	32	40	40	42	0	38
	63	7	310	1	76	1	8	6	11	5	8	6	24	19	21	18	16	2	29	32	35	31	29	5	32	40	36	33	34	3	127
	63	8	720	6	255	18	20	19	20	25	34	21	35	57	38	41	31	12	43	47	67	49	59	7	87	68	60	58	97	3	261
	63	9	550	5	153	1	19	34	13	10	14	0	37	33	39	19	18	4	60	38	39	32	31	5	42	62	51	46	26	9	256
	63	10	540	1	175	0	7	1	2	0	2	0	41	7	11	4	6	0	54	34	28	34	21	3	31	39	35	22	25	0	73
	64	1	670	5	240	3	18	28	27	15	25	7	12	24	20	16	23	2	51	41	48	69	70	3	49	77	86	65	39	1	352
	64	3	680	1	258	7	21	22	32	29	36	9	45	45	48	67	60	1	41	40	37	34	54	6	48	59	43	148	65	6	591
	64	4	780	1	188	6	25	24	17	31	27	0	19	14	18	17	16	1	25	21	18	16	29	0	32	20	34	27	24	4	168
	64	5	620	0	43	1	7	4	6	4	2	6	10	9	3	5	20	0	12	4	5	4	6	0	8	12	14	14	9	0	72
	64	6	810	9	278	0	9	6	4	29	30	3	44	30	35	37	16	6	54	41	46	85	39	4	86	55	40	45	41	4	192
	64	7	950	2	76	0	5	5	1	1	1	0	5	1	0	6	3	0	4	9	1	3	1	0	6	10	13	11	13	1	38
	64	8	500	42	279	37	40	56	50	57	51	29	60	50	57	46	50	39	99	84	68	74	49	38	104	101	86	67	#	40	358
	64	9	780	0	53	1	6	20	0	2	1	0	21	37	19	41	31	0	35	45	61	37	74	0	34	26	16	11	58	0	42
	67	2	650	5	293	0	18	18	35	15	24	0	45	23	36	45	23	1	112	126	58	108	96	1	63	87	101	75	65	5	411
	67	3	740	1	148	0	6	3	2	1	2	1	37	22	29	20	16	0	79	55	44	45	44	2	84	53	45	41	48	9	167
	67	4	270	0	152	1	22	21	11	7	15	0	30	27	29	27	28	0	45	38	39	35	49	0	67	43	39	50	62	0	60
	67	5	400	9	193	10	22	22	21	22	22	9	36	33	34	29	36	11	60	58	55	60	56	9	57	32	49	43	50	7	211
	67	7	800	1	367	0	17	50	61	37	24	1	60	59	65	63	57	0	69	61	66	58	68	0	99	66	61	55	57	3	85
	67	8	910	0	334	0	5	22	16	13	3	0	27	28	25	28	47	0	32	42	30	34	34	0	37	31	42	30	36	4	201
	67	9	600	4	174	6	101	87	99	82	96	5	92	96	112	105	96	0	89	98	75	94	100	2	92	76	101	78	95	2	359
	67	10	830	0	62	0	2	0	1	1	0	0	3	3	2	1	2	0	11	6	7	9	10	0	17	25	15	8	13	0	18
	67	11	200	1	249	0	5	3	1	3	0	0	12	20	8	23	8	0	23	12	22	10	20	0	14	8	15	17	12	0	6
	67	12	310	0	94	0	0	0	0	0	0	0	6	3	1	1	3	0	11	4	3	5	1	0	13	10	14	4	6	0	67
	67	13	650	5	96	3	12	7	5	12	5	0	8	6	5	3	10	4	16	12	23	17	9	4	40	27	27	36	22	1	155
	67	14	780	0	94	0	2	3	2	3	1	0	8	5	1	4	1	0	30	33	20	34	23	0	32	34	28	24	17	0	41
	70	1	550	1	131	0	7	0	3	2	2	1	4	5	4	5	0	0	8	16	5	8	15	0	9	12	11	17	18	0	67
	70	2	650	0	222	0	1	9	9	4	10	0	18	10	19	23	17	0	49	27	26	34	15	0	66	71	41	54	62	0	57
	70	3	900	0	321	0	12	6	0	0	0	0	31	16	22	16	17	0	65	20	30	50	85	0	86	88	69	60	35	0	165
	70	4	670	9	246	6	46	29	32	21	30	9	31	44	38	75	37	2	86	58	53	46	50	6	78	42	45	41	52	3	302
	70	5	650	2	77	3	3	8	0	1	5	2	10	4	5	5	3	3	9	16	5	5	15	1	20	25	13	19	16	0	80
	70	6	775	0	227	3	4	6	2	7	3	4	11	10	7	13	11	0	14	34	15	12	10	0	21	10	15	8	12	0	99
	70	7	775	0	511	0	37	31	26	20	25	0	53	42	27	39	27	0	95	64	91	67	66	0	124	135	115	106	95	0	438
	70	8	770	0	137	0	1	2	1	1	1	0	3	4	1	1	2	0	3	1	4	0	1	1	5	5	8	14	3	1	23
	70	9	500	0	54	1	2	3	4	6	6	0	8	11	4	7	1	0	14	16	5	10	9	0	23	20	12	19	28	0	144
	70	10	700	0	106	7	22	20	30	15	22	3	32	32	20	16	14	6	41	37	46	42	23	5	31	37	37	40	19	1	115
inj-BP4h	91	1	850	0	54	0	0	0	0	0	0	0	7	7	6	8	4	0	21	13	19	6	7	0	26	22	10	11	21	0	16
	91	2	850	3	105	3	6	6	9	7	6	2	19	15	15	8	6	4	25	32	12	30	28	9	48	38	52	49	48	2	184
	91	3	900	4	73	8	7	7	4	8	5	5	21	7	17	8	13	8	15	17	6	12	16	5	17	20	15	13	18		
	91	4	1090	0	26	0	9	6	8	4	3	3	12	7	3	12	7	0	31	38	22	18	28	3	69	49	56	25	33	1	271
	91	5	520	6	63	8	6	20	10	9	3	3	10	16	22	16	9	3	14	6	22	26	11	3	12	8	16	18	12	2	150
	91	6	650	1	57	0	2	2	2	2	1	1	5	14	6	3	4	2	25	28	22	29	15	3	25	31	26	31	33	0	52
	91	7	770	0	37	0	2	1	2	1	1	0	4	6	9	2	17	0	18	14	28	16	14	3	28	14	21	15	19	3	167
	91	8	350	2	112	2	10	9	7	8	21	1	31	19	14	16	16	0	22	20	19	24	26	1	35	38	33	33	33	2	100
	91	9	440	4	122	2	4	5	6	7	1	5	17	22	18	12	13	5	39	34	29	21	33	4	64	28	44	61	60	3	110
	91	10	570	0	114	0	13	9	8	17	6	4	30	20	26	15	25	0	22	31	21	17	12	0	24	22	30	26	21	1	95
	91	11	760	2	59	1	12	5	10	6	4	1	14	11	13	15	5	2	21	11	8	7	13	2	33	26	45	36	28	2	127
	91	13	960	0	42	0	0	1	0	0	2	0	2	2	2	0	2	0	8	8	5	1	4	0	9	3	8	9	13	0	4
	92	2	610	2	40	15	16	15	13	14	18	14	39	23	21	18	11	13	45	43	38	33	25	11	29	52	43	57	50	1	160
	92	3	540	0	110	0	6	0	10	2	0	1	7	6	2	2	1	0	12	10	5	3	10	2	14	20	13	14	9	0	14
	92	4	790	3	200	2	9	3	3	3	0	1	8	8	5	2	15	1	18	25	14	15	3	0	30	35	23	24	9		

Note – Table is continued on the next page.

	Rat #	Neuron	Depth	Brush		1.4g vF						4g vF						10g vF						26g vF						Pinch	
				BL		BL	1	2	3	4	5	BL	1	2	3	4	5	BL	1	2	3	4	5	BL	1	2	3	4	5	BL	
inj-BP4h	92	5	640	3	127	5	7	3	13	7	11	3	27	29	38	12	17	5	42	38	37	59	38	6	60	47	67	72	63	5	129
	92	6	950	1	46	1	5	8	4	2	2	1	9	5	5	9	10	0	12	10	13	11	15	1	11	18	24	28	23	3	145
	92	7	500	0	105	0	3	1	6	0	4	0	9	4	4	7	3	0	23	37	14	38	40	0	23	11	5	14	23	0	5
	92	10	700	0	31	0	1	0	0	0	0	0	3	3	2	4	7	16	24	18	10	11	11	0	29	16	9	9	3	0	9
	93	1	840	41	314	45	50	30	36	31	36	19	75	64	60	50	48	22	50	89	62	79	36	17	61	68	65	66	31	22	488
	93	2	450	0	23	0	0	0	0	0	0	0	0	1	0	0	0	0	7	0	0	0	0	0	3	0	0	0	0	0	1
	93	3	520	0	22	0	1	5	2	5	1	0	5	5	3	1	2	0	14	6	9	5	3	0	15	8	7	5	9	0	69
	93	5	720	2	70	1	12	6	8	4	7	1	18	9	11	14	10	1	18	10	8	11	6	1	18	15	11	16	11	2	147
	93	6	900	0	80	1	3	2	0	5	1	0	5	5	3	8	2	0	23	13	7	7	8	0	26	9	32	12	14	2	70
	93	7	600	0	19	0	3	4	2	2	2	0	5	3	2	3	3	0	10	9	5	3	3	0	15	6	11	9	7	0	40
	93	8	850	1	76	5	8	5	12	24	17	6	26	23	23	17	20	2	9	11	6	12	13	2	10	5	18	15	18	0	38
	93	9	770	0	72	0	5	3	8	6	4	0	6	16	9	11	12	0	36	8	21	10	10	0	21	17	11	17	19	0	35
	93	10	840	1	120	3	11	8	8	5	8	3	12	29	13	14	6	5	12	25	7	2	7	4	16	20	21	16	16	3	69
	93	11	940	0	32	0	8	4	2	4	3	0	14	11	10	9	7	0	35	35	34	24	28	0	41	55	72	70	58	0	171
	93	13	600	3	122	6	9	3	15	18	9	12	24	14	26	17	23	4	38	34	36	33	30	3	49	32	35	19	30	5	134
	93	13	600	2	65	5	5	4	14	11	4	6	22	12	15	11	9	10	29	33	30	22	17	9	34	21	32	19	11	6	51
	117	1	120	0	112	0	4	1	1	3	3	0	5	4	9	1	8	0	14	8	13	7	12	0	11	12	8	6	17	0	8
	117	2	320	0	59	0	6	4	5	5	5	0	10	9	10	8	9	0	13	17	17	16	19	0	25	27	19	21	16	0	8
	117	3	710	0	113	1	15	20	28	14	26	4	27	29	25	34	34	2	53	52	27	28	27	4	82	84	67	59	54	4	292
	117	4	720	0	91	0	6	2	9	8	3	0	7	7	4	9	7	0	27	24	24	16	6	0	21	10	17	25	17	0	100
	117	5	615	15	135	15	66	31	30	28	34	16	34	39	20	32	22	18	20	33	24	19	6	20	35	40	47	47	73	13	218
	117	7	700	0	140	0	4	9	3	3	5	0	12	10	5	6	12	0	19	20	26	24	20	0	33	33	29	22	28	0	67
	117	8	520	11	97	8	8	8	20	17	11	17	9	21	13	24	26	10	22	24	18	27	22	10	16	34	31	29	37	8	81
	117	9	650	1	112	2	12	4	1	6	3	1	21	10	4	9	5	0	28	19	19	19	20	2	38	61	45	31	40	2	113
	117	10	580	14	69	11	31	31	20	31	30	12	48	25	38	27	15	12	38	28	22	34	27	12	26	26	20	27	12	17	145
	117	11	680	0	56	0	4	1	0	0	1	0	11	16	9	7	9	0	22	9	6	9	5	0	26	12	9	17	12	0	13
	117	12	490	1	92	3	11	8	8	15	16	4	25	18	20	19	16	12	22	23	18	17	18	11	20	15	25	25	21	7	131
	117	13	550	0	94	0	5	3	2	6	4	1	11	6	12	6	16	1	20	16	10	13	15	2	24	19	18	17	12	0	29
	117	14	465	9	53	12	14	6	3	15	6	14	8	10	16	20	12	7	13	10	12	9	9	7	12	24	14	17	19	8	64
	118	1	580	11	145	8	47	38	12	37	12	16	49	58	33	33	18	8	33	39	40	34	52	20	85	63	85	64	65	7	401
	118	2	825	0	31	0	1	3	3	2	0	0	3	1	2	2	4	0	1	0	2	3	4	0	3	4	3	3	1	0	3
	118	3	450	1	83	0	8	11	10	11	13	4	30	1	2	4	8	2	17	5	8	19	19	2	31	33	48	35	35	0	75
	118	4	750	0	7	1	6	11	2	3	2	0	8	22	13	17	9	0	24	15	7	10	13	0	25	20	23	23	16	1	217
	118	5	880	17	113	13	18	14	11	20	16	14	24	21	22	11	15	22	20	25	23	22	29	19	17	21	16	18	19	18	101
	118	6	420	0	67	0	6	10	5	4	0	1	15	23	16	19	12	4	24	18	21	15	10	1	36	15	11	23	34	2	25
	118	7	650	1	176	2	16	9	38	6	9	0	35	17	14	12	13	1	19	22	37	27	21	0	59	52	61	84	70	8	651
	118	8	780	0	97	0	1	2	3	0	1	3	21	13	6	13	8	0	28	22	18	19	17	0	46	36	26	28	37	0	122
	118	9	680	4	106	9	33	25	13	21	25	2	14	18	15	13	26	12	75	41	38	34	26	10	37	22	13	17	11	7	98
	118	10	720	5	87	5	9	17	14	16	21	5	38	17	22	29	16	5	47	26	36	47	21	7	58	53	68	62	54	6	315
	118	12	620	3	88	4	11	11	11	7	6	4	15	26	29	26	12	4	20	30	27	18	18	4	18	52	56	44	36	10	144
	118	13	800	0	57	0	2	2	3	4	1	0	8	7	5	7	3	0	4	9	8	8	10	0	9	11	10	6	8	0	36
	118	14	670	1	44	0	7	8	6	3	5	0	6	5	19	12	13	1	24	21	22	23	23	1	17	14	17	13	18	1	67
inj-BP8h	124	1	450	16	438	12	65	65	69	48	40	16	90	83	88	64	83	7	103	96	83	85	91	6	126	109	123	115	129	4	461
	124	2	520	3	44	5	7	10	7	10	6	4	19	30	11	27	26	8	20	38	25	33	22	6	41	53	45	33	32	2	164
	124	3	650	1	196	1	14	11	7	12	6	1	16	23	9	11	21	0	25	25	20	16	14	0	28	27	17	26	31	0	82
	124	5	810	13	215	19	24	35	17	26	29	20	38	31	31	19	31	17	35	32	25	39	30	12	49	45	38	32	38		
	124	6	320	0	225	0	0	0	0	0	0	0	69	60	75	44	66	0	63	78	55	78	45	0	68	83	59	70	69	0	241
	124	7	720	13	145	4	12	10	13	20	10	9	36	33	24	21	23	7	25	18	17	21	23	7	39	39	41	39	52	3	79
	124	8	680	14	225	4	22	39	22	15	19	6	53	73	70	68	64	3	70	53	70	39	69	8	63	34	49	50	43	1	230
	124	9	530	3	46	8	47	40	53	38	36	3	41	52	46	34	36	7	65	65	70	49	61	1	53	68	36	22	47	3	300
	124	10	520	3	183	9	24	18	10	20	16	2	21	18	17	25	10	10	36	39	31	30	28	12	74	69	71	47	65	13	376
	125	1	450	19	124	30	67	33	58	42	74	11	76	97	58	91	71	20	95	78	73	66	75	8	73	68	59	42	37	12	186
	125	3	390	0	135	0	5	6	8	5	5	0	11	12	10	7	8	0	13	10	14	10	10	0	16	16	18	12	10	0	27
	125	4	450	6	156	6	35	18	11	4	8	13	26	34	41	25	28	6	41	34	34	27	27	7	42	68	35	74	57	6	105
	125	5	470	1	85	0	34	12	8	14	14	3	25	13	6	17	34	2	45	27	28	24	19	7	59	45	14	30	37	2	88

Note – Table is continued on the next page.

	Rat #	Neuron	Depth	Brush		1.4g vF						4g vF						10g vF						26g vF						Pinch	
				BL		BL	1	2	3	4	5	BL	1	2	3	4	5	BL	1	2	3	4	5	BL	1	2	3	4	5	BL	
inj-BP8h	125	6	600	3	99	0	13	2	13	6	13	0	25	17	13	15	22	1	46	45	46	44	50	1	55	99	66	68	31	1	512
	125	7	550	3	160	4	13	4	8	4	7	7	16	11	10	8	25	1	38	39	50	47	39	2	50	75	105	93	71	2	616
	125	8	540	7	179	5	44	48	45	34	28	5	73	50	56	70	47	1	68	58	45	58	50	5	85	97	83	62	62	1	580
	125	9	600	4	190	1	12	17	13	13	17	1	89	#	93	75	64	2	42	23	34	34	20	1	72	55	70	76	85	1	229
	125	11	560	2	164	2	40	31	30	42	38	7	28	57	61	46	35	7	50	49	66	61	69	17	37	58	46	49	49	4	244
	125	12	530	2	66	2	29	19	24	12	21	3	24	47	31	26	28	5	20	38	31	13	30	3	11	24	27	39	24	3	66
	125	13	400	0	333	0	2	6	6	1	3	0	9	10	5	12	7	7	19	20	24	29	18	4	19	17	35	20	13	0	36
	126	1	425	8	79	6	15	5	11	10	8	8	16	13	14	8	3	3	9	4	11	8	23	12	10	6	13	11	14	12	118
	126	2	1000	27	344	36	31	47	34	26	45	21	71	85	84	77	64	41	93	97	91	93	92	20	126	139	129	127	142	7	390
	126	3	820	7	153	9	46	30	17	21	15	4	31	30	24	34	19	13	29	40	29	19	16	8	29	35	31	28	19	14	351
	126	6	560	0	78	0	13	11	6	4	5	3	24	19	19	7	25	1	27	29	24	26	26	0	31	28	31	27	30	0	133
	126	7	750	0	131	1	25	20	43	15	8	3	47	54	56	51	63	2	80	47	44	63	58	3	58	58	51	32	33	3	155
	126	8	820	0	75	0	3	5	9	5	2	4	9	15	13	11	15	0	18	26	21	14	26	2	36	24	18	38	33		
	126	9	450	0	383	0	1	0	3	1	0	0	2	5	4	1	2	0	11	34	37	38	40	0	16	23	18	18	23	0	76
	126	10	440	0	132	0	2	6	2	7	1	0	15	57	22	26	23	0	43	60	41	30	47	0	56	37	38	37	17	0	153
	126	11	650	0	78	0	4	5	3	1	2	0	1	0	0	1	3	0	11	3	5	4	6	0	15	24	15	8	15	0	119
	126	12	900	0	97	0	1	3	3	4	7	0	10	13	26	28	32	0	28	44	35	37	47	0	25	39	46	33	26	0	11
	127	1	720	26	206	29	22	37	24	22	38	28	31	29	30	30	27	21	38	37	36	27	44	18	44	42	38	39	30	3	304
	127	2	870	14	240	33	33	27	33	34	22	28	58	50	50	26	46	33	95	65	77	73	66	24	121	103	99	105	120	44	375
	127	3	950	0	113	0	1	1	2	1	2	0	0	3	0	3	1	0	20	9	7	6	6	0	49	45	23	18	15	0	112
	127	4	1020	0	92	0	2	0	1	1	0	0	4	1	2	2	1	0	13	8	3	4	2	0	30	39	44	10	32	0	93
	127	5	900	9	456	17	29	15	14	14	30	7	29	44	53	33	28	6	52	72	55	37	46	8	65	54	41	45	37	7	137
	127	7	800	0	137	1	8	4	2	1	1	1	14	24	11	23	11	3	48	44	43	36	36	0	60	42	46	75	73	1	315
	127	8	900	0	99	0	24	14	16	13	18	0	24	21	16	9	14	0	16	16	13	8	6	0	11	6	9	6	7	0	34
	127	9	780	9	176	10	11	5	11	24	10	11	37	40	21	29	40	10	67	76	109	124	131	40	149	127	170	175	161	3	367
	127	10	900	0	29	0	2	1	0	5	2	0	1	9	5	3	0	4	20	49	34	17	43	0	50	69	62	72	69	0	413
	127	12	810	9	92	8	15	15	16	9	10	4	13	15	11	13	18	11	21	14	10	15	12	4	34	24	24	25	39	17	136
	127	13	860	10	179	7	22	13	20	14	10	7	33	23	23	27	11	10	60	41	49	44	42	10	65	60	50	54	55	17	232
	128	1	440	2	134	3	17	21	12	27	18	2	28	31	29	20	37	2	31	39	47	29	41	1	35	46	45	39	30	0	203
	128	2	570	0	220	3	19	16	14	12	9	3	24	29	27	27	30	1	47	45	37	43	51	18	78	86	70	65	57	6	340
	128	4	700	1	137	0	5	7	9	9	11	0	13	14	10	6	11	0	7	6	3	5	7	0	13	3	11	7	10	0	14
	128	5	800	0	97	0	4	0	2	1	0	0	11	8	6	6	6	0	50	48	48	48	40	1	35	40	41	44	24	0	106
	128	6	360	0	203	0	10	19	13	13	12	0	66	12	63	51	63	0	68	63	42	44	35	0	69	92	102	104	102	0	169
	128	7	775	6	225	6	18	23	24	11	18	6	34	26	35	28	31	6	18	12	17	25	16	7	15	23	36	27	44	8	274
	128	8	925	2	75	4	23	22	23	34	27	2	33	22	27	42	36	1	61	43	42	32	48	4	59	63	52	45	53	1	199
	128	9	1010	0	110	1	5	10	11	5	8	0	6	6	7	10	12	1	24	14	19	29	26	1	63	68	62	49	48	0	368
	128	10	450	0	27	0	8	10	9	7	8	0	11	23	16	16	20	1	26	21	29	19	24	0	16	36	33	31	20	0	230
	128	11	550	2	181	0	7	14	6	7	14	1	20	18	24	17	8	0	32	33	30	34	23	7	32	28	42	36	24	3	139
	128	13	780	12	270	9	16	23	30	28	22	16	35	25	28	28	34	8	97	60	65	86	80	24	87	115	84	104	107	5	440
inj-BPd1	83	1	670	0	129	3	6	11	11	12	9	7	16	12	23	19	16	4	20	18	22	30	28	8	43	27	44	32	42	5	329
	83	2	620	8	362	1	7	21	19	12	21	6	16	36	50	21	21	3	28	35	36	41	51	1	51	66	68	73	53	4	245
	83	3	620	0	139	4	10	10	10	10	9	3	27	16	20	20	18	3	20	24	17	11	16	5	21	16	14	19	19	0	34
	83	4	470	1	81	0	2	2	1	5	1	3	18	5	7	10	10	2	27	36	19	35	23	11	74	62	84	74	69	7	355
	83	5	830	0	42	0	0	0	0	0	0	0	2	1	3	0	1	0	23	27	23	33	22	0	53	55	57	56	51	0	308
	83	6	620	0	100	0	10	6	5	9	6	0	19	9	17	11	11	0	31	16	22	32	14	0	80	46	34	54	44	0	75
	83	8	420	2	15	2	10	5	2	5	4	0	3	5	3	6	5	2	6	6	7	5	6	1	16	13	21	19	16	2	41
	83	9	480	10	129	12	27	19	13	41	25	7	49	38	40	35	54	13	39	75	75	77	67	13	64	83	78	69	90	5	640
	83	10	670	4	276	0	20	29	15	18	18	2	32	30	29	31	37	1	46	55	48	39	39	1	54	54	47	50	62	0	238
	83	11	780	0	193	0	22	16	13	25	15	0	19	12	16	12	11	0	74	58	58	40	63	0	45	83	97	44	105	0	340
	86	4	500	1	163	0	20	23	19	17	13	0	30	29	20	19	20	4	33	30	25	17	23	0	51	29	29	21	23	0	185
	86	5	760	5	178	10	12	18	29	19	34	8	39	46	40	39	32	9	35	46	35	33	38	6	34	57	44	63	56	21	432
	86	6	800	1	134	0	2	1	2	1	1	0	3	5	2	9	3	0	10	15	5	16	9	3	51	42	51	41	42	2	161
	86	7	520	2	216	1	13	11	7	7	6	1	37	14	6	12	24	3	39	22	26	29	27	1	51	58	48	53	59	2	157
	86	8	720	0	204	0	19	6	21	26	18	1	36	48	44	19	55	0	75	48	48	59	33	0	38	50	39	38	47	0	257
	86	9	830	4	213	3	2	15	2	2	2	0	9	6	15	8	4	2	4	11	5	13	11	1	15	18	11	9	18	0	65

Note – Table is continued on the next page.

	Rat #	Neuron	Depth	Brush		1.4g vF						4g vF						10g vF						26g vF						Pinch	
				BL		BL	1	2	3	4	5	BL	1	2	3	4	5	BL	1	2	3	4	5	BL	1	2	3	4	5	BL	
inj-BPd1	86	10	700	1	298	1	27	12	30	7	8	8	68	61	36	25	42	3	43	60	50	43	70	0	68	78	28	64	63	7	354
	86	11	820	0	60	0	3	4	7	7	4	0	10	10	12	9	4	0	19	18	21	18	14	0	27	25	21	17	15	0	58
	87	1	710	0	48	0	1	3	2	2	1	0	2	2	4	1	1	0	4	12	3	5	8	0	5	4	6	8	5	0	9
	87	2	350	0	131	0	0	0	0	0	0	0	14	17	17	6	18	0	29	36	42	35	40	0	41	33	28	31	33	0	59
	87	3	560	0	193	0	5	3	2	2	5	0	4	8	3	6	4	0	28	20	13	20	21	0	28	17	15	23	27	0	14
	87	4	820	0	251	0	0	2	8	5	3	0	9	14	12	7	10	0	13	22	55	21	34	0	24	30	39	34	19	0	257
	87	5	410	0	195	0	4	3	6	3	3	0	12	13	17	4	15	0	35	10	31	15	7	0	27	29	17	21	16	0	70
	87	6	750	0	236	0	11	10	7	7	3	0	24	19	20	29	11	0	77	38	43	27	48	0	66	59	50	47	56	0	288
	87	7		0	52	0	1	1	1	1	1	0	2	0	2	2	3	0	6	7	4	7	5	0	9	6	4	5	5	0	8
	87	8	700	0	111	0	2	3	1	0	1	0	17	16	12	16	21	0	13	16	40	28	14	0	28	14	29	17	33	0	68
	119	1	370	0	77	0	4	4	1	3	3	0	3	4	1	4	3	0	9	19	15	15	17	0	50	36	17	19	24	1	497
	119	2	790	0	52	0	1	2	0	3	0	0	10	6	3	1	3	0	39	26	20	35	24	0	45	57	45	59	44	1	206
	119	3	720	0	136	0	8	11	3	5	3	0	32	22	16	30	20	0	36	27	31	31	33	0	58	38	61	48	31	0	214
	119	4	660	1	41	3	4	3	5	5	5	1	11	7	11	9	9	0	29	11	17	18	22	0	40	20	57	59	55	0	225
	119	5	830	0	142	0	8	0	3	3	1	0	23	10	5	8	14	0	80	55	30	34	43	0	47	56	55	60	59	0	292
	119	6	300	0	148	0	42	43	34	28	30	0	26	59	48	41	40	0	58	56	37	50	42	0	44	41	24	27	7	0	3
	120	1	520	0	113	0	1	4	2	9	7	0	8	14	7	15	7	0	43	21	68	39	25	0	38	31	58	39	31	2	46
	120	2	680	4	155	4	7	8	7	4	11	1	17	2	3	4	4	5	33	72	65	89	122	3	65	75	79	72	97	1	307
	120	3	800	34	321	21	41	39	48	36	44	15	64	68	62	57	53	11	92	65	63	69	75	14	94	120	127	112	119		
	120	4	740	0	134	0	5	4	3	6	2	0	8	9	5	7	16	0	39	28	10	14	16	0	59	34	19	21	12	0	36
	120	5	740	1	211	0	14	10	6	10	7	0	34	21	39	16	19	1	51	41	29	22	30	2	55	66	61	43	53	5	178
	120	6	520	1	109	1	16	18	15	49	31	1	37	30	30	41	56	5	54	76	42	72	40	0	21	8	26	12	13	0	309
	120	7	740	0	231	0	67	51	15	2	0	0	7	0	0	0	0	0	29	34	23	26	26	0	56	45	49	43	48	0	37
	120	8	570	3	227	1	4	8	9	9	7	0	17	12	16	14	8	0	30	34	29	17	24	1	65	54	48	43	48	0	318
	120	9	590	12	188	7	5	11	12	6	19	7	64	29	18	19	16	5	64	57	48	35	40	11	73	63	64	54	76	3	412
	120	10	750	0	160	0	5	6	5	5	2	1	11	7	10	4	10	1	25	12	14	25	16	0	35	26	34	30	29	0	98
	120	11	500	0	262	0	40	47	40	34	29	0	59	52	34	25	33	0	41	42	46	44	49	0	45	48	36	41	41	2	206
	120	12	730	0	69	0	3	5	1	0	1	0	29	26	23	21	20	0	25	30	35	24	23	0	36	48	28	20	27	0	101
	120	13	710	3	302	0	22	40	43	7	28	3	37	27	19	34	9	2	48	39	41	73	75	0	33	35	39	52	52	0	131
	122	1	440	10	106	9	17	8	18	9	14	5	18	13	11	19	5	6	19	27	23	25	24	4	24	29	23	30	26	2	76
	122	2	520	1	82	0	1	6	2	1	0	1	7	3	6	6	0	1	29	16	12	6	13	0	29	20	23	21	18	3	124
	122	3	560	1	154	0	3	5	5	6	8	8	33	24	17	16	14	3	38	31	20	24	35	3	72	44	55	38	32	3	177
	122	4	640	5	179	6	6	10	7	9	6	8	28	24	40	15	16	4	41	24	24	24	21	4	40	28	27	24	34	4	280
	122	7	625	0	145	0	2	2	6	2	4	0	11	11	8	10	8	0	29	34	39	30	40	0	70	75	77	71	72	0	271
	122	8	720	0	133	0	5	8	5	9	3	2	13	11	2	29	14	0	34	31	15	14	24	1	26	47	42	30	19		
	122	10	520	7	72	12	11	10	18	17	12	8	15	14	18	12	12	9	12	15	14	22	23	3	41	38	39	50	60	3	216
	122	11	570	16	306	13	45	64	63	54	37	16	90	87	61	54	81	28	53	61	69	62	46	53	111	73	65	59	72	13	284
	122	12	500	1	81	3	24	17	23	11	14	9	39	32	22	25	31	6	31	35	34	30	24	2	53	41	53	33	44	11	191
	122	13	750	0	59	0	1	0	0	0	0	0	25	7	16	24	19	0	58	65	52	45	47	0	53	56	49	60	55	0	307

Note – Missing data points are from neurons that were lost during recording before completing the stimulation protocol.

Table D.3. Spike counts on day 7 for TSP4 treatment study (Chapter 4).

	Rat #	Neuron	Depth	Brush		1.4g vF						4g vF						10g vF						26g vF						Pinch	
				BL		BL	1	2	3	4	5	BL	1	2	3	4	5	BL	1	2	3	4	5	BL	1	2	3	4	5	BL	
Strep + Sham	270	1	970	0	32	0	2	0	0	4	2	0	12	7	5	5	3	0	16	23	17	13	15	0	35	37	32	29	29	0	41
	270	2	610	9	58	8	16	9	13	7	7	7	17	11	10	7	14	8	14	11	8	14	20	4	10	6	6	8	13	5	120
	270	3	670	22	124	26	34	32	38	33	42	20	22	68	37	53	32	22	34	34	51	34	47	16	59	55	75	62	62	41	417
	270	4	740	0	22	0	0	0	0	1	1	0	0	0	0	1	3	0	13	8	9	3	8	0	15	22	16	35	35	0	105
	270	5	870	3	30	7	4	6	6	8	6	3	11	11	7	7	9	2	17	10	13	9	16	3	31	17	16	18	18	3	24
	270	6	600	17	173	17	13	19	9	5	10	8	17	25	9	14	12	0	6	8	4	4	8	14	25	42	35	36	35	1	155
	270	7	770	0	44	0	0	1	0	1	0	0	0	0	0	1	0	0	13	4	9	10	10	6	16	18	16	34	20	0	345
	270	8	780	9	140	14	21	25	21	20	18	6	25	23	25	13	26	8	37	30	19	36	26	10	53	38	30	30	20	12	87
	270	9	800	6	60	8	7	9	8	8	10	8	14	21	16	14	14	9	20	16	13	18	19	13	21	18	18	17	17	5	102
	270	10	940	0	158	1	5	1	3	2	1	0	2	8	1	9	8	1	7	8	4	11	20	0	14	14	18	14	16	1	74
	270	11	590	9	52	16	19	24	13	7	16	16	21	24	17	12	11	15	20	17	9	13	13	13	24	34	20	13	26	1	48
	270	12	660	19	189	32	44	18	20	35	19	21	26	21	15	13	29	23	45	29	29	31	27	16	37	42	42	40	39	12	271
	270	13	700	0	98	0	10	7	3	3	1	0	14	22	15	8	6	0	35	43	24	21	13	0	33	36	24	26	20	0	168
	270	14	800	0	300	0	15	10	13	8	7	0	16	14	14	17	9	0	48	40	51	57	27	0	55	34	33	30	23	0	103
20µg TSP4 + Phys	274	1	530	0	90	0	3	2	5	3	2	0	6	1	8	5	3	0	21	11	13	11	10	0	17	9	12	11	8	0	23
	274	2	800	0	110	0	3	0	3	3	1	0	8	14	6	10	18	0	33	27	28	29	34								
	274	4	550	22	349	2	38	25	20	11	38	13	51	39	38	34	41	3	34	31	25	28	26								
	274	5	730	5	286	4	21	15	9	34	13	14	35	31	58	41	37	18	77	52	49	79	60	11	102	63	89	50	60	9	474
	274	6	620	11	131	12	15	24	9	16	12	6	33	19	21	17	16	14	34	24	32	27	29	5	31	46	33	51	45	10	592
	274	7	600	10	177	7	12	11	12	14	9	11	20	34	41	43	33	2	59	57	42	64	50	2	65	64	59	50	67	3	200
	274	8	140	1	94	0	4	0	2	2	1	0	25	13	12	9	19	0	12	9	6	6	8	0	29	58	24	39	27	0	519
	274	9	650	10	295	2	42	22	31	28	26	8	55	38	35	48	48	13	49	47	33	56	54	23	68	76	76	74	84	23	379
	274	10	450	25	322	36	47	52	39	39	60	35	58	76	84	41	52	33	68	76	73	59	68	34	77	86	72	62	67	25	376
	274	11	500	1	332	0	29	7	10	9	6	0	30	22	24	31	27	0	57	67	51	41	85	0	96	68	62	80	54	2	507
	274	12	640	3	431	4	11	20	22	34	11	1	51	46	42	47	65	8	102	86	91	92	86	2	110	108	99	108	114	2	597
	274	13	510	1	170	9	11	13	19	19	22	9	42	32	30	49	27	15	57	55	49	45	52	10	55	70	36	51	47	6	155
	274	14	710	0	620	0	23	84	45	15	40	0	57	107	48	56	58	0	46	93	111	68	72	0	133	108	105	102	100	0	496
	274	15	510	0	319	0	2	2	5	5	4	0	42	36	51	75	78	1	97	93	88	84	78	1	107	144	100	116	124	0	554
60µg TSP4 + Phys	280	1	615	1	186	4	14	12	26	35	6	6	24	17	23	15	20	3	36	38	40	43	31	5	34	32	32	64	24	1	345
	280	2	760	0	98	0	4	9	10	14	10	0	22	13	7	15	11	0	26	16	18	21	16	0	26	23	26	24	18	0	505
	280	3	300	1	74	3	6	7	4	3	3	4	16	25	20	11	22	3	50	34	44	44	21	2	65	75	79	94	96	1	439
	280	4	600	21	402	24	40	26	38	41	37	23	68	64	104	97	76	11	97	167	96	104	57	2	55	58	58	47	59	0	184
	280	5	660	8	157	5	24	4	20	13	28	3	38	23	14	20	25	4	30	25	30	24	43	0	49	52	34	53	40	0	228
	280	6	670	11	224	26	27	29	24	52	27	28	27	32	32	37	38	28	34	41	38	50	31	18	59	64	83	67	81	16	890
	280	7	530	3	147	7	15	15	17	19	9	5	28	33	30	28	41	5	54	54	44	34	45	7	65	67	59	55	57	7	393
	280	8	600	5	235	4	59	59	44	53	58	1	69	56	55	34	55	1	51	36	39	43	43	0	51	43	20	32	33	1	137
	280	9	750	5	257	20	52	48	46	45	33	15	58	48	50	50	45	13	59	51	43	51	54	2	70	47	50	32	50	14	172
	280	10	970	0	118	0	0	1	15	0	1	0	26	1	23	15	25	0	36	24	24	30	25	0	30	31	28	24	32	0	137
	280	11	1000	1	116	0	0	4	1	3	1	0	30	26	13	22	29	0	35	46	42	39	25	0	60	40	50	55	57	0	149
	280	12	470	2	399	2	28	18	41	26	24	1	78	43	69	56	43	0	108	104	83	87	107	3	140	116	118	124	92	0	305
	280	13	820	1	47	0	1	2	0	1	0	0	11	8	6	13	15	1	19	18	15	13	13	0	23	23	20	20	22	0	142
60µg TSP4 + Inj	281	1	860	0	19	0	0	3	1	0	1	0	17	13	13	7	12	0	32	17	28	19	13	0	35	32	16	24	25	0	234
	281	2	860	2	201	0	14	35	49	35	39	3	35	68	45	49	58	4	61	47	62	33	70	6	48	65	78	51	82	0	177
	281	3	970	1	81	1	2	2	0	1	0	2	6	15	6	12	5	1	35	41	47	28	30	1	61	32	40	43	51	2	183
	281	4	610	0	441	1	36	18	21	6	31	0	55	45	43	45	48	1	64	70	62	37	56	2	65	80	84	75	71	0	351
	281	5	780	1	292	4	46	36	37	32	33	0	56	65	45	56	52	7	52	47	62	39	35	2	78	63	63	48	39	1	261
	281	6	700	10	353	29	45	40	37	30	39	15	64	74	74	86	56	25	84	51	51	69	58	15	70	53	78	74	59	7	451
	281	7	550	0	188	1	3	9	4	9	5	1	24	25	35	23	18	2	62	45	51	49	46	4	78	75	70	74	76	4	410
	281	8	830	3	91	4	12	12	10	12	10	4	13	15	11	20	19	9	33	33	22	24	24	2	30	20	20	22	20	12	240
	281	9	800	0	229	0	6	9	19	26	20	0	72	56	49	42	37	0	54	69	58	66	60	0	89	53	52	55	41	0	88
	281	10	560	3	208	0	10	6	2	3	7	0	34	27	16	34	38	0	76	65	63	45	48	0	73	64	76	39	54	0	279
	281	11	650	11	154	8	8	10	12	13	12	9	67	62	94	49	46	7	84	76	113	67	124	7	180	172	138	178	175	4	671
	281	12	700	17	284	9	34	12	28	25	22	7	60	58	43	41	29	7	82	68	68	74	69	8	110	108	91	85	101	15	484

Note – Missing data points are from neurons that were lost during recording before completing the stimulation protocol.

Table D.4. Spike counts for optimization of burst SCS parameters on day 7 after painful nerve root compression (Chapter 6).

			SCS Parameters								Spikes/10sec		
Rat #	Neuron	Stim #	Pulse #	Pulse Hz	Pulse Width	Burst Hz	Amplitude	Charge per Burst	Spike2 Waveform ID	Neuron Type	BL	Pre-SCS	Post-SCS
69	2	1	7	500	1000	40	90%	8.82	01	WDR	14	190	94
69	2	1	7	500	1000	40	90%	8.82	02	WDR	7	98	78
69	2	1	7	500	1000	40	90%	8.82	04	WDR	66	466	234
69	2	1	7	500	1000	40	90%	8.82	05	WDR	4	82	76
69	2	1	7	500	1000	40	90%	8.82	06	WDR	6	99	100
69	2	2	5	500	1000	40	90%	6.30	01	WDR	11	156	137
69	2	2	5	500	1000	40	90%	6.30	02	WDR	6	175	126
69	2	2	5	500	1000	40	90%	6.30	04	WDR	24	142	122
69	2	2	5	500	1000	40	90%	6.30	05+07	WDR	22	98	105
69	2	2	5	500	1000	40	90%	6.30	06	WDR	1	56	30
69	2	2	5	500	1000	40	90%	6.30	08	WDR	5	64	56
69	3	1	5	500	1000	40	90%	6.30	01	WDR	9	200	178
69	3	1	5	500	1000	40	90%	6.30	02	WDR	5	75	51
69	3	1	5	500	1000	40	90%	6.30	03	HT	0	30	19
69	3	1	5	500	1000	40	90%	6.30	05	WDR	8	77	63
69	3	2	7	500	1000	40	90%	8.82	01	NC	0	94	29
69	3	2	7	500	1000	40	90%	8.82	02	NC	6	158	104
69	3	2	7	500	1000	40	90%	8.82	03	NC	8	105	128
69	3	2	7	500	1000	40	90%	8.82	05	NC	0	13	43
69	3	2	7	500	1000	40	90%	8.82	06	NC	0	30	8
69	3	2	7	500	1000	40	90%	8.82	07	NC	2	43	4
69	3	2	7	500	1000	40	90%	8.82	09	NC	3	78	46
69	3	3	3	500	1000	40	90%	3.78	02	NC	0	82	84
69	3	3	3	500	1000	40	90%	3.78	03	NC	7	271	461
69	3	3	3	500	1000	40	90%	3.78	05	NC	4	41	24
69	3	5	7	500	500	40	90%	8.82	02	NC	16	143	67
69	3	5	7	500	500	40	90%	8.82	03	NC	3	613	477
69	3	5	7	500	500	40	90%	8.82	04	NC	3	121	60
69	3	5	7	500	500	40	90%	8.82	06	NC	10	113	65
71	4	1	5	500	1000	40	90%	6.30	02	WDR	1	56	50
71	4	1	5	500	1000	40	90%	6.30	0F	HT	35	68	75
71	4	2	7	500	1000	40	90%	8.82	01	WDR	0	58	19
71	4	2	7	500	1000	40	90%	8.82	02	HT	61	152	116
71	4	3	3	500	1000	40	90%	3.78	02	WDR	2	42	33
71	4	4	7	500	500	40	90%	4.41	01	NC	11	142	79
71	4	4	7	500	500	40	90%	4.41	02+03	NC	32	144	118
71	5	1	7	500	1000	40	90%	8.82	01	HT	0	73	34
71	5	1	7	500	1000	40	90%	8.82	02	HT	2	22	16
71	5	2	5	500	1000	40	90%	6.30	01	HT	1	239	107
71	5	2	5	500	1000	40	90%	6.30	02	HT	10	64	72
71	5	3	3	500	1000	40	90%	3.78	01	HT	0	192	230
71	6	1	7	500	500	40	90%	4.41	01	WDR	22	300	238
71	6	1	7	500	500	40	90%	4.41	02	WDR	47	521	277
71	6	1	7	500	500	40	90%	4.41	03	WDR	37	292	208
71	6	1	7	500	500	40	90%	4.41	07	HT	5	56	20
71	6	1	7	500	500	40	90%	4.41	09	WDR	34	355	307
71	6	1	7	500	500	40	90%	4.41	0A	WDR	14	222	125
71	6	1	7	500	500	40	90%	4.41	0B	HT	3	151	176
71	6	2	7	500	1000	40	90%	8.82	0E	WDR	34	155	61
71	6	2	7	500	1000	40	90%	8.82	0F	WDR	26	177	110

Note – Table is continued on the next page.

			SCS Parameters								Spikes/10sec		
Rat #	Neuron	Stim #	Pulse #	Pulse Hz	Pulse Width	Burst Hz	Amplitude	Charge per Burst	Spike2 Waveform ID	Neuron Type	BL	Pre-SCS	Post-SCS
71	6	2	7	500	1000	40	90%	8.82	10	WDR	13	137	60
71	6	2	7	500	1000	40	90%	8.82	16	HT	5	50	10
71	6	2	7	500	1000	40	90%	8.82	17	WDR	5	28	17
71	6	3	7	500	750	40	90%	6.62	01+07	NC	43	129	121
71	6	3	7	500	750	40	90%	6.62	02+04	NC	38	134	79
71	6	3	7	500	750	40	90%	6.62	06	NC	37	128	99
71	6	5	7	500	250	40	90%	2.21	01+06	NC	74	177	140
71	6	5	7	500	250	40	90%	2.21	02	NC	12	77	67
71	6	5	7	500	250	40	90%	2.21	03	NC	6	40	27
71	6	5	7	500	250	40	90%	2.21	04	NC	27	105	91
71	6	5	7	500	250	40	90%	2.21	05	NC	0	25	31
71	6	5	7	500	250	40	90%	2.21	07	NC	10	22	24
71	7	1	7	500	250	40	90%	2.21	01	WDR	14	625	599
71	7	1	7	500	250	40	90%	2.21	02	WDR	28	308	309
71	7	1	7	500	250	40	90%	2.21	03	WDR	1	46	44
71	7	1	7	500	250	40	90%	2.21	06	WDR	2	62	51
71	7	1	7	500	250	40	90%	2.21	08	NC	0	53	54
71	7	2	7	500	1000	40	90%	8.82	01+03	NC	2	542	322
71	7	2	7	500	1000	40	90%	8.82	02	NC	4	170	200
71	7	2	7	500	1000	40	90%	8.82	05	NC	3	99	65
71	7	2	7	500	1000	40	90%	8.82	06	NC	2	118	51
71	7	2	7	500	1000	40	90%	8.82	07	NC	4	52	39
71	7	3	7	500	500	40	90%	4.41	01	NC	4	371	296
71	7	3	7	500	500	40	90%	4.41	02	NC	2	197	116
71	7	3	7	500	500	40	90%	4.41	03+06	NC	4	132	69
71	7	3	7	500	500	40	90%	4.41	04	NC	5	55	38
71	7	3	7	500	500	40	90%	4.41	07	NC	2	218	174
71	7	4	7	500	750	40	90%	6.62	01+03	NC	12	814	609
71	7	4	7	500	750	40	90%	6.62	05	NC	7	101	86
71	7	4	7	500	750	40	90%	6.62	06	NC	5	42	23
71	7	4	7	500	750	40	90%	6.62	08	NC	2	61	36
73	8	1	7	500	750	40	90%	6.14	01	HT	3	667	548
73	8	1	7	500	500	40	90%	4.10	01	HT	7	681	610
73	8	1	7	500	250	40	90%	2.05	01	HT	10	525	470
73	8	1	7	500	1000	40	90%	8.19	01	HT	7	246	287
73	9	1	7	500	250	40	90%	2.05	02	NC	9	99	136
73	9	1	7	500	250	40	90%	2.05	03	NC	2	17	16
73	9	1	7	500	250	40	90%	2.05	05	NC	3	79	146
73	9	1	7	500	250	40	90%	2.05	06	NC	1	39	24
73	9	2	7	500	1000	40	90%	8.19	01	NC	1	151	77
73	9	2	7	500	1000	40	90%	8.19	03	NC	0	52	17
73	9	2	7	500	1000	40	90%	8.19	06	NC	0	48	30
73	9	2	7	500	1000	40	90%	8.19	07	NC	1	45	35
73	9	2	7	500	1000	40	90%	8.19	08	NC	0	104	60
73	9	4	7	500	500	40	90%	4.10	01	NC	1	82	55
73	9	4	7	500	500	40	90%	4.10	02	NC	7	98	83
73	9	4	7	500	500	40	90%	4.10	03	NC	6	114	43
73	9	4	7	500	500	40	90%	4.10	0E	NC	6	60	65
73	9	5	7	500	750	40	90%	6.14	01	NC	11	71	46
73	9	5	7	500	750	40	90%	6.14	04	NC	5	176	134

Note – Table is continued on the next page.

			SCS Parameters								Spikes/10sec		
Rat #	Neuron	Stim #	Pulse #	Pulse Hz	Pulse Width	Burst Hz	Amplitude	Charge per Burst	Spike2 Waveform ID	Neuron Type	BL	Pre-SCS	Post-SCS
73	9	5	7	500	750	40	90%	6.14	07	NC	0	32	22
73	9	5	7	500	750	40	90%	6.14	0C	NC	5	150	134
73	9	6	7	500	1000	60	90%	8.19	02	NC	2	84	106
73	9	6	7	500	1000	60	90%	8.19	03	NC	13	502	376
73	9	6	7	500	1000	60	90%	8.19	04	NC	0	19	28
73	9	6	7	500	1000	60	90%	8.19	0D	NC	1	25	35
88	1	1	7	500	1000	40	90%	7.70	01	WDR	8	252	215
88	1	1	7	500	1000	40	90%	7.70	02	WDR	40	477	422
88	1	1	7	500	1000	40	90%	7.70	03	WDR	10	233	222
88	1	1	7	500	1000	40	90%	7.70	04	WDR	18	251	226
88	1	1	7	500	1000	40	90%	7.70	05	WDR	25	285	246
88	1	2	5	500	1000	40	90%	5.50	01+05	WDR	72	451	349
88	1	2	5	500	1000	40	90%	5.50	02	WDR	35	137	147
88	1	2	5	500	1000	40	90%	5.50	03+04	WDR	67	259	238
88	1	2	5	500	1000	40	90%	5.50	06	WDR	8	43	40
88	1	2	5	500	1000	40	90%	5.50	07	WDR	47	326	257
88	1	3	3	500	1000	40	90%	3.30	01	WDR	48	254	192
88	1	3	3	500	1000	40	90%	3.30	02	WDR	80	530	367
88	1	3	3	500	1000	40	90%	3.30	03	HT	12	102	66
88	1	3	3	500	1000	40	90%	3.30	04	WDR	26	235	151
88	2	1	7	500	500	40	90%	3.85	01	WDR	47	322	228
88	2	1	7	500	500	40	90%	3.85	03+07	WDR	58	321	157
88	2	1	7	500	500	40	90%	3.85	06	WDR	14	251	189
88	2	1	7	500	500	40	90%	3.85	0A	WDR	3	67	31
88	2	2	7	500	1000	40	90%	7.70	01+03	WDR	92	659	506
88	2	2	7	500	1000	40	90%	7.70	02	WDR	10	56	47
88	2	2	7	500	1000	40	90%	7.70	06	WDR	18	174	129
88	2	3	7	500	250	40	90%	1.93	01	WDR	4	145	124
88	2	3	7	500	250	40	90%	1.93	02	WDR	26	298	272
88	2	3	7	500	250	40	90%	1.93	03	WDR	10	118	94
88	2	3	7	500	250	40	90%	1.93	06	WDR	2	107	95
88	2	4	7	500	750	40	90%	5.77	01	WDR	7	171	121
88	2	4	7	500	750	40	90%	5.77	02	WDR	28	209	131
89	1	1	7	500	1000	40	90%	9.45	01+06	WDR	16	630	291
89	1	1	7	500	1000	40	90%	9.45	03	WDR	11	824	108
89	1	1	7	500	1000	40	90%	9.45	08	HT	0	48	12
89	1	1	7	500	1000	40	90%	9.45	09	WDR	17	59	172
89	1	2	3	500	1000	40	90%	4.05	01+05	WDR	10	640	609
89	1	2	3	500	1000	40	90%	4.05	02	WDR	6	255	286
89	1	2	3	500	1000	40	90%	4.05	03	WDR	10	320	362
89	1	3	5	500	1000	40	90%	6.75	01+02	WDR	20	539	353
89	1	3	5	500	1000	40	90%	6.75	03	WDR	15	296	219
89	1	3	5	500	1000	40	90%	6.75	04	HT	5	75	48
89	1	4	7	500	1000	60	90%	9.45	01+06	WDR	47	689	195
89	1	4	7	500	1000	60	90%	9.45	03+05	WDR	13	821	870
89	1	5	7	500	1000	40	90%	9.45	01+06	WDR	33	597	448
89	1	5	7	500	1000	40	90%	9.45	02	WDR	4	168	130
89	1	5	7	500	1000	40	90%	9.45	04	HT	5	101	118
89	1	5	7	500	1000	40	90%	9.45	05	HT	0	36	25
89	2	1	7	500	1000	20	90%	9.45	01	HT	118	250	139

Note – Table is continued on the next page.

			SCS Parameters								Spikes/10sec		
Rat #	Neuron	Stim #	Pulse #	Pulse Hz	Pulse Width	Burst Hz	Amplitude	Charge per Burst	Spike2 Waveform ID	Neuron Type	BL	Pre-SCS	Post-SCS
89	2	2	7	500	1000	40	90%	9.45	01	HT	44	145	102
89	2	3	7	500	1000	60	90%	9.45	01	HT	77	277	183
89	3	1	5	333	1000	40	90%	6.75	01	WDR	31	360	337
89	3	1	5	333	1000	40	90%	6.75	02	WDR	38	121	119
89	3	1	5	333	1000	40	90%	6.75	03	WDR	9	181	162
89	3	1	5	333	1000	40	90%	6.75	04	HT	7	30	22
89	3	1	5	333	1000	40	90%	6.75	05	WDR	7	108	65
89	3	2	5	250	1000	40	90%	6.75	01	WDR	12	200	140
89	3	2	5	250	1000	40	90%	6.75	02	WDR	27	154	138
89	3	2	5	250	1000	40	90%	6.75	04	WDR	14	173	190
89	3	2	5	250	1000	40	90%	6.75	05	WDR	2	31	99
89	3	2	5	250	1000	40	90%	6.75	06	WDR	11	92	98
89	3	3	5	500	1000	40	90%	6.75	01	WDR	38	316	195
89	3	3	5	500	1000	40	90%	6.75	02	WDR	15	460	274
89	3	3	5	500	1000	40	90%	6.75	03	WDR	14	302	195
89	3	3	5	500	1000	40	90%	6.75	07	WDR	6	139	101
89	3	4	7	500	1000	60	90%	9.45	01	WDR	102	371	300
89	3	4	7	500	1000	60	90%	9.45	02+03	WDR	16	316	303
89	3	4	7	500	1000	60	90%	9.45	04	WDR	24	727	375
89	3	5	7	500	1000	20	90%	9.45	01+06	WDR	23	433	374
89	3	5	7	500	1000	20	90%	9.45	03	WDR	4	139	83
89	3	5	7	500	1000	20	90%	9.45	04+07	WDR	62	596	592
89	3	5	7	500	1000	20	90%	9.45	05	WDR	5	126	74
89	3	6	7	500	1000	40	90%	9.45	02	WDR	238	861	716
89	3	6	7	500	1000	40	90%	9.45	04	WDR	17	207	154
89	3	6	7	500	1000	40	90%	9.45	07	HT	31	165	96
89	4	1	7	500	1000	40	90%	9.45	01	HT	0	404	373
89	4	1	7	500	1000	40	90%	9.45	02	HT	0	95	77
89	4	1	7	500	1000	40	90%	9.45	03	HT	0	337	387
89	4	1	7	500	1000	40	90%	9.45	04	HT	0	140	85
89	4	1	7	500	1000	40	90%	9.45	05	HT	0	110	88
89	4	2	7	500	500	40	90%	4.73	01+05	HT	0	210	137
89	4	2	7	500	500	40	90%	4.73	03	HT	0	124	162
89	4	2	7	500	500	40	90%	4.73	04	HT	0	243	297
89	4	2	7	500	500	40	90%	4.73	07	HT	0	185	304
89	4	3	7	500	750	40	90%	7.09	01	HT	0	322	196
89	4	3	7	500	750	40	90%	7.09	02	HT	0	177	146
89	4	3	7	500	750	40	90%	7.09	03	HT	0	109	119
89	4	3	7	500	750	40	90%	7.09	05	HT	0	96	34
89	4	3	7	500	750	40	90%	7.09	06	HT	0	182	120
89	4	3	7	500	750	40	90%	7.09	08	HT	0	97	40
89	4	4	7	500	250	40	90%	2.36	01+05	HT	0	266	215
89	4	4	7	500	250	40	90%	2.36	02	HT	0	56	66
89	4	4	7	500	250	40	90%	2.36	03	HT	0	121	146
89	4	4	7	500	250	40	90%	2.36	04	HT	0	219	253
89	4	4	7	500	250	40	90%	2.36	08	HT	0	115	108
89	4	5	5	500	1000	40	90%	6.75	01	HT	0	224	181
89	4	5	5	500	1000	40	90%	6.75	02	HT	0	184	80
89	4	5	5	500	1000	40	90%	6.75	03	HT	0	116	54
89	4	5	5	500	1000	40	90%	6.75	05	HT	0	226	170

Note – Table is continued on the next page.

			SCS Parameters								Spikes/10sec		
Rat #	Neuron	Stim #	Pulse #	Pulse Hz	Pulse Width	Burst Hz	Amplitude	Charge per Burst	Spike2 Waveform ID	Neuron Type	BL	Pre-SCS	Post-SCS
89	4	5	5	500	1000	40	90%	6.75	08	HT	0	265	177
89	4	6	5	250	1000	40	90%	6.75	01	HT	0	318	255
89	4	6	5	250	1000	40	90%	6.75	02	HT	0	147	139
89	4	6	5	250	1000	40	90%	6.75	03	HT	0	200	276
89	4	6	5	250	1000	40	90%	6.75	04	HT	0	100	107
89	4	6	5	250	1000	40	90%	6.75	05	HT	0	243	219
89	4	7	5	333	1000	40	90%	6.75	01	HT	0	399	393
89	4	7	5	333	1000	40	90%	6.75	02	HT	0	139	158
89	4	7	5	333	1000	40	90%	6.75	04	HT	0	73	55
89	4	7	5	333	1000	40	90%	6.75	05	HT	0	343	400
89	4	7	5	333	1000	40	90%	6.75	06	HT	0	164	186
90	1	1	7	500	1000	20	90%	10.70	01	WDR	0	417	167
90	1	2	7	500	1000	40	90%	10.70	01	WDR	0	644	170
90	2	1	7	500	1000	40	90%	10.70	01	WDR	23	438	115
90	2	1	7	500	1000	40	90%	10.70	02+04	WDR	8	487	151
90	2	1	7	500	1000	40	90%	10.70	03	HT	14	75	135
90	2	1	7	500	1000	40	90%	10.70	05	WDR	54	283	217
90	2	2	7	500	1000	40	60%	7.14	01+03	WDR	54	597	595
90	2	2	7	500	1000	40	60%	7.14	02	WDR	38	505	549
90	2	2	7	500	1000	40	60%	7.14	04	WDR	2	94	63
90	2	3	7	500	1000	40	30%	3.57	01	WDR	47	272	348
90	2	3	7	500	1000	40	30%	3.57	02	WDR	89	558	394
90	2	3	7	500	1000	40	30%	3.57	03	WDR	26	324	287
90	2	3	7	500	1000	40	30%	3.57	05	WDR	28	243	221
90	3	1	5	333	1000	40	90%	7.65	01+04+05	WDR	13	477	543
90	3	1	5	333	1000	40	90%	7.65	02	WDR	0	33	21
90	3	1	5	333	1000	40	90%	7.65	03	HT	1	19	31
90	3	2	5	500	1000	40	90%	7.65	01+03+06	WDR	18	367	343
90	3	2	5	500	1000	40	90%	7.65	02	WDR	10	379	270
90	3	2	5	500	1000	40	90%	7.65	04	WDR	11	156	81
90	3	3	5	250	1000	40	90%	7.65	01+03+06	WDR	6	315	218
90	3	3	5	250	1000	40	90%	7.65	02	WDR	4	79	61
90	3	3	5	250	1000	40	90%	7.65	04	HT	0	61	53
90	3	4	7	500	1000	40	60%	7.14	01+03	WDR	6	415	208
90	3	4	7	500	1000	40	60%	7.14	02	WDR	2	91	51
90	3	4	7	500	1000	40	60%	7.14	06	HT	0	63	27
90	3	4	7	500	1000	40	60%	7.14	05	WDR	0	89	97
90	3	5	7	500	1000	40	30%	3.57	01	WDR	10	526	446
90	3	5	7	500	1000	40	30%	3.57	02	WDR	0	45	26
90	3	5	7	500	1000	40	30%	3.57	06	WDR	0	93	53
90	4	1	7	500	1000	40	90%	10.70	01	WDR	13	132	111
90	4	1	7	500	1000	40	90%	10.70	02	WDR	1	35	22
90	4	2	7	500	1000	60	90%	10.70	01	WDR	24	100	104
90	4	2	7	500	1000	60	90%	10.70	04	WDR	3	88	80
90	4	3	7	500	1000	20	90%	10.70	01	WDR	8	119	35
90	4	3	7	500	1000	20	90%	10.70	02	WDR	31	104	81
90	4	3	7	500	1000	20	90%	10.70	04	WDR	5	77	72
91	1	1	7	500	1000	40	60%	6.72	01+03	WDR	0	307	232
91	1	1	7	500	1000	40	60%	6.72	02	HT	0	217	231
91	1	3	7	500	1000	40	30%	3.36	01	HT	0	65	34

Note – Table is continued on the next page.

			SCS Parameters								Spikes/10sec		
Rat #	Neuron	Stim #	Pulse #	Pulse Hz	Pulse Width	Burst Hz	Amplitude	Charge per Burst	Spike2 Waveform ID	Neuron Type	BL	Pre-SCS	Post-SCS
91	1	3	7	500	1000	40	30%	3.36	02	WDR	26	84	63
91	1	3	7	500	1000	40	30%	3.36	03	WDR	1	46	51
91	1	3	7	500	1000	40	30%	3.36	04	WDR	13	55	46
91	1	4	7	500	1000	40	90%	10.10	01	WDR	48	237	149
91	1	4	7	500	1000	40	90%	10.10	02	WDR	4	240	186
91	1	4	7	500	1000	40	90%	10.10	05	WDR	30	69	33
91	1	4	7	500	1000	40	90%	10.10	06+07	HT	24	257	159
91	2	1	7	500	1000	20	90%	10.10	01+02	HT	0	117	24
91	2	1	7	500	1000	20	90%	10.10	03+05	WDR	2	200	180
91	2	1	7	500	1000	20	90%	10.10	04	WDR	20	109	51
91	2	2	7	500	1000	40	90%	10.10	01	WDR	1	229	237
91	2	2	7	500	1000	40	90%	10.10	02	HT	10	37	18
91	2	2	7	500	1000	40	90%	10.10	03	HT	3	113	59
91	2	2	7	500	1000	40	90%	10.10	05	WDR	13	103	70
91	3	1	5	500	1000	40	90%	7.20	01+02	WDR	11	575	428
91	3	2	5	333	1000	40	90%	7.20	01	WDR	19	331	264
91	3	3	5	250	1000	40	90%	7.20	01	WDR	22	725	444
91	3	4	7	500	1000	40	90%	10.10	01	WDR	35	470	371
91	3	5	3	500	1000	40	90%	4.32	01+03	WDR	20	423	228
91	3	5	3	500	1000	40	90%	4.32	02	WDR	16	193	177
91	4	1	7	500	1000	40	60%	6.72	01	HT	28	119	84
91	4	1	7	500	1000	40	60%	6.72	02	WDR	8	22	19
91	4	2	7	500	1000	40	90%	10.10	01	WDR	20	268	234
91	4	2	7	500	1000	40	90%	10.10	02+03	HT	12	252	166
91	4	2	7	500	1000	40	90%	10.10	05	WDR	0	105	53
91	4	3	7	500	1000	40	30%	3.36	01+07	WDR	10	93	208
91	4	3	7	500	1000	40	30%	3.36	02	WDR	36	103	139
91	4	3	7	500	1000	40	30%	3.36	03	WDR	6	26	43
91	4	4	7	500	1000	60	90%	10.10	01+03	HT	49	129	94
91	4	4	7	500	1000	60	90%	10.10	06+07	WDR	12	73	123
91	4	4	7	500	1000	60	90%	10.10	08	WDR	6	122	73
91	4	5	7	500	1000	20	90%	10.10	01	WDR	80	354	468
91	4	5	7	500	1000	20	90%	10.10	02	WDR	48	347	460
91	4	5	7	500	1000	20	90%	10.10	05+07	WDR	20	326	428
92	1	1	7	500	1000	40	90%	9.10	01	WDR	0	74	28
92	1	2	7	500	750	40	90%	6.83	01	WDR	0	69	57
92	1	3	7	500	500	40	90%	4.55	01	WDR	0	154	133
92	1	4	7	500	250	40	90%	2.28	01+02+04	WDR	0	211	178
92	1	5	7	500	1000	60	90%	9.10	01	WDR	0	118	77
92	1	6	7	500	1000	20	90%	9.10	01+02	WDR	0	82	88
92	2	1	7	500	1000	40	90%	9.10	01	WDR	15	134	65
92	2	1	7	500	1000	40	90%	9.10	02+03+04	WDR	48	318	269
92	2	2	7	500	1000	40	60%	6.02	01	WDR	12	59	58
92	2	2	7	500	1000	40	60%	6.02	02	WDR	64	554	491
92	2	3	7	500	1000	40	30%	3.01	01	WDR	111	171	194
92	2	3	7	500	1000	40	30%	3.01	02	WDR	89	272	249
92	2	3	7	500	1000	40	30%	3.01	03+06	WDR	96	216	250
92	2	4	5	500	1000	40	90%	6.50	01	WDR	77	257	192
92	2	4	5	500	1000	40	90%	6.50	03+09	WDR	29	205	184

Note – Table is continued on the next page.

			SCS Parameters								Spikes/10sec		
Rat #	Neuron	Stim #	Pulse #	Pulse Hz	Pulse Width	Burst Hz	Amplitude	Charge per Burst	Spike2 Waveform ID	Neuron Type	BL	Pre-SCS	Post-SCS
92	2	4	5	500	1000	40	90%	6.50	04	WDR	27	240	134
92	2	5	5	333	1000	40	90%	6.50	01+04	WDR	31	309	287
92	2	5	5	333	1000	40	90%	6.50	02	WDR	18	200	253
92	2	5	5	333	1000	40	90%	6.50	03	WDR	18	194	123
92	2	6	5	250	1000	40	90%	6.50	01+02	WDR	30	335	181
92	2	6	5	250	1000	40	90%	6.50	04	WDR	22	126	90

Table D.5. Spike counts after burst or tonic SCS on day 7 following painful nerve root compression (Chapter 7).

Mode	Rat #	Neuron	pre-SCS baseline															0min post-SCS												
			Brush		1.4g vF					26g vF					Pinch			1.4g						26g						Pinch	
			BL		1	2	3	4	5	1	2	3	4	5	BL			BL	1	2	3	4	5	BL	1	2	3	4	5	BL	
Burst	207	1	1	582	2	5	9	5	2	54	75	41	67	55	1	694		4	6	10	14	7	8	4	54	41	45	47	46	14	308
		3	0	86	6	6	6	6	3	52	45	33	39	43	0	195		0	6	7	7	5	6	0	35	44	40	20	31	0	185
		4	0	13	0	2	0	0	0	4	2	7	4	4	0	63		0	0	1	2	2	0	1	6	5	4	3	3	0	38
		4	2	224	12	11	12	13	7	64	54	55	62	76	14	481		2	6	9	6	8	8	0	41	35	25	25	16	8	292
		5	2	9	0	0	0	0	1	6	4	1	2	4	0	57		0	2	0	1	0	0	1	0	5	0	4	3	2	58
		5	6	86	7	6	14	13	15	22	37	39	17	49	2	255		0	5	6	2	6	2	0	13	24	6	27	13	16	217
		6	3	332	4	27	3	4	29	87	77	85	76	82	5	498		3	2	7	3	15	3	0	26	44	26	41	27	3	264
		7	10	165	16	22	17	29	23	37	33	32	49	34	21	357		1	13	15	9	5	7	1	14	27	21	19	15	16	168
	208	9	0	161	9	13	17	13	9	50	45	42	41	33	0	175		1	10	14	13	13	6	2	44	33	37	51	39	4	235
		10	0	147	5	8	4	4	6	29	23	22	27	38	0	165		0	4	2	1	1	3	0	18	4	7	13	6	0	105
		11	10	258	20	27	15	24	20	107	91	83	78	118	8	881		7	7	12	9	15	13	7	60	86	89	94	50	3	690
		12	2	26	6	6	6	2	2	10	19	21	16	16	2	144		2	7	3	4	1	2	4	11	11	13	7	15	2	45
		14	0	140	3	2	4	6	2	50	44	40	48	47	0	243		1	6	4	6	6	4	2	13	14	15	15	12	0	51
		14	3	173	7	4	3	6	6	27	12	21	16	22	2	79		0	4	3	3	2	3	0	4	8	2	6	7	0	29
		15	0	16	4	2	2	2	4	7	6	20	5	8	0	205		0	4	2	2	1	1	1	26	8	21	15	5	0	135
	209	16	6	157	6	9	22	22	5	56	72	61	49	49	7	193		14	16	15	14	7	18	7	45	49	39	67	39	11	167
		17	2	50	2	2	1	5	2	14	6	24	22	16	1	308		15	15	14	10	10	10	7	15	12	10	13	13	15	289
		17	2	123	8	4	3	5	4	27	19	27	28	29	0	183		3	2	8	4	4	9	4	18	16	14	13	17	3	60
		18	14	305	48	36	35	43	43	68	65	83	56	68	20	822		2	4	12	4	9	7	5	25	11	12	33	16	10	285
		19	1	200	33	28	28	23	27	38	65	58	45	82	6	380		3	17	17	9	14	16	0	36	38	29	29	19	2	183
		21	4	341	11	5	7	22	10	100	73	67	73	72	4	673		7	12	17	12	16	4	11	66	67	59	51	58	22	553
		22	7	92	11	9	11	9	9	32	28	20	25	32	3	752		13	22	18	15	16	12	26	45	42	39	37	31	4	262
	210	23	2	260	11	12	12	9	17	67	68	72	68	48	0	212		5	26	30	17	14	21	5	46	62	46	44	37	5	260
		24	2	24	6	5	1	3	3	24	9	11	12	8	2	310		0	2	0	0	1	1	0	15	23	31	26	16	0	163
		24	2	24	5	3	3	1	4	12	12	11	19	17	12	138		0	7	2	5	2	3	3	14	9	13	12	13	11	112
		25	18	289	50	70	48	49	34	114	126	110	95	136	19	872		22	54	29	25	32	31	7	74	91	64	106	77	19	611
		26	0	32	2	4	9	9	3	53	63	50	44	43	0	301		1	2	6	1	3	0	1	40	45	49	45	42	3	250
		27	13	264	83	35	30	90	86	148	148	137	133	103	14	890		1	15	41	12	45	65	5	56	97	80	102	46	8	663
	211	29	5	17	4	3	3	3	8	12	7	14	12	12	3	153		3	1	1	6	4	2	1	19	8	6	6	5	3	101
		29	21	106	41	23	24	24	27	43	42	28	36	35	10	322		2	8	5	10	7	15	6	20	11	14	23	15	13	278
		30	1	53	3	14	8	10	5	26	19	24	16	19	2	247		0	4	5	3	1	2	0	33	17	17	12	22	2	159
		31	8	124	7	25	15	7	13	47	36	31	41	44	9	301		1	8	8	4	0	2	7	21	16	18	14	16	3	156
		33	2	64	5	1	1	8	11	58	48	53	34	35	0	512		14	31	17	22	17	16	36	67	45	39	30	55	5	331
		34	0	95	4	4	4	3	2	14	9	15	13	21	2	221		3	2	1	0	7	2	3	14	17	8	15	11	4	255
		34	4	65	13	8	7	7	8	18	15	13	9	20	1	359		0	7	7	7	7	9	12	26	22	14	18	22	10	275
	212	35	1	105	12	3	3	8	18	111	77	84	61	64	7	676		20	21	18	35	30	34	14	48	37	32	31	34	10	203
		36	5	175	6	10	19	18	12	52	93	54	50	51	7	561		20	34	22	30	27	30	16	67	43	42	37	35	30	534
		37	2	60	5	9	11	11	9	25	33	22	29	24	1	243		6	9	9	6	6	3	1	42	34	33	29	28	15	209
		38	0	3	0	0	0	0	0	0	1	0	0	1	0	240		0	0	0	0	1	0	0	0	2	1	0	0	0	196
		39	0	17	1	1	1	1	2	27	39	39	28	35	0	494		0	1	0	0	2	0	0	11	21	11	5	13	0	38
		41	8	86	9	8	17	21	4	49	34	24	45	41	5	824		7	14	16	13	8	8	6	21	34	33	27	31	6	358
	215	42	4	44	4	8	5	12	20	73	86	77	68	87	8	544		8	1	10	16	8	15	5	30	61	27	51	63	22	349
		43	1	110	0	30	19	9	12	46	42	41	35	36	1	223		0	3	11	7	15	7	0	21	19	44	20	17	9	203
		44	8	30	13	5	9	17	10	83	97	63	64	65	6	615		3	5	1	6	7	7	3	72	71	70	61	33	4	323
		45	0	0	0	0	0	0	0	74	68	64	68	52	0	791		0	0	0	0	0	0	0	48	55	53	68	66	0	452
	216	46	1	84	4	2	1	6	2	39	30	25	24	35	1	509		2	3	2	2	0	4	2	21	20	11	18	10	1	202
		47	0	5	0	0	0	0	0	7	4	4	4	5	0	159		0	0	0	0	0	0	0	1	0	2	1	0	0	110
		48	0	30	4	7	2	3	11	17	17	15	7	24	0	196		1	3	0	3	2	2	0	11	8	10	6	29	0	32
		49	2	99	8	4	1	2	8	27	28	18	18	23	0	431		0	0	10	8	3	12	2	21	13	16	15	28	1	135

Note – Table is continued on the next page.

Mode	Rat #	Neuron	2min post-SCS														5min post-SCS													
			1.4g						26g						Pinch		1.4g						26g						Pinch	
			BL	1	2	3	4	5	BL	1	2	3	4	5	BL		BL	1	2	3	4	5	BL	1	2	3	4	5	BL	
Burst	207	1	9	26	20	18	29	17	9	58	56	41	45	56	3	419	5	67	34	38	38	39	5	71	84	78	58	72	5	281
		3	0	8	6	9	6	7	0	37	22	34	22	27	0	97	0	3	6	11	7	5	0	26	17	26	21	22	0	139
		4	0	2	1	3	0	0	2	6	12	6	8	10	1	49	0	0	1	0	0	1	1	5	5	7	10	10	0	46
		4	3	28	10	11	12	6	8	46	26	35	41	37	0	297	3	18	8	6	6	10	4	34	31	32	38	41	2	361
		5	1	0	0	0	0	0	0	1	11	2	1	6	0	57	1	3	1	0	0	0	0	11	8	3	4	7	2	85
		5	4	8	3	13	10	3	0	41	45	33	21	52	3	139	2	5	7	3	4	8	3	41	31	50	42	50	5	243
		6																												
		7	3	8	7	7	6	5	5	28	25	15	17	18	2	61	2	12	6	10	7	9	5	71	52	31	33	38	3	253
	208	9	1	10	15	7	13	14	1	47	52	53	37	49	7	267	1	26	15	12	17	3	4	41	28	33	39	54	1	184
		10	0	3	1	6	2	4	0	4	6	10	5	6	2	66	0	2	1	2	0	8	0	21	7	4	16	27	0	147
		11	6	21	17	12	19	16	6	73	101	97	80	87	10	541	12	25	24	28	32	24	13	100	87	113	88	78	9	828
		12	1	9	9	6	4	4	6	30	21	19	19	22	2	138	2	8	4	16	9	5	6	29	21	26	21	31	4	178
		14	0	8	6	4	4	2	0	23	18	8	20	14	0	93	0	9	5	2	3	5	0	29	19	24	21	15	0	88
		14	0	5	3	4	1	1	0	6	9	7	10	3	1	33	0	4	2	1	0	4	0	6	9	7	10	7	0	28
		15	0	5	6	3	3	8	1	22	15	18	21	24	0	151	0	5	9	3	3	7	0	33	20	39	20	23	0	162
	209	16	12	2	10	25	9	7	12	51	48	46	41	41	8	185	2	12	12	6	11	9	7	41	38	40	46	37	19	235
		17	5	5	2	6	4	6	3	20	12	8	15	15	0	192	6	10	6	2	3	2	3	23	13	7	3	6	0	210
		17	1	9	7	1	4	4	1	22	21	11	10	16	0	84	0	5	1	4	7	5	3	30	18	14	9	15	1	68
		18	11	20	24	16	13	19	4	59	65	32	44	40	5	417	2	9	7	4	4	11	3	19	23	28	28	16	3	193
		19	0	24	27	17	23	17	1	49	33	65	43	51	6	456	3	21	27	18	9	12	0	44	35	32	23	37	2	467
		21	6	20	13	8	22	8	0	58	58	51	62	49	0	502	6	11	14	3	10	20	14	75	80	72	62	62	20	737
		22	1	14	9	10	9	9	3	37	17	19	21	17	4	298	1	7	7	9	4	7	0	28	26	18	17	18	2	318
	210	23	1	22	13	17	16	17	3	61	38	43	36	38	8	249							3	46	45	33	34	35	5	225
		24	0	1	1	6	2	1	3	18	30	14	9	6	1	205	2	1	6	3	4	2	1	12	5	8	24	18	5	329
		24	4	6	2	7	3	3	2	14	13	10	12	5	6	123	10	2	5	9	2	5	17	28	25	20	28	28	19	152
		25	24	50	49	53	35	61	16	73	77	71	69	91	20	808	16	34	61	50	36	49	13	116	89	108	114	95	23	813
		26	2	3	7	8	5	4	2	47	62	46	56	56	2	296	0	1	0	0	2	0	3	36	60	75	63	53	1	299
		27	1	24	62	40	77	45	4	92	119	95	100	100	2	1035	6	30	52	64	45	58	2	122	137	121	131	116	12	1033
	211	29	5	7	1	5	4	4	2	12	8	7	13	11	8	65	2	13	3	6	7	3	7	23	18	21	19	14	5	197
		29	6	14	3	12	9	12	12	26	16	15	32	18	20	151	6	7	6	9	9	14	4	18	15	23	13	18	11	195
		30	0	6	7	3	4	2	1	22	27	18	18	18	0	128	1	5	8	13	9	17	0	26	32	27	16	26	16	581
		31	2	5	4	6	4	7	4	16	20	12	19	14	4	200														
		33	19	17	18	19	11	14	23	44	46	28	30	45	34	505	12	9	14	17	7	10	3	16	20	26	24	24	8	433
		34							10	21	21	17	13	23	4	185	6	8	19	5	7	4	5	22	20	30	33	31	2	240
		34							4	30	22	20	20	34	0	206	6	10	16	11	13	7	16	27	29	43	36	36	0	263
	212	35	0	7	0	11	4	9	12	111	57	45	45	12	31	598	0	5	5	8	5	13	0	61	71	48	73	54	1	273
		36	28	35	26	26	30	34	21	60	57	48	69	55	30	333	31	39	40	36	42	35	39	98	85	90	80	66	39	595
		37	2	8	10	7	21	10	3	41	36	39	36	29	9	222							2	38	31	38	34	29	1	262
		38	0	0	1	0	0	1	0	1	0	0	1	0	0	233	0	0	0	0	1	0	0	0	0	1	0	0	0	255
		39	0	0	0	2	2	1	0	15	44	8	4	5	0	211	0	3	2	3	2	1	0	83	51	35	38	31	0	235
		41	5	12	13	7	25	9	14	23	22	20	17	22	7	458	4	12	9	27	13	25	5	41	32	42	50	23	15	638
	215	42	5	12	3	8	3	5	6	50	60	49	61	51	5	547	6	37	6	6	12	22	5	119	69	69	81	83	4	644
		43	1	12	8	12	17	11	1	40	26	29	22	18	0	104	0	10	7	20	25	15	1	35	23	25	44	22	1	147
		44	5	3	6	6	4	13	6	64	73	69	74	55	4	414	2	1	4	12	8	12	6	87	68	74	65	66	6	557
		45	0	0	0	0	0	0	7	58	52	56	53	49	92	773	0	0	0	0	0	0	0	65	53	48	50	54	0	564
	216	46	3	7	1	2	3	4	2	30	32	20	25	21	5	411	1	0	3	0	6	3	3	22	28	22	33	20	1	401
		47	0	0	0	0	0	0	0	1	0	1	3	2	0	76	0	0	0	1	0	0	0	8	4	1	3	3	0	164
		48	0	2	5	6	5	4	0	22	13	20	18	26	0	96	2	6	3	5	10	13	3	29	22	23	40	25	1	157
		49	0	10	6	8	3	6	2	36	17	14	22	21	4	308	0	6	9	4	7	6	1	25	21	20	25	28	3	338

Note – Table is continued on the next page.

Mode	Rat #	Neuron	10min post-SCS														15min post-SCS													
			1.4g						26g						Pinch		1.4g						26g						Pinch	
			BL	1	2	3	4	5	BL	1	2	3	4	5	BL		BL	1	2	3	4	5	BL	1	2	3	4	5	BL	
Burst	207	1	11	74	35	72	47	51	11	134	132	150	66	83	15	668	16	59	53	47	45	52	16	114	78	102	81	78	17	450
		3	0	4	7	4	7	5	0	18	22	23	21	17	0	142	1	13	6	7	11	6	0	38	30	28	28	35	4	217
		4	1	1	1	1	2	2	0	8	7	20	8	11	1	81	4	0	0	1	0	1	0	6	5	10	5	8	0	38
		4	6	14	10	11	17	12	4	39	30	51	47	33	3	490	0	6	5	4	7	5	1	42	50	31	43	46	0	330
		5	0	1	0	0	1	1	1	7	4	3	4	5	0	103	0	1	3	5	5	0	0	5	3	2	6	6	0	94
		5	6	9	9	10	8	11	4	31	34	37	24	31	0	321	2	9	8	10	4	6	1	26	22	23	43	24	1	189
		6																												
		7	5	25	15	14	13	17	4	51	59	73	65	42	6	230	1	18	8	12	11	7	3	36	49	54	50	55	1	217
	208	9	3	31	30	22	20	6	4	56	43	43	42	41	9	285	4	11	20	26	16	30	7	51	50	49	28	45	9	322
		10	3	2	2	4	10	1	8	39	32	15	49	10	4	85	0	6	9	5	7	5	6	35	20	22	36	16	5	106
		11	2	25	29	30	25	23	4	104	111	91	108	79	7	506	15	60	55	44	39	72	13	95	115	158	151	78	13	920
		12	6	21	18	8	22	9	6	10	7	2	6	9	10	261	4	5	2	12	6	8	6	16	12	28	11	6	8	187
		14	0	9	9	6	11	3	3	43	46	36	26	43	1	162	3	21	4	12	7	3	1	35	29	42	44	18	1	104
		14	1	13	12	19	12	5	6	24	16	15	16	17	6	174	6	18	9	21	10	8	2	28	13	18	19	14	4	153
		15	0	6	2	7	4	5	2	35	20	31	21	12	0	216	3	12	6	4	2	3	4	48	41	23	27	21	3	324
	209	16	6	13	8	8	10	4	6	46	49	32	42	43	8	300	9	16	10	10	6	12	6	64	48	52	50	47	9	355
		17	4	6	7	2	9	2	0	18	9	15	11	5	5	333	11	11	11	4	7	10	1	23	20	51	33	22	2	410
		17	0	5	4	4	11	0	0	23	19	20	17	13	7	111	2	13	7	3	10	6	0	39	17	28	18	21	1	157
		18	4	11	7	6	7	14	6	48	37	42	51	45	4	408	7	36	27	11	20	17	13	63	38	49	47	53	9	545
		19	5	23	17	18	29	11	0	54	56	64	70	55	4	415	11	28	22	39	30	20	2	49	49	47	46	52	3	390
		21	7	10	8	18	15	13	11	58	78	64	57	45	7	522	10	12	27	7	3	14	5	67	78	47	52	69	3	626
		22	0	8	7	8	3	1	0	21	16	18	12	19	3	386	0	8	4	8	7	5	1	40	27	41	27	29	11	449
	210	23	1	19	20	19	15	11	2	31	54	38	37	34	4	212	2	16	16	15	16	22	5	36	42	40	27	29	6	223
		24	0	4	1	3	1	2	2	29	13	11	11	4	2	342	0	1	4	2	1	0	0	12	32	9	17	25	4	304
		24	4	1	5	2	3	7	7	23	21	14	16	13	4	206	1	6	2	2	3	3	8	26	18	14	17	27	10	199
		25	26	42	36	41	33	44	22	139	130	112	109	104	32	1010	27	43	44	39	29	50	17	175	141	137	96	111	41	1032
		26	1	0	0	0	0	0	0	65	47	55	57	99	0	373	0	1	0	1	0	0	2	68	64	73	67	76	2	254
		27																												
	211	29	2	2	6	5	5	5	2	19	9	10	13	16	8	97	0	6	1	1	5	3	2	16	19	17	6	14	0	128
		29	8	20	21	23	30	26	10	35	42	36	69	82	13	336	16	14	16	16	25	18	25	78	57	48	26	81	18	402
		30	14	19	29	19	16	13	33	59	73	69	63	65	21	523	17	27	22	16	19	19	16	57	53	61	54	54	6	419
		31																												
		33	12	22	14	15	11	9	18	39	40	42	40	36	3	544	12	14	16	14	6	14	12	41	32	33	26	35	3	616
		34	0	6	11	2	1	1	2	20	27	35	18	22	2	162														
		34	11	17	21	15	11	9	13	48	55	38	34	37	1	295														
	212	35	1	3	2	2	4	0	1	32	43	29	30	19	3	290	3	3	13	7	7	8	0	46	31	32	33	35	3	335
		36	33	37	42	53	33	43	51	79	71	63	50	60	51	568	25	24	20	26	32	24	33	46	57	53	49	38	26	404
		37	6	15	15	9	8	10	7	29	35	28	28	24	14	225	5	7	5	7	6	11	7	34	20	28	28	32	18	174
		38	1	0	0	1	0	0	1	1	3	1	4	2	0	224	0	0	1	0	0	2	0	7	2	3	4	1	0	183
		39	0	2	3	1	0	8	0	21	48	35	36	36	0	311	0	2	1	2	5	5	0	64	55	54	45	45	0	288
		41	13	13	14	17	16	18	9	42	46	26	52	37	12	471	10	12	9	14	14	16	18	34	28	47	49	34	12	553
	215	42	6	14	23	11	7	10	16	77	77	64	65	58	13	564	7	25	26	12	19	8	11	70	60	78	63	65	14	571
		43	0	4	17	13	8	18	0	28	33	25	38	11	0	160	6	26	27	14	27	28	5	41	60	46	46	57	3	236
		44	5	10	15	6	16	12	11	86	78	70	60	65	5	448	3	7	8	14	6	9	4	90	64	63	78	60	7	475
		45	0	0	0	0	0	0	0	42	45	49	52	42	0	572	0	0	0	0	0	0	0	44	47	52	50	54	0	650
	216	46	4	1	4	5	2	7	7	39	38	30	32	36	4	367	4	3	4	3	6	1	2	41	41	33	31	25	6	524
		47	0	1	1	0	0	2	0	2	7	5	4	6	0	168	0	0	0	0	0	1	0	6	6	3	5	4	0	128
		48	1	12	11	8	5	8	3	34	30	28	22	24	0	160	1	11	13	7	4	9	2	34	27	41	35	40	2	211
		49	1	7	7	4	2	7	1	43	38	29	29	35	2	368	1	9	8	7	6	5	0	31	19	31	27	25	1	503

Note – Table is continued on the next page.

Mode	Rat #	Neuron	pre-SCS baseline															0min post-SCS												
			Brush		1.4g vF					26g vF					Pinch			1.4g						26g						Pinch	
			BL		1	2	3	4	5	1	2	3	4	5	BL			BL	1	2	3	4	5	BL	1	2	3	4	5	BL	
Tonic	207	1	4	582	7	10	9	5	14	40	29	27	26	27	10	260		14	17	17	16	5	14	14	28	48	33	34	38	10	148
		2	2	92	1	2	6	2	2	39	30	21	42	43	2	398		13	14	8	1	2	4	2	37	13	30	20	20	17	317
		3	1	62	13	6	7	11	6	38	30	28	28	35	4	217		9	27	16	12	16	10	12	27	28	32	49	48	11	299
		4	0	11	0	1	2	0	1	1	3	1	6	10	0	94		1	1	0	0	0	0	0	12	7	12	17	11	2	66
		4	4	189	12	13	8	9	5	35	37	45	87	73	6	443		13	18	15	14	12	4	6	46	48	42	43	44	7	395
		5	0	8	0	1	0	1	1	3	5	0	5	5	0	79		0	0	0	0	0	1	1	2	6	0	1	5	1	65
		5	10	133	5	23	15	13	11	38	33	26	53	72	3	290		12	12	7	15	10	4	10	62	46	34	33	67	9	233
		6	7	284	9	14	12	29	31	105	76	129	97	87	4	729		6	10	7	7	14	32	7	56	47	62	55	67	12	613
		7	4	393	15	17	13	10	18	63	96	117	99	74	2	456		2	16	11	10	16	5	4	77	88	81	69	46	3	394
		8	1	231	12	15	17	8	38	74	50	61	50	42	0	192		0	9	4	9	9	22	0	80	81	44	52	50	0	222
	208	9	6	230	31	27	11	14	30	72	106	31	54	99	8	361		11	13	10	5	15	16	3	32	15	21	12	19	4	315
		10	6	43	10	7	7	8	8	14	17	13	16	8	3	150		1	7	8	9	8	9	4	25	20	7	14	15	4	138
		11	0	258	15	29	28	16	22	81	111	117	83	70	2	558		7	27	18	17	5	15	5	88	48	54	84	79	12	332
		12	6	86	7	4	6	4	11	32	18	23	24	18	3	199		4	5	11	9	5	18	8	35	20	26	25	18	2	189
		13	0	4	0	2	0	0	0	43	34	28	44	45	0	241		0	7	3	0	5	3	0	13	12	9	18	9	0	41
		14	0	146	9	4	7	5	6	42	33	28	27	22	0	205								1	25	40	24	33	29	0	183
	209	17	2	33	7	3	2	1	7	11	7	9	2	10	0	255		1	1	1	6	1	5	1	10	14	9	10	7	1	121
		17	3	112	9	6	11	11	11	22	27	15	18	15	1	226		2	7	1	8	5	6	0	15	8	14	11	14	7	180
		18	1	164	8	8	16	9	12	58	53	44	45	34	4	516		3	19	16	10	7	7	2	44	48	41	43	35	11	435
		19	0	223	58	58	41	46	34	68	73	47	42	47	0	564		1	15	12	13	13	8	0	24	25	18	27	21	9	228
		20	37	212	38	41	44	42	44	68	70	63	57	58	41	411		28	33	32	34	28	35	17	29	23	30	25	25	17	285
		21	4	281	21	24	22	33	23	100	96	84	87	77	17	890		12	38	13	25	21	37	28	84	56	55	69	73	26	353
		22	14	111	16	20	18	12	16	39	48	44	56	63	18	598		3	11	9	10	10	10	5	22	26	18	24	21	11	214
	210	23	5	154	11	26	17	19	19	43	43	39	37	32	3	210		1	18	12	16	21	13	3	46	37	22	29	28	2	114
		24	0	7	1	3	3	2	2	29	6	6	17	7	0	217		0	1	2	0	1	2	3	20	11	9	21	5	10	232
		24	1	13	3	4	4	1	1	15	10	10	9	6	0	206		0	7	4	2	1	2	7	11	14	8	12	7	11	155
		25	11	414	19	12	31	24	17	163	116	109	112	94	11	812		7	21	17	9	12	14	19	57	94	99	75	62	15	657
		26	0	4	1	1	2	0	1	41	45	46	21	42	0	273		1	1	1	0	1	1	1	29	29	36	57	47	0	186
		27	1	194	11	19	16	7	16	88	85	77	66	78	0	711		4	20	30	9	21	15	2	56	28	43	51	48	4	568
		28	0	258	27	32	27	22	20	65	85	53	50	70	2	854		0	30	31	22	14	10	2	54	91	24	38	72	0	303
		28	0	5	0	2	2	1	3	2	3	1	1	1	1	42		0	2	1	1	1	1	0	2	0	0	2	1	0	9
	211	29	2	15	2	4	2	1	3	16	9	9	13	15	4	140		3	0	1	0	1	1	2	11	11	9	7	15	2	90
		29	19	154	36	21	25	38	20	87	76	60	58	56	7	491		4	2	4	3	4	2	7	15	17	10	12	8	7	164
		30	4	286	10	22	20	21	14	77	69	88	89	78	8	611		1	30	28	34	31	21	8	58	59	56	48	63	8	336
		31	0	2	0	0	0	0	0	18	21	28	18	44	0	840		0	0	0	0	0	0	0	6	8	4	11	10	1	329
		32	0	8	1	3	0	1	2	3	4	5	1	1	1	572														3	363
		33	4	70	7	10	7	12	13	49	40	36	35	29	4	705		12	12	14	15	18	7	13	50	42	27	42	39	7	394
		34	5	117	5	3	13	1	0	5	11	20	14	11	4	225		5	8	5	1	2	2	8	16	15	12	14	11	7	219
		34	0	37	8	8	2	5	5	20	18	22	25	18	0	399		2	4	10	7	9	8	8	34	23	24	20	24	23	310
	212	35	4	39	8	11	5	6	0	51	47	44	33	24	1	370		3	3	4	5	0	6	0	17	18	19	14	23	2	289
		36	30	366	39	40	28	44	35	117	125	125	86	138	29	814		22	24	24	20	21	17	26	83	63	85	69	60	52	471
		37	6	101	15	4	7	11	5	21	33	25	30	18	9	246		4	6	11	8	4	4	8	22	15	15	23	12	9	190
		39	0	88	6	4	6	3	1	65	65	35	32	43	0	483		0	0	2	4	4	5	1	58	35	28	45	21	0	237
		41	2	80	21	7	13	15	3	42	39	46	33	53	7	694		17	19	16	8	18	20	10	27	17	20	21	15	15	292
	215	42	3	140	37	40	19	11	13	106	105	108	121	92	2	708		1	4	4	4	3	0	3	15	16	16	30	9	5	108
		43	3	103	9	15	10	22	19	49	46	35	42	36	0	205		1	16	12	6	4	29	0	23	49	26	17	17	5	163
		44	0	17	1	0	1	1	0	56	58	58	50	55	0	386		0	0	1	2	1	1	0	42	50	50	44	37	0	218
	216	46	3	43	5	10	3	10	7	54	51	42	39	36	6	457		1	7	9	7	5	7	4	31	30	29	21	31	4	423
		47	0	8	1	1	1	2	3	13	12	13	14	13	0	60		0	0	0	0	1	0	0	4	4	1	3	5	0	45
		48	0	32	4	6	4	5	1	21	21	16	17	15	0	152		0	3	4	3	1	5	0	13	15	15	15	12	1	82
		49	0	36	3	3	1	2	0	25	15	34	27	29	0	396		0	0	0	0	0	1	0	5	5	0	2	6	0	276

Note – Table is continued on the next page.

Mode	Rat #	Neuron	2min post-SCS														5min post-SCS													
			1.4g						26g						Pinch		1.4g						26g						Pinch	
			BL	1	2	3	4	5	BL	1	2	3	4	5	BL		BL	1	2	3	4	5	BL	1	2	3	4	5	BL	
Tonic	207	1	35	37	31	47	35	17	11	44	42	41	46	35	12	284	10	31	35	30	27	31	15	53	42	50	33	39	14	283
		2	0	7	4	3	1	3	0	34	20	21	18	13	2	287	1	10	4	7	2	10	2	36	38	13	19	49	0	387
		3	20	25	24	25	18	23	3	45	16	40	29	12	11	295	14	10	18	20	24	29	10	30	24	35	21	27	20	233
		4	0	3	1	0	1	0	1	10	11	5	17	10	1	86	0	2	3	0	0	1	0	12	12	9	10	10	0	136
		4	2	13	18	14	11	8	12	53	51	37	36	44	8	334	22	30	14	23	26	27	22	47	63	58	78	56	8	475
		5	0	1	1	0	1	0	1	4	3	1	8	3	2	17	1	3	2	0	2	0	0	11	9	9	5	9	0	128
		5	9	9	16	10	10	9	13	65	55	36	48	62	23	429	14	28	36	22	25	19	30	62	48	78	75	83	9	396
		6	3	12	7	6	17	10	6	67	69	65	71	65	6	341	10	30	26	24	20	11	9	48	64	59	55	65	3	525
		7	4	30	25	23	12	14	3	83	64	79	61	61	4	418	1	9	22	20	19	25	4	66	70	64	71	70	3	429
		8	0	3	14	0	9	38	1	52	53	61	52	54	2	204	7	40	22	6	22	44	1	67	56	51	57	48	0	204
	208	9	10	6	14	13	25	16	8	19	26	23	30	18	9	177	15	16	21	13	13	23	1	39	35	22	34	26	10	227
		10	5	7	11	8	7	8	8	27	14	19	15	12	6	148	8	17	13	1	1	5	3	26	35	8	24	24	6	144
		11	4	13	13	15	15	6	2	84	73	82	43	55	6	459	3	25	19	21	9	44	4	69	101	84	88	93	2	379
		12	1	8	13	6	9	5	12	41	25	19	20	24	13	139	4	9	4	1	7	5	6	23	17	24	24	15	6	201
		13	0	0	0	0	0	0	0	11	44	31	20	19	0	193														
		14	1	17	8	11	6	11	3	37	30	42	27	30	0	81	1	6	5	3	14	7	2	39	24	23	28	21	1	65
	209	17	3	5	7	4	1	3	0	21	20	24	14	9	24	292	3	3	4	0	5	3	0	23	19	11	10	11	4	204
		17	3	4	5	4	3	7	0	17	18	9	11	8	7	179	3	2	3	11	3	9	0	27	15	20	30	14	0	130
		18	5	23	13	13	12	10	4	42	41	38	34	36	7	292	5	13	16	12	10	13	7	49	47	27	35	29	8	382
		19	3	7	16	13	3	20	0	11	22	22	18	32	0	201	0	14	11	8	13	16	0	22	37	72	17	60	7	384
		20	13	34	27	29	31	25	31	31	28	34	29	34	36	293	10	25	23	24	24	22	10	25	23	24	24	22	33	312
		21	10	9	34	16	22	29	22	71	66	50	75	44	32	390	5	8	2	8	20	17	4	61	53	66	74	55	16	528
		22	4	11	6	4	14	11	2	30	21	28	19	22	5	207	2	12	10	8	7	6	0	21	17	18	22	25	2	343
	210	23	1	15	6	15	11	11	2	39	34	39	28	20	7	213	0	9	16	14	17	14	3	48	37	31	37	34	5	161
		24	1	2	5	0	5	1	3	21	7	17	12	12	2	136	0	0	0	0	1	0	1	9	20	9	12	6	1	161
		24	3	2	5	3	0	3	8	20	6	15	14	17	10	142	3	5	3	3	2	4	3	17	13	13	11	5	3	164
		25	12	20	7	35	37	25	1	109	88	17	129	85	15	674	9	20	14	14	14	13	10	118	96	110	88	116	17	809
		26							2	36	36	76	52	43	5	353	8	2	5	7	5	11	2	73	75	57	85	71	1	290
		27	2	20	35	29	19	15	16	87	102	112	107	79	6	452	4	22	24	21	39	20	8	78	73	77	83	88	11	712
		28	1	15	15	8	23	11	0	61	65	58	36	68	0	449	0	28	11	12	10	13	0	61	79	60	64	89	0	615
		28	1	0	1	1	2	2	1	1	0	1	4	1	0	11	0	3	1	2	0	4	0	0	2	2	3	3	0	24
	211	29	3	4	0	5	3	0	5	6	8	17	11	10	0	92	1	2	4	0	1	2	4	8	10	9	14	5	1	100
		29	8	9	10	4	10	6	9	24	21	22	14	16	7	219	4	15	12	7	7	13	3	23	36	42	29	30	4	204
		30	8	10	13	20	4	14	14	65	73	41	50	43	1	206	10	17	18	26	12	12	15	31	25	28	25	32	11	308
		31	0	0	0	0	0	0	0	16	5	16	14	24	0	368	0	0	0	0	0	0	1	44	43	40	44	64	0	639
		32													2	329													3	393
		33	11	17	20	14	21	17	9	35	29	31	31	39	16	435	16	20	14	12	18	17	5	48	25	73	51	35	4	478
		34	6	2	7	2	3	6	7	21	10	18	13	17	2	214	0	9	14	3	15	6	4	18	20	19	15	16	3	314
		34	2	15	9	10	9	10	20	47	32	34	27	33	0	318	5	16	12	13	16	13	24	38	29	33	34	31	1	351
	212	35	2	0	2	3	7	5	5	33	14	14	12	15	3	298	1	7	0	13	3	0	1	27	24	13	19	25	3	296
		36							17	79	64	54	62	69	18	493	11	27	10	14	14	20	23	58	67	50	54	50	22	631
		37	3	10	1	11	5	1	6	13	11	21	15	17	2	216	3	7	2	0	8	6	6	7	4	18	10	12	2	124
		39	0	2	8	3	1	7	0	52	45	36	25	27	0	195	0	6	3	4	1	5	0	51	48	32	53	42	0	315
		41	4	6	8	3	4	21	3	27	37	33	26	43	15	453	10	15	16	10	20	17	10	46	44	46	42	23	1	441
	215	42	2	10	7	0	5	3	4	45	19	10	10	11	2	478	2	16	4	8	9	11	2	35	59	81	59	46	6	556
		43	0	6	16	18	24	13	0	23	21	37	16	21	3	211	2	3	16	3	1	6	2	23	20	24	16	17	6	149
		44	0	1	1	1	1	3	0	53	56	54	43	50	1	334	0	1	1	2	2	2	0	39	61	51	45	44	0	344
	216	46	3	8	5	10	5	10	4	46	40	35	34	29	4	437	8	6	10	5	8	6	6	54	41	45	33	20	4	362
		47	0	0	0	1	0	0	0	3	2	0	2	2	0	64	0	0	0	0	0	3	0	8	4	4	1	6	0	104
		48	3	6	4	9	7	1	3	12	31	24	20	21	0	168	2	8	11	7	7	4	5	23	26	15	33	14	1	247
		49	0	1	0	1	1	1	0	8	11	5	6	6	0	190	0	3	1	1	0	2	1	13	11	15	16	3	0	250

Note – Table is continued on the next page.

Mode	Rat #	Neuron	10min post-SCS														15min post-SCS													
			1.4g						26g						Pinch		1.4g						26g						Pinch	
			BL	1	2	3	4	5	BL	1	2	3	4	5	BL		BL	1	2	3	4	5	BL	1	2	3	4	5	BL	
Tonic	207	1	4	22	11	13	10	21	5	28	23	17	17	30	8	169	2	8	12	8	7	16	2	19	24	23	25	24	6	137
		2	0	9	4	5	5	7	3	24	22	7	17	14	7	349	3	8	9	7	2	7	2	14	23	21	13	17	9	149
		3	8	18	27	23	27	15	6	24	36	24	26	31	12	322	1	5	6	4	5	9	0	15	14	14	22	12	6	229
		4	0	1	0	1	0	0	1	11	7	7	9	14	1	197	1	0	0	0	0	0	1	13	11	8	15	12	1	53
		4	5	14	10	10	10	8	8	62	66	40	51	67	12	579	20	17	16	27	9	14	33	76	46	68	85	68	11	367
		5	0	0	1	0	2	2	0	3	7	4	3	6	6	50	1	1	0	1	0	1	2	1	2	4	4	3	0	75
		5	6	18	11	15	18	23	14	60	96	70	57	66	39	455	6	27	22	27	25	38	30	59	90	54	86	92	10	361
		6	16	23	49	46	12	8	3	59	58	58	76	62	4	607	7	36	16	16	8	15	11	61	72	62	75	90	6	588
		7	3	29	30	31	20	15	3	76	54	79	62	89	4	451	2	25	26	24	20	17	5	75	65	67	100	80	2	439
		8	1	13	10	9	3	12	0	76	52	60	47	61	0	214														
	208	9	3	15	29	24	21	18	15	57	38	22	27	24	9	268	6	24	23	30	12	31	8	39	39	23	10	19	10	264
		10	4	7	9	2	9	8	8	49	13	19	18	12	4	118	0	4	2	4	2	2	2	19	5	17	21	18	2	62
		11	5	24	10	56	41	12	1	89	72	58	50	59	7	681	14	20	27	15	24	20	6	107	91	83	78	118	8	881
		12	8	8	6	2	10	5	10	41	30	23	24	19	7	172	3	7	6	8	7	6	1	49	16	18	28	21	7	224
		13																												
		14	2	15	12	2	10	5	4	35	32	24	29	22	1	107	0	10	1	2	5	7	3	47	29	32	20	32	0	170
	209	17	1	5	3	0	2	3	1	24	15	13	11	16	0	161	0	17	1	7	2	0	4	16	26	11	22	38	1	266
		17	0	7	4	3	6	6	0	26	15	13	11	13	0	164	0	14	5	7	7	4	1	33	38	19	25	24	1	244
		18	11	23	33	19	16	14	3	51	49	46	50	45	10	575	7	22	22	20	19	8	4	63	35	42	49	73	10	630
		19	1	9	9	11	8	8	0	40	30	34	47	42	1	338	0	25	8	26	0	12	0	36	11	31	31	46	0	400
		20	21	24	18	29	27	25	16	30	14	26	14	15	34	329	7	10	11	10	19	13	8	13	6	7	12	12	20	156
		21	2	21	15	26	20	13	17	77	61	58	63	63	10	887	4	11	5	7	22	10	4	100	73	67	73	72	4	673
		22	1	7	4	8	4	5	1	42	21	33	25	36	12	479	0	6	5	3	2	5	2	48	48	59	41	57	9	585
	210	23	1	17	12	19	14	16	5	29	37	33	25	32	2	160	5	9	17	11	17	9	7	39	34	19	42	27	7	196
		24	0	2	0	2	3	1	1	9	9	15	10	7	0	220	1	0	1	0	0	0	0	6	24	9	18	3	1	211
		24	0	4	7	2	1	2	5	18	13	17	13	13	1	193	3	6	4	3	1	0	10	17	19	19	23	14	2	165
		25	18	38	21	17	34	18	13	79	87	106	100	92	26	790	11	43	51	23	50	40	19	71	71	125	82	120	31	742
		26	15	13	7	6	3	7	8	77	71	54	56	64	5	451	2	3	1	0	3	0	0	57	41	81	69	56	5	301
		27	2	26	18	24	33	8	1	85	78	102	132	133	6	770	16	63	24	13	28	43	2	93	130	109	89	103	6	1058
		28	4	17	30	9	26	14	0	59	55	65	85	57	1	527							0	37	64	72	43	64	0	448
		28	0	0	2	3	1	2	1	3	1	0	1	1	1	84	0	0	0	0	0	5	0	3	7	6	4	3	0	93
	211	29	1	1	1	1	0	1	0	6	10	8	11	7	1	68	3	5	2	4	2	2	3	20	11	14	12	16	0	129
		29	2	2	7	4	10	7	6	61	40	43	64	53	7	308	10	14	15	16	8	17	8	67	49	39	46	62	7	340
		30	4	13	17	12	7	14	3	26	9	11	22	15	2	362	0	9	10	16	22	9	3	29	16	25	16	17	3	175
		31	0	4	5	5	5	4	1	46	54	36	32	36	0	954														
		32													3	499													3	385
		33	12	11	10	14	13	18	9	34	36	29	24	39	1	508	17	15	28	24	17	33	16	49	60	54	41	58	5	521
		34	2	5	4	16	3	4	3	20	10	20	15	8	2	245	13	4	26	3	27	10	5	24	20	25	22	22	2	305
		34	1	12	14	10	5	2	10	48	33	38	42	25	1	283	16	9	15	18	15	12	21	44	39	49	39	36	0	303
	212	35	0	7	2	3	6	8	0	6	6	4	6	11	0	295	2	3	0	1	5	3	1	26	15	15	14	27	1	194
		36	6	14	17	13	9	7	11	95	57	76	54	53	15	569	8	3	10	16	8	20	13	51	47	50	35	55	19	589
		37	1	0	3	0	1	2	3	1	3	8	6	4	4	74	4	4	4	8	9	10	6	20	18	12	18	20	8	277
		39	0	6	4	12	5	6	0	43	46	64	47	42	0	340	0	18	6	2	11	9	2	65	66	66	62	74	0	510
		41	4	13	11	15	15	9	10	50	36	41	33	45	5	570	2	8	1	11	4	15	8	32	31	34	33	51	8	578
	215	42	9	7	13	8	2	6	10	60	58	63	60	63	7	674	4	18	11	2	8	3	8	74	67	58	58	58	12	617
		43	0	49	19	11	20	20	2	46	40	43	28	38	8	223	1	26	12	22	33	16	4	39	28	34	31	30	3	235
		44	3	3	2	12	2	5	2	49	51	53	49	51	0	304	2	5	7	6	2	2	7	83	76	72	74	68	8	457
	216	46	6	5	11	11	9	8	5	53	56	46	43	34	5	545	3	4	4	4	9	13	6	42	46	43	51	43	6	459
		47	0	0	1	0	0	0	0	2	2	6	4	5	0	94	0	0	0	0	2	2	0	8	8	6	5	11	0	54
		48	2	20	6	5	2	0	2	29	11	46	33	33	4	169	3	12	8	4	3	11	1	27	21	34	20	30	1	166
		49	0	0	2	1	2	3	0	26	20	15	8	4	0	351	0	1	0	1	0	0	0	10	11	9	4	16	0	266

Note – Missing data points are from neurons that were lost during recording before completing the stimulation protocol.

Table D.6. Spike counts after burst or tonic SCS on day 7 following painful nerve root compression with spinal superfusion of bicuculline (Chapter 7).

Mode	Rat #	Neuron	pre-SCS baseline															0min post-SCS												
			Brush		1.4g vF					26g vF					Pinch			1.4g						26g					Pinch	
			BL		1	2	3	4	5	1	2	3	4	5	BL		BL	1	2	3	4	5	BL	1	2	3	4	5	BL	
Burst	250	7	0	88	3	15	14	2	6	33	35	40	19	40	0	135	0	3	2	9	0	2	0	44	51	49	26	41	0	72
		9	18	173	59	55	64	84	70	226	213	206	146	203	73	1200	0	31	30	48	12	32	0	184	179	82	23	76	7	204
		11	0	96	5	3	8	1	2	39	42	42	26	34	1	142	0	14	9	13	12	10	0	30	25	28	24	29	0	207
		12	14	226	54	78	68	64	73	157	149	162	178	174	7	860	45	111	103	37	54	53	11	92	69	49	114	70	80	675
		13	4	190	18	10	16	16	33	63	32	47	34	43	0	569	2	19	21	5	6	13	0	54	43	46	27	19	66	767
	251	14	19	301	33	22	33	33	22	138	53	69	111	84	23	519	9	23	32	25	12	15	24	44	61	41	43	31	14	372
		15	34	916	146	156	139	92	121	297	294	292	249	241	8	1848	8	49	57	42	36	36	4	158	140	96	100	95	9	495
		16	9	317	18	11	24	27	13	105	40	108	77	75	2	485	5	4	12	6	12	7	10	43	22	38	103	79	8	477
		17	0	282	19	21	96	65	68	120	96	94	78	79	1	728	0	52	3	11	14	49	2	27	55	47	35	47	1	404
		18	5	150	8	14	5	9	12	69	57	58	49	70	15	506	4	32	14	10	18	17	4	64	47	33	26	22	10	335
Tonic	250	7	8	326	25	44	21	33	15	59	78	103	88	100	3	130	3	9	5	2	6	4	0	12	27	11	10	12	0	19
		8	0	28	9	15	7	3	39	30	14	27	47	81	6	261	0	6	1	2	5	1	0	25	25	18	13	21	0	96
		11	0	119	8	15	14	6	9	39	37	52	46	36	0	153	0	10	13	18	9	23	2	35	33	24	31	32	0	247
		12	0	5	0	0	0	0	0	0	0	0	0	0	0	139	0	6	0	0	0	1	0	2	1	1	4	5	0	111
		12	10	231	11	25	25	14	19	26	44	20	39	29	1	283	7	17	15	17	17	18	0	44	28	15	11	24	1	144
		13	3	185	24	19	14	19	15	96	115	101	70	113	0	641	0	16	44	11	2	12	0	73	82	153	111	124	5	579
	251	16	10	394	41	39	45	40	48	37	88	69	46	51	9	589	1	7	12	11	22	12	8	41	49	54	45	47	16	341
		17	0	509	26	21	44	57	70	147	134	90	95	110	2	828	3	63	13	18	19	25	1	54	33	69	33	47	0	616
		18	4	303	39	15	17	31	11	74	88	81	91	66	9	571	10	6	20	4	14	14	5	58	36	30	36	36	5	248
		19	0	18	1	2	0	3	4	10	5	66	61	17	0	756	1	12	0	11	3	18	0	14	17	14	17	4	0	553

Mode	Rat #	Neuron	2min post-SCS														5min post-SCS													
				1.4g						26g					Pinch			1.4g						26g					Pinch	
			BL	1	2	3	4	5	BL	1	2	3	4	5	BL		BL	1	2	3	4	5	BL	1	2	3	4	5	BL	
Burst	250	7	2	21	6	22	14	14	10	20	50	72	68	41	5	144	7	19	34	10	16	10	0	31	10	25	51	27	0	100
		9	0	1	1	3	1	1	0	169	113	282	210	102	0	729	0	1	0	0	1	2	0	159	125	100	102	52	0	680
		11	3	16	16	10	9	6	0	32	26	28	33	28	2	183	0	9	10	3	7	7	0	46	36	13	20	30	1	155
		12	20	49	55	15	71	49	3	78	79	84	76	53	5	357	25	114	122	79	83	55	35	113	97	108	104	80	8	909
		13	9	26	26	30	62	40	1	44	77	36	51	13			0	35	28	32	20	12	1	45	43	44	44	68		
	251	14	6	14	11	11	20	15	13	26	15	42	37	30	26	342	2	13	5	7	14	7	6	18	16	14	13	13	0	236
		15	4	29	28	28	21	25	8	85	113	79	73	98	19	1214	15	86	47	42	41	49	0	90	78	73	57	22	3	1659
		16	3	17	19	15	9	6	6	61	48	28	45	38	15	493	4	13	20	62	18	38	7	97	141	126	135	136	8	793
		17	1	5	13	0	2	21	1	86	74	60	54	86	3	433	3	60	34	10	8	12	3	26	74	86	99	79	3	456
		18	5	14	14	24	22	11	8	75	51	69	65	55	8	290	6	27	32	24	13	35	14	77	76	63	86	55	5	466
Tonic	250	7	0	4	1	8	1	4	0	24	18	21	31	11	0	38	1	12	4	28	12	7	0	40	39	51	44	59	2	186
		8	0	5	1	3	1	1	8	39	33	47	21	40	8	272	0	14	18	5	7	0	2	49	20	24	21	30	0	190
		11	0	14	8	8	21	14	4	25	30	33	19	45	0	238	1	6	11	14	13	11	0	27	21	33	43	38	5	204
		12	0	4	0	2	0	5	1	1	6	11	0	5	1	169	10	34	23	32	37	28	29	43	36	37	28	46	11	218
		12	1	22	14	28	4	16	20	45	36	45	68	44	0	270	8	1	4	4	12	0	4	12	7	5	11	1	0	97
		13	7	15	18	28	18	18	3	90	82	57	57	50	8	406	0	15	14	18	6	19	0	93	58	103	101	107	2	470
	251	16	9	27	46	18	12	39	24	47	52	57	115	36	28	523	6	10	8	12	13	3	5	38	48	64	49	79	3	379
		17	1	12	16	3	17	10	0	40	87	60	65	41	2	437	1	26	26	9	6	61	3	111	92	101	83	56	2	672
		18	3	10	8	9	12	28	4	38	72	64	21	33	3	189	5	21	34	8	30	12	3	62	45	72	33	60	4	406
		19	0	0	7	0	0	1	0	7	16	15	20	17	0	391	0	5	0	0	0	0	0	22	10	3	6	7	0	648

Note – Table is continued on the next page.

Mode	Rat #	Neuron	10min post-SCS														15min post-SCS													
				1.4g						26g					Pinch			1.4g						26g					Pinch	
			BL	1	2	3	4	5	BL	1	2	3	4	5	BL		BL	1	2	3	4	5	BL	1	2	3	4	5	BL	
Burst	250	7	0	3	19	8	8	6	0	24	28	15	25	50	0	103	0	11	8	13	4	26	0	38	13	23	35	36	1	216
		9																												
		11	0	7	7	15	8	14	0	13	17	19	22	26	6	88	0	12	8	11	9	13	0	45	17	18	26	40	0	101
		12	25	90	107	106	94	34	17	103	129	103	107	123	17	583	25	54	78	68	64	73	18	157	149	162	178	174	7	860
		13	2	28	17	38	12	20	9	51	52	50	33	58			15	18	23	22	23	18	2	85	114	73	91	69	3	496
	251	14	3	10	9	6	7	6	8	46	39	31	51	63	8	120	0	17	8	14	2	0							2	190
		15													12	1772														
		16	4	48	18	54	32	26	7	102	103	92	89	87	6	531	6	8	8	13	42	21	4	80	97	73	45	59	9	450
		17	3	35	68	17	11	66	4	70	106	91	85	129	4	713	5	17	46	50	23	52	3	137	76	87	101	104	7	726
		18	7	30	24	16	14	35	5	91	98	30	66	106	11	386	5	39	15	17	31	11	2	74	88	81	91	66	9	571
Tonic	250	7	2	13	11	7	1	8	0	25	24	20	14	11	0	54	0	5	9	8	3	4	0	14	6	13	6	14	0	37
		8	0	5	8	1	1	1	0	36	43	29	29	21	11	173	4	14	17	6	3	3	5	19	22	9	4	8	1	206
		11	0	9	18	8	11	6	1	65	44	41	34	8	0	349	0	21	8	13	13	4	0	59	46	39	31	35	1	217
		12	22	18	22	25	23	36	9	37	20	29	29	40	7	168	7	20	50	32	29	27	13	46	45	23	37	32	0	248
		12	4	14	15	10	17	17	1	42	29	29	51	29	0	135	5	11	12	20	10	13	12	49	29	38	13	47	9	192
		13	3	20	15	24	14	10	0	98	58	63	71	95	6	650	0	24	19	14	19	15	0	96	80	54	44	78	0	641
	251	16	6	14	24	53	26	53	12	67	60	54	39	75	6	237	6	24	10	3	10	2	7	67	81	82	61	74	2	331
		17	0	46	67	34	3	93	2	101	114	118	98	102	1	668	0	19	21	96	65	68	5	120	96	94	78	79	1	728
		18	0	19	17	9	20	21	2	62	39	37	44	39	2	296	0	24	28	17	11	5	2	86	117	71	86	86	3	467
		19	0	1	10	3	0	4	0	11	19	8	5	1	0	749	0	11	6	8	2	11	0	22	13	14	27	24	0	914

Note – Missing data points are from neurons that were lost during recording before completing the stimulation protocol.

Table D.7. Spike counts after burst or tonic SCS on day 7 following painful nerve root compression with spinal superfusion of CGP35348 (Chapter 7).

Mode	Rat #	Neuron	pre-SCS baseline															0min post-SCS												
			Brush		1.4g vF					26g vF					Pinch			1.4g						26g						Pinch	
			BL		1	2	3	4	5	1	2	3	4	5	BL			BL	1	2	3	4	5	BL	1	2	3	4	5	BL	
Burst	249	1	9	120	21	25	16	24	26	50	51	47	85	81	20	517		0	7	10	2	9	4	3	10	25	17	13	14	5	213
		2	17	117	20	26	21	20	21	31	33	40	59	62	17	705		9	9	14	18	23	9	10	34	29	19	28	39	13	208
		4	11	72	15	18	14	13	18	35	35	35	66	39	11	671		23	21	22	27	24	22	16	57	37	48	28	28	15	344
		5	15	224	26	37	24	33	32	96	85	93	95	124	16	851		12	20	17	21	9	14	4	88	58	76	69	95	8	772
		6	13	172	24	26	35	36	17	100	59	67	74	78	14	763		11	20	22	24	25	28	25	29	39	38	42	41	20	488
	252	20	12	206	18	19	21	16	25	43	49	33	27	34	18	500		12	21	19	15	23	15	13	31	42	46	31	33	21	475
		21	10	652	93	112	130	116	99	196	137	143	123	146	23	616		6	105	93	61	85	157	6	84	100	87	110	106	6	314
		22	2	460	49	52	72	56	79	124	122	108	113	104	1	745		8	27	20	26	35	38	8	66	50	53	42	24	2	158
		23	23	154	24	34	17	20	13	42	49	43	56	45	16	366		3	9	5	3	6	8	0	12	11	14	9	12	1	94
	265	24	0	161	8	13	10	10	16	27	18	19	13	11	0	159		0	7	7	5	4	4	0	20	8	18	22	19	0	150
		25	0	38	3	0	3	3	0	15	20	11	22	12	0	507		0	18	3	14	5	6	0	20	8	8	21	20	0	324
		26	8	349	45	60	49	42	54	94	71	87	96	93	8	716		11	46	65	57	49	45	10	90	80	59	72	74	7	433
		27	4	50	6	3	5	5	9	46	32	30	29	30	3	134		1	3	2	6	2	2	1	43	32	26	25	17	4	98
		28	1	16	7	3	3	6	3	44	55	32	47	42	0	500		2	3	3	2	2	1	0	14	23	20	23	17	11	281
		29	12	306	47	39	26	28	17	94	116	75	98	105	17	1094		11	12	21	12	13	13	16	43	53	39	48	51	9	423
	266	30	5	251	18	13	11	16	30	52	51	58	51	51	6	340		3	17	16	12	14	18	4	49	49	38	35	49	4	279
		32	8	70	12	8	7	8	9	27	18	22	19	26	2	291		9	8	14	7	11	7	4	13	17	16	13	16	0	124
		34	2	601	12	8	14	12	15	87	81	79	65	71	3	556		0	7	3	7	5	6	1	34	46	54	44	38	0	205
	267	36	1	62	4	3	1	4	1	60	62	45	34	45	2	507		1	4	4	2	3	3	0	40	41	28	24	20	3	320
		37	0	16	3	5	3	3	2	58	82	61	41	47	0	340		0	19	8	6	0	1	0	49	48	24	26	22	1	260
	268	38	2	76	8	5	9	6	6	33	36	32	31	17	2	111		4	15	5	4	8	6	2	33	12	6	12	29	2	75
		39	0	62	30	28	27	28	26	81	71	71	70	65	6	832		2	92	22	32	19	29	1	48	75	71	33	46	22	555
		40	0	8	0	0	0	0	0	10	7	12	9	14	0	299		0	1	0	1	0	0	0	6	7	15	7	5	0	118
		41	0	0	0	0	0	0	0	25	24	19	14	20	0	355		0	0	1	0	0	1	0	13	16	7	9	10	0	333
	269	44	8	241	34	17	28	28	44	86	76	80	63	77	9	540		3	15	4	5	11	5	5	27	25	19	17	16	17	187
		46	1	97	11	12	5	7	14	35	44	44	31	35	0	351		0	7	5	3	3	4	2	22	26	35	23	17	0	155
		47	0	71	1	4	3	6	1	29	31	18	24	23	0	425		0	1	2	1	0	0	0	13	7	9	8	10	0	235
		48	0	19	2	5	3	3	2	36	17	29	42	35	2	365		0	1	2	0	2	2	0	10	7	9	6	10	1	120
		49	10	457	63	68	58	50	72	138	107	128	98	106	16	530		7	22	15	32	15	12	3	62	75	68	137	53	8	373

Note – Table is continued on the next page.

Mode	Rat #	Neuron	2min post-SCS														5min post-SCS													
			1.4g						26g						Pinch		1.4g						26g						Pinch	
			BL	1	2	3	4	5	BL	1	2	3	4	5	BL		BL	1	2	3	4	5	BL	1	2	3	4	5	BL	
Burst	249	1	1	13	18	8	8	14	1	28	27	29	36	31	2	611	3	20	7	9	8	5	3	15	17	10	11	14	0	188
		2	8	18	24	11	16	21	8	33	28	28	33	36	13	227	16	27	22	11	27	20	17	61	31	33	20	36	28	620
		4	23	34	18	26	21	21	17	32	37	30	53	41	10	457	29	36	28	34	30	26	26	48	46	51	58	57	9	531
		5	10	20	34	33	28	21	20	77	65	74	74	93	18	788	22	19	38	48	24	33	26	97	107	81	109	92	34	883
		6	7	15	2	11	19	10	9	38	41	32	40	47	15	630	17	17	23	27	23	23	22	60	45	49	40	37	23	617
	252	20	17	23	16	22	17	17	6	45	19	31	23	48	13	434	19	25	45	25	18	15	14	30	36	47	36	53	8	395
		21	0	95	82	73	56	57	3	173	146	107	105	59	4	344	2	78	57	65	77	84	0	91	82	42	45	90	1	336
		22	7	10	28	10	25	20	1	33	20	33	18	20	5	56	5	41	45	41	35	27	3	37	41	22	28	20	0	109
		23	0	7	4	5	5	3	26	37	26	26	27	27	0	127	7	15	16	11	11	11	3	28	19	17	30	27	1	264
	265	24	0	8	7	6	4	3	0	14	25	19	16	11	0	85	0	2	11	6	9	10	0	18	24	27	26	18	1	118
		25	1	14	8	5	6	3	0	10	25	18	12	12	0	375	0	3	2	3	1	3	0	38	46	36	27	23	0	399
		26	11	49	46	46	49	56	8	76	69	87	85	71	5	393	9	41	45	39	28	51	8	91	59	68	68	54	11	469
		27	1	1	6	10	7	9	0	29	37	26	25	24	2	105	5	5	2	10	6	6	5	36	34	37	31	27	3	193
		28	2	7	1	3	4	3	1	10	22	24	21	14	0	260	1	7	5	3	3	4	0	30	29	25	33	28	1	374
		29	8	11	15	10	16	14	9	31	39	46	53	33	11	328	16	28	19	8	15	18	9	45	41	38	27	47	13	480
	266	30	2	5	11	14	6	12	1	35	48	37	42	40	7	237	5	14	23	14	15	17	5	53	55	37	63	47	5	314
		32	4	9	8	5	9	7	0	10	15	12	16	10	0	124	11	17	11	9	10	10	3	17	18	18	24	35	1	222
		34	2	3	8	9	5	4	2	45	40	41	40	48	1	223	1	6	6	5	8	3	3	49	52	58	27	35	1	345
	267	36	0	4	2	5	3	5	2	27	48	28	32	49	0	360	3	6	9	11	7	5	3	67	51	53	43	69	1	420
		37	2	17	6	10	8	2	1	67	33	30	24	5	0	302	2	13	1	2	1	2	0	49	26	48	35	36	0	341
	268	38	3	11	6	10	13	10	4	13	21	19	11	28	3	72	0	4	1	12	9	11	4	23	25	24	19	24	4	61
		39	0	7	26	13	22	21	5	34	31	32	28	35	0	208	7	19	40	15	23	24	3	98	84	70	81	77	4	692
		40	0	3	3	2	0	1	0	4	14	5	12	5	0	142	0	1	0	0	0	0	0	11	7	5	7	11	0	152
		41	0	3	3	1	0	0	0	30	14	18	21	15	0	350	0	0	0	1	0	1	0	24	27	17	14	28	0	402
	269	44	5	37	19	23	27	29	3	49	60	54	58	57	7	285	4	23	27	32	31	30	2	35	26	37	42	57	11	355
		46	0	6	5	2	3	3	2	32	12	26	14	28	0	249	0	4	1	4	2	3	2	38	32	30	32	38	0	272
		47	1	1	1	0	2	1	0	17	12	8	12	12	0	257	0	1	2	3	2	1	0	25	23	21	26	24	0	335
		48	0	2	1	2	0	2	0	20	18	23	19	9	1	189	0	2	4	3	1	3	0	26	17	42	18	22	0	286
		49	3	13	70	55	22	34	0	79	48	72	66	147	7	229	9	25	36	84	94	91	7	161	71	53	107	133	7	618

Note – Table is continued on the next page.

Mode	Rat #	Neuron	10min post-SCS														15min post-SCS													
			1.4g						26g						Pinch		1.4g						26g						Pinch	
			BL	1	2	3	4	5	BL	1	2	3	4	5	BL		BL	1	2	3	4	5	BL	1	2	3	4	5	BL	
Burst	249	1	0	5	2	12	8	13	2	19	19	23	20	23	1	90	31	67	47	51	45	38	22	79	70	75	97	78	14	653
		2	25	27	19	22	21	15	13	44	38	53	32	29	10	456	25	34	30	37	30	38	35	58	57	65	52	41	20	697
		4	26	31	32	21	32	21	22	36	36	32	43	56	7	480	37	43	33	29	32	39	25	65	73	62	69	58	13	514
		5	19	49	42	36	27	48	19	84	81	68	88	87	11	1120	15	46	39	24	24	28	17	111	136	107	101	108	34	1099
		6	24	33	37	24	43	85	28	44	45	50	47	50	20	712	19	22	31	21	22	34	25	58	72	67	65	66	20	708
	252	20	16	26	29	10	18	17	6	31	39	46	43	46	6	360	11	13	19	5	5	11	3	22	29	32	32	24	5	404
		21	3	125	139	144	148	44	0	156	112	122	89	87	0	281	7	79	99	69	100	56	1	183	131	133	110	74	1	506
		22	7	42	30	42	49	44	2	26	28	35	33	34	1	125	4	25	45	48	21	41	0	45	21	28	32	27	2	152
		23	7	16	13	7	9	10	2	29	27	25	24	20	0	273	8	16	13	15	21	12	2	32	27	20	21	26	0	345
	265	24	0	10	3	7	4	5	0	29	16	13	24	7	0	168	3	7	9	6	2	4	0	20	17	13	21	15	3	152
		25	0	11	9	1	1	1	0	25	43	52	45	59	0	444	0	9	8	1	3	4	0	19	21	22	17	29	0	363
		26	12	58	59	56	51	51	7	117	119	133	64	83	4	598	10	75	33	66	42	45	13	106	96	72	142	138	8	504
		27	4	10	6	12	7	5	4	42	26	30	27	29	2	220	3	6	9	6	8	11	11	38	34	41	42	29	4	210
		28	4	14	12	8	3	6	0	45	52	52	46	46	1	507	0	5	8	5	2	6	0	62	58	47	57	66	4	512
		29	7	23	13	20	23	12	10	46	55	58	47	51	8	513	19	23	23	13	18	19	12	70	63	57	40	40	13	504
	266	30	6	17	14	14	24	27	1	46	52	59	34	54	7	434	7	14	34	22	20	28	6	61	80	92	75	64	6	403
		32	13	19	15	14	16	11	5	29	35	25	31	29	0	214	22	23	21	20	22	22	10	25	32	33	38	30	0	306
		34	3	6	5	7	6	7	1	50	43	38	30	33	1	301	0	9	8	4	5	4	0	54	61	54	62	50	0	461
	267	36	1	6	5	7	4	7	3	69	66	36	45	59	3	342	2	8	7	6	5	5	4	57	35	36	41	37	2	381
		37	1	6	0	3	0	0	0	39	20	37	20	39	0	313														
	268	38	4	11	9	5	8	5	1	28	16	20	27	31	4	99	4	8	4	5	6	14	3	32	20	22	27	32	4	122
		39	6	53	16	21	59	27	1	105	92	69	72	80	8	763	5	30	28	27	28	26	1	81	71	71	70	65	6	832
		40	0	4	2	5	0	0	0	16	10	10	11	8	0	162	0	4	2	11	2	1	0	8	6	6	7	7	0	180
		41	0	3	0	1	0	0	0	42	14	18	18	15	0	275	1	5	5	3	1	1	0	36	38	31	31	28	0	363
	269	44	7	25	30	29	18	23	2	60	49	44	59	50	9	451	5	27	16	19	23	13	7	36	26	30	29	44	4	298
		46	0	5	3	5	8	6	0	45	49	39	39	40	0	235	3	7	6	7	8	7	0	78	48	43	51	49	1	308
		47	0	8	3	1	2	2	0	33	21	29	40	34	0	442	0	1	1	1	2	3	0	31	27	34	33	25	0	380
		48	0	3	1	0	0	4	0	19	35	40	34	36	0	311	3	3	3	2	0	4	1	28	26	23	23	27	0	364
		49	9	59	75	23	99	72	5	138	142	127	123	122	8	519	10	61	63	68	50	72	12	138	107	128	98	106	16	530

Note – Table is continued on the next page.

Mode	Rat #	Neuron	pre-SCS baseline															0min post-SCS												
			Brush		1.4g vF					26g vF					Pinch			1.4g						26g						Pinch	
			BL		1	2	3	4	5	1	2	3	4	5	BL		BL	1	2	3	4	5	BL	1	2	3	4	5	BL	
Tonic	249	1	16	183	34	39	29	24	25	48	51	37	52	43	15	329	14	26	28	22	27	28	11	66	68	59	49	61	6	462
		2	15	121	18	21	14	16	18	43	43	27	21	30	18	273	8	9	6	18	11	10	10	41	25	33	27	30	2	306
		3	0	102	5	11	8	10	7	27	25	27	16	38	2	564	2	8	13	14	9	9	0	42	32	34	43	22	0	662
		4	37	186	43	33	29	32	39	65	73	62	69	58	13	514	16	24	12	4	9	11	7	37	40	52	35	53	1	320
		5	9	191	28	33	14	28	20	56	74	52	61	64	4	733	2	15	20	13	12	10	1	67	93	35	90	66	6	829
		6	9	204	18	28	31	28	36	45	43	40	34	25	9	408	45	49	41	39	49	32	31	59	48	49	52	51	48	713
	252	20	0	93	1	7	20	3	9	15	11	9	15	24	2	374	0	3	7	3	1	5	0	14	9	10	6	8	0	188
		21	2	689	145	142	120	118	172	110	86	123	88	136	5	456	14	138	140	133	105	109	18	169	96	95	106	76	10	450
		22	4	388	68	65	65	64	74	81	99	66	72	62	3	726														
		23	7	125	16	13	15	21	12	37	32	25	26	31	0	345	4	13	8	13	13	8	2	28	23	14	20	20	0	296
	265	24	0	222	3	4	3	1	4	33	35	15	23	14	0	153	0	4	4	0	0	2	0	14	5	3	8	4	0	203
		25	0	11	1	1	1	1	1	23	27	16	23	27	0	388	6	23	19	12	14	6	2	17	38	20	16	29	0	381
		26	2	416	11	20	22	34	36	105	123	112	90	143	4	580	3	18	55	10	32	46	3	109	101	100	96	105	5	530
		27	2	88	8	18	6	6	3	37	30	34	26	31	5	173	0	11	6	7	7	9	4	30	24	17	24	13	5	162
		28	1	107	4	2	2	2	7	40	44	49	26	37	0	452	19	24	19	19	20	16	14	56	56	65	59	57	2	592
		29	13	119	23	23	13	18	19	70	63	57	40	40	13	504	0	1	3	1	3	2	0	8	16	15	13	20	0	207
	266	30	12	224	16	19	21	32	16	47	76	56	45	56	6	291	9	15	20	12	20	19	4	59	39	37	35	37	6	282
		32	0	28	4	6	4	3	2	12	15	20	20	13	0	288	4	23	10	11	9	8	3	22	12	13	19	21	0	180
		33	8	177	47	45	23	43	16	74	72	83	63	64	6	527	3	7	14	10	14	9	2	49	33	22	35	36	0	281
	267	34	1	380	6	7	8	9	24	43	44	64	51	48	0	503	0	7	8	7	3	8	0	41	45	39	38	34	0	421
		36	0	13	0	1	0	0	0	11	6	25	14	15	0	249	3	4	4	2	3	6	2	31	16	33	24	54	0	356
	268	38	11	176	16	24	14	14	11	59	53	60	61	64	5	39	5	10	3	14	8	11	3	42	40	22	15	39	5	46
		39	4	329	29	27	27	31	26	79	73	67	65	65	1	824	2	24	14	8	20	32	0	104	77	72	69	117	2	821
		40	0	6	0	2	0	0	0	45	48	39	50	30	0	324	3	5	1	1	5	0	1	32	36	29	22	28	0	219
		41	1	9	5	3	3	1	1	36	38	31	31	28	0	363	0	4	3	2	1	0	0	29	14	18	27	26	0	422
	269	45	3	162	20	21	19	27	14	52	50	53	52	43	3	722	1	9	4	12	4	11	1	58	45	53	39	54	8	604
		46	0	70	3	3	3	2	3	18	24	19	22	22	0	189	0	7	6	3	6	4	1	33	34	24	21	31	1	270
		47	0	55	1	1	1	2	3	31	27	34	33	25	0	380	0	1	1	0	2	1	0	26	23	29	24	37	0	316
		48	0	44	4	5	1	8	4	31	27	31	28	28	0	406	1	5	0	2	2	1	0	32	28	37	43	21	1	362
		49	10	475	61	63	68	51	74	147	117	133	106	129	16	557	16	52	29	43	48	64	8	154	148	128	94	142	8	521

Note – Table is continued on the next page.

Mode	Rat #	Neuron	2min post-SCS														5min post-SCS													
			1.4g						26g						Pinch		1.4g						26g						Pinch	
			BL	1	2	3	4	5	BL	1	2	3	4	5	BL		BL	1	2	3	4	5	BL	1	2	3	4	5	BL	
Tonic	249	1	17	28	30	35	25	19	12	33	43	65	58	47	13	444	18	26	31	22	36	21	12	54	43	47	27	45	12	429
		2	0	12	5	8	10	20	5	23	43	40	36	34	12	290	6	14	21	12	9	13	3	27	36	31	30	22	6	330
		3	9	18	14	15	17	5	1	24	18	29	20	28	14	676														
		4	15	24	21	15	12	16	7	28	27	19	37	60	1	501	23	22	22	19	13	11	9	43	66	33	44	70	1	418
		5	18	22	17	12	29	6	6	79	114	97	69	73	8	993	1	16	9	15	14	14	5	75	120	112	111	102	11	942
		6	25	38	39	31	32	36	30	33	54	38	53	54	32	597	13	23	18	24	24	28	20	50	47	43	36	36	22	468
	252	20	13	34	29	17	19	25	10	59	64	44	35	45	3	285	12	46	35	35	18	17	16	50	44	41	49	53	21	459
		21	7	65	40	40	53	22	6	87	104	67	55	93	7	367	17	127	154	88	116	107	8	101	116	125	128	67	1	299
		22	5	73	53	42	39	44	2	77	115	99	102	89	3	694	14	78	65	95	75	84	4	105	136	97	110	101	1	664
		23	11	20	14	14	12	11	6	28	23	23	25	33	1	334	14	30	23	23	24	28							13	430
	265	24	0	12	10	10	7	7	0	15	33	29	10	17	0	214	0	9	12	8	7	6	0	33	31	21	23	9	0	264
		25	0	10	2	2	1	1	0	15	27	11	16	34	0	416	0	3	3	2	5	3	0	15	37	12	25	31	0	352
		26	4	55	50	62	23	40	3	108	79	82	140	115	0	567	3	39	33	44	54	77	1	93	98	100	79	78	1	407
		27	3	4	3	6	6	4	4	44	15	32	29	25	2	169	8	7	6	18	14	9	6	41	32	21	28	26	8	238
		28	6	10	12	8	8	5	1	47	41	41	35	52	1	649	3	9	9	7	5	9	1	33	27	63	64	63	0	571
		29	2	10	7	4	8	6	2	25	26	25	27	36	0	195	2	7	3	9	12	5	1	32	39	29	40	48	4	360
	266	30	6	22	20	15	20	17	5	61	35	40	48	51	3	325	13	20	29	25	24	27	7	62	47	57	42	60	9	356
		32	8	10	10	10	10	9	0	22	20	20	17	24	0	162	3	16	10	11	9	13	1	17	22	28	20	33	0	199
		33	1	6	4	12	16	18	2	46	40	39	36	40	2	339	0	12	23	12	19	9	0	58	58	68	55	52	3	425
	267	34	1	7	3	3	3	5	0	57	41	44	40	39	1	455	2	3	3	5	5	6	1	54	57	57	43	46	0	336
		36	3	9	2	1	2	2	4	31	23	23	12	38	1	480	1	4	5	1	2	9	0	50	36	30	24	19	0	386
	268	38	6	6	11	20	12	8	0	19	26	26	19	15	3	89	3	17	10	7	8	9	0	32	15	19	21	17	0	147
		39	1	36	11	21	15	25	1	78	90	101	106	95	2	848	4	54	20	24	18	38	7	96	96	115	118	103	10	1015
		40	2	2	7	3	2	4	0	23	25	35	32	35	2	315	0	9	3	4	1	4	0	21	29	29	31	43	0	342
		41	0	6	4	1	3	5	1	27	30	29	30	44	0	329	7	26	7	4	5	3	2	36	25	24	34	63	0	407
	269	45																												
		46	0	0	2	4	3	6	3	41	40	18	38	33	3	381	3	7	3	4	6	4	0	39	34	28	25	60	1	315
		47	0	0	2	4	2	2	0	19	18	14	30	19	0	306	0	1	2	2	2	2	0	29	18	23	16	22	0	412
		48	0	1	3	3	1	1	0	14	39	11	25	19	0	391	4	6	6	13	16	18	9	48	45	27	25	19	1	421
		49	10	60	66	68	68	63	8	161	135	92	150	129	3	361	1	63	70	80	68	82	3	143	172	136	139	126	3	551

Note – Table is continued on the next page.

Mode	Rat #	Neuron	10min post-SCS														15min post-SCS													
			1.4g						26g						Pinch		1.4g						26g						Pinch	
			BL	1	2	3	4	5	BL	1	2	3	4	5	BL		BL	1	2	3	4	5	BL	1	2	3	4	5	BL	
Tonic	249	1	22	43	46	36	36	29	17	47	37	25	29	31	13	345	20	36	41	22	17	33	20	75	36	30	34	37	18	327
		2	17	24	23	21	22	15	15	53	28	23	37	39	6	441	16	39	33	20	30	27	18	42	44	28	34	56	10	415
		3																												
		4	19	30	19	15	18	13	9	55	45	34	41	35	3	529	24	26	23	22	20	18	13	88	73	60	75	65	3	458
		5	21	37	23	32	31	44	11	101	120	72	80	77	15	1197	22	41	58	27	46	43	21	114	84	118	96	84	15	935
		6	28	38	34	35	46	35	36	75	71	60	57	57	16	743	25	32	32	31	29	25	26	58	50	54	47	55	19	625
	252	20	28	47	44	23	39	22	15	82	70	63	44	64	10	468	11	18	19	21	16	25	17	43	49	33	27	34	18	500
		21	8	134	120	69	80	93	4	156	96	94	96	71	1	422	7	126	68	59	62	67	2	92	59	59	62	70	3	364
		22	9	60	31	65	33	38	4	91	49	90	89	52	4	809	13	49	52	72	56	79	9	124	122	108	113	104	1	745
		23	12	19	24	19	19	15	7	40	20	23	25	20	8	459	13	22	15	21	11	22	6	40	20	26	29	29	0	417
	265	24	0	9	11	11	3	6	0	24	22	12	19	25	0	252	0	20	15	15	5	4	0	24	27	19	8	17	0	193
		25	0	6	13	6	4	10	0	19	40	10	23	21	0	423	0	10	12	8	5	7	1	24	19	26	33	42	0	401
		26	0	27	69	35	55	44	2	89	70	76	100	125	1	570	8	63	39	49	52	52	4	83	63	97	79	104	5	513
		27	4	17	15	8	4	13	4	44	26	24	25	23	6	220	4	7	10	9	8	10	5	38	29	21	11	23	7	256
		28	3	3	2	6	1	4	0	44	40	42	28	37	0	445	1	7	3	3	6	3	1	44	55	32	47	42	0	500
		29	5	6	11	9	8	15	1	30	50	39	38	49	3	190	5	6	5	4	5	6	0	33	34	29	22	39	1	339
	266	30	12	20	29	21	15	27	0	63	39	54	41	73	9	381	16	30	26	34	26	25	8	47	54	62	42	51	4	348
		32	5	18	17	16	10	14	3	48	42	39	48	32	1	231	17	28	22	25	23	18	9	36	31	46	43	49	0	279
		33	4	12	11	11	9	13	3	48	46	51	51	40	5	361	0	4	11	4	5	12	2	48	59	57	33	50	2	305
	267	34	0	5	11	10	16	2	1	52	63	45	50	45	0	483	1	5	7	12	27	8	1	68	50	56	35	31	3	676
		36	0	6	9	8	6	10	0	40	36	42	46	49	0	458	1	12	14	8	11	8	2	85	68	38	54	57	2	536
	268	38	3	8	11	11	11	13	4	25	18	19	10	21	2	98	2	8	5	9	6	6	2	33	36	32	31	17	2	111
		39	2	76	54	29	21	23	8	115	105	89	111	133	6	849	7	24	43	17	45	26	6	106	102	102	97	85	13	831
		40	1	8	6	1	5	3	1	34	23	38	29	29	0	298	0	1	2	0	0	0	0	13	15	11	8	21	1	339
		41	0	14	5	4	0	1	0	39	42	27	37	50	0	432	9	20	17	11	12	16	0	68	55	41	41	44	3	450
	269	45																												
		46	2	11	10	6	7	9	0	65	58	49	61	49	2	351	2	9	10	11	7	13	7	37	49	50	37	28	0	313
		47	0	1	1	2	1	0	0	44	46	36	31	34	0	335	1	2	2	0	4	0	0	38	29	12	22	45	0	382
		48	0	0	6	3	1	3	0	25	37	42	44	57	3	399	0	2	5	2	2	3	0	36	17	29	42	35	2	365
		49	16	90	25	86	82	67	12	190	160	171	131	153	16	541	14	72	72	47	89	82	11	140	90	82	113	77	15	691

Note – Missing data points are from neurons that were lost during recording before completing the stimulation protocol.

Table D.8. Spike counts after burst or tonic SCS on day 7 following painful facet joint injury (Chapter 7).

Mode	Rat #	Neuron	pre-SCS baseline															0min post-SCS												
			Brush		1.4g vF					26g vF					Pinch			1.4g						26g						Pinch	
			BL		1	2	3	4	5	1	2	3	4	5	BL		BL	1	2	3	4	5	BL	1	2	3	4	5	BL	
Burst	213	1	8	158	9	15	15	16	14	54	39	35	44	37	6	908	8	21	17	20	11	28	12	52	43	41	52	34	20	719
		2	0	10	1	1	0	2	1	31	16	16	20	17	0	162	0	1	0	0	0	0	0	10	6	4	2	5	0	52
		3	0	81	55	37	25	50	21	58	66	75	65	96	0	414	1	8	9	16	6	4	0	46	55	53	57	41	0	305
	214	7	6	268	40	32	26	35	39	78	50	68	70	44	13	340	5	14	11	9	11	8	6	71	47	59	46	42	5	158
		8	0	0	0	0	0	0	0	2	5	1	3	4	0	200	0	0	0	0	0	0	0	6	10	5	6	6	0	81
		9	0	44	5	4	3	4	2	32	33	36	31	35	0	293	0	0	0	0	0	1	0	8	0	2	7	3	0	89
		10	1	136	22	12	16	14	16	58	56	62	73	80	6	1297	9	19	19	19	19	25	5	105	101	81	85	88	10	684
	217	11	0	22	11	11	22	5	8	43	34	22	18	24	0	254	0	12	14	14	6	2	2	55	39	44	27	37	0	169
		12	7	74	42	32	19	24	20	63	42	53	49	48	8	356	6	17	16	5	9	28	8	53	43	20	34	13	7	131
		13	17	95	33	15	25	20	16	95	93	45	69	74	0	773	0	9	3	0	2	0	9	46	47	40	37	25	0	458
		14	10	225	30	29	20	17	24	59	56	55	55	95	12	839	7	18	17	13	24	20	13	51	39	46	39	44	8	666
		15	4	255	37	52	35	38	25	70	51	45	45	45	7	551	7	28	23	27	22	34	8	79	65	57	59	49	15	524
	218	16	14	138	16	7	17	13	19	57	51	69	58	54	14	764	10	13	9	9	9	4	6	16	11	28	11	20	7	419
		17	3	155	19	16	11	26	12	49	45	50	36	27	5	475	4	9	21	7	2	5	2	34	39	38	39	33	3	291
		18	0	42	13	2	11	2	4	24	20	18	18	19	0	341	0	0	0	0	1	0	0	10	8	10	9	11	0	218
		19	0	283	17	7	7	9	5	93	87	76	64	52	0	686	1	33	21	22	25	10	5	95	56	53	51	46	0	449
		21	0	8	0	0	0	0	0	29	34	34	38	46	0	302	0	0	0	0	0	0	0	50	37	38	47	55	0	372
		22	0	154	18	16	12	17	17	56	54	53	60	43	2	226	0	16	8	11	14	16	0	71	57	34	44	38	4	220
		23	0	69	1	1	2	1	1	16	32	33	38	21	0	893	2	6	2	1	2	1	0	12	21	15	12	13	1	279
		23	1	113	7	6	11	8	9	50	59	47	57	48	1	382	1	13	3	2	7	6	2	40	40	37	41	50	3	173
	219	24	0	171	50	31	20	35	15	85	81	86	69	94	0	551	1	21	16	6	14	6	0	29	43	42	42	31	3	318
		25	23	124	33	26	34	29	31	42	45	38	41	39	11	500	0	0	0	0	1	2	4	16	12	12	5	10	4	303
		26	0	149	7	12	7	7	6	49	42	35	38	36	0	350	1	5	7	8	7	4	0	25	15	22	11	23	0	159
		27	1	148	22	23	18	8	13	40	37	54	33	44	0	477	1	8	10	4	7	10	0	30	23	33	30	31	0	215
		28	0	91	5	4	1	4	5	59	50	56	37	43	3	658	27	38	24	30	35	42	12	54	52	48	50	49	0	430
		30	0	50	8	4	8	2	9	33	28	36	28	31	0	153	0	2	15	4	15	11	0	22	15	29	21	22	0	106
	220	31	0	159	79	52	51	37	50	101	81	74	71	73	5	540	2	20	10	9	17	17	1	34	24	14	9	31	0	121
		32	3	67	2	2	4	5	1	27	18	22	14	24	4	147	0	3	4	0	4	0	1	17	15	19	11	11	1	33
		33	2	430	22	14	11	13	20	74	64	93	77	71	1	812	4	50	22	9	44	15	1	90	74	59	47	58	1	629
		34	1	133	17	14	12	8	10	60	54	69	100	84	0	666	0	18	10	17	11	10	4	56	42	29	42	31	0	202
	221	36	1	205	12	28	37	27	17	85	106	93	123	102	27	680	26	43	26	28	37	31	10	99	108	125	94	78	42	674
		38	4	387	7	11	14	13	12	46	63	76	55	81	2	480	4	16	14	11	10	14	3	76	47	64	60	67	4	228
		40	0	316	38	33	25	22	27	112	71	126	93	86	0	264	0	23	32	26	14	19	0	107	87	74	70	74	1	140
		41	0	121	11	6	3	3	1	26	21	14	17	20	0	142	0	2	1	2	1	3	0	13	28	19	15	18	0	91
	222	42	0	268	1	4	8	40	38	46	25	31	19	50	0	110	0	5	23	6	19	20	0	47	28	23	16	14	0	49

Note – Table is continued on the next page.

Mode	Rat #	Neuron	2min post-SCS														5min post-SCS													
			1.4g						26g						Pinch		1.4g						26g						Pinch	
			BL	1	2	3	4	5	BL	1	2	3	4	5	BL		BL	1	2	3	4	5	BL	1	2	3	4	5	BL	
Burst	213	1	13	23	14	29	14	21	8	57	45	51	36	37	29	514	14	22	19	25	32	21	15	65	43	53	61	64	13	725
		2	0	0	0	0	0	0	0	19	12	15	11	5	0	50	0	0	0	0	0	0	0	9	12	5	6	13	0	94
		3	1	7	4	15	10	7	0	40	31	26	27	19	2	286	1	3	6	20	4	19	0	34	87	57	38	40	0	330
	214	7	13	21	17	19	15	15	15	44	43	41	56	44	2	245	2	14	13	18	8	16	2	53	46	61	31	27	10	232
		8	0	0	0	0	0	0	0	5	2	1	0	1	0	68	0	0	0	0	0	0	0	9	6	4	7	4	0	97
		9	0	0	0	0	0	0	0	10	9	5	2	3	0	105	0	0	0	0	0	0	0	7	7	3	4	5	0	184
		10	10	27	21	22	21	24	3	105	77	85	81	96	9	662	5	22	18	26	26	21	6	172	151	129	132	114	4	803
	217	11	13	41	35	15	13	25	12	57	51	30	37	56	24	310	1	17	11	16	12	15	1	39	33	27	21	36	3	271
		12	5	22	15	10	19	8	1	44	33	33	32	30	8	185	8	22	16	13	22	11	13	35	36	23	32	28	11	242
		13	1	16	6	5	4	3	0	52	56	33	30	50	0	442	3	13	15	17	12	11	0	96	67	56	47	62	0	696
		14	10	25	27	17	22	15	8	47	81	40	32	39	12	669	14	16	15	24	16	24	13	51	60	73	58	44	10	646
		15	0	31	34	30	30	27	5	49	37	46	66	59	6	591	11	25	26	16	18	21	5	54	55	34	39	40	3	337
	218	16	0	1	0	2	2	0	0	6	17	10	22	14	2	444	0	0	0	0	2	1	0	10	17	20	18	21	0	466
		17	5	7	25	5	6	14	7	44	22	36	26	27	3	247	14	26	27	13	18	18	7	68	43	29	44	20	8	348
		18	0	0	0	0	1	1	0	14	15	16	14	18	0	283	0	0	0	0	0	0	0	15	15	17	17	19	0	267
		19	0	38	40	21	22	26	0	96	82	58	62	54	0	522	25	73	59	29	53	52	21	125	106	85	75	79	0	667
		21	0	0	0	0	0	0	0	76	42	46	31	19	0	459	0	0	0	0	0	0	0	29	16	87	58	65	0	320
		22	1	21	18	25	14	17	0	45	51	64	64	58	2	224	0	12	10	11	23	20	7	69	52	46	25	49	2	265
		23	0	1	1	2	1	3	0	22	29	16	14	20	0	347	1	4	1	0	0	0	1	22	23	14	23	26	0	507
		23	0	6	7	10	8	13	0	49	41	41	29	35	0	194	1	6	5	6	3	3	1	52	49	47	43	46	0	284
	219	24	0	17	8	4	11	24	3	55	48	56	51	64	0	355	3	28	32	13	23	23	5	65	64	64	47	62	3	326
		25	0	1	3	2	2	5	3	22	23	20	23	23	3	180	0	0	0	2	1	3	0	19	20	20	25	20	6	313
		26	0	7	1	6	7	5	0	25	30	24	36	28	0	193	0	9	6	2	6	7	0	22	39	32	44	31	0	366
		27	2	10	13	4	9	15	2	27	23	39	23	23	1	241	1	1	3	2	3	4	0	9	5	7	8	9	1	267
		28	6	15	15	20	27	34	2	37	41	44	39	42	23	465	0	5	4	10	9	11	6	52	53	49	53	58	12	514
		30	0	1	3	4	4	3	0	11	21	36	46	32	0	104	0	1	5	3	1	6	0	46	32	36	30	30	0	93
	220	31	4	12	10	15	18	13	2	18	22	25	23	28	2	170	6	18	15	24	20	23	6	34	28	26	24	24	4	182
		32	0	7	0	1	3	6	0	23	16	19	13	7	1	90	1	1	4	0	5	2	1	30	10	22	10	12	1	134
		33	0	61	26	29	17	8	0	106	81	70	33	31	2	642	3	67	24	17	30	22	2	101	99	62	63	60	1	757
		34	4	19	17	9	16	13	6	40	47	30	37	36	9	247	3	14	7	11	18	9	5	46	68	86	83	57	0	530
	221	36	17	20	30	18	6	11	3	85	53	81	76	80	0	942	35	41	42	40	49	17	27	101	90	98	36	74	0	665
		38	3	13	7	10	12	9	5	83	79	81	53	67	6	309	3	15	10	11	7	12	3	82	79	70	78	91	4	496
		40	0	29	22	26	23	19	1	129	83	92	76	89	1	219	5	33	21	29	27	22	1	103	87	90	81	78	1	202
		41	0	2	4	0	1	1	0	23	22	13	18	17	0	170	0	1	1	0	0	0	0	26	24	15	17	15	0	203
	222	42	0	6	7	7	8	4	0	34	21	19	20	13	0	112	0	8	11	1	4	9	1	29	14	12	13	14	1	108

Note – Table is continued on the next page.

Mode	Rat #	Neuron	10min post-SCS														15min post-SCS													
			1.4g						26g						Pinch		1.4g						26g						Pinch	
			BL	1	2	3	4	5	BL	1	2	3	4	5	BL		BL	1	2	3	4	5	BL	1	2	3	4	5	BL	
Burst	213	1	18	21	25	28	26	29	22	67	63	55	72	54	14	674	7	22	35	23	16	21	30	75	58	60	78	56	20	896
		2																												
		3	4	9	22	36	8	32	5	25	61	36	52	45	2	322	4	44	11	12	22	8	7	40	64	96	65	82	0	322
	214	7	8	24	21	33	22	19	4	40	46	41	72	55	9	317	7	11	15	23	20	12	4	36	45	59	39	44	8	325
		8	0	0	0	0	0	0	0	4	4	2	6	5	0	115	0	0	0	0	0	1	0	11	5	3	4	3	0	106
		9	0	0	0	0	0	0	0	22	16	7	10	9	0	200	0	1	1	0	0	0	0	34	34	30	23	29	0	214
		10	4	24	19	16	24	20	9	132	129	111	98	96	6	1188	1	32	24	16	21	22	6	179	135	132	125	116	10	1062
	217	11	3	12	10	10	7	4	1	38	25	23	28	20	3	157	0	11	7	11	9	18	7	45	44	42	23	33	16	283
		12	5	27	18	28	11	5	1	52	37	29	32	48	0	357	5	24	26	12	22	24	1	57	53	44	45	38	5	311
		13	7	21	11	21	13	15	18	56	54	84	28	84	0	669	10	19	15	18	17	18	10	75	62	46	59	65	0	669
		14	14	23	20	17	22	28	15	58	68	80	76	63	13	783	17	27	17	30	22	21	11	63	61	68	46	61	24	919
		15	4	36	32	39	33	39	4	47	49	36	48	54	5	418	1	19	28	18	11	12	2	41	45	47	65	65	0	313
	218	16	0	0	0	0	1	1	0	30	25	24	21	32	0	557	1	2	1	0	1	1	0	25	22	9	29	17	0	583
		17	2	8	11	26	16	24	15	46	43	26	41	46	5	415	9	17	15	18	18	15	7	60	47	47	35	39	6	438
		18	0	0	0	0	0	0	0	9	12	16	17	18	0	231	0	0	0	0	0	0	0	16	15	17	12	14	0	301
		19	4	21	30	17	21	19	2	97	94	81	58	53	0	613	27	111	53	67	37	38	7	77	62	47	70	71	6	643
		21	0	0	0	0	0	0	0	53	54	53	50	73	0	556	0	0	0	0	0	0	0	81	41	89	65	70	0	368
		22	0	15	21	25	29	10	7	76	65	62	52	48	4	279	2	22	12	11	18	21	2	45	71	62	60	47	2	320
		23	0	1	1	0	1	3	3	26	18	32	22	29	1	650	1	6	6	1	3	2	0	24	30	34	31	25	0	593
		23	1	5	4	7	5	7	3	60	37	47	49	38	2	365	0	7	10	3	6	1	1	50	53	48	39	41	1	393
	219	24	6	17	10	9	19	8	1	34	50	42	55	51	6	427	4	13	11	12	13	14	2	35	34	23	23	33	6	379
		25	0	0	0	0	0	0	0	20	26	26	29	36	4	420	0	0	0	0	0	0	1	19	27	16	17	22	2	442
		26	0	5	4	1	7	4	0	54	44	55	31	46	0	317	0	0	0	0	4	3	0	23	69	53	51	55	0	346
		27	1	2	8	6	4	5	3	23	31	27	27	29	12	366	1	4	2	2	6	5	0	14	22	15	19	13	2	192
		28	0	3	5	4	7	8	3	45	56	47	47	48	9	571	2	11	18	20	14	19	6	43	47	47	40	60	17	589
		30	0	13	5	12	6	14	0	40	32	36	39	32	0	148	0	3	6	4	3	4	0	19	21	21	33	26	0	164
	220	31	2	19	38	23	20	16	1	32	40	41	31	20	4	259	1	42	5	24	17	21	8	61	44	36	38	42	6	442
		32	2	1	4	4	5	2	3	24	27	13	17	19	2	114	1	0	3	4	1	5	1	30	20	16	16	19	9	144
		33	6	31	48	46	31	28	2	84	92	77	54	44	0	638	3	18	40	28	27	15	0	104	80	87	70	69	7	536
		34	2	13	16	16	11	18	5	46	85	105	96	106	7	586	2	11	16	9	8	12	0	61	76	87	74	82	3	646
	221	36	26	21	50	27	32	35	24	91	117	109	78	93	5	830	54	48	53	35	59	34	1	66	113	80	69	94	10	746
		38	0	14	11	7	6	19	2	108	93	90	97	96	1	460	2	12	19	3	8	19	5	92	87	65	74	79	1	654
		40	0	25	28	20	18	27	0	140	77	78	65	102	0	308	0	39	30	18	30	17	0	94	71	69	81	68	0	350
		41	0	1	2	0	1	1	0	23	23	20	15	22	0	139	0	6	4	1	2	2	0	29	19	20	14	24	0	159
	222	42	0	15	6	4	0	5	0	27	20	11	15	21	0	92	0	8	7	3	9	39	1	15	18	17	20	46	3	162

Note – Table is continued on the next page.

Mode	Rat #	Neuron	pre-SCS baseline															0min post-SCS													
			Brush		1.4g vF					26g vF					Pinch		1.4g						26g						Pinch	
			BL		1	2	3	4	5	1	2	3	4	5	BL		BL	1	2	3	4	5	BL	1	2	3	4	5	BL	
Tonic	213	1	6	115	28	11	17	22	11	92	78	52	57	70	2	1034	2	7	2	8	7	5	7	41	49	23	17	35	4	441
		3	7		44	11	12	22	8	40	64	96	65	82	0	322	3	23	34	3	6	4	2	22	28	39	42	20	0	167
		5	0	0	0	0	0	0	0	22	14	9	8	25	0	157	0	0	0	0	0	0	0	20	8	18	2	3	0	73
	214	6	0	227	19	22	20	14	18	38	46	65	62	53	0	234	2	30	45	43	27	31	4	39	72	39	61	54	3	216
		7	9	165	18	23	17	20	23	33	43	52	35	50	6	146	0	3	5	2	6	5	1	13	9	7	9	3	2	46
		8	0	1	0	0	0	0	0	13	12	11	14	14	0	172	0	0	0	0	0	0	1	1	3	4	3	6	0	45
		9	0	0	0	0	0	0	0	34	34	30	23	29	0	271	0	0	0	0	0	0	0	19	10	9	9	5	0	180
		10	5	179	6	8	10	11	7	33	47	35	56	32	6	318	9	17	15	22	7	18	10	39	30	42	41	38	4	254
	217	11	0	19	3	3	2	2	1	47	38	37	37	32	0	209	0	1	7	3	7	1	0	38	27	19	18	34	0	57
		12	4	99	36	34	20	20	23	45	43	40	30	37	1	398	4	19	15	12	14	13	2	57	42	34	38	31	2	309
		13	0	13	1	0	0	1	1	46	60	42	48	60	0	846	1	5	2	2	4	1	2	46	36	25	29	35	0	458
		14	12	190	30	35	26	19	22	56	85	102	86	74	16	832	15	14	17	22	18	24	14	75	56	98	85	86	24	644
		15	7	384	54	49	47	47	47	94	116	101	108	118	19	1104	11	56	64	63	42	54	21	98	115	69	92	78	22	595
	218	16	2	104	5	6	4	2	3	65	65	68	56	54	4	949	2	3	2	0	4	4	1	38	35	30	36	29	2	613
		17	4	367	28	39	20	17	35	72	55	46	54	33	7	372	4	20	7	19	10	8	1	46	38	38	32	41	2	307
		19	9	335	41	35	41	32	33	89	64	79	60	71	4	764	1	31	17	19	15	15	0	50	33	36	40	40	0	425
		20	2	96	37	37	29	24	38	63	75	55	73	55	0	210	0	22	14	31	14	16	0	57	55	67	54	53	0	60
		21	0	31	41	30	37	12	44	98	95	91	69	130	0	450	0	0	0	9	1	0	0	61	57	49	63	26	0	552
		22	1	269	17	17	32	36	16	56	57	61	59	45	0	296	2	19	15	39	21	16	4	52	58	40	42	45	2	173
		23	0	57	0	3	2	1	1	29	39	30	28	29	1	692	0	4	2	1	1	0	0	12	11	10	16	7	0	334
		23	0	121	5	3	9	6	9	56	56	55	46	45	0	420	0	10	8	5	1	5	0	39	48	44	26	30	0	240
	219	24	6	149	29	26	36	28	22	51	36	42	48	43	12	307	3	7	7	5	11	8	3	10	19	23	22	27	7	261
		25	9	106	9	10	5	14	15	60	40	31	44	45	5	374	1	5	5	3	11	19	12	32	36	38	38	28	23	431
		26	0	71	3	2	5	1	3	50	44	51	29	36	0	278	0	6	8	6	5	4	0	43	52	33	25	30	2	180
		27	0	170	6	10	9	8	11	36	27	35	58	58	1	459	2	6	11	8	14	11	3	47	49	50	49	61	0	222
		28	2	76	10	7	6	12	14	56	55	56	49	60	2	671	0	11	8	19	20	28	14	42	46	39	41	41	2	448
		29	0	43	4	3	4	2	2	10	7	12	9	9	0	408	1	1	3	0	3	2	0	12	7	7	6	6	0	372
		30	0	102	3	4	3	4	1	27	27	24	23	22	0	146	3	5	4	6	5	6	0	35	13	26	30	19	0	76
	220	31	4	190	29	13	30	19	23	48	36	42	44	54	3	330	0	22	23	18	25	14	5	42	40	35	29	39	2	269
		32	0	34	3	2	2	3	4	26	16	19	19	16	0	85	0	1	4	2	7	3	0	16	15	5	5	15	0	23
		33	2	454	54	25	20	18	25	92	85	89	58	64	1	684	8	40	19	24	14	11	0	79	78	51	41	60	4	641
		34	0	119	11	10	7	24	3	42	46	38	16	28	0	338	0	18	20	13	6	14	0	28	22	17	19	12	0	115
	221	36	0	221	10	15	9	11	5	60	52	56	61	71	1	776	4	30	25	12	9	16	3	45	69	63	57	52	0	352
		37	0	9	0	0	1	0	2	64	76	56	60	51	0	672	0	0	0	0	0	0	0	47	45	46	57	46	0	604
		38	3	250	10	6	5	9	14	81	77	91	107	100	3	932	2	15	19	12	16	13	2	95	76	52	85	67	6	401
		40	0	185	10	11	15	14	17	64	68	48	62	62	0	228	1	25	8	12	13	15	1	69	27	49	50	62	0	156
		41	0	99	0	0	0	1	1	23	13	17	13	17	0	190	0	0	0	0	1	0	0	17	20	19	9	23	0	98
	222	42	0	325	4	6	5	4	4	34	31	22	27	25	0	232	1	16	4	1	3	4	0	28	18	14	8	11	0	62

Note – Table is continued on the next page.

Mode	Rat #	Neuron	2min post-SCS														5min post-SCS													
			1.4g						26g						Pinch		1.4g						26g						Pinch	
			BL	1	2	3	4	5	BL	1	2	3	4	5	BL		BL	1	2	3	4	5	BL	1	2	3	4	5	BL	
Tonic	213	1	4	11	11	11	5	5	3	37	40	30	38	36	7	543	3	11	14	10	13	10	6	65	78	53	53	45	8	698
		3	0	4	3	4	2	2	1	23	21	19	24	22	0	99	4	8	2	11	5	11	0	22	21	34	23	19	0	122
		5	0	0	0	0	0	0	0	19	17	11	10	12	0	95	0	0	0	0	0	0	0	10	6	13	5	16	0	195
	214	6	5	34	27	27	27	46	3	44	56	63	40	46	4	273	9	31	17	16	19	33	7	68	76	49	31	66	11	157
		7	0	7	7	6	6	5	1	10	8	12	11	11	4	59	1	2	6	5	4	1	2	24	31	11	19	14	3	78
		8	0	0	0	0	0	0	0	2	6	7	4	5	0	44	0	0	0	0	0	0	0	2	9	2	5	1	0	130
		9	0	0	1	0	0	0	0	22	20	15	14	11	0	135	0	1	0	0	1	0	0	18	12	9	6	11	0	199
		10	1	14	15	17	18	14	6	29	43	33	36	35	6	266	5	21	15	13	12	9	5	38	36	33	29	30	20	361
	217	11	0	12	8	16	8	7	0	33	43	34	29	25	0	70	0	12	13	7	7	17	0	51	39	29	33	26	0	170
		12	3	26	18	12	12	30	5	62	56	54	40	36	7	269	2	5	19	17	14	19	5	42	31	44	36	33	3	246
		13	0	2	2	1	2	1	2	45	34	50	50	18	0	404	0	6	6	2	3	6	0	46	36	46	58	63	0	655
		14	11	26	32	21	23	16	14	100	64	92	72	78	14	852	22	34	26	32	27	27	20	74	91	85	79	78	28	991
		15	24	60	63	42	39	43	14	96	74	69	64	68	20	550	5	52	33	41	54	48	13	80	70	78	64	68	11	673
	218	16	3	1	0	2	4	0	0	29	39	45	32	23	3	604	1	0	1	0	2	1	1	39	44	45	45	42	1	645
		17	5	9	11	7	10	10	2	43	39	27	12	13	8	302	6	15	29	44	17	15	1	66	40	38	35	26	1	340
		19	0	21	42	27	24	20	1	86	79	63	49	50	1	416													0	457
		20	0	36	38	38	29	39	0	48	56	59	62	59	0	67	1	43	53	46	30	38	0	67	65	74	75	71	1	193
		21	0	0	2	7	9	4	0	89	58	8	62	89	0	557	0	38	35	37	2	6	0	69	19	23	51	42	0	490
		22	0	12	16	8	12	18	0	65	68	53	74	44	6	257	1	7	7	20	15	11	1	52	66	53	48	48	1	220
		23	1	1	1	2	0	1	0	18	16	13	20	12	1	405	0	3	2	0	1	0	0	17	23	6	29	16	0	559
		23	1	5	4	5	3	4	3	51	39	29	24	36	1	227	1	4	9	4	5	8	1	43	39	32	39	48	0	304
	219	24	4	6	11	10	9	2	1	31	27	16	32	16	3	222	3	9	6	4	4	10	5	28	32	23	33	40	1	252
		25	3	12	8	14	27	14	5	25	28	38	26	27	21	328	1	1	1	1	1	3	8	32	24	24	27	27	3	381
		26	1	12	2	14	1	9	0	55	50	43	37	52	0	290	1	16	8	6	19	4	1	54	52	46	41	38	1	383
		27	0	12	5	6	15	7	4	37	41	36	31	37	0	401	11	21	15	8	9	10	2	39	42	40	38	50	3	511
		28	0	9	29	34	39	28	4	46	37	37	52	43	26	452	3	8	8	16	22	25	18	48	38	45	45	43	33	617
		29	0	2	5	3	3	3	0	12	6	11	23	15	1	338	1	2	1	2	3	3	0	10	8	31	27	32	1	378
		30	0	2	4	5	6	5	0	33	33	35	31	30	1	162	0	6	4	4	4	9	0	39	27	24	33	37	0	203
	220	31	6	34	27	23	25	34	2	65	64	41	45	46	7	355														
		32	0	4	4	2	4	3	0	11	9	19	12	23	0	43	3	2	4	1	3	2	0	16	18	16	14	11	0	129
		33	2	25	33	15	28	15	1	79	97	55	30	39	7	520	2	33	36	37	31	20	8	99	86	81	71	71	5	689
		34	0	10	9	13	10	13	0	25	38	22	26	32	0	189	0	11	15	14	12	10	3	35	21	21	24	23	0	308
	221	36	29	53	27	30	32	32	20	58	82	91	40	80	2	553	6	24	17	26	20	4	3	54	55	61	36	52	0	600
		37	0	0	0	0	0	0	0	51	53	52	51	41	0	504	0	0	0	0	0	0	0	50	63	42	38	50	0	545
		38	3	12	20	35	48	26	2	97	68	78	83	101	37	486	6	6	14	8	22	8	3	76	71	69	88	64	2	574
		40	0	24	11	16	17	18	0	97	32	29	41	49	0	176	0	29	17	21	21	25	0	104	67	43	55	70	0	257
		41	0	1	0	3	2	1	0	22	18	16	17	19	0	94	1	4	3	1	2	1	0	32	23	19	19	25	0	135
	222	42	1	7	4	5	6	2	1	25	15	14	13	8	0	106	0	20	8	12	1	41	0	35	19	14	26	28	0	129

Note – Table is continued on the next page.

Mode	Rat #	Neuron	10min post-SCS														15min post-SCS													
			1.4g						26g						Pinch		1.4g						26g						Pinch	
			BL	1	2	3	4	5	BL	1	2	3	4	5	BL		BL	1	2	3	4	5	BL	1	2	3	4	5	BL	
Tonic	213	1	10	10	13	20	9	15	6	62	56	52	72	59	12	923	7	11	22	8	20	14	12	72	63	58	51	41	16	761
		3	1	6	6	2	3	3	6	14	16	24	33	14	0	150	0	8	10	6	9	4	0	20	10	9	11	10	0	161
		5	0	0	0	0	0	0	0	21	14	17	10	18	0	140	0	0	0	0	0	0	0	17	17	9	14	18	0	172
	214	6	1	15	16	26	16	17	6	28	21	29	25	27	14	121	0	17	16	13	22	19	0	28	29	32	41	46	23	205
		7	1	4	8	7	6	8	3	20	10	7	3	10	4	89	2	1	4	2	4	0	0	12	13	9	7	7	2	37
		8	1	1	0	0	1	1	0	6	10	8	4	5	6	143	0	0	0	0	0	0	0	1	0	1	2	0	0	90
		9	0	0	1	0	0	0	0	16	11	12	12	11	0	257	0	1	0	0	0	0	0	24	16	7	13	16	0	255
		10	2	14	11	11	8	10	2	27	22	27	24	14	6	258	4	13	9	13	10	11	1	27	28	40	27	39	5	286
	217	11	0	22	31	51	50	27	0	45	59	35	34	39	0	198	0	36	22	21	21	12	0	75	45	35	46	41	0	222
		12	2	22	17	22	10	12	2	48	32	16	37	26	4	248	1	5	18	11	8	3	0	35	27	29	24	46	2	328
		13	9	17	10	10	18	11	10	67	56	74	86	61	0	729	17	33	15	25	20	16	13	95	93	45	69	74	0	773
		14	17	28	45	29	43	30	20	57	64	45	67	74	18	807	25	34	32	30	31	17	9	85	70	89	90	55	9	930
		15	6	41	37	43	42	45	5	95	88	69	73	56	17	595	3	28	41	30	33	43	11	67	61	57	52	68	6	515
	218	16	1	3	1	0	0	1	0	41	51	35	51	47	1	607	1	0	0	0	1	0	0	37	20	33	28	27	1	666
		17	4	29	15	13	13	20	0	41	38	21	23	32	2	379	22	35	53	21	28	22	4	59	51	118	48	77	0	580
		19																												
		20	0	36	40	28	20	26	0	69	61	63	55	53	0	192	0	32	44	42	32	25	1	79	67	62	71	50	3	107
		21	0	32	23	7	36	17	0	41	32	44	70	45	0	300	0	31	25	28	4	39	0	52	82	26	83	80	0	461
		22	2	16	12	9	22	18	0	61	66	59	49	70	6	313	3	9	11	17	16	25	0	52	62	57	64	56	2	254
		23	18	20	18	20	20	9	12	29	21	18	17	24	18	1050	3	1	3	13	5	2	2	19	22	23	21	17	7	965
		23	0	7	7	5	12	9	1	46	46	32	40	39	0	490	0	11	7	11	5	6	2	57	66	45	49	44	0	449
	219	24	2	9	13	23	13	21	3	27	42	51	43	46	3	240	4	18	16	16	18	12	2	41	34	35	36	38	3	381
		25	0	2	1	2	1	4	4	23	25	21	25	29	7	450	14	18	24	21	19	18	19	33	47	46	47	47	11	484
		26	7	8	31	20	5	12	0	58	60	42	53	53	1	446	0	3	4	2	3	2	0	41	53	33	41	42	3	377
		27	1	7	10	9	5	11	3	41	52	37	66	43	2	492	7	22	17	11	16	12	1	49	32	31	34	41	4	633
		28	2	1	6	3	9	9	6	40	49	45	37	42	23	604	4	5	6	6	5	10	0	35	40	32	37	45	10	402
		29	2	8	7	17	7	8	2	24	14	20	22	17	0	188	5	12	22	11	20	19	7	21	35	26	33	19	5	333
		30	0	4	6	2	8	2	0	22	26	23	23	37	2	109	0	1	0	0	0	1	0	24	29	20	17	24	1	154
	220	31																												
		32	4	3	2	2	1	1	1	19	30	20	12	10	7	149	2	1	1	5	2	1	0	22	17	13	19	17	2	122
		33	0	18	13	26	34	37	5	83	83	61	82	59	8	714	2	63	25	29	41	16	5	67	90	109	75	70	6	781
		34	1	12	22	21	18	11	1	55	59	67	63	52	0	601	6	39	17	14	11	12	2	57	39	59	80	92	2	265
	221	36	6	22	33	12	9	13	5	64	55	43	56	51	2	523	31	44	39	50	29	36	27	65	73	66	72	55	0	549
		37	0	0	0	0	0	0	0	50	64	55	66	67	0	423	0	0	0	0	0	0	0	18	19	15	37	37	0	340
		38	2	12	11	14	12	12	4	57	74	68	55	62	1	432	5	10	9	10	14	5	1	86	61	57	65	67	1	607
		40	0	27	22	13	13	9	0	107	42	61	53	61	0	276	0	32	21	26	26	29	0	149	97	112	92	77	0	253
		41	0	2	0	0	1	2	0	14	26	23	25	15	0	243	0	3	2	1	1	4	0	26	24	27	22	19	0	163
	222	42	1	17	17	1	3	7	3	16	13	10	13	9	1	175	3	6	0	5	10	6	0	45	20	30	22	21	0	118

Note – Missing data points are from neurons that were lost during recording before completing the stimulation protocol.

APPENDIX E

Customized Matlab Codes

This appendix includes the Matlab codes that were used in the studies throughout this thesis. A Matlab code was used for densitometric quantification of fluorescent immunolabeling in the studies in Chapters 4 and 5 (Section E.1). This code requires that all images be located in the same file directory. Prior to running this script, the detection threshold (0-255) should be defined separately for both the red and green channels based on the threshold to detect positive labeling in tissue from naïve rats. The code detects all of the pixels that exceed those defined threshold in the red and green channels, and also identifies pixels with colocalized red and green labeling. The code generates an Excel file containing the filenames of each image. The output variables can be manually copied and pasted from the Matlab Variable Editor into the Excel file to correlate each image filename with the fraction of positively-labeled red, green, and colocalized pixels in that image.

Section E.2 details the code used to generate the maximum intensity projections (MIP) from each set of three images in confocal image stacks of spinal cord sections labeled with synaptic markers. This code was used for the studies in Chapter 5. Image stacks should be contained in sequentially named folders (i.e., stack1, stack2, stack3, etc). The code loads all images within a stack folder using the naming convention “image#” (i.e., image1, image2, image3, etc). If the image stacks or image files are named using a different convention, the code should be altered at the indicated lines in Section E.2 in

order to recognize the image stack folders and image filenames. The code loads each set of three images and separately compares the pixel intensity in the three images at each pixel location in each channel. A new image is constructed by taking the highest-intensity red and green pixels at each pixel location from the three constituent images, and the resulting MIP is saved with a new filename.

Section E.3 includes the Matlab code used to quantify the percent area of tissue in immunolabeled spinal cord sections for studies in Chapter 5. The code allows a user to iteratively set a threshold to create a black and white mask that discriminates immunolabeled tissue (white) from holes, gaps, and unlabeled regions in the image (black). The code then quantifies the fraction of pixels in the image that represents immunolabeled tissue, and outputs the result to the Matlab workspace.

E.1 Densitometry Code

```
clear all;
close all;

%Identify and load images based on common prefix
D = dir('*.tif');
IPfname = 'NDC_TSP4_GFAP_07-9-13';
OPfile = strcat(IPfname, '.xls');
fid = fopen(OPfile, 'w');

%Set thresholds for red and green channels
red_thresh = 115;
green_thresh = 165;
% higher value corresponds to more positive pixels
h1 = waitbar(0,'Please wait...');

for k=1:length(D);
    %Read file in
    file=D(k).name;
    %Load the image
    imag_orig = imread(file);
    imag_red = imag_orig(:,:,1);%grab the green/red labeled image
    imag_green = imag_orig(:,:,2);%grab the green labeled image
    %Take the inverse of the image
    imag_red = uint8(-double(imag_red) + 255);
```

```
imag_green = uint8(-double(imag_green) + 255);
%Calculate number of pixels
[a b]=size(imag_red);
tsize=a*b;
low=double(min(imag_red(:)));
high=double(max(imag_red(:)));
whiteSpace = 0.85*high;


%calc percent of positive pixels in tissue for red signal
backg=sum(sum(imag_red > whiteSpace));
posp=sum(sum(imag_red < red_thresh));
red_avg(k)=mean(imag_red(imag_red<red_thresh));
percpos(k)=  posp/(tsize-backg);

%calc percent of positive pixels in tissue for green signal
backg_green=sum(sum(imag_green > whiteSpace));
posp_green=sum(sum(imag_green < green_thresh));
percpos_green(k) = posp_green/(tsize-backg_green);
green_avg(k)=mean(imag_green(imag_green<green_thresh));


%map out pos and neg pixels
pmap_red=(imag_red < red_thresh);
nmap=(imag_red > whiteSpace);
pmap_green = (imag_green < green_thresh);

%make positive pixels  green, and background pixels blue
imag1(:,:,1) = zeros(a,b);
imag1(:,:,2) = pmap_red;
imag1(:,:,3) = zeros(a,b);
imag2(:,:,1) = zeros(a,b);
imag2(:,:,2) = pmap_green;
imag2(:,:,3) = zeros(a,b);


%Create a new image for the co-localization
[R, C] = find(pmap_red == 0);%
imag_co = imag2;
for ind = 1:length(R)
    imag_co(R(ind),C(ind),2) = 0;
end

%calculate the number of green positive pixels relative to total
%number of pixels that express red(gfap/map2, etc.)
tot_green(k) = length(find(pmap_green == 1));
tot_co(k) = length(find(imag_co(:,:,2) == 1));
col_per_red(k) = tot_co(k)/posp; %amount col per red area
perc_co(k) = tot_co(k)/(tsize-backg_green);

%Print name of image in Excel file
fprintf(fid, '%s \n', D(k).name);

%Image the red and green channels with positive pixels
```

```
    imag_red_channel = imag_orig;
    imag_red_channel(:,:,2:3)=0;
    imag_green_channel = imag_orig;
    imag_green_channel(:,:,[1,3])=0;
    figure; image(imag_red_channel)
    figure; image(imag1)
    figure; image(imag_green_channel)
    figure; image(imag2)


    %saveas(h, ['colocalize-' D(k).name], 'jpg')
    waitbar(k/length(D))
    clear imag imag1 imag2 R C
end

%Format output to copy and paste into Excel file
out1=percpos_green';  %overall fraction green pixels
out2=percpos';   %overall fraction red pixels
out3=perc_co';   %overall fraction colocalized pixels
out4=col_per_red';   %colocalized pixels as fraction of red-positive
close(h1)
status = fclose(fid);
```

E.2 Create Maximum Intensity Projections from Confocal Image Stacks

```
for k=1:INSERT NUMBER OF STACKS

    %name of folder containing image stack MODIFY STACK NAMES HERE:
    foldername=['stack', num2str(k)];

%set working file directory to the location of the image stack
cd(['E:\Nate\Imaging and Staining\synapse counting\BPD4 synapses\',
foldername])

%specify image naming convention (* = wildcard character so that the
directory function (dir) will locate all filenames containing "image"
followed by any other character or number) MODIFY IMAGE NAMES HERE:
di = dir('image*.tif');

%load all images from image stack (comment out lines if stack is fewer
than 12 images)
A = imread(di(1).name);
B = imread(di(2).name);
C = imread(di(3).name);
D = imread(di(4).name);
E = imread(di(5).name);
F = imread(di(6).name);
G = imread(di(7).name);
H = imread(di(8).name);
I = imread(di(9).name);
J = imread(di(10).name);
K = imread(di(11).name);
L = imread(di(12).name);
```

```
MIParray1 = zeros(size(A));
MIParray2 = zeros(size(A));
MIParray3 = zeros(size(A));
MIParray4 = zeros(size(A));

%select the pixel at each coordinate location with the highest
intensity from among the 3 constituent images
for i=1:3
    for j=1:size(A,1)
        for k=1:size(A,2)
            MIParray1(j,k,i) = max([A(j,k,i) B(j,k,i) C(j,k,i)]);
            MIParray2(j,k,i) = max([D(j,k,i) E(j,k,i) F(j,k,i)]);
            MIParray3(j,k,i) = max([G(j,k,i) H(j,k,i) I(j,k,i)]);
            MIParray4(j,k,i) = max([J(j,k,i) K(j,k,i) L(j,k,i)]);
        end
    end
end

MIPimg1 = uint8(MIParray1);
MIPimg2 = uint8(MIParray2);
MIPimg3 = uint8(MIParray3);
MIPimg4 = uint8(MIParray4);
imwrite(MIPimg1,'MIP_um1.tif','tif','compression','none')
imwrite(MIPimg2,'MIP_um2.tif','tif','compression','none')
imwrite(MIPimg3,'MIP_um3.tif','tif','compression','none')
imwrite(MIPimg4,'MIP_um4.tif','tif','compression','none')

clearvars -except k
close all
end
```

E.3 Quantify the Percentage of Tissue Area in Immunolabeled Sections

```
%specify the filenames of each maximum intensity projection for which
the tissue area will be quantified
names=['MIP_um1.tif'; 'MIP_um2.tif'; 'MIP_um3.tif'];
file = names(k,:);
t=imread(file);

%Load image and follow command line prompts to interactively choose
threshold for detection of tissue area
if k==1
    trig=0;
    while trig==0;
        close all
        bwthresh=input('select b/w threshold (start at 0.06): ');
        tt=im2bw(t,bwthresh); %adjust BW threshold based on image
brightness to get good mask
        figure;
        subplot(1,2,1),imshow(t)
        subplot(1,2,2),imshow(tt)
        trig=input('0 to reset baseline, 1 to move on: ');
    end
```

```
else
    tt=im2bw(t,bwthresh);
%     figure;
%     subplot(1,2,1),imshow(t)
%     subplot(1,2,2),imshow(tt)
end

%% Find regions with area and all pixels in each region
S=regionprops(tt,'Area','PixelList');
c=struct2cell(S);
A=(cell2mat(c(1,:)))';

%Find regions with pixel count under threshold and fill in as
background
thresh1=100;
fill1=tt;
for i=1:numel(A)
    if A(i)<thresh1
        pix=c{2,i};

        for j=1:size(pix,1)
            fill1(pix(j,2),pix(j,1))=0;
        end
    end
end

%Invert image and repeat filling process for tissue areas
ttt=imcomplement(fill1);
S2=regionprops(ttt,'Area','PixelList');
c2=struct2cell(S2);
A2=(cell2mat(c2(1,:)))';

thresh2=100;
fill2=ttt;
for i=1:numel(A2)
    if A2(i)<thresh2
        pix=c2{2,i};

        for j=1:size(pix,1)
            fill2(pix(j,2),pix(j,1))=0;
        end
    end
end

tissArea(k)=bwarea(imcomplement(fill2))/numel(fill2);

figure;
subplot(2,2,1),imshow(t)
subplot(2,2,2),imshow(tt)
subplot(2,2,3),imshow(imcomplement(fill2))
%Read out threshold value and tissue area percentage
bwthresh
tissArea
```

APPENDIX F

Protein Quantification in the DRG and Spinal Cord using Western Blot

This appendix itemizes the quantification of proteins from the dorsal root ganglia (DRG) and spinal cord tissue for the studies using Western blot in Chapters 4 and 5. Table F.1 details the quantification of proteins in the spinal cord tissue from the rats that underwent sham or painful facet joint injury followed by intra-articular injections of bupivacaine (BP) or a saline vehicle (VEH) in the studies presented in Chapter 4. Injections were administered immediately (*inj-BP0h*, *inj-VEH0h*, *sham-VEH0h*) or at day 4 (*inj-BPd4*, *inj-VEHd4*, *sham-VEHd4*) after injury. Quantified proteins included glutamatergic signaling proteins (ERK, pERK, NR1, pNR1, mGluR5, GLAST, GLT1) and glial fibrillary acidic protein (GFAP) as an indicator of astrocyte activation. The levels of each protein in each rat were normalized to β-tubulin to control for the amount of protein loaded for each sample, and then normalized to the average of the sham group for each treatment time point.

Quantification of β-tubulin, TSP4, and TSP4 normalized to the average of the sham group in the DRG and spinal cord at days 1 and 7 after sham or painful facet joint injury are summarized in Table F.2 (for studies in Chapter 5). Similarly, Table F.3 includes the quantification of β-tubulin TSP4 in the spinal cord at day 7 after painful facet joint injury with daily administration of TSP4 antisense or mismatch

oligonucleotides, for studies that are also included in Chapter 5. Table F.3 also includes TSP4 normalized to the average of the group receiving mismatch oligonucleotides.

Table F.1. Western blot quantification of glutamatergic signaling proteins and GFAP on day 7 for bupivacaine treatment study, normalized to sham for each treatment time point (Chapter 4).

	Rat #	ERK	pERK	NR1	pNR1	mGluR5	GLAST	GLT1	GFAP
inj-BP0h	41	1.20	0.80	0.61	0.33	0.92	1.11	0.75	1.23
	42	0.54	1.52	0.87	0.36	1.52	1.27	0.84	2.36
	43	0.80	0.89	0.68	1.43	1.41	1.00	1.02	1.17
	46	0.79	0.84	1.14	n/a	0.71	0.21	0.84	2.12
	49	1.29	n/a	1.63	0.17	0.67	0.60	n/a	2.65
	51	0.77	0.63	0.76	0.13	1.26	0.63	0.73	1.92
inj-VEH0h	45	0.83	0.72	0.65	8.11	1.58	1.88	0.67	1.85
	48	0.77	1.58	0.87	1.32	1.15	1.60	0.78	1.75
	50	0.63	3.44	1.10	n/a	1.15	0.93	n/a	2.62
	52	0.75	1.95	1.25	2.99	1.66	1.44	0.66	2.27
	53	1.04	2.02	1.33	7.63	1.86	1.62	0.76	2.06
	54	0.90	1.76	1.29	5.62	2.14	1.64	0.46	2.16
	72	0.90	1.51	1.33	1.01	1.90	1.30	0.38	1.40
sham-VEH0h	78	0.88	0.71	1.33	0.05	0.98	1.20	n/a	1.14
	79	n/a	1.23	0.95	0.07	0.83	0.79	n/a	0.77
	80	0.96	0.53	1.10	0.30	0.90	0.97	0.90	0.79
	81	0.67	0.61	1.25	0.17	1.29	0.88	1.32	0.90
	133	1.10	1.16	0.53	2.05	n/a	n/a	0.94	1.05
	134	1.39	1.75	0.84	3.36	n/a	1.16	0.84	1.35
inj-BPd4	53a	0.95	1.19	1.74	1.35	1.38	2.18	0.36	1.33
	56	0.87	n/a	0.58	1.21	1.41	2.07	0.35	1.03
	63	1.06	2.24	1.17	1.59	1.90	3.02	0.66	1.95
	64	1.05	1.32	0.58	1.22	1.71	1.90	0.35	1.03
	70	1.27	1.49	0.85	1.92	1.68	1.96	0.52	1.09
inj-VEHd4	52a	1.12	1.05	0.88	1.43	1.28	2.74	0.57	1.06
	54a	0.80	1.63	0.90	0.68	1.59	2.02	0.24	1.04
	65	1.20	1.52	2.06	1.45	1.53	3.75	0.19	1.39
	66	1.31	1.73	0.62	2.46	2.45	3.30	0.25	2.05
	67	1.34	1.36	1.99	n/a	2.48	3.19	0.54	1.17
	69	1.09	2.83	1.15	1.51	1.74	3.98	0.25	2.06
	71	n/a	1.17	n/a	1.75	n/a	2.46	n/a	1.27
sham-VEHd4	132	0.85	0.99	1.86	0.96	0.70	0.62	0.53	0.86
	135	1.08	1.79	0.79	1.55	0.98	1.18	0.95	1.01
	136	1.25	0.52	0.76	1.21	1.28	1.12	0.93	1.19
	137	0.99	0.73	0.60	1.01	1.04	1.34	1.03	1.28
	138	0.93	0.92	0.38	0.84	0.92	0.84	1.16	0.81
	139	0.98	1.26	0.75	0.75	1.01	1.01	1.20	0.96
	140	0.92	0.80	1.86	0.68	1.07	0.90	1.19	0.89

n/a = data not collected due to inconsistent protein transfer pattern

Table F.2. Western blot quantification of DRG and spinal TSP4 on day 7 after sham or painful facet joint injury (Chapter 5).

	Group	Rat #	β-tubulin	TSP4	TSP4 Normalized to Average of Sham for Each Time Point
DRG D1	Injury	273	38.44	0.29	0.45
	Injury	278	46.17	0.18	0.23
	Injury	279	38.51	0.33	0.52
	Injury	280	41.97	0.63	0.90
	Injury	287	35.67	0.23	0.39
	Injury	292	38.44	0.40	0.63
	Injury	296	41.89	0.58	0.83
	Sham	274	29.85	0.50	1.01
	Sham	275	33.73	0.80	1.43
	Sham	281	37.21	0.35	0.57
	Sham	293	28.91	0.57	1.19
	Sham	300	33.64	0.45	0.81
DRG D7	Injury	249	54.63	1.53	0.42
	Injury	254	37.32	0.64	0.25
	Injury	255	44.32	0.79	0.26
	Injury	264	53.57	1.43	0.40
	Injury	265	40.29	2.27	0.84
	Injury	266	41.19	2.35	0.85
	Injury	268	49.95	1.83	0.54
	Injury	271	44.70	0.39	0.13
	Sham	253	36.27	4.07	1.67
	Sham	256	39.55	3.91	1.47
	Sham	257	36.58	1.53	0.62
	Sham	262	36.58	3.36	1.36
	Sham	263	26.97	1.17	0.64
	Sham	267	28.73	0.46	0.24
Spinal Cord D1	Injury	273	29.60	21.60	0.99
	Injury	278	29.00	27.30	1.28
	Injury	279	28.60	26.40	1.26
	Injury	280	29.70	26.90	1.23
	Injury	287	29.70	24.60	1.13
	Injury	292	30.70	27.70	1.23
	Injury	296	31.00	29.20	1.28
	Injury	299	26.90	25.10	1.27
	Sham	272	25.50	22.80	1.22
	Sham	274	22.00	18.30	1.13
	Sham	275	27.80	18.20	0.89
	Sham	281	27.50	15.40	0.76
	Sham	293	29.20	17.50	0.82
	Sham	300	32.60	28.20	1.18

Note – Table is continued on the next page.

	Group	Rat #	β-tubulin	TSP4	TSP4 Normalized to Average of Sham for Each Time Point
Spinal Cord D7	Injury	248	17.92	1.97	1.54
	Injury	254	18.65	1.48	1.11
	Injury	255	21.54	1.53	1.00
	Injury	264	20.26	0.31	1.34
	Injury	265	18.76	0.38	1.78
	Injury	268	22.70	0.34	1.31
	Injury	271	19.25	0.36	1.64
	Sham	252	17.93	1.31	1.02
	Sham	253	15.06	1.41	1.31
	Sham	256	17.76	1.20	0.95
	Sham	257	19.95	1.29	0.91
	Sham	262	7.11	0.04	0.49
	Sham	263	15.28	0.21	1.20
	Sham	267	20.21	0.20	0.87
	Sham	270	16.21	0.23	1.24

Table F.3. Western blot quantification of spinal TSP4 on day 7 after painful facet injury with administration of antisense or mismatch oligonucleotides (Chapter 5).

	Rat #	β-tubulin	TSP4	TSP4 Normalized to Average of Mismatch
Injury + TSP4 Antisense Oligonucleotides	229	18.21	0.35	0.60
	231	20.43	0.58	0.88
	236	18.94	0.34	0.56
	237	25.54	0.68	0.83
	241	23.91	0.35	0.46
Injury + TSP4 Mismatch Oligonucleotides	232	21.92	0.37	0.53
	233	17.79	0.74	1.30
	234	20.15	0.79	1.22
	238	25.24	0.87	1.07
	239	24.15	0.82	1.06
	240	26.70	0.71	0.83

APPENDIX G

Quantification of Immunolabeled Proteins in the Spinal Cord

This appendix summarizes the quantification of immunolabeled proteins in the spinal cord in the studies presented in Chapters 4 and 5. Immunolabeling was quantified by densitometry using a custom Matlab code (see Section E.1 of Appendix E), and data in each table are presented as the fraction of positively-labeled pixels in each image. In each table, images are identified by the group, rat number, and image number that includes the side of the spinal cord (L or R for the left or right side) and the tissue section number (consecutive sections were numbered 1-6 on each slide). Table G.1 details the quantification of phosphorylated NMDA receptor subunit NR1 (pNR1), metabotropic glutamate receptor mGluR5, and glial fibrillary acidic protein (GFAP). Proteins were quantified in the superficial dorsal horn at day 7 after sham or painful facet joint injury followed by intra-articular bupivacaine (BP) or saline vehicle (VEH) injections either immediately (*inj-BP0h*, *inj-VEH0h*, *sham-VEH0h*) or at day 4 (*inj-BPd4*, *inj-VEHd4*, *sham-VEHd4*) after injury, in the studies presented in Chapter 4. Figure G.1 presents representative images of spinal dorsal horns labeled for mGluR5 and GFAP, and Figure G.2 presents representative images of spinal dorsal horns labeled for pNR1 and GFAP from each rat in each group.

Tables G.2 and G.3 summarize the quantification of thrombospondin-4 (TSP4), GFAP, and colocalized TSP4 and GFAP (Coloc) in the superficial dorsal horn (DH), dorsal columns, and deep dorsal horn in the studies presented in Chapter 5. Table G.2 presents the quantification of TSP4 and GFAP at day 7 after sham or painful facet joint injury. Figure G.3 presents representative images of TSP4- and GFAP-labeled superficial dorsal horns, deep dorsal horns, and dorsal columns of spinal cords from each rat at day 7 after sham or painful facet joint injury. Table G.3 lists the quantification of TSP4 and GFAP at day 7 after sham or painful facet joint injury followed by BP or VEH injections immediately (*inj-BP0h*, *inj-VEH0h*, *sham-VEH0h*) or at day 4 (*inj-BPd4*, *inj-VEHd4*, *sham-VEHd4*) after injury. Figures G.4-G.6 present representative TSP4- and GFAP-labeled images of the superficial dorsal horn (G.4), deep dorsal horn (G.5), and dorsal columns (G.6) of spinal cords from each rat in each group.

Table G.1. Densitometric quantification of pNR1, mGluR5, and GFAP at day 7 for bupivacaine treatment study (Chapter 4).

injBP-0h					sham-VEH0h				
Rat #	Image	pNR1	mGluR5	GFAP	Rat #	Image	pNR1	mGluR5	GFAP
147	L1	0.18	0.22	0.22	159	L1	0.14	0.26	0.07
	L2	0.22	0.29	0.29		L2		0.31	
	L3	0.15	0.37	0.37		L3	0.23	0.29	0.07
	L4	0.13	0.37	0.37		L4	0.19	0.24	0.04
	L5	0.18	0.28	0.28		L5	0.29	0.34	0.06
	L6	0.15	0.21	0.21		L6	0.26	0.31	0.10
	R1	0.14	0.29	0.29		R1	0.21	0.29	0.12
	R2	0.08	0.31	0.31		R2	0.26	0.29	0.09
	R3	0.20	0.30	0.30		R3	0.25	0.33	0.13
	R4	0.12	0.23	0.23		R4	0.28	0.30	0.12
	R5	0.18	0.31	0.31		R5	0.26	0.35	0.13
	R6	0.20	0.26	0.26		R6	0.26	0.36	0.12
148	L1	0.20	0.27	0.27	160	L1	0.13	0.36	0.08
	L2	0.29	0.42	0.42		L2	0.14	0.26	0.03
	L3	0.23	0.27	0.27		L3	0.26	0.19	0.04
	L4	0.34	0.32	0.32		L4		0.26	0.07
	L5	0.35	0.34	0.34		L5		0.24	0.11
	L6	0.18	0.35	0.35		L6	0.27	0.21	0.07
	R1	0.08	0.24	0.24		R1	0.21	0.15	0.02
	R2	0.22	0.17	0.17		R2	0.13	0.31	0.05
	R3	0.23	0.15	0.15		R3	0.24	0.21	0.08
	R4	0.40	0.18	0.18		R4			
	R5	0.33	0.22	0.22		R5		0.17	0.09
	R6	0.28	0.21	0.21		R6		0.16	0.05
149	L1	0.22	0.21	0.21	161	L1	0.21	0.26	0.12
	L2	0.19	0.20	0.20		L2	0.21	0.32	0.17
	L3	0.25	0.33	0.33		L3	0.19	0.31	0.13
	L4	0.33	0.30	0.30		L4	0.21	0.31	0.16
	L5	0.16	0.40	0.40		L5	0.14	0.35	0.13
	L6	0.26	0.34	0.34		L6	0.21	0.38	0.14
	R1	0.20	0.30	0.30		R1	0.13	0.20	0.10
	R2	0.28	0.30	0.30		R2	0.25	0.31	0.19
	R3	0.33	0.30	0.30		R3	0.20	0.25	0.11
	R4	0.12	0.31	0.31		R4	0.12	0.27	0.16
	R5	0.22				R5	0.23	0.37	0.15
	R6	0.34	0.23	0.23		R6	0.19	0.27	0.14

Note – Table is continued on the next page. Missing values are due to tissue sections that were torn or folded, preventing quantification of immunolabeling in the dorsal horn.

injBP-0h (continued)					sham-VEH0h (continued)				
Rat #	Image	pNR1	mGluR5	GFAP	Rat #	Image	pNR1	mGluR5	GFAP
150	L1	0.27	0.29	0.29	162	L1	0.15	0.23	0.09
	L2	0.28	0.40	0.40		L2	0.23	0.27	0.10
	L3	0.18	0.33	0.33		L3	0.23	0.43	0.09
	L4	0.26				L4	0.19	0.30	0.08
	L5	0.21	0.29	0.29		L5		0.33	0.14
	L6	0.27	0.36	0.36		L6	0.38	0.45	
	R1	0.25	0.35	0.35		R1	0.23	0.37	0.11
	R2	0.29	0.39	0.39		R2	0.22	0.30	0.12
	R3	0.26	0.48	0.48		R3	0.26	0.37	0.13
	R4	0.35	0.20	0.20		R4		0.28	0.14
	R5	0.23	0.34	0.34		R5	0.28	0.35	0.15
	R6	0.21	0.35	0.35		R6	0.26	0.25	0.14
151	L1	0.19	0.20	0.20	163	L1	0.29	0.30	0.13
	L2	0.15	0.38	0.38		L2	0.27	0.36	0.11
	L3	0.23	0.18	0.18		L3	0.24	0.40	0.14
	L4	0.07	0.22	0.22		L4	0.24	0.50	
	L5	0.11	0.28	0.28		L5	0.37	0.43	0.14
	L6	0.18	0.30	0.30		L6	0.29	0.43	0.17
	R1	0.25	0.21	0.21		R1	0.34	0.35	0.13
	R2	0.22	0.35	0.35		R2	0.30	0.43	0.07
	R3	0.27	0.34	0.34		R3	0.30	0.42	0.14
	R4	0.25	0.31	0.31		R4	0.38	0.42	0.07
	R5	0.01	0.31	0.31		R5	0.32	0.41	0.11
	R6	0.29	0.20	0.20		R6	0.33	0.35	0.15
152	L1	0.11	0.30	0.30	164	L1	0.24	0.35	0.12
	L2	0.16	0.39	0.39		L2	0.22	0.32	0.11
	L3	0.16	0.23	0.23		L3		0.38	0.18
	L4		0.22	0.22		L4			
	L5	0.14	0.34	0.34		L5	0.31	0.35	0.12
	L6	0.20	0.39	0.39		L6	0.26	0.40	0.14
	R1	0.22	0.17	0.17		R1	0.30	0.25	0.08
	R2	0.20	0.39	0.39		R2	0.20	0.34	0.08
	R3	0.19	0.27	0.27		R3		0.31	0.13
	R4	0.11	0.19	0.19		R4		0.43	
	R5	0.18	0.37	0.37		R5	0.32	0.38	0.14
	R6	0.36	0.41	0.41		R6	0.20	0.32	0.12

Note – Table is continued on the next page. Missing values are due to tissue sections that were torn or folded, preventing quantification of immunolabeling in the dorsal horn.

inj-VEH0h					inj-BPd4				
Rat #	**Image**	**pNR1**	**mGluR5**	**GFAP**	**Rat #**	**Image**	**pNR1**	**mGluR5**	**GFAP**
171	L1	0.22	0.25	0.12	153	L1	0.26	0.16	0.08
	L2	0.17	0.35	0.18		L2	0.20	0.34	
	L3	0.21	0.41	0.16		L3	0.24	0.31	
	L4	0.30	0.33	0.12		L4	0.30	0.30	0.07
	L5	0.29	0.44	0.14		L5	0.30	0.30	0.05
	L6	0.20	0.40	0.13		L6	0.35	0.30	0.05
	R1	0.29	0.28	0.09		R1	0.23		0.09
	R2	0.18	0.39	0.15		R2	0.22	0.29	
	R3	0.16	0.39	0.19		R3	0.23	0.23	
	R4		0.32	0.08		R4	0.17	0.21	0.10
	R5	0.26	0.37	0.16		R5	0.28	0.37	0.04
	R6	0.23	0.36	0.12		R6	0.21	0.28	0.05
172	L1	0.33	0.44	0.13	154	L1	0.12	0.31	0.06
	L2	0.27	0.52	0.14		L2	0.27	0.42	0.09
	L3	0.27	0.43	0.14		L3	0.18	0.35	0.10
	L4	0.26	0.33	0.12		L4	0.25		
	L5	0.33	0.47	0.15		L5	0.26	0.37	0.09
	L6	0.27	0.42	0.20		L6	0.25	0.32	
	R1	0.23	0.41	0.13		R1	0.17		
	R2	0.37	0.42	0.16		R2	0.38	0.23	0.07
	R3	0.35	0.41	0.13		R3	0.21	0.16	0.07
	R4	0.31	0.34	0.18		R4	0.24		
	R5		0.41	0.11		R5	0.20	0.30	0.06
	R6	0.27	0.45	0.16		R6	0.14	0.32	0.07
173	L1	0.38	0.36	0.08	155	L1	0.36	0.27	0.08
	L2	0.39	0.36	0.09		L2	0.28	0.26	0.16
	L3	0.38	0.35	0.05		L3	0.28	0.32	0.12
	L4	0.45	0.48	0.13		L4	0.29	0.21	0.11
	L5	0.27	0.44	0.12		L5	0.19	0.35	0.12
	L6	0.33	0.27	0.09		L6	0.23	0.34	0.11
	R1	0.23	0.44	0.16		R1	0.16	0.26	0.13
	R2	0.25	0.41	0.14		R2	0.34	0.43	0.15
	R3	0.32	0.40	0.10		R3	0.34	0.29	0.16
	R4	0.35	0.47	0.30		R4	0.27	0.33	0.18
	R5	0.25	0.43	0.14		R5	0.34	0.43	0.16
	R6	0.36	0.29	0.17		R6	0.23	0.40	0.12

Note – Table is continued on the next page. Missing values are due to tissue sections that were torn or folded, preventing quantification of immunolabeling in the dorsal horn.

inj-VEH0h (continued)					inj-BPd4 (continued)				
Rat #	Image	pNR1	mGluR5	GFAP	Rat #	Image	pNR1	mGluR5	GFAP
174	L1		0.29	0.14	156	L1	0.29	0.35	0.16
	L2	0.27	0.36	0.18		L2	0.27	0.40	0.12
	L3		0.30	0.20		L3	0.34	0.35	0.18
	L4		0.29	0.20		L4	0.33	0.18	0.10
	L5		0.33	0.16		L5	0.28		
	L6	0.21	0.32	0.19		L6	0.33		0.19
	R1		0.42	0.10		R1	0.37	0.29	0.08
	R2	0.21	0.40	0.09		R2	0.15	0.39	0.10
	R3	0.20	0.39	0.12		R3	0.24	0.40	0.15
	R4		0.34	0.13		R4	0.31	0.36	
	R5	0.24	0.33	0.13		R5	0.34	0.24	0.15
	R6	0.28	0.37	0.12		R6	0.40		0.12
175	L1		0.37	0.12	157	L1	0.20	0.27	0.08
	L2		0.37			L2	0.30	0.33	0.08
	L3		0.34			L3	0.19	0.28	
	L4	0.38	0.21	0.08		L4	0.26	0.31	0.14
	L5	0.27	0.42	0.09		L5	0.33	0.37	0.12
	L6		0.37			L6	0.27	0.34	0.15
	R1		0.13	0.05		R1		0.31	0.10
	R2	0.26	0.36			R2	0.18	0.32	0.14
	R3		0.28	0.11		R3		0.21	
	R4	0.29	0.28	0.05		R4	0.29	0.27	0.09
	R5	0.29	0.46	0.18		R5	0.33	0.35	0.12
	R6	0.24	0.33	0.11		R6	0.30	0.32	0.13
176	L1	0.16	0.35	0.09	158	L1	0.34	0.30	0.08
	L2	0.22	0.46	0.08		L2	0.30	0.33	0.10
	L3	0.19	0.32	0.12		L3	0.24	0.28	0.08
	L4	0.25	0.30	0.06		L4	0.32	0.41	0.13
	L5		0.44	0.07		L5	0.30	0.35	0.15
	L6	0.25	0.47	0.08		L6	0.26	0.40	0.17
	R1	0.29	0.25	0.08		R1	0.30	0.23	0.12
	R2	0.29	0.35	0.07		R2	0.34	0.30	0.17
	R3	0.21	0.28	0.10		R3	0.24	0.33	0.16
	R4	0.20	0.28	0.05		R4	0.31	0.32	0.17
	R5		0.42	0.07		R5	0.44	0.33	0.13
	R6	0.23	0.36	0.10		R6	0.35	0.35	0.12

Note – Table is continued on the next page. Missing values are due to tissue sections that were torn or folded, preventing quantification of immunolabeling in the dorsal horn.

sham-VEHd4					inj-VEHd4				
Rat #	**Image**	**pNR1**	**mGluR5**	**GFAP**	**Rat #**	**Image**	**pNR1**	**mGluR5**	**GFAP**
165	L1	0.13	0.40		177	L1	0.15	0.33	0.07
	L2	0.14	0.30	0.09		L2	0.39	0.36	0.06
	L3	0.35	0.25	0.09		L3	0.37	0.34	0.11
	L4	0.08	0.33	0.07		L4	0.29	0.31	0.12
	L5	0.15	0.29	0.11		L5	0.30	0.37	0.07
	L6	0.34	0.36	0.14		L6	0.22	0.41	0.13
	R1	0.19	0.27	0.11		R1		0.42	0.06
	R2	0.27	0.28	0.06		R2	0.30	0.39	0.12
	R3	0.29	0.26	0.06		R3	0.24	0.37	0.14
	R4	0.15	0.29	0.08		R4	0.20	0.36	0.11
	R5	0.19	0.23	0.03		R5	0.27	0.38	0.15
	R6	0.31	0.33	0.09		R6	0.18	0.37	0.08
166	L1	0.21	0.16	0.11	178	L1		0.38	0.09
	L2	0.27	0.30	0.19		L2	0.23	0.40	0.08
	L3	0.22	0.35	0.11		L3	0.24	0.38	0.10
	L4	0.23	0.28	0.12		L4	0.24	0.28	
	L5	0.20	0.32	0.09		L5	0.14	0.30	0.12
	L6	0.24	0.31	0.12		L6		0.41	0.08
	R1	0.24	0.34	0.10		R1	0.15	0.32	0.13
	R2	0.16	0.36	0.20		R2	0.25	0.37	0.13
	R3	0.26		0.17		R3	0.23	0.32	0.09
	R4		0.28	0.10		R4	0.20	0.29	0.20
	R5		0.38	0.12		R5	0.18	0.27	0.08
	R6		0.35	0.13		R6	0.28	0.32	0.13
167	L1		0.28		179	L1	0.41	0.30	0.08
	L2		0.27			L2	0.35	0.35	0.14
	L3	0.23	0.19	0.05		L3	0.31	0.27	0.13
	L4	0.10	0.32	0.09		L4	0.28	0.33	0.12
	L5	0.11	0.31	0.07		L5	0.32	0.40	0.12
	L6	0.09	0.19	0.02		L6	0.30	0.35	0.15
	R1		0.23	0.12		R1	0.29	0.38	0.14
	R2	0.26	0.20	0.06		R2	0.32	0.39	0.08
	R3	0.25	0.27	0.04		R3	0.32	0.32	0.13
	R4	0.14	0.29	0.08		R4	0.28	0.36	0.08
	R5	0.22	0.29	0.05		R5	0.37	0.42	0.13
	R6	0.23	0.28	0.06		R6	0.39	0.35	0.12

Note – Table is continued on the next page. Missing values are due to tissue sections that were torn or folded, preventing quantification of immunolabeling in the dorsal horn.

sham-VEHd4 (continued)					inj-VEHd4 (continued)				
Rat #	Image	pNR1	mGluR5	GFAP	Rat #	Image	pNR1	mGluR5	GFAP
168	L1	0.23	0.19	0.05	180	L1	0.35	0.36	0.14
	L2	0.17	0.24	0.05		L2	0.29	0.36	0.10
	L3	0.12	0.39	0.08		L3	0.31	0.42	0.10
	L4	0.15	0.21	0.05		L4		0.31	0.07
	L5	0.31	0.18	0.01		L5		0.28	0.05
	L6	0.21	0.39	0.06		L6		0.35	0.11
	R1	0.26	0.22	0.05		R1	0.29	0.42	0.09
	R2	0.29	0.17	0.12		R2	0.31	0.38	0.13
	R3	0.26	0.33	0.12		R3	0.33	0.38	0.19
	R4	0.10	0.28	0.06		R4		0.32	0.12
	R5	0.23	0.44	0.10		R5		0.38	0.14
	R6	0.13	0.23	0.03		R6	0.42	0.42	0.16
169	L1	0.21	0.27	0.11	182	L1	0.34		0.14
	L2	0.11	0.24	0.11		L2	0.34	0.27	0.10
	L3	0.16	0.29	0.09		L3	0.30	0.37	0.17
	L4	0.23	0.31	0.14		L4	0.31	0.29	0.12
	L5	0.16	0.37	0.07		L5	0.32	0.34	0.15
	L6	0.16	0.37	0.07		L6	0.34	0.28	0.13
	R1	0.25		0.07		R1		0.33	0.14
	R2	0.24		0.12		R2	0.27	0.28	0.19
	R3	0.19		0.13		R3	0.43	0.37	0.15
	R4	0.16		0.09		R4	0.23	0.34	0.14
	R5	0.22		0.12		R5	0.33	0.33	0.13
	R6	0.24		0.16		R6	0.30	0.42	0.19
170	L1	0.23	0.25						
	L2	0.15	0.26	0.10					
	L3	0.14	0.19	0.09					
	L4	0.24	0.33	0.18					
	L5	0.23	0.27						
	L6		0.25	0.15					
	R1	0.25	0.33	0.11					
	R2	0.29	0.16	0.12					
	R3	0.17	0.17	0.12					
	R4	0.21	0.38	0.13					
	R5	0.16	0.32	0.09					
	R6		0.31						

Note – Missing values are due to tissue sections that were torn or folded, preventing quantification of immunolabeling in the dorsal horn.

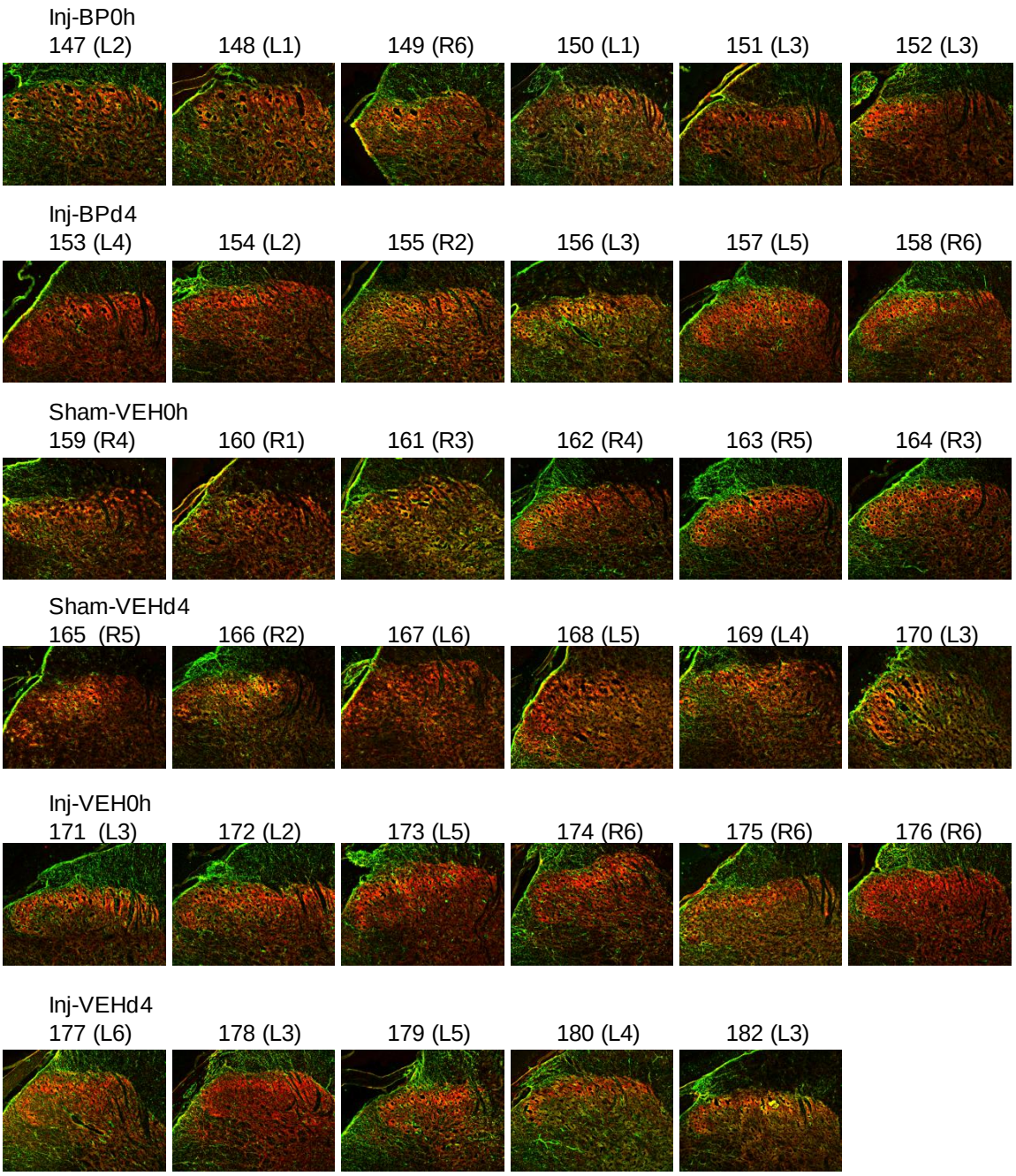

Figure G.1. Immunolabeling of mGluR5 (green) and GFAP (red) in the spinal dorsal horn at day 7 for the bupivacaine treatment study. Proteins were evaluated after sham or painful facet joint injury followed by intra-articular bupivacaine (BP) or saline vehicle (VEH) injections either immediately (*inj-BP0h*, *inj-VEH0h*, *sham-VEH0h*) or at day 4 (*inj-BPd4*, *inj-VEHd4*, *sham-VEHd4*). Representative images are indicated by the rat number, and an image number that includes the right (R) or left (L) side of the spinal cord and the section of tissue (consecutive sections were labeled 1-6 for each rat).

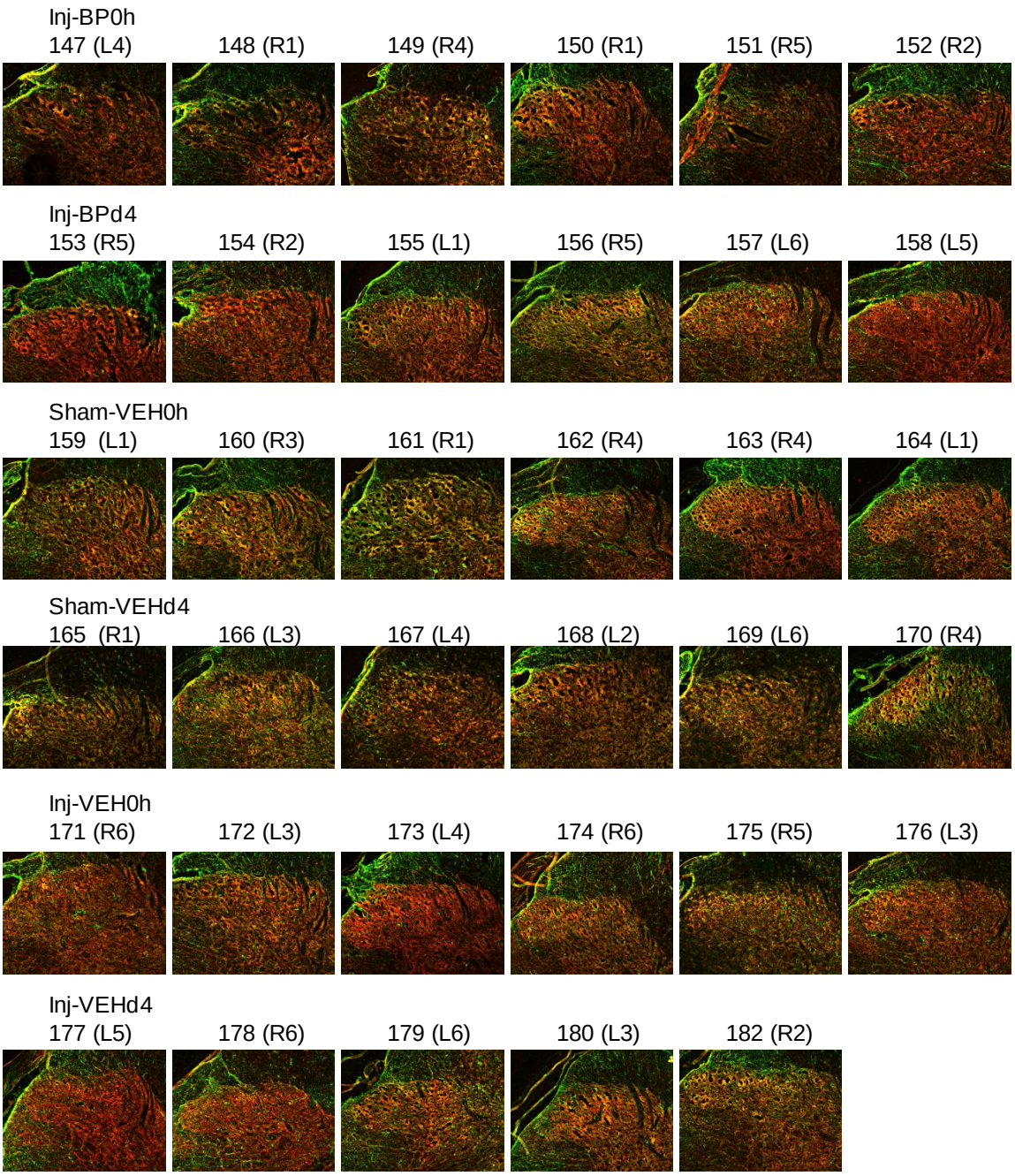

Figure G.2. Immunolabeling of pNR1 (green) and GFAP (red) in the spinal dorsal horn at day 7 for the bupivacaine treatment study. Proteins were evaluated after sham or painful facet joint injury followed by intra-articular bupivacaine (BP) or saline vehicle (VEH) injections either immediately (*inj-BP0h, inj-VEH0h, sham-VEH0h*) or at day 4 (*inj-BPd4, inj-VEHd4, sham-VEHd4*). Representative images are indicated by the rat number, and an image number that includes the right (R) or left (L) side of the spinal cord and the section of tissue (consecutive sections were labeled 1-6 for each rat).

Table G.2. Densitometric quantification of TSP4 and GFAP at day 7 after sham or painful facet joint injury (Chapter 5).

Superficial DH						Dorsal Columns					
	Rat #	Image	TSP4	GFAP	Coloc.		Rat #	Image	TSP4	GFAP	Coloc.
Injury	47	L1	0.085	0.109	0.027	Injury	47	L2	0.077	0.032	0.017
		R1	0.020	0.069	0.003			L4	0.059	0.062	0.006
		L2	0.166	0.109	0.029			R4	0.043	0.029	0.002
		R2	0.104	0.080	0.012			L5	0.137	0.055	0.006
		L3	0.048	0.092	0.012			R5	0.046	0.115	0.006
		R3	0.032	0.058	0.002			L6	0.059	0.045	0.003
		L4	0.020	0.028	0.001			R6	0.090	0.081	0.010
		R4	0.013	0.075	0.003		48	L1	0.161	0.140	0.055
		L5	0.370	0.124	0.078			R1	0.098	0.076	0.005
		R5	0.039	0.156	0.016			L2	0.143	0.135	0.037
		R6	0.096	0.051	0.010			R2	0.109	0.137	0.021
	48	L1	0.024	0.071	0.006			L3	0.168	0.171	0.046
		R1	0.026	0.077	0.006			R3	0.201	0.147	0.030
		L2	0.752	0.217	0.161			L4	0.111	0.114	0.019
		R2	0.444	0.132	0.085			R4	0.118	0.151	0.031
		L3	0.142	0.138	0.033		49	L1	0.047	0.021	0.001
		R3	0.487	0.143	0.081			R1	0.072	0.035	0.002
	49	R1	0.020	0.028	0.002			L2	0.068	0.030	0.003
		L2	0.086	0.050	0.010			L3	0.059	0.020	0.001
		R2	0.131	0.085	0.029			R3	0.088	0.031	0.003
		R3	0.069	0.039	0.009			R4	0.048	0.043	0.001
		R4	0.034	0.036	0.003			L5	0.098	0.075	0.008
		L5	0.321	0.068	0.033			R5	0.089	0.061	0.007
		R5	0.179	0.065	0.019		53	L1	0.142	0.078	0.018
		L6	0.286	0.042	0.019			R1	0.236	0.132	0.056
	53	L2	0.279	0.150	0.066			L2	0.255	0.142	0.082
		L3	0.016	0.132	0.003			R2	0.063	0.043	0.004
		L4	0.008	0.053	0.001			L4	0.042	0.089	0.009
		R4	0.004	0.062	0.001			R4	0.039	0.101	0.010
		L5	0.256	0.123	0.042			L5	0.120	0.102	0.022
		R5	0.061	0.030	0.002			R5	0.165	0.107	0.027
	54	L3	0.182	0.061	0.018			L6	0.145	0.067	0.010
		R3	0.399	0.199	0.128			R6	0.111	0.059	0.006
		L4	0.022	0.135	0.010		54	L2	0.300	0.116	0.050
		R4	0.128	0.109	0.023			R2	0.128	0.066	0.014
		L5	0.131	0.109	0.024			L3	0.138	0.124	0.041
		R5	0.034	0.082	0.007			L5	0.132	0.131	0.033
	59	L1	0.016	0.043	0.001			R6	0.022	0.046	0.001
		R1	0.003	0.048	0.001		59	L1	0.032	0.077	0.002
		L2	0.194	0.148	0.049			R1	0.049	0.096	0.007
		R2	0.229	0.156	0.060			L2	0.097	0.116	0.011
		L3	0.056	0.077	0.010			R2	0.069	0.154	0.014
		R3	0.044	0.053	0.008			L3	0.106	0.126	0.014
		L5	0.303	0.112	0.054			R3	0.083	0.098	0.009
		R5	0.029	0.045	0.005			L5	0.110	0.166	0.035
								L6	0.029	0.029	0.001

Note – Table is continued on the next page.

Superficial DH (continued)						Dorsal Columns (continued)					
	Rat #	Image	TSP4	GFAP	Coloc.		Rat #	Image	TSP4	GFAP	Coloc.
Sham	50	L2	0.012	0.030	0.001	Sham	50	L1	0.039	0.049	0.003
		R2	0.061	0.017	0.003			L2	0.107	0.077	0.023
		L4	0.014	0.035	0.000			R2	0.035	0.076	0.003
		R4	0.017	0.020	0.000			R3	0.057	0.029	0.002
		L5	0.169	0.054	0.008			L4	0.056	0.018	0.002
		R5	0.292	0.065	0.023			R4	0.044	0.039	0.000
		L6	0.064	0.053	0.006			R5	0.121	0.066	0.008
		R6	0.009	0.033	0.000			L6	0.081	0.082	0.010
	55	L1	0.045	0.138	0.015			R6	0.019	0.052	0.001
		L2	0.221	0.106	0.043		55	L1	0.048	0.089	0.008
		R2	0.035	0.086	0.013			R1	0.066	0.112	0.016
		R3	0.020	0.095	0.005			L3	0.094	0.087	0.014
		L4	0.043	0.131	0.016			R3	0.091	0.081	0.011
		R4	0.052	0.070	0.010			L4	0.051	0.086	0.006
		L5	0.197	0.077	0.018			R4	0.049	0.060	0.008
		R5	0.196	0.081	0.030			L5	0.086	0.118	0.017
		L6	0.185	0.070	0.015		56	L1	0.043	0.132	0.010
	56	L1	0.085	0.140	0.026			R1	0.101	0.091	0.010
		R1	0.102	0.075	0.013			L2	0.130	0.106	0.013
		L2	0.115	0.116	0.021			R2	0.116	0.090	0.010
		R2	0.170	0.110	0.029			L3	0.049	0.086	0.008
		L3	0.069	0.091	0.013			R3	0.059	0.161	0.020
		L4	0.100	0.126	0.027			L4	0.050	0.105	0.010
		R4	0.059	0.072	0.011			R4	0.060	0.092	0.010
		L5	0.057	0.075	0.011			R6	0.194	0.074	0.012
		L6	0.158	0.078	0.021		60	R2	0.055	0.057	0.004
	60	L2	0.117	0.060	0.014			R3	0.077	0.089	0.014
		R2	0.113	0.097	0.028			L4	0.029	0.037	0.001
		L3	0.111	0.037	0.006			L5	0.085	0.077	0.014
		R3	0.071	0.132	0.017			L6	0.065	0.069	0.007
		L4	0.012	0.029	0.001			R6	0.024	0.052	0.005
		R4	0.030	0.038	0.002						
		L5	0.088	0.077	0.015						
		R5	0.114	0.040	0.008						
		L6	0.018	0.036	0.001						
		R6	0.066	0.034	0.003						

Note – Table is continued on the next page.

Deep DH						Deep DH (continued)					
	Rat #	Image	TSP4	GFAP	Coloc.		Rat #	Image	TSP4	GFAP	Coloc.
Injury	47	R1	0.003	0.053	0.000	Injury	59	L1	0.003	0.033	0.000
		R2	0.029	0.060	0.005			R1	0.005	0.039	0.000
		L3	0.024	0.080	0.002			R2	0.010	0.039	0.001
		R3	0.017	0.037	0.000			L3	0.005	0.049	0.001
		L4	0.013	0.035	0.003			L4	0.012	0.013	0.000
		R4	0.048	0.027	0.004			R4	0.005	0.031	0.000
		L5	0.043	0.060	0.006			L5	0.006	0.031	0.000
		R5	0.048	0.075	0.013	Sham		R5	0.005	0.034	0.001
		L6	0.041	0.048	0.003			L6	0.015	0.028	0.001
		R6	0.018	0.042	0.001		50	R1	0.010	0.023	0.000
	48	L1	0.021	0.019	0.000			L2	0.028	0.037	0.003
		R1	0.025	0.013	0.000			L3	0.057	0.008	0.001
		L2	0.023	0.039	0.001			R3	0.011	0.002	0.000
		R2	0.009	0.046	0.001			L4	0.029	0.013	0.000
		L3	0.067	0.041	0.003			R4	0.023	0.010	0.000
		R3	0.014	0.045	0.001			L5	0.077	0.037	0.005
		R4	0.083	0.017	0.001			R5	0.045	0.037	0.002
	49	R1	0.027	0.003	0.000			L6	0.005	0.013	0.000
		R2	0.026	0.028	0.001			R6	0.005	0.025	0.000
		L3	0.037	0.008	0.000		55	L2	0.016	0.017	0.000
		R3	0.020	0.012	0.000			R2	0.035	0.052	0.003
		L4	0.057	0.030	0.002			L3	0.010	0.075	0.001
		R4	0.018	0.020	0.000			R3	0.020	0.021	0.000
		L5	0.035	0.015	0.001			L4	0.004	0.018	0.000
		R5	0.072	0.077	0.010			R4	0.004	0.021	0.000
		R6	0.044	0.013	0.000			L5	0.013	0.007	0.001
	53	L1	0.028	0.011	0.000			R5	0.034	0.044	0.003
		R1	0.023	0.018	0.000			L6	0.016	0.024	0.000
		L2	0.014	0.047	0.000			R6	0.026	0.036	0.001
		R2	0.061	0.010	0.001		56	L1	0.028	0.041	0.001
		L4	0.007	0.019	0.000			R1	0.026	0.054	0.002
		R4	0.002	0.023	0.000			L2	0.065	0.038	0.005
		R5	0.024	0.032	0.001			L4	0.017	0.026	0.000
		L6	0.013	0.012	0.000			R4	0.007	0.018	0.000
		R6	0.018	0.015	0.000			L5	0.014	0.005	0.000
	54	L2	0.040	0.009	0.000			R5	0.069	0.022	0.005
		R2	0.057	0.008	0.000			L6	0.003	0.009	0.000
		L3	0.086	0.011	0.002		60	R1	0.013	0.016	0.001
		R3	0.050	0.013	0.001			L2	0.022	0.053	0.001
		L4	0.004	0.054	0.003			R2	0.063	0.049	0.011
		R4	0.002	0.017	0.000			L3	0.020	0.035	0.001
		R5	0.006	0.018	0.000			R3	0.017	0.086	0.003
		L6	0.053	0.024	0.003			R4	0.033	0.007	0.000
		R6	0.029	0.017	0.000			L5	0.029	0.026	0.002
								R5	0.049	0.028	0.004
								L6	0.014	0.025	0.001
								R6	0.032	0.020	0.002

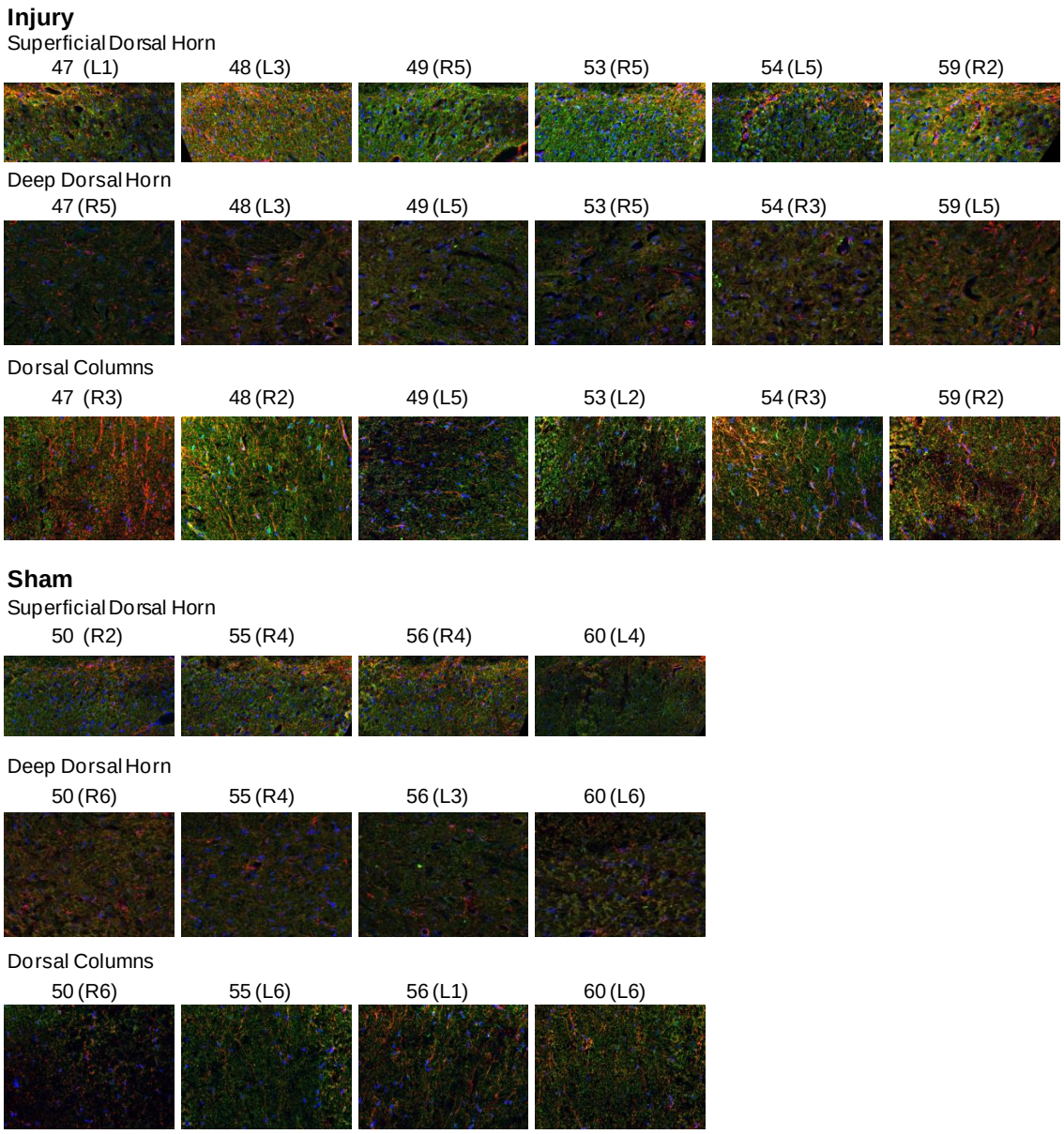

Figure G.3. Immunolabeling of TSP4 (green) and GFAP (red) in the spinal cord at day 7 after sham or painful facet joint injury. TSP4 and GFAP labeling were evaluated in the superficial dorsal horn, deep dorsal horn, and dorsal columns of the spinal cord. Representative images are indicated by the rat number, and an image number that includes the right (R) or left (L) side of the spinal cord and the section of tissue (consecutive sections were labeled 1-6 for each rat).

Table G.3. Densitometric quantification of TSP4 and GFAP at day 7 for bupivacaine treatment study (Chapter 5).

Superficial DH						Dorsal Columns					
	Rat #	Section	TSP4	GFAP	Coloc.		Rat #	Section	TSP4	GFAP	Coloc.
inj-VEH0h	171	L2	0.143	0.061	0.027	inj-VEH0h	171	L2	0.223	0.121	0.024
		R2	0.199	0.094	0.041			R2	0.265	0.201	0.050
		L3	0.061	0.047	0.007			L3	0.125	0.088	0.003
		R3	0.123	0.047	0.015			R3	0.171	0.108	0.008
		L4	0.027	0.018	0.002			L5	0.189	0.158	0.022
		R4	0.011	0.022	0.000			R5	0.229	0.143	0.028
		L5	0.169	0.061	0.026			L6	0.287	0.132	0.017
		R5	0.277	0.088	0.043		172	L2	0.152	0.096	0.003
		L6	0.253	0.165	0.081			R2	0.176	0.137	0.006
		R6	0.092	0.040	0.007			L3	0.280	0.077	0.004
	172	L2	0.254	0.133	0.064			L4	0.110	0.065	0.003
		R2	0.138	0.088	0.020			L5	0.344	0.190	0.041
		L4	0.098	0.052	0.014			R5	0.299	0.248	0.077
		L5	0.297	0.089	0.038			L6	0.178	0.066	0.004
		R5	0.153	0.071	0.016		173	L1	0.059	0.078	0.002
		L6	0.060	0.075	0.007			R1	0.023	0.217	0.009
		R6	0.218	0.032	0.007			L2	0.130	0.223	0.026
	173	L1	0.009	0.012	0.000			R2	0.087	0.196	0.013
		R1	0.039	0.167	0.016			L3	0.085	0.192	0.010
		L2	0.098	0.154	0.035			R3	0.140	0.204	0.031
		R2	0.046	0.086	0.010			L4	0.092	0.173	0.014
		L3	0.047	0.128	0.015			L5	0.117	0.270	0.039
		R3	0.096	0.138	0.036			R5	0.259	0.318	0.089
		L4	0.054	0.064	0.008			L6	0.119	0.210	0.021
		R4	0.049	0.052	0.004			R6	0.178	0.229	0.038
		L5	0.270	0.160	0.079			R4	0.075	0.109	0.006
		R5	0.228	0.110	0.043		174	L1	0.268	0.083	0.003
		L6	0.061	0.109	0.014			R1	0.108	0.246	0.007
		R6	0.091	0.090	0.015			L2	0.092	0.209	0.023
	174	L1	0.100	0.031	0.003			R2	0.171	0.283	0.049
		L2	0.230	0.178	0.083			L3	0.079	0.204	0.013
		R2	0.354	0.206	0.114			R3	0.162	0.257	0.036
		L3	0.098	0.125	0.032			L5	0.286	0.230	0.039
		L4	0.201	0.110	0.023			R5	0.280	0.249	0.034
		L5	0.205	0.094	0.025			L6	0.241	0.171	0.013
		R5	0.214	0.124	0.035		175	L1	0.015	0.242	0.005
		L6	0.091	0.035	0.004			L2	0.112	0.334	0.046
		R6	0.004	0.055	0.001			R2	0.123	0.366	0.047
	175	L1	0.012	0.143	0.004			L3	0.081	0.331	0.036
		L2	0.098	0.177	0.039			R3	0.148	0.354	0.065
		R2	0.042	0.210	0.022			R4	0.072	0.148	0.008
		L3	0.020	0.125	0.006			R5	0.098	0.244	0.040
		L4	0.006	0.104	0.001			R6	0.124	0.171	0.025
		R4	0.038	0.042	0.004		176	L1	0.070	0.196	0.006
		L5	0.092	0.168	0.039			R2	0.137	0.269	0.023
		R5	0.104	0.214	0.053			R5	0.015	0.278	0.001
		L6	0.036	0.042	0.004	sham-VEH0h	159	L1	0.004	0.055	0.000
		R6	0.114	0.091	0.020			R1	0.005	0.052	0.000
	176	L1	0.012	0.086	0.002			L2	0.029	0.180	0.005
		L2	0.017	0.132	0.003			R2	0.024	0.144	0.003
		R2	0.003	0.074	0.000			L3	0.018	0.168	0.002
		R5	0.001	0.084	0.000			R3	0.021	0.162	0.002
sham-VEH0h	159	L1	0.003	0.018	0.000			L4	0.012	0.102	0.001
		R1	0.003	0.014	0.000			L5	0.015	0.151	0.001
		L2	0.010	0.082	0.003			R5	0.020	0.137	0.002
		R2	0.050	0.094	0.015			L6	0.039	0.131	0.001
		L3	0.038	0.116	0.020			R6	0.014	0.113	0.000
		R3	0.006	0.063	0.002		160	L2	0.015	0.212	0.004
		L4	0.019	0.038	0.002			R2	0.019	0.247	0.005
		R4	0.004	0.011	0.000			L3	0.023	0.176	0.002
		L5	0.026	0.106	0.007			R3	0.029	0.214	0.005
		R5	0.009	0.094	0.002			L4	0.005	0.092	0.000
		L6	0.004	0.073	0.001			R4	0.012	0.109	0.001
		R6	0.001	0.065	0.000			L5	0.023	0.215	0.003

Note – Table is continued on the next page.

Superficial DH (continued)						Dorsal Columns (continued)					
	Rat #	Section	TSP4	GFAP	Coloc.		Rat #	Section	TSP4	GFAP	Coloc.
sham-VEH0h	160	L2	0.013	0.072	0.004	sham-VEH0h	160	L6	0.077	0.056	0.003
		R2	0.011	0.061	0.003		161	L1	0.094	0.109	0.005
		R3	0.001	0.064	0.000			R1	0.087	0.091	0.004
		R4	0.000	0.030	0.000			L2	0.054	0.159	0.007
		L5	0.008	0.066	0.001			R2	0.047	0.158	0.007
		R5	0.006	0.089	0.001			R3	0.076	0.127	0.006
		L6	0.002	0.052	0.000			L4	0.028	0.117	0.003
	161	R1	0.009	0.009	0.000			R4	0.034	0.133	0.003
		L2	0.036	0.043	0.007			L5	0.071	0.182	0.017
		R2	0.010	0.026	0.001			R5	0.063	0.241	0.019
		L3	0.058	0.051	0.009			R6	0.115	0.182	0.010
		R3	0.011	0.031	0.001		162	R2	0.026	0.246	0.008
		L4	0.024	0.040	0.003			L3	0.047	0.149	0.004
		R4	0.019	0.031	0.001			R3	0.042	0.155	0.002
		L5	0.062	0.097	0.017			R4	0.055	0.154	0.004
		R5	0.037	0.097	0.011			L5	0.026	0.172	0.002
		L6	0.051	0.055	0.010			R5	0.032	0.191	0.005
		R6	0.053	0.036	0.006			L6	0.064	0.198	0.006
	162	R1	0.037	0.034	0.002			R6	0.042	0.218	0.004
		L3	0.022	0.070	0.007		163	L1	0.100	0.079	0.002
		R3	0.034	0.119	0.008			R1	0.020	0.009	0.000
		R4	0.002	0.056	0.000			L2	0.335	0.295	0.076
		L5	0.051	0.087	0.013			R2	0.237	0.352	0.077
		R5	0.026	0.086	0.007			L3	0.202	0.310	0.045
		L6	0.011	0.102	0.003			R3	0.228	0.259	0.030
		R6	0.010	0.104	0.002			L5	0.117	0.188	0.003
	163	L1	0.032	0.007	0.001			R5	0.166	0.097	0.007
		R1	0.026	0.003	0.000			L6	0.222	0.220	0.027
		L3	0.112	0.085	0.020			R6	0.191	0.271	0.027
		R3	0.042	0.125	0.012			L4	0.056	0.189	0.006
		L5	0.112	0.011	0.003		164	L4	0.151	0.015	0.001
		R5	0.104	0.011	0.002			R4	0.206	0.014	0.001
		L6	0.108	0.116	0.025			L5	0.069	0.106	0.005
		R6	0.054	0.136	0.017			R6	0.152	0.155	0.033
	164	L4	0.009	0.015	0.000			L1	0.046	0.076	0.003
		R4	0.002	0.033	0.000			R1	0.062	0.063	0.001
		L5	0.420	0.116	0.077			R2	0.164	0.126	0.010
		R5	0.097	0.089	0.018	inj-BP0h	147	L1	0.074	0.047	0.001
		R6	0.078	0.026	0.006			R1	0.048	0.062	0.001
inj-BP0h	147	L1	0.031	0.040	0.003			L2	0.031	0.091	0.001
		R1	0.015	0.039	0.003			R2	0.076	0.110	0.004
		L2	0.054	0.094	0.015			L3	0.154	0.103	0.005
		R2	0.084	0.076	0.016			R3	0.179	0.102	0.008
		L3	0.113	0.022	0.005			L4	0.122	0.090	0.004
		L4	0.042	0.057	0.009			R4	0.044	0.074	0.003
		R4	0.025	0.034	0.003			L5	0.206	0.081	0.013
		L5	0.173	0.020	0.008			R5	0.117	0.062	0.007
		R5	0.109	0.027	0.009			R6	0.096	0.075	0.004
		L6	0.079	0.019	0.005		148	L1	0.060	0.071	0.002
		R6	0.030	0.023	0.001			R1	0.077	0.117	0.003
	148	L1	0.004	0.011	0.000			L2	0.157	0.115	0.011
		R1	0.019	0.033	0.002			R2	0.088	0.075	0.003
		L2	0.066	0.050	0.008			L3	0.116	0.188	0.014
		R2	0.085	0.023	0.005			R3	0.059	0.153	0.007
		L3	0.071	0.037	0.009			L4	0.032	0.165	0.005
		R3	0.026	0.037	0.003			R4	0.044	0.143	0.004
		L4	0.010	0.043	0.001			L5	0.026	0.115	0.003
		R4	0.023	0.028	0.002			R5	0.021	0.146	0.002
		L5	0.103	0.097	0.023			R6	0.088	0.206	0.016
		R5	0.088	0.085	0.018		149	L1	0.074	0.108	0.002
		L6	0.123	0.103	0.032			R1	0.029	0.094	0.000
		R6	0.125	0.063	0.022			L2	0.065	0.170	0.009

Note – Table is continued on the next page.

Superficial DH (continued)						Dorsal Columns (continued)					
	Rat #	Section	TSP4	GFAP	Coloc.		Rat #	Section	TSP4	GFAP	Coloc.
inj-BP0h	149	R1	0.053	0.032	0.002	inj-BP0h	149	R2	0.054	0.113	0.003
		L2	0.088	0.110	0.023			R3	0.139	0.149	0.014
		R2	0.084	0.034	0.005			R4	0.050	0.087	0.001
		L3	0.066	0.099	0.017			L5	0.062	0.164	0.012
		R3	0.094	0.062	0.012			R5	0.015	0.113	0.002
		L5	0.375	0.153	0.099			L6	0.168	0.038	0.002
		R5	0.039	0.035	0.003			R6	0.183	0.027	0.002
		L6	0.022	0.025	0.003			L3	0.108	0.174	0.014
		R6	0.042	0.009	0.001		150	R1	0.010	0.115	0.001
	150	L1	0.004	0.046	0.000			L2	0.021	0.240	0.006
		R1	0.004	0.042	0.000			R2	0.007	0.246	0.002
		L2	0.006	0.102	0.001			L3	0.006	0.211	0.001
		R2	0.003	0.146	0.002			R3	0.009	0.193	0.002
		L3	0.001	0.070	0.000			L4	0.005	0.134	0.000
		R3	0.000	0.116	0.000			R4	0.003	0.105	0.000
		L4	0.001	0.034	0.000			L5	0.029	0.090	0.001
		R4	0.000	0.050	0.000			R5	0.024	0.039	0.000
		L5	0.010	0.028	0.000			R6	0.009	0.109	0.001
		R5	0.007	0.039	0.001		151	L1	0.051	0.080	0.001
		L6	0.002	0.014	0.000			R1	0.043	0.086	0.000
		R6	0.000	0.125	0.000			L2	0.060	0.113	0.008
	151	L1	0.004	0.017	0.000			L3	0.066	0.125	0.005
		R1	0.003	0.023	0.000			R3	0.144	0.197	0.035
		L2	0.024	0.052	0.004			L5	0.030	0.102	0.001
		R2	0.047	0.045	0.003			R5	0.022	0.075	0.001
		L3	0.093	0.069	0.014			L6	0.005	0.079	0.000
		R3	0.048	0.082	0.007			R6	0.060	0.096	0.002
		L5	0.012	0.013	0.000		152	L1	0.004	0.135	0.000
		L6	0.013	0.018	0.001			R1	0.005	0.131	0.001
		R6	0.022	0.037	0.002			L2	0.020	0.128	0.002
	152	R1	0.001	0.041	0.000			R2	0.022	0.209	0.004
		L2	0.017	0.130	0.008			L3	0.010	0.214	0.001
		R2	0.021	0.147	0.011			R3	0.019	0.202	0.002
		L3	0.001	0.095	0.000			L4	0.009	0.178	0.001
		R3	0.003	0.089	0.000			R4	0.007	0.083	0.001
		L4	0.001	0.057	0.000			L6	0.076	0.203	0.016
		R4	0.001	0.065	0.000			R6	0.063	0.175	0.013
		L6	0.083	0.132	0.031	inj-VEHd4	177	L1	0.068	0.085	0.012
		R6	0.044	0.123	0.015			R1	0.056	0.048	0.006
inj-VEHd4	177	L1	0.061	0.125	0.020			L2	0.041	0.103	0.009
		R1	0.084	0.125	0.027			R2	0.063	0.106	0.013
		L2	0.141	0.167	0.053			L3	0.057	0.113	0.011
		R2	0.061	0.193	0.032			R3	0.056	0.095	0.011
		L3	0.145	0.181	0.051			L4	0.026	0.093	0.006
		R3	0.019	0.178	0.011			R4	0.013	0.035	0.001
		L4	0.032	0.108	0.011			L5	0.090	0.174	0.036
		R4	0.021	0.133	0.009			L6	0.040	0.097	0.009
		L5	0.130	0.208	0.062			R6	0.030	0.102	0.007
		R5	0.054	0.201	0.027		178	L1	0.017	0.070	0.002
		L6	0.070	0.173	0.025			R1	0.008	0.063	0.001
		R6	0.008	0.132	0.003			L2	0.048	0.141	0.018
	178	L1	0.001	0.053	0.000			R2	0.088	0.105	0.021
		R1	0.001	0.050	0.000			L3	0.042	0.113	0.010
		L2	0.095	0.158	0.040			R3	0.035	0.080	0.007
		R2	0.089	0.148	0.039			L5	0.097	0.127	0.029
		L3	0.031	0.088	0.008			L6	0.028	0.066	0.005
		R3	0.011	0.086	0.003			R6	0.048	0.093	0.011
		L4	0.005	0.052	0.001		179	L1	0.066	0.079	0.017
		R4	0.001	0.033	0.000			L2	0.031	0.153	0.015
		L5	0.019	0.131	0.007			R2	0.066	0.159	0.028
		R5	0.014	0.123	0.006			L3	0.030	0.096	0.007
		L6	0.007	0.063	0.002			R3	0.028	0.117	0.007
		R6	0.009	0.067	0.002			R4	0.193	0.081	0.036

Note – Table is continued on the next page.

Superficial DH (continued)						Dorsal Columns (continued)					
	Rat #	Section	TSP4	GFAP	Coloc.		Rat #	Section	TSP4	GFAP	Coloc.
inj-VEHd4	179	L1	0.009	0.032	0.001	inj-VEHd4	179	L5	0.069	0.068	0.015
		R1	0.069	0.060	0.012			R5	0.068	0.095	0.016
		L2	0.068	0.214	0.038			R6	0.044	0.076	0.007
		R2	0.019	0.147	0.010		180	L1	0.017	0.032	0.001
		L3	0.020	0.063	0.006			R1	0.012	0.030	0.000
		L4	0.031	0.097	0.008			L3	0.019	0.041	0.001
		L5	0.057	0.186	0.021			R3	0.026	0.049	0.002
		R5	0.032	0.112	0.010			L4	0.029	0.040	0.003
		L6	0.064	0.191	0.023			R4	0.030	0.042	0.003
		R6	0.016	0.070	0.003			L5	0.126	0.076	0.017
	180	L1	0.021	0.042	0.004			L6	0.064	0.044	0.003
		R1	0.005	0.048	0.001			R6	0.047	0.051	0.003
		L3	0.006	0.041	0.001		182	L2	0.028	0.051	0.003
		R3	0.010	0.120	0.003			R2	0.024	0.044	0.002
		L4	0.034	0.066	0.009			L3	0.097	0.075	0.012
		R4	0.010	0.070	0.003			R3	0.074	0.081	0.011
		L5	0.068	0.129	0.026			L4	0.062	0.065	0.005
		R5	0.016	0.114	0.005			R4	0.076	0.073	0.007
		L6	0.007	0.049	0.001			R5	0.009	0.049	0.001
		R6	0.013	0.099	0.004			L6	0.023	0.059	0.002
	182	L1	0.011	0.043	0.002	sham-VEHd4	165	L1	0.025	0.034	0.002
		R1	0.009	0.034	0.002			R1	0.014	0.020	0.001
		L2	0.027	0.065	0.007			L2	0.015	0.046	0.001
		R2	0.013	0.053	0.003			L3	0.009	0.047	0.000
		L3	0.045	0.102	0.013			R3	0.013	0.038	0.001
		R3	0.065	0.097	0.018			L4	0.028	0.050	0.003
		L4	0.058	0.089	0.017			R4	0.017	0.043	0.002
		R4	0.028	0.084	0.008			L5	0.018	0.045	0.002
		L5	0.013	0.074	0.003			L6	0.056	0.042	0.001
		R5	0.008	0.070	0.002			R6	0.030	0.035	0.000
		L6	0.048	0.080	0.011		166	L1	0.051	0.059	0.006
sham-VEHd4	165	L1	0.014	0.036	0.002			R1	0.009	0.036	0.001
		R1	0.006	0.021	0.000			L2	0.025	0.061	0.002
		L2	0.015	0.040	0.004			R2	0.020	0.042	0.001
		R2	0.011	0.035	0.001			L3	0.019	0.033	0.001
		L3	0.004	0.037	0.000			R3	0.023	0.040	0.001
		R3	0.028	0.049	0.004			L4	0.000	0.010	0.000
		L4	0.032	0.045	0.004			L5	0.000	0.013	0.000
		L5	0.032	0.042	0.006			L6	0.001	0.021	0.000
		R5	0.020	0.079	0.006			R6	0.000	0.016	0.000
		L6	0.016	0.027	0.001		167	R2	0.009	0.002	0.000
		R6	0.005	0.038	0.000			L3	0.006	0.004	0.000
	166	L1	0.019	0.076	0.006			R3	0.005	0.008	0.000
		L2	0.017	0.076	0.006			L4	0.006	0.005	0.000
		R2	0.017	0.061	0.002			R4	0.007	0.002	0.000
		L3	0.003	0.051	0.001			L5	0.005	0.004	0.000
		R3	0.004	0.050	0.001			R5	0.004	0.004	0.000
		L4	0.000	0.009	0.000			L6	0.005	0.007	0.000
		R4	0.000	0.001	0.000			R6	0.004	0.007	0.000
	167	L1	0.000	0.000	0.000		168	L1	0.010	0.024	0.000
		R1	0.001	0.000	0.000			R1	0.007	0.009	0.000
		L2	0.008	0.002	0.000			L2	0.023	0.043	0.002
		R2	0.003	0.001	0.000			R2	0.014	0.023	0.001
		L3	0.004	0.008	0.000			L3	0.020	0.059	0.001
		R3	0.002	0.008	0.000			R3	0.006	0.032	0.000
		L4	0.002	0.001	0.000			L4	0.008	0.011	0.000
		L5	0.001	0.004	0.000			R4	0.001	0.023	0.000
		R5	0.001	0.014	0.000			L5	0.043	0.045	0.004
		L6	0.002	0.008	0.000			R5	0.017	0.037	0.002
		R6	0.001	0.009	0.000			L6	0.027	0.074	0.002
	168	L1	0.000	0.010	0.000			R6	0.018	0.071	0.001
		R1	0.001	0.002	0.000		169	L1	0.002	0.004	0.000
		L2	0.001	0.040	0.000			R1	0.005	0.005	0.000
		R2	0.002	0.023	0.000			L2	0.015	0.016	0.000
		L3	0.005	0.064	0.003			R2	0.011	0.011	0.000
		R3	0.001	0.032	0.000			L3	0.022	0.020	0.000
		L5	0.011	0.034	0.001			R3	0.014	0.017	0.000
		R5	0.001	0.037	0.000			L4	0.029	0.019	0.001

Note – Table is continued on the next page.

Superficial DH (continued)						Dorsal Columns (continued)					
	Rat #	Section	TSP4	GFAP	Coloc.		Rat #	Section	TSP4	GFAP	Coloc.
sham-VEHd4	169	L1	0.001	0.015	0.000	shan-VEHd4	169	R4	0.019	0.014	0.000
		L2	0.015	0.035	0.003			L5	0.028	0.018	0.001
		R2	0.009	0.008	0.000			R5	0.042	0.034	0.002
		L3	0.008	0.038	0.001			L6	0.026	0.036	0.001
		R3	0.003	0.011	0.000			R6	0.018	0.051	0.001
		L4	0.030	0.053	0.008		170	L2	0.046	0.045	0.003
		R4	0.012	0.008	0.000			R2	0.045	0.050	0.003
		L5	0.064	0.067	0.017			L3	0.050	0.016	0.000
		R5	0.030	0.011	0.001			L4	0.067	0.022	0.002
		L6	0.035	0.061	0.007			R4	0.042	0.028	0.001
		R6	0.006	0.033	0.000			L5	0.019	0.010	0.000
	170	L2	0.076	0.046	0.006	inj-BPd4	153	L2	0.008	0.043	0.001
		R2	0.054	0.063	0.012			L3	0.053	0.115	0.016
		L3	0.107	0.064	0.018			R3	0.059	0.157	0.018
		L4	0.009	0.028	0.001			L4	0.009	0.053	0.001
		R4	0.006	0.016	0.000			L5	0.005	0.046	0.001
		L5	0.046	0.021	0.001			R5	0.113	0.235	0.063
inj-BPd4	153	L2	0.023	0.169	0.014			L6	0.014	0.070	0.004
		R2	0.003	0.024	0.001			R6	0.039	0.099	0.015
		L3	0.012	0.039	0.004		154	L1	0.030	0.071	0.003
		R3	0.005	0.036	0.001			R1	0.036	0.060	0.004
		L4	0.006	0.016	0.002			L2	0.033	0.061	0.005
		L5	0.011	0.099	0.006			R2	0.054	0.109	0.011
		R5	0.006	0.099	0.002			L4	0.026	0.050	0.002
		L6	0.021	0.071	0.010			L5	0.017	0.094	0.003
		R6	0.010	0.099	0.003			R5	0.027	0.073	0.005
	154	L1	0.013	0.062	0.003			L6	0.106	0.126	0.020
		R1	0.020	0.030	0.002		155	L2	0.005	0.028	0.001
		L2	0.049	0.107	0.022			R2	0.005	0.019	0.000
		R2	0.013	0.068	0.004			L3	0.005	0.029	0.000
		R3	0.295	0.245	0.169			R3	0.003	0.031	0.000
		L4	0.004	0.015	0.000			L5	0.017	0.061	0.001
		L5	0.017	0.077	0.008			R5	0.005	0.033	0.000
		R5	0.004	0.072	0.001		156	L2	0.005	0.020	0.000
		L6	0.007	0.016	0.000			R2	0.058	0.083	0.014
		R6	0.021	0.052	0.010			R3	0.015	0.044	0.002
	155	L2	0.013	0.078	0.004			R5	0.015	0.029	0.001
		R2	0.001	0.029	0.000			L6	0.012	0.027	0.000
		L3	0.007	0.059	0.002			R6	0.023	0.022	0.001
		R3	0.001	0.030	0.000		157	L2	0.012	0.038	0.001
		L4	0.001	0.020	0.000			L3	0.013	0.029	0.001
		L5	0.002	0.037	0.000			L5	0.023	0.054	0.002
		R5	0.005	0.015	0.000			R5	0.019	0.053	0.002
	156	R2	0.001	0.049	0.000			R6	0.017	0.042	0.002
		L3	0.001	0.040	0.000		158	R1	0.018	0.037	0.001
		R3	0.001	0.039	0.000			L2	0.060	0.089	0.012
		L4	0.012	0.051	0.003			R2	0.055	0.067	0.010
		R4	0.001	0.041	0.000			L3	0.020	0.039	0.002
		L5	0.031	0.104	0.010			R3	0.024	0.064	0.003
		R6	0.003	0.029	0.000			L4	0.034	0.031	0.001
	157	L2	0.033	0.212	0.024			L5	0.038	0.063	0.003
		R2	0.016	0.147	0.009			R5	0.028	0.052	0.002
		L3	0.017	0.210	0.013			L6	0.025	0.045	0.003
		R3	0.007	0.128	0.004			R6	0.024	0.053	0.003
		R5	0.019	0.127	0.006						
		L6	0.020	0.083	0.004						
		R6	0.021	0.114	0.007						
	158	L1	0.008	0.066	0.005						
		R1	0.003	0.066	0.001						
		L2	0.031	0.184	0.017						
		R2	0.108	0.193	0.064						
		L3	0.002	0.126	0.001						
		R3	0.002	0.128	0.001						
		L5	0.057	0.102	0.033						
		R5	0.063	0.102	0.024						
		L6	0.036	0.110	0.012						
		R6	0.029	0.071	0.006						

Note – Table is continued on the next page.

Deep DH						Deep DH (continued)					
	Rat #	Section	TSP4	GFAP	Coloc.		Rat #	Section	TSP4	GFAP	Coloc.
inj-VEH0h	171	L2	0.140	0.086	0.009	inj-BP0h	148	L1	0.024	0.077	0.001
		L3	0.069	0.050	0.003			L2	0.096	0.028	0.001
		L4	0.094	0.085	0.005			L3	0.049	0.074	0.005
		L5	0.103	0.112	0.006			L4	0.023	0.094	0.002
		L6	0.099	0.072	0.003			L5	0.083	0.098	0.015
	172	L2	0.110	0.039	0.008			L6	0.061	0.089	0.007
		L4	0.175	0.118	0.003		149	L1	0.032	0.097	0.002
		L5	0.062	0.017	0.002			L2	0.048	0.142	0.008
	173	L1	0.012	0.089	0.001			L3	0.082	0.090	0.005
		L2	0.023	0.138	0.002			L4	0.017	0.027	0.000
		L3	0.026	0.129	0.002			L5	0.062	0.084	0.009
		L4	0.018	0.124	0.001			L6	0.005	0.058	0.000
		L5	0.054	0.134	0.005		150	L1	0.019	0.045	0.001
		L6	0.041	0.152	0.004			L2	0.002	0.125	0.001
	174	L1	0.040	0.032	0.001			L3	0.002	0.112	0.000
		L3	0.019	0.141	0.002			L5	0.015	0.046	0.000
		L4	0.123	0.120	0.005		151	L1	0.021	0.060	0.000
	175	L1	0.007	0.179	0.000			R1	0.039	0.083	0.001
		L2	0.015	0.197	0.002			R2	0.017	0.078	0.001
		L3	0.006	0.147	0.000			R2	0.039	0.047	0.001
		L4	0.059	0.085	0.001			L3	0.045	0.023	0.001
		L5	0.004	0.180	0.000			R3	0.045	0.048	0.001
		L6	0.146	0.049	0.001			R5	0.019	0.007	0.000
	176	L5	0.021	0.122	0.000			L6	0.003	0.038	0.000
sham-VEH0h	159	L2	0.012	0.101	0.001			R6	0.008	0.054	0.000
		L3	0.010	0.073	0.001		152	L2	0.005	0.113	0.000
		L4	0.014	0.088	0.001			L3	0.002	0.097	0.000
		L5	0.012	0.094	0.002			L4	0.002	0.094	0.000
		L6	0.010	0.093	0.001			L5	0.013	0.130	0.002
	160	L2	0.011	0.095	0.001			L6	0.018	0.118	0.003
		L3	0.006	0.095	0.000	inj-VEHd4	177	L1	0.025	0.034	0.003
		L5	0.008	0.091	0.000			L2	0.044	0.039	0.005
		L6	0.008	0.076	0.000			L4	0.009	0.037	0.001
	161	L1	0.012	0.061	0.000			L5	0.009	0.036	0.001
		R1	0.023	0.047	0.000		178	L1	0.005	0.045	0.001
		L2	0.016	0.078	0.001			L2	0.023	0.047	0.003
		L3	0.020	0.090	0.001			L3	0.004	0.033	0.001
		L5	0.041	0.088	0.008			L4	0.009	0.037	0.001
		L6	0.037	0.089	0.004			L5	0.001	0.032	0.000
	162	L1	0.064	0.057	0.000			L6	0.013	0.037	0.001
		L2	0.030	0.167	0.005		179	L1	0.044	0.045	0.008
		L3	0.030	0.121	0.002			L2	0.001	0.034	0.000
		L4	0.012	0.133	0.001			L6	0.036	0.043	0.004
		L5	0.011	0.106	0.000		180	L1	0.021	0.025	0.001
		L6	0.014	0.113	0.001			L3	0.006	0.038	0.001
	163	L2	0.025	0.134	0.001			L4	0.043	0.026	0.004
		L3	0.086	0.089	0.003			L5	0.035	0.065	0.006
		L4	0.017	0.116	0.001			L6	0.010	0.050	0.003
		L5	0.078	0.004	0.000		182	L1	0.018	0.036	0.002
		L6	0.020	0.114	0.001			L2	0.012	0.024	0.001
	164	L5	0.075	0.047	0.002			L3	0.028	0.026	0.002
		L6	0.070	0.031	0.001			L4	0.035	0.025	0.002
inj-BP0h	147	L1	0.025	0.038	0.001			L5	0.018	0.060	0.003
		R1	0.013	0.039	0.000			L6	0.022	0.028	0.001
		L2	0.054	0.039	0.002	sham-VEHd4	165	L2	0.013	0.016	0.000
		R2	0.075	0.027	0.001			L3	0.011	0.013	0.000
		R3	0.114	0.058	0.003			L4	0.009	0.008	0.000
		L4	0.006	0.031	0.000			L5	0.019	0.018	0.001
		R4	0.011	0.028	0.000			L6	0.011	0.019	0.000
		L5	0.081	0.005	0.000		166	L1	0.005	0.037	0.001
		R5	0.077	0.006	0.001			L2	0.010	0.038	0.001
		L6	0.030	0.006	0.000			L3	0.009	0.027	0.001
		R6	0.070	0.025	0.000			L6	0.001	0.020	0.000

Note – Table is continued on the next page.

Deep DH (continued)					
	Rat #	Section	TSP4	GFAP	Coloc.
sham-VEHd4	167	L3	0.006	0.002	0.000
		L4	0.003	0.003	0.000
		L5	0.006	0.004	0.000
		L6	0.004	0.005	0.000
	168	L1	0.002	0.004	0.000
		L2	0.004	0.006	0.000
		L3	0.003	0.027	0.000
		L5	0.008	0.016	0.000
	169	L1	0.003	0.001	0.000
		L2	0.012	0.005	0.000
		L3	0.003	0.006	0.000
		L4	0.013	0.004	0.000
		L5	0.021	0.008	0.000
	170	L2	0.057	0.044	0.004
		L4	0.006	0.021	0.000
inj-BPd4	153	L2	0.008	0.006	0.000
		L5	0.004	0.006	0.000
	154	L1	0.017	0.008	0.000
		L2	0.021	0.018	0.002
		L4	0.002	0.004	0.000
		L5	0.004	0.010	0.000
		L6	0.020	0.007	0.000
	155	L3	0.002	0.021	0.000
		L4	0.001	0.016	0.000
	156	L1	0.004	0.005	0.000
		L2	0.004	0.008	0.000
		L3	0.003	0.011	0.000
		L4	0.011	0.034	0.001
		L6	0.011	0.017	0.001
	157	L2	0.048	0.065	0.013
		L3	0.016	0.032	0.004
		L5	0.028	0.064	0.006
	158	L1	0.009	0.023	0.001
		L2	0.029	0.037	0.003
		L3	0.006	0.027	0.001
		L4	0.012	0.012	0.001
		L5	0.019	0.019	0.001
		L6	0.016	0.027	0.002

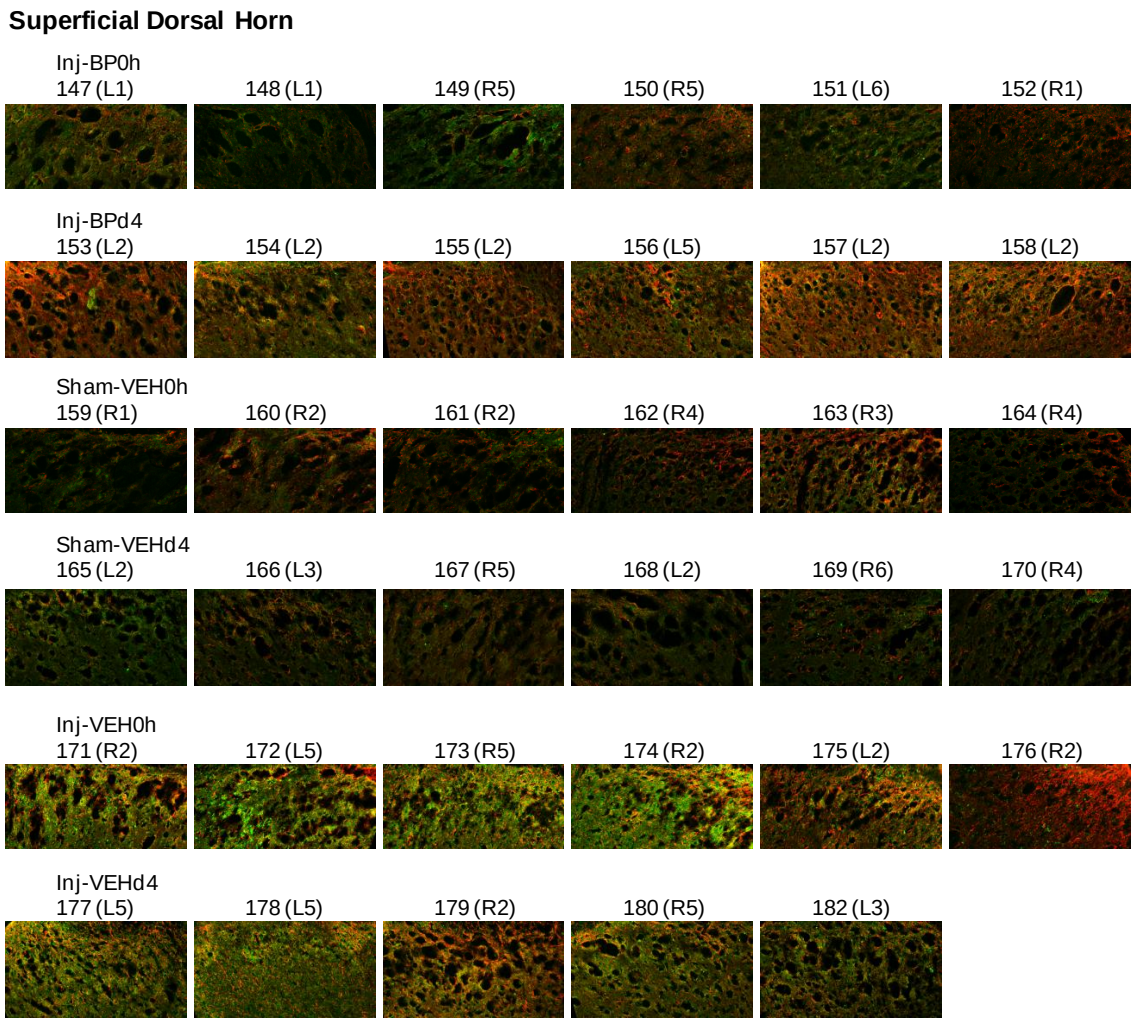

Figure G.4. Immunolabeling of TSP4 (green) and GFAP (red) in the superficial dorsal horn at day 7 for the bupivacaine treatment study. TSP4 and GFAP labeling were evaluated after sham or painful facet joint injury followed by intra-articular bupivacaine (BP) or saline vehicle (VEH) injections either immediately (*inj-BP0h*, *inj-VEH0h*, *sham-VEH0h*) or at day 4 (*inj-BPd4*, *inj-VEHd4*, *sham-VEHd4*). Representative images are indicated by the rat number, and an image number that includes the right (R) or left (L) side of the spinal cord and the section of tissue (consecutive sections were labeled 1-6 for each rat).

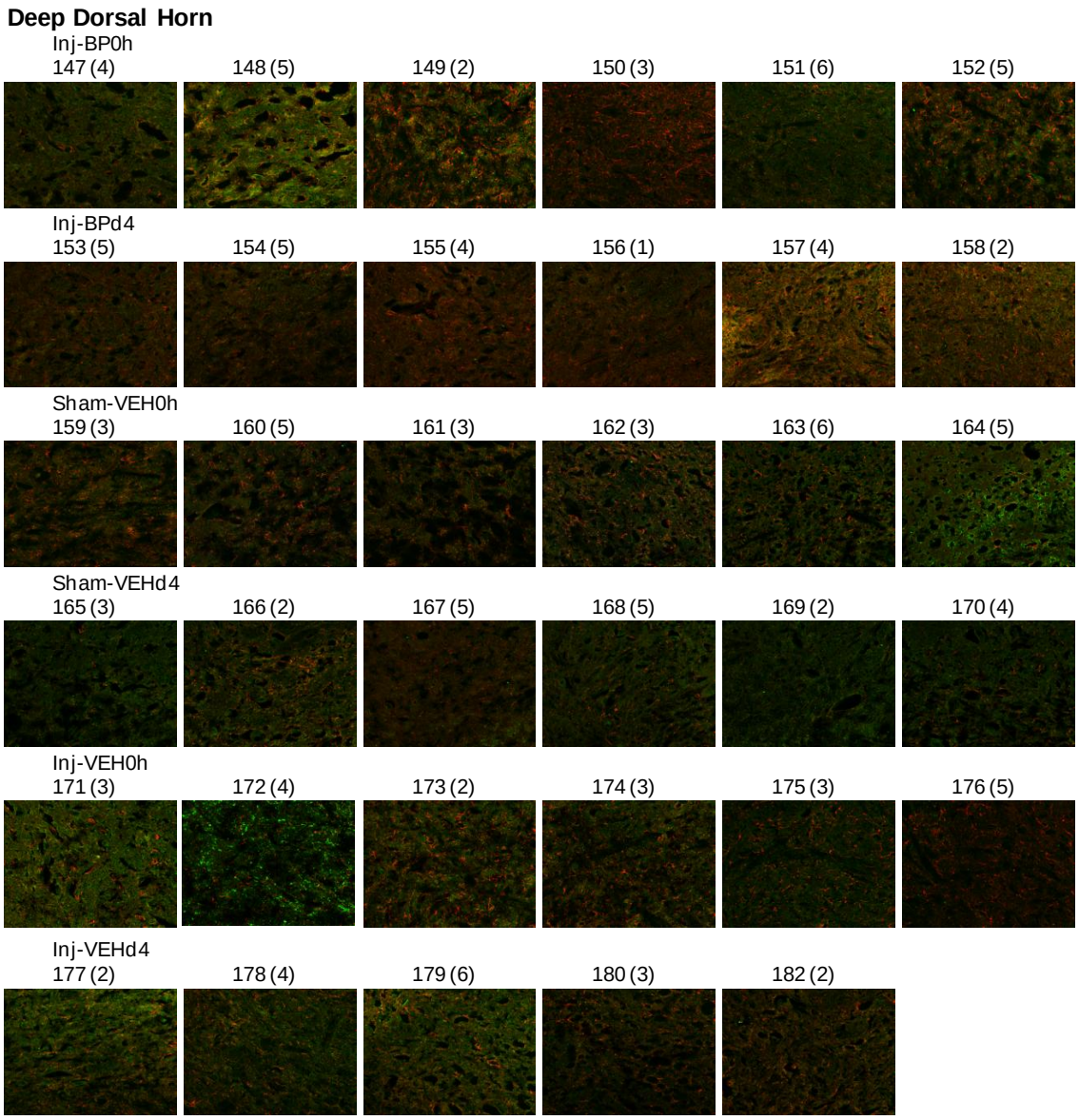

Figure G.5. Immunolabeling of TSP4 (green) and GFAP (red) in the deep dorsal horn at day 7 for the bupivacaine treatment study. TSP4 and GFAP labeling were evaluated after sham or painful facet joint injury followed by intra-articular bupivacaine (BP) or saline vehicle (VEH) injections either immediately (*inj-BP0h, inj-VEH0h, sham-VEH0h*) or at day 4 (*inj-BPd4, inj-VEHd4, sham-VEHd4*). Representative images are indicated by the rat number and section of tissue (consecutive sections were labeled 1-6 for each rat).

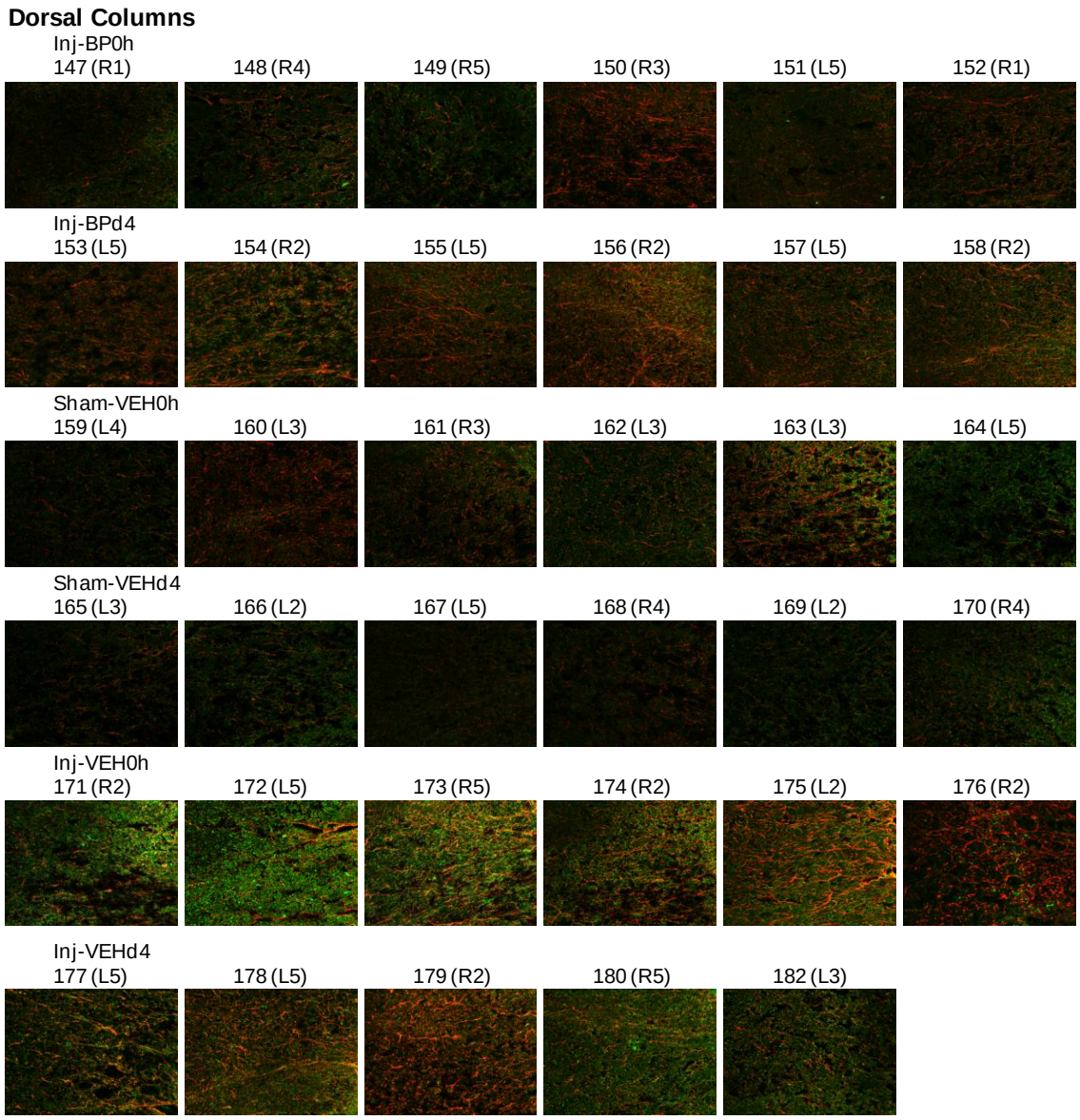

Figure G.6. Immunolabeling of TSP4 (green) and GFAP (red) in the dorsal columns at day 7 for the bupivacaine treatment study. TSP4 and GFAP labeling were evaluated after sham or painful facet joint injury followed by intra-articular bupivacaine (BP) or saline vehicle (VEH) injections either immediately (*inj-BP0h, inj-VEH0h, sham-VEH0h*) or at day 4 (*inj-BPd4, inj-VEHd4, sham-VEHd4*). Representative images are indicated by the rat number, and an image number that includes the right (R) or left (L) side of the spinal cord and the section of tissue (consecutive sections were labeled 1-6 for each rat).

APPENDIX H

Protocol for Counting Excitatory Synaptic Puncta

This appendix details the protocol used for counting excitatory synapses from confocal microscopy images of immunolabeled spinal cord sections. The protocol, detailed in Section H.1, is based on previously published methods (Ippolito and Eroglu, 2010). Spinal cord sections were labeled for synapsin, a presynaptic structural protein, and homer, a postsynaptic protein found in excitatory synapses. Detailed methods for immunolabeling and confocal imaging of synaptic proteins are presented in Section 5.3.5 of Chapter 5. Confocal image stacks were acquired with up to 12 images at increments of 0.33μm in the z-axis. Each sequence of three images (i.e., images 1-3, images 4-6, etc.) was combined to create a maximum intensity projection (MIP) corresponding to 1μm of tissue depth using a custom MATLAB code (see Section E.2 of Appendix E).

H.1. Protocol for Counting Synaptic Puncta

1. Open an MIP in ImageJ (NIH; Bethesda, MD) with the Puncta Analyzer plug-in installed. The Puncta Analyzer plug-in requires ImageJ version 1.29 or older.
2. Select a region of interest or select the entire image and initialize the Punta Analyzer plug-in.

3. In the opening dialogue box, select the boxes for the red and green channels, and select the boxes to subtract background in the red and green channels (Fig. H.1).

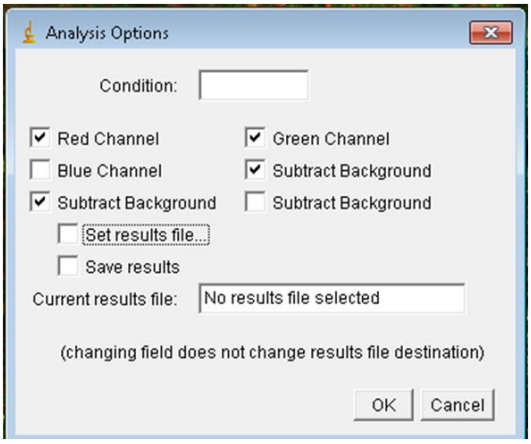

Fig. H.1. Puncta Analyzer initialization dialogue box. The red and green channels are selected for synapsin- (red) and homer-labeled (green) images, and background subtraction is selected for each channel.

4. For the first (red) channel, subtract background by selecting a rolling ball radius of 50 and deselecting the check box marked "White Background" (Fig. H.2).

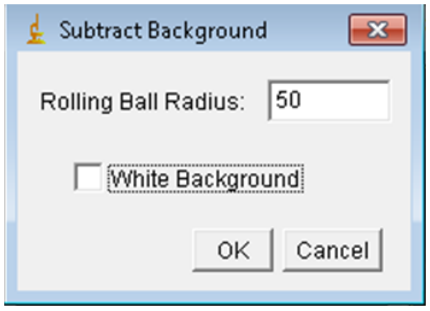

Fig. H.2. Background subtraction dialogue box. Select a rolling ball radius of 50 for background subtraction. The grayscale images have a black background, so deselect the check box for white background.

5. Move the slider bar to set the threshold for positive labeling in the red channel. The threshold should be set such that puncta in the spinal cord are discriminated from background labeling. The grayscale image with an overlayed depiction of positively-

labeled pixels can be compared with the original two-color image to determine if the selected threshold value discriminates positively-labeled puncta (Fig. H.3).

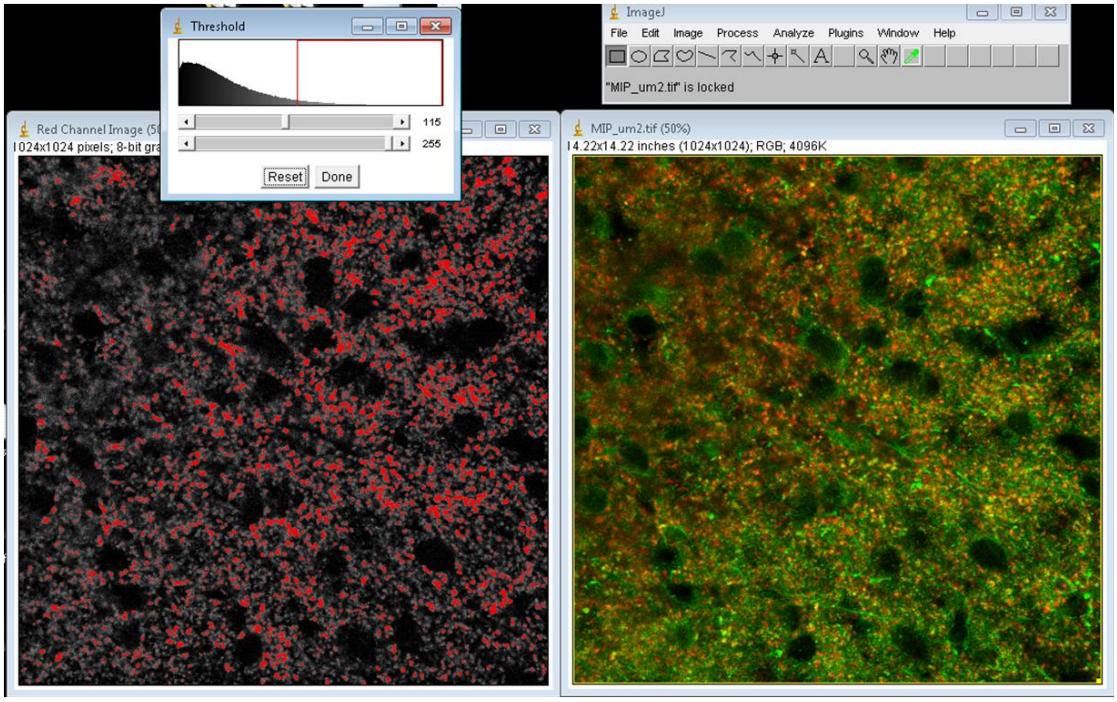

Fig. H.3. Detection threshold for synaptic puncta. Choose a detection threshold that discriminates positively-labeled puncta (shown in red on the grayscale image to the left) from the background of the image. Use the original image (right) to confirm detection of positively-labeled puncta.

6. Once a threshold value is selected, the next dialogue box determines the sensitivity of the detection algorithm to the size of positively-labeled puncta. Choose a minimum size of 4 pixels to discount all puncta with clusters of 3 or fewer pixels (Fig. H.4).
7. Repeat steps 4-6 for the green channel.
8. The generated results file reports the number of red, green, and colocalized puncta. Save the results as a .TXT file and save the new .TIFF image showing the locations of detected puncta overlaid on the original image. Record the red threshold, green threshold, and number of colocalized puncta in a separate Microsoft Excel table.

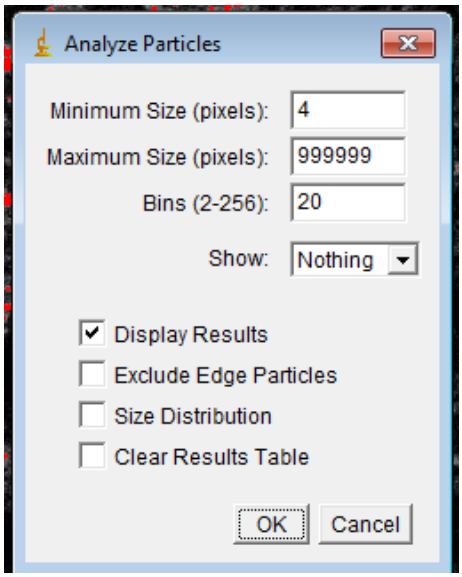

Fig. H.4. Puncta size dialogue box. Set the "Minimum Size" to 4 pixels to detect only those puncta comprised of 4 or more positively-labeled pixels clustered together. Check the box marked "Display Results" to output the number of puncta for the red and green channels and the number of colocalized puncta.

9. Determine the area of the tissue as a percentage of the total image area, excluding any holes or gaps in the tissue. A custom MATLAB code was written to find the area of the tissue parenchyma (see Section E.3 of Appendix E). For each image, choose a detection threshold that best discriminates the labeled tissue from holes or gaps in the tissue section (Fig. H.5). Record the chosen threshold value and the percentage of the image area identified as tissue.
10. Divide the number of colocalized synaptic puncta by the tissue area percentage to calculate the synapse number normalized to the tissue area, or the synapse density.

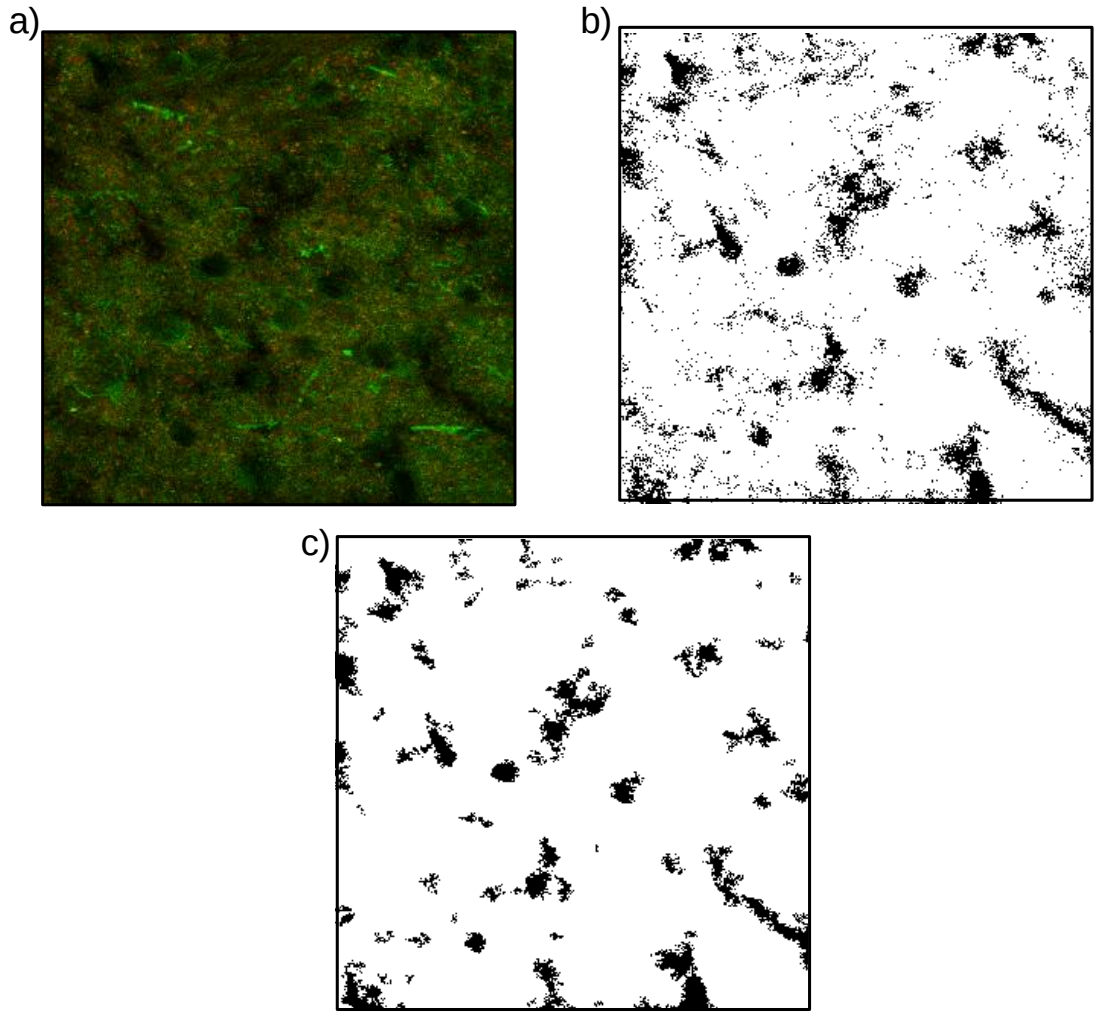

Fig. H.5. Detection of tissue area. A black and white mask is applied to the original image **(a)** by converting each pixel to black or white depending on its fluorescence intensity. **(b)** The black/white intensity threshold can be iteratively determined to discriminate tissue (white) from holes and gaps in the tissue (black). The threshold was set to 0.065 for this representative image. **(c)** After smoothing the black and white mask, the black areas correspond to the unlabeled regions in the original image.

APPENDIX I

Quantification of Synaptic Puncta in the Spinal Dorsal Horn

This appendix summarizes the quantification of excitatory synapses in the spinal dorsal horn. The protocol for synapse counting is presented in detail in Section H.1 of Appendix H. The tables in this appendix include the number of synapses identified in each image of the spinal dorsal horn, along with the group, rat number, and tissue section number (consecutive sections were numbered 1-6 on each slide). The percentage of tissue parenchyma in each image was measured using a custom MATLAB code (see Section E.3 of Appendix E) and used to calculate the normalized number of synapses per area. The fraction of the image detected as tissue area (Area), the threshold used for detection of tissue area (Area Coefficient), and the normalized synapse number (Normalized Synapses) are presented for each image in all tables. Tables I.2-I.4 also include the red and green channel thresholds (Red Threshold and Green Threshold) used for detecting synaptic puncta.

Table I.1 details the synapse counts from the superficial and deep dorsal horn at day 7 after sham or painful facet joint injury in the studies presented in Chapter 5. Table I.2 presents synapse counts in the superficial dorsal horn at day 7 after painful facet joint injury for rats that received TSP4 antisense or mismatch oligonucleotides, and Table I.3 presents synapse counts in the superficial dorsal horn at day 7 after painful facet joint

injury for rats that received and gabapentin (*Inj-GBP*) or vehicle treatment (*Inj-VEH*); both tables correspond to studies presented in Chapter 5. Lastly, Table I.4 lists synapse counts in the superficial dorsal horn at day 7 after sham or painful facet joint injury in rats that received intra-articular bupivacaine (BP) or saline vehicle (VEH) either immediately (*inj-BP0h*, *inj-VEH0h*, *sham-VEH0h*) or at day 4 (*inj-BPd4*, *inj-VEHd4*, *sham-VEHd4*) after injury, in studies presented in Chapter 5.

Table I.1. Quantification of synapses at day 7 after sham or painful facet joint injury (Chapter 5).

Group		Rat #	Slice	Side	Stack	Synapses	Area	Area Coefficient	Normalized Synapses
Superficial Dorsal Horn	Injury	47	4	L	41	314	0.800	0.065	392.35
			5	L	43	176	0.717	0.065	245.36
			1	R	81	521	0.727	0.07	717.04
			2	R	83	175	0.689	0.07	253.84
		48	2	R	37	91	0.669	0.055	136.00
			2	R	79	323	0.598	0.075	539.95
			3	R	77a	207	0.834	0.075	248.08
		49	7	L	21	203	0.607	0.06	334.60
			8	L	23	346	0.787	0.075	439.70
			2	R	61a	190	0.652	0.065	291.50
		52	4	L	25	456	0.801	0.07	569.43
			5	L	27	197	0.591	0.065	333.39
			5	R	65	422	0.483	0.075	873.89
			6	L	67	127	0.739	0.075	171.76
		53	9	R	85	242	0.617	0.07	392.28
			7	R	45a	93	0.762	0.07	122.06
		54	4	L	5	202	0.740	0.05	272.97
			5	L	7	189	0.440	0.055	429.74
			10	R	49	178	0.743	0.065	239.47
			11	L	51	67	0.561	0.07	119.34
			6	R	87	170	0.655	0.075	259.54
	Sham	50	8	L	29	119	0.534	0.06	222.93
			9	L	31	45	0.675	0.055	66.66
			1	L	69	161	0.802	0.065	200.65
			2	R	71	171	0.860	0.07	198.93
		55	7	L	17	128	0.645	0.05	198.36
			8	L	19	339	0.814	0.06	416.56
			2	L	53	246	0.693	0.07	355.18
			9	L	55	150	0.881	0.06	170.36
		56	4	L	13	114	0.526	0.06	216.73
			7	R	57	122	0.711	0.065	171.49
			8	R	59	136	0.721	0.07	188.63
		60	4	L	33	107	0.594	0.06	180.26
			5	L	35	152	0.804	0.06	189.01
			11	L	73	128	0.741	0.06	172.72
			6	R	75	258	0.776	0.065	332.69
Deep Dorsal Horn	Injury	47	4	L	42	141	0.641	0.06	220.07
			5	L	44	42	0.624	0.05	67.34
			1	R	82	81	0.815	0.075	99.36
			2	R	84	427	0.795	0.07	537.38
		48	2	R	38	56	0.774	0.05	72.36
			4	L	40	100	0.688	0.06	145.29
			3	R	78	279	0.810	0.07	344.66
			2	R	80	57	0.729	0.055	78.19
		49	7	L	22	189	0.718	0.055	263.34
			8	L	24	26	0.641	0.07	40.56
			2	R	62a	134	0.518	0.075	258.54

Note – Table is continued on the next page.

Group		Rat #	Slice	Side	Stack	Synapses	Area	Area Coefficient	Normalized Synapses
Deep Dorsal Horn (continued)	Injury	52	4	L	26	12	0.586	0.06	20.50
			5	L	28	204	0.596	0.065	342.05
			5	R	66	405	0.680	0.07	595.41
			6	L	68	107	0.674	0.06	158.75
		53	1	L	2	119	0.681	0.05	174.74
			2	L	3	53	0.647	0.05	81.98
			9	R	86	166	0.640	0.07	259.29
			7	R	46a	49	0.734	0.06	66.74
		54	4	L	6	280	0.819	0.05	341.88
			5	L	8	107	0.792	0.05	135.14
			10	R	50	155	0.584	0.065	265.41
			6	L	88	152	0.690	0.06	220.23
	Sham	50	8	L	30	37	0.819	0.05	45.17
			9	L	32	89	0.731	0.05	121.72
			1	L	70	242	0.726	0.06	333.47
			2	R	72	295	0.890	0.07	331.65
		55	7	L	18	284	0.714	0.07	397.76
			8	L	20	169	0.784	0.06	215.53
			2	L	54	282	0.766	0.07	368.24
			9	L	56	177	0.754	0.06	234.81
		56	5	L	16	50	0.817	0.06	61.19
			7	R	58	214	0.664	0.065	322.29
			8	R	60	508	0.731	0.075	694.75
		60	4	L	34	175	0.610	0.06	286.70
			5	L	36	30	0.506	0.05	59.32
			11	L	74	44	0.653	0.06	67.36
			6	R	76	141	0.853	0.065	165.34

Table I.2. Quantification of synapses at day 7 after painful facet injury and prior treatment with TSP4 antisense or mismatch oligonucleotides (Chapter 5).

Group	Rat #	Slice	Stack	Synapses	Red Threshold	Green Threshold	Area	Area Coefficient	Normalized Synapses
Antisense Oligonucleotide Treatment	253	1	1	542	85	105	0.888	0.07	610.43
		2	2	330	90	100	0.880	0.06	375.17
		3	3	516	95	95	0.912	0.07	566.04
		4	4	418	95	110	0.809	0.06	516.75
		5	5	531	95	105	0.929	0.06	571.34
		6	6	259	105	80	0.930	0.06	278.43
	254	1	7	194	68	80	0.888	0.045	218.44
		2	8	264	100	110	0.978	0.065	269.94
		3	9	304	70	80	0.839	0.055	362.29
		4	10	186	60	60	0.892	0.047	208.64
		5	11	240	80	75	0.661	0.05	363.03
		6	12	275	75	75	0.871	0.045	315.91
	255	1	39	161	50	65	0.680	0.025	236.83
		2	40	223	48	60	0.713	0.03	312.81
		3	41	171	45	53	0.718	0.018	238.33
		4	42	497	75	85	0.725	0.037	685.42
		5	43	367	75	90	0.776	0.03	472.94
		6	44	319	90	90	0.825	0.05	386.48
	256	1	45	295	75	85	0.743	0.027	397.04
		2	46	241	80	85	0.713	0.022	337.87
		3	47	251	70	75	0.764	0.04	328.71
		4	48	397	82	90	0.753	0.035	527.15
		5	49	315	68	83	0.722	0.025	436.17
		6	50	207	50	75	0.769	0.025	269.15
	259	1	69	702	95	100	0.828	0.05	847.83
		2	70	347	90	90	0.869	0.06	399.13
		3	71	147	70	62	0.883	0.04	166.57
		4	73	550	70	73	0.850	0.04	647.36
		5	74	331	80	75	0.936	0.05	353.78
	260	1	75	767	125	130	0.954	0.06	804.40
		2	76	816	125	130	0.901	0.06	905.56
		3	77	124	77	73	0.871	0.025	142.45
		4	78	468	115	115	0.892	0.05	524.49
		5	79	594	130	115	0.837	0.045	709.68
		6	80	276	60	60	0.926	0.027	298.22
Mismatch Oligonucleotide Treatment	257	1	27	330	85	85	0.644	0.04	512.42
		2	28	570	95	95	0.796	0.055	716.44
		3	29	225	70	60	0.781	0.035	288.17
		4	30	534	95	85	0.691	0.035	772.68
		5	31	392	80	77	0.756	0.035	518.31
		6	32	259	60	50	0.760	0.035	340.70

Note – Table is continued on the next page.

Group	Rat #	Slice	Stack	Synapses	Red Threshold	Green Threshold	Area	Area Coefficient	Normalized Synapses
Mismatch Oligonucleotide Treatment (continued)	258	1	33	479	100	105	0.740	0.055	647.30
		2	34	442	77	85	0.797	0.045	554.58
		3	35	232	80	75	0.823	0.032	281.93
		4	36	538	75	95	0.822	0.03	654.26
		5	37	533	75	90	0.775	0.03	687.56
		6	38	253	50	80	0.760	0.03	332.72
	261	1	13	499	60	70	0.930	0.06	536.33
		2	14	749	105	110	0.861	0.065	870.12
		3	15	549	100	105	0.952	0.065	576.98
		4	16	446	55	65	0.909	0.055	490.54
		5	17	1091	100	120	0.973	0.06	1121.62
		6	18	519	100	115	0.909	0.075	570.83
	262	1	19	299	70	55	0.903	0.055	331.08
		2	20	737	105	95	0.972	0.065	758.54
		3	21	404	75	80	0.940	0.06	429.79
		4	22	328	50	50	0.750	0.045	437.51
		5	23	548	105	95	0.934	0.07	586.66
		6	24	340	67	70	0.840	0.05	404.76
	263	1	57	484	82	97	0.676	0.065	715.98
		2	58	646	82	102	0.692	0.06	933.26
		3	59	310	75	87	0.737	0.055	420.85
		4	60	375	73	82	0.561	0.05	668.33
		5	61	691	80	90	0.876	0.06	789.08
		6	62	254	80	80	0.792	0.055	320.87
	264	1	63	949	115	100	0.911	0.065	1041.48
		2	64	450	95	90	0.902	0.05	498.78
		3	65	248	73	77	0.832	0.045	297.97
		4	66	923	135	130	0.843	0.07	1094.51
		5	67	966	135	130	0.966	0.07	1000.52
		6	68	442	90	85	0.825	0.05	535.76

Table I.3. Quantification of synapses at day 7 for gabapentin treatment study (Chapter 5).

Group	Rat #	Stack	Synapses	Red Threshold	Green Threshold	Area	Area Coefficient	Normalized Synapses
Inj-GBP	301	1	187	115	160	0.508	0.07	367.97
		2	153	100	160	0.661	0.07	231.47
		6	141	75	145	0.584	0.055	241.31
	303	4	243	95	185	0.566	0.07	429.10
		5	220	95	165	0.730	0.06	301.58
		7	132	90	150	0.825	0.055	160.06
		8	132	95	155	0.733	0.06	180.20
	305	41	46	70	110	0.405	0.055	113.47
		42	124	90	115	0.602	0.06	205.91
		46	152	90	120	0.746	0.05	203.70
		47	247	95	130	0.646	0.06	382.23
	306	43	111	90	120	0.672	0.06	165.23
		44	75	85	110	0.625	0.055	119.94
		45	159	100	135	0.781	0.06	203.48
		48	107	85	145	0.726	0.065	147.40
	307	33	57	90	125	0.550	0.065	103.64
		34	96	90	125	0.480	0.06	200.00
		36	64	90	125	0.369	0.06	173.44
	308	35	144	95	155	0.762	0.07	188.90
		37	179	85	130	0.649	0.06	275.98
		38	154	85	125	0.466	0.065	330.19
Inj-VEH	302	26	124	80	115	0.496	0.07	250.20
		29	61	85	130	0.434	0.065	140.49
		30	122	90	135	0.543	0.078	224.84
	304	27	179	90	120	0.497	0.06	360.09
		28	339	90	145	0.643	0.07	526.89
		31	229	90	135	0.614	0.065	373.15
	337	17	124	82	150	0.437	0.065	283.95
		18	252	90	135	0.566	0.06	444.92
		19	154	80	135	0.311	0.075	494.70
		22	243	95	140	0.428	0.075	568.29
	338	20	303	100	130	0.460	0.07	659.27
		21	109	90	140	0.421	0.07	259.09
		23	235	95	185	0.402	0.11	585.16
		24	239	90	125	0.562	0.065	424.96
	339	9	94	75	125	0.341	0.075	275.42
		10	123	85	125	0.539	0.07	228.12
		13	389	105	120	0.562	0.07	691.92
		14	152	85	130	0.549	0.07	276.87
	341	11	198	85	120	0.510	0.07	388.39
		12	73	80	135	0.540	0.065	135.14
		15	217	85	155	0.584	0.08	371.32
		16	336	90	145	0.596	0.07	564.14

Table I.4. Quantification of synapses at day 7 for bupivacaine treatment study (Chapter 5).

Group	Rat #	Slice	Stack	Synapses	Red Threshold	Green Threshold	Area	Area Coefficient	Normalized Synapses
inj-VEH0h	171	1	25	351	75	103	0.582	0.07	602.99
		2	26	330	90	90	0.839	0.07	393.56
		4	27	538	105	100	0.754	0.07	713.15
		5	28	802	115	110	0.896	0.075	895.29
	172	1	29	1258	115	95	0.916	0.07	1372.76
		4	30	572	100	105	0.969	0.075	590.48
	173	1	1	329	80	70	0.724	0.075	454.23
		2	2	260	75	60	0.840	0.065	309.45
		3	3	277	73	67	0.930	0.075	297.98
	173	4	16	535	100	90	0.955	0.07	560.39
		5	17	604	110	85	0.973	0.07	620.76
		6	18	390	95	78	0.942	0.07	414.19
	174	1	19	713	115	90	0.799	0.07	892.81
		2	20	569	115	95	0.932	0.07	610.52
		3	21	350	90	80	0.925	0.075	378.21
		4	22	449	105	85	0.939	0.075	478.27
		5	23	724	115	90	0.956	0.07	757.01
		6	24	453	90	78	0.921	0.065	491.70
	175	1	4	240	73	70	0.847	0.06	283.29
		2	5	216	82	75	0.937	0.07	230.57
		3	6	275	73	75	0.977	0.06	281.62
		4	7	624	115	90	0.902	0.065	692.10
		5	8	630	110	90	0.967	0.07	651.70
		6	9	685	95	90	0.899	0.07	762.30
	176	1	10	1016	110	95	0.941	0.07	1080.05
		2	11	945	115	100	0.972	0.07	972.62
		3	12	486	100	97	0.917	0.065	529.93
		4	13	547	90	60	0.854	0.06	640.29
		5	14	726	110	75	0.901	0.06	805.68
		6	15	710	100	87	0.857	0.06	828.37
inj-BP0h	147	1	31	162	70	75	0.473	0.07	342.78
		2	32	170	55	60	0.587	0.07	289.81
		3	33	208	65	70	0.674	0.065	308.61
		4	34	282	90	95	0.845	0.065	333.57
		5	35	212	77	75	0.713	0.065	297.42
		6	36	131	70	65	0.681	0.05	192.51
	148	1	43	327	75	80	0.766	0.055	426.84
		2	44	407	68	70	0.771	0.06	528.02
		3	45	122	70	60	0.789	0.05	154.61
		4	46	426	90	87	0.731	0.06	583.08
		5	47	303	73	70	0.790	0.05	383.69
		6	48	223	70	60	0.749	0.05	297.77
	149	1	49	376	100	85	0.906	0.06	415.10
		2	50	185	75	65	0.809	0.055	228.71
		3	51	253	80	55	0.860	0.055	294.05
		4	52	860	120	100	0.854	0.07	1006.67
		5	53	150	80	65	0.887	0.055	169.15
		6	54	426	120	110	0.891	0.07	477.95

Note – Table is continued on the next page.

Group	Rat #	Slice	Stack	Synapses	Red Threshold	Green Threshold	Area	Area Coefficient	Normalized Synapses
inj-BP0h (continued)	150	1	55	300	90	82	0.811	0.055	370.00
		2	56	335	80	70	0.856	0.05	391.45
		3	57	171	75	85	0.852	0.06	200.63
		4	58	338	115	100	0.889	0.06	380.29
		5	59	167	85	75	0.895	0.06	186.53
		6	60	384	115	100	0.847	0.06	453.26
	151	1	37	310	65	63	0.890	0.06	348.43
		2	38	312	64	70	0.809	0.065	385.52
		3	39	224	70	72	0.821	0.065	272.77
		4	40	250	100	80	0.819	0.06	305.40
		5	41	188	45	50	0.778	0.04	241.55
		6	42	78	58	50	0.720	0.035	108.36
	152	1	61	645	125	105	0.951	0.07	678.09
		2	62	336	115	105	0.925	0.07	363.24
		3	63	309	85	80	0.890	0.06	347.11
		4	64	225	90	75	0.910	0.06	247.28
		5	65	193	72	78	0.920	0.07	209.85
		6	66	255	87	65	0.845	0.06	301.81
sham-VEH0h	159	1	67	431	105	93	0.890	0.07	484.54
		2	68	77	75	70	0.811	0.055	94.96
		3	69	69	75	70	0.846	0.06	81.57
		4	70	650	105	115	0.923	0.075	704.61
		5	71	166	110	90	0.898	0.07	184.96
		6	72	282	85	70	0.917	0.065	307.63
	160	1	73	381	105	115	0.841	0.06	452.92
		2	74	261	105	90	0.840	0.06	310.79
		3	75	176	68	65	0.906	0.05	194.26
		4	76	383	90	85	0.838	0.06	457.10
		5	77	65	72	68	0.839	0.07	77.44
	161	1	80	79	80	75	0.949	0.07	83.28
		2	81	145	73	70	0.829	0.055	174.85
		3	82	57	67	60	0.839	0.04	67.91
		4	83	396	100	95	0.836	0.06	473.97
		5	84	305	105	90	0.815	0.06	374.19
		6	85	187	65	70	0.652	0.06	286.72
	162	1	86	514	115	105	0.912	0.07	563.84
		2	87	733	115	120	0.980	0.075	747.65
		3	88	374	100	95	0.926	0.06	403.89
		4	89	488	90	88	0.934	0.075	522.26
		5	90	294	105	100	0.938	0.075	313.40
	163	1	91	180	95	85	0.934	0.07	192.82
		2	92	139	82	85	0.678	0.06	205.17
		3	93	189	85	85	0.781	0.06	241.94
		4	94	187	90	92	0.720	0.06	259.90
		5	95	320	125	100	0.752	0.06	425.59
		6	96	191	90	85	0.696	0.055	274.35
	164	1	97	210	90	100	0.876	0.06	239.86
		2	98	293	100	103	0.858	0.06	341.41
		3	99	253	75	75	0.857	0.06	295.08
		4	100	351	75	80	0.823	0.07	426.44
		5	101	607	105	90	0.893	0.07	679.50
		6	102	287	85	70	0.973	0.07	294.87

Note – Table is continued on the next page.

Group	Rat #	Slice	Stack	Synapses	Red Threshold	Green Threshold	Area	Area Coefficient	Normalized Synapses
inj-VEHd4	177	1	1	328	64	65	0.853	0.075	384.75
		2	2	438	85	80	0.948	0.075	461.98
		3	3	263	85	70	0.882	0.07	298.32
		4	4	278	85	75	0.937	0.075	296.79
		5	5	474	95	80	0.931	0.075	509.24
		6	6	554	100	75	0.919	0.065	603.16
	178	1	7	720	100	85	0.955	0.07	754.24
		2	8	593	90	85	0.954	0.075	621.59
		3	9	595	100	80	0.937	0.06	634.87
		4	10	904	100	85	0.966	0.07	935.82
		5	11	429	80	72	0.961	0.075	446.64
		6	12	338	85	70	0.872	0.07	387.79
	179	1	13	200	75	62	0.837	0.075	239.06
		2	14	150	80	60	0.630	0.07	238.28
		3	15	503	100	75	0.867	0.07	580.36
		4	16	363	80	65	0.887	0.075	409.15
		5	17	263	75	60	0.881	0.075	298.46
		6	18	700	90	80	0.731	0.075	958.25
	180	1	19	503	100	85	0.851	0.075	591.14
		2	20	324	85	73	0.854	0.075	379.39
		3	21	613	100	90	0.892	0.075	687.61
		4	22	401	85	67	0.852	0.075	470.88
		5	23	266	75	50	0.847	0.05	313.94
		6	24	446	100	85	0.887	0.065	502.99
	182	1	25	557	100	80	0.967	0.09	576.19
		2	26	689	105	85	0.868	0.075	793.96
		3	27	334	85	70	0.888	0.08	376.30
		4	28	709	115	95	0.797	0.075	889.59
		5	29	691	100	85	0.856	0.075	806.96
		6	30	216	80	60	0.671	0.068	321.81
inj-BPd4	153	1	31	167	85	70	0.832	0.075	200.70
		2	32	252	60	50	0.672	0.06	374.89
		3	33	564	95	80	0.857	0.075	657.96
		4	42	623	105	95	0.908	0.09	686.43
		5	43	576	115	100	0.741	0.075	777.22
	154	1	36	859	125	110	0.838	0.075	1025.06
		2	37	670	125	120	0.890	0.08	753.23
		3	38	439	85	75	0.701	0.075	626.25
		4	39	688	105	115	0.893	0.08	770.78
		5	40	685	105	105	0.793	0.08	863.37
		6	41	210	105	85	0.760	0.075	276.28
	155	1	44	283	70	70	0.853	0.09	331.69
		2	45	361	75	65	0.849	0.08	425.11
		3	46	311	75	62	0.906	0.08	343.27
		4	47	113	90	75	0.970	0.085	116.46
		5	48	481	105	85	0.961	0.08	500.57
		6	49	227	95	75	0.948	0.08	239.43
	156	1	50	701	95	85	0.770	0.08	910.63
		2	51	611	105	90	0.862	0.08	708.90
		3	52	262	85	70	0.815	0.07	321.43
		4	53	580	115	90	0.655	0.075	886.04
		5	54	561	115	105	0.880	0.075	637.64
		6	55	264	105	90	0.834	0.06	316.43

Note – Table is continued on the next page.

Group	Rat #	Slice	Stack	Synapses	Red Threshold	Green Threshold	Area	Area Coefficient	Normalized Synapses
inj-BPd4 (continued)	157	1	56	406	85	85	0.696	0.075	583.17
		2	57	490	105	90	0.888	0.075	551.62
		3	58	434	85	75	0.932	0.07	465.57
		4	59	515	100	90	0.801	0.065	643.27
		5	60	863	115	105	0.929	0.075	928.76
		6	61	465	105	85	0.857	0.08	542.59
	158	1	62	502	112	100	0.669	0.075	749.93
		2	63	760	90	82	0.904	0.075	840.71
		3	64	307	83	75	0.855	0.07	358.98
		4	65	529	115	108	0.865	0.08	611.35
		5	66	712	115	100	0.802	0.075	887.56
		6	67	580	105	100	0.946	0.08	612.85
sham-VEHd4	165	1	68	263	80	75	0.759	0.035	346.33
		2	69	129	80	65	0.519	0.045	248.60
		3	70	199	85	75	0.632	0.045	314.67
		4	71	382	120	115	0.655	0.075	583.12
		5	72	702	110	90	0.767	0.045	915.13
		6	73	304	92	80	0.747	0.03	406.74
	166	1	74	525	125	110	0.813	0.06	645.44
		2	75	791	125	125	0.729	0.055	1085.79
		3	76	268	115	100	0.794	0.045	337.45
		4	77	277	105	105	0.799	0.04	346.77
		5	78	467	105	90	0.761	0.035	613.42
		6	79	359	105	90	0.746	0.03	481.30
	167	1	80	103	100	67	0.615	0.03	167.40
		2	81	177	100	85	0.789	0.04	224.25
		3	82	100	95	70	0.782	0.04	127.94
		4	83	409	120	100	0.785	0.045	521.35
		5	84	308	115	110	0.781	0.04	394.21
		6	85	123	90	80	0.714	0.035	172.32
	168	1	86	195	125	115	0.643	0.04	303.45
		2	87	357	125	110	0.748	0.04	477.40
		3	88	236	90	80	0.810	0.035	291.43
		5	89	333	90	115	0.679	0.035	490.57
		6	90	184	100	85	0.727	0.03	253.16
	169	1	91	46	75	70	0.707	0.03	65.11
		2	92	220	90	85	0.932	0.07	235.95
		4	93	235	95	75	0.884	0.04	265.96
		5	94	231	100	85	0.824	0.045	280.34
		6	95	131	90	72	0.753	0.04	173.97
	170	1	96	337	98	87	0.522	0.065	646.09
		2	97	302	130	115	0.700	0.035	431.68
		3	98	168	95	62	0.514	0.05	327.17
		4	99	410	135	115	0.715	0.04	573.19
		5	100	272	90	85	0.743	0.04	366.03
		6	101	91	90	75	0.702	0.04	129.61

APPENDIX J

Mechanical Hyperalgesia after Nerve Root Compression

This appendix summarizes the temporal mechanical hyperalgesia responses in the forepaws for each rat that underwent a painful C7 dorsal nerve root compression in the studies of spinal cord stimulation in Chapters 6 and 7. Mechanical hyperalgesia is reported as the paw withdrawal threshold (PWT) for the ipsilateral and contralateral forepaws of each rat on each testing day, including the average baseline response (BL). Paw withdrawal thresholds for each forepaw were averaged based on three separate rounds of testing on each day. Table J.1 details the PWTs for all the rats included in studies using burst or tonic spinal cord stimulation; painful nerve root compression was applied seven days before spinal cord stimulation and hyperalgesia was assessed at baseline and on days 1, 3, 5, and 7 after nerve root compression.

Table J.1. Paw withdrawal thresholds after painful nerve root compression for spinal cord stimulation at day 7 (Chapters 6 and 7).

		Ipsilateral Forepaw					Contralateral Forepaw				
	Rat #	BL	D1	D3	D5	D7	BL	D1	D3	D5	D7
Painful Nerve Root Compression	J69	6.67	3.33	4.00	4.00	4.67	11.67	11.00	10.00	17.00	12.67
	J71	15.00	2.13	1.13	4.00	5.33	6.67	11.00	15.00	13.33	9.33
	J73	15.67	4.00	4.47	6.67	5.33	14.00	11.67	16.33	18.67	12.67
	J88	8.33	0.87	2.67	2.67	3.53	8.50	7.33	8.67	8.33	9.33
	J89	3.67	0.60	1.80	0.87	1.53	4.00	3.13	6.67	6.00	2.00
	J90	11.00	2.47	5.33	7.33	6.67	14.83	14.67	13.33	11.00	18.67
	J91	11.33	11.67	3.33	1.80	2.27	16.17	26.00	26.00	8.00	7.33
	J92	4.00	0.60	0.60	1.40	1.33	4.00	8.00	1.80	1.80	3.13
	207	8.67	4.67	3.33	2.67	4.00	9.50	8.00	7.33	7.33	7.33
	208	12.17	4.67	6.67	4.00	4.00	14.17	15.00	10.00	8.00	8.00
	209	13.50	6.00	8.00	10.00	8.67	19.67	13.33	11.67	18.67	18.67
	210	19.67	4.00	4.00	4.00	5.33	20.50	15.00	10.00	10.00	11.00
	211	13.33	5.33	4.67	4.00	4.00	12.17	18.67	11.00	13.33	11.67
	212	16.00	6.00	6.00	5.33	5.33	20.33	26.00	26.00	15.00	18.67
	215	17.83	8.00	6.00	4.67	3.33	14.17	17.00	13.33	11.00	11.67
	216	20.50	6.67	4.67	6.67	5.33	19.67	22.33	13.33	15.00	11.67
	249	8.67	2.47	1.60	1.80	3.33	12.67	15.00	8.33	6.67	8.00
	250	18.67	8.00	10.33	5.33	4.00	18.67	11.67	14.67	18.67	15.00
	251	12.67	2.47	1.33	2.47	2.20	13.33	15.00	6.00	9.67	9.67
	252	11.00	0.60	1.33	1.33	3.33	11.00	9.67	7.33	10.33	11.00
	265	22.33	2.67	4.00	4.00	7.00	24.17	22.33	22.33	18.67	22.33
	266	18.50	4.00	4.00	4.00	4.00	16.00	11.67	8.67	13.33	18.67
	267	10.33	0.60	2.67	2.67	3.33	9.17	9.33	12.67	8.67	13.33
	268	14.50	1.80	2.67	2.67	1.80	12.17	18.67	15.00	11.00	18.67
	269	22.33	2.67	4.67	1.80	4.00	16.83	12.67	15.00	15.00	15.00

Note - Rats #J69-J92 were labeled according to Jenell Smith's rat numbering scheme. Rats #207-269 were labeled according to the numbering scheme used in the remainder of this thesis. Rats #J69-J92 were used in the studies presented in Chapter 6, and rats #207-269 were used in the studies presented in Chapter 7.

APPENDIX K

Joint Distraction Mechanics, Hyperalgesia, and Synapse Density in the Dorsal Horn at Day 14 after Painful Facet Joint Injury

This appendix summarizes the data presented in Chapter 8, including the quantification of mechanical hyperalgesia and excitatory and inhibitory synapses in the spinal cord on day 14 after either a sham surgery or painful facet joint injury. Table K.1 summarizes the force, displacement, and strain data measured across the C6/C7 facet joint for each rat that underwent joint distraction. Table K.2 lists the paw withdrawal thresholds for each rat at baseline (BL) and on days 1, 3, 5, 7, 10, and 14 after the sham or painful facet joint injury procedures.

Table K.3 presents the quantification of excitatory synapses in the superficial dorsal horn at day 14 in those same groups. Excitatory synapses were quantified by immunolabeling the colocalization of the pre-synaptic marker, synapsin (red), and the post-synaptic marker, homer (green), as described in detail in Section 5.3.5 of Chapter 5 and in Section H.1 of Appendix H. In two separate rounds of quantification, the number of synapses was identified in each image, and the percentage of tissue parenchyma was measured using a custom MATLAB code (see Section E.3 of Appendix E) (Crosby et al., 2014c). The percentage of the image detected as tissue area (Area) was then used to calculate the number of synapses normalized to the tissue area for each image (synapse density). The synapse densities in the injury group were normalized to the average of the

synapse densities in the sham group for each round. The normalized synapse densities from the two rounds of quantification were averaged to yield a single synapse density for each tissue section. Table K.3 presents the synapse number and percentage of area for each image of the spinal dorsal horn for each rat, along with the group, rat number, and tissue section number. The table also lists the normalized synapse densities from each round of labeling, and the average of the two rounds for each tissue section.

Table K.4 summarizes the quantification of inhibitory synapses in the superficial dorsal horn at day 14 after sham or painful facet joint injury. Inhibitory synapses were quantified by immunolabeling gephyrin (red), a post-synaptic protein in inhibitory synapses, and bassoon (green), a pre-synaptic structural protein, using the same protocol described in Section H.1 of Appendix H for excitatory synapses. The number of synapses identified in each image of the spinal dorsal horn is presented for each rat, along with the group, rat number, tissue section number (consecutive sections were numbered 1-6 on each slide), and the side of the spinal cord (left, L, or right, R). The table also includes the red and green channel thresholds (Red Threshold and Green Threshold) used for detecting synaptic puncta. The percentage of tissue parenchyma in each image was measured using a custom MATLAB code (see Section E.3 of Appendix E) (Crosby et al., 2014c). The percentage of the image detected as tissue area (Area) was then used to calculate the number of synapses normalized to the tissue area (Normalized Synapses) for each image.

Table K.1. Facet joint distraction mechanics for rats that were tested for hyperalgesia through day 14 after painful facet joint injury (Chapter 8).

Group	Rat #	Load (N)	Vertebral Distraction (mm)	Average Capsule Distraction (mm)	Maximum MPS (%)	Average MPS (%)	Maximum x-strain (%)	Average x-strain (%)	Maximum y-strain (%)	Average y-strain (%)
Injury	100	3.35	0.72	0.44	23.6	21.9	19.0	15.8	7.0	2.5
	101	3.16	0.83	0.37	25.3	23.4	21.3	17.0	1.3	-1.9
	102	3.33	0.69	0.31	22.3	19.0	17.9	13.8	11.9	6.3
	103	4.04	0.64	0.33	23.2	18.0	15.5	12.3	7.9	-0.7
	104	2.92	0.68	0.33	34.3	24.2	24.6	15.5	7.1	2.3
	105	3.06	0.60	0.54	56.6	39.7	41.1	31.1	-0.5	-7.2

Table K.2. Paw withdrawal thresholds through day 14 after sham or painful facet joint injury (Chapter 8).

Group	Rat #	BL	D1	D3	D5	D7	D10	D14
Injury	100	7.60	3.67	5.00	6.00	6.00	8.33	7.67
	101	11.80	6.33	4.00	2.00	2.33	1.70	2.00
	102	18.30	4.00	6.33	4.00	3.33	3.67	3.67
	103	12.80	6.67	4.67	6.33	3.33	4.67	4.67
	104	10.60	6.00	5.33	6.33	7.67	6.00	6.67
	105	12.00	6.67	5.33	3.67	4.33	3.47	3.33
Sham	106	10.10	9.00	8.33	9.83	9.67	8.00	10.17
	107	10.90	8.33	16.17	15.17	10.33	10.67	10.50
	108	7.60	10.17	9.33	7.00	7.33	12.50	14.00
	109	18.90	13.33	9.17	11.33	9.67	8.67	10.83
	110	10.50	10.75	10.50	9.00	11.33	10.50	11.33

Table K.3. Quantification of excitatory synapses in the superficial dorsal horn at day 14 after sham or painful facet joint injury (Chapter 8).

			Round 1			Round 2			Average
Group	Rat #	Slice	Synapses	Area (%)	Synapse Density Normalized to Sham Avg	Synapses	Area (%)	Synapse Density Normalized to Sham Avg	Synapse Density Normalized to Sham Avg
Injury	100	1	254	0.7865	3.067	---	---	---	3.067
		2	113	0.8078	1.330	547	0.8608	3.898	2.614
		3	---	---	---	188	0.7598	1.518	1.518
		4	81	0.7719	0.997	70	0.9351	0.459	0.728
		5	---	---	---	173	0.85	1.249	1.249
		5	65	0.6447	0.959	302	0.8323	2.226	1.593
		6	57	0.6261	0.864	---	---	---	0.864
	101	1	80	0.7294	1.045	---	---	---	1.045
		2	70	0.8412	0.788	397	0.9182	2.653	1.720
		2	---	---	---	236	0.9106	1.590	1.590
		3	101	0.62	1.548	148	0.8476	1.071	1.310
		3	---	---	---	100	0.9091	0.675	0.675
		4	65	0.655	0.940	57	0.7704	0.454	0.697
		5	---	---	---	427	0.8792	2.980	2.980
		6	---	---	---	219	0.8127	1.653	1.653
	102	1	40	0.495	0.769	---	---	---	0.769
		2	84	0.6328	1.263	90	0.6292	0.878	1.070
		3	1	0.4491	0.019	170	0.6533	1.596	0.808
		4	256	0.5859	4.150	172	0.8148	1.295	2.723
		5	22	0.6774	0.304	224	0.8292	1.657	0.981
		6	37	0.5658	0.617	570	0.8488	4.120	2.369
	103	1	3	0.4492	0.066	54	0.8232	0.402	0.234
		2	32	0.7445	0.408	79	0.9047	0.536	0.472
		3	91	0.7701	1.121	74	0.8875	0.512	0.816
		5	5	0.6985	0.066	153	0.801	1.172	0.619
		5	---	---	---	62	0.7707	0.494	0.494
		6	248	0.8058	2.925	58	0.8468	0.420	1.673
	104	1	222	0.5198	4.056	---	---	---	4.056
		2	36	0.6666	0.513	---	---	---	0.513
		3	120	0.6632	1.718	---	---	---	1.718
		4	134	0.6306	2.018	---	---	---	2.018
		5	29	0.7282	0.378	---	---	---	0.378
		6	144	0.52512	2.604	---	---	---	2.604
	105	1	76	0.7011	1.026	103	0.79	0.800	0.913
		2	50	0.416	1.140	141	0.7995	1.082	1.111
		3	69	0.59	1.111	60	0.3832	0.961	1.036
		4	30	0.59	0.484	163	0.6585	1.519	1.001
		5	---	---	---	107	0.9534	0.689	0.689
		6	146	0.4968	2.792	29	0.4482	0.397	1.594

Note – Table is continued on the next page. Missing values are from sections that were torn, folded over, or came off the slide during immunolabeling. These data were collected and analyzed by Ben Bulka.

			Round 1			Round 2			Average
Group	Rat #	Slice	Synapses	Area (%)	Synapse Density Normalized to Sham Avg	Synapses	Area (%)	Synapse Density Normalized to Sham Avg	Synapse Density Normalized to Sham Avg
Sham	106	1	8	0.6942	0.114	248	0.9125	1.667	0.891
		2	5	0.5791	0.085	239	0.8593	1.706	0.896
		3	140	0.7085	1.880	127	0.9	0.866	1.373
		4	74	0.5239	1.339	201	0.8957	1.377	1.358
		5	---	---	---	180	0.9189	1.202	1.202
		6	---	---	---	49	0.745	0.404	0.404
	107	1	101	0.6926	1.415	34	0.8854	0.236	0.825
		2	---	---	---	119	0.8984	0.813	0.813
		3	---	---	---	63	0.7605	0.508	0.508
		4	143	0.6958	1.956	86	0.9419	0.560	1.258
		5	---	---	---	72	0.939	0.470	0.470
		6	154	0.7513	1.947	158	0.882	1.099	1.523
	108	1	163	0.9764	1.586	9	0.4627	0.119	0.853
		2	---	---	---	54	0.8335	0.397	0.397
		2	112	0.9611	1.111	24	0.5816	0.253	0.682
		4	123	0.8039	1.453	---	---	---	1.453
		6	73	0.9665	0.722	---	---	---	0.722
	109	1	24	0.6896	0.332	243	0.8645	1.724	1.028
		2	114	0.8203	1.320	371	0.8904	2.556	1.938
		3	49	0.603	0.769	332	0.9369	2.174	1.472
		4	83	0.676	1.168	176	0.8675	1.245	1.206
		5	66	0.8496	0.741	122	0.8806	0.850	0.795
		6	10	0.9326	0.104	112	0.9169	0.749	0.427
	110	1	---	---	---	119	0.8667	0.842	0.842
		2	---	---	---	184	0.7673	1.471	1.471
		3	---	---	---	106	0.8971	0.725	0.725
		4	---	---	---	88	0.8071	0.669	0.669
		5	---	---	---	212	0.9279	1.402	1.402
		6	---	---	---	122	0.8929	0.838	0.838

Note –Missing values are from sections that were torn, folded over, or came off the slide during immunolabeling. These data were collected and analyzed by Ben Bulka.

Table K.4. Quantification of inhibitory synapses in the superficial dorsal horn at day 14 after sham or painful facet joint injury (Chapter 8).

Group	Rat #	Slice	Side	Stack	Synapses	Red Threshold	Green Threshold	Area	Normalized Synapses
Injury	100	1	L	7	169	110	115	0.963	175
		2	L	8	485	115	120	0.708	686
		3	L	9	1570	130	115	0.963	1630
		4	L	10	1133	115	120	0.455	2488
		5	L	11	117	115	100	0.681	172
	101	1	L	1	1376	110	100	0.968	1421
		2	L	2	726	120	110	0.965	752
		3	L	3	1503	120	90	0.992	1516
		4	L	4	657	110	110	0.985	667
		5	L	5	514	120	120	0.979	525
		6	L	6	801	120	115	0.976	820
	102	1	L	18	1722	145	110	0.925	1861
		2	L	19	1122	110	115	0.953	1177
		3	L	20	684	125	90	0.827	827
		4	L	21	1253	135	100	0.936	1338
		5	L	22	1443	130	90	0.947	1524
		6	L	23	359	130	110	0.658	546
	104	1	L	12	267	140	120	0.895	298
		2	L	13	1294	125	110	0.959	1349
		3	L	14	944	130	85	0.948	996
		4	L	15	582	120	85	0.961	606
		5	L	16	504	120	90	0.800	630
		6	L	17	1403	135	90	0.941	1490
	105	1	L	24	845	145	115	0.913	926
		2	L	25	901	130	115	0.800	1127
		3	L	26	970	130	100	0.834	1163
		4	L	27	737	135	95	0.844	873
		5	L	28	251	130	105	0.901	278
		6	L	29	1040	120	100	0.834	1247
Sham	106	1	L	34	2239	130	110	0.991	2259
		2	L	35	2590	125	110	0.995	2604
		3	L	36	2176	125	105	0.981	2219
		4	L	37	2556	150	120	0.996	2566
		5	L	38	2384	135	95	0.994	2400
		6	L	39	2108	130	110	0.990	2130
	107	2	L	30	1290	140	115	0.982	1313
		3	L	31	1524	140	130	0.985	1547
		5	L	32	3259	125	100	0.990	3293
		6	L	33	1660	130	115	0.966	1718
	108	1	L	45	359	125	105	0.990	363
		2	L	46	973	125	90	0.989	984
		3	L	47	826	125	100	0.990	835
		4	L	48	1519	135	125	0.996	1526
		5	L	49	2181	130	120	0.993	2196
		6	L	50	987	120	120	0.996	991
	109	1	L	40	1030	135	130	0.453	2274
		2	L	41	1983	135	125	0.975	2033
		3	L	42	1552	140	120	0.996	1559
		5	L	43	531	125	105	0.246	2159
	110	1	L	51	2199	125	125	0.982	2239
		2	L	52	2057	135	110	0.960	2142
		3	L	53	1965	130	120	0.986	1993
		4	L	54	2107	135	125	0.928	2270
		5	L	55	2309	140	120	0.982	2352
		6	L	56	2250	130	115	0.998	2256

Note – These data were collected and analyzed by Ben Bulka.

REFERENCES

Adams JC, Lawler J. The thrombospondins. *Int J Biochem Cell B* 2004; 36:961-968.

Adams JC. Thrombospondins: multifunctional regulators of cell interactions. *Annu Rev Cell Dev Biol* 2001; 17:25-51.

Alo KM, Redko V, Charnov J. Four year follow-up of dual electrode spinal cord stimulation for chronic pain. *Neuromodulation* 2002; 5:79-88.

Alo KM, Yland MJ, Charnov JH, Redko V. Multiple program spinal cord stimulation in the treatment of chronic pain: follow-up of multiple program SCS. *Neuromodulation* 1999; 2(4):266-272.

Alo KM, Yland MJ, Kramer DL, Charnov JH, Redko V. Computer assisted and patient interactive programming of dual octrode spinal cord stimulation in the treatment of chronic pain. *Neuromodulation* 1998; 1(1): 30-45.

Antonacci MD, Mody DR, Heggeness MH. Innervation of the human vertebral body: a histologic study. *J Spinal Disord Tech* 1998; 11(6):526-531.

Aprill C. Cervical zygapophyseal joint pain patterns II: a clinical evaluation. *Spine* 1990; 15(6):458-461.

Araujo MC, Sinnott CJ, Strichartz GR. Multiple phases of relief from experimental mechanical allodynia by systemic lidocaine: responses to early and late infusions. *Pain* 2003; 103:21-29.

Arber S, Caroni P. Thrombospondin-4, an extracellular matrix protein expressed in the developing and adult nervous system promotes neurite outgrowth. *J Cell Biol* 1995; 131(4):1083-1094.

Bailey AL, Ribeiro-Da-Silva A. Transient loss of terminals from non-peptidergic nociceptive fibers in the substantia gelatinosa of spinal cord following chronic constriction injury of the sciatic nerve. *Neuroscience* 2006; 138:675-690.

Banic B, Petersen-Felix S, Andersen OK, Radanov BP, Villiger PM, Arendt-Nielsen L, Curatolo M. Evidence for spinal cord hypersensitivity in chronic pain after whiplash injury and in fibromyalgia. *Pain* 2004; 107:7–15.

Barnsley L, Bogduk N. Medial branch blocks are specific for the diagnosis of cervical zygapophyseal joint pain. *Region Anesth* 1993; 18(6):343-350.

Barnsley L, Lord SM, Wallis BJ, Bogduk N. The prevalence of chronic cervical zygapophysial joint pain after whiplash. *Spine* 1995; 20(1):20-25.

Baron R. Mechanisms of disease: neuropathic pain – a clinical perspective. *Nat Clin Pract Neuro* 2006; 2:95-106.

Basarsky TA, Parpura V, Haydon PG. Hippocampal synaptogenesis in cell culture: developmental time course of synapse formation, calcium influx, and synaptic protein distribution. *J Neurosci* 1994; 14(11):6402-6411.

Basbaum AI, Bautista DM, Scherrer G, Julius D. Cellular and molecular mechanisms of pain. *Cell* 2009; 139:267-284.

Beaman DN, Graziano GP, Glover RA, Wojtys EM, Chang V. Substance P innervation of lumbar spine facet joints. *Spine* 1993; 18(8):1044-1049.

Beck H, Schröck H, Sandkühler J. Controlled superfusion of the rat spinal cord for studying non-synaptic transmission: an autoradiographic analysis. *J Neurosci Meth* 1995; 58(1):193-202.

Bell GK, Kidd D, North RB. Cost-effectiveness analysis of spinal cord stimulation in treatment of failed back surgery syndrome. *J Pain Symptom Manag* 1997; 13(5):286-295.

Benveniste EN. Inflammatory cytokines within the central nervous sytem: sources, function, and mechanism of action. *Am J Physiol* 1992; 263(1):C1-C16.

Benzel EC. The Cervical Spine. Lippincott Williams & Wilkins, Philadelphia, 2012.

Blenk KH, Janig W, Michaelis M, Vogel C. Prolonged injury discharge in unmyelinated nerve fibres following transection of the sural nerve in rats. *Neurosci Lett* 1996; 215(3):185–188.

Blom SM, Pfister JP, Santello M, Senn W, Nevian T. Nerve injury-induced neuropathic pain causes disinhibition of the anterior cingulate cortex. *J Neurosci* 2014; 34(17):5754-5764.

Bogduk N, Marsland A. The cervical zygapophysial joints as a source of neck pain. *Spine* 1988; 13(6):610-617.

Bogduk N, Yoganandan N. Biomechanics of the cervical spine part 3: minor injuries. *Clin Biomech* 2001; 16:267-275.

Bove SE, Laemont KD, Brooker RM, Osborn MN, Sanchez BM, Guzman RE, Hook KE, Juneau PL, Connor JR, Kilgore KS. Surgically induced osteoarthritis in the rat results in the development of both osteoarthritis-like joint pain and secondary hyperalgesia. *Osteoarthr Cartilage* 2006; 14:1041-1048.

Brakeman PR, Lanahan AA, O'Brien R, Roche K, Barnes CA, Huganir RL, Worley PF. Homer: a protein that selectively binds metabotropic glutamate receptors. *Nature* 1997; 386:284-288.

Braz JM, Nassar MA, Wood JN, Basbaum AI. Parallel "pain" pathways arise from subpopulations of primary afferent nociceptor. *Neuron* 2005; 47(6):787-793.

Brenner GJ, Ji RR, Shaffer S, Woolf CJ. Peripheral noxious stimulation induces phosphorylation of the NMDA receptor NR1 subunit at the PKC-dependent site, serine-896, in spinal cord dorsal horn neurons. *Eur J Neurosci* 2004; 20(2):375-384.

Brocker DT, Grill WM. Principles of electrical stimulation of neural tissue. *Handb Clin Neurol* 2013; 116:3-18.

Brumley MR, Hentall ID, Pinzon A, Kadam BH, Blythe A, Sanchez FJ, Taberner AM, Noga BR. Serotonin concentrations in the lumbosacral spinal cord of the adult rat following microinjection or dorsal surface application. *J Neurophysiol* 2007; 98(3):1440-1450.

Buesa I, Ortiz V, Aguilera L, Torre F, Zimmermann M, Azkue JJ. Disinhibition of spinal responses to primary afferent input by antagonism at GABA receptors in urethane-anaesthetised rats is dependent on NMDA and metabotropic glutamate receptors. *Neuropharmacology* 2006; 50(5):585-594.

Buesa I, Urrutia A, Bilbao J, Aguilera L, Zimmermann M, Azkue JJ. Morphine-induced depression of spinal excitation is not altered following acute disruption of $GABA_A$ or $GABA_B$ receptor activity. *Eur J Pain* 2008; 12(6):677-685.

Burnstock G. P2X receptors in sensory neurones. *Brit J Anaesth* 2000; 84(4):476-488.

Buyten JP, Zundert J, Vueghs P, Vanduffel L. Efficacy of spinal cord stimulation: 10 years of experience in a pain centre in Belgium. *Eur J Pain* 2001; 5(3):299-307.

Buyten V, Al-Kaisy A, Smet I, Palmisani S, Smith T. High-frequency spinal cord stimulation for the treatment of chronic back pain patients: results of a prospective multicenter European clinical study. *Neuromodulation* 2013; 16(1):59-66.

Cameron T. Safety and efficacy of spinal cord stimulation for the treatment of chronic pain: a 20-year literature review. *J Neurosurg* 2004; 100(3):254-267.

Cata JP, Weng HR, Chen JH, Dougherty PM. Altered discharges of spinal wide dynamic range neurons and down-regulation of glutamate transporter expression in rats with paclitaxel-induced hyperalgesia. *Neuroscience* 2006; 138(1):329-338.

Cavanaugh DJ, Lee H, Lo L, Shields SD, Zylka MJ, Basbaum AI, Anderson DJ. Distinct subsets of unmyelinated primary sensory fibers mediate behavioral responses to noxious thermal and mechanical stimuli. *P Natl Acad Sci USA* 2009; 106(22):9075-9080.

Cavanaugh JM, El-Bohy A, Hardy WN, Getchell TV, Getchell ML, King AI Sensory innervation of soft tissues of the lumbar spine in the rat. *J Orthop Res* 1989; 7(3):378-388.

Chang YW, Winkelstein BA. Schwann cell proliferation and macrophage infiltration are evident at day 14 after painful cervical nerve root compression in the rat. *J Neurotraum* 2011; 28:2429-2438.

Chaplan SR, Bach FW, Pogrel JW, Chung JM, Yaksh TL. Quantitative assessment of tactile allodynia in the rat paw. *J Neurosci Meth* 1994; 53(1):55-63.

Chen C, Lu Y, Cavanaugh JM, Kallakuri S, Patwardhan A. Recording of neural activity from goat cervical facet joint capsule using custom-designed miniature electrodes. *Spine* 2005; 30(12):1367-1372.

Chen C, Lu Y, Kallakuri S, Patwardhan A, Cavanaugh JM. Distribution of A-delta and C-fiber receptors in the cervical facet joint capsule and their response to stretch. *J Bone Joint Surg Am* 2006; 88:1807-1816.

Chen DW, Hu CC, Chang YH, Lee MS, Chang CJ, Hsieh PH. Intra-articular bupivacaine reduces postoperative pain and meperidine use after total hip arthroplasty: a randomized double-blind study. *J Arthroplasty* 2014; in press.

Chen L, Huang LM. Protein kinase C reduces Mg2+ block of NMDA-receptor channels as a mechanism of modulation. *Nature* 1992; 356:521-523.

Chen SR, Pan HL. Activation of muscarinic receptors inhibits spinal dorsal horn projection neurons: role of $GABA_B$ receptors. *Neuroscience* 2004; 125(1):141-148.

Chen Y, Akin O, Nern A, Tsui CY, Pecot MY, Zipursky SL. Cell-type-specific labeling of synapses in vivo through synaptic tagging with recombination. *Neuron* 2014; 81(2):280-293.

Chen YW, Zhao P, Borup R, Hoffman EP. Expression profiling in the muscular dystrophies: identification of novel aspects of molecular pathophysiology. *J Cell Biol* 2000; 151:1321-1336.

Chi SI, Levine JD, Basbaum AI. Effects of injury discharge on the persistent expression of spinal cord fos-like immunoreactivity produced by sciatic nerve transection in the rat. *Brain Res* 1993; 617(2):220-224.

Chien A, Eliav E, Sterling M. The development of sensory hypoesthesia after whiplash injury. *Clin J Pain* 2010; 26(8):722-728.

Chou AK, Muhammad R, Huang SM, Chen JT, We CL, Lin CR, Lee TH, Lin SH, Lu CY, Yang LC. Altered synaptophysin expression in the rat spinal cord after chronic constriction injury of sciatic nerve. *Neurosci Lett* 2002; 333:155-158.

Christensen MD, Hulsebosch CE. Chronic central pain after spinal cord injury. *Neurotrauma* 1997; 14:517-537.

Christopherson KS, Ullian EM, Stokes CCA, Mullowney CE, Hell JW, Agah A, Lawler J, Mosher DF, Bornstein P, Barres BA. Thrombospondins are astrocyte-secreted proteins that promote CNS synaptogenesis. *Cell* 2005; 120(3):421-433.

Chung K, McNeill DL, Hulsebosch CE, Coggeshall RE. Changes in dorsal horn synaptic disc numbers following unilateral dorsal rhizotomy. *J Comp Neurol* 1989; 283:568-577.

Coderre TJ, Katz J, Vaccarino AL, Melzack R. Contribution of central neuroplasticity to pathological pain: review of clinical and experimental evidence. *Pain* 1993; 52:259-285.

Coghill AC, Mayer DJ, Price DD. Wide dynamic range but not nociceptive-specific neurons encode multidimensional features of prolonged repetitive heat pain. *J Neurophysiol* 1993; 69:703-716.

Compton AK, Shah B, Hayek SM. Spinal cord stimuilation: a review. *Curr Pain Headache Rep* 2012; 16:35-42.

Cook AJ, Woolf CJ, Wall PD, McMahon SB. Dynamic receptive field plasticity in rat spinal cord dorsal horn following C-primary afferent input. *Nature* 1987; 325:151-153.

Costigan M, Scholz J, Woolf CJ. Neuropathic pain: a maladaptive response of the nervous system to damage. *Annu Rev Neurosci* 2009:32:1-32.

Croft AC. Whiplash injury: the current model. *J Am Chiropr Assoc* 2000; July, 32-42.

Crosby ND, Gilliland TM, Winkelstein BA. Early afferent activity from the facet joint after painful trauma to its capsule potentiates neuronal excitability and glutamate signaling in the spinal cord. *Pain* 2014a; 155(9):1878-1887.

Crosby ND, Goodman Keiser MD, Smith JR, Zeeman ME, Winkelstein BA. Stimulation parameters define the effectiveness of burst spinal cord stimulation in a rat model of neuropathic pain. *Neuromodulation* 2014b; DOI: 10.1111/ner12221.

Crosby ND, Weisshaar CL, Winkelstein BA. Spinal neuronal plasticity is evident within 1 day after a painful cervical facet joint injury. *Neurosci Lett* 2013; 542:102-106.

Crosby ND, Zaucke F, Kras JV, Dong L, Luo ZD, Winkelstein BA. Thrombospondin-4 and excitatory synaptogenesis promote spinal sensitization after painful mechanical joint injury. *J Neurosci* 2014c; Submitted.

Cui JG, Linderoth B, Meyerson BA. Effects of spinal cord stimulation on touch-evoked allodynia involve GABAergic mechanisms: an experimental study in the mononeuropathic rat. *Pain* 1996; 66(2):287-295.

Cui JG, O'Connor WT, Ungerstedt U, Linderoth B, Meyerson BA. Spinal cord stimulation attenuates augmented dorsal horn release of excitatory amino acids in mononeuropathy via a GABAergic mechanism. *Pain* 1997; 73(1):87-95.

Curatolo M, Arendt-Nielsen L, Petersen-Felix S. Evidence, mechanisms, and clinical implications of central hypersensitivity in chronic after whiplash injury. *Clin J Pain* 2004; 20:469-476.

Curatolo M, Petersen-Felix S, Arendt-Nielsen L, Giani C, Zbinden AM, Radanov BP. Central hypersensitivity in chronic pain after whiplash injury. *Clin J Pain* 2001; 17(4):306-315.

Curtis DR, Duggan AW, Felix D, Johnston GAR. Bicuculline and central GABA receptors. *Nature* 1970; 228:676–677.

D'Mello R, Dickenson AH. Spinal cord mechanisms of pain. *Br J Anesth* 2008; 101(1):8-16.

Danbolt NC. Glutamate uptake. *Prog Neurobiol* 2001; 65(1):1-105.

Daniele CA, MacDermott AB. Low-threshold primary afferent drive onto GABAergic interneurons in the superficial dorsal horn of the mouse. *J Neurosci* 2009; 29:686-695.

Daulhac L, Maffre V, Mallet C, Etienne M, Privat AM, Kowalski-Chauvel A, Seva C, Fialip J, Eschalier A. Phosphorylation of spinal N-methyl-D-aspartate receptor NR1 subunits by extracellular signal-regulated kinase in dorsal horn neurons and microglia contributes to diabetes-induced painful neuropathy. *Eur J Pain* 2011; 15:169e.1-169e.12.

Davoody L, Quiton RL, Lucas JM, Ji Y, Keller A, Masri R. Conditioned place preference reveals tonic pain in an animal model of central pain. *J Pain* 2011; 12(8):868-874.

De Camilli P, Cameron R, Greengard P. Synapsin 1, a nerve terminal specific phosphoprotein: its general distribution in synapses of the central and peripheral nervous system demonstrated by immunofluorescence in frozen and plastic sections. *J Cell Biol* 1983; 96:1337-1354.

De Ridder D, Plazier M, Kamerling N, Menovsky T, Vanneste S. Burst spinal cord stimulation for limb and back pain. *World Neurosurg* 2013; 80:642-649.

De Ridder D, Vanneste S, Plazier M, van der Loo E, Menovsky T. Burst spinal cord stimulation: toward paresthesia-free pain suppression. *Neurosurgery* 2010; 66:986-990.

De Vos CC, Bom MJ, Vanneste S, Lenders MWPM, de Ridder D. Burst spinal cord stimulation evaluated in patients with failed back surgery syndrome and painful diabetic neuropathy. *Neuromodulation* 2013; doi:10.1111/ner12116.

Deng B, Begeman PC, Yang KH Tashman S, King AI. Kinematics of human cadaver cervical spine during low speed read-end impacts. *Stapp Car C* 2000; 44:171-188.

Deriemer SA, Strong JA, Albert KA, Greengard P, Kaczmarek LK. Enhancement of calcium current in Aplysia neurons by phorbol ester and protein kinase C. *Nature* 1985; 313:313-316.

Devor M, Wall PD, Catalan N. Systemic lidocaine silences ectopic neuroma and DRG discharge without blocking nerve conduction. *Pain* 1992; 48:261-268.

Devor M. Ectopic discharge in A-beta afferents as a source of neuropathic pain. *Exp Brain Res* 2009; 196:115-128.

Devor M. Response of nerves to injury in relation to neuropathic pain. In: McMahon SB, Koltzenburg M (Eds.), Wall and Melzack's Textbook of Pain, Churchill Livingstone, London, 2005, pp. 905-927.

Dingledine R, Borges K, Bowie D, Traynelis SF. The glutamate receptor ion channels. *Pharmacol Rev* 1999; 51(1):7-62.

Djouhri L, Koutsikou S, Fang X, McMullan S, Lawson SN. Spontaneous pain, both neuropathic and inflammatory, is related to frequency of spontaneous firing in intact C-fiber nociceptors. *Neurobiol Dis* 2006; 26:1281-1292.

Dong L, Crosby ND, Winkelstein BA. Gabapentin alleviates facet-mediated pain through reduced neuronal hyperexcitability and astrocytic activation in the spinal cord. *J Pain* 2013a; 14(12):1564-1572.

Dong L, Guarino BB, Jordan-Sciutto KL, Winkelstein BA. Activating Transcription Factor 4, a mediator of the integrated stress response, is increased in the dorsal root ganglia following painful facet joint distraction. *Neuroscience*, 2011; 193:377-86.

Dong L, Quindlen JC, Lipschutz DE, Winkelstein BA. Whiplash-like facet joint loading initiates glutamatergic responses in the DRG and spinal cord associated with behavioral hypersensitivity. *Brain Res* 2012; 21:51-63.

Dong L, Smith JR, Winkelstein BA. Ketorolac reduces spinal astrocytic activation and PAR1 expression associated with attenuation of pain following facet joint injury. *J Neurotraum* 2013b; 30:818-825.

Dong L, Winkelstein BA. Simulated whiplash modulates expression of the glutamatergic system in the spinal cord suggesting spinal plasticity is associated with painful dynamic cervical facet loading. *J Neurotrauma* 2010; 27(1):163-174.

Dong L. Inflammatory and neuronal mechanisms of facet-mediated pain in the context of neck injury. Doctoral dissertation, University of Pennsylvania, Philadelphia, Pennsylvania, 2013.

Dooley DJ, Donovan CM, Meder WP, Whetzel SZ. Preferential action of gabapentin and pregabalin at P/Q-type voltage-sensitive calcium channels: inhibition of K+-evoked [3H]-norepinephrine release from rat neocortical slices. *Synapse* 2002; 45(3):171-190.

Dostrovsky JO, Craig AD. Ascending projection systems. In: McMahon SB, Koltzenburg M (Eds.), Wall and Melzack's Textbook of Pain, 5th ed., Churchill Livingstone, London, 2006.

Dougherty PM, Garrison CJ, Carlton SM. Differential influence of local anesthetic upon two models of experimentally induced peripheral mononeuropathy in the rat. *Brain Res* 1992; 570(1):109-115.

Downie WW, Leatham PA, Rhind VM, Wright V, Branco JA, Anderson JA. Studies with pain rating scales. *Ann Rheum Dis* 1978; 37(4):378-381.

Drew GM, Siddall PJ, Duggan AW. Mechanical allodynia following contusion injury of the rat spinal cord is associated with loss of GABAergic inhibition in the dorsal horn. *Pain* 2004; 109(3):379-388.

Drottning M, Staff PH, Levin L, Malt UF. Acute emotional response to common whiplash predicts subsequent pain complaints: a prospective study of 107 subjects sustaining whiplash injury. *Nord J Psychiat* 1995; 49(4):293-300.

Dubuisson D. Effect of dorsal-column stimulation on gelatinosa and marginal neurons of cat spinal cord. *J Neurosurg* 1989; 70:257-265.

Dunkle ET, Zaucke F, Clegg DO. Thrombospondin-4 and matrix three-dimensionality in axon growth and adhesion in the developing retina. *Exp Eye Res* 2007; 84:707-717.

Duquette M, Nadler M, Okuhara D, Thompson J, Shuttleworth T, Lawler J. Members of the thrombospondin gene family bind stromal interaction molecule 1 and regulate calcium channel activity. *Matrix Biol* 2014; DOI:10.1016/j.matbio.2014.05.004.

Dwyer A, Aprill C, Bogduk N. Cervical zygapophyseal joint pain patterns I: a study in normal volunteers. *Spine* 1990; 15(6):453-457.

Dyhre H, Lang M, Wallin R, Renck H. The duration of action of bupivacaine, levobupivacaine, ropivacaine and pethidine in peripheral nerve block in the rat. *Acta Anaesthesiol Scand* 1997; 41:1346-1352.

Ehlers MD. Synapse formation: astrocytes spout off. *Curr Biol* 2005; 15(4):R134-R137.

Eroglu C, Allen NJ, Susman MW, O'Rourke NA, Park CY, Ozkan E, Chakraborty C, Mulinyawe SB, Annis DS, Huberman AD, Green EM, Lawler J, Dolmetsch R, Garcia KC, Smith J, Luo ZD, Rosenthal A, Mosher DF, Barres BA. Gabapentin receptor a2d-1 is a neuronal thrombospondin receptor responsible for excitatory CNS synaptogenesis. *Cell* 2009; 139:380-392.

Fernandez E, Turk DC. Sensory and affective components of pain: separation and synthesis. *Psychol Bull* 1992; 112:205-217.

Field KJ, White WJ, Lang CM. Anaesthetic effects of chloral hydrate, pentobarbitone and urethane in adult male rats. *Lab Anim* 1993; 27(3):258-269.

Field MJ, Holloman EF, McCleary S, Hughes J, Singh L. Evaluation of gabapentin and S-(+)-3-isobutylgaba in a rat model of postoperative pain. *JPET* 1997; 282:1242-1246.

Finnerup NB, Nikolajsen L, Jensen TS. Are we neglecting spinal reorganization following nerve damage? *Pain* 2012; 153:269-272.

Fischer TZ, Tan AM, Waxman SG. Thalamic neuron hyperexcitability and enlarged receptive fields in the STZ model of diabetic pain. *Brain Res* 2009; 1268:154-161.

Freeman MD, Croft AC, Rossignol AM, Weaver DS, Reiser M. A review and methodologic critique of the literature refuting whiplash syndrome. *Spine* 1999; 24(1):86-96.

Gissen AJ, Covino BG, Gregus J. Differential sensitivity of fast and slow fibers in mammalian nerve: effect of etidocaine and bupivacaine on fast/slow fibers. *Anesth Analg* 1982; 61(7):570-575.

Gonzales-Darder JM, Barbera J, Abellan MJ. Effect of prior anesthesia on autotomy following sciatic transection in rats. *Pain* 1986; 24:87-91.

Gracely RH, Lynch SA, Bennett GJ. Painful neuropathy: altered central processing maintained dynamically by peripheral input. *Pain* 1992; 51(2):175-194.

Grant G, Koerber HR. Spinal cord cytoarchitecture. In: Paxinos G (Ed.)The Rat Nervous System, 3rd ed., Elsevier, London, 2004.

Grant G, Robertson B. Primary afferent projections to the spinal cord. In: Paxinos G (Ed.) The Rat Nervous System, 3rd ed., Elsevier, London, 2004.

Greenspan JD, Craft RM, LeResche L, Arendt-Nielsen L, Berkley KJ, Fillingim RB, Gold MS, Holdcroft A, Lautenbacher S, Mayer EA, Mogil JS, Murphy AZ, Traub RJ. Studying sex and gender differences in pain and analgesia: a consensus report. Pain 2007; 132:S26-S45.

Grudt TJ, Williams JT, Travagli RA. Inhibition by 5-hydroxytryptamine and noradrenaline in substantia gelatinosa of guinea-pig spinal trigeminal nucleus. *J Physiol* 1995; 485:113–120.

Guan Y, Wacnik PW, Yang F, Carteret AF, Chung CY, Meyer RA, Raja SN. Spinal cord stimulation-induced analgesia: electrical stimulation of dorsal column and dorsal roots

attenuates dorsal horn neuronal excitability in neuropathic rats. *Anesthesiology* 2010; 113:1392-1405.

Guan Y. Spinal cord stimulation: neurophysiological and neurochemical mechanisms of action. *Curr Pain Headache Rep* 2012; 16:271-225.

Guyton AC, Hall JE. Textbook of physiology. WB Saunders, Philadelphia, 1996.

Hains BC, Johnson KM, Eaton MJ, Willis WD, Hulsebosch CE. Serotonergic neural precursor cell grafts attenuate bilateral hyperexcitability of dorsal horn neurons after spinal hemisection in rat. *Neuroscience* 2003a; 116(4):1097-1110.

Hains BC, Klein JP, Saab CY, Craner MJ, Black JA, Waxman SG. Upregulation of sodium channel $Na_V1.3$ and functional involvement in neuronal hyperexcitability associated with central neuropathic pain after spinal cord injury. *J Neurosci* 2003b; 23(26):8881-8892.

Hains BC, Willis WD, Hulsebosch CE. Temporal plasticity of dorsal horn somatosensory neurons after acute and chronic spinal cord hemisection in rat. *Brain Res* 2003c; 970(1):238-241.

Hanai F, Matsui N, Hongo N. Changes in responses of wide dynamic range neurons in the spinal dorsal horn after dorsal root or dorsal root ganglion compression. *Spine* 1996; 21(12):1408-1414.

Hansen U, Platz N, Becker A, Bruckner P, Paulsson M, Zaucke F. A secreted variant of cartilage oligomeric matrix protein carrying a chondrodysplasia-causing mutation (p.H587R) disrupts collagen fibrillogenesis. *Arthritis Rheum* 2011; 63:159-167.

Hao JX, Yu YX, Seiger Å, Wiesenfeld-Hallin Z. Systemic tocainide relieves mechanical hypersensitivity and normalizes the responses of hyperexcitable dorsal horn wide-dynamic-range neurons after transient spinal cord ischemia in rats. *Exp Brain Res* 1992; 91(2):229-235.

Hathaway CB, Hu JW, Bereiter DA. Distribution of Fos-like immunoreactivity in the caudal brainstem of the rat following noxious chemical stimulation of the temporomandibular joint. *J Comp Neurol* 1995; 356:444-456.

Herren-Gerber R, Weiss S, Arendt-Nielsen L, Petersen-Felix S, Di Stefano G, Radanov B, Curatolo M. Modulation of central hypersensitivity by nociceptive input in chronic pain after whiplash injury. *Pain* 2004; 5:366-376.

Hogg-Johnson S, van der Velde G, Carroll LJ, Holm LW, Cassidy JD, Guzman J, Cote P, Haldeman S, Ammendolia C, Carragee E, Hurwitz E, Nordin M, Peloso P. The burden and determinants of neck pain in the general population. *Spine* 2008; 33(4):S39-S51.

Holm LW, Carroll LJ, Cassidy JD, Hogg-Johnson S, Côté P, Guzman J, Peloso P, Nordin M, Hurwitz E, van der Velde G, Carragee E, Haldeman S. The burden and determinants of neck pain in whiplash-associated disorders after traffic collisions: results of the bone and joint decade 2000–2010 task force on neck pain and its associated disorders. *J Manip Physiol Ther* 2008; 33:S52–S59.

Holsheimer J. Which neuronal elements are activated directly by spinal cord stimulation. *Neuromodulation* 2002; 5:25-31.

Holtmaat A, Randall J, Cane M. Optical imaging of structural and functional synaptic plasticity in vivo. *Eur J Pharmacol* 2013; 719(1):128-136.

Honore P, Rogers SD, Schwei MJ, Salak-Johnson JL, Luger NM, Sabino MC, Clohisy DR, Mantyh PW. Murine models of inflammatory, neuropathic and cancer pain each generates a unique set of neurochemical changes in the spinal cord and sensory neurons. *Neuroscience* 2000; 98:585-598.

Hubbard RD, Chen Z, Winkelstein BA. Transient cervical nerve root compression modulates pain: load thresholds for allodynia and sustained changes in spinal neuropeptide expression. *J Biomech* 2008; 41(3):677-85.

Hubbard RD, Winkelstein BA. Transient cervical nerve root compression in the rat induces bilateral forepaw allodynia and spinal glial activation: mechanical factors in painful neck injuries. *Spine* 2005; 30:1924-1932.

Hughes DI, Scott DT, Todd AJ, Riddell JS (2003) Lack of evidence for sprouting of Aβ afferents into the superficial laminas of the spinal cord dorsal horn after nerve section. *J Neurosci* 2003; 23(29):9491-9499.

Inami S, Shiga T, Tsujino A, Yabuki T, Okado N, Ochiai N. Immunohistochemical demonstration of nerve fibers in the synovial fold of the human cervical facet joint. *J Orthop Res* 2001; 19(4):593-596.

Ippolito DM, Eroglu C. Quantifying synapses: an immunohistochemistry-based assay to quantify synapse number. *J Vis Exp* 2010; 45:2270.

Jaken RJP, Joosten EAJ, Knuwer M, Miller R, van der Meulen I, Marcus MAE, Deumens R. Synaptic plasticity in the substantia gelatinosa in a model of chronic neuropathic pain. *Neurosci Lett* 2010; 469(1):30-33.

Jansen GB , Edlund C, Grane P, Hildingsson C, Karlberg M, Link H. Whiplash injuries: diagnosis and early management. *Eur Spine J* 2008; 17.

Jaumard NV, Udupa JK, Welch WC, Winkelstein BA. Kinematic magnetic resonance imaging to define the cervical facet joint space for the spine in neutral and torsion. *Spine* 2014; 39(8):664-672.

Johansen JP, Fields HL, Manning BH. The affective component of pain in rodents: direct evidence for a contribution of the anterior cingulate cortex. *P Natl Acad Sci USA* 2001; 98(14):8077-8082.

Kain SR, Adams M, Kondepudi A, Yang TT, Ward WW, Kitts P. Green fluorescent protein as a reporter of gene expression and protein localization. *Biotechniques* 1995; 19(4):650-655.

Kallakuri S, Singh A, Chen C, Cavanaugh JM. Demonstration of substance P, calcitonin gene-related peptide, and protein gene product 9.5 containing nerve fibers in human cervical facet joint capsules. *Spine* 2004; 29(11):1182-1186.

Kallakuri S, Singh A, Lu Y, Chen C, Patwardhan A, Cavanaugh JM. Tensile stretching of cervical facet joint capsule and related axonal changes. *Eur Spine J* 2008; 17:556-563.

Kaneoka K, Ono K, Inami S, Hayashi K. Motion analysis of cervical vertebrae during whiplash loading. *Spine* 1999; 24(8):763-769.

Kawasaki Y, Kohno T, Zhuang ZY, Brenner GJ, Wang H, van der Meer C, Befort K, Woolf CJ, Ji RR. Ionotropic and metabotropic receptors, protein kinase A, protein kinase C, and Src contribute to C-fiber-induced ERK activation and cAMP response element-binding protein phosphorylation in dorsal horn neurons, leading to central sensitization. *J Neurosci* 2004; 24(38):8310-8321.

Kawasaki-Yatsugi S, Nagakura Y, Ogino S, Sekizawa T, Kiso T, Takahashi M, Ishikawa G, Ito H, Shimizu Y. Automated measurement of spontaneous pain-associated limb movement and drug efficacy evaluation in a rat model of neuropathic pain. *Eur J Pain* 2012; 16(10):1426-1436.

Kim DS, Figueroa KW, Li KW, Boroujerdi A, Yolo T, Luo ZD. Profiling of dynamically changed gene expression in dorsal root ganglia post peripheral nerve injury and a critical role of injury-induced glial fibrillary acetic protein in maintenance of pain behaviors. *Pain* 2009; 143(1):114-122.

Kim DS, Li KW, Boroujerdi A, Yu YP, Zhou CY, Deng P, Park J, Zhang X, Lee J, Corpe M, Sharp K, Steward O, Eroglu C, Barres B, Zaucke F, Xu ZC, Luo ZD. Thrombospondin-4 contributes to spinal sensitization and neuropathic pain states. *J Neurosci* 2012; 32(26):8977-8987.

King T, Vera-Portocarrero L, Gutierrez T, Vanderah TW, Dussor G, Lai J, Fields HL, Porreca F. Unmasking the tonic-aversive state in neuropathic pain. *Nat Neurosci* 2009; 12(11):1364-1366.

Kirvela OA, Kotilainen E. Successful treatment of whiplash-type injury induced severe pain syndrome with epidural stimulation: a case report. *Pain* 1999; 80(1):441-443.

Kitagawa J, Kanda K, Sugiura M, Tsuboi Y, Ogawa A, Shimizu K, Koyama N, Kamo H, Watanabe T, Ren K, Iwata K. Effect of chronic inflammation on dorsal horn nociceptive neurons in aged rats. *J Neurophysiol* 2005; 93:3594-3604.

Kiyatkin A, Aksamitiene E. Multistrip Western blotting to increase quantitative data output. *Methods Mol Biol* 2009; 536:149-161.

Klein SM, Greengrass RA, Steele SM, D'Ercole FJ, Speer KP, Gleason DH, DeLong ER, Warner DS. A comparison of 0.5% bupivacaine, 0.5% ropivacaine, and 0.75% ropivacaine for interscalene brachial plexus block. *Anesth Analg* 1998; 87:1316-1319.

Koelbaek-Johansen M, Graven-Nielsen T, Schou Olesen A, Arendt-Nielsen L. Generalised muscular hyperalgesia in chronic whiplash syndrome. *Pain* 1999; 83(2):229-234.

Koga K, Furue H, Rashid MH, Takaki A, Katafuchi T, Yoshimura M. Selective activation of primary afferent fibers evaluated by sine-wave electrical stimulation. *Mol Pain* 2005; 1:13-23.

Koltzenburg M, Lundberg LE, Torebjork HE. Dynamic and static components of mechanical hyperalgesia in human hairy skin. *Pain* 1992; 51:207-219.

Koltzenburg M, Wahren LK, Torebjork HE. Dynamic changes of mechanical hyperalgesia in neuropathic pain states and healthy subjects depend on the ongoing activity of unmyelinated nociceptive afferents. *Pflugers Arch* 1992; 420:R452.

Kosek E, Januszewska A. Mechanisms of pain referral in patients with whiplash associated disorder. *Eur J Pain* 2008; 12(5):650-660.

Kras JV, Dong L, Winkelstein BA. Increased interleukin-1 & prostaglandin E2 expression in the spinal cord at day 1 after painful facet joint injury: evidence of early spinal inflammation. *Spine* 2014a; 39(3):207-212.

Kras JV, Tanaka K, Gilliland TM, Winkelstein BA. An anatomical and immunohistochemical characterization of afferents innervating the C6/C7 facet joint after painful joint loading in the rat. *Spine* 2013a; 38(6):E325-E331.

Kras JV, Weisshaar CL, Kartha S, Pall PS, Winkelstein BA. Intra-articular nerve growth factor regulates the development of injury-induced facet joint pain and central sensitization via peptidergic afferent signaling in the joint. *J Neurosci* 2014b; submitted.

Kras JV, Weisshaar CL, Quindlen JA, Winkelstein BA. Brain-derived neurotrophic factor is upregulated in the cervical DRG & spinal cord and contributes to the maintenance of pain from facet joint injury. *J Neurosci Res* 2013b; 91:1312-1321.

Kreis PG, Fishman SM. Spinal cord stimulation: percutaneous implantation techniques. New York, NY: Oxford University Press; 2009.

Kucukdereli H, Allen NJ, Lee AT, Feng A, Ozlu MI, Conatser LM, Chakraborty C, Workman G, Weaver M, Sage EH, Barres BA, Eroglu C. Control of excitatory CNS synaptogenesis by astrocyte-secreted proteins Hevin and SPARC. *P Natl Acad Sci USA* 2011; 108(32):E440-E449.

Kumar K, Malik S, Demeria D. Treatment of chronic pain with spinal cord stimulation versus alternative therapies: cost-effectiveness analysis. *Neurosurgery* 2002; 51(1):106-116.

LaBuda CJ, Fuchs PN. A behavioral test paradigm to measure the aversive quality of inflammatory and neuropathic pain in rats. *Exp Neurol* 2000; 163(2):490-494.

Lam DK, Sessle BJ, Hu JW. Surgical incision can alter capsaicin-induced central sensitization in rat brainstem nociceptive neurons. *Neuroscience* 2008; 156:737-747.

LaMotte RH, Shain CN, Simone DA, Tsai EFP. Neurogenic hyperalgesia: psychophysical studies of underlying mechanisms. *J Neurophysiol* 1991; 66:190-211.

Lander P. Selective cervical nerve blocks. In: Schweitzer ME, Laredo JD, editors. New techniques in interventional musculoskeletal radiology, first edition. New York: Informa Healthcare; 2007.

Lang GT. Cervical Anatomy of the Cervical Spine, Thieme Medical Publishers, New York, 1993.

Latremoliere A, Woolf CJ. Central sensitization: a generator of pain hypersensitivity by central neural plasticity. *J Pain* 2009;10:895-926.

Lee KE, Davis MB, Mejilla RM, Winkelstein BA. In vivo cervical facet capsule distraction: mechanical implications for whiplash and neck pain. *Stapp Car C* 2004; 48:373-395.

Lee KE, Davis MB, Winkelstein BA. Capsular ligament involvement in the development of mechanical hyperalgesia after facet joint loading: behavioral and inflammatory outcomes in a rodent model of pain. *J Neurotraum* 2008a;25:1383-1393.

Lee KE, Thinnes JH, Gokhin DS, Winkelstein BA. A novel rodent neck pain model of facet-mediated behavioral hypersensitivity: implications for persistent pain and whiplash injury. *J Neurosci Meth* 2004b; 137:151-159.

Lee KE, Winkelstein BA. Joint distraction magnitude is associated with different behavioral outcomes and substance P levels for cervical facet joint loading in the rat. *J Pain* 2009; 10:436-445.

Levin BE, Hubschmann OR. Dorsal column stimulation effect on human cerebrospinal fluid and plasma catecholamines. *Neurology* 1980; 30(1):65.

Li J, Simone DA, Larson AA. Windup leads to characteristics of central sensitization. *Pain* 1999; 79(1):75-82.

Li KW, Kim DS, Zaucke F, Luo ZD. Trigeminal nerve injury-induced thrombospondin-4 up-regulation contributes to orofacial neuropathic pain states in a rat model. *Eur J Pain* 2014; 18(4):489-495.

Li KW, Yu YP, Zhou C, Kim DS, Lin B, Sharp K, Steward O, Luo ZD. Calcium channel α2δ1 proteins mediate trigeminal neuropathic pain states associated with aberrant excitatory synaptogenesis. *J Biol Chem* 2014; 289(10):7025-7037.

Liaw WJ, Stephens RL Jr, Binns BC, Chu Y, Sepkuty JP, Johns RA, Rothstein JD, Tao YX. Spinal glutamate uptake is critical for maintaining normal sensory transmission in rat spinal cord. *Pain* 2005; 115(1):60-70.

Lin JY, Peng B, Yang ZW, Min S. Number of synapses increased in the rat spinal dorsal horn after sciatic nerve transection: a stereological study. *Brain Res Bull* 2011; 84:430-433.

Lin MZ, Glenn JS, Tsien RY. A drug-controllable tag for visualizing newly synthesized proteins in cells and whole animals. *P Natl Acad Sci USA* 2008; 105(22):7744-7749.

Lin SC, Yeh JH, Chen CL, Chou SH, Tsai YJ. Effects of local lidocaine treatment before and after median nerve injury on mechanical hypersensitivity and microglia activation in rat cuneate nucleus. *Eur J Pain* 2011; 15:359-367.

Lind G, Meyerson BA, Winter J, Linderoth B. Intrathecal baclofen as adjuvant therapy to enhance the effect of spinal cord stimulation in neuropathic pain: a pilot study. *Eur J Pain* 2004; 8(4):377-383.

Lind G, Schechtmann G, Winter J, Meyerson BA, Linderoth B. Baclofen-enhanced spinal cord stimulation and intrathecal baclofen alone for neuropathic pain: Long-term outcome of a pilot study. *Eur J Pain* 2008; 12(1):132-136.

Linderoth B, Foreman RD. Physiology of spinal cord stimulation: review and update. *Neuromod* 1999; 2(3):150-164.

Linderoth B, Gazelius B, Fanck J, Brodin E. Dorsal column stimulation induces release of serotonin and substance P in the cat dorsal horn. *Neurosurgery* 1992; 31:289-296.

Linderoth B, Stiller CO, Gunasekera L, O'Conner WT, Ungerstedt U, Brodin E. Gamma-aminobutyric acid is released in the dorsal horn by electrical spinal cord stimulation: an in vivo microdialysis study in the rat. *Neurosurgery* 1994; 34(3):484-489.

Linton SJ, Hellsing AL, Hallden K. A population based study of spinal pain among 35-45-year old individuals. *Spine* 1998; 23:1457-1463.

Liu C, Wall PD, Ben-Dor E, Michaelis M, Amir R, Devor M. Tactile allodynia in the absence of C-fiber activation: altered firing properties of DRG neurons following spinal nerve injury. *Pain* 2000; 85:503-521.

Liu XJ, Salter MW. Glutamate receptor phosphorylation and trafficking in pain plasticity in spinal cord dorsal horn. *Eur J Neurosci* 2010; 32:278-289.

Lo FS, Zhau S, Erzurumlu RS. Astrocytes promote peripheral nerve injury-induced reactive synaptogenesis in the neonatal CNS. *J Neurophysiol* 2011; 106:2876-2887.

Lord SM, Barnsley L, Bogduk N. Percutaneous radiofrequency neurotomy in the treatment of cervical zygapophysial joint pain: a caution. *Neurosurgery* 1995; 36(4):732-739.

Lord SM, Barnsley L, Wallis BJ, Bogduk N. Chronic cervical zygapophysial joint pain after whiplash: a placebo-controlled prevalence study. *Spine* 1996; 21:1737-1744.

Lord SM, Barnsley L, Wallis BJ, McDonald GJ, Bogduk N. Percutaneous radio-frequency neurotomy for chronic cervical zygapophyseal-joint pain. *N Engl J Med* 1996; 335(23):1721-1726.

Lu Y, Chen C, Kallakuri S, Patwardhan A, Cavanaugh JM. Neural response of cervical facet joint capsule to stretch: a study of whiplash pain mechanisms. *Stapp Car C* 2005a; 49:49-65.

Lu Y, Chen C, Kallakuri S, Patwardhan A, Cavanaugh JM. Neurophysiological and biomechanical characterization of goat cervical facet joint capsules. *J Orthop Res* 2005b; 23(4):779-787.

Luan F, Yang KH, Deng B, Begeman PC, Tashman S, King AI. Qualitative analysis of neck kinematics during low-speed rear-end impact. *Clin Biomech* 2000; 15(9):649-657.

Luo ZD, Calcutt NA, Higuera ES, Valder CR, Song YH, Svensson CI, Myers RR. Injury type-specific calcium channel a2d-1 subunit upregulation in rat neuropathic pain models correlates with antiallodynic effects of gabapentin. *J Pharmacol* 2002; 303:1199-1205.

Malcangio M, Bowery NG. GABA and its receptors in the spinal cord. *Trends Pharmacol Sci* 1996; 17(12):457-462.

Manchikanti L, Boswell M, Singh V, Pampati V, Damron K, Beyer C. Prevalence of facet joint pain in chronic spinal pain of cervical, thoracic, and lumbar regions. *BMC Musculoskel Dis* 2004; 5:15.

Manchikanti L, Pampati V, Singh V, Falco FJE. Assessment of the escalating growth of facet joint interventions in the Medicare population in the United States from 2000-2011. *Pain Physician* 2013; 16:E365-E378.

Manchikanti L, Singh V, Falco FJE, Cash KM, Fellows B. Cervical medial branch blocks for chronic cerical facet joint pain. *Spine* 2008; 33(17):1813-1820.

Manola L, Holsheimer J, Veltnik PH, Bradley K, Peterson D. Theoretical investigation into longitudinal cathodal field steering in spinal cord stimulation. *Neuromodulation* 2007; 10:120-132.

Martin BI, Deyo TA, Mirza SK, Turner JA, Comstock BA, Hollingworth W, Sullivan SD. Expenditures and health status among adults with back and neck problems. *J Amer Med Assoc* 2008; 299(6):656-664.

Martindale JC, Wilson AW, Reeve AJ, Chessell IP, Headley PM. Chronic secondary hypersensitivity of dorsal horn neurons following inflammation of the knee joint. *Pain* 2007; 133:79-86.

Mayer ML, Westbrook GL, Guthrie PB. Voltage-dependent block by Mg2+ of NMDA responses in spinal cord neurons. *Nature* 1984; 309:261-263.

McLain RF, Pickar JG. Mechanoreceptor endings in human thoracic and lumbar facet joints. *Spine* 1998; 23(2):168-173.

McLain RF. Mechanoreceptor endings in cervical facet joints. *Iowa Orthopaedic J* 1993; 13:149-154.

McMahon SB. NGF as a mediator of inflammatory pain. *Philos Trans R Soc Lond B Biol Sci* 1996; 351:431-440.

Melzack R, Wall PD. Pain mechanisms: a new theory. *Science* 1965; 150:971-979.

Melzack R. The short-form McGill pain questionnaire. *Pain* 1987; 30(2):191-197.

Mendell LM. Constructing and deconstructing the gate theory of pain. *Pain* 2014; 155(2):210-216.

Meyer RA, Ringkamp M, Campbell JN, Raja SN. Peripheral mechanisms of cutaneous nociception. In: McMahon SB, Koltzenburg M (Eds.), Wall and Melzack's Textbook of Pain, 5th ed., Churchill Livingstone, London, 2006.

Michaelis M, Blenk K, Janig W, Vogel C. Development of spontaneous activity and mechanosensitivity in axotomized afferent nerve fibers during the first hours after nerve transection in rats. *J Neurophysiol* 1995; 74:1020-1027.

Miki K, Iwata K, Tsuboi Y, Morimoto T, Kondo E, Dai Y, Ren K, Noguchi K. Dorsal column-thalamic pathway is involved in thalamic hyperexcitability following peripheral nerve injury: a lesion study in rats with experimental mononeuropathy. *Pain* 2000; 85(1):263-271.

Millan MJ. Descending control of pain. *Prog Neurobiol* 2002; 66(6):355-474.

Milligan ED, Watkins LR. Pathological and protective roles of glia in chronic pain. *Nat Rev* 2009; 10:23-36.

Mogil JS, Chanda ML. The case for the inclusion of female subjects in basic science studies of pain. Pain 2005; 117(1):1-5.

Mogil JS, Crager SE. What should we be measuring in behavioral studies of chronic pain in animals? *Pain* 2004; 112(1):12-15.

Mogil JS. Animal models of pain: progress and challenges. *Nat Rev Neurosci* 2009; 10(4):283-294.

Molander C, Xu Q, Rivero-Melian C, Grant G. Cytoarchitectonic organization of the spinal cord in the rat: II. The cervical and upper thoracic cord. *J Comp Neurol* 1989; 289:375-385.

Moog M, Quintner J, Hall T, Zusman M. The late whiplash syndrome: a psychophysical study. *Eur J Pain* 2002; 6(4):283-294.

Moore KA, Kohno T, Karchewski LA, Scholz J, Baba H, Woolf CJ. Partial peripheral nerve injury promotes a selective loss of GABAergic inhibition in the superficial dorsal horn of the spinal cord. *J Neurosci* 2002; 22(15):6724-6731.

Munglani R. Neurobiological mechanisms underlying chronic whiplash associated pain: the peripheral maintenance of central sensitization. *J Musculoskelet Pain* 2000; 8(1):169-178.

Narikawa K, Furue H, Kumamoto E, Yoshimura M. In vivo patch-clamp analysis of IPSCs evoked in rat substantia gelatinosa neurons by cutaneous mechanical stimulation. *J Neurophysiol* 2000; 84:2171-2174.

Neher E, Sakaba T. Multiple roles of calcium ions in the regulation of neurotransmitter release. *Neuron* 2008; 59(6):861-872.

Newman PK. Whiplash injury. *Brit Med J* 1990; 301(6749):395-396.

Nicholson KJ, Gilliland TM, Winkelstein BA. Upregulation of GLT-1 by treatment with ceftriaxone alleviates radicular pain by reducing spinal astrocyte activation and neuronal hyperexcitability. *J Neurosci Res* 2014a; 92:116-129.

Nicholson KJ, Zhang S, Gilliland TM, Winkelstein BA. Riluzole effects on behavioral sensitivity and the development of axonal damage and spinal modifications that occur after painful nerve root compression: laboratory investigation. *J Neurosurg: Spine* 2014b; 20(6):751-762.

North RA, Yoshimura M. The actions of noradrenaline on neurones of the rat substantia gelatinosa *in vitro. J Physiol* 1984; 349:43–55.

Oakley JC, Prager JP. Spinal cord stimulation: mechanisms of action. *Spine* 2002; 27(22):2574-2583.

Ohnmeiss DD, Rashbaum RF, Bogdanffy GM. Prospective outcome evaluation of spinal cord stimulation in patients with intractable leg pain. *Spine* 1996; 21(11):1344-1350.

Ohtori S, Takahashi K, Chiba T, Yamagata M, Sameda H, Moriya H. Sensory innervation of the cervical facet joints in rats. *Spine* 2001; 26:147-150.

Olpe HR, Karlsson G, Pozza MF, Brugger F, Steinmann M, Van Riezen H, Fagg G, Hall RG, Froestl W, Bittiger H. CGP 35348: a centrally active blocker of $GABA_B$ receptors. *Eur J Pharmacol* 1990; 187:27-38.

Ono K, Kaneoka K, Wittek A, Kajzer J. Cervical injury mechanism based on the analysis of human cervical vertebral motion and head-neck-torso kinematics during low speed rear impacts. *Stapp Car C* 1997; 41:339-356.

Panjabi MM, Cholewicki J, Nibu K, Babat LB, Dvorak J. Simulation of whiplash trauma using whole cervical spine specimens. *Spine* 1998a; 23:17-24.

Panjabi MM, Cholewicki J, Nibu K, Grauer J, Vahldiek M. Capsular ligament stretches during in vitro whiplash simulations. *J Spinal Disord* 1998b; 11:227-232.

Panjabi MM, Cholewicki J, Nibu K, Grauer JN, Babat LB, Dvorak J. Mechanism of whiplash injury. *Clin Biomech* 1998c; 13:239-249.

Pearson AM, Ivancic PC, Ito S, Panjabi MM. Facet joint kinematics and injury mechanisms during simulated whiplash. *Spine* 2004; 29(4):390-397.

Peeters GG, Verhagen AP, de Bie RA, Oostendorp RA. The efficacy of conservative treatment in patients with whiplash injury: a systematic review of clinical trials. *Spine* 2001; 26(4):E64-E73.

Pekny M, Nilsson M. Astrocyte activation and reactive gliosis. *Glia* 2005; 50(4):427-434.

Peng B, Lin JY, Shang Y, Yang ZW, Wang YP. Plasticity in the synaptic number associated with neuropathic pain in the rat spinal dorsal horn: a stereological study. *Neurosci Lett* 2010; 486(1):24-28.

Petrenko AB, Yamakura T, Baba H, Shimoji K. The role of N-methyl-D-aspartate (NMDA) receptors in pain: a review. *Anesth Analg* 2003; 97:1108-1116.

Pettersson K, Toolanen G. High-dose methylprednisolone prevents extensive sick leave after whiplash injury: a prospective, randomized, double-blind study. *Spine* 1998; 23(9):984-989.

Polgár E, Todd AJ. Tactile allodynia can occur in the spared nerve injury model in the rat without selective loss of GABA or GABA< sub> A</sub> receptors from synapses in laminae I–II of the ipsilateral spinal dorsal horn. *Neuroscience* 2008; 156(1):193-202.

Porreca F, Ossipov MH, Gebhart GF. Chronic pain and medullary descending facilitation. *Trends Neurosci* 2002; 25(6):319-325.

Poulsen D, Park JW, Jeon NL, Robinson MB, Rothstein JD. Presynaptic regulation of astroglial excitatory neurotransmitter transporter GLT1. *Neuron* 2009; 61:880-894.

Price DD. Psychological and neural mechanisms of the affective dimension of pain. *Science* 2000; 288(5472):1769-1772.

Qin C, Martinez M, Tang R, Huynh J, Goodman Keiser M, Farber JP, Carman JC, Wienecke GM, Niederauer G, Foreman RD. Is constant current of constant voltage spinal cord stimulation superior for the suppression of nociceptive visceral and somatic stimuli? A rat model. *Neuromodulation* 2011; 15:132-143.

Queen SA, Kesslak JP, Bridges R J. Regional distribution of sodium-dependent excitatory amino acid transporters in rat spinal cord. *J Spinal Cord Med* 2007; 30(3):263-271.

Quinlan KP, Annest JL, Myers B, Ryan G, Hill H. Neck strains and sprains among motor vehicle occupants—United States, 2000. *Accident Anal Prev* 2004; 36(1):21-27.

Quinn KP, Bauman JA, Crosby ND, Winkelstein BA. Anomalous fiber realignment during tensile loading of the rat facet capsular ligament identifies mechanically induced damage and physiological dysfunction. *J Biomech* 2010a; 43(10):1870-1875.

Quinn KP, Dong L, Golder FJ, Winkelstein BA. Neuronal hyperexcitability in the dorsal horn after painful facet joint injury. *Pain* 2010b; 151:414-421.

Ramos KM, Lewis MT, Morgan KN, Crysdale NY, Kroll JL, Taylor FR, Harrison JA, Sloane EM, Maier SF, Watkins LR. Spinal upregulation of glutamate transporter GLT-1 by ceftriaxone: therapeutic efficacy in a range of experimental nervous system disorders. *Neuroscience* 2010; 169(4):1888-1900.

Ren K, Dubner R. Central nervous system plasticity and persistent pain. *J Orofac Pain* 1998; 13:155-163.

Rexed B. The cytoarchitectonic organization of the spinal cord in the cat. *J Comp Neurol* 1952; 96:415-495.

Rhalmi S, Yahia LH, Newman N, Isler M. Immunohistochemical study of nerves in lumbar spine ligaments. *Spine* 1993; 18(2):264-267.

Risher WC, Eroglu C. Thrombospondins as key regulators of synaptogenesis in the central nervous system. *Matrix Biol* 2012; 31(3):170-177.

Rizvi S, Kumar K. A case for spinal cord stimulation therapy – don't delay. *Practical Pain Management* 2013; 13:48-61.

Roehr B. New Report Details Uphill Battle to Solve the U.S.'s Pain Problem. Scientific American, July, 2011.

Rose MA, Kam PCA. Gabapentin: pharmacology and its use in pain management. *Anaesthesia* 2002; 57:451-462.

Rosenfeld M, Gunnarsson R, Borenstein P. Early intervention in whiplash-associated disorders: a comparison of two treatment protocols. *Spine* 2000; 25(14):1782-1787.

Rothman SM, Hubbard RD, Lee KE, Winkelstein BA. Detection, transmission, and perception of pain. In: Slipman CW, Derby R, Simeone FA, Mayer TG (Eds.) Interventional spine: an algorithmic approach, Saunders, Philadelphia, 2008, pp 29-38.

Rothman SM, Winkelstein BA. Cytokine antagonism reduces pain and modulates spinal astrocytic reactivity after cervical nerve root compression. *Ann Biomed Eng* 2010; 38:2563-2576.

Rothman SM, Winkelstein BA. Chemical and mechanical nerve root insults induce differential behavioral sensitivity and glial activation that are enhanced in combination. *Brain Res* 2007; 1181:30-43.

Roy DF, Fleury J, Fontaine SB, Dussault RG. Clinical evaluation of cervical facet joint infiltration. *J Can Assoc Radiol* 1988; 39:118-120.

Sankarasubramanian V, Buitenweg JR, Holsheimer J, Veltnik P. Triple leads programmed to perform as longitudinal guarded cathodes in spinal cord stimulation: a modeling study. *Neuromodulation* 2011; 14:401-411.

Schechtmann G, Song Z, Ultenius C, Meyerson BA, Linderoth B. Cholinergic mechanisms involved in the pain relieving effect of spinal cord stimulation in a model of neuropathy. *Pain* 2008; 139:136-145.

Schwarzer AC, Wang SC, Bogduk N, McNaught PJ, Laurent R. Prevalence and clinical features of lumbar zygapophysial joint pain: a study in an Australian population with chronic low back pain. *Ann Rheum Dis* 1995; 54:100-106.

Seltzer Z, Beilin B, Ginzburg R, Paran Y, Shimko T. The role of injury discharge in the induction of neuropathic pain behavior in rats. *Pain* 1991a; 46:327-336.

Seltzer Z, Cohn S, Ginzburg R, Beilin B. Modulation of neuropathic pain behavior in rats by spinal disinhibition and NMDA receptor blockade of injury discharge. *Pain* 1991b; 45:69-75.

Sengupta P. The laboratory rat: relating its age with humans. *Int J Prev Med* 2013; 4(6):624.

Shankarappa SA, Tsui JH, Kim KN, Reznor G, Dohlman JG, Langer R, Kohane DS. Prolonged nerve blockade delays the onset of neuropathic pain. *P Natl Acad Sci USA* 2012; 109(43):17555-17560.

Sheather-Reid RB, Cohen ML. Psychophysical evidence for a neuropathic component of chronic neck pain. *Pain* 1998; 75(2):341-347.

Sheng M, Lin JW. Glutamatergic synapses: molecular organization. In: eLS. John Wiley & Sons Ltd, Chichester, 2001; doi:10.1038/npg.els.0000235.

Shi M, Wang JY, Luo F. Depression shows divergent effects on evoked and spontaneous pain behaviors in rats. *J Pain* 2010; 11(3):219-229.

Shimoji K, Shimizu H, Maruyama Y, Matsuki M, Kuribayashi H, Fujioka H. Dorsal column stimulation in man: facilitation of primary afferent depolarization. *Anesth Analg* 1982; 61:410-413.

Siegmund GP, Myers BS, Davis MB, Bohnet HF, Winkelstein BA. Mechanical evidence of cervical facet capsule injury during whiplash: a cadaveric study using combined shear, compression, and extension loading. *Spine* 2001; 26(19):2095-2101.

Siegmund GP, Winkelstein BA, Ivancic PC. The anatomy and biomechanics of acute and chronic whiplash injury. *Traffic Inj Prev* 2009; 10:101-112.

Simpson BA. Spinal cord stimulation. *Brit J Neurosurg* 1997; 11(1):5-11.

Sivilotti L, Woolf CJ. The Contribution of GABA~ A and Glycine Receptors to Central Sensitization: Disinhibition and Touch-Evoked Allodynia in the Spinal Cord. *J Neurophysiol* 1994; 72(1):169-179.

Smith JR, Syré PP, Oake S, Nicholson KJ, Weisshaar CL, Cruz K, Bucki R, Baumann B, Janmey PA, Winkelstein BA. Salmon and human thrombin differentially regulate radicular pain, glial-induced inflammation and spinal neuronal excitability through the protease-activated receptor-1. *PLoS One* 2013*;* 8:e80006.

Smits H, van Kleef M, Holsheimer J, Joosten EAJ. Experimental spinal cord stimulation and neuropathic pain: Mechanisms of action, technical aspects, and effectiveness. *Pain Practice* 2013; 13:154-168.

Snider WD, McMahon SB. Tackling pain at the source: new ideas about nociceptors. *Neuron* 1998; 20(4):629-632.

Soliman AC, Yu JS, Coderre TJ. mGlu and NMDA receptor contributions to capsaicin-induced thermal and mechanical hypersensitivity. *Neuropharmacology* 2005; 48(3):325-332.

Song Z, Meyerson BA, Linderoth B. Spinal 5-HT receptors that contribute to the pain-relieving effects of spinal cord stimulation in a rat model of neuropathy. *Pain* 2011; 152(7):1666-1673.

Sonohata M, Furue H, Katafuchi T, Yasaka T, Doi A, Kumamoto E, Yoshimura M. Actions of noradrenaline on substantia gelatinosa neurones in the rat spinal cord revealed by in vivo patch recording. *J Physiol* 2004; 555:515–526.

Spitzer WO. Scientific monograph of the Quebec task force on whiplash-associated disorders: redefining'whiplash'and its management. *Spine* 1995; 20:1-73.

Steeds CE. The anatomy and physiology of pain. *Surgery* 2009; 27(12):507-511.

Stefani A, Spadoni F, Bernardi G. Gabapentin inhibits calcium currents in isolated rat brain neurons. *Neuropharmacology* 1998; 37(1):83-91.

Stemper BD, Yoganandan N, Pintar FA. Gender-and region-dependent local facet joint kinematics in rear impact: implications in whiplash injury. Spine 2004; 29(16):1764-1771.

Stenina OI, Desai SY, Krukovets I, Kight K, Janigro D, Topol EJ, Plow EF. Thrombospondin-4 and its variants: expression and differential effects on endothelial cells. *Circulation* 2003; 108:1514-1519.

Sterling M, Hendrikz J, Kenardy J, Kristjansson E, Dumas JP, Niere K, Cote J, deSerres S, Rivest K, Jull G. Assessment and validation of prognostic models for poor functional recovery 2 months after whiplash injury: a multicentre inception cohort study. *Pain* 2012; 153:1727-1734.

Sterling M, Jull G, Vicenzino B, Kenardy J. Sensory hypersensitivity occurs soon after whiplash injury and is associated with poor recovery. Pain 2003; 104(3):509-517.

Stiller CO, Cui JG, O'Conner WT, Brodin E, Meyerson BA, Linderoth B. Release of γ-aminobutyric acid in the dorsal horn and suppression of tactile allodynia by spinal cord stimulation in mononeuropathic rats. *Neurosurgery* 1996; 39(2):367-375.

Stojanovic MP, Abdi S. Spinal cord stimulation. *Pain Physician* 2002; 5:156-166.

Sufka KJ. Conditioned place preference paradigm: a novel approach for analgesic drug assessment against chronic pain. *Pain* 1994; 58(3):355-366.

Sun Q, Tu H, Xing GG, Han JS, Wan Y. Ectopic discharges from injured nerve fibers are highly correlated with tactile allodynia only in early but not late stage in rats with spinal nerve ligation. *Exp Neurol* 2005; 191:128-136.

Sundararajan S, Prasad P, Demetropoulos CK, Tashman S, Begeman PC, Yang KH, King AI. Effect of head-neck position on cervical facet stretch of post mortem human subjects during low speed rear end impacts. *Stapp Car C* 2004; 48:331-372.

Sung B, Lim G, Mao J. Altered Expression and Uptake Activity of Spinal Glutamate Transporters after Nerve Injury Contribute to the Pathogenesis of Neuropathic Pain in Rats. *J Neurosci* 2003; 23(7)2899-2910.

Tabatabai M, Booth AM. Mechanism of action of local anesthetics on synaptic transmission in the rat. *Anesth Analg* 1990; 71:149-157.

Takahashi Y, Chiba T, Kurokawa M, Aoki Y. Dermatomes and the central organization of dermatomes and body surface regions in the spinal cord dorsal horn in rats. *J Compar Neurol* 2003; 462(1):29-41.

Tang R, Martinez M, Goodman-Keiser M, Farber JP, Qin C, Foreman RD. Comparison of burst and tonic spinal cord stimulation on spinal neural processing in an animal model. *Neuromodulation* 2014; 17(2):143-151.

Todd AJ, Koerber HR. Neuroanatomical substrates of spinal nociception. In: McMahon SB, Koltzenburg M (Eds.), Wall and Melzack's Textbook of Pain, 5th ed., Churchill Livingstone, London, 2006.

Todd AJ. Neuronal circuitry for pain processing in the dorsal horn. *Nat Rev Neurosci* 2010; 11(12):823-836.

Tran MD, Neary JT. Purinergic signaling induces thrombospondin-1 expression in astrocytes. *P Natl Acad Sci USA* 2006; 103(24):9321-9326.

Tretter V, Mukherjee J, Maric HM, Schindelin H, Sieghart W, Moss SJ. Gephyrin, the enigmatic organizer at GABAergic synapses. *Fr Cell Neurosci* 2012; 6:23.

Ullian EM, Sapperstein SK, Christopherson KS, Barres BA. Control of synapse number by glia. *Science* 2001; 291:657-661.

Ultenius C, Linderoth B, Meyerson BA, Wallin J. Spinal NMDA receptor phosphorylation correlates with the presence of neuropathic signs following peripheral nerve injury in the rat. *Neurosci Lett* 2006; 399(1):85-90.

Van Oosterwijck J, Nijs J, Meeus M, Paul L. Evidence for central sensitization in chronic whiplash: a systematic literature review. *Eur J Pain* 2013; 17(3):299-312.

Vanegas H, Schaible HG. Descending control of persistent pain: inhibitory or facilitatory? *Brain Res Rev* 2004; 46(3):295-309.

Vierck CJ, Hansson PT, Yezierski RP. Clinical and pre-clinical pain assessment: are we measuring the same thing? *Pain* 2008; 135(1):7-10.

Wall PD, Waxman S, Basbaum AI. Ongoing activity in peripheral nerve: injury discharge. *Exp Neurol* 1974; 45:576-589.

Wall PD, Woolf CJ. The brief and the prolonged facilitatory effects of unmyelinated afferent input on the rat spinal cord are independently influenced by peripheral nerve section. *Neuroscience* 1986; 17(4):1199-1205.

Wang HJ, Wang W, Patel KP, Rozanski GJ, Zucker IH. Spinal cord GABA receptors modulate the exercise pressor reflex in decerebrate rats. *Am J Physiol-Reg I* 2013; 305(1):R42-R49.

Watkins LR, Milligan ED, Maier SF. Glial activation: a driving force for pathological pain. *Trends Neurosci* 2001; 24(8):450-455.

Watson C, Paxinos G, Kayalioglu G, Heise C. Atlas of the rat spinal cord, in: Watson C, Paxinos G, Kayalioglu G (Eds.), The Spinal Cord, Academic Press, London, 2009, pp. 238-306.

Wei J, Yang HB, Qin JB, Kong FJ, Yang TB. Single-dose intra-articular bupivacaine after knee arthroscopic surgery: a meta-analysis of randomized placebo-controlled studies. *Knee Surg Sports Traumatol Arthrosc* 2013; doi:10.1007/s00167-013-2543-7.

Weisshaar CL, Dong L, Bowman AS, Perez FM, Guarino BB, Sweitzer SM, Winkelstein BA. Metabotropic glutamate receptor-5 and protein kinase C-epsilon increase in dorsal root ganglion neurons and spinal glial activation in an adolescent rat model of painful neck injury. *J Neurotrauma* 2010; 27(12):2261-2271.

Weisshaar CL, Winkelstein BA. Ablating spinal NK1-bearing neurons eliminates the development of pain and reduces spinal neuronal hyperexcitability and inflammation from mechanical joint injury in the rat. *J Pain* 2014; 15(4):378-386.

Wells J, Tripp LN. Time course of reactive synaptogenesis in the subcortical somatosensory system. *J Comp Neurol* 1987; 255(3):466-475.

Wesselink WA, Boom HBK. Analysis of current density and related parameters in spinal cord stimulation. *IEEE T Rehabil Eng* 1998; 6:200-207.

Wilson SG, Mogil JS. Measuring pain in the (knockout) mouse: big challenges in a small mammal. *Behav Brain Res* 2001; 125(1):65-73.

Winkelstein BA, Nightingale RW, Richardson WJ, Myers BS. The cervical facet capsule and its role in whiplash injury: a biomechanical investigation. *Spine* 2000; 25(10):1238-1246.

Winkelstein BA, Santos DG. An intact facet capsular ligament modulates behavioral sensitivity and spinal glial activation produced by cervical facet joint tension. *Spine* 2008; 33(8):856-862.

Winkelstein BA. Mechanisms of central sensitization, neuroimmunology & injury biomechanics in persistent pain: implications for musculoskeletal disorders. *J Electromyogr Kines* 2004; 14(1):87-93.

Woolf CJ, Chong MS. Preemptive analgesia – treating postoperative pain by preventing the establishment of central sensitization. *Anesth Analg* 1993; 77:362-379.

Woolf CJ, Salter MW. Neuronal plasticity: increasing the gain in pain. *Science* 2000; 288(5472):1765-1769.

Woolf CJ, Shortland P, Coggeshall RE. Peripheral nerve injury triggers central sprouting of myelinated afferents. *Nature* 1992; 355:75-78.

Woolf CJ, Shortland P, Reynolds M, Ridings J, Doubell T, Coggeshall RE. Reorganization of central terminals of myelinated primary afferents in the rat dorsal horn following peripheral axotomy. *J Comp Neurol* 1995; 360:121-134.

Woolf CJ, Thompson SW. The induction and maintenance of central sensitization is dependent on N-methyl-D-aspartic acid receptor activation; implications for the treatment of post-injury pain hypersensitivity states. *Pain* 1991; 44(3):293-299.

Woolf CJ, Wall PD. Relative effectiveness of C primary afferent fibers of different origins in evoking a prolonged facilitation of the flexor reflex in the rat. *J Neurosci* 1986; 6(5):1433-1442.

Woolf CJ. Central sensitization: implications for the diagnosis and treatment of pain. *Pain* 2011; 152(3):S2-S15.

Woolf CJ. Evidence for a central component of post-injury pain hypersensitivity. *Nature* 1983; 306:686-688.

Xie W, Strong JA, Meij JTA, Zhang J, Yu L. Neuropathic pain: early spontaneous afferent activity is the trigger. *Pain* 2005; 116:243-256.

Xin W, Weng H, Dougherty PM. Plasticity in expression of the glutamate transporter GLT-1 and GLAST in spinal dorsal horn glial cells following partial sciatic nerve ligation. *Mol Pain* 2009; 5:15.

Xu XJ, Dalsgaard CJ, Wiesenfeld-Hallin Z. Intrathecal CP-96,345 blocks reflex facilitation induced in rats by substance P and C-fiber-conditioning stimulation. Eur J Pharmacol 1992; 216(3):337-344.

Xu T, Jiang W, Du D, Xu Y, Hu Q, Shen Q. Role of spinal metabotropic glutamate receptor subtype 5 in the development of tolerance to morphine-induced antinociception in rat. *Neurosci Lett* 2007; 420:155-159.

Yakhnitsa V, Linderoth B, Meyerson BA. Spinal cord stimulation attenuates dorsal horn neuronal hyperexcitability in a rat model of mononeuropathy. *Pain* 1999; 79:223-233.

Yaksh TL, Luo ZD. Anatomy of the Pain Processing System. In: Waldman S (Ed.) International Pain Management, 2nd ed., WB Saunders, Philadelphia, 2001.

Yaksh TL. Central pharmacology of nociceptive transmission. In: McMahon SB, Koltzenburg M (Eds.), Wall and Melzack's Textbook of Pain, 5th ed., Churchill Livingstone, London, 2006.

Yaksh TL. Spinal systems and pain processing: development of novel analgesic drugs with mechanistically defined models. *Trends Pharmacol Sci* 1999; 20(8):329-337.

Yamashita T, Cavanaugh JM, El-Bohy AA, Getchell TV, King AI. Mechanosensitive afferent units in the lumbar facet joint. *J Bone Joint Surg* 1990; 72:865–870.

Yamashita T, Cavanaugh JM, Özaktay AC, Avramov AI, Getchell TV, King AI. Effect of substance P on mechanosensitive units of tissues around and in the lumbar facet joint. *J Orthop Res* 1993; 11(2):205-214.

Yamashita T, Minaki Y, Özaktay AC, Cavanaugh JM, King AI. A morphological study of the fibrous capsule of the human lumbar facet joint. *Spine* 1996; 21(5):538-543.

Young MR, Fleetwood-Walker SM, Dickinson T, Blackburn-Munro G, Sparrow H, Birch PJ, Bountra C. Behavioural and electrophysiological evidence supporting a role for group I metabotropic glutamate receptors in the mediation of nociceptive inputs to the rat spinal cord. *Brain Res* 1997; 777(1-2):161-169.

Zeilhofer HU, Willis WD. GABA and Glycine in Spinal Nociceptive Processing. In: Gebhardt GF, Schmidt RF (Eds.) Encyclopedia of Pain, Springer Berlin, Heidelberg, Germany, 2013, pp. 1337-1344.

Zeng J, Kim D, Li KW, Sharp K, Steward O, Zaucke F, Luo ZD. Thrombospondin-4 contributes to spinal cord injury-induced changes in nociception. *Eur J Pain* 2013; 17(10):1458-1464.

Zhang H, Xie W, Xie Y. Spinal cord injury triggers sensitization of wide dynamic range dorsal horn neurons in segments rostral to the injury. *Brain Res* 2005; 1055(1):103-110.

Zhang HM, Chen SR, Cai YQ, Richardson TE, Driver LC, Lopez-Berestein G, Pan HL. Signaling mechanisms mediating muscarinic enhancement of GABAergic synaptic transmission in the spinal cord. *Neuroscience* 2009; 158(4):1577-1588.

Zhang S, Nicholson KJ, Smith JR, Syré PP, Gilliland TM, Winkelstein BA. The roles of mechanical compression and chemical irritation in regulating spinal neuronal signaling in painful cervical nerve root injury. *Stapp Car C* 2013; 57:219-242.

Zhang TC, Janik JJ, Grill WM. Mechanisms and models of spinal cord stimulation for the treatment of neuropathic pain. *Brain Res* 2014; http://dx.doi.org/10.1016/j.brainres. 2014.04.039.

Zimmerman M. Ethical guidelines for investigations of experimental pain in conscious animals. *Pain* 1983; 16:109-110.